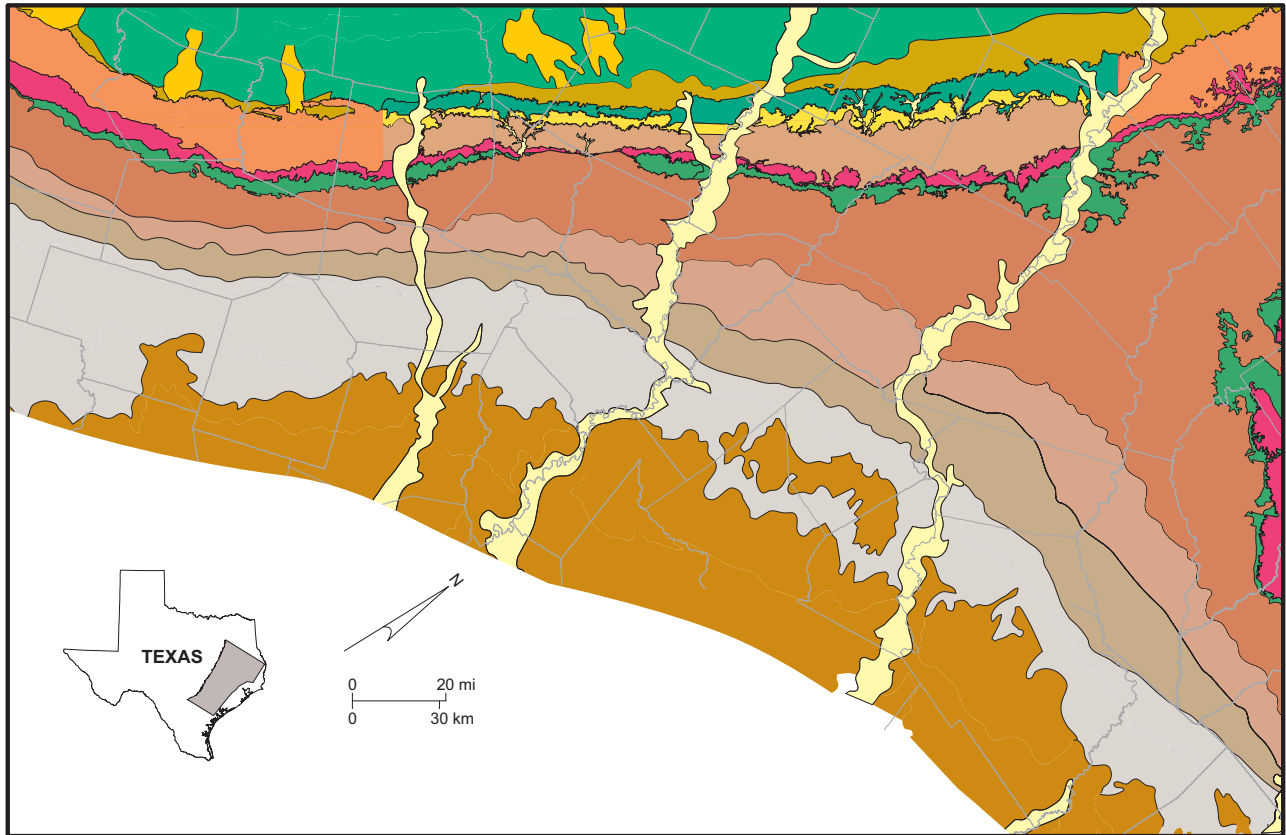


GROUNDWATER AVAILABILITY MODEL FOR THE CENTRAL PART OF THE CARRIZO-WILCOX AQUIFER IN TEXAS



Prepared for
Texas Water Development Board

By Alan R. Dutton, Bob Harden¹, Jean-Philippe Nicot, and David O'Rourke²

**Bureau of Economic Geology
Scott W. Tinker, Director**

John A. and Katherine G. Jackson School of Geosciences
The University of Texas at Austin
Austin, Texas 78713-8924

¹ R. W. Harden and Associates, Inc.

² HDR Engineering Services, Inc.

**GROUNDWATER AVAILABILITY MODEL
FOR THE CENTRAL PART OF THE
CARRIZO-WILCOX AQUIFER IN TEXAS**

Prepared for
Texas Water Development Board

Under
Contract No. 2001-483-378

By Alan R. Dutton, Bob Harden¹, Jean-Philippe Nicot, and David O'Rourke²

**Bureau of Economic Geology
Scott W. Tinker, Director**

John A. and Katherine G. Jackson School of Geosciences
The University of Texas at Austin
Austin, Texas 78713-8924

¹ R. W. Harden and Associates, Inc.

² HDR Engineering Services, Inc.

CONTENTS

Abstract	1
1.0 Introduction	4
2.0 Study area	8
2.1 Physiography and Climate.....	13
2.2 Geology	19
3.0 Previous Work.....	29
4.0 Hydrologic setting	32
4.1 Hydrostratigraphy.....	32
4.2 Structure	34
4.3 Water Quality	53
4.4 Water Levels and Regional Groundwater Flow	57
4.4.1 Data and Methods.....	58
4.4.2 Predevelopment or Steady-State Distribution of Hydraulic Head	61
4.4.3 Postdevelopment Changes in Hydraulic Head	68
4.5 Recharge.....	79
4.5.1 Field Methods.....	84
4.5.2 Field Results	85
4.6 Interaction of Surface Water and Groundwater	91
4.6.1 Low-Flow Studies	93
4.6.2 Base-Flow Studies.....	95
4.6.3 Surface-Water Reservoirs.....	101
4.7 Groundwater Evapotranspiration	103

4.8	Hydraulic Properties.....	103
4.9	Well Discharge.....	114
5.0	Conceptual Model of Groundwater Flow.....	125
6.0	Model Design.....	129
6.1	Code and Processor.....	129
6.2	Layers and Grid.....	130
6.3	Boundary Conditions.....	138
6.3.1	Recharge.....	140
6.3.2	Interaction of Surface Water and Groundwater.....	144
6.3.2.1	Stream-Flow Routing.....	144
6.3.2.2	Surface-Water Reservoirs.....	146
6.3.3	Evapotranspiration.....	147
6.3.4	General-Head Boundary.....	148
6.3.5	Horizontal-Flow Barrier.....	150
6.3.6	Wells.....	151
6.4	Model Parameters.....	164
7.0	Modeling Approach.....	173
8.0	Steady-State Model.....	177
8.1	Calibration.....	177
8.2	Sensitivity Analysis.....	187
8.3	Water Budget.....	193
9.0	Transient Model.....	197
9.1	Calibration and Verification.....	197
9.2	Water Budget.....	220

9.3	Sensitivity Analysis.....	228
10.0	Predictions.....	234
10.1	Predictive Results.....	234
10.2	Water Budget.....	255
11.0	Limitations of the Model.....	265
11.1	Input Data.....	265
11.2	Assumptions.....	268
11.3	Scale of Application.....	271
12.0	Future Improvements.....	273
13.0	Conclusions.....	276
14.0	Acknowledgments.....	280
15.0	References.....	282
	Appendix A.....	A-1
	Appendix B.....	B-1
	Appendix C.....	C-1
	Appendix D.....	D-1

Figures

1.	Location of the Carrizo–Wilcox aquifer in Texas showing the overlapping position of the three regional models.....	6
2.	Location of the study area relative to roads, major cities and towns, lakes, and rivers.....	9
3.	Extent of previous models of groundwater flow in the Carrizo–Wilcox aquifer in the study area.....	10

4.	Location of groundwater conservation districts in the study area.....	11
5.	Location of Regional Water Planning Groups in the study area.....	12
6.	Land-surface elevation in the study area relative to divides between surface-water drainage basins	14
7.	Average annual precipitation (1940 through 1997) in the study area	16
8.	Historical annual precipitation measured at rain gages at Seguin, Smithville, Cameron, Athens, and Nacogdoches	17
9.	Average net lake evaporation rate in the study area.....	18
10.	Generalized stratigraphic chart for the study	20
11.	Generalized map of surface geology in the study area.....	21
12.	Thickness of major sandstones in the Simsboro Formation in the study area.....	23
13.	Thickness of major sandstones in the Carrizo Formation in the study area.....	26
14.	Geologic structure in the study area.....	35
15.	Vertical strike-oriented profile of the formations making up the Carrizo–Wilcox aquifer and adjacent formations.	36
16.	Vertical dip-oriented profile of the formations making up the Carrizo–Wilcox aquifer and adjacent formations.	38
17.	Elevation of the base of the Hooper Formation (base of Wilcox Group)	43
18.	Elevation of the base of the Simsboro Formation (top of Hooper Formation).....	45
19.	Elevation of the base of the Calvert Bluff Formation (top of Simsboro Formation).....	46

20. Elevation of the base of the Carrizo Formation (top of Calvert Bluff Formation)	47
21. Elevation of the top of the Carrizo Formation (base of the Reklaw Formation)	48
22. Elevation of the top of the Reklaw Formation	49
23. Total thickness of the Hooper Formation.....	50
24. Total thickness of the Simsboro Formation	51
25. Total thickness of the Calvert Bluff Formation.....	52
26. Total thickness of the Carrizo Formation.....	54
27. Total dissolved solids (TDS) content of groundwater in the Carrizo–Wilcox aquifer and in the saline section downdip of the aquifer	56
28. Water-level elevation under “predevelopment” conditions in the Simsboro aquifer	62
29. Water-level elevation under “predevelopment” conditions in the Carrizo aquifer.....	63
30. Water-level elevation under “predevelopment” conditions in the Queen City aquifer.....	67
31. Water-level elevation in the Simsboro aquifer measured during 1987 to 1990 and used for the 1990 model-year calibration.....	69
32. Water-level elevation in the Simsboro aquifer measured during 1995 to 2000 and used for the 2000 model-year calibration.....	70
33. Water-level elevation in the Carrizo aquifer measured during 1987 to 1990 and used for the 1990 model-year calibration.....	71

34. Water-level elevation in the Carrizo aquifer measured during 1995 to 2000 and used for the 2000 model-year calibration.....	72
35. Hydrographs for 10 representative wells in the Hooper Formation.....	74
36. Locations of water wells for which hydrographs are presented.....	75
37. Hydrographs for 10 representative wells in the Simsboro Formation.....	76
38. Hydrographs for 10 representative wells in the Calvert Bluff Formation.....	77
39. Hydrographs for 10 representative wells in the Carrizo Formation.....	78
40. Recharge rates estimated in previous hydrologic studies of the Carrizo–Wilcox aquifer.....	80
41. Map of soil permeability in the recharge area of the model.....	82
42. Variation with depth in water content in soil cores.....	86
43. Variation with depth in soil-water chloride in soil cores	88
44. Location of stream-flow gages used for base-flow separation.....	98
45. Comparison of total discharge and estimated base flow for Plum Creek near Luling, Texas.....	99
46. Base-flow increase across the Carrizo–Wilcox outcrop, unitized by area of drainage basin in the outcrop.....	100
47. Histograms of hydraulic conductivity in the Carrizo, Calvert Bluff, Simsboro, and Hooper, and of specific storage in the Carrizo–Wilcox aquifer.....	105
48. Map of average hydraulic conductivity in the Hooper Formation	109
49. Map of average hydraulic conductivity in the Simsboro Formation.....	111
50. Map of average hydraulic conductivity in the Calvert Bluff Formation.....	112
51. Map of average hydraulic conductivity in the Carrizo Formation	113

52.	Total groundwater withdrawals from the Carrizo–Wilcox aquifer in the study area.....	115
53.	Conceptual model of the aquifer showing how the hydrostratigraphy translates into the computer model of the aquifer	126
54.	Location of active cells in model layer 6, representing groundwater in the Hooper Formation, and the position of boundary cells.....	132
55.	Location of active cells in model layer 5, representing groundwater in the Simsboro Formation, and the position of boundary cells.....	133
56.	Location of active cells in model layer 4, representing the Calvert Bluff Formation, and the position of boundary cells.....	134
57.	Location of active cells in model layer 3, representing the Carrizo Formation, and the position of boundary cells.....	135
58.	Location of active cells in model layer 2, representing the Reklaw Formation, and the position of boundary cells.....	136
59.	Location of active cells in model layer 1, representing alluvium in the Colorado, Brazos, and Trinity River systems, and the position of boundary cells.....	137
60.	Distribution of groundwater withdrawal in 2000 for municipal and manufacturing and power supplies.....	152
61.	Map of population density in rural parts of the study area, excluding cities and towns with more than 500 people.....	156
62.	Variation in total rate of groundwater withdrawal in 1990 in Carrizo aquifer, Calvert Bluff aquitard, Simsboro aquifer, and Hooper aquitard.....	158

63.	Variation in total rate of groundwater withdrawal in 2000 in Carrizo aquifer, Calvert Bluff aquitard, Simsboro aquifer, and Hooper aquitard.....	160
64.	Storativity assigned to model cells representing the Hooper aquitard	168
65.	Storativity assigned to model cells representing the Simsboro aquifer.....	169
66.	Storativity assigned to model cells representing the Calvert Bluff aquitard.....	170
67.	Storativity assigned to model cells representing the Carrizo aquifer.....	171
68.	Storativity assigned to model cells representing the Reklaw aquitard.....	172
69.	Recharge rate estimated on the basis of soil properties and results of previous studies	180
70.	Histogram of recharge rates applied in the model.....	181
71.	Simulated water levels for the Simsboro aquifer in the study area under predevelopment or steady-state (1950) conditions and comparison with measured contours.....	182
72.	Simulated water levels for the Carrizo aquifer in the study area under predevelopment or steady-state (1950) conditions and comparison with measured contours.....	183
73.	Comparison of simulated and measured water levels in the steady-state simulation of model layers representing the Carrizo–Wilcox aquifer	184
74.	Location of water-level measurements used in calibration of the steady-state version of the model.....	185
75.	Map of residual differences between simulated and measured water levels for the Simsboro aquifer (layer 5) for the steady-state calibration.....	188
76.	Map of residual differences between simulated and measured water levels for the Carrizo aquifer (layer 3) for the steady-state calibration.....	189

77.	Sensitivity of predicted water levels in the Simsboro aquifer (layer 5) of the steady-state model to changes in parameter values for the Simsboro aquifer (layer 5), Carrizo aquifer (layer 3), and recharge rate, streambed conductance, and the GHB boundary on the Reklaw aquitard (layer 2).....	192
78.	Sensitivity of predicted water levels in the Carrizo aquifer (layer 3) of the steady-state model to changes in parameter values for the Carrizo aquifer (layer 3), Simsboro aquifer (layer 5), and recharge rate, streambed conductance, and the GHB boundary on the Reklaw aquitard (layer 2).....	194
79.	Block diagram of the Carrizo–Wilcox aquifer representing the components of the steady-state model.....	196
80.	Maps for the Simsboro aquifer (layer 5) showing simulated and observed 1990 water level and drawdown from 1950 through 1990	199
81.	Map of residual differences simulated and measured water levels for the Simsboro aquifer (layer 5) for the 1990 calibration	200
82.	Comparison of simulated and observed water levels for the 1990 calibration.....	201
83.	Location of wells used to develop the 1990 calibration of the model.....	202
84.	Maps for the Carrizo aquifer (layer 3) showing simulated and observed 1990 water level and drawdown from 1950 to 1990.....	204
85.	Map of residual differences between simulated and measured water levels for the Carrizo aquifer (layer 3) for the 1990 calibration.....	205
86.	Maps of water level in the Hooper Formation (layer 6) in 1990 and 2000.....	206
87.	Maps of water level in the Calvert Bluff Formation (layer 4) in 1990 and 2000.....	207

88.	Comparison of simulated and observed water levels for the 2000 calibration.....	208
89.	Location of wells used to develop the 2000 calibration of the model.....	209
90.	Maps for the Simsboro aquifer (layer 5) showing simulated and observed 2000 water level and drawdown from 1950 through 2000	210
91.	Map of residual differences between simulated and measured water levels for the Simsboro aquifer (layer 5) for the 2000 calibration	211
92.	Maps for the Carrizo aquifer (layer 3) showing simulated and observed 2000 water level and drawdown from 1950 through 2000	213
93.	Map of residual differences between simulated and measured water levels for the Carrizo aquifer (layer 3) for the 2000 calibration.....	214
94.	Comparison of simulated and observed water-level hydrographs for 10 wells in the Hooper aquitard (layer 6).....	216
95.	Comparison of simulated and observed water-level hydrographs for 10 wells in the Simsboro aquifer (layer 5)	217
96.	Comparison of simulated and observed water-level hydrographs for 10 wells in the Calvert Bluff aquitard (layer 4).....	218
97.	Comparison of simulated and observed water-level hydrographs for 10 wells in the Carrizo aquifer (layer 3).....	219
98.	Changes in simulated ET and base-flow discharge to stream with variation in recharge and pumping rates.....	221
99.	Map of aquifer discharge simulated as groundwater evapotranspiration for 2000.....	224

100. Block diagram of the Carrizo–Wilcox aquifer representing the components of the transient model for 2000	226
101. Sensitivity of predicted water levels in the Simsboro aquifer (layer 5) in the transient model to changes in parameter values for the Simsboro aquifer (layer 5), Carrizo aquifer (layer 3), and other parts of the model.....	229
102. Sensitivity of predicted water levels in the Carrizo aquifer (layer 3) in the transient model to changes in parameter values for the Carrizo aquifer (layer 3), Simsboro aquifer (layer 5), Carrizo aquifer (layer 3), and other parts of the model.....	230
103. Sensitivity of simulated water levels to order-of-magnitude changes in storativity for the Carrizo aquifer (layer 3) and Simsboro aquifer (layer 5)	231
104. Sensitivity of simulated water levels in the Carrizo and Simsboro aquifers to differences in storativity.....	233
105. Simulated hydrographs showing predicted water levels through 2050 for wells in the Hooper aquitard (layer 6)	235
106. Simulated hydrographs showing predicted water levels through 2050 for wells in the Simsboro aquifer (layer 5)	236
107. Simulated hydrographs showing predicted water levels through 2050 for wells in the Calvert Bluff aquitard (layer 4)	237
108. Simulated hydrographs showing predicted water levels through 2050 for wells in the Carrizo aquifer (layer 3)	238
109. Maps for the Simsboro aquifer (layer 5) showing predicted 2010 water level and drawdown from 2000 through 2010 assuming drought-of-record recharge from 2008 through 2010.....	240

110. Maps for the Simsboro aquifer (layer 5) showing predicted 2020 water level and drawdown from 2000 through 2020 assuming drought-of-record recharge from 2018 through 2020.....	241
111. Maps for the Simsboro aquifer (layer 5) showing predicted 2030 water level and drawdown from 2000 through 2030 assuming drought-of-record recharge from 2028 through 2030.....	242
112. Maps for the Simsboro aquifer (layer 5) showing predicted 2040 water level and drawdown from 2000 through 2040 assuming drought-of-record recharge from 2038 through 2040.....	243
113. Maps for the Simsboro aquifer (layer 5) showing predicted 2050 water level and drawdown from 2000 through 2050 assuming drought-of-record recharge from 2048 through 2050.....	244
114. Maps for the Carrizo aquifer (layer 3) showing predicted 2010 water level and drawdown from 2000 through 2010 assuming drought-of-record recharge from 2008 through 2010.....	247
115. Maps for the Carrizo aquifer (layer 3) showing predicted 2020 water level and drawdown from 2000 through 2020 assuming drought-of-record recharge from 2018 through 2020.....	248
116. Maps for the Carrizo aquifer (layer 3) showing predicted 2030 water level and drawdown from 2000 through 2030 assuming drought-of-record recharge from 2028 through 2030.....	249
117. Maps for the Carrizo aquifer (layer 3) showing predicted 2040 water level and drawdown from 2000 through 2040 assuming drought-of-record recharge from 2038 through 2040.....	250

118. Maps for the Carrizo aquifer (layer 3) showing predicted 2050 water level and drawdown from 2000 through 2050 assuming drought-of-record recharge from 2048 through 2050.....	251
119. Maps for groundwater in the Hooper Formation (layer 6) showing predicted 2050 water level and drawdown from 2000 through 2050 assuming drought-of-record recharge from 2048 through 2050	253
120. Maps for groundwater in the Calvert Bluff Formation (layer 4) showing predicted 2050 water level and drawdown from 2000 through 2050 assuming drought-of-record recharge from 2048 through 2050	254
121. Difference for the end of 2050 in simulated water levels in Carrizo aquifer (layer 3) and Simsboro aquifer (layer 5) assuming average versus drought-of-record rates of recharge	256
122. Block diagram of the Carrizo–Wilcox aquifer representing the components of the predictive model for 2050	260

Tables

1. Water content, chloride concentration, and estimated recharge based on unsaturated zone chloride concentrations, chloride concentrations in groundwater and associated recharge rates, and age of the chloride profile.....	87
2. Results of ^3He , ^4He , ^{20}Ne , ^{40}Ar , and N_2 measurements, and calculated tritogenic helium-3 ($^3\text{He}^*$) and $^3\text{H}/^3\text{He}$ ages	90
3. Average flow of streams in study area	94
4. Summary of low-flow studies in Cibolo Creek.....	96
5. Characteristics of reservoirs in study area.....	102

6.	Summary of hydraulic conductivity of the central Carrizo–Wilcox aquifer in the study area.....	106
7.	Rates of groundwater withdrawal from the Carrizo–Wilcox aquifer as assigned within the study area	116
8.	Rate of groundwater withdrawal for municipal public water supply and rural domestic, mining, manufacturing, irrigation, power, and stock-water supply from the Carrizo–Wilcox aquifer as assigned in the model	117
9.	Projection parameters for the model grid and hydrogeologic data	139
10.	Calibrated values of minimum and maximum recharge rate by layer	141
11.	Summary of model calibration and verification statistics	186
12.	Simulated groundwater discharge to streams.....	190
13.	Water budget for the calibrated steady-state model.....	195
14a.	Water budget for the calibrated steady-state and transient models.....	222
14b.	Water budget for the transient model for drought years 1988 and 1996.....	223
15.	Simulated leakage of water to the Carrizo–Wilcox aquifer from surface- water reservoirs	227
16.	Water budget for the predictive model.....	257
17.	Simulated groundwater discharge to streams for the predictive model	262
18.	Sensitivity of predicted 2050 water budget (with drought of record) to changes in storativity and pumping rate.....	263

ABSTRACT

This report documents one of three overlapping, quasi-three-dimensional, numerical models of the occurrence and movement of groundwater in the Carrizo–Wilcox aquifer in Texas. The model was developed as part of a Texas Groundwater Availability Modeling (GAM) program to assist in evaluating groundwater availability and water levels in response to potential droughts and future pumping, including new well fields. Formations of the Paleocene-Eocene-age Wilcox Group, along with the overlying Carrizo Formation, make up a major aquifer system in Texas. This model covers the central section of the Carrizo–Wilcox aquifer as defined by the surface-water divide between the San Antonio and Guadalupe Rivers to the southwest and the surface-water divide between the Trinity and Neches Rivers to the northeast. Groundwater withdrawal from the central part of the Carrizo–Wilcox aquifer accounted for approximately 36 percent of all pumping from the aquifer in 2000.

The model is based on data on geological structure and depositional setting of the aquifer, hydrological properties, water-use survey estimates of historical groundwater withdrawals, and base flow of rivers and streams. New insights into how the downdip circulation of freshwater is affected by fault zones and a deep-basin geopressured zone are based on maps of total dissolved solids and equivalent water levels from the outcrop to depths of more than 10,000 ft. In addition, results of field studies using “environmental” tracers yielded regional estimates of recharge rates that broadly match estimates from previous models.

The six-layer model was developed using MODFLOW-96 and includes four layers representing groundwater in the Simsboro and Carrizo Formations, the main flow units of the

Carrizo–Wilcox aquifer system, and in the Hooper and Calvert Bluff Formations, which locally act as confining layers or aquitards within the Carrizo–Wilcox aquifer. During the past 2 decades, about 90 percent of the water pumped from the aquifer was from the Simsboro and Carrizo Formations. Another confining unit, representing the overlying Reklaw Formation, was included as a bounding layer in which water levels in the Queen City aquifer were applied. We also included a layer representing alluvium along the Colorado, Brazos, and Trinity Rivers in the outcrop of the Carrizo–Wilcox aquifer. The Simsboro and Carrizo Formations contribute base flow to these rivers, but discharge is indirect, through the alluvium, rather than directly to stream beds.

A steady-state model representing “predevelopment” (no pumping) conditions was calibrated against water levels measured prior to 1950 and historical low-flow measurements in streams. A transient version of the model with 1-yr-long stress periods was calibrated against water-level hydrographs and stream-flow data for the period from 1950 through 1990, with an emphasis on 1990 data. The calibrated model was verified by comparison with water levels recorded during the 1990s, with an emphasis on 2000 data. During the 1980s and 1990s the years with the smallest rainfall were 1988 and 1996 in the study area. Model runs were made with monthly stress periods for the 36 months from 1987 through 1989 and from 1995 through 1997 to check how simulated water level responds to short-term variation in recharge and pumping rates. Recharge rates, vertical hydraulic conductivity, specific storage, specific yield, and boundary-flux properties were calibrated using the model. We considered horizontal hydraulic conductivity to be one of the more well-known attributes of the aquifer, given the number of pumping- and specific-capacity tests and the quality of regional mapping of the distribution and thickness of sandstones that make up the permeable

architecture of the aquifer. Uncertainty in calibrated water levels is less than or equal to 10 percent of the range of water-level measurements.

To demonstrate the use of the groundwater model as an evaluative and predictive tool, several simulations were made of future water-level changes with assumed periods of normal and drought-of-record precipitation. Future rates of groundwater withdrawal were assigned on the basis of demand numbers from eight Regional Water Planning Groups.

Groundwater pumpage is expected to continue to increase between 2000 and 2050, but at a slower rate than that of the past decade. Pumping rates will continue to increase from the Bryan-College Station well field but will be fairly steady from the Lufkin-Angelina County well field. Additional well fields, including municipal well fields, will be established or grow. Many municipalities and industries will meet future needs by drilling new wells and increasing their withdrawal from the Carrizo–Wilcox aquifer. Mining operations will continue to extract a significant volume of groundwater, but after increasing in withdrawal rate during the period from 1990 through 2010, pumping rates related to mining are expected to remain steady or decrease. Overall, total pumping from the Carrizo–Wilcox aquifer in the study area is expected to increase from 194,000 acre-feet per year in 2000 to over 360,000 acre-feet per year in 2050.

The simulated decline of water level related to groundwater pumping will occur mainly through a decrease in artesian storage. The pressure head of groundwater is simulated to remain above the top of aquifer layers except where the confined aquifer is at shallow depths near the outcrop. The model also suggests that the major rivers will continue to receive groundwater discharge even with increased pumping and under drought conditions. Model predictions for 2050 using average recharge versus drought-of-record recharge result in only a few feet of simulated water-level differences in the outcrop.

1.0 INTRODUCTION

The Carrizo–Wilcox aquifer is one of nine major aquifers in Texas and extends across the state from the Rio Grande in the south, northeastward into Arkansas and Louisiana, parallel to the Gulf Coast aquifer (Ashworth and Hopkins, 1995). This aquifer supplies water to approximately 60 counties. Groundwater production is predominantly for municipal public-water supply, manufacturing, and rural domestic use. The largest areas of municipal use are in the Bryan-College Station, Lufkin-Nacogdoches, and Tyler areas, all of which use groundwater from the Carrizo–Wilcox aquifer. A significant volume of groundwater in the central part of the aquifer is extracted as part of lignite mining operations. Irrigation pumping from the Carrizo–Wilcox aquifer is greatest in the Wintergarden region in South Texas. Water use in 1997 amounted to 430,000 acre-feet/yr, exceeded only by the Gulf Coast and Ogallala aquifers (Texas Water Development Board [TWDB], 2002).

Planning for water needs for the period from 2000 through 2050 is critical for the State of Texas because of the frequency of droughts. The State Water Plan (TWDB, 2002) describes the development, management, and conservation of water resources and preparation for potential droughts (TWDB, 2002). The most recently published State Water Plan differs from previous Texas water plans in that it is a result of a bottom-up rather than top-down approach and represents the management strategies adopted by the 16 Regional Water Planning Groups in Texas. Estimating groundwater availability for the 50-yr planning period in Texas involves aquifer management goals, environmental issues, rules and regulations, and scientific understanding of how an aquifer works (Mace and others, 2000b).

Groundwater availability assessment is important for the Carrizo–Wilcox aquifer. Pumping from the aquifer in the area between the Neches and San Antonio Rivers, for example, increased 170 percent between 1980 and 2000. In the area between the Colorado

and Brazos Rivers, pumpage increased from 10,600 to 37,900 acre-feet/yr between 1951 and 1996, primarily as a result of mining needs (Dutton, 1999).

Numerical modeling is a useful tool for assessing groundwater availability during the next 50 yr under proposed pumpage scenarios and potential future drought conditions. The Groundwater Availability Model (GAM) program involves development of GAM models for each of the major and minor aquifers in the state. Three separate numerical models (Northern, Central, and Southern) were developed for the Carrizo–Wilcox aquifer in Texas, with large overlap regions between the models (fig. 1). This report documents the development of the GAM model for the central part of the Carrizo–Wilcox aquifer.

The format for the models developed under the GAM program has been standardized. Each model includes the development of a conceptual model of groundwater flow in the model area, which forms the basis for the numerical model of the region. The numerical model requires information on the initial and boundary conditions and the hydraulic properties in the aquifer. A steady-state model is developed that represents predevelopment conditions. In addition, a transient model is developed and simulated results are compared with measured water levels in 1990, as well as water-level changes through time. The model is verified by simulating the period from 1990 through 2000 and comparing the simulated water levels with measured values in 2000, as well as with water-level changes for that period. Comparison of simulated and estimated base flow of streams is also part of model calibration. Sensitivity analyses are performed in the steady-state and transient models and help determine important controls on groundwater flow and assess uncertainties in model parameters. The calibrated model is then used to predict aquifer conditions during the 50-yr planning cycle (2000 to 2050). Groundwater withdrawal for the 50-yr period was derived from a TWDB analysis of the demands and supplies of surface water and groundwater,

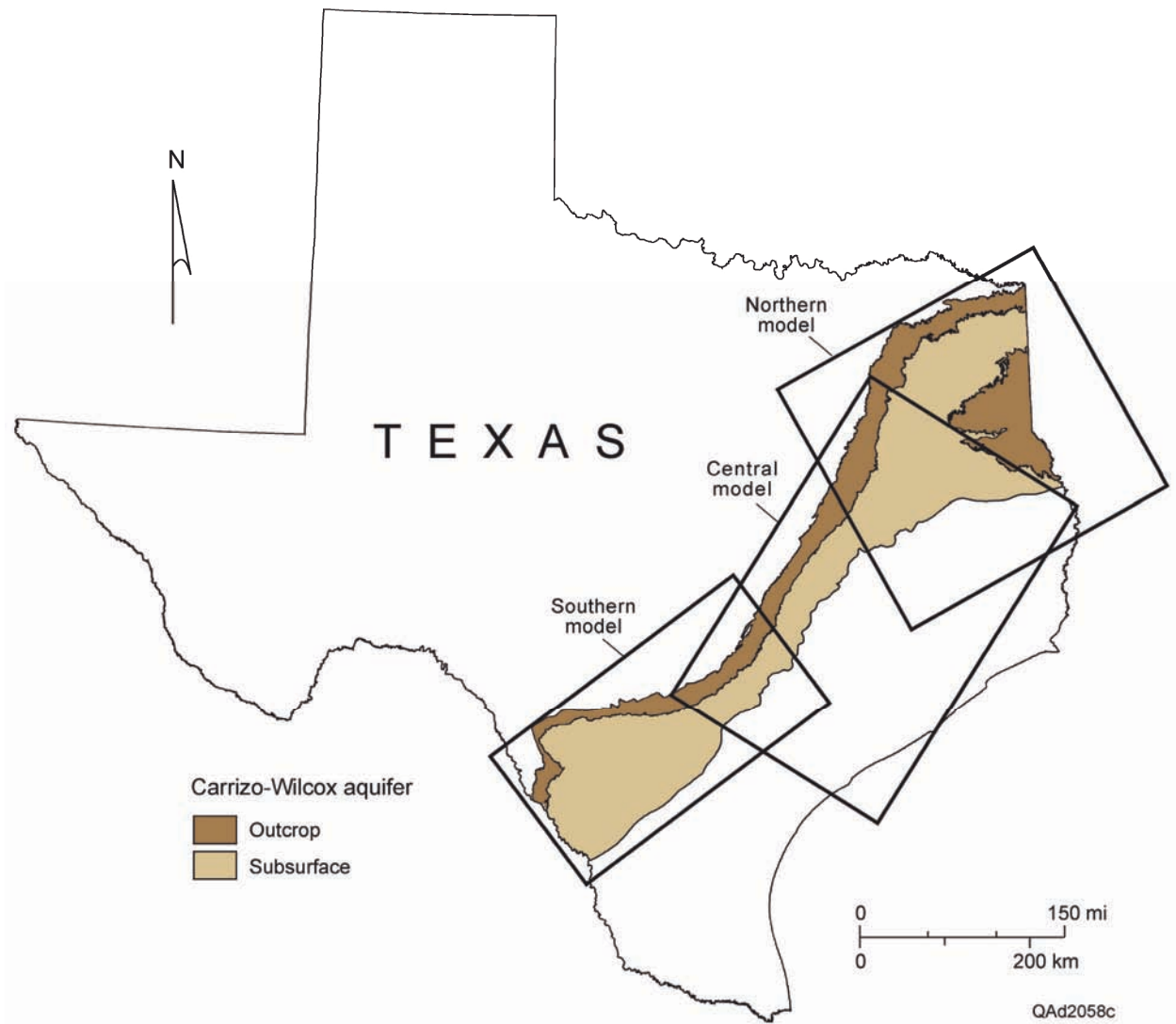


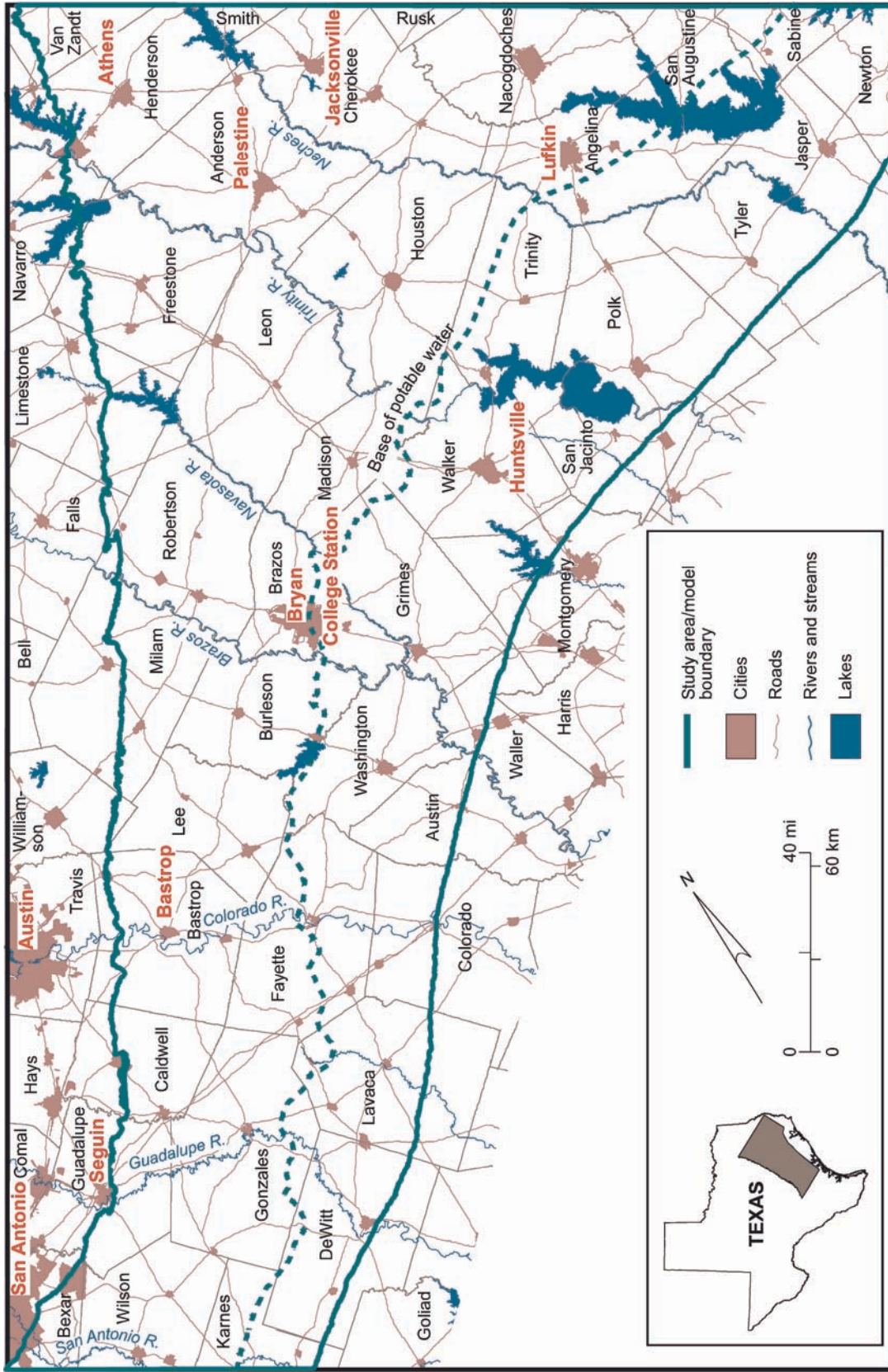
Figure 1. Location of the Carrizo–Wilcox aquifer in Texas showing the overlapping position of the three regional models.

along with possible water-management strategies, projected by the Regional Water Planning Groups. Input from stakeholders was incorporated into the modeling process through quarterly stakeholder advisory forums. The model developed for the Central Carrizo–Wilcox aquifer is described in this report according to the requirements of the GAM program. The model developed in this study is available for Groundwater Conservation Districts, Regional Water Planning Groups, River Authorities, and others to assess the groundwater availability in the Central Carrizo–Wilcox aquifer. The report and model are posted on the GAM web page at <http://www.twdb.state.tx.us/GAM>.

2.0 STUDY AREA

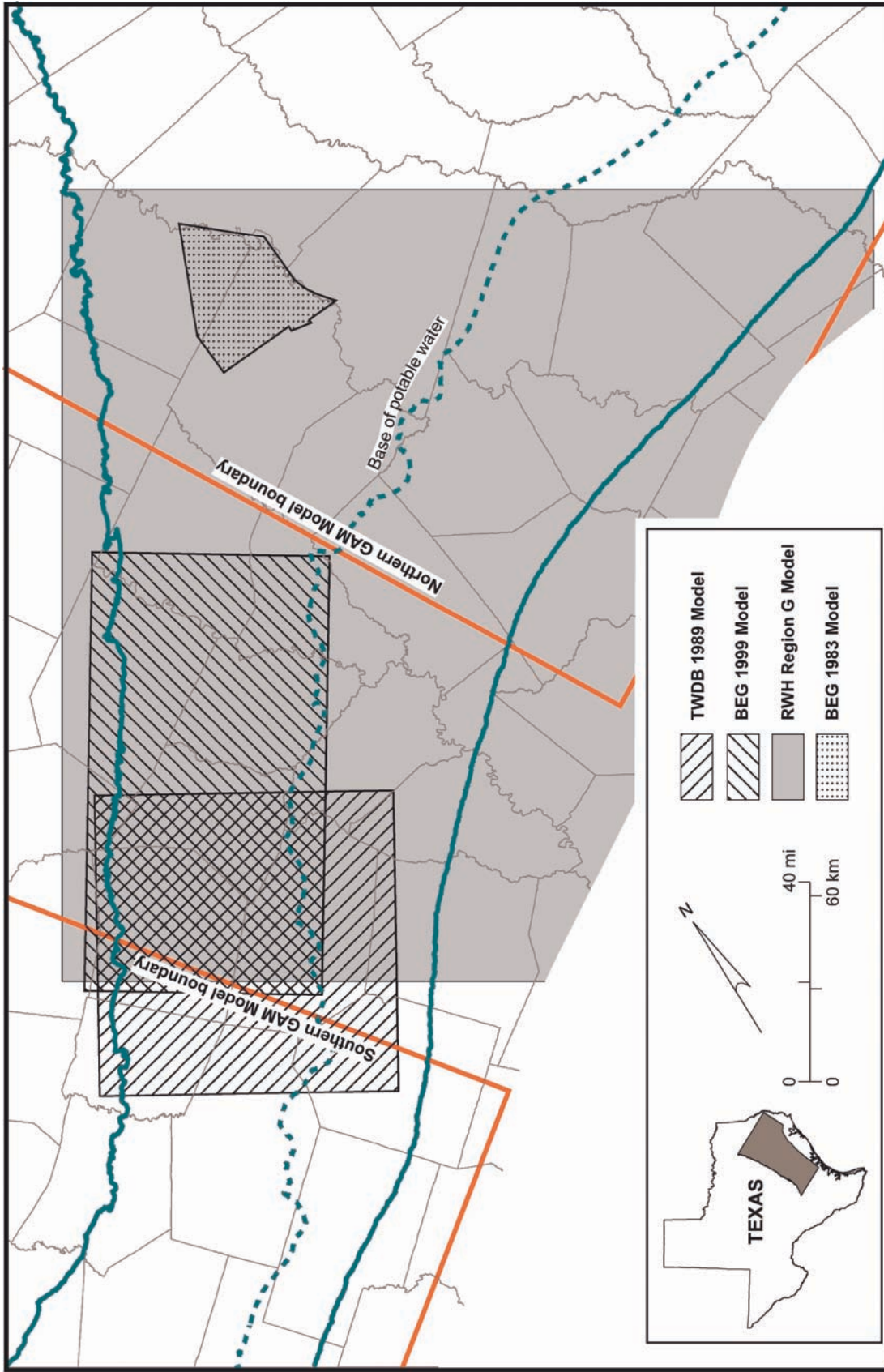
The study area overlaps with the areas of the southern and northern models of the Carrizo–Wilcox aquifer developed concurrently with the model of the central part of the aquifer in Texas (fig. 1). This report focuses on the central part of the Carrizo–Wilcox aquifer in Texas. The southwestern boundary of the study area falls along the course of the San Antonio River (fig. 2). The boundary to the northwest is at the limit of the outcrop of the formations that make up the Carrizo–Wilcox aquifer. The northeastern boundary of the study area runs from the aquifer outcrop in Van Zandt County, across part of the East Texas Basin and the Sabine Uplift, and then continues into the deep part of the Carrizo–Wilcox aquifer. The southeastern boundary of the study area was placed approximately 10 to 40 mi downdip of the base of freshwater in the aquifer and coincides with a major fault zone, as discussed in Section 4.2. Application of the southern or northern Carrizo–Wilcox aquifer models may provide more representative results than this central model near the southwestern and northeastern lateral boundaries (fig. 3).

Parts of more than 30 counties are included in the study area (fig. 2). The study area includes all or parts of 18 groundwater conservation districts (fig. 4), several of which have pending confirmation. Parts of eight regional water planning areas are within the study area (fig. 5): Region C, North East Texas D, Brazos G, Region H, East Texas I, Lower Colorado K, South Central Texas L, and Lavaca P regions. Information on the water plans of these regions may be found at www.state.tx.us/assistance/rwpg/main-docs/regional-plans-index.htm. The study area also includes parts of eight River Authority jurisdictions: the Angelina and Neches River Authority, Brazos River Authority, Guadalupe-Blanco

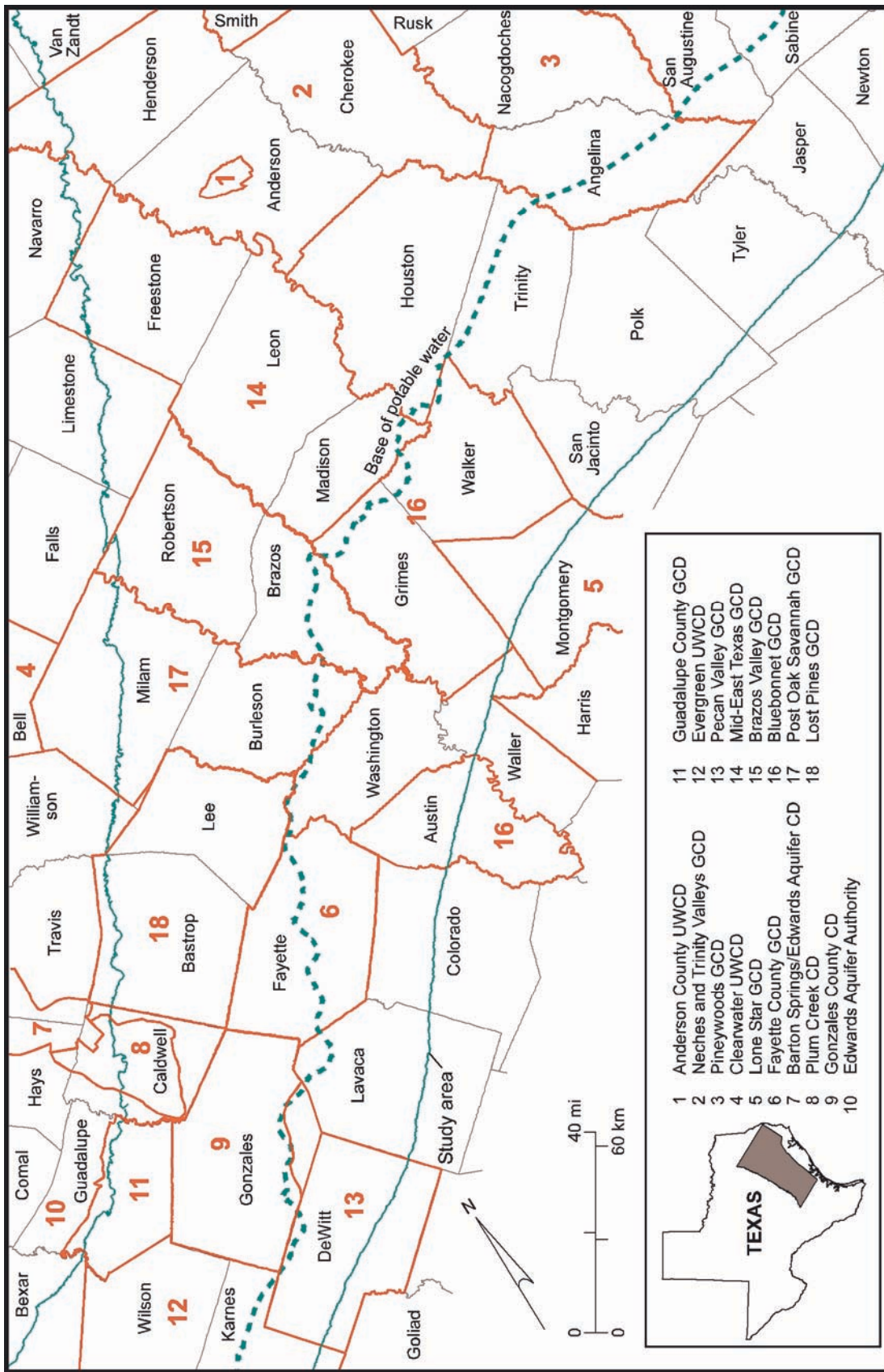


QA41795c

Figure 2. Location of the study area relative to roads, major cities and towns, lakes, and rivers. The study area extends beyond the limit of potable water in the Carrizo–Wilcox aquifer.



QAd1811(g)je
 Figure 3. Extent of previous models of groundwater flow in the Carrizo–Wilcox aquifer in the study area. Models are identified in the text.



QA47797c

Figure 4. Location of groundwater conservation districts in the study area (November 2002). Taken and modified from <http://www.twdb.state.tx.us/mapping/index.htm>.

River Authority, Lavaca-Navidad River Authority, Lower Colorado River Authority, Lower Neches River Authority, San Antonio River Authority, and Trinity River Authority.

2.1 Physiography and Climate

The study area lies entirely within the Interior Coastal Plains, part of the Gulf Coastal Plain (Wermund, 1996a). To the west is the Blackland Prairies and farther west is the limestone escarpment at the eastern edge of the Hill Country. To the southeast are the Coastal Prairies. Land-surface elevations across the study area range from almost 750 ft (all elevations in this report are given relative to mean sea level [msl]) in the southwest, closer to the Balcones Escarpment, to less than 150 ft in river bottomlands (fig. 6). The valleys of the Brazos, Colorado, and Trinity Rivers are deeper and broader than those of the San Antonio, Guadalupe, Navasota, and Neches Rivers. Ground-surface elevation overlying the Carrizo–Wilcox aquifer is highest in the study area in the upland areas between Trinity and Neches Rivers and between Neches and Angelina Rivers (fig. 6).

The Interior Coastal Plains is underlain at the surface mostly by deposits of poorly consolidated sandstone, mudstone, and shale. Although the sandstones are friable and poorly cemented, they are somewhat resistant to erosion and form hills of low relief with slopes of 3 to 10 percent that may rise as much as 100 ft above the adjacent areas (Henry and Basciano, 1979). The sandstone hills are the outcrop of fluvial and deltaic channel deposits that make up the aquifer in the subsurface. The strike of the sandstone hills within the Simsboro, Carrizo, and Queen City Formations forms long sandy ridges separated by topographic trends of areas with slightly lower elevation, which are underlain by the

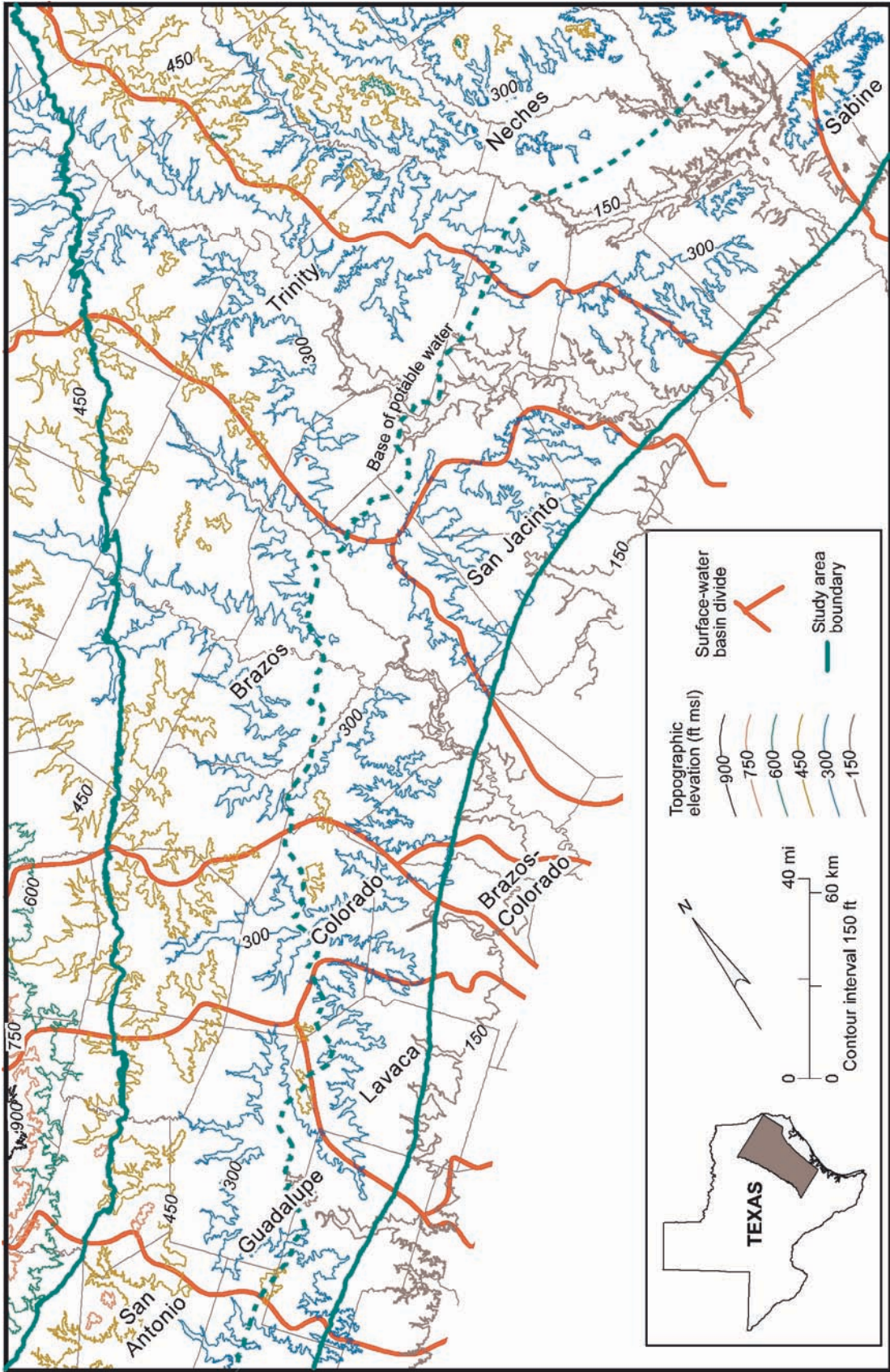
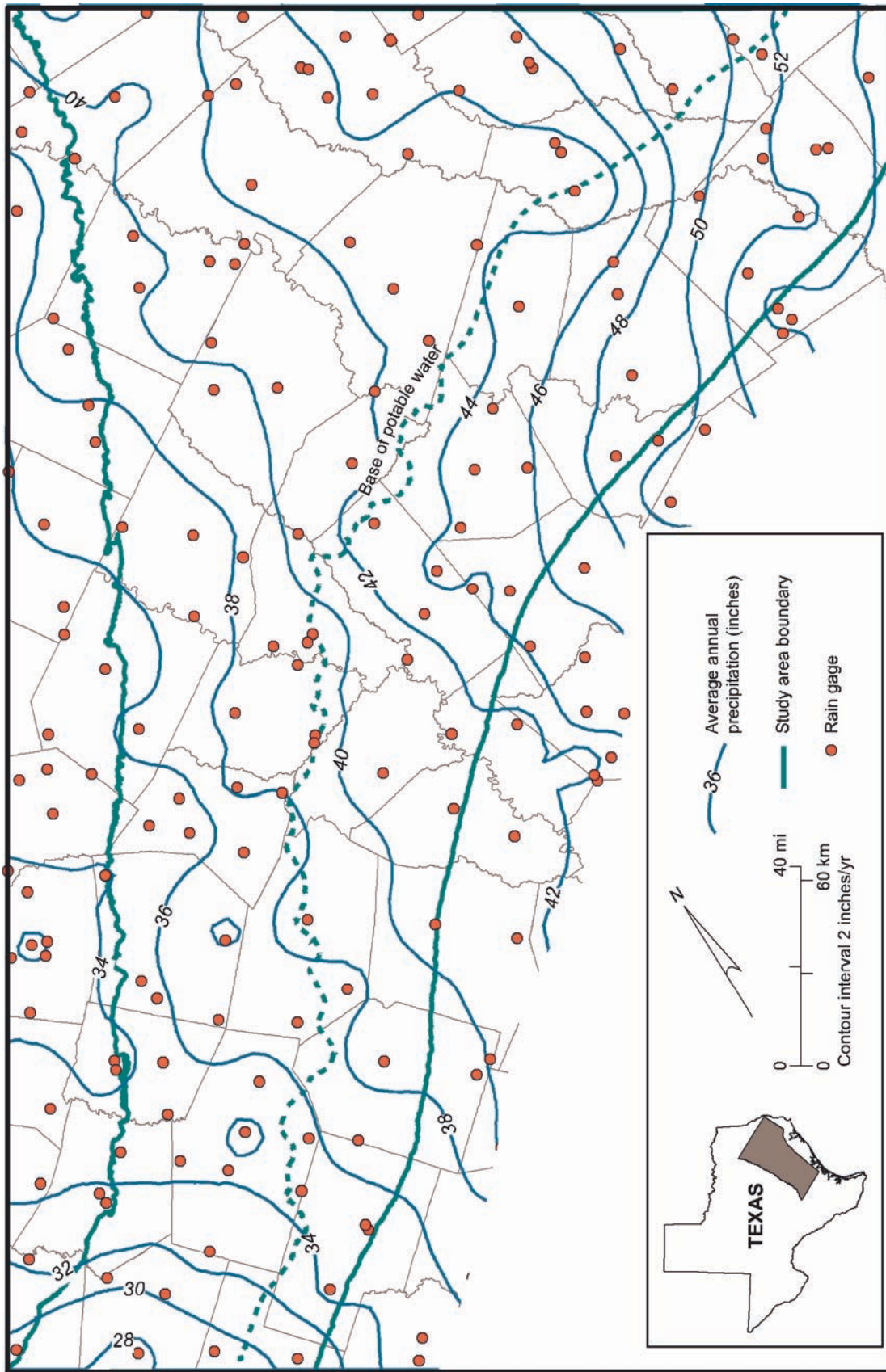


Figure 6. Land-surface elevation in the study area relative to divides between surface-water drainage basins. The study area is within the Interior Coastal Plains physiographic province. River basins from Wermund (1996b).

muddy substrates of the Hooper, Calvert Bluff, and Reklaw Formations. Relief between the upland divides and river bottomlands of about 100 ft is typical across the study area.

Climate of the study area is subhumid (Larkin and Bomar, 1983). Precipitation gradually decreases from east to west from more than 52 inches/yr to less than 28 inches/yr (fig. 7), following the regional trend across the Gulf Coastal Plain. Annual precipitation for the period from 1940 through 1997 across the study area averaged about 41.7 inches/yr. Average annual precipitation during the period from 1900 through 1997 ranged from 14 inches/yr in 1917 to 60.4 inches/yr in 1973. The period from 1954 through 1956 included 3 of the 10 driest years since 1940 and can be defined as the drought of record for the area (fig. 8). The driest years during the decades of the 1980s and 1990s were 1988 (average of 29.4 inches/yr) and 1996 (average of 38.1 inches/yr). Mean annual air temperature ranges from 65° F in the north to 70° F in the south (Larkin and Bomar, 1983). Evaporation increases from east to west across the study area. Average annual (1950–1979) gross lake evaporation is about 1.5 times average annual precipitation and ranges from 46 inches in the east to 63 inches in the west. Net lake-surface evaporation (gross lake evaporation minus precipitation) is less than zero (negative) in the eastern third of the study area (fig. 9), where precipitation rate is high; there is more precipitation than evaporation. The positive value of net lake evaporation in the western part of the study area means there is a potential on average each year for more evaporation than precipitation. Precipitation between October and May, however, is subject to less evaporation.



OA41792c

Figure 7. Average annual precipitation (1940 through 1997) in the study area. Data from www.twdb.state.tx.us/mapping/gisdata.htm.

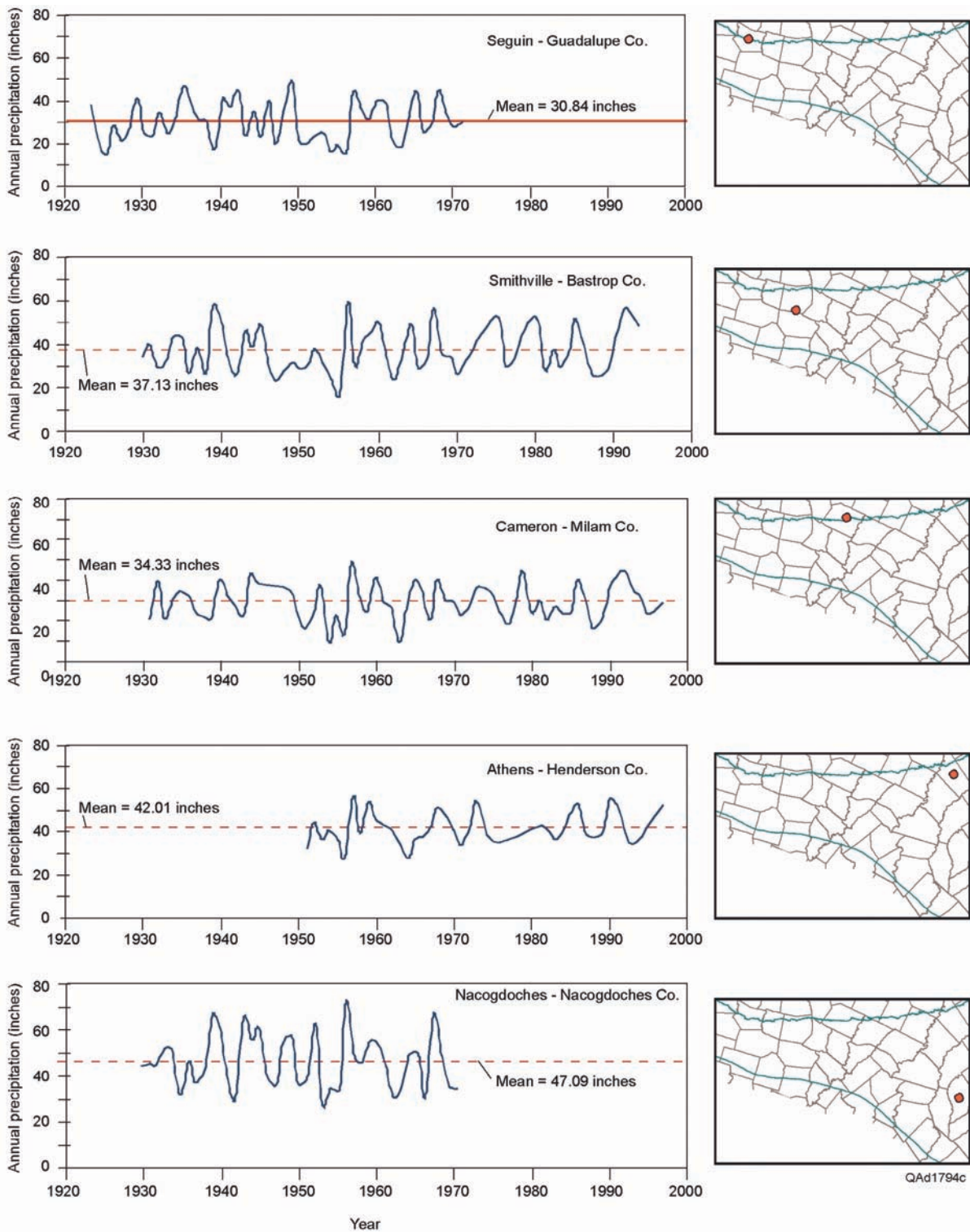
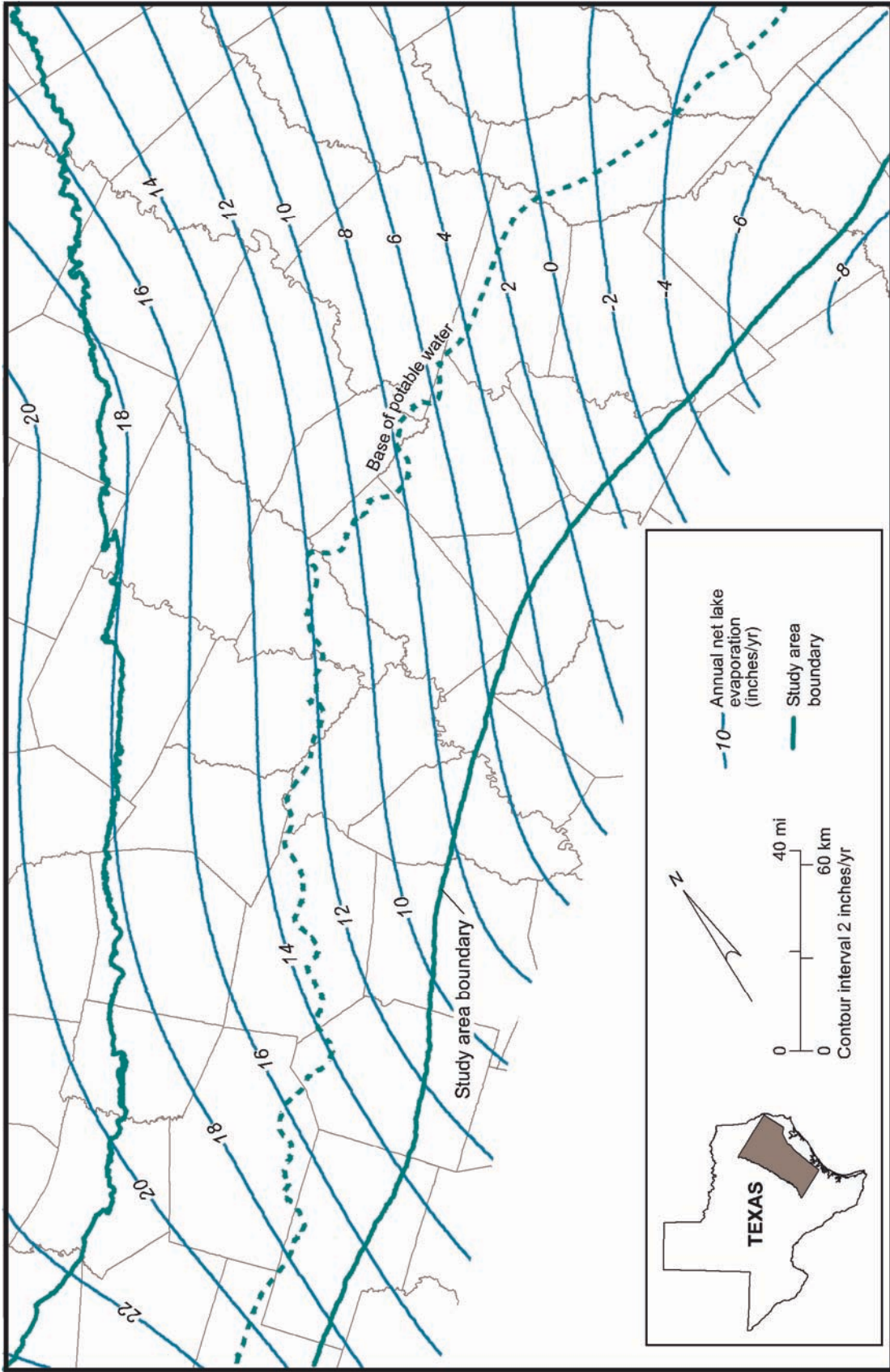


Figure 8. Historical annual precipitation measured at rain gages at Seguin, Smithville, Cameron, Athens, and Nacogdoches. Data from <http://lwf.ncdc.noaa.gov/oa/climate/online/coop-precip.html>.



QA41816C

Figure 9. Average net lake evaporation rate in the study area. Data from <http://hyper20.twdb.state.tx.us/Evaporation/evap.html>.

2.2 Geology

The Carrizo–Wilcox aquifer is made up of the Wilcox Group and the overlying Carrizo Formation of the Claiborne Group (figs. 10, 11). The Carrizo Formation is included in the Wilcox Group in the deep subsurface (Bebout and others, 1982; Hamlin, 1988; Xue and Galloway, 1995). Between the Trinity and Colorado Rivers the Wilcox Group is formally subdivided into three formations, which are, from oldest to youngest, the Hooper, Simsboro, and Calvert Bluff Formations (Kaiser, 1978; Ayers and Lewis, 1985; Xue and Galloway, 1995). The Carrizo and Simsboro Formations make up the main aquifer units. More than 80 percent of the Carrizo and Simsboro Formations in the study area consist of porous and permeable sandstone (Ayers and Lewis, 1985).

The outcrop of each formation that makes up the Carrizo–Wilcox aquifer (the Hooper, Simsboro, Calvert Bluff, and Carrizo Formations) between the Trinity and Colorado Rivers is generally 1 to 3 mi in width except for the thicker Calvert Bluff Formation that has an outcrop typically 4 to 6 mi in width (fig. 11). This reflects cumulative formation thicknesses near the outcrop that are less than 500 ft and a coastward formational dip of 0.25° to 2° (20 to 180 ft/mi) (Henry and Basciano, 1979). The width of the undifferentiated Wilcox Group outcrop south of the Colorado River and north of the Trinity River is approximately 10 to 15 mi wide.

The Hooper Formation represents the initial progradation of the Wilcox Group fluvial-deltaic systems into the Houston Embayment of the Gulf of Mexico basin and consists of interbedded shale and sandstones in subequal amounts, with minor amounts of lignite. It coarsens upward from shale-dominated prodelta deposits of the Rockdale delta to sand-dominated upper delta plain and fluvial deposits in the outcrop area (Ayers and Lewis, 1985) and delta-front/prodelta facies in the downdip part of the study area.

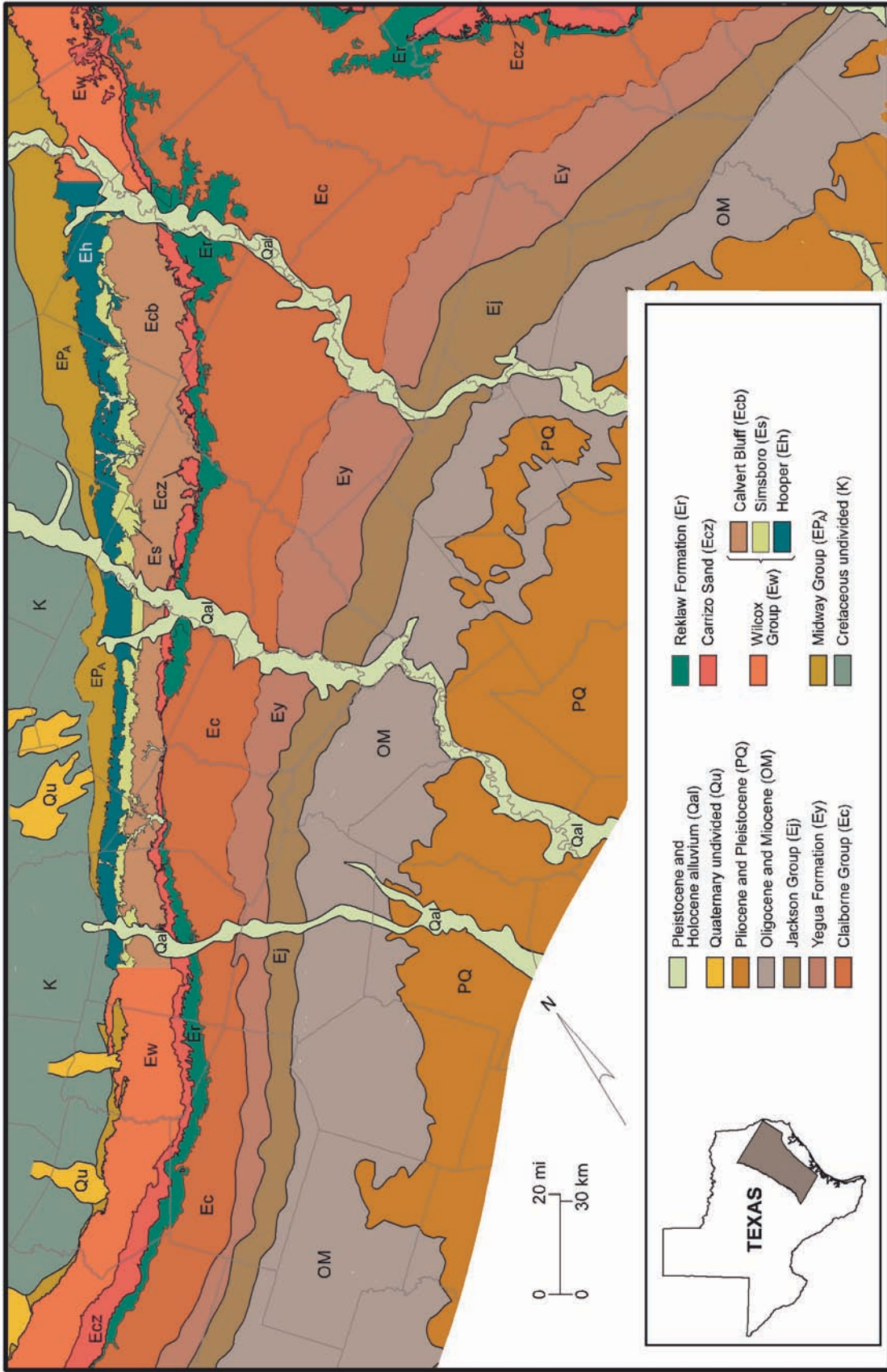
ERA	Series	Southwest Carrizo-Wilcox aquifer		Central Carrizo-Wilcox aquifer (this study)		Northeast Carrizo-Wilcox aquifer		
		Stratigraphy	Model layer	Stratigraphy	Model layer	Stratigraphy	Model layer	
QUATERNARY	Focene	Alluvium	X	Alluvium	1	Alluvium	X	
		Jackson Group		Jackson Group	X			
		Yegua Fm.		Yegua Fm.				
		Laredo Fm.		Cook Mtn. Fm.				
		Sparta Sand		Sparta Sand				
		Weches Fm.		Weches Fm.				
	TERTIARY	M	Claiborne Group	X	Claiborne Group	X	Claiborne Group	X
			El Pico Clay		Queen City Sand		Queen City Sand	
			Bigford Fm.		Reklaw Fm.		Reklaw Fm.	
			Carrizo Sand		Upper Wilcox		Carrizo Sand	
			Middle Wilcox		Calvert Bluff		Calvert Bluff	
			Lower Wilcox		Simsboro		Hooper	
Paleocene	L	Midway Formation	X	Midway Formation	X	Midway Formation	X	
		Wilcox Group		Wilcox Group		Wilcox Group		
		Upper Wilcox		Upper Wilcox		Upper Wilcox		
		Middle Wilcox		Middle Wilcox		Middle Wilcox		
		Lower Wilcox		Lower Wilcox		Lower Wilcox		
		Hooper		Hooper		Hooper		

QAd1793c



Not modeled

Figure 10. Generalized stratigraphic chart for the study area (after Ayers and Lewis, 1985; Hamlin, 1988; Kaiser, 1978; Intera and Parsons Engineering Science, 2002a, b).

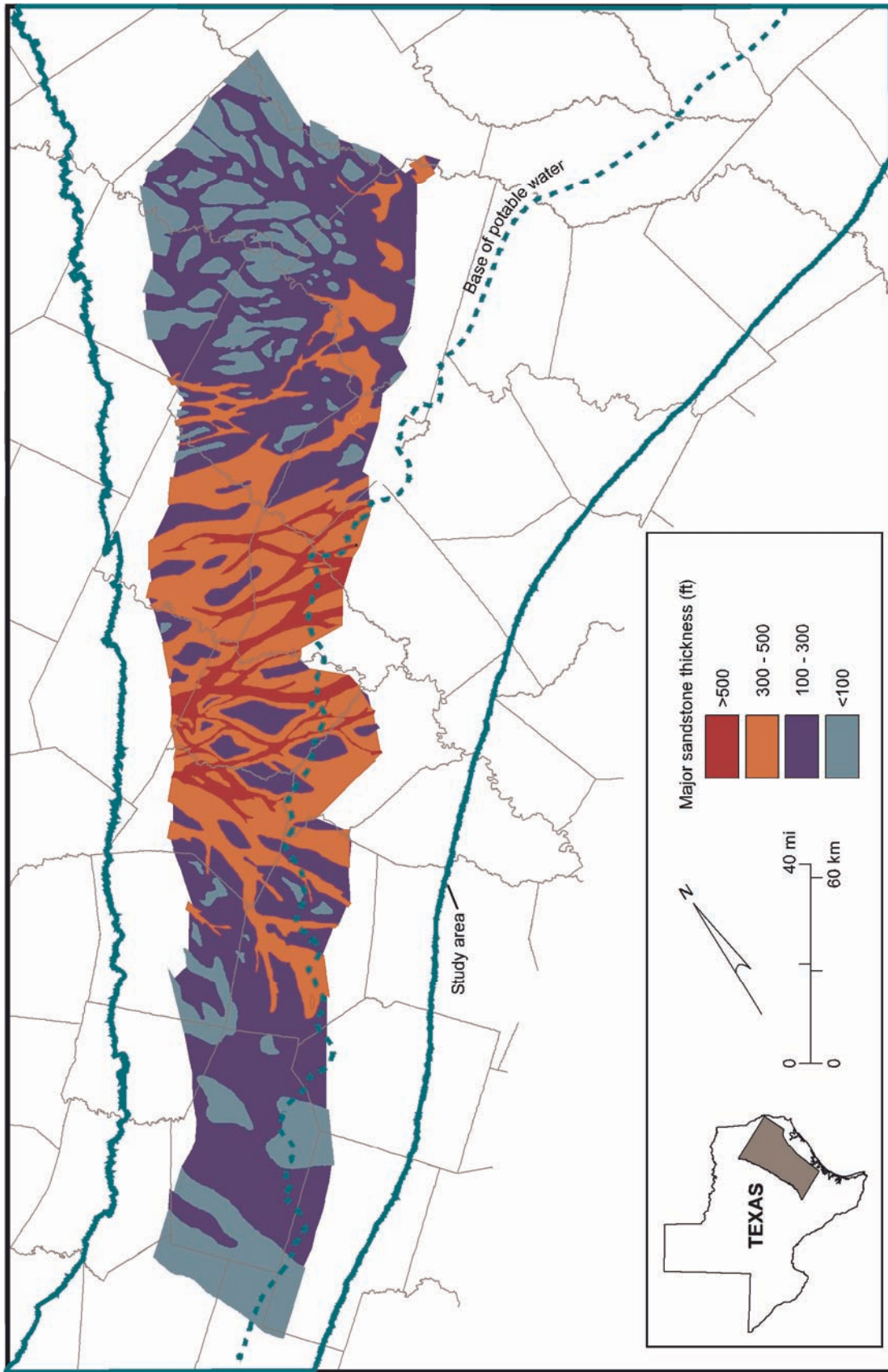


QA41815c

Figure 11. Generalized map of surface geology in the study area. The Wilcox Group is not subdivided into formations south of the Colorado River or north of the Trinity River. Claiborne Group shown on map does not include Yegua Formation, Reklaw Formation, and Carrizo Sand. Modified from Bureau of Economic Geology (1992).

Sandstone thickness trends are dominantly dip elongate, being northwest-southeast oriented in the central and northern parts of the study area and more southerly in the southern part of the model area. Thickness of “major sands” ranges from 40 ft to narrow bands of more than 200 ft in the shallow subsurface, with these narrow bands widening and thickening to more than 300 ft, broadly, in the middip region of the model area, and then thinning to near zero in most of the downdip model area (Ayers and Lewis, 1985). Sandstone percent ranges from less than 20 percent adjacent to major axes of deposition to 50 percent at axes. Thick sandstone bodies do not extend downdip beyond the base of freshwater except in the areas of Lavaca, Austin, and Waller Counties.

The Simsboro Formation is predominantly a sand-rich formation (fig. 12) composed of a multistory, multilateral sand deposit (Henry and others, 1979). The Simsboro Formation was deposited in environments ranging from fluvial and upper delta floodplain near the outcrop (Fisher and McGowen, 1967; Ayers and Lewis, 1985) to delta front and prodelta at the downdip margins of the study area. Its deposits have been referred to as making up the Rockdale Delta System (Fisher and McGowen, 1967). The Rockdale Delta, which lies between the Colorado and Trinity Rivers, has more than 500 ft of sandstone in the Simsboro Formation (fig. 12). Thick sandstones extend well past the base of freshwater. Sandstone thickness patterns consist of narrow, dip-oriented trends of more than 500 ft alternating with areas of less than 100 ft in the updip and middip regions, thinning to less than 100 ft in the downdip part of the study area. More north- to south-oriented sandstone trends of generally less than 200 ft exist in the northern part of the model area, composing the Mt. Pleasant Fluvial System of Fisher and McGowen (1967). Thick Simsboro sandstones between the Colorado and Trinity Rivers separate the more muddy and thin-bedded sands of the lower and upper Wilcox Group (fig. 10). Whereas sandstone generally makes up 80 percent of



Q-A41799c

Figure 12. Thickness of major sandstones in the Simsboro Formation in the study area. Modified from Ayers and Lewis (1985).

the Simsboro Formation, it is generally only 20 to 40 percent of the underlying Hooper Formation and overlying Calvert Bluff Formations. Hooper and Calvert Bluff Formations, however, have as much as 50 percent sandstone locally and are locally important groundwater-bearing units.

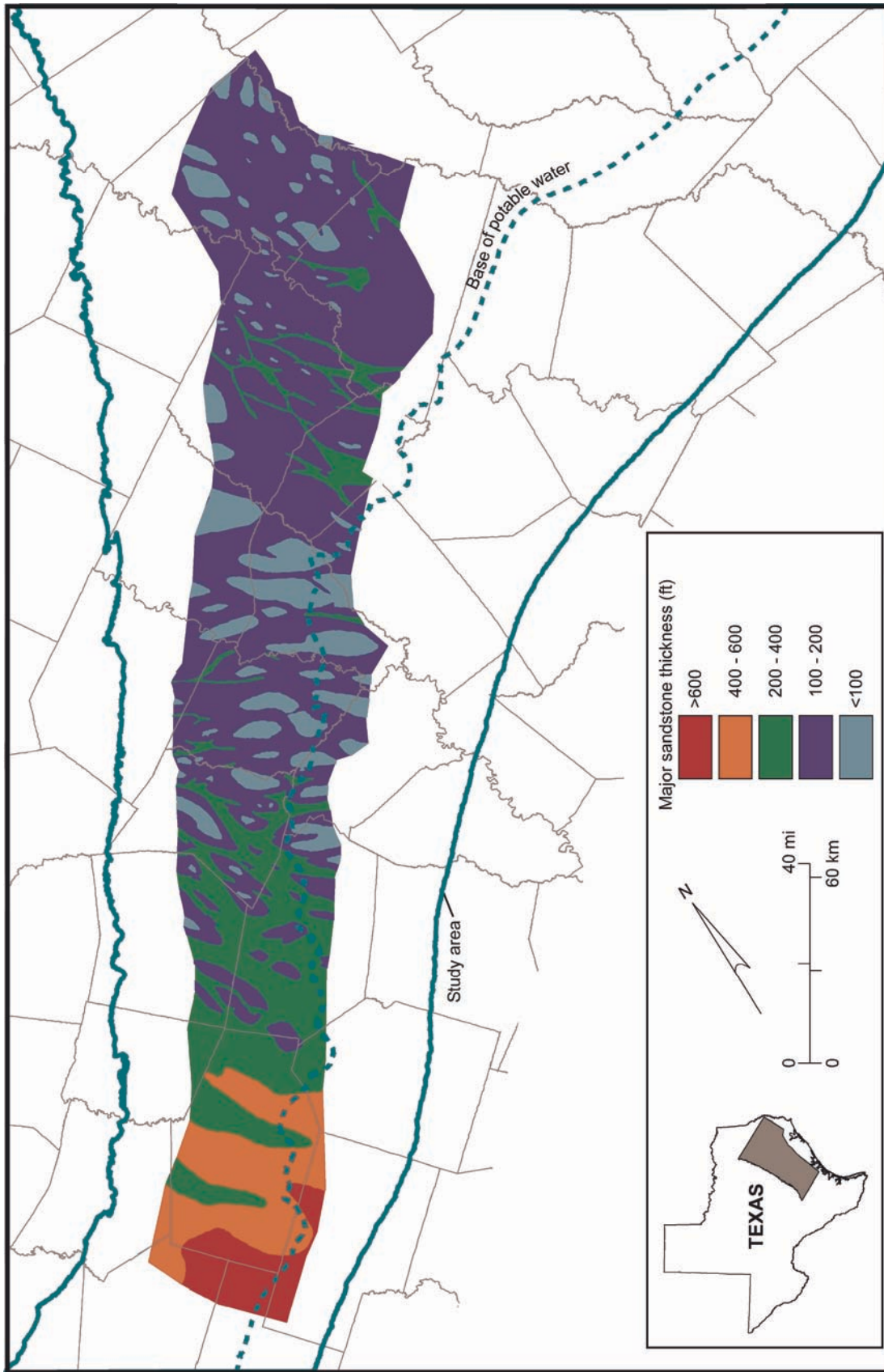
Multilateral sands are less abundant, and the Wilcox Group is not formally subdivided where the Rockdale Delta System dies out to the south and north (fig. 12). South of the Colorado River, Simsboro-equivalent deposits change to strike-oriented, nearshore, marine-dominated facies (the San Marcos Strandplain Bay system of Fisher and McGowen, 1967), which do not make up a major sand system and are not differentiated from the rest of the Wilcox Group (Barnes, 1992; Henry and others, 1979). The geological map (fig. 11) breaks out the Hooper, Simsboro, and Calvert Bluff Formations of the Wilcox Group between the Colorado and Trinity Rivers. Mapping does not formally define separate formations of the Wilcox Group south of the Colorado River or north of the Trinity River.

The Calvert Bluff, like the Hooper Formation, consists mainly of low-permeability claystone and lignite deposits (Ayers and Lewis, 1985), which function like confining layers that retard the vertical movement of water within the Carrizo–Wilcox aquifer across the study area. Where present in sufficient thickness, however, sandstones can yield appreciable quantities of water in the Calvert Bluff. The communities of Bastrop, Elgin, and Milano, for example, have had public water-supply wells in the Calvert Bluff or Hooper Formations. Sandstone and shale are interbedded in subequal parts, with intermixed lignite beds, a significant resource in Central and East Texas (Kaiser, 1978). Multistory sandstone bodies that are 50 to 100 ft thick in the updip area reflect fluvial to upper delta-plain deposition. By 10 to 15 mi downdip of the outcrop, these have changed to distributary facies, which terminate in delta-front and prodelta facies in the downdip part of the model area. Narrow

axes where sandstone thickness of greater than 200 ft near the outcrop give way to broader axes of more than 400 ft of sandstone in the mid-dip region, change to a broad, strike-oriented thickness trend near the downdip limit of freshwater that finally thins to less than 100 ft in the downdip part of the model area (Ayers and Lewis, 1985). Greatest sandstone thickness occurs in the southern part of the study area and in central Leon, eastern Madison, and eastern Walker Counties, reflecting diversion of Rockdale Delta deposition around former loci of deposition in the underlying Simsboro Formation.

The Carrizo Formation is hydrologically connected to the underlying Wilcox Group; the two units collectively are referred to as the Carrizo–Wilcox aquifer, the subject of this study. The Carrizo Formation is the oldest part of the Claiborne Group in the Central Texas study area (fig. 10) and is considered part of the Wilcox Group in the subsurface (Bebout and others, 1982). By the time of Carrizo Formation deposition, the center of sand deposition had shifted to the south of the San Marcos Arch, feeding the Rosita Delta System (Ayers and Lewis, 1985). Within the central and northeastern parts of the study area, sand thickness is strongly dip oriented (northwest to southeast). Total thickness of sandstone in the Carrizo Formation is typically between 100 and 200 ft, typically less than in the Simsboro Formation. Sandstone thickness in the Carrizo Formation, however, increases to several hundreds of feet to the southwest in Gonzales, Wilson, DeWitt, and Karnes Counties (fig. 13) (Hamlin, 1988), where the remaining activity of the Rockdale Delta was focused. Ayers and Lewis (1985, p. 7) mapped the top of the Carrizo Sand at the top of an upward-fining sequence called the Newby Member of the Reklaw Formation.

Framework mineralogy in the Carrizo–Wilcox aquifer was characterized by Loucks and others (1986), who documented an increase in feldspar content in Wilcox sandstone from South Texas through East Texas. Under the classification of Folk (1968), Carrizo–Wilcox



QAd1800c

Figure 13. Thickness of major sandstones in the Carrizo Formation in the study area. Modified from Ayers and Lewis (1985).

sandstones vary from subarkose, arkose, and lithic arkose in the lower coast (quartz ~60 to 85 percent and feldspar-to-rock fragments ratios of >3:1 to <1:1) to subarkose, arkose, lithic arkose, and feldspathic litharenite in the upper coast (quartz ~40 to 80 percent and feldspar:rock fragment ratios of 3:1 to slightly greater than 1:3). Authigenic clay grain coatings, feldspar, kaolinite, and minor carbonate cements dominate diagenetic events at depths of less than 5,000 ft. Quartz cement is a dominant diagenetic phase at depths of between about 5,000 and 8,000 ft, and iron-rich carbonate cement is dominant at depths below 8,000 ft. Feldspar corrosion and dissolution are common soil-forming processes in the unsaturated zone, with formation of kaolinitic and smectitic clay coats on other framework grains (Dutton, 1990).

Underlying the Carrizo–Wilcox aquifer is the marine shale of the Paleocene Midway Formation (figs. 10, 11). The Midway is transitional between the fully marine deposits of the Upper Cretaceous and the foredelta and lower delta floodplain deposits of the Hooper Formation (Fisher and McGowen, 1967; Ayers and Lewis, 1985).

Deposits of the Claiborne Group that overlies the Wilcox Group also reflect several episodes of fluvial and deltaic progradation, marked by thick sandstones of the Queen City and Sparta Formations, interspersed with relative marine advances marked by the marine shale of the Reklaw, Weches, and Cook Mountain Formations. Low-permeability marine shale of the Reklaw Formation restricts groundwater movement between the Carrizo Formation and the overlying aquifer in the Queen City Formation in the Claiborne Group (fig. 10). The Carrizo and Reklaw Formations are broken out of the Claiborne Group in the geological map (fig. 11) because they are included as separate hydrological layers in the model.

Pleistocene and Holocene (Quaternary) alluvium floors the valleys of the Colorado, Brazos, and Trinity Rivers. Alluvial deposits contain highly permeable sands and gravels, as well as low-permeability silts and clays. Various terrace levels record the history of floodplain evolution in the coastal plain over the past several million years (Hall, 1990).

3.0 PREVIOUS WORK

This study has built on previous hydrogeologic investigations and regional computer models of the Carrizo–Wilcox aquifer (fig. 3). The scale of previous models ranges from the local to regional. All models have treated the base of the Wilcox Group (base of Hooper Formation) as a no-flow boundary, making the assumption that there is negligible exchange of groundwater with the underlying Midway Group. Other boundary conditions varied between models.

Fogg and others (1983) developed a model of the Carrizo–Wilcox aquifer in the Trinity River Basin (Leon and Freestone Counties) using the TERZAGI code (BEG 1983 Model, fig. 3). The main purpose of this study was to evaluate how to represent hydraulic conductivities of highly heterogeneous aquifers.

Thorkildsen and others (1989) simulated groundwater flow in the Carrizo–Wilcox aquifer in the Colorado River basin (TWDB 1989 Model, fig. 3). This study compiled well data, geologic information, and hydraulic parameters, developed a groundwater model, and evaluated aquifer response to various future pumpage scenarios. The model of Thorkildsen and others (1989) subdivided the Carrizo–Wilcox aquifer into four layers, and the model was bounded by a no-flow boundary at the outcrop limit and a constant-head boundary at the downdip limit. Steady-state calibration was based on 1985 water levels. Transient simulations were run for 1985 through 2029 to evaluate aquifer response to future pumpage. Thorkildsen and Price (1991, unpublished simulations) used models to evaluate groundwater availability in the Carrizo–Wilcox aquifer between the Colorado and Trinity Rivers; however, there is little documentation of these models. The models of the Carrizo–Wilcox

aquifer by Thorkildsen and others (1989) and Thorkildsen and Price (1991; unpublished simulations) have model blocks that represent areas of 4 and 16 mi², respectively.

The U.S. Geological Survey's RASA (Regional Aquifer System Analysis) program includes the development of large-scale regional models of aquifers along the coastal plain rimming the Gulf of Mexico, including the Carrizo–Wilcox aquifer in Texas (Ryder, 1988; Williamson and others, 1990; Ryder and Ardis, 1991). The Carrizo–Wilcox aquifer is represented as two layers. The code used for these models was developed by Kuiper (1985). The primary objective of these models was to evaluate the regional groundwater flow system, including the hydrogeologic framework and hydraulic attributes of the units. The model developed by Ryder (1988) was restricted to steady-state simulations representing predevelopment conditions. The model developed by Williamson and others (1990) included steady-state and transient simulations (1935 through 1980). In addition to steady-state and transient (1910 through 1982), Ryder and Ardis (1991) also conducted predictive simulations to evaluate aquifer response to potential future pumpage scenarios. This model used a constant-head, updip boundary condition, which probably results in overestimation of recharge rate under future pumpage conditions because the constant-head boundary condition provides an inexhaustible supply of water. The models by Ryder (Ryder, 1988; Ryder and Ardis, 1991) have model blocks that represent an area of 25 mi².

Dutton (1999) prepared a predictive model of the groundwater in Hooper, Simsboro, Calvert Bluff, and Carrizo Formations between the Colorado and Brazos Rivers (BEG 1999 Model, fig. 3). No-flow boundaries to the north and south were located beyond the Colorado and Brazos Rivers, assumed to be hydrologic boundaries. The model excluded pumping in the area of the well field of the cities of Bryan and College Station and did not take into account the effect of this well field on the model area. The downdip boundary was set 10 to

20 mi beyond the limit of freshwater; a vertical gradient in hydraulic head was prescribed along the downdip boundary. Hydraulic conductivity was assigned on the basis of the distribution of sand deposits (Ayers and Lewis, 1985). Various assumed water-development projects were simulated for the period from 2000 through 2050. Model results suggested that lateral and downdip boundaries had some effect on model results.

R. W. Harden and Associates, Inc., developed a model of the aquifer between the Colorado and Neches Rivers for the Brazos Region G Regional Water Planning Group (RWH Region G Model, fig. 3). The MODFLOW code was used for the simulations and the Carrizo–Wilcox aquifer was subdivided into five layers, representing the Hooper, Simsboro, Calvert Bluff, and Carrizo Formations and the Newby Member of the Reklaw Formation. A downdip model boundary was set very far away from the area of interest so as not to affect model results directly. Hydraulic conductivity was assigned on the basis of the distribution of sand deposits (Ayers and Lewis, 1985). The model included steady-state simulations (1950, 1985) and predictive simulations (2000 through 2050).

While the present model has been in development, simultaneous efforts were under way to construct parallel models of the Carrizo–Wilcox aquifers in northern and southern parts of the aquifer in Texas (fig. 3) (Intera and Parsons Engineering Science, 2002a, b). Geology, hydrology, climate, and history of groundwater use differ somewhat between the northern, central, and southern parts of the Carrizo–Wilcox aquifer in Texas. The models overlap large areas (figs. 1, 3), and model development was coordinated to make the results as consistent as possible.

4.0 HYDROLOGIC SETTING

In this section on hydrogeologic setting, we discuss information on the aquifer and its properties that has been compiled and analyzed for building the groundwater model. Groundwater conditions in counties included in the study area have been previously documented (for example, Anders, 1957, 1960; Arnow, 1959; Dillard, 1963; Peckham, 1965; Shafer, 1965, 1966, 1974; Follett, 1966, 1970, 1974; Tarver, 1966, 1968; Thompson, 1966, 1972; Cronin and Wilson, 1967; Rogers, 1967; Wilson, 1967; Guyton and Associates, 1970, 1972; White, 1973; Henry and Basciano, 1979; Henry and others, 1979; Ayers and Lewis, 1985; Dutton, 1985, 1990; Rettman, 1987; Sandeen, 1987; Thorkildsen and others, 1989; Baker and others 1990; Duffin, 1991; Thorkildsen and Price, 1991). We developed the hydrogeologic setting on the basis of these and additional studies we conducted in support of this modeling effort. Additional studies include remapping structural elevations of the aquifer layers, developing water-level hydrographs and maps of the potentiometric surface, estimating base flow to rivers and streams, investigating recharge rates, and mapping total dissolved solids.

4.1 Hydrostratigraphy

The Carrizo–Wilcox aquifer system in the Central Texas study area is composed of four hydrostratigraphic units with distinct hydraulic properties: the Hooper, Simsboro, and Calvert Bluff Formations of the Wilcox Group and the Carrizo Sand of the Claiborne Group (fig. 10). In general, the Simsboro and Carrizo Formations contain thicker, more laterally continuous and more permeable sands (figs. 12, 13) and, therefore, are more important hydrostratigraphic units when determining groundwater availability. Calvert Bluff and

Hooper Formations typically are made up of clay, silt, and sand mixtures, as well as lignite deposits. Because of their relatively low vertical permeability, the Hooper and Calvert Bluff Formations act as leaky aquitards that confine fluid pressures in the Simsboro and Carrizo aquifers and restrict groundwater movement between the layers. Although the Hooper and Calvert Bluff Formations contain sand units, they are generally finer and less continuous than the sands of the Simsboro and Carrizo Formations. The four units of the Carrizo–Wilcox aquifer system in the Central Texas study area were modeled as individual layers (fig. 10).

Deposits of the Claiborne Group that overlies the Wilcox Group also reflect several episodes of fluvial and deltaic progradation, marked by thick sandstones of the Queen City, Sparta, and Yegua Formations. The formations dominated by progradational sandstones are interlayered with relative marine advances marked by marine shales of the Reklaw, Weches, and Cook Mountain Formations. Low-permeability marine shale of the Reklaw Formation, for example, restricts groundwater movement between aquifers in the Carrizo Formation and overlying Queen City Formation in the Claiborne Group (fig. 10).

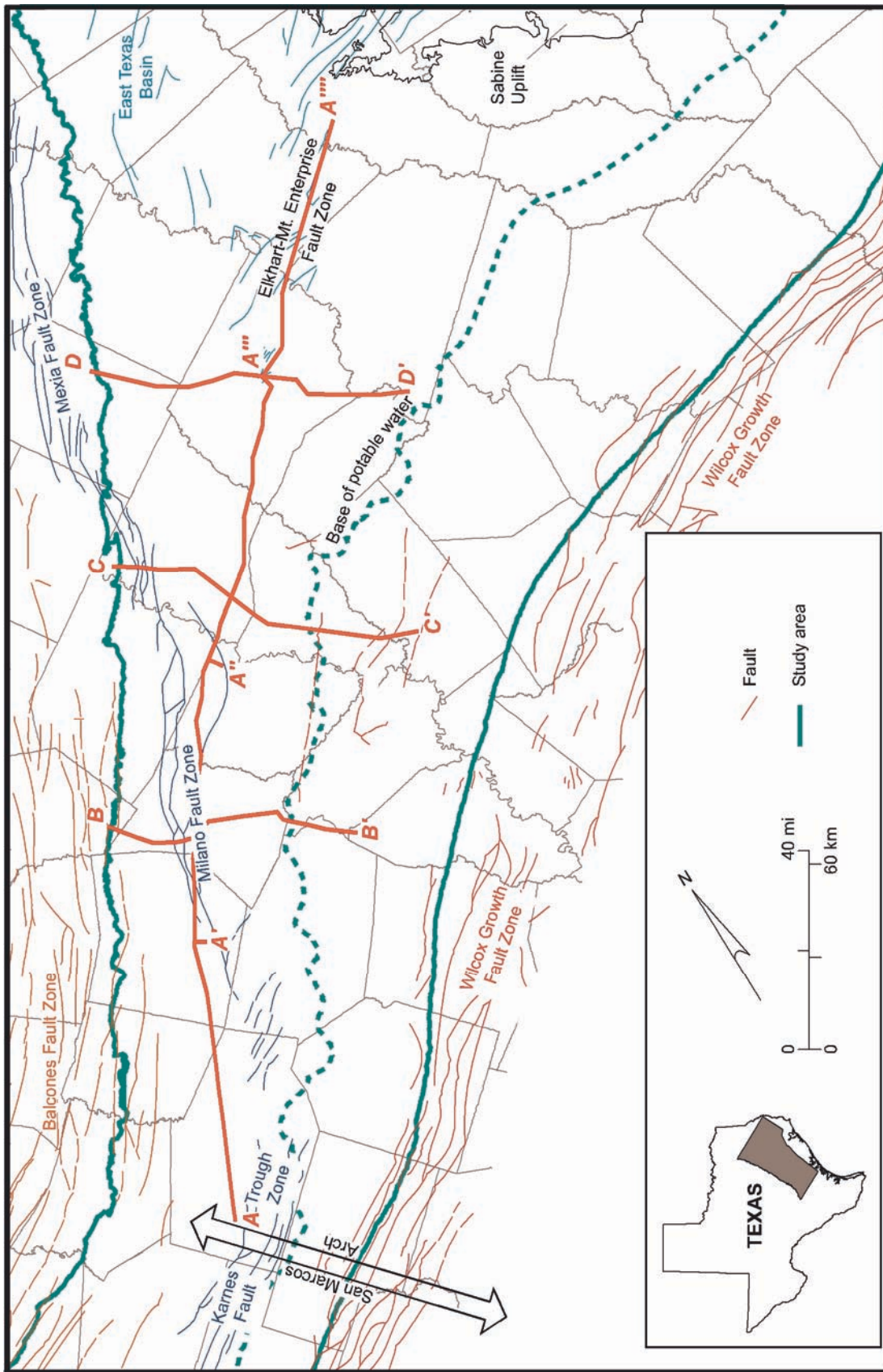
There is appreciable use of groundwater in the Brazos River alluvium for irrigation, and this deposit has been named a minor aquifer by the Texas Water Development Board (Ashworth and Hopkins, 1995; Hovorka and Dutton, 2001). Pleistocene and Holocene (Quaternary) alluvium also underlies the valleys of the Colorado and Trinity Rivers. Alluvium exchanges water between the Carrizo–Wilcox aquifer and the rivers. Groundwater in the bedrock formations can discharge into the alluvium, and water moves between the alluvial deposits and the surface-water channels. Alluvium can also store water that is recharged to the banks of rivers during flood flow; bank storage is released back to the rivers during low flow. Because of such interaction, alluvium in those three river valleys was included as a layer in the model. Because river alluvium was not the focus of this study,

this model should not be used to assess water resources of the alluvium without additional calibration of the modeled hydrologic properties of the alluvium.

4.2 Structure

Depositional patterns of Carrizo–Wilcox sediments have been influenced by the tectonic evolution of the Gulf of Mexico basin since its opening more than 180 million years ago. Early history of the basin included rifting and creation of numerous subbasins. During the Jurassic, marine flooding and restricted circulation resulted in accumulation of halite beds in these subbasins (Jackson, 1982). Subsidence continued as the rifted continental crust cooled. The sediment column records the effects of changes in relative rates of sediment progradation, basin subsidence, and sea-level change. More than 50,000 ft of sediment has accumulated in the Gulf of Mexico basin (Salvador, 1991).

The San Marcos Arch (fig. 14) is a structurally high basement feature beneath the central part of the Texas Coastal Plain separating the East Texas and South Texas basins, areas that had greater rates of subsidence. The Carrizo Formation and Wilcox Group drape over the San Marcos Arch. The structural effect on the Carrizo–Wilcox aquifer is obscured in figure 15, however, because the line of section turns from southwest to south and the San Marcos Arch plunges (increases in depth) toward the coast. The Sabine Uplift, which lies at the northern edge of the study area and extends into Louisiana, is another broad structural dome. Its topographic expression influenced sediment deposition in the East Texas Basin during the Tertiary (Fogg and others, 1991). The East Texas Basin is one of the major subbasins formed early in the Mesozoic, and it had significant thicknesses of halite deposition. Subsidence, tilting, and differential loading by Cenozoic sediments caused the



QAd1798c

Figure 14. Geologic structure in the study area. Modified from Ewing (1990). Lines of sections shown in figures 15 and 16.

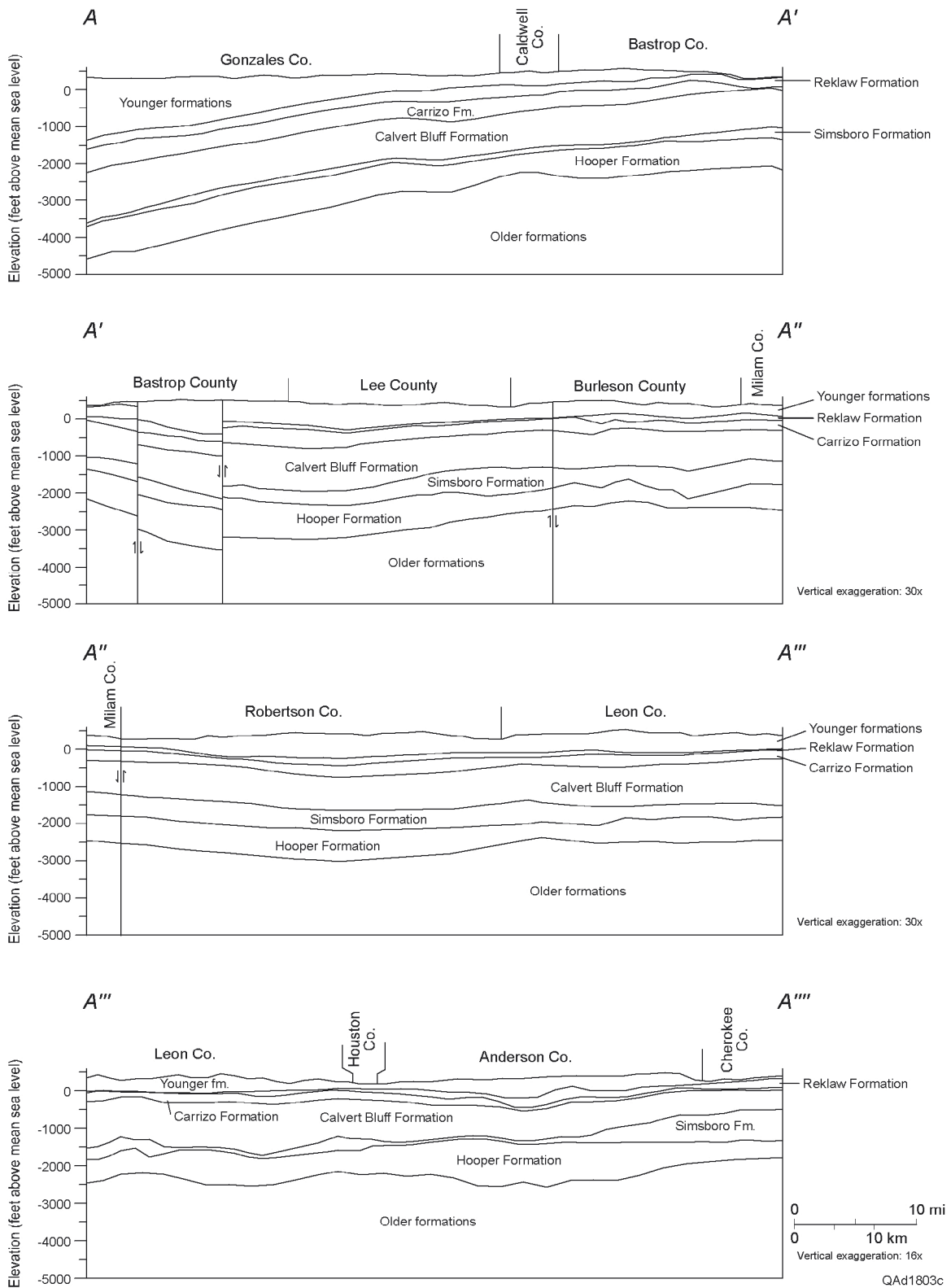


Figure 15. Vertical strike-oriented profile of the formations making up the Carrizo–Wilcox aquifer and adjacent formations. Strike section A–A''' shown in figure 14.

displacement of halite beds and the formation of various salt-tectonic features such as salt ridges and salt diapirs or domes (Jackson, 1982).

The Wilcox Group was the first major progradation during the Cenozoic. The Carrizo–Wilcox aquifer, therefore, occurs in a regional setting in which formation dip and thickness increase toward the Gulf of Mexico basin (fig. 16). Dip of the older formations increased as they were buried by younger sediments and as the basin subsided. As subsidence continued during progradation and deposition, formation thickness increased toward the Gulf.

Various fault zones are associated with the basin history of crustal warping, subsidence, and sediment loading. From coastward to inland, these include (1) the Wilcox Growth Fault Zone, (2) the Karnes-Milano-Mexia Fault Zone, and (3) the Balcones Fault Zone (fig. 14).

The Wilcox Growth Fault zone lies at the eastern limit of the study area (fig. 14). The growth or listric faults formed as thick packages of Wilcox sediment prograded onto the uncompacted marine clay and mud deposited in the subsiding basin beyond the Cretaceous shelf edge. Continued downward slippage on the gulfward side of the faults and sustained sediment deposition resulted in the Wilcox Group thickening across the growth fault zone (Hatcher, 1995). Petroleum exploration drilling and geophysical studies within the study area have indicated that many of these large, listric growth faults can offset sediments by 3,000 ft or more. The listric fault planes are curved, the dip of the faults decreases with depth, and the faults die out in the deeply buried shale beds. Complex fault patterns evolved, with antithetic faults forming various closed structures. The growth fault zone forms structural traps that hold major oil and gas reservoirs in the Wilcox Group (Fisher and McGowen, 1967; Galloway and others, 1983; Kisters and others, 1989). A few Wilcox Group oil fields

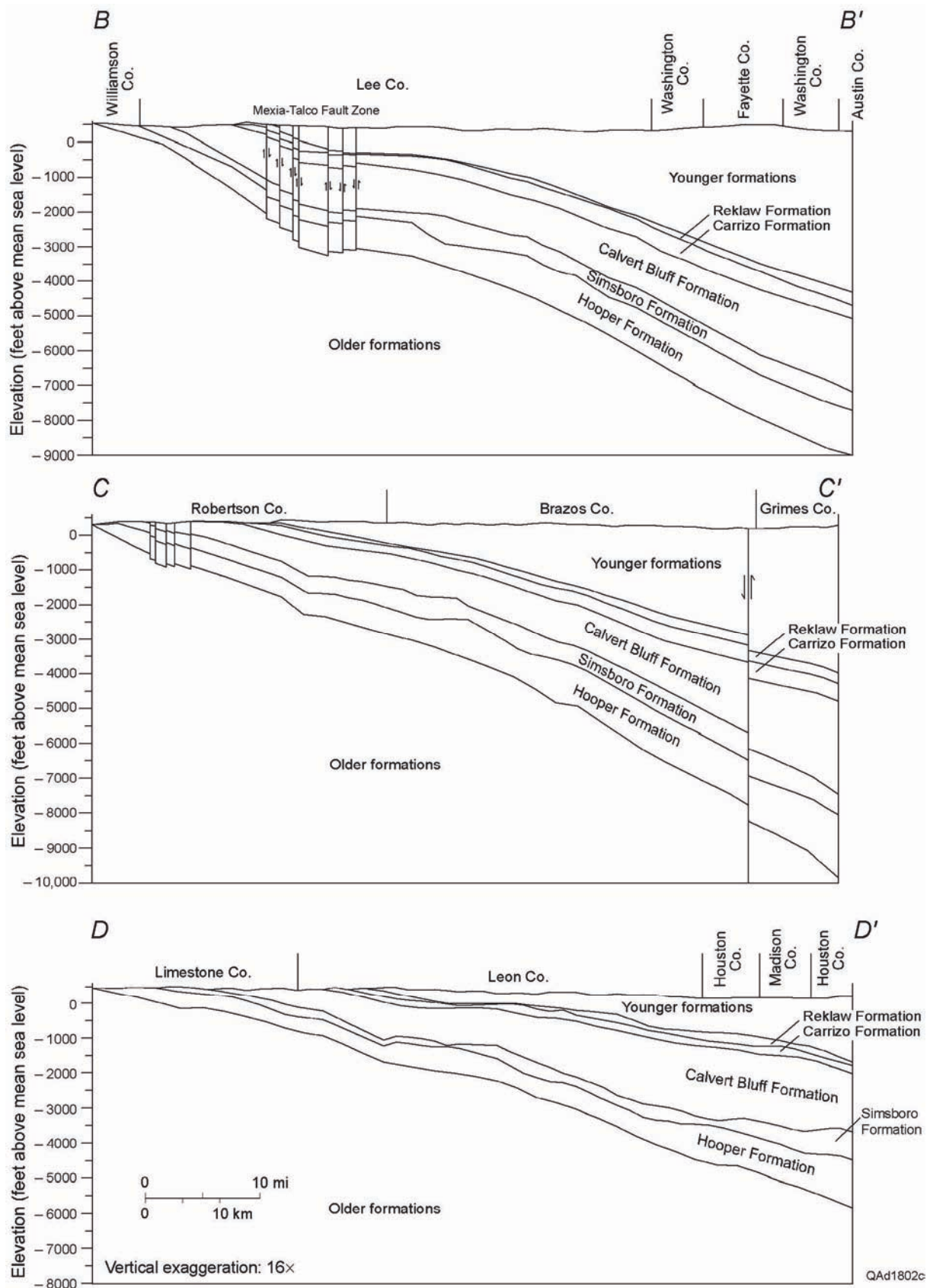


Figure 16. Vertical dip-oriented profile of the formations making up the Carrizo–Wilcox aquifer and adjacent formations. Dip sections B–B', C–C', and D–D' shown in figure 14.

associated with other faults lie updip of the growth fault zone (Fisher and McGowen, 1967; Galloway and others, 1983).

Displacement of halite beds resulting from subsidence, tilting, and sediment loading is the likely mechanism resulting in a zone of normal faults that offset Carrizo–Wilcox strata in the study area, including the Karnes Trough Fault Zone, Milano Fault Zone, and Mexia Fault Zone (fig. 14) (Jackson, 1982; Ewing, 1990). These fault zones in this report are collectively referred to as the Karnes-Milano-Mexia Fault Zone. The fault zone marks the updip limit of the Jurassic Louann Salt (Jackson, 1982). Displacement along the Karnes-Milano-Mexia Fault Zone occurred throughout Mesozoic deposition along the Gulf Coast and continued at least through the Eocene, resulting in noticeable syndepositional features. Numerous faults with as much as 800 ft of displacement that exhibit no syndepositional features are also present throughout the Karnes-Milano-Mexia Fault Zone (Jackson, 1982). In the central and southwest portions of the model, the Karnes-Milano-Mexia Fault Zone displaces sediments by more than 1,000 ft in some areas, restricting the hydraulic communication between outcrop and downdip sections of the aquifer (fig. 16a, b). The Karnes-Milano-Mexia Fault Zone goes updip of the Carrizo–Wilcox aquifer near the northwestern corner of the study area (fig. 14).

Flexure across the structural high between the East Texas Basin and the Gulf of Mexico basin formed extensional faults and associated graben structures of the Elkhart-Mt. Enterprise Fault Zone (fig. 14). This fault zone offsets Carrizo–Wilcox sediments by several hundred feet (Jackson, 1982).

The Balcones Fault Zone consists of numerous fault strands that swing from northwesterly in the southern part of the model area to north-northwesterly in the central and northern part of the area (fig. 14). Faults in this trend are of normal displacement, dominantly

dipping to the southeast (basinward), although some northwest-dipping synthetic faults occur (Collins and Laubach, 1990). Fault strands are spaced roughly 1 to 3 mi apart and have throws of 15 to 300 ft (Nance and others, 1994; Collins, 1995). Although the Balcones trend follows the thrust-fault trends of the late Paleozoic Ouachita orogen (Ewing, 1990), activity is limited to the Late Cretaceous and Tertiary (Collins and Laubach, 1990). The zone results from tilting along the perimeter of the Gulf Coast basin, flexure, and gulfward extension (Murray, 1961; Collins and others, 1992). Some evidence points toward movement of this system as recently as Plio-Pleistocene times (Collins and Laubach, 1990).

Structure of the aquifer system also consists of the physical dimensions of the aquifer and its confining layers: the six surfaces describing the elevations of the tops and bottoms and the position of the sides of the model layers. Of all the input data, aquifer-system geometry is probably the best characterized. Structure of the top and bottom of the aquifer is defined by numerous wells, topography of the land surface is mapped, water levels are repeatedly measured to define the top of the aquifer in the outcrop zone, and geologic maps show the lateral extent of formation outcrops. Although formation thickness was not defined exactly at every point in the aquifer, the uncertainty is acceptable and generally does not greatly impact results of a model.

Construction of structural surfaces of layer elevations for input to the computer model required compilation and digitizing of structure information from a number of sources. Sources on subsurface structure included Bebout and others (1982), Ayers and Lewis (1985), Thorkildsen (unpublished data on Carrizo–Wilcox aquifer groundwater modeling and water-quality analysis, East Texas), Kaiser (1990), and Hosman and Weiss (1991). In addition, we used tabulated geologic determinations from geophysical logs contained in the Bureau of Economic Geology Geophysical Log Library. A three-arc second digital elevation

model (DEM) of the study area was downloaded from a U.S. Geological Survey (USGS) Website. DEM data were used to define the top elevations of aquifers in their outcrop. Several hundred new stratigraphic picks were made from geophysical logs of oil and gas wells in Anderson, Caldwell, Gonzales, Guadalupe, and Houston Counties. Locations of logs were digitized from Ayers and Lewis (1985) and estimated from county highway maps.

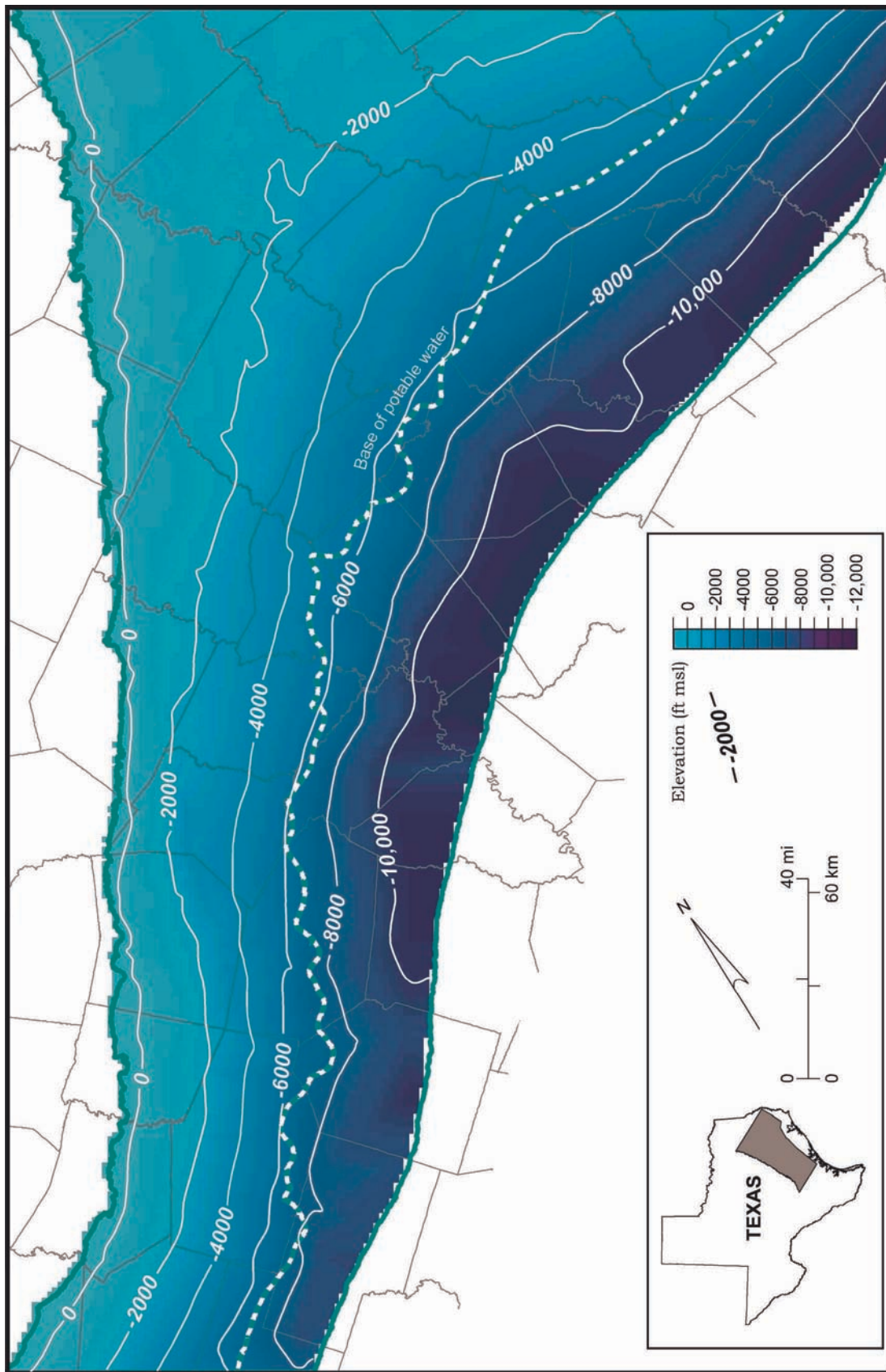
These several data sets are spatially dissimilar, so merging them required both GIS and geostatistical software packages. Construction of layer structure surfaces made use of data as follows:

- Base of Hooper Formation included information from Ayers and Lewis (1985), Thorkildsen (unpublished data), Hosman and Weiss (1991), and outcrop DEM data.
- Base of Simsboro Formation included information from Ayers and Lewis (1985), Kaiser (1990), and outcrop DEM data. The Thorkildsen (unpublished) data were used in areas not otherwise covered.
- Base of Calvert Bluff Formation included information from Ayers and Lewis (1985) and outcrop DEM data. The Thorkildsen (unpublished) data were inserted in areas not otherwise covered.
- Base of Carrizo Formation included information from Ayers and Lewis (1985), Thorkildsen (unpublished data), Hosman and Weiss (1991), and outcrop DEM data.
- Base of Reklaw Formation included information from Ayers and Lewis (1985), Thorkildsen (unpublished data), and outcrop DEM data. The surface formed by these data was extrapolated to areas in the eastern corner of the model.
- Top of Reklaw Formation included information from Ayers and Lewis (1985), Thorkildsen (unpublished data), and outcrop DEM data.

Layer elevations were checked for vertical consistency by mapping layer thickness calculated using a triangulated irregular network method. False points inserted at appropriate locations corrected areas having a vertical discrepancy. Layer elevations were extended to areas lacking geophysical control data by kriging layer thickness, recalculating layer elevations from the kriged surface, and merging the recalculated elevation surface into data-poor areas.

Alluvial deposits associated with the Colorado, Brazos, and Trinity Rivers most likely have a significant impact on the interaction of surface water and groundwater in the outcrop of the Carrizo–Wilcox aquifer. Areal limits of the alluvium associated with the Colorado, Brazos, and Trinity Rivers were digitized from McGowen and others (1987), Proctor and others (1988), Proctor and others (1993a, b), and Shelby and others (1993). The upper surface of the alluvium was taken as ground surface and assigned by draping USGS DEM data onto model cell centroids in the areas underlain by alluvium. Thickness of alluvium was estimated from data on well depth and well-screen position (Wilson, 1967; http://www.twdb.state.tx.us/data/waterwell/well_info.html). The lower surface of alluvium was mapped by subtracting alluvium thickness from DEM for each model cell.

Elevation of the base of the Wilcox Group (base of Hooper Formation) ranges from ground surface at the updip limit of the formation to as much as 12,000 ft below sea level at the downdip limit of the study area (fig. 17). Maps of layer elevation shown in figures 17 through 21 indicate a fixed position of the base of freshwater. The base of freshwater shown on these illustrations is taken from the TWDB map of the freshwater extent of the Carrizo–Wilcox aquifer and is included in the structure maps for reference. The base of freshwater in the Hooper Formation lies some distance farther updip than that shown on the map, which is defined mainly by the downdip limit of freshwater in the Carrizo Formation.

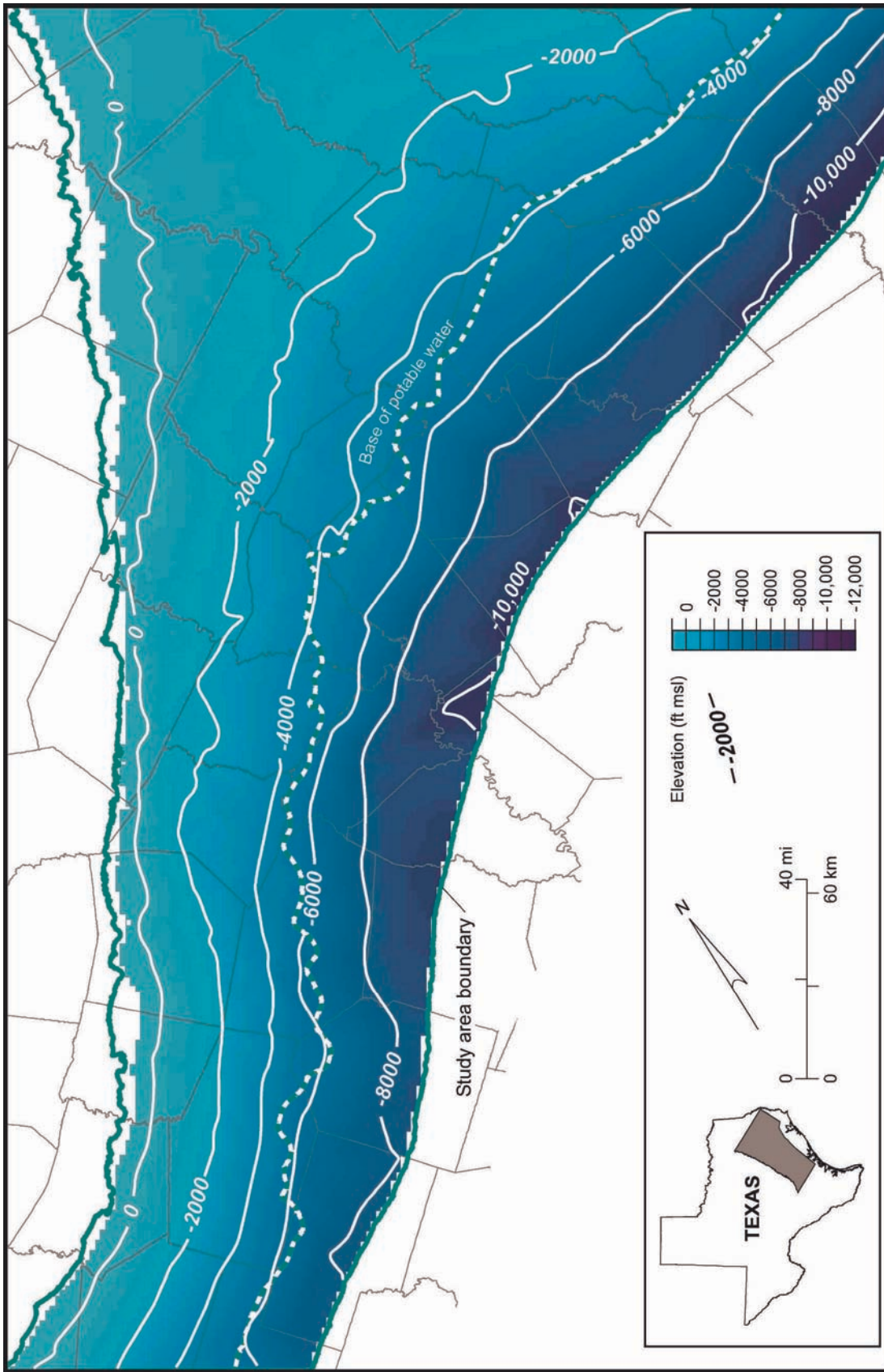


QA41810C

Figure 17. Elevation of the base of the Hooper Formation (base of Wilcox Group).

Structural elevations of the Simsboro and Calvert Bluff Formations (figs. 18, 19) show the same general features of a surface gently dipping to the southeast toward the Gulf of Mexico. The strike of contours on the structural surfaces changes from north-northeast to east and reflects basement structure. The contours strike eastward south of the East Texas Basin and Sabine Uplift. The East Texas Basin lies between the 0-ft elevation contours of the base and top of the Carrizo Formation (figs. 20, 21, respectively) in the northern part of the study area—between the outcrops of the Carrizo Formation to the northwest and northeast. The top of the Reklaw Formation (fig. 22) shows the same major structural features as do the underlying formational contacts. The saddle in the structure of the Reklaw Formation top in Anderson County, lying between the 0-ft elevation contours, marks the southern end of the East Texas Basin.

Thicknesses of each formation were tallied from the geophysical log sources, compiled in a database, and contoured in figures 23 through 26. Each formation thickens southeastward toward the Gulf of Mexico. The freshwater section of the Hooper Formation is mainly less than 1,200 ft thick (fig. 23). Thickness of the Simsboro Formation is greatest (up to 500 ft; fig. 24) in the central part of the study area where the center of deposition was in the Rockdale Delta (Fisher and McGowen, 1967). Because the focus of the model was on the freshwater aquifer, not as much data were compiled for the part of the study area downdip (eastward) of the base of freshwater. This fact and interpolation between different data sets make the mapped thickness of the Simsboro Formation in the deepest part of the study area appear irregular. The thickest part of the Simsboro Formation lies in the northeastern corner of the study area. Thickness of the Calvert Bluff likewise increases downdip and toward the Gulf of Mexico (fig. 25). The thickest part of the Calvert Bluff is in the central part of the study area.



QAd1811c

Figure 18. Elevation of the base of the Simsboro Formation (top of Hooper Formation).

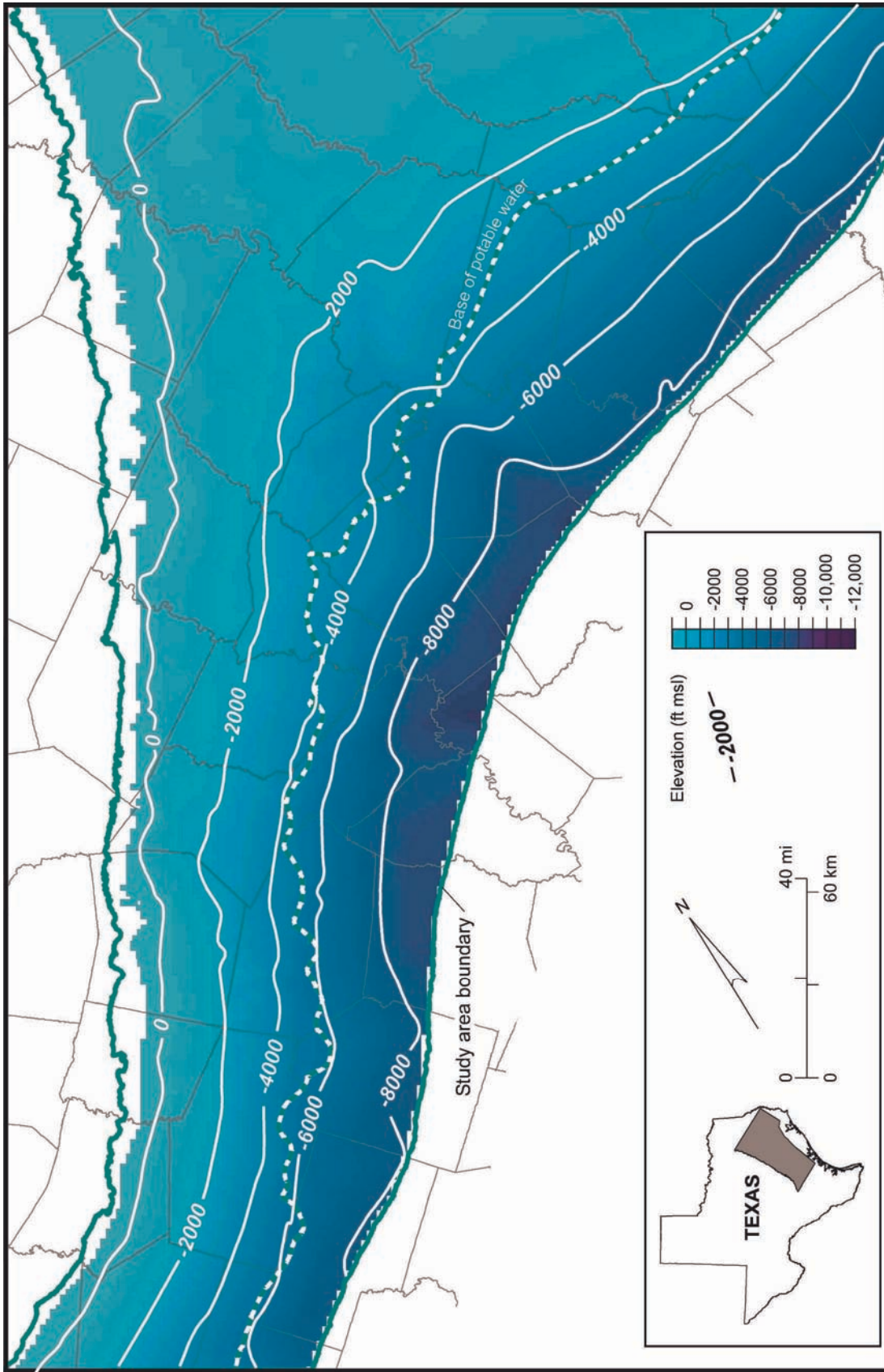


Figure 19. Elevation of the base of the Calvert Bluff Formation (top of Simsboro Formation).

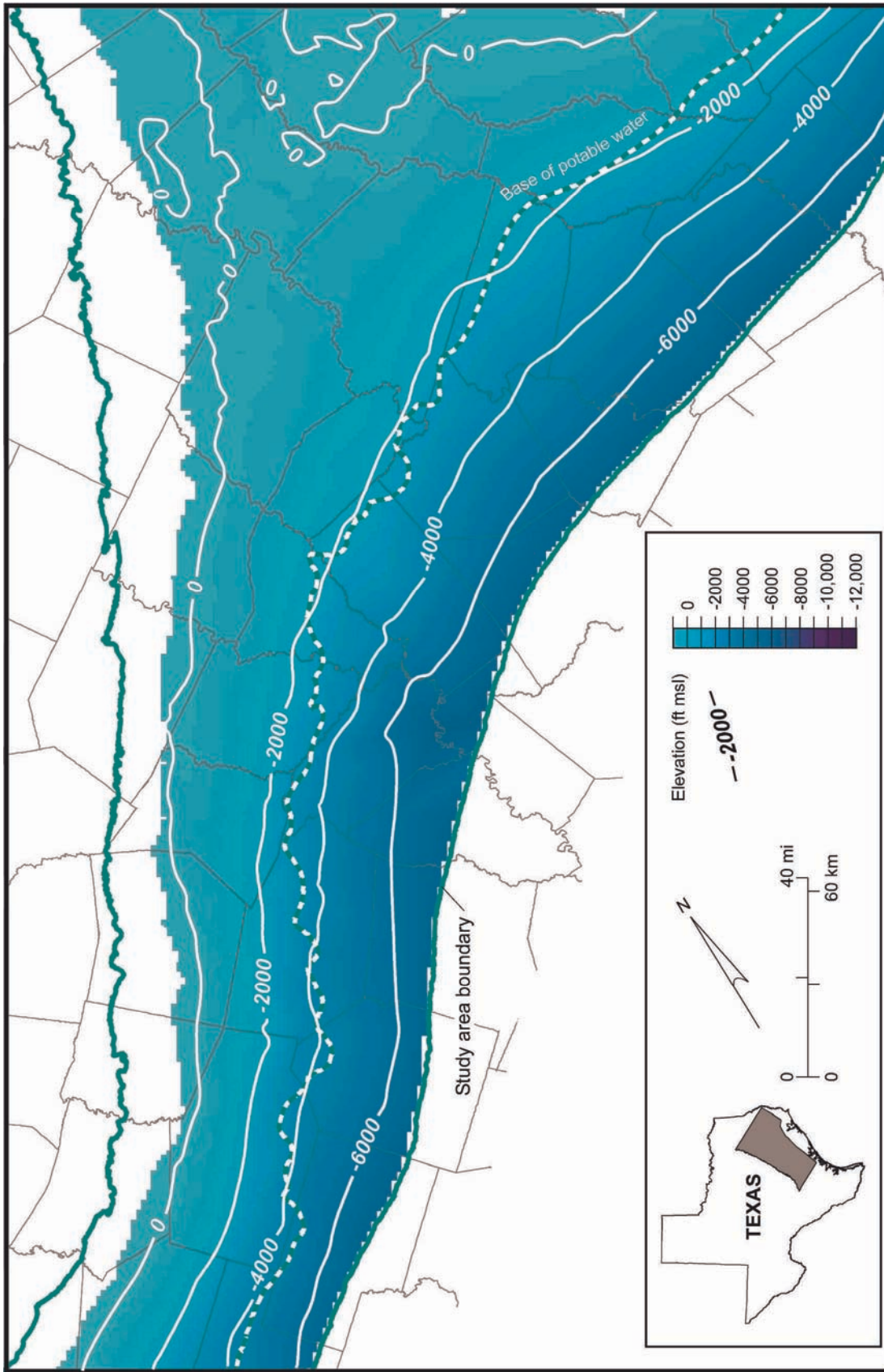
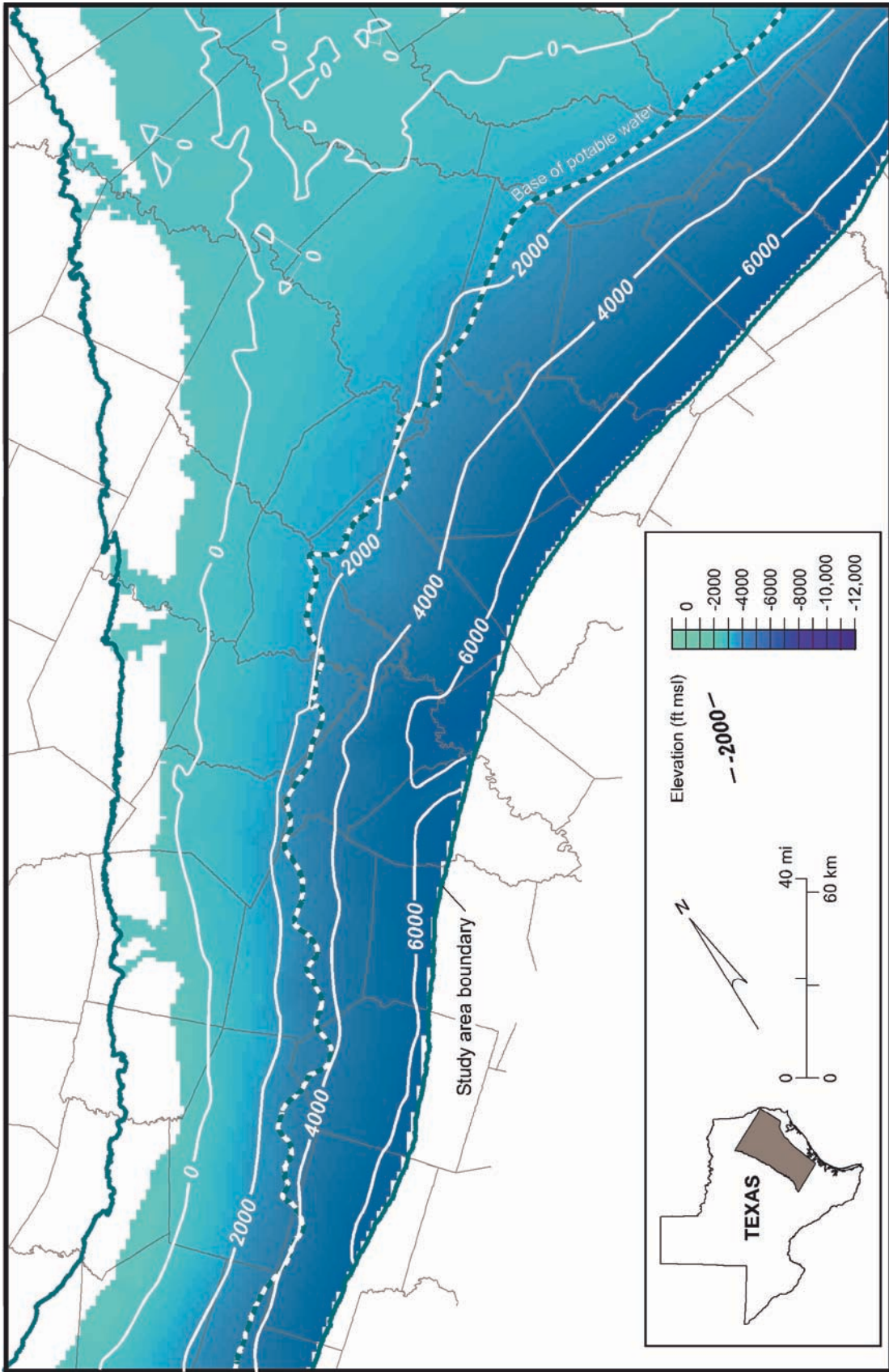
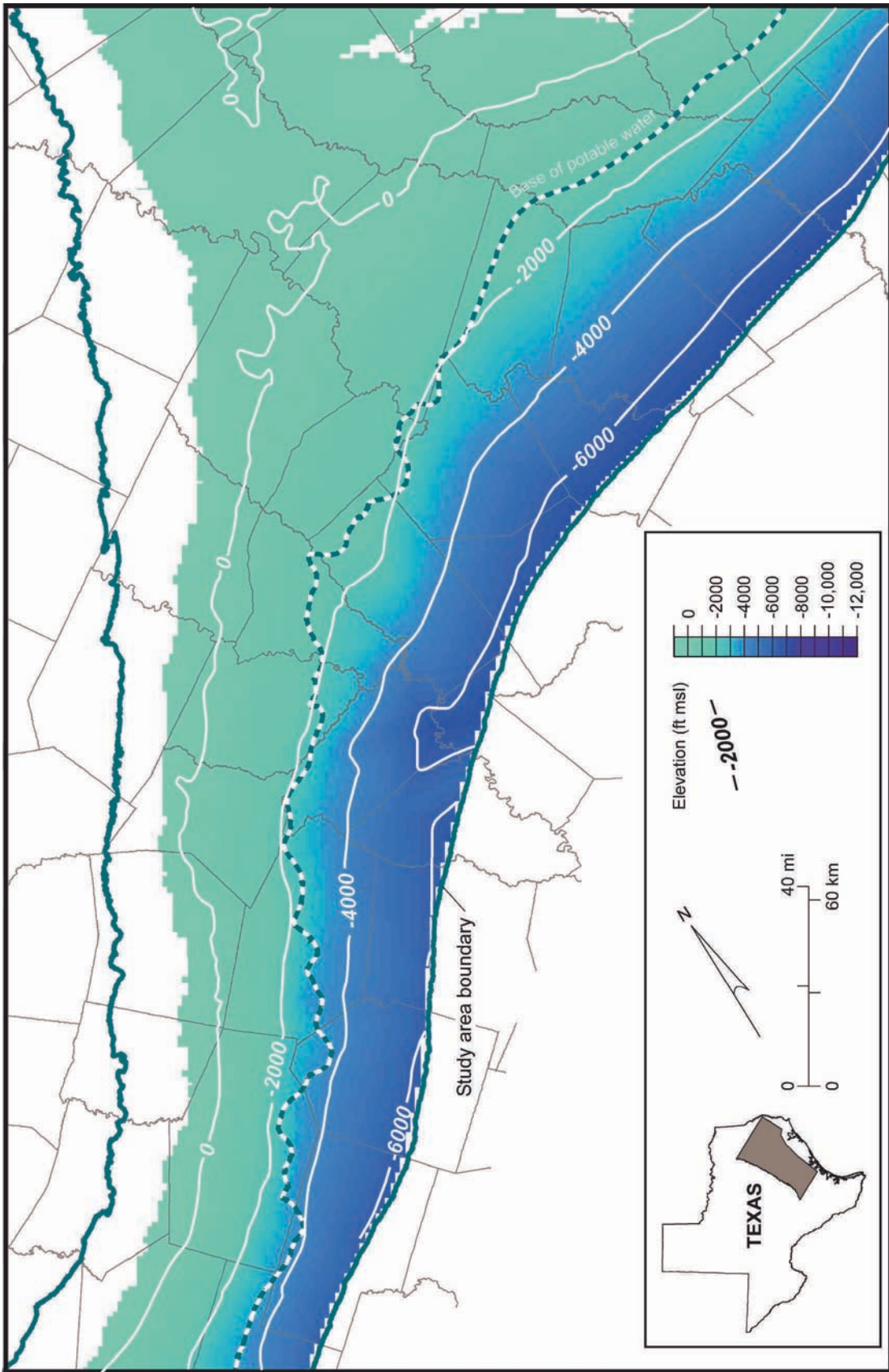


Figure 20. Elevation of the base of the Carrizo Formation (top of Calvert Bluff Formation).



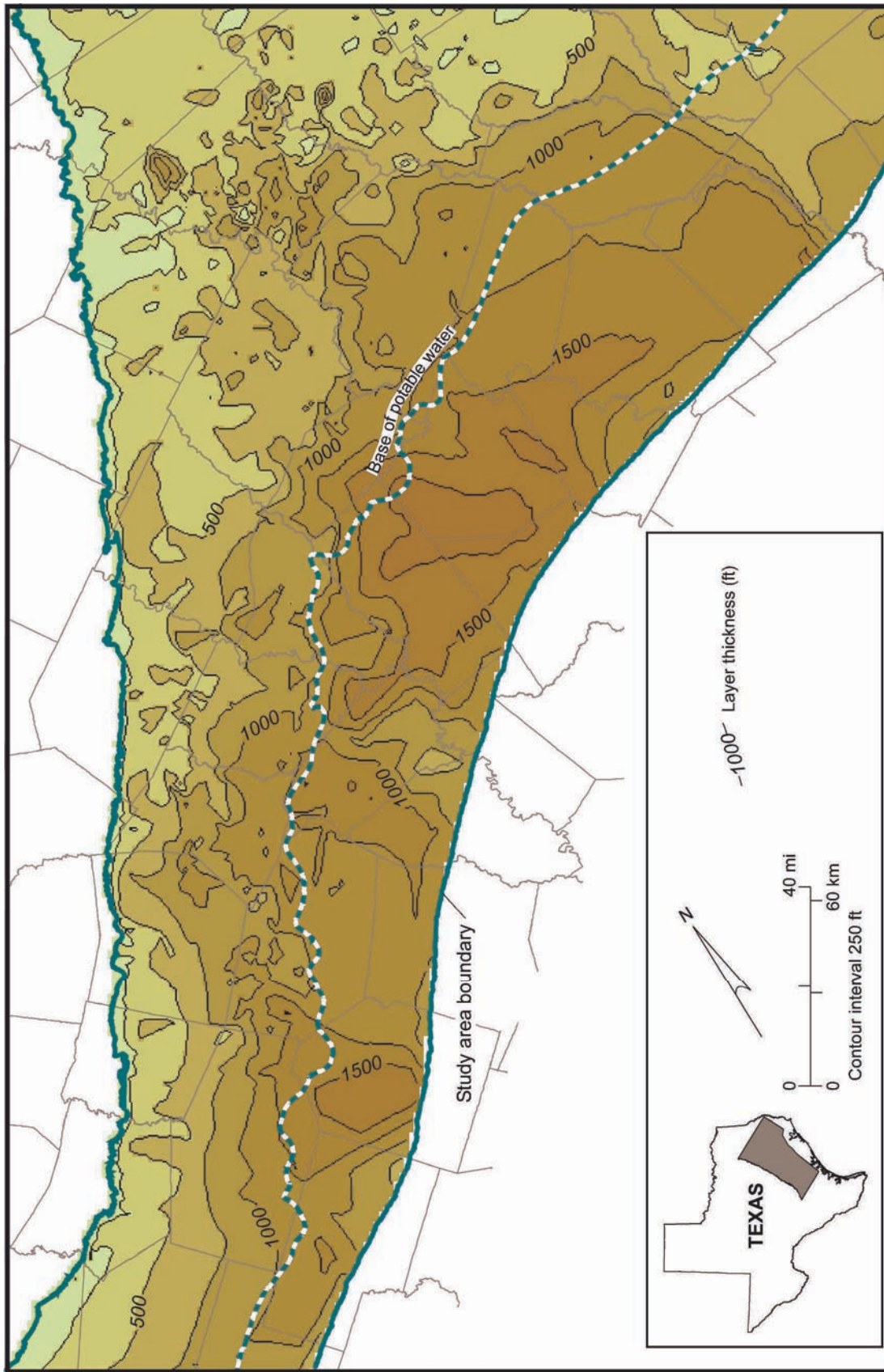
QAD1814C

Figure 21. Elevation of the top of the Carrizo Formation (base of the Reklaw Formation).



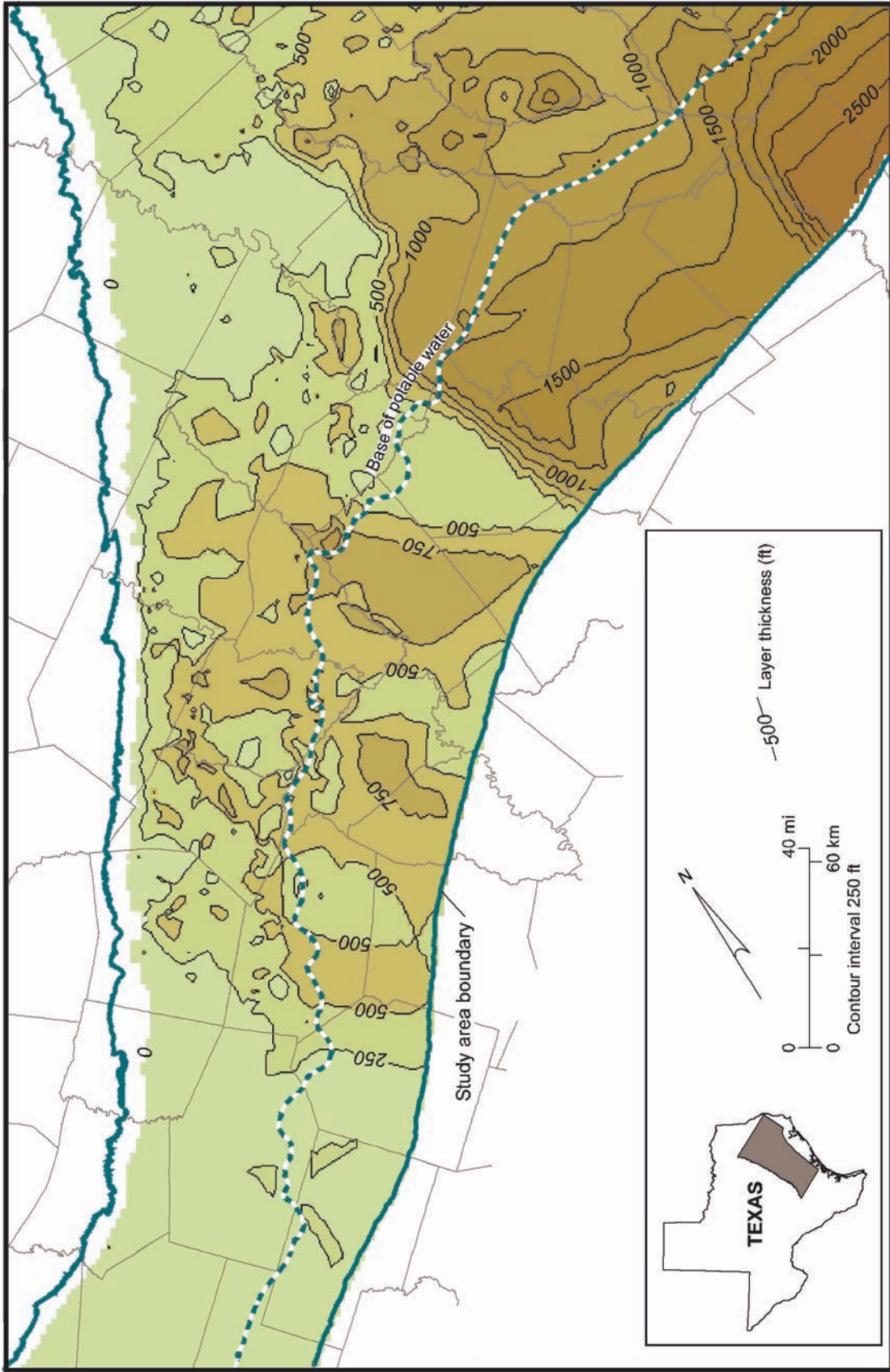
QA42279X

Figure 22. Elevation of the top of the Reklaw Formation.



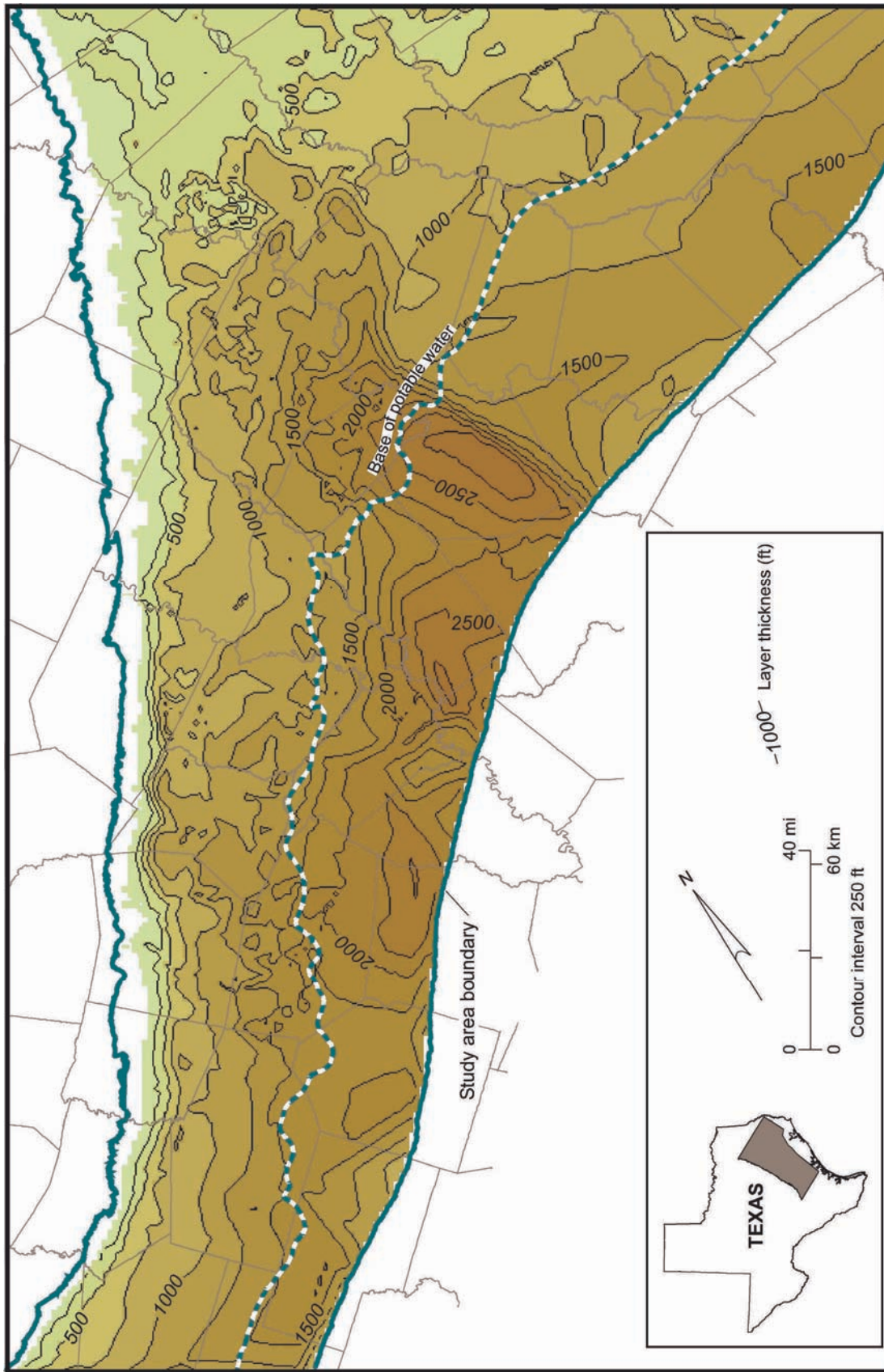
QAd1817c

Figure 23. Total thickness of the Hooper Formation.



QA41820c

Figure 24. Total thickness of the Simsboro Formation.



QA41819c

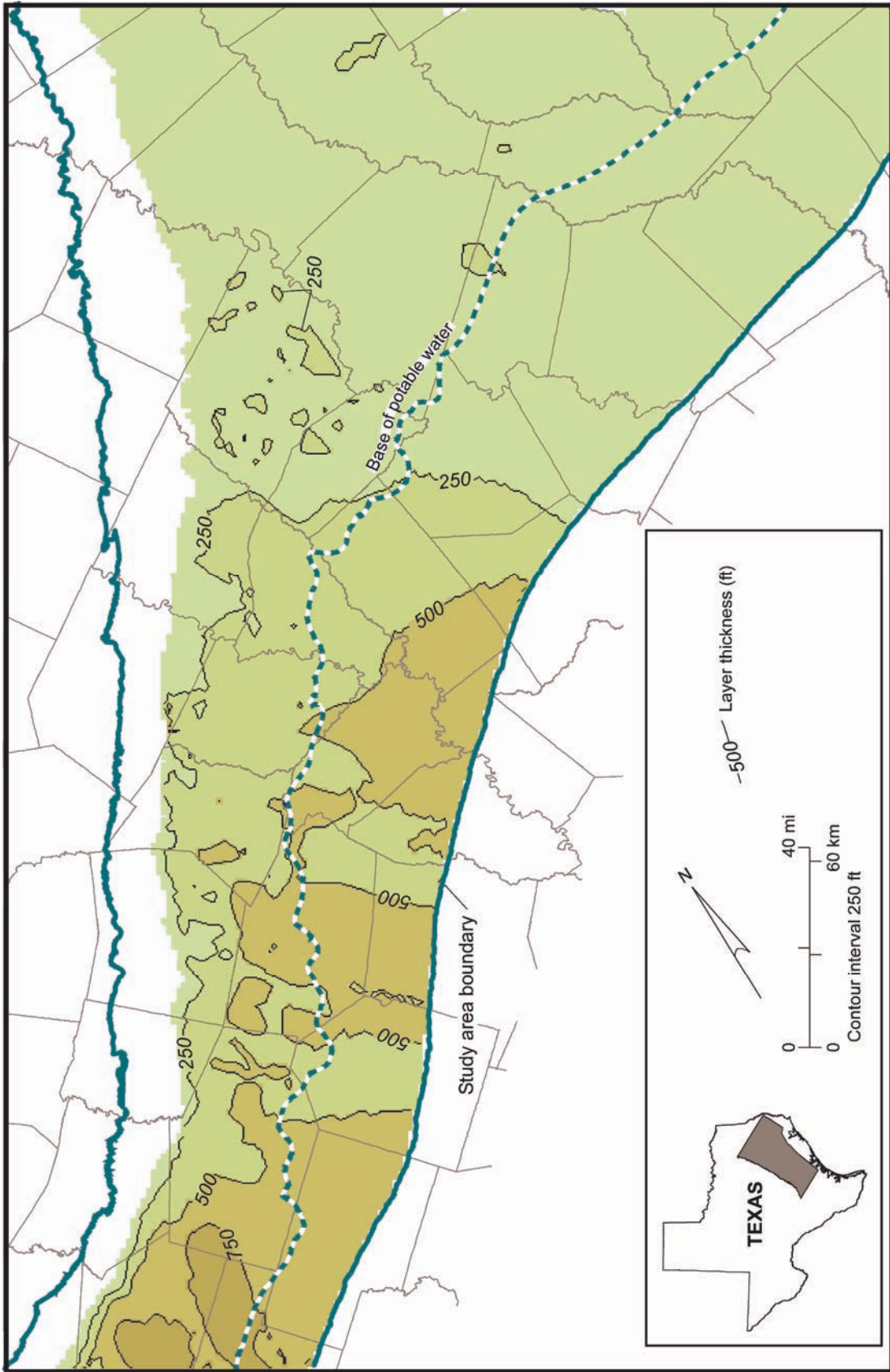
Figure 25. Total thickness of the Calvert Bluff Formation.

Thickness of the Carrizo Formation does not vary downdip as much as in the other formations (fig. 26). Its thickness increases, however, toward the south across the study area. The center of deposition of Carrizo sediments had shifted southward, unlike the earlier Wilcox sediments (Hamlin, 1988). Thickness of the Reklaw Formation in the study area ranges from less than 100 ft to locally more than 300 ft. In the East Texas Basin the formation is from 100 ft to more than 300 ft thick. Thickness of Colorado River alluvium ranges from about 30 to 70 ft in Bastrop County. Alluvium thickness beneath the floodplains of the Brazos and Trinity Rivers in the study area averages about 30 to 50 ft in Milam, Robertson, Henderson, Freestone, and Anderson Counties.

4.3 Water Quality

Water-quality data were compiled from both hydrologic and petroleum-industry sources. Data on total dissolved solids for fresh groundwater in the aquifer were compiled from the TWDB online groundwater database; reports on public water-supply wells compiled by the Texas Commission on Environmental Quality (TCEQ), formerly the Texas Natural Resources Conservation Commission (TNRCC); permit files at the Railroad Commission of Texas (RRC); and individual water-supply companies and well owners. Data on formation waters in Wilcox reservoirs were purchased from IHS Energy Group, Houston. Charge balance for 89 percent of freshwater chemical analyses and 92 percent of formation waters is within ± 5 percent.

Data on total dissolved solids (TDS) were posted using ArcView® and manually contoured. Data are insufficient to allow regional mapping of water quality by layer;



QAd1818c

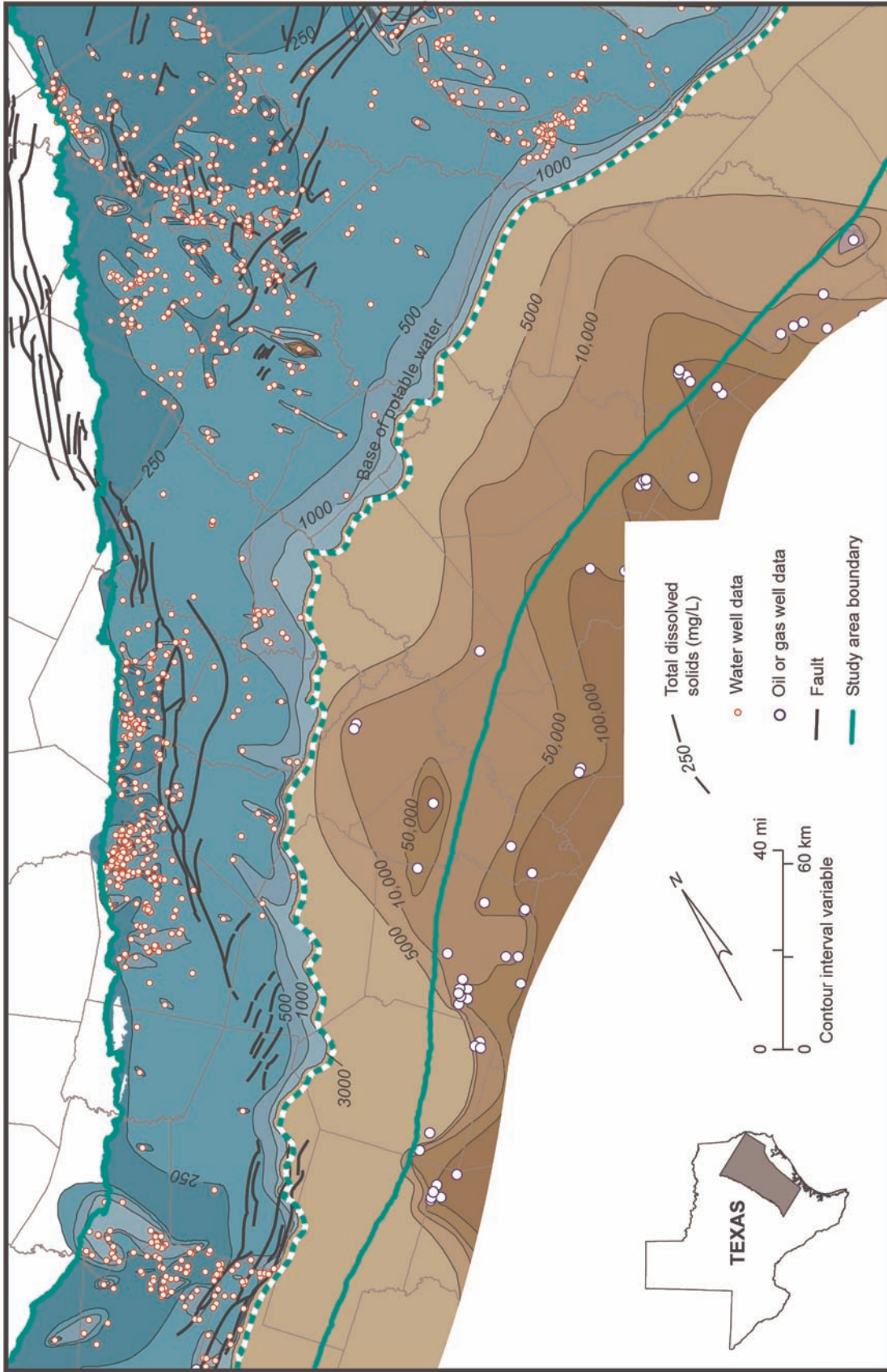
Figure 26. Total thickness of the Carrizo Formation.

figure 27 is a composite map of TDS in the Carrizo–Wilcox aquifer. The downdip limit of the base of potentially potable water in the aquifer as defined by the TWDB was represented by the contour of 3,000 mg/L TDS.

TDS in the outcrop of sand-rich parts of the Carrizo–Wilcox aquifer of Central Texas varies generally from 100 mg/L near the water table to 300 mg/L (fig. 27). Locally TDS can exceed 1,000 mg/L. Most of the confined part of the aquifer has TDS of <500 mg/L, especially in well-interconnected sand-rich zones. Hydrochemical types (Piper, 1944), highly variable in the shallow subsurface, tend to change toward the sodium-bicarbonate (NaHCO_3) type as groundwater moves farther downdip in the aquifer. This trend follows a typical pattern of Gulf Coast groundwaters, with ion exchange and incongruent solution of minerals prevalent reactions (Foster, 1950). Salinity variation might also result from leakage of poor-quality water from low-permeability, sand-poor deposits (Henry and others, 1979; Dutton, 1985).

Downdip of the 500 mg/L TDS contour, salinity increases rapidly at 250 to 450 mg/L/mi to the limit of potable water at 3,000 mg/L. Salinity continues to increase at a rate of as much as 1,000 mg/L/mi across the brackish-water zone between 3,000 and 10,000 mg/L and as much as 12,000 mg/L/mi across the saline zone between 10,000 and 100,000 mg/L (fig. 27). In the central and north part of the study area, TDS varies between 10,000 and 50,000 mg/L updip of the growth fault zone. In the south, groundwater with TDS of less than 5,000 mg/L extends into the growth fault zone (Dutton and others, 2002).

The chemical composition of the formation waters associated with oil fields matches that of three water types (sodium-acetate, sodium-chloride, and calcium-chloride waters) identified by Morton and Land (1987) and Land and Macpherson (1992) as typical of



QAAd1823(b)c

Figure 27. Total dissolved solids (TDS) content of groundwater in the Carrizo–Wilcox aquifer and in the saline section downdip of the aquifer.

the Cenozoic saline section beneath the Texas Coastal Plain. Land and Macpherson (1992) suggested that sodium-chloride water originated from dissolution of halite by groundwater and that sodium-acetate water derived from seawater by sulfate reduction and other mineralogic reactions, including dilution by water released from the smectite-to-illite change. The calcium-chloride water was derived from water moving up faults from the underlying Mesozoic section (Land and Macpherson, 1992).

The downdip extent of freshwater in the Carrizo–Wilcox aquifer may be affected partly by the Karnes-Milano-Mexia Fault Zone, which breaks up the continuity of transmissive sandstones between the outcrop and the deeper, subsurface part of the aquifer (Dutton and others, 2002). Through the middle of the study area, displacement of faults is as much as 1,000 ft (Ayers and Lewis, 1985). The continuity of major sandstones in the Simsboro and Carrizo Formations is disrupted, and locally the Carrizo Formation does not crop out. The width of the freshwater zone in the Carrizo–Wilcox aquifer, as seen in plan view and measured from the outcrop to the downdip limit of freshwater, is only 20 to 30 mi in Central Texas (fig. 27). The major faults die out southwest, where the aquifer is as much as 80 mi wide. To the northeast, the fault zone passes updip of the outcrop and does not affect fluid flow in the Carrizo–Wilcox aquifer. In East Texas the freshwater zone is recharged on both the western and eastern sides of the East Texas Basin and is more than 60 mi wide (fig. 27).

4.4 Water Levels and Regional Groundwater Flow

Subsurface fluid-pressure regimes in the Gulf of Mexico basin include hydropressured, transitional, and geopressured zones (Parker, 1974; Jones, 1975; Bethke,

1986). Hydropressed conditions are typical of near-surface aquifers; their pressure-depth gradient plots along a trend of approximately 0.43 psi/ft. The geopressed zone has pressure-depth gradients of more than 0.7 psi/ft (Loucks and others, 1986).

4.4.1 Data and Methods

To construct maps of the potentiometric surface of the Carrizo–Wilcox aquifer, we pooled data from the freshwater part of the aquifer and from the adjacent, more saline part of the Wilcox Group. Data for the freshwater part of the Carrizo–Wilcox aquifer and the Queen City aquifer were obtained from records of water levels measured in water wells listed in the Texas Water Development Board (TWDB) online groundwater database (<http://www.twdb.state.tx.us>). We selected the earliest measurements in each part of the study area to best represent predevelopment or pseudo-steady-state water levels. Most of the water levels used in the maps were measured in the 1950s, but some were measured as early as the 1930s. Contouring of the water-level measurements took into account topographic elevation of the ground surface.

The process of selecting water levels for calibration and verification of the model involved several steps.

- (1) A Microsoft Access database containing TWDB water-level records was compiled for the counties in the study area.
- (2) Data quality was reviewed. Wells with three or more historical water-level measurements were candidates for use. For the steady-state calibration, water-level measurements of various dates were selected on a county-by-county basis to include the earliest available measurements. This was necessary because pumping that may have affected water levels started at various times in the study area.

- (3) Hydrographs were constructed and inspected for candidate wells. Well hydrographs were discarded if they showed erratic trends near the calibration or verification dates (1990 and 2000, respectively).
- (4) Calibration data were assigned to model layers mainly on the basis of the TWDB aquifer code. Where the aquifer code was insufficient (e.g., designated as Wilcox Group), we also compared the calculated elevation of the base of the well against layer elevation; elevation of screened intervals where reported was also checked.
- (5) During calibration and verification, we continued to check assignment of well hydrographs by layers. Most changes were for wells assigned to a layer on the basis of total well depth. Some cases were found where the well was drilled only a short distance into a layer; if screen information was reported it might show that the well had been completed in the overlying aquifer unit. It is possible that some wells assigned to one model layer may be screened in an overlying layer.

Water-level measurements from the Bryan-College Station well field were included in the calibration data set. Static water-level measurements from the Simsboro Formation prior to well-field development form an important water-level calibration point in the deep artesian portion of the aquifer. Water-level measurements taken when a well is not pumping are considered static water-level measurements. Simulated water levels reflect drawdown caused by groundwater withdrawal assigned to model cells. Adjusting static water levels for the Bryan-College Station well field is appropriate for comparison with simulated results for model cells. The adjustment followed the method of Anderson and Woessner (1992 , p. 147 –149). An initial water-level recovery was estimated using known transmissivity, average pumping rate, and assumed elapsed recovery time. Initial recovery was projected to

an equivalent for a 1-mi grid cell. The correction factor is small relative to measured and simulated changes in water level.

To extend the maps of water-level elevation farther downdip across the saline part of the study area, data on fluid pressure from Wilcox gas wells were compiled from Lasser, Inc. (2000). We extracted data on bottom-hole pressure, cumulative gas production, and measurement depth for 583 Wilcox gas wells in the study area. We checked pressure decline against production and found that the earliest pressure readings sufficed to help us estimate original pressure for each well. Some pressure readings are obviously affected by production in nearby wells. To cull much of the reduced-pressure data we took the highest pressure readings in a 400-mi² area (20- × 20-mi area), leaving 31 data points. We then calculated the equivalent water pressure (P_w) by subtracting capillary pressure (P_c) from recorded bottom-hole gas pressure (P_g) using equation 1 (modified from Amyx and others, 1960, p. 138, equations 3 through 6):

$$P_w = P_g - P_c = P_g - H(\rho_w - \rho_g) \quad (1)$$

where ρ_w and ρ_g are water and gas densities, respectively, and H is the height of the gas column between the measurement point and the reservoir's gas-water contact. Gas density was calculated by applying a gas compressibility (z) factor (Brill and Beggs, 1974).

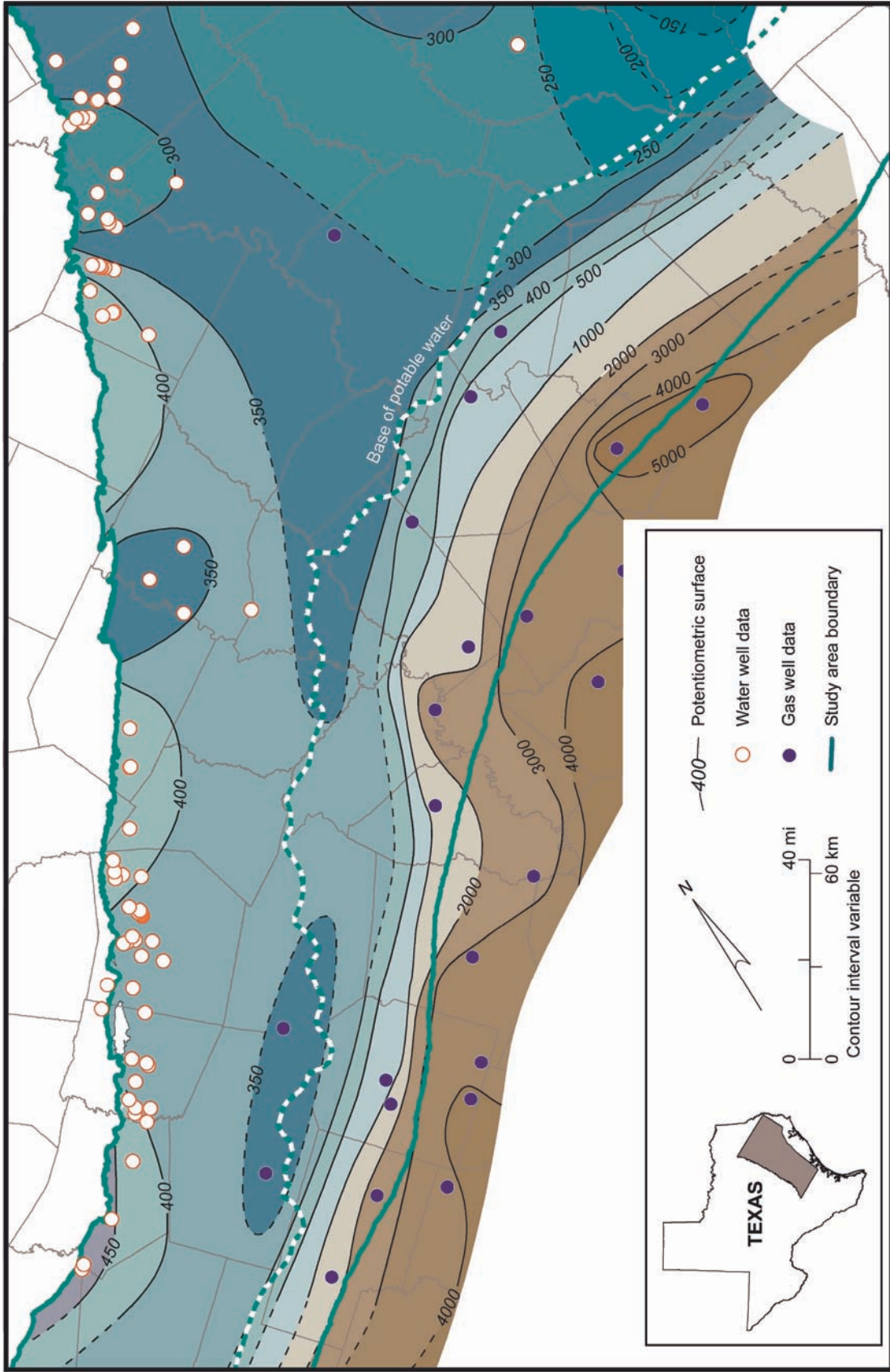
Capillary pressure increases with height above the gas-water contact. We found few data on elevation of the gas-water contact for the gas fields included in the culled list. We assumed that the typical measuring point for pressure data in Wilcox gas fields in the study area was 100 ft above the gas-water contact (Kosters and others, 1989). In one field the measuring point was 30 ft above the gas-water contact. If our 100-ft value overestimates height of the measuring point above the gas-water contact, the map of potentiometric surface in the downdip gas fields underestimates actual hydraulic head. Finally, we estimated

hydraulic head by (1) dividing water pressure by the specific weight of saline water, assumed to be 0.465 psi/ft, and (2) adding pressure head to the elevation head at the measurement point. We merged the same mapped potentiometric surface of the Wilcox geopressed zone with those of the updip aquifers in the Simsboro and the Carrizo Formations (figs. 28, 29).

4.4.2 Predevelopment or Steady-State Distribution of Hydraulic Head

Before aquifer development, water levels in and near the outcrop generally follow topography (figs. 28, 29). Hydraulic head in the freshwater-bearing aquifer is higher beneath upland areas and drainage divides than beneath river valleys and the area downdip of the outcrop (figs. 28, 29; Fogg and Kreitler, 1982; Fogg and others, 1991; Thorkildsen and Price, 1991; Dutton, 1999). Hydraulic head is also higher (>300 ft; figs. 28, 29), where the Carrizo–Wilcox aquifer is recharged at its outcrop across the Sabine Uplift area (Fogg and others, 1991). The Carrizo–Wilcox aquifer in the East Texas Basin area is recharged from both the Sabine Uplift and the aquifer outcrop on the northwestern side of the basin. Between the Sabine Uplift and the aquifer outcrop on the west side of the basin, water-level elevations in both the Simsboro and Carrizo Formations are less than 300 ft (figs. 28, 29). Hydraulic head decreases toward the northeast corner of the study area, reflecting the topographic elevation of less than 100 ft msl in the Angelina River valley.

These patterns of water-level elevation suggest that groundwater moves from the upland areas toward river bottomlands in the outcrop and also downdip to deeper parts of the aquifer. Groundwater in the Simsboro and Carrizo Formations generally is unconfined where the formations crop out and confined where the formations are overlain by the Calvert Bluff and Reklaw Formations (fig. 11). The fact that water levels are highest in the outcrop



QA41824c

Figure 28. Water-level elevation under "predevelopment" conditions in the Simsboro aquifer based on measurements made between 1936 and 1953.

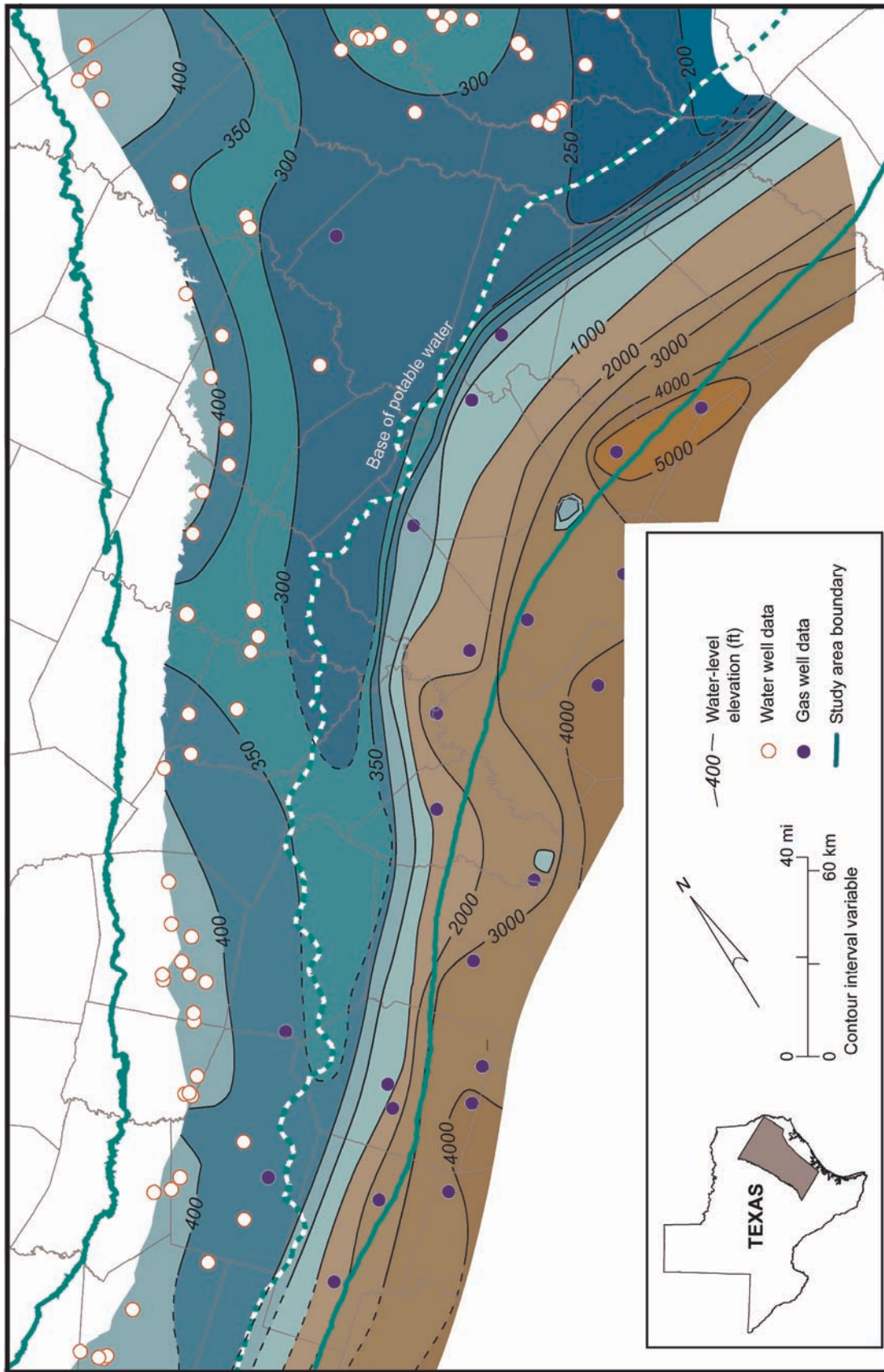


Figure 29. Water-level elevation under “predevelopment” conditions in the Carrizo aquifer based on measurements made between 1901 and 1955. QAD1825c

beneath the upland areas indicates that most recharge naturally occurs there under historical and present conditions.

Hydraulic head in the aquifer system is continuously distributed in three spatial dimensions. Figures 28 and 29 show the horizontal component of the hydraulic-head distribution and indicate the potential for lateral flow of groundwater in the Simsboro and Carrizo aquifers. The potential for vertical movement of groundwater between the units of the Carrizo–Wilcox aquifer is proportional to the vertical gradient in hydraulic head. Vertical gradients in hydraulic head between the Queen City and Carrizo–Wilcox aquifers in the East Texas Basin, including parts of Anderson, Cherokee, Freestone, Henderson, and Leon Counties in the model area, show the potential for downward leakage from the Queen City aquifer to the Carrizo–Wilcox aquifer everywhere except beneath major stream valleys (Fogg and Kreitler, 1982). The groundwater model by Dutton (1999) found that under steady-state conditions, cross-formational movement of groundwater was downward beneath upland areas and upward beneath the major stream valleys. Groundwater withdrawal from the aquifers can locally change the vertical gradient.

Fluid pressure in the deepest part of the modeled area is transitional between hydro pressured and geopressured conditions. A transition interval between hydro pressured and truly geopressured conditions is typical of Gulf of Mexico deposits. Geopressure is thought to result from a combination of (1) rapid burial of uncompacted sediments, (2) presence of low-permeability sediments and fault zones that restrict movement or release of deeply buried fluid, and (3) conversion of bound water to pore water from the temperature-controlled mineralogic phase change of smectite to illite (Bethke, 1986; Harrison and Summa, 1991). Bethke (1986) concluded that a low-permeability seal is critical for development and preservation of geopressured conditions in the Gulf of Mexico Basin;

geopressure would have bled off without bounding seals. The updip limit of the geopressured zone occurs in the thick shale section and shale-bounded growth fault zone that lies downdip of the Cretaceous shelf margin around the Gulf of Mexico Basin.

Hydraulic head calculated for formation water in equilibrium with gas pressures in Wilcox reservoirs varies from less than 400 ft to more than 5,000 ft across the study area (figs. 28, 29). A hydraulic-head minimum appears to lie near or within a zone about 10 to 12 mi downdip of the base of freshwater. The gradient in hydraulic head in the confined part of the Carrizo–Wilcox aquifer is approximately 0.001 to 0.002, directed toward the Gulf of Mexico. The gradient reverses direction and is steeper, approximately 0.02 to approximately 0.04, directed inland from the geopressured zone.

Given the decrease in hydraulic head with groundwater flow downdip from the aquifer outcrop (downdip-directed gradient) and the presence of geopressured conditions in the deep Wilcox Group, hydraulic head must reach a minimum in the Carrizo–Wilcox aquifer at some point downdip of the outcrop, beyond which the hydraulic-head gradient reverses and head increases across the geopressured zone toward the Gulf of Mexico. We show the “valley” of minimum hydraulic head, located between the aquifer and the geopressured zone, sloping or dipping to the northeast, toward the area of the Sabine River valley with the lowest topographic elevation in the study area. The presence of a hydraulic-head minimum indicates that there is appreciable vertical flow between formations. It is possible that the vertical component may be greater than the lateral component of groundwater flow in that zone.

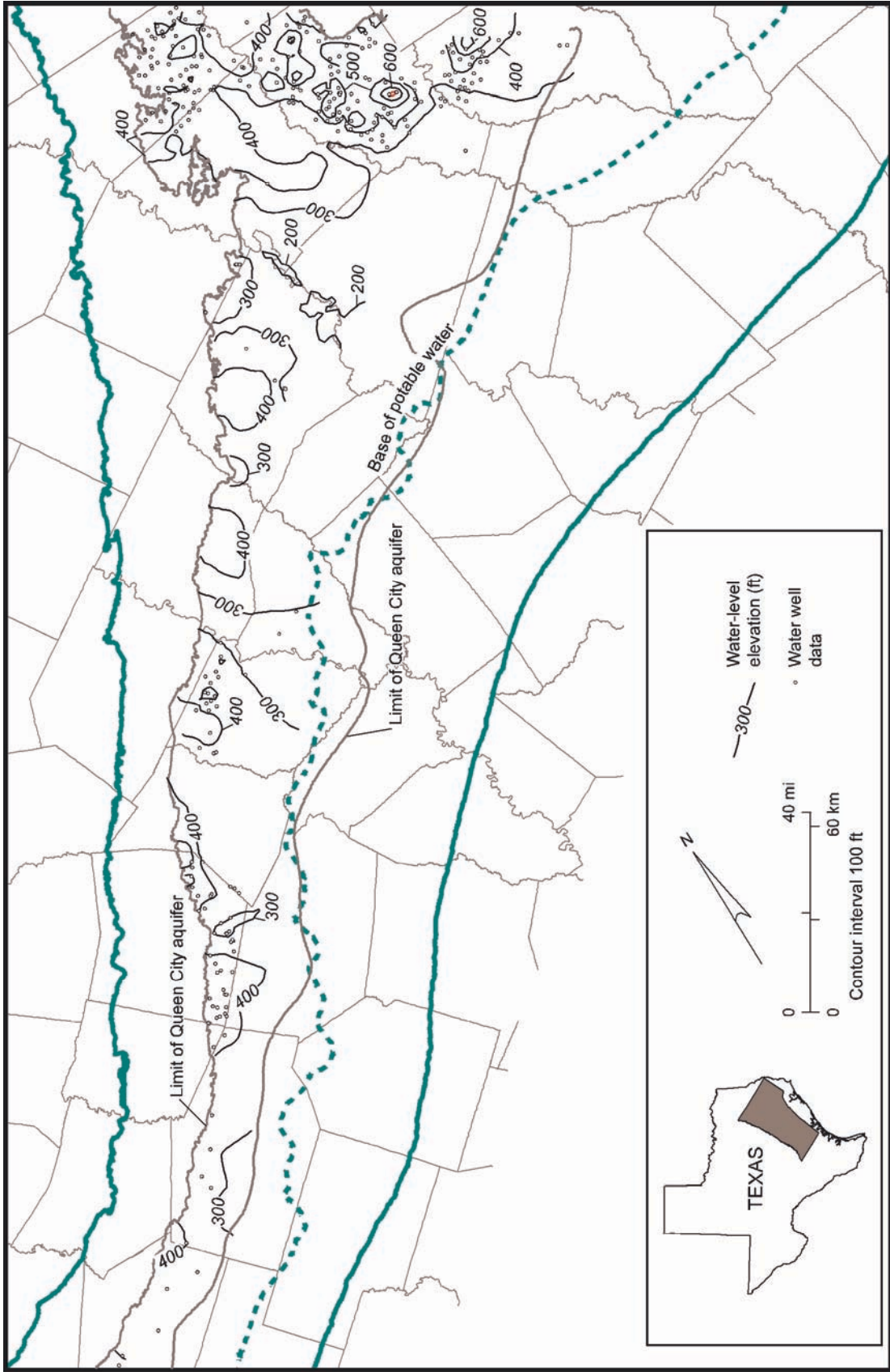
The updip-directed gradient in hydraulic head and salinity implies some fluid movement out of the geopressured zone under initial reservoir conditions. As pointed out by Bethke (1986) if there had been much fluid movement, geopressure would have bled off

through geologic time, and saline formation waters would extend much closer to the outcrop. The amount of updip and vertical movement of fluid from the geopressured zone may be limited by fluid density, formation dip, and hydraulic conductivity. Additional work needs to be done on a local scale to quantify the mass flux of water and solutes out of the geopressured zone (Harrison and Summa, 1991).

One implication of the reversal in gradient in hydraulic head is that there may have been a stagnation zone (Tóth, 1978) in the area downdip of the base of freshwater. Rate of lateral movement of groundwater within this stagnation zone may have been close to zero. Very slow rate of flow is also a consequence of the density of fluid and the dip of the formation structure.

As previously noted, significant reductions in reservoir pressure have occurred with production of gas from the Wilcox gas fields in the growth fault zone. The regional gradient in hydraulic head between the geopressured zone and the freshwater part of the Carrizo–Wilcox aquifer has undoubtedly changed. It was beyond the scope of this study to map the historic or transient change in fluid pressures in the Wilcox gas fields.

Water-level elevations in the Queen City aquifer generally lie between 200 and 400 ft in the area south of the Trinity River, lower in valleys and higher in upland areas (fig. 30). The Queen City aquifer is the first major aquifer overlying the Carrizo–Wilcox aquifer. Water levels in the Queen City aquifer in the study area are highest beneath areas of higher topography between the Trinity and Neches Rivers and between the Neches and Angelina Rivers (fig. 6).



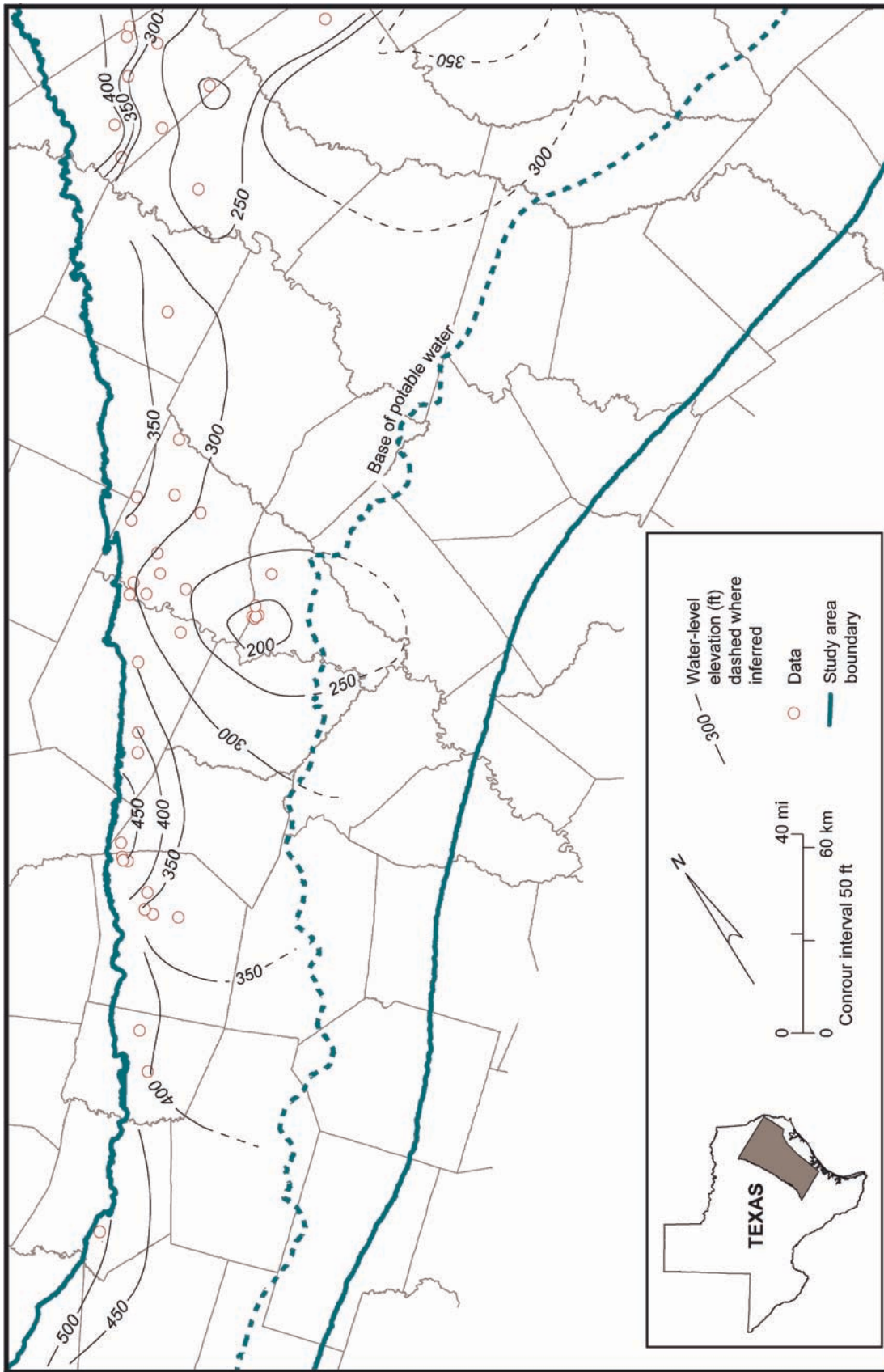
QA-02285x

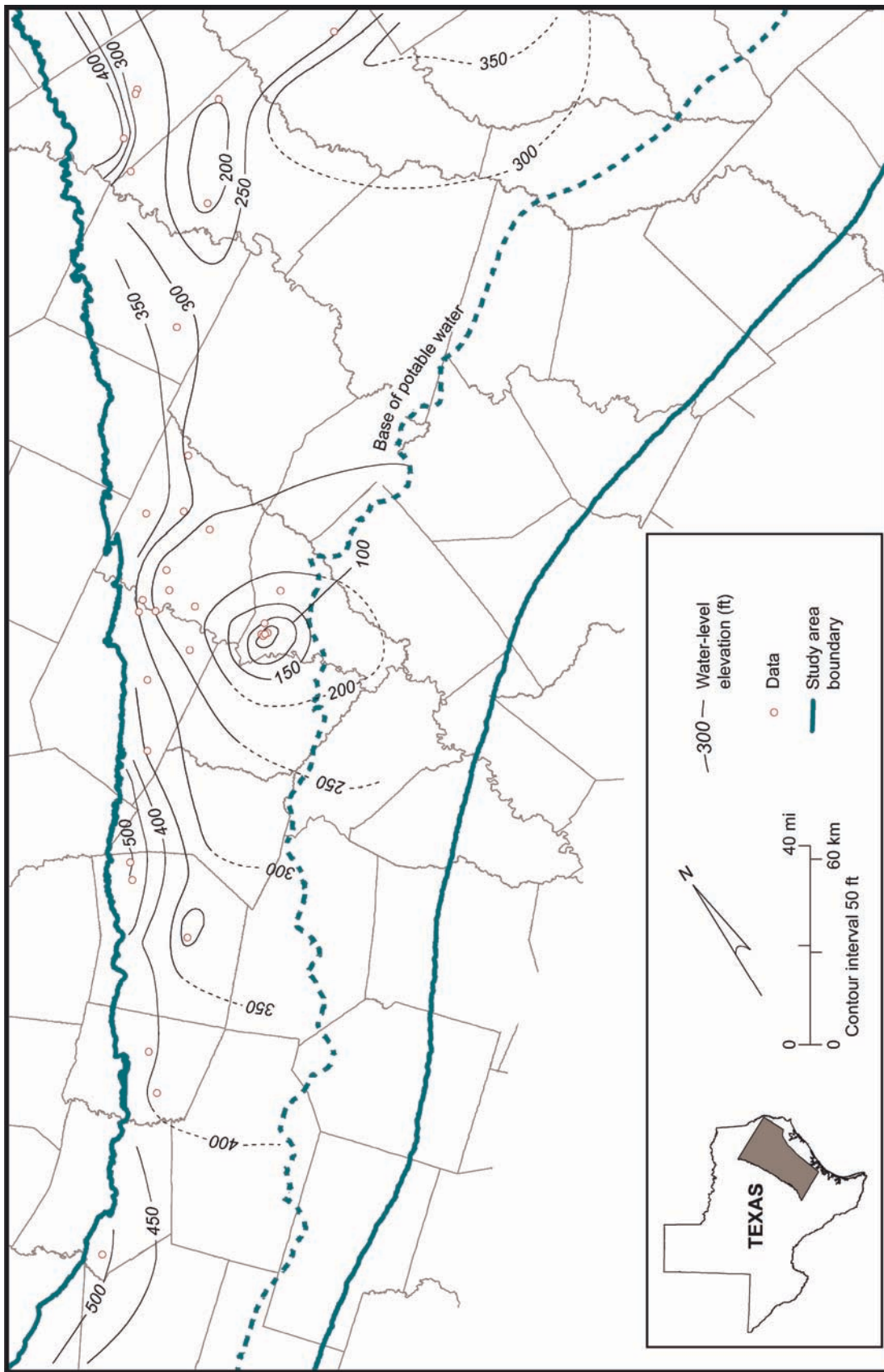
Figure 30. Water-level elevation under “predevelopment” conditions in the Queen City aquifer.

4.4.3 Postdevelopment Changes in Hydraulic Head

Groundwater has been produced from the Carrizo–Wilcox aquifer for more than 50 yr. The Bryan-College Station well field, for example, was developed in the 1950s. At the center of the Bryan-College Station well fields water-level elevations in the Simsboro aquifer that were initially about 350 to 355 ft above mean sea level (msl) had decreased to about 160 to 165 ft msl by 1990 (fig. 31) and to about 10 to 20 ft msl by 2000 (fig. 32). At the center of the Lufkin-Angelina County well field in the Carrizo aquifer, hydraulic head had decreased from a predevelopment level of about 270 ft msl to more than 260 ft below sea level by 1990 (fig. 33) and to more than 300 ft below sea level by 2000 (fig. 34). The maps of hydraulic head in 1990 and 2000 (figs. 31 through 34) show the continued effect of recharge from the Sabine Uplift area, with water-level measurements of more than 300 ft msl. The maps also show a drop in water level in northern Cherokee and southern Smith Counties and parts of adjacent counties that are a result of pumping beyond the northern boundary of the study area.

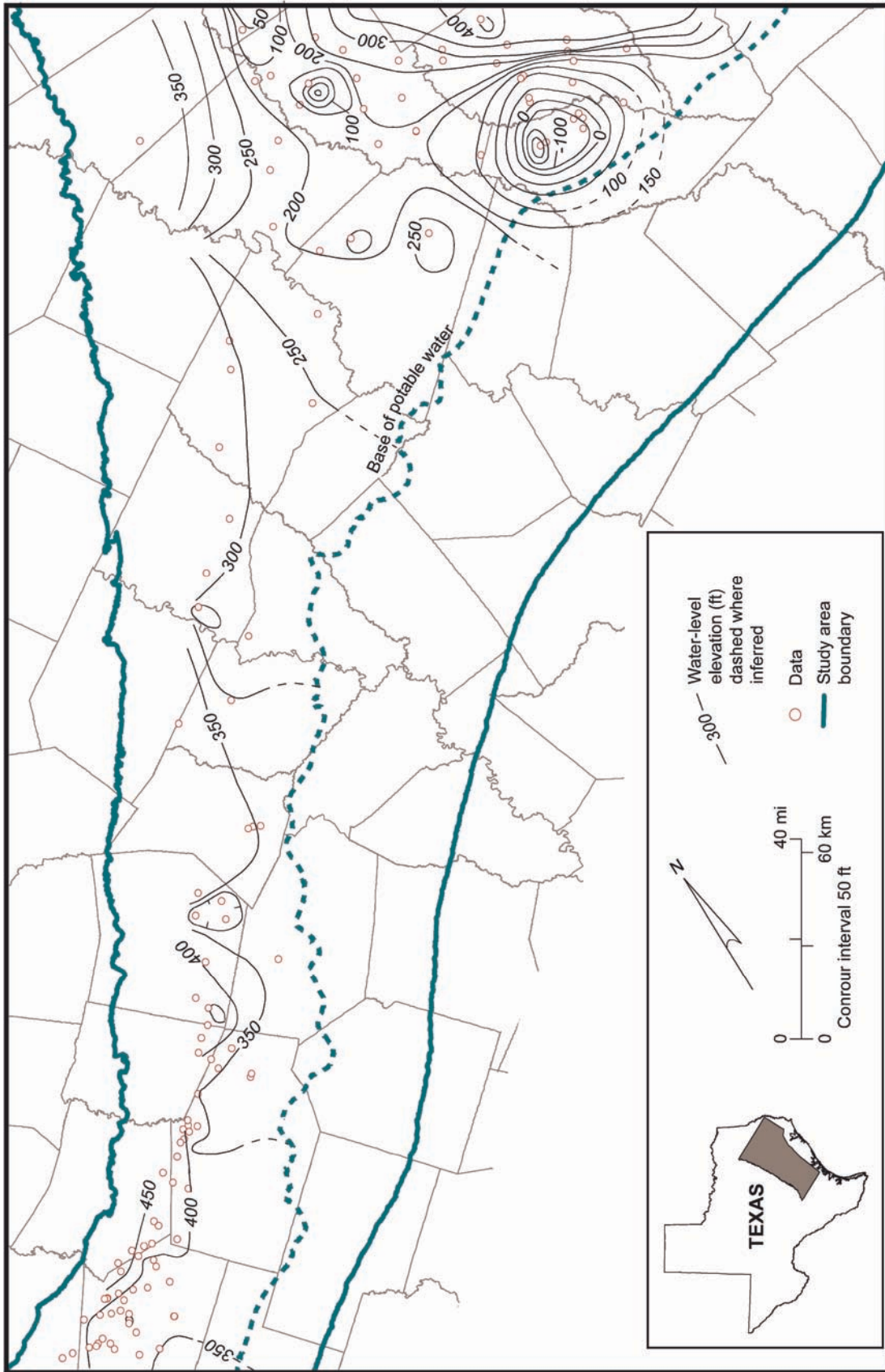
Decline in water level in the confined part of the aquifer downdip of the outcrop results from a decrease in artesian pressure in the aquifer. The top of the aquifers (figs. 18 through 21) lies far beneath the levels to which water rises in the artesian wells of the Carrizo–Wilcox aquifer. When groundwater is pumped from the aquifer, much if not most of the loss of hydraulic head comes from small changes in pressure applied to grains of sand and clay and other sediment, as well as the binding cement that make up the matrix of the aquifer.





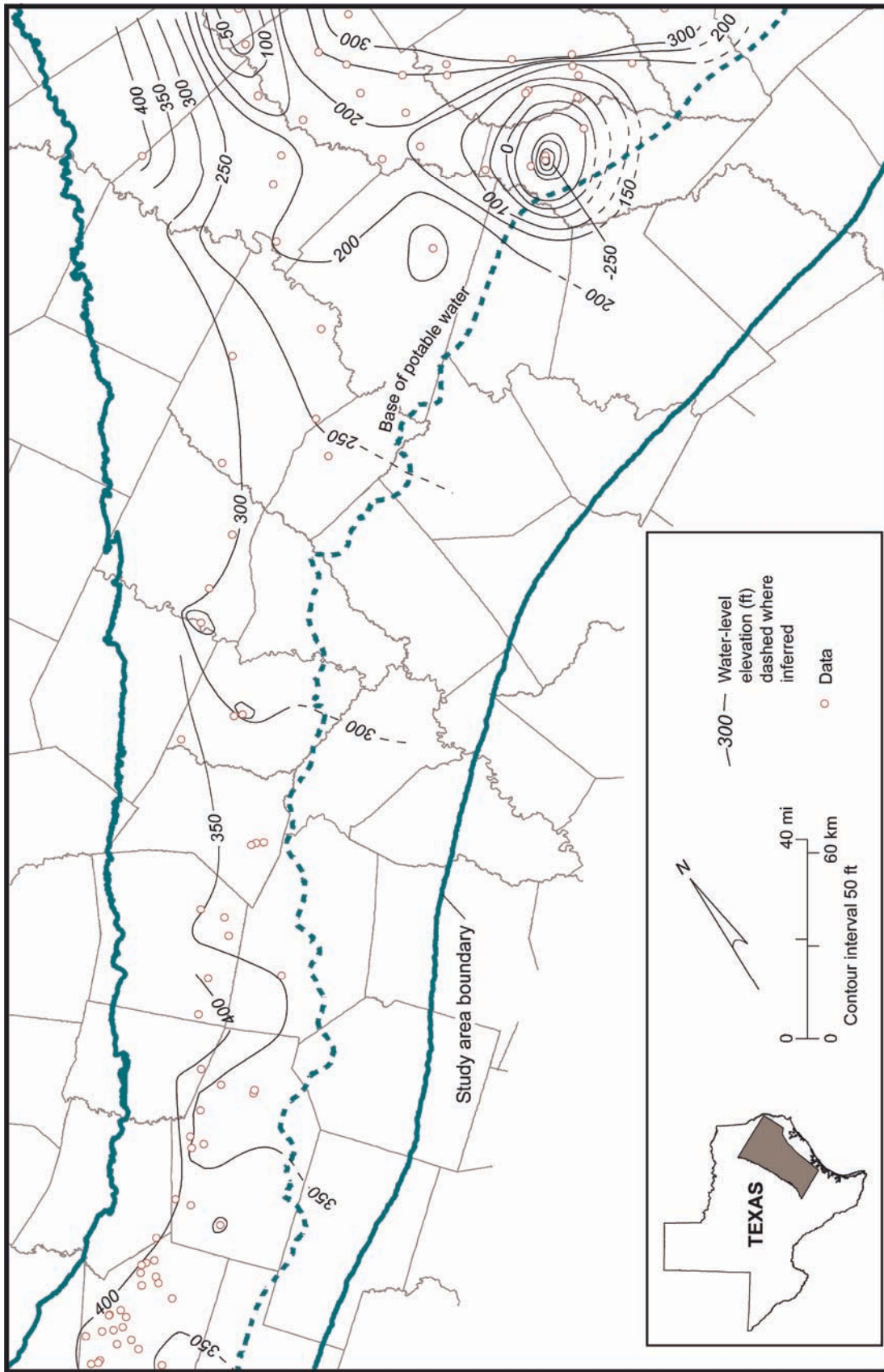
QAd1828c

Figure 32. Water-level elevation in the Simsboro aquifer measured during 1995 through 2000 and used for the 2000 model-year calibration.



QA41827c

Figure 33. Water-level elevation in the Carrizo aquifer measured during 1987 through 1990 and used for the 1990 model-year calibration.

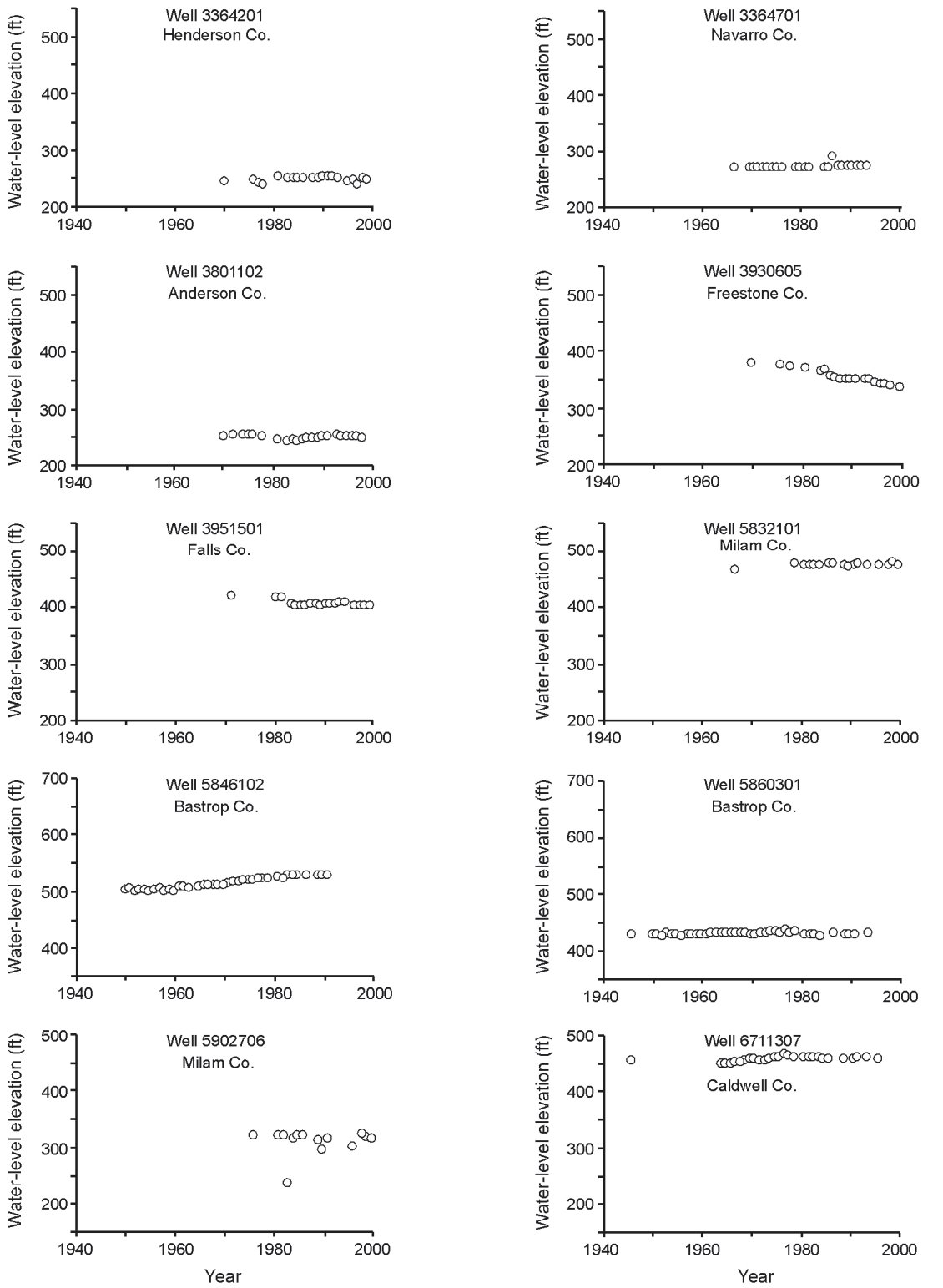


QA41829c

Figure 34. Water-level elevation in the Carrizo aquifer measured during 1995 through 2000 and used for the 2000 model-year calibration.

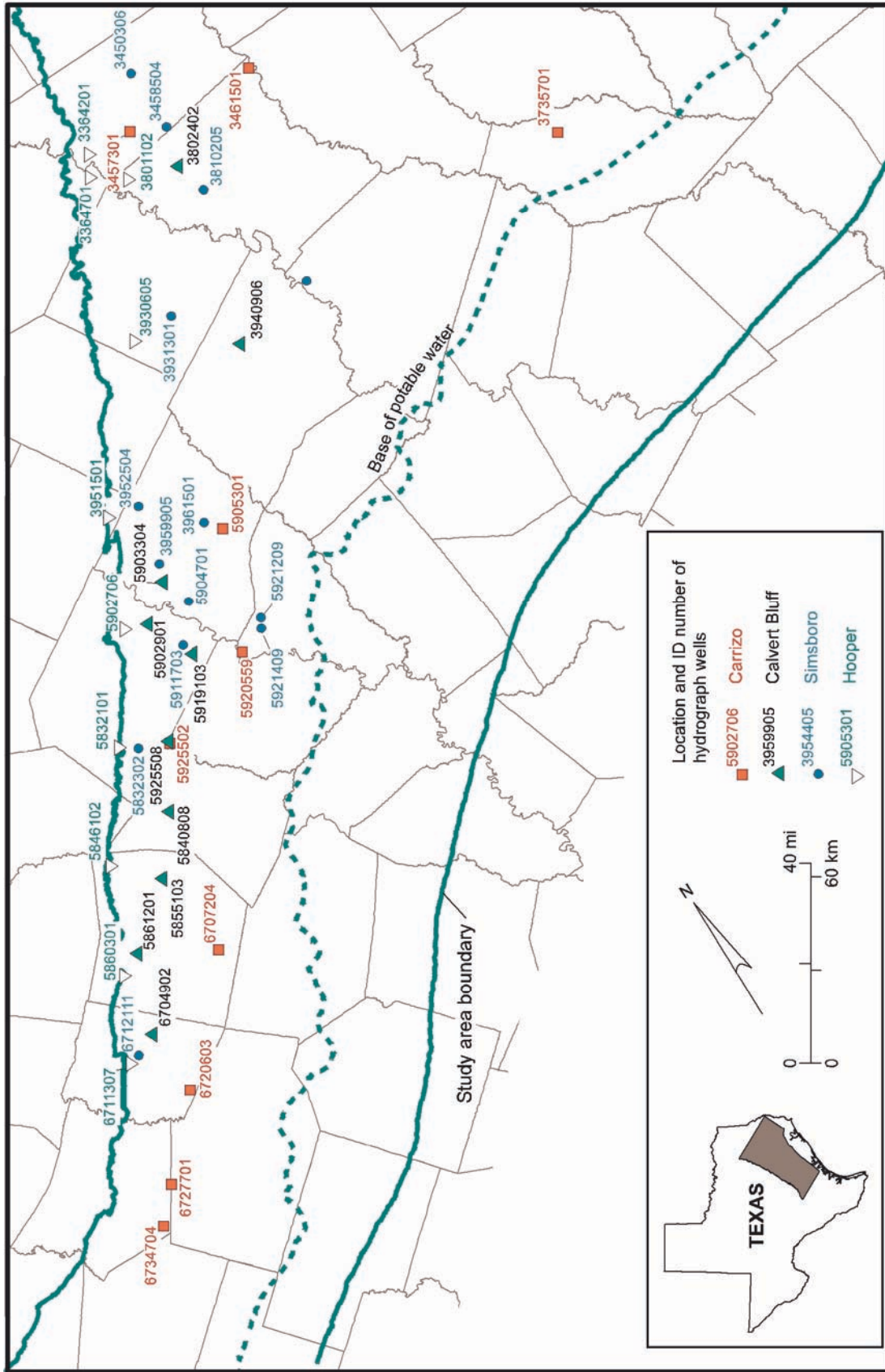
Most hydrographs of water level in the Hooper Formation show only slight variations over the past 20 to 30 yr (fig. 35) because there has not been much pumping from that part of the Carrizo–Wilcox aquifer. A well in Bastrop County shows a slight water-level rise and a well in Freestone County shows a slight water-level fall. Most of the wells in which water-level measurements in the Hooper Formation are available are close to its outcrop (fig. 36). Hydrographs for the Simsboro aquifer show more fluctuation and generally a decline in water levels (fig. 37). These patterns reflect greater rates of pumping from the Simsboro Formation than from the Hooper Formation. Hydrographs of Calvert Bluff water levels show a range of characteristics: steady levels, gentle declines, and fluctuations (fig. 38). Water levels in Angelina County, at the northern edge of the study area, have shown some of the greatest changes (fig. 39). In general, however, outside of the areas of large withdrawals of groundwater, water-level change in most of the Carrizo–Wilcox aquifer has been slight and gradual.

We also looked at hydrographs of water levels in the Queen City aquifer to evaluate whether water-level fluctuations needed to be taken into account in setting the model's upper boundary. In general, water levels in the Queen City aquifer have remained steady throughout the past several decades. Of 126 well records examined, only 6 cases were seen in which water-level decline was significant, as much as 105 ft. Wells showing appreciable decline include 3469901 (Smith County), 3727103 (Nacogdoches County), 3841701 (Leon County), 3956301 (Leon County), 3955302 (Leon County), and 6708604 (Fayette County). Water-level records from other nearby wells do not show much decline, indicating that these reported changes are local and not regional.



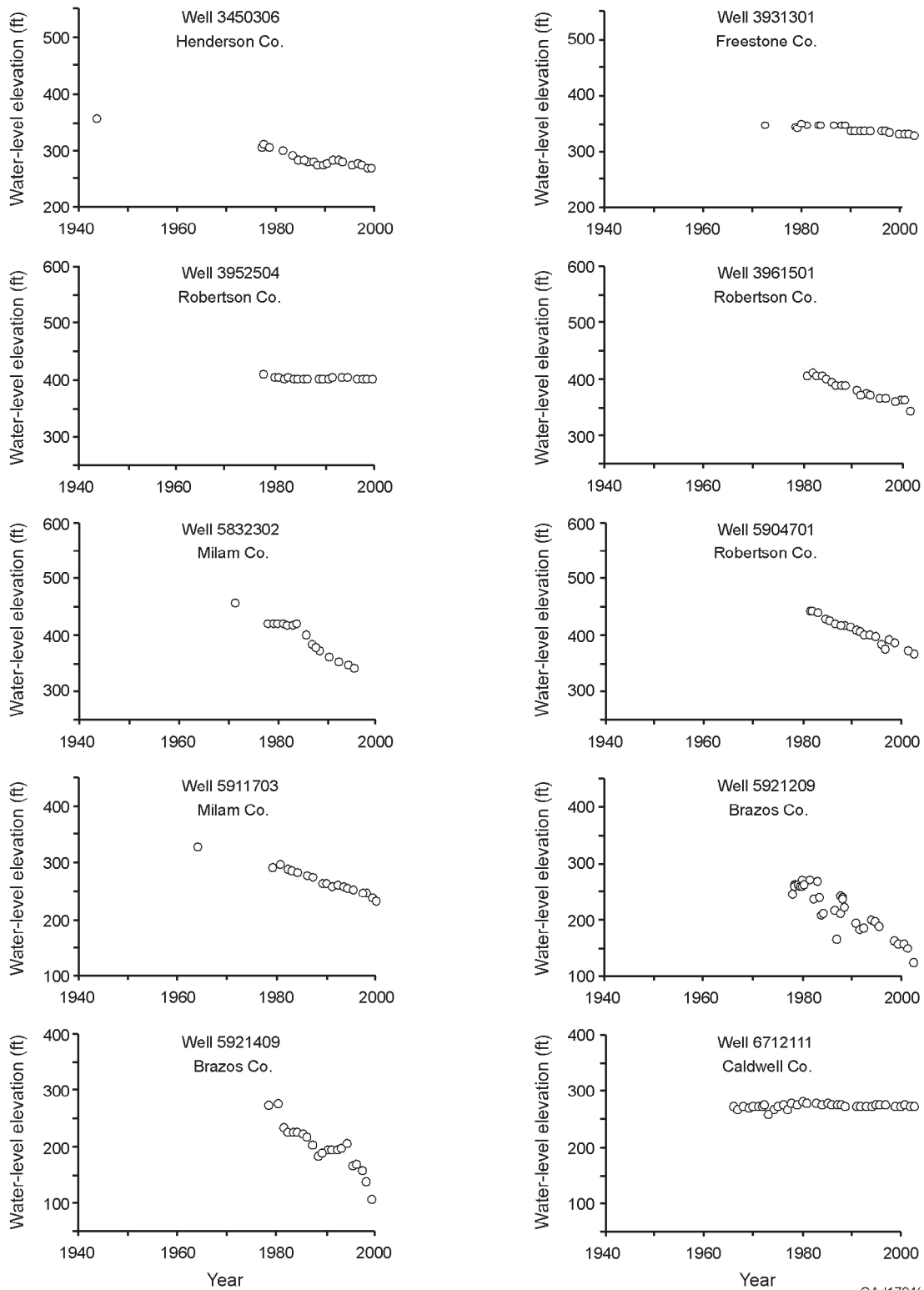
QAd1794(d)c

Figure 35. Hydrographs for 10 representative wells in the Hooper Formation (layer 6). Locations of wells shown in figure 36.



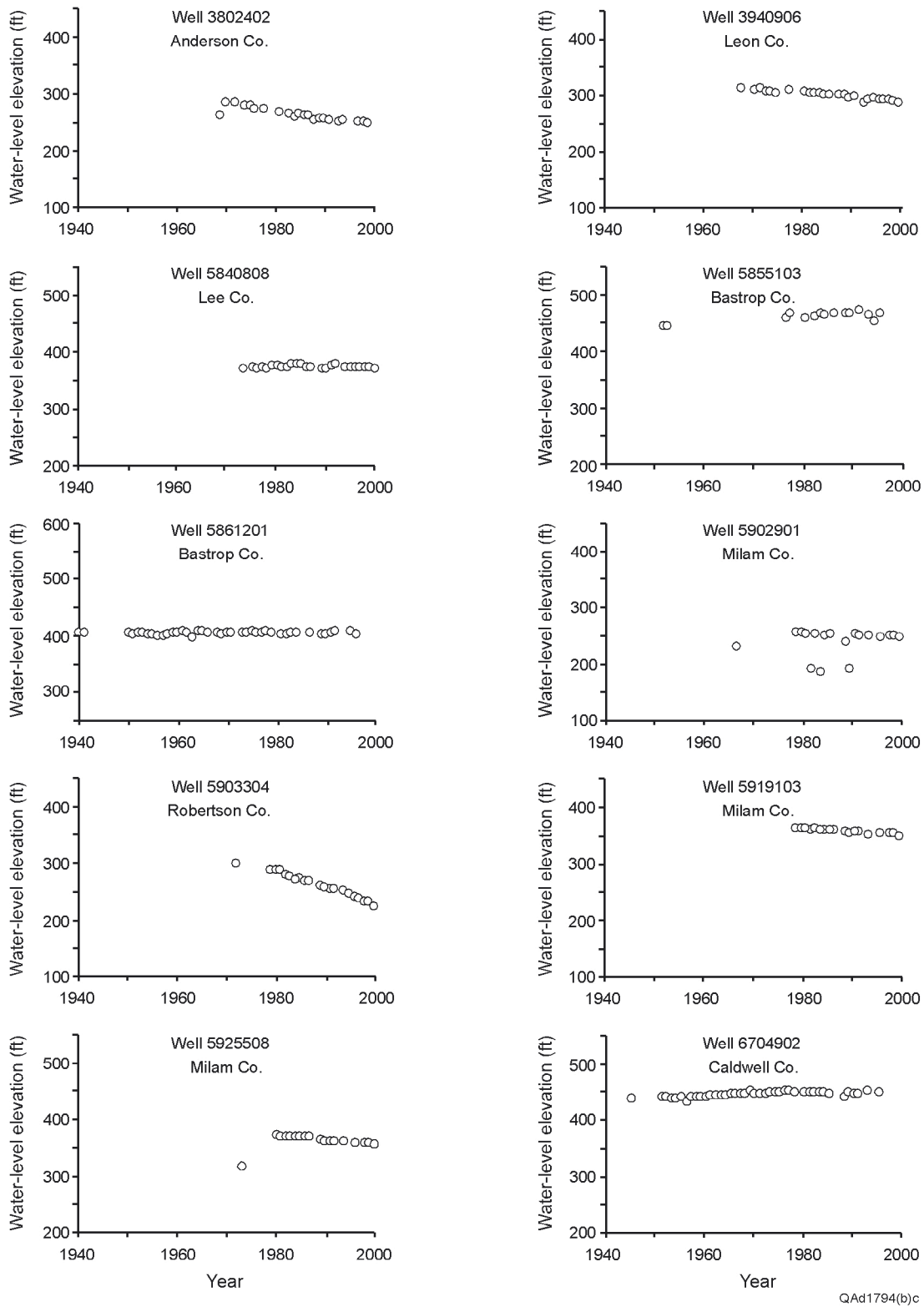
QA1822(a)c

Figure 36. Locations of water wells for which hydrographs are presented.



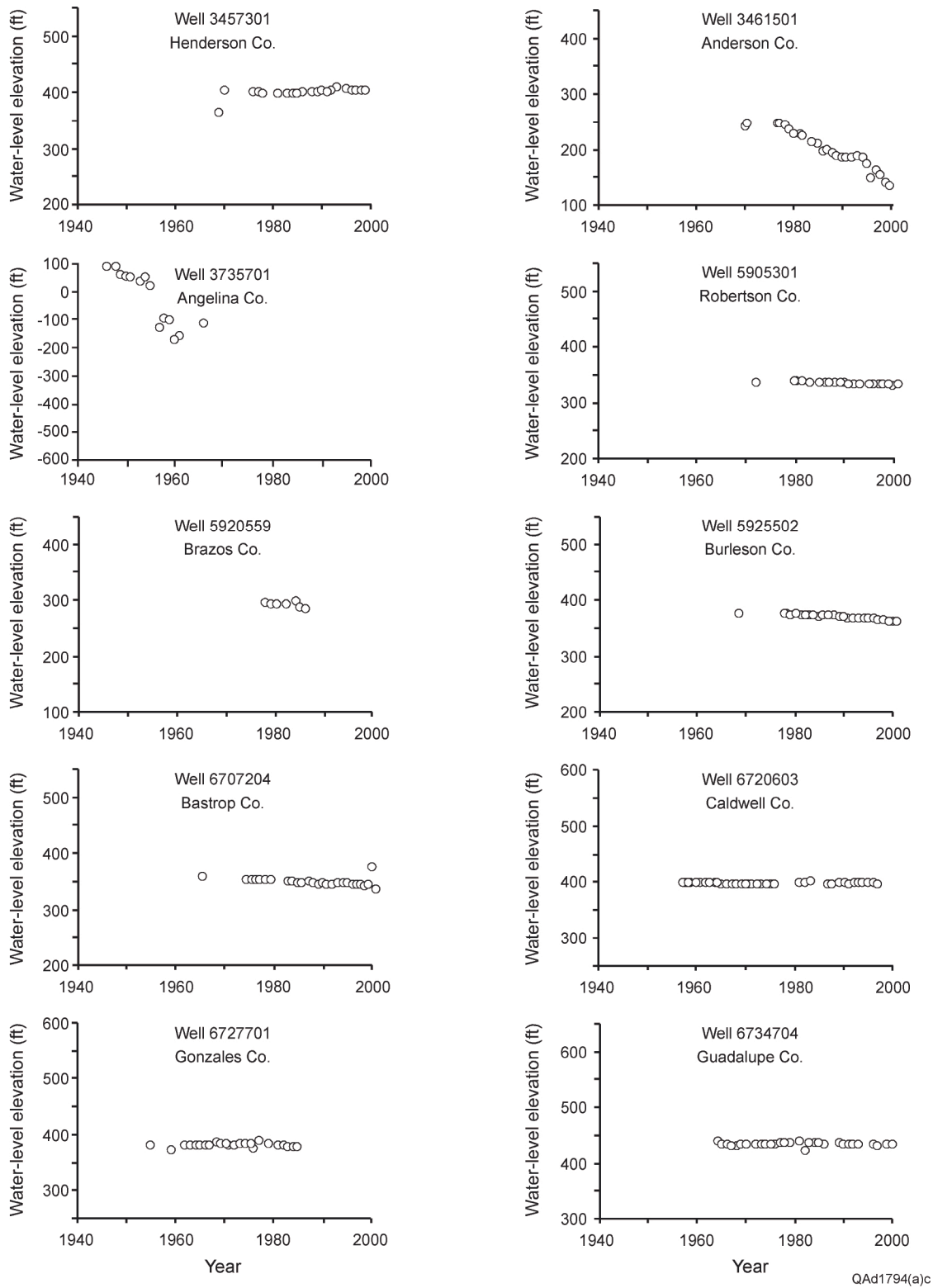
QAAd1794(c)c

Figure 37. Hydrographs for 10 representative wells in the Simsboro Formation. Locations of wells shown in figure 36.



QAd1794(b)c

Figure 38. Hydrographs for 10 representative wells in the Calvert Bluff Formation. Locations of wells shown in figure 36.



QAd1794(a)c

Figure 39. Hydrographs for 10 representative wells in the Carrizo Formation. Locations of wells shown in figure 36.

4.5 Recharge

Recharge occurs when water moving downward from the ground surface reaches the water table of the aquifer. Recharge to the Carrizo–Wilcox aquifer in this study area occurs mostly from deep drainage of water through the soil and unsaturated zone. To the southwest in the Carrizo aquifer, significant recharge occurs as loss of surface water flow from streams crossing the aquifer outcrop (Intera and Parsons Engineering Science, 2002b). In this report, we do not include cross-formational movement of groundwater as recharge.

Recharge rates have been estimated in several previous studies of the Carrizo–Wilcox aquifer, most of which were modeling studies (Scanlon and others, 2002). Few direct or field measurements have been made previously. Estimates of recharge rate range from 0.1 to more than 5 inches/yr (fig. 40). Thorkildsen and Price (1991) estimated an average rate of 1 inch/yr for the Carrizo–Wilcox outcrop on the basis of model calibration. Dutton (1999) calculated an area-weighted recharge rate close to 1 inch/yr, with higher rates in the Simsboro and Carrizo aquifers and much lower rates in the Hooper and Calvert Bluff aquitards. Dutton (1999) followed Ryder (1988) and Ryder and Ardis (1991) in assuming that recharge in upland areas of the Simsboro and Carrizo aquifers is 2 to 4 inches/yr.

In general, only a small amount of annual rainfall reaches the water table because most rainfall runs off, is evaporated from soils or surface-water bodies, or is transpired by plants. Plant transpiration and soil-water evaporation are collectively referred to as evapotranspiration (ET). Dutton (1990) estimated that about 10 percent of precipitation may end up as recharge. With smaller recharge rates, the percent of precipitation that is recharged to groundwater in the Hooper or Calvert Bluff aquitard is smaller.

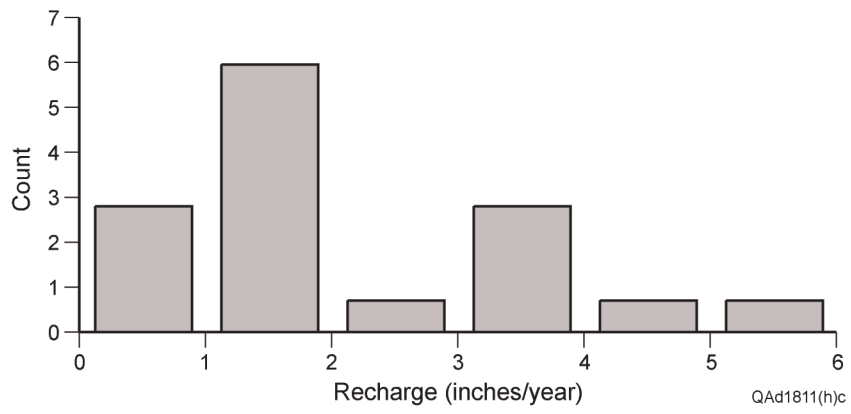


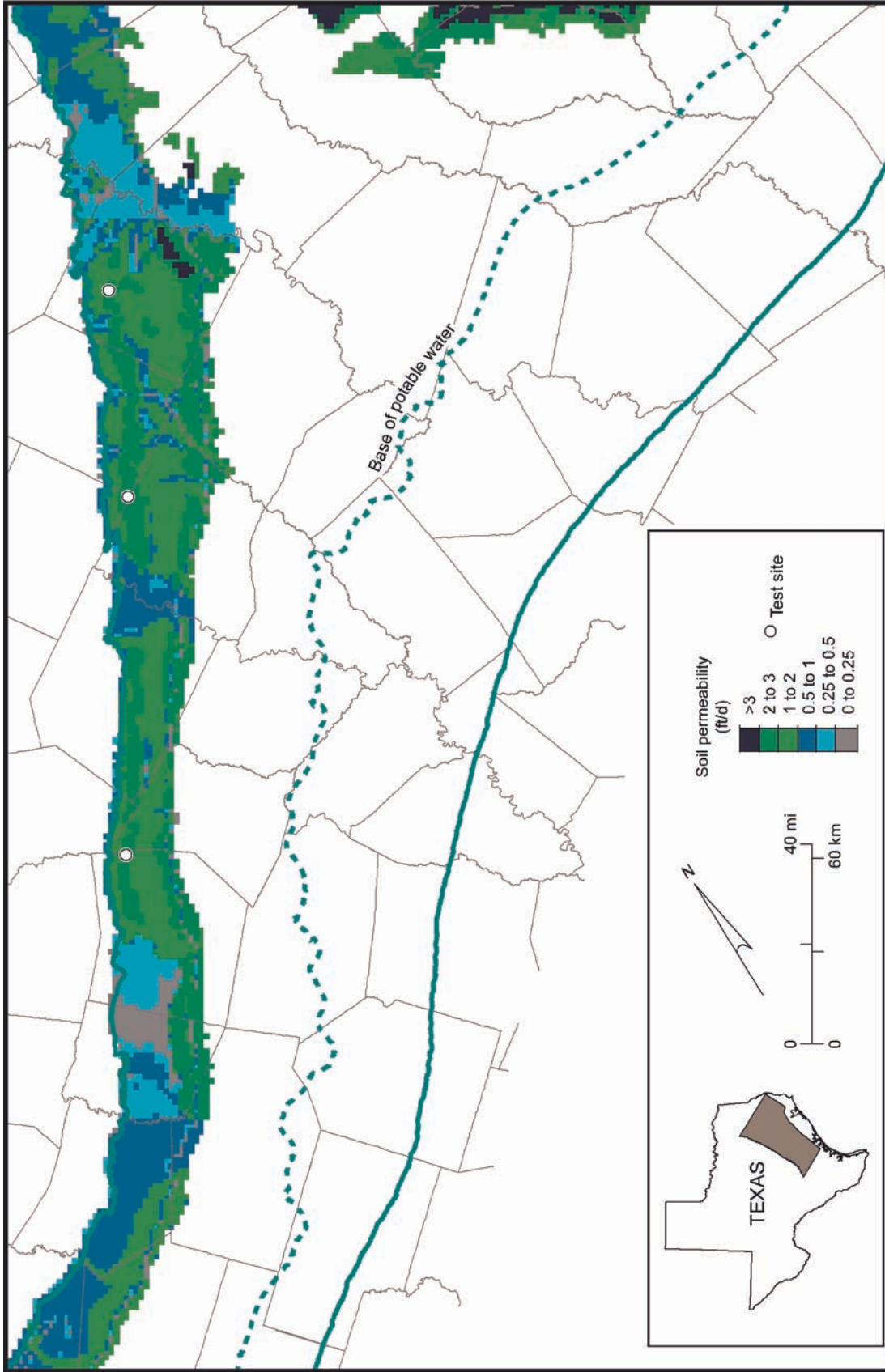
Figure 40. Recharge rates estimated in previous hydrologic studies of the Carrizo–Wilcox aquifer. Data from Scanlon and others (2002).

Rejected recharge is the concept that much of the water that reaches the water table as recharge in the unconfined part of the aquifer does not travel downdip into the confined part of the aquifer. Rejected recharge leaves the unconfined part of the aquifer by discharge to seeps and springs in valleys, discharge to rivers and streams, and evapotranspiration in river bottomland areas. Rejected recharge generally does not include withdrawal of groundwater by wells in the unconfined aquifer. The water that cycles through the unconfined aquifer, therefore, is not available for withdrawal by wells in the confined part of the aquifer.

Captured recharge is the concept that drawdown of water levels in the confined part of the aquifer increases the gradient in hydraulic head and draws more groundwater from the unconfined to confined parts of the aquifer. In addition, drawdown of water levels in the unconfined aquifer, owing to pumping of wells in either the unconfined or confined parts of the aquifer, results in a decrease in the discharge of groundwater to rivers and streams and may reduce actual evapotranspiration. Groundwater that is “captured” by the confined aquifer reflects a change in the water budget of the aquifer.

As mentioned previously, seasonal trends in precipitation and evapotranspiration vary across the study area (figs. 7, 9). Precipitation during October through May is less subject to ET and can move deeper into the soil profile (Dutton, 1982; Dutton, 1990). Recharge, therefore, might be greater during the period between October and May than at other times of the year.

Previous studies indicate that there is more recharge through the predominantly sandy Simsboro and Carrizo Formations than through the clay-rich Hooper, Calvert Bluff, and Reklaw Formations. Hydrologic properties of the soils developed on these formations reflect the predominant grain texture of the underlying formations. Figure 41 shows the spatial variation in vertical permeability of soil as mapped from the TNRIS State Soil Geographic



QA42286x

Figure 41. Map of soil permeability in the recharge area of the model. Permeability calibrated as vertical harmonic mean using thickness and permeabilities of soil layers. Test sites for using environmental tracers for estimating recharge rate were located in the outcrop of the Simsboro aquifer in Bastrop, Lee, Robertson, and Freestone Counties.

Database (STATSGO) data. Most soils are described with A, B, and C soil horizons. The STATSGO data include information on thickness and permeability of the three horizons. We calculated the harmonic mean of permeability, in which permeability is limited by thick horizons of low permeability. This approach takes into account the presence of clay-rich B horizons that commonly form so-called “hardpans” in the soils of the Wilcox Group and Carrizo Formation (Dutton, 1990). Figure 41 shows that soil permeability is typically more than 2 ft/d in the outcrop of the Simsboro and Carrizo Formations and about 1 ft/d in the outcrop of the Hooper and Calvert Bluff Formations. Soil permeability is also more than 2 ft/d in the outcrop of much of the Reklaw Formation. South of the Colorado River and north of the Trinity River, soil permeability is fairly uniform throughout the Wilcox Group. As previously mentioned, the major sands that define the Simsboro Formation are mainly between the Colorado and Trinity Rivers.

Recharge rates vary during seasonal, annual, and longer time periods and differ across the outcrop according to vegetation, slope, soils, and other factors. However, the movement of water downward from soil through the thick (>30-ft) unsaturated zone above the Simsboro and Carrizo aquifers is controlled more by the hydrological properties of the unsaturated zone than the annual precipitation rate. Fluctuation in recharge rate at the water table is much less than fluctuation in annual precipitation. In addition, fluctuation in recharge rate lags fluctuation in precipitation rate owing to time of travel through the unsaturated zone. Fluctuation in annual rate of precipitation results mainly in changes in amount of water stored in the unsaturated zone. In this report we refer to typical or representative rates of recharge. As the preceding discussion shows, however, a single number does not adequately describe differences in recharge rates across the study area. Additional work is needed to document the average and variability of recharge rates.

4.5.1 Field Methods

Field measurements were made to (1) assess results of previous model-based estimates of recharge rate for use in this model; (2) evaluate whether recharge rates assigned in the model should be less than 1 inch/yr, 1 to 4 inches/yr, or more than 4 inches/yr; and (3) begin developing improved techniques for quantifying recharge rate using field data. Details of the field tests and results are given in appendix A. Data were collected at seven locations across three test areas: Bastrop and Lee Counties, Robertson County, and Freestone County (fig. 41). The approach was to analyze “environmental tracers” extracted from soil core. The environmental tracers included chloride in soil water and tritium (^3H) and tritium/helium in groundwater. Cores were collected using a hollow-stem auger on a CME Mobile 75 drilling rig. Cores were taken continuously with depth until auger refusal or until the water table was encountered. No drilling fluid was used to avoid contamination of samples.

Sediment samples were collected for laboratory measurement of water content and chloride concentrations. Chloride extracted from soil cores was analyzed by ion chromatography (detection limit 0.1 mg/L) at the New Mexico Bureau of Mines. Gravimetric water content was measured in the laboratory at the Bureau of Economic Geology by oven drying samples at 105°C for 24 to 72 hr. Groundwater samples were collected from all seven test holes for tritium analysis and from three wells for tritium/helium analysis. Tritium samples were analyzed at the University of Miami Tritium Laboratory. Helium concentrations and helium isotope ratios ($^3\text{He}/^4\text{He}$) in the samples were measured at the University of Utah.

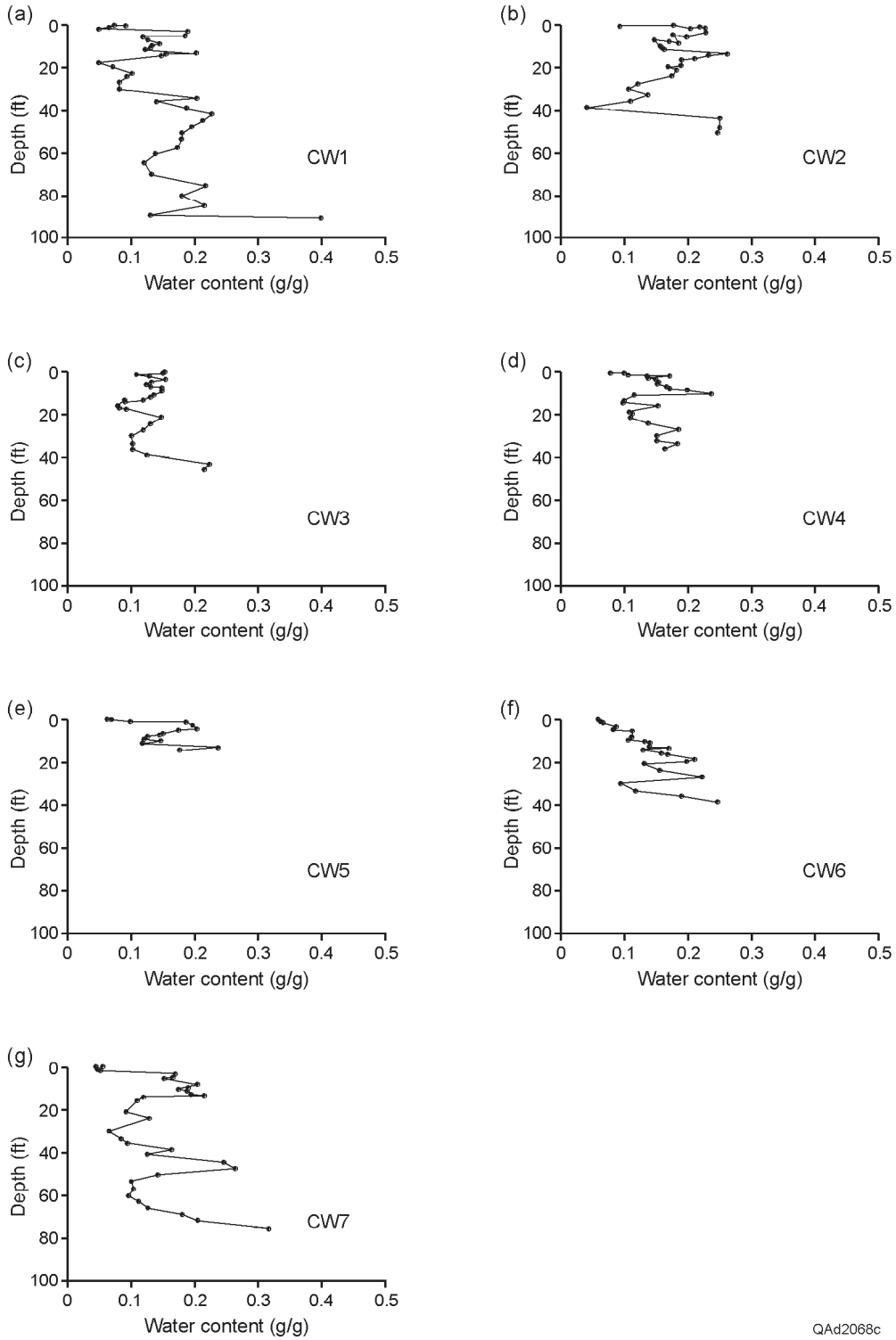
4.5.2 Field Results

Average water content in each soil profile was not highly variable and ranged from 0.13 to 0.18 g/g (fig. 42, table 1). Minimum water content ranged from 4 to 8 percent by weight. Maximum water content ranged from 22 to 40 percent by weight, indicating that some soil samples were close to water saturation. Spatial variability in water content could be qualitatively related to soil texture. Water content was highest near the water table in most profiles. Average chloride concentration in the unsaturated zone ranged from 23 to 519 mg/L (fig. 43, table 1). Chloride concentration was highly variable at each location; there was no systematic variation in chloride concentration with depth.

Recharge rates (R) were calculated from the ratio between chloride concentration in rainfall and in the soil samples using equation 2:

$$R = Cl_p/Cl_s \times P \quad (2)$$

where Cl_p and Cl_s are concentrations of chloride in precipitation and soil water, respectively, and P is precipitation rate. Recharge rates were calculated for that part of soil profiles that generally represents the last 50 yr. In some cases recharge rates appear to show that a 50-yr transit time corresponds to a very narrow depth interval. Recharge rates estimated from the soil-chloride data ranged from 0.2 to 1.4 inches/yr. The time required for chloride to accumulate in the various soil profiles ranged from approximately 100 to 2,800 yr. Primary assumptions of the chloride mass balance approach are that water movement is downward and that there are no subsurface sources or sinks of chloride. The first assumption is valid because in broad areas between surface-water bodies, the main direction of water movement

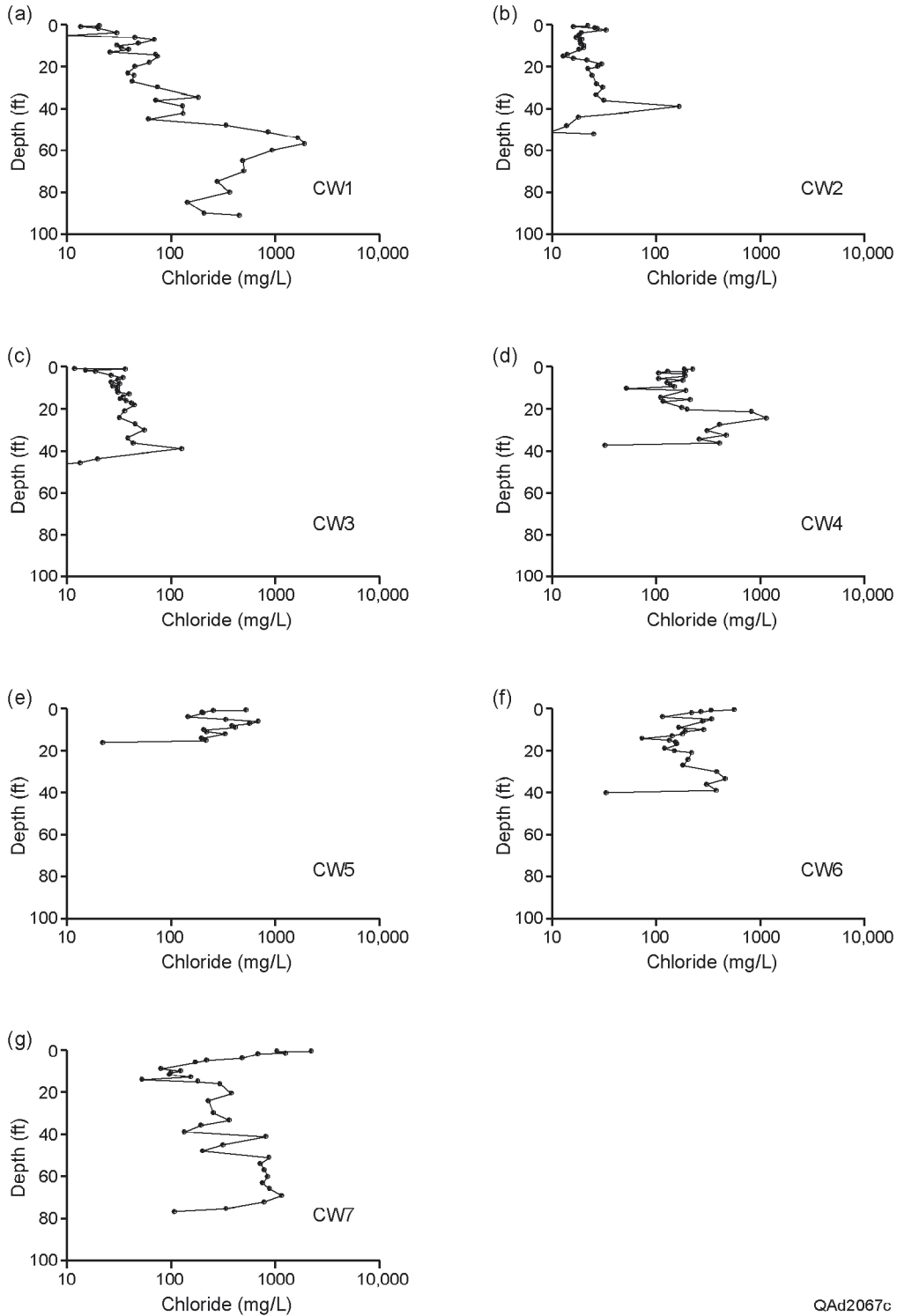


QAd2068c

Figure 42. Variation with depth in water content in soil cores. CW1 and CW2 from Bastrop and Lee Counties, respectively, CW6 and CW7 from Robertson County, and CW3 to CW5 from Freestone County (figure 41).

Table 1. Water content, chloride concentration, and estimated recharge based on unsaturated zone (uz) chloride concentrations, chloride concentrations in groundwater (gw) and associated recharge rates, and age of the chloride profile.

Borehole no.	Water content uz (g/g)			Chloride uz (mg/L)			Recharge rate (uz) (in/yr)	Cl (gw) (mg/L)	Recharge rate (gw) (inches/yr)	Age (yr)
	Mean	Min.	Max.	Mean	Min.	Max.				
CW-1	0.21	0.08	0.34	245	10	1907	0.79	180	0.20	2815
CW-2	0.18	0.04	0.26	23	11	37	1.42	25	1.34	110
CW-3	0.13	0.08	0.22	35	12	125	1.02	5	6.22	112
CW-4	0.14	0.08	0.24	259	51	1131	0.24	32	1.06	846
CW-5	0.15	0.06	0.24	325	145	684	0.20	22	1.54	360
CW-6	0.13	0.06	0.25	239	72	560	0.20	33	1.02	700
CW-7	0.14	0.05	0.32	518	52	2206	0.20	107	0.31	2480



QAAd2067c

Figure 43. Variation with depth in soil-water chloride in soil cores. CW1 and CW2 from Bastrop and Lee Counties, respectively, CW6 and CW7 from Robertson County, and CW3 to CW5 from Freestone County (figure 41).

is vertical and the direction in the hydrogeologic setting of the study area, the direction of net flow of water in the unsaturated zone, is downward. The second assumption is also reasonable for these tests in the Simsboro Formation outcrop (Dutton, 1985, 1990).

Chloride concentration was generally lower (5 to 180 mg/L) in groundwater than in the unsaturated zone (table 1, appendix A). Recharge rates calculated using equation 2 for groundwater chloride ranged from 0.2 to 6.2 inches/yr, generally higher than those based on unsaturated-zone chloride (CW3-CW6). Recharge rates from the two data sets were similar for samples from CW2 and CW7. Low recharge rates calculated for CW1 may be unrepresentative of recharge in this area because groundwater was confined (under slight artesian pressure) in this borehole. The low recharge rate for CW7 may reflect additional chloride from old pore fluids (Dutton, 1985) because clay content was high in this borehole. The higher recharge rate at CW3 may represent focused recharge because surface water was ponded nearby. Preferential flow may result in low chloride concentrations in the groundwater, reflecting higher rates of recharge. Representative recharge rates based on groundwater chloride concentrations range from 1 to 1.5 inches/yr.

Groundwater tritium concentrations ranged from 0.76 to 3.57 TU (table 2) Tritium levels were greater than the detection limit (~ 0.2 TU) and indicate that a component of water was recharged during the last 50 yr. The age of groundwater was calculated using analyses of tritium/helium from boreholes CW3 and CW4; analytical results for the CW6 sample were invalid. Residence time of the water was calculated to be 2.2 for the CW3 samples and 34.5 yr for the CW4 sample. The ages represent the time of ^3He accumulation since it was isolated from the unsaturated zone. Water velocities were calculated by dividing the depth of the sample beneath the water table by the estimated groundwater age, yielding velocities of 0.4 (CW4) to 4 ft/yr (CW3). Recharge rates were calculated by multiplying velocities by

Table 2. Results of ^3He , ^4He , ^{20}Ne , ^{40}Ar , and N_2 measurements, and calculated tritiogenic helium-3 ($^3\text{He}^*$) and $^3\text{H}/^3\text{He}$ ages.

BH no.	^3H (TU)	^3H error (2σ TU)	R/Ra [†]	^4He cc STP/g [‡]	^{20}Ne cc STP/g	^{40}Ar cc STP/g	N_2 cc STP/g	$^3\text{He}^*$ TU	Age (yr)
CW-1	0.76	0.18							
CW-2	3.25	0.22							
CW-3	3.3	0.22	1.072	4.41E-08	1.99E-07	4.72E-04	0.0150	0.4	2.2
CW-4	3.57	0.24	1.072	9.35E-08	2.97E-07	7.04E-04	0.0251	21.4	34.5
CW-5	2.43	0.2							
CW-6	3.05	0.2	0.986	5.80E-08	2.59E-07	5.66E-04	0.0184	-7.1	
CW-7	1.1	0.18							

[†] R is the $^3\text{H}/^4\text{He}$ ratio of the sample; Ra is the $^3\text{H}/^4\text{He}$ ratio of the air standard

[‡] STP Standard temperature and pressure

^3H error reported as two standard deviations (2σ)

average porosity (assumed to be 35 percent). A recharge rate of 1.6 inches/yr estimated for CW4 is similar to that from the groundwater chloride concentration (32 mg/L). A recharge rate of 16.7 inches/yr was estimated for CW3 samples, and was much higher than the rate estimated from groundwater chloride concentration. Rates in excess of 4 inches/yr probably reflect a component of recharge that is locally focused from surface ponds.

Preliminary field results indicate that the sampled parts of the Simsboro Formation have similar recharge rates in that there was more variability within sample areas than between areas. Judging by these results, average recharge rate in this part of the Simsboro appears to range from about 1 to 4 inches/yr. These data are consistent with previous model estimates (fig. 40). Groundwater chloride concentration seems to provide a reliable basis for recharge estimation in this study area. Unsaturated-zone chloride concentration generally gave lower estimates of recharge rate than did groundwater chloride. Further study is needed to evaluate the application of these environmental-tracer techniques for the estimation of recharge rate in the study area.

4.6 Interaction of Surface Water and Groundwater

A large amount of the recharge that occurs in the upland outcrop of the Carrizo–Wilcox aquifer moves along short flow paths within the outcrop toward discharge areas beneath the topographically low lying areas in river bottomlands. Some flow paths are very short and issue in springs that form the headwaters of local streams. Most natural groundwater discharge may be to springs and seeps and to evapotranspiration in river bottomlands. Groundwater in the bedrock Carrizo–Wilcox aquifer also moves into the Quaternary alluvial deposits that floor the valleys of the Colorado, Brazos, and Trinity

Rivers. Groundwater discharge to the streams and rivers that cross the outcrop of the Carrizo–Wilcox aquifer makes up the base flow of these surface waters. Most of the discharge is probably from the Simsboro and Carrizo aquifers, and less is from the Hooper and Calvert Bluff aquitards. Estimates of natural groundwater discharge, therefore, require analysis of the flow of these surface waters.

The following streams and rivers occur in the study area and were included in the model: San Antonio River, Cibolo Creek, Guadalupe River, San Marcos River, Plum Creek, Cedar Creek, Colorado River, Big Sandy Creek, Middle Yegua Creek, East Yegua Creek, Little River, Brazos River, Little Brazos River, Walnut Creek, Duck Creek, Steele Creek, Navasota River, Big Creek, Upper Keechi Creek, Tehuacana Creek, and Trinity River (fig. 2). Cronin and Wilson (1967) summarized hydrogeologic information about alluvium beneath the Brazos River valley. Much more hydrogeologic information is available about the Brazos River alluvium, designated a minor aquifer, than for alluvium in the Colorado or Trinity River valleys.

Where the water table is above the streambed and slopes toward the stream, the stream receives groundwater from the aquifer; that is called a gaining reach (i.e., it gains flow as it moves through the reach). Where the water table is beneath the streambed and slopes away from the stream, the stream loses water to the aquifer; that is called a losing reach. Where impounded surface-water rises above the base-level elevation of groundwater in the river valleys, water can leak out of the reservoir and be a source of recharge.

Base flow is the contribution of groundwater to gaining reaches of a stream or river. After runoff from storm events has drained away, the natural surface-water flow that continues is base flow from groundwater. Streams can have an intermittent base flow, which is usually associated with wet winters and dry, hot summers. Larger streams and rivers might

have a perennial base flow. Direct exchange between surface and groundwater is limited to the outcrop.

Slade and others (2002) compiled the results of 366 gain-loss studies since 1918 that included 249 individual stream reaches throughout Texas. A total of five gain-loss studies were conducted on two streams in the study area: the Colorado River and Cibolo Creek. Results presented here are for stream reaches that cross the outcrop area. Table 3 reports the average annual flow at gages nearest the upstream extent of the Wilcox Group outcrop. Streams having headwaters within the outcrop of the Carrizo–Wilcox aquifer by definition have zero inflow from upstream.

Two methods were used to characterize interaction of surface and ground waters: low-flow studies and base-flow separation. First, details of historical low-flow studies conducted on any streams across the Carrizo–Wilcox aquifer within the model domain were reviewed. Second, data from stream gages located on the outcrop were analyzed using techniques of base-flow separation to obtain quantitative estimates of groundwater discharge to the streams.

4.6.1 Low-Flow Studies

Low-flow studies involve flow measurements at many locations on a stream within a short period of time, ideally when flow is low and no significant surface runoff occurs. Low-flow studies were conducted on the Colorado River in 1918 and on Cibolo Creek in 1949, 1963, and 1968. To use these results we estimated where gage sites were located relative to the outcrop of the aquifer. In all four studies, surface-water flow increased downstream as the stream crossed the aquifer outcrop, indicating gaining conditions at the time the studies were performed.

Table 3. Average flow of streams in study area.

Modeled stream name	Initial flow (acre-feet/yr)	Referenced gage
San Antonio River	40,861	USGS 08178565 San Antonio River at Loop 410 at San Antonio, TX
Cibolo Creek	16,606	USGS 08185000 Cibolo Creek at Selma, TX
Guadalupe River	330,192	USGS 08168500 Guadalupe River above Comal River at New Braunfels, TX
San Marcos River	283,749	USGS 08172000 San Marcos River at Luling, TX
Plum Creek	35,777	USGS 08172400 Plum Creek at Lockhart, TX
Cedar Creek	0	NA
Colorado River	1,622,898	USGS 08158000 Colorado River at Austin, TX
Big Sandy Creek	0	NA
Middle Yegua Creek	0	NA
East Yegua Creek	0	NA
Little River	1,264,803	USGS 08106500 Little River at Cameron, TX
Brazos River	2,052,843	USGS 08098290 Brazos River near Highbank, TX
Little Brazos River	0	NA
Walnut Creek	0	NA
Duck Creek	0	NA
Steele Creek	0	NA
Navasota River	79,970	USGS 08110325 Navasota River above Groesbeck, TX
Big Creek	0	NA
Upper Keechi Creek	0	NA
Tehuacana Creek	63,217	USGS 08064700 Tehuacana Creek near Streetman, TX
Trinity River	3,765,815	USGS 08065000 Trinity River near Oakwood, TX

In the 1918 Colorado River study, flow across the aquifer outcrop increased from about 61 to 97 cubic feet per second (cfs), an increase of 36 cfs. Flow at the Smithville gage during this low-flow study was 101 cfs. A flow of 101 cfs is exceeded 99.9 percent of the time at the Smithville gage. This indicates that even during conditions of extremely low flow, the Colorado River has been a gaining reach across the outcrop of the Carrizo–Wilcox aquifer. A flow study in August 1985 included only the downstream half of the outcrop area and, in contrast to the 1918 study, resulted in an average *loss* of 1,832 acre feet per year per river mile. There were, however, releases of large volumes of water from Highland Lakes reservoirs during the 1985 study, so study results are not representative of low-flow conditions. The 1985 study data, therefore, were not used in this analysis.

Three Cibolo Creek studies spanned a range of flow conditions across the outcrop of the Carrizo–Wilcox aquifer. In each case, flow increased across the outcrop (table 4). Cibolo Creek has been a consistently gaining reach across the outcrop of the Carrizo–Wilcox aquifer over a wide range of flow conditions.

4.6.2 Base-Flow Studies

The part of a stream's flow that is not directly influenced by runoff is considered to be its base flow. Base flow is an accumulation of groundwater discharge across the bed and banks of a stream. Base-flow separation was performed on daily stream-flow data using the Base Flow Index (BFI) program, jointly maintained by the USGS and U.S. Bureau of Reclamation (Wahl, 2001). BFI uses the Standard Hydrologic Institute Method for base-flow separation; this method identifies sudden rises in the hydrograph typical of storm-induced runoff and separates the total stream flow into a daily time series of base flow and storm flow for each gage. Base-flow separation is a standard graphical technique that provides an

Table 4. Summary of low-flow studies in Cibolo Creek.

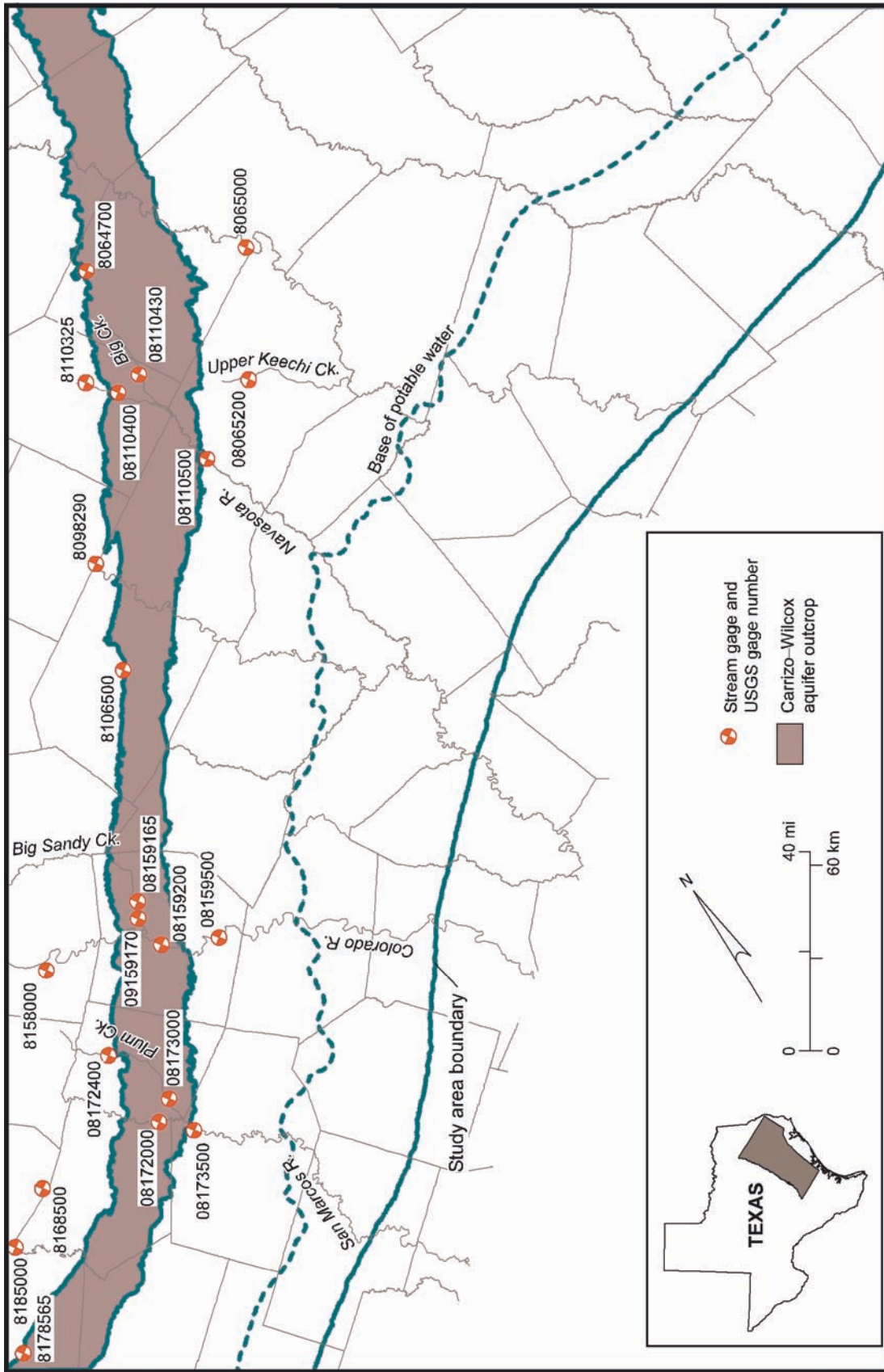
Year of study	Gain (cfs)	Rate of gain (cfs/mi)	Measured low flow (cfs)	Percent of time flow is exceeded
1949	~10	0.4	14	81
1963	~11	0.5	17	73
1968	~25	1	62	18

estimate of groundwater discharge. For a given day, the program may under- or overpredict base flow; however, the long-term accuracy of the method is commonly accepted. Details of the base-flow separation are given in appendix B.

Seven study reaches were identified that have pairs of stream gages located either entirely on or very near the boundary of the Carrizo–Wilcox outcrop (fig. 44). By isolating study reaches located entirely on the outcrop, we minimized the influence of hydrologic factors external to the base flow from the Carrizo aquifer. The difference in base flow between the upstream and downstream gages is an estimate of the amount of groundwater discharge between the two gages. Estimates of base flow for the Colorado and Navasota Rivers were adjusted to take into account water withdrawals and return flows located between the gages, using information from Water Availability Models (WAM) prepared for the TCEQ. Both adjustments were small relative to total base flow.

Base flow can be small compared with total flow. Base flow in Plum Creek, a tributary of the San Marcos River, for example, is typically less than 10 cfs, whereas total flow can exceed 150 cfs (fig. 45).

Base-flow discharge was converted to unit values by dividing the change in base flow between stations by the intervening area of the watershed on the outcrop (fig. 44). Base-flow duration curves were made from unit daily values. These curves show the percentage of time that each base-flow value was exceeded during the period of record (fig. 46). The shape of the curves is similar for most of the various gaged streams and watersheds. The median (50-percent exceedance) increase in base flow for the appropriate study reach, unitized by area of the drainage basin underlain by the Simsboro and Carrizo aquifers, was used to estimate calibration targets for groundwater discharge for like-sized ungaged streams in the steady-state model. For example, data for the Colorado River were used to estimate targets



QA41814(a)c

Figure 44. Location of stream-flow gages used for base-flow separation and stream inflow estimates.

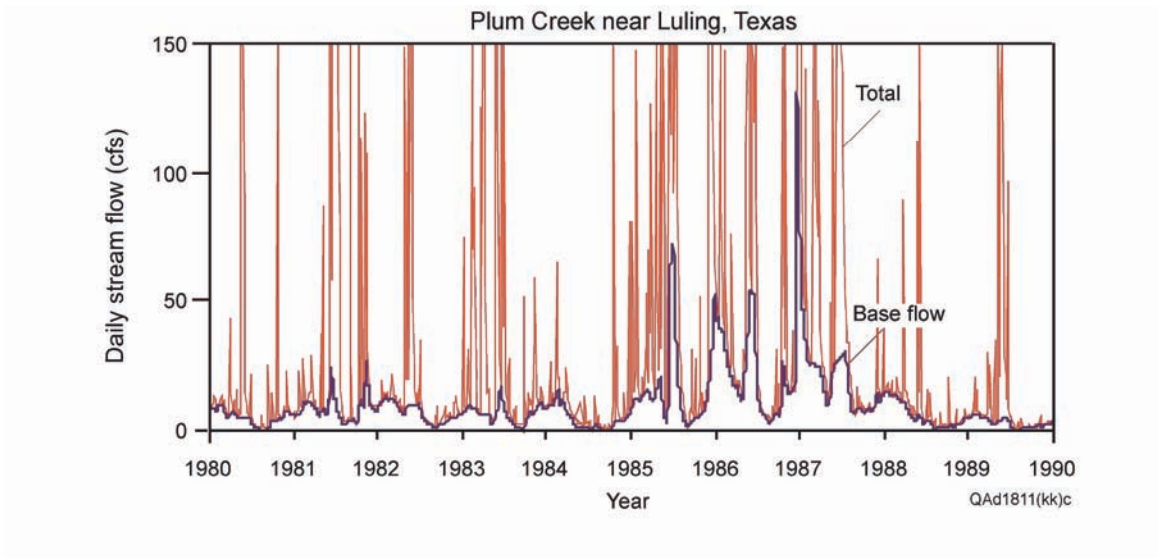


Figure 45. Comparison of total discharge and estimated base flow for Plum Creek near Luling, Texas (gage no. 08173000).

for the Brazos and Trinity Rivers, whereas data for Plum Creek were used to estimate targets for Cedar Creek. The median unit base-flow increase (cfs/mi²) for the appropriate study reach was multiplied by a simple function of the outcrop area of these aquifers in the watershed for the corresponding ungaged stream basins.

4.6.3 Surface-Water Reservoirs

Several lakes and reservoirs are also present: Braunig Lake, Calaveras Lake, Lake Bastrop, Alcoa Lake, Twin Oaks Reservoir, Lake Limestone, Richland-Chambers Reservoir, Fairfield Lake, and Cedar Creek Reservoir (fig. 2). Table 5 lists characteristics of these lakes and reservoirs. Most of these reservoirs overlay the outcrop of the Calvert Bluff Formation (Braunig Lake, Calaveras Lake, Lake Bastrop, Alcoa Lake, Twin Oaks Reservoir, Fairfield Lake) or extend from the Hooper Formation to the Calvert Bluff Formation, overlapping the outcrop of the Simsboro Formation (Lake Limestone, Richland-Chambers Reservoir, Cedar Creek Reservoir). Water-level fluctuations are small, and water levels can be considered constant through time. All the reservoirs lose water to the underlying aquifers or aquitards, but the exact amount is hard to quantify. The relationship between Lake Limestone and the Navasota River provides a way to estimate this reservoir's leakage. Median daily base flow at the first USGS gage station downstream of the reservoir increased by about 7 to 10 cfs after the reservoir was impounded in 1981. Most of the measured increase in base flow may be attributed to reservoir releases (Certificate of Adjudication 12-5165, held by the Brazos River Authority for Lake Limestone, mandates a minimum pass-through release of 6 cfs). The remaining 1 to 4 cfs base-flow increase may be used as an estimate of reservoir seepage at this location.

Table 5. Characteristics of reservoirs in study area.

ID#	Reservoir	Owner	Date impounded	Water-level fluctuations (ft)	Size (acres)
1	Lake Bastrop	Lower Colorado River Authority	1964	1-2	906
2	Alcoa Lake	ALCOA	1952	small	914
3	Twin Oaks Reservoir	Texas Power and Light	1982		1,460
4	Lake Limestone	Brazos River Authority	1978	1-3	13,680
5	Richland-Chambers Reservoir	Tarrant County Water Control	1987	3	44,000
6	Fairfield Lake	Texas Utilities Electric	1969	4	2,353
7	Cedar Creek Reservoir	Tarrant County Water Control	1965	4	34,300
8	Braunig Lake	City of San Antonio	1964	1-2	1,350
9	Calaveras Lake	City of San Antonio	1969	1-2	3,450

4.7 Groundwater Evapotranspiration

As previously mentioned, some recharge leaves the unconfined part of the aquifer by evapotranspiration (ET) in river bottomland areas. In this report this process is referred to as *groundwater evapotranspiration* to distinguish it from ET that takes place in soils across the upland areas. The groundwater model simulates the occurrence and movement of water beneath the water table. ET in the soil zone of the upland areas, along with runoff, reduces the amount of precipitation that drains downward from the root zone to eventually reach the water table. Such ET is not included in the model. Discharge of groundwater from shallow water tables in river bottomlands by the process of evapotranspiration is included in the model. Groundwater ET may be a major component of rejected recharge. The maximum rate of groundwater ET most likely parallels average net lake evaporation rate (fig. 9).

4.8 Hydraulic Properties

Typical of sediments deposited in fluvial and deltaic environments, hydrogeologic properties of the Carrizo–Wilcox aquifer are heterogeneous on local and regional scales (for example, figs. 12, 13). Sand, silt, clay, and lignite are the most common materials found in the Carrizo–Wilcox aquifer. Hydrogeologic properties vary with sediment texture. On a regional scale, hydraulic conductivity of aquifers and confining layers (aquitards) differ vertically and laterally. There is appreciable lateral heterogeneity in hydrogeologic properties related to original depositional systems and subsequent burial diagenesis of the sediments that make up the Carrizo–Wilcox aquifer. Much of the heterogeneity reflects the variations in thickness of sandstones (figs. 12, 13). The thick major sands may have greater hydraulic conductivity than thinner sands, as well as greater lateral continuity (Fogg and others, 1983).

We assume that the aquifer and aquitard materials are isotropic in the horizontal direction. This means that horizontal hydraulic conductivity is the same regardless of direction. Vertical anisotropy (K_v/K_h), the ratio of vertical (K_v) to horizontal (K_h) hydraulic conductivity, expresses the degree to which vertical movement of groundwater may be restricted. Vertical anisotropy is related to the presence of sedimentary structures, bedding, and interbedded low-permeability layers. Mace and others (2000) compiled data on the hydraulic properties of the Carrizo–Wilcox aquifer. Vertical anisotropy is poorly quantified and is generally estimated during model calibration (Fogg and others, 1983; Anderson and Woessner, 1992). Thickness of Carrizo–Wilcox sediments is also variable. Variations in aquifer thickness and hydraulic conductivity produce a range in transmissivity.

Average (geometric mean) hydraulic conductivities of Simsboro and Carrizo sandstones, as calculated from the Mace and others (2000c) data, are similar and higher than those of Hooper and Calvert Bluff sandstones (fig. 47). Average hydraulic conductivity from field tests is about 25 ft/d in the Simsboro Formation and about 20 ft/d in the Carrizo Formation, four to five times greater than average test results in the Hooper and Calvert Bluff Formations (table 6). Average transmissivity of screened parts of the Simsboro and Carrizo Formations are about 1,150 and 500 ft²/d, respectively, about five to ten times greater than in the Hooper and Calvert Bluff Formations (table 6). The range of hydraulic conductivity data is generally about three orders of magnitude (fig. 47).

Previous studies have shown that simulation of groundwater flow in a heterogeneous aquifer can be sensitive to the spatial distribution of hydraulic conductivity. Our approach to mapping hydraulic conductivity followed these four steps (appendix C):

- (1) We posted the hydraulic-conductivity values compiled by Mace and others (2000c).

Additional work was needed to assign Mace and others (2000c) data to specific

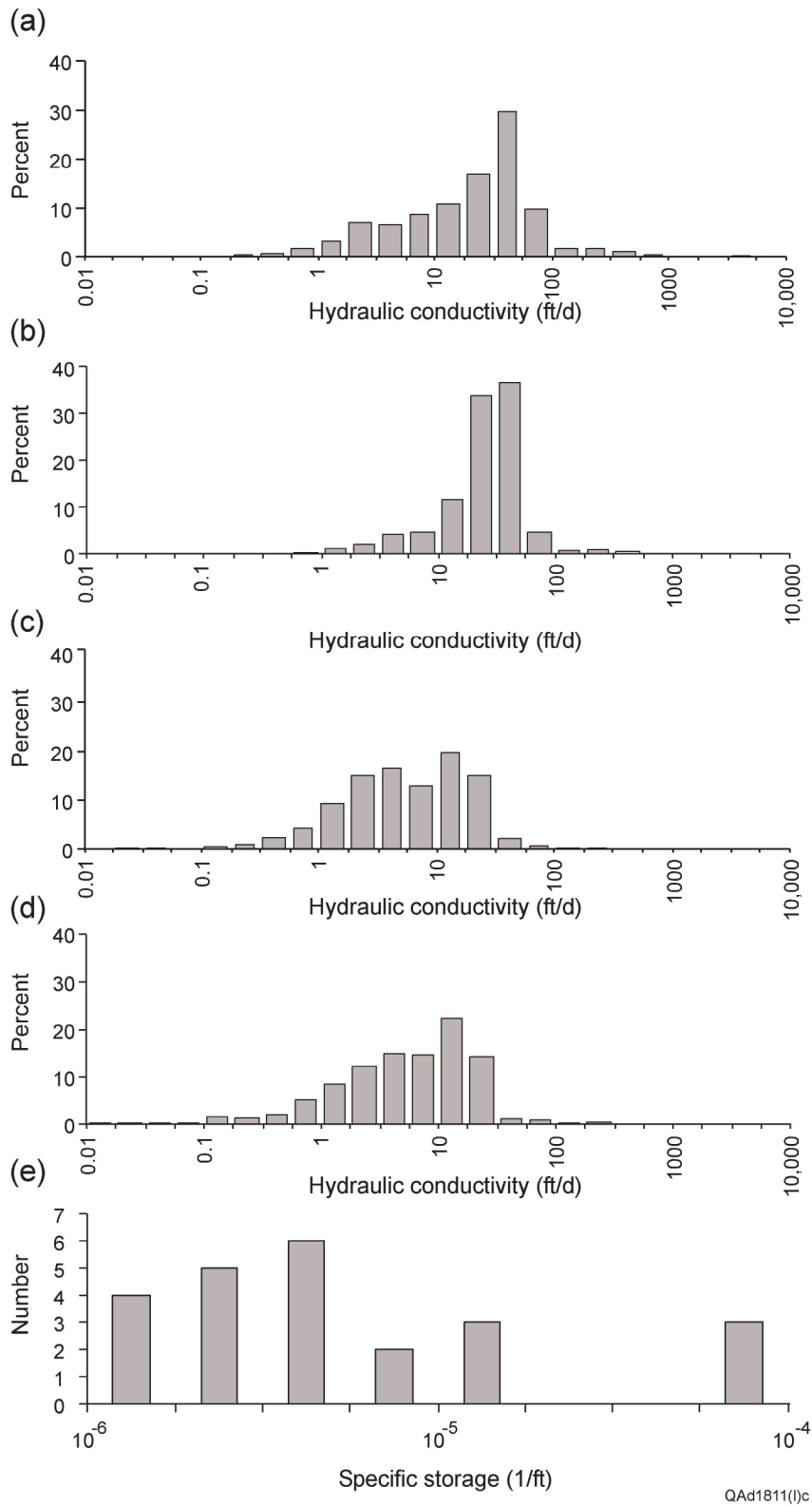


Figure 47. Histograms of hydraulic conductivity in the (a) Carrizo, (b) Simsboro, (c) Calvert Bluff, and (d) Hooper, and (e) specific storage in the Carrizo–Wilcox aquifer. Data from Mace and others (2000).

Table 6. Summary of hydraulic conductivity of the central Carrizo-Wilcox aquifer in the study area.

	Carrizo	Calvert Bluff	Simsboro	Hooper
<u>Model cells</u>				
Horizontal hydraulic conductivity geometric mean (K_h) (ft/d)	6.2	0.9	2.6	0.9
Vertical hydraulic conductivity geometric mean (K_v) (ft/d)	1.3×10^{-3}	9.7×10^{-5}	9.5×10^{-4}	3.5×10^{-5}
Vertical anisotropy geometric mean (K_v/K_h) within layer	2.1×10^{-4}	1.1×10^{-4}	3.7×10^{-4}	7.1×10^{-5}
Vertical anisotropy arithmetic mean (K_v/K_h) within layer	1.2×10^{-3}	2.2×10^{-4}	8.6×10^{-4}	3.4×10^{-3}
Min K_v/K_h	$3. \times 10^{-5}$	$1. \times 10^{-5}$	$4. \times 10^{-5}$	$1. \times 10^{-5}$
Max K_v/K_h	0.85	3.3×10^{-3}	0.03	0.1
<u>Field data (Mace and others, 2000; see fig. 47)</u>				
Horizontal hydraulic conductivity geometric mean (K_h) (ft/d)	19.3	5.6	24.8	5.4

model layers on the basis of well depth, screened interval, and designated aquifer code. Data were posted on maps as the logarithm (base 10) of the reported hydraulic conductivity.

- (2) We overlaid the posted values on maps of the net thickness of sandstone in the aquifer layers. To account for the entire study area we used appropriate sandstone-thickness maps from Bebout and others (1982), Ayers and Lewis (1985), and Xue (1994). To supplement these maps, we posted and contoured values of sandstone thickness for a part of Gonzales County.
- (3) We contoured hydraulic conductivity using the thickness of sandstones as an interpretive guide. Our conceptual model is that hydraulic conductivity is greatest in the thickest part of the fluvial channel axes because (a) that is where the coarse-grained sands are concentrated and low-permeability silts and clays tend to be absent and (b) thick sandstones tend to be better interconnected and have a higher effective hydraulic conductivity (Fogg and others, 1983). We found qualitative but mappable local correlation between sandstone thickness and hydraulic conductivity.
- (4) The contoured maps of hydraulic conductivity were digitized, along with the maps of sandstone thickness, and values of hydraulic conductivity and sandstone thickness were interpolated for each cell of the model.

Because the entire thickness of the aquifer at any location is not made up of sandstone, we calculated average values of horizontal (K_h) and vertical (K_v) hydraulic conductivity using equations 3 and 4:

$$K_h = (K_{hs} \times b_s + K_{hc} \times b_c)/B \quad (3)$$

$$K_v = B/[(b_s/K_{vs}) + (b_c/K_{vc})] \quad (4)$$

where K_{hs} and b_s are the horizontal hydraulic conductivity and total layer thickness of sand, respectively; K_{hc} and b_c are horizontal hydraulic conductivity and total layer thickness of clay, silt, and lignite, respectively; and B is total layer thickness. We assumed that local vertical anisotropy is 0.1 for sandstone beds and 0.01 for clay, silt, and lignite beds. We used digitized maps of sandstone thickness and of layer thickness; total thickness of clay, silt, and lignite was estimated from layer thickness minus sandstone thickness.

This approach to assigning hydraulic conductivity to model cells results in average values that are less than the average of measured values (table 6). For example, the average horizontal hydraulic conductivity assigned to the Carrizo Formation in the study area is 6.2 ft/d, whereas the measured average is 19.3 ft/d. Initial values calculated for the Bryan-College Station well field slightly overestimated known hydraulic conductivity. Maximum hydraulic conductivity of thick deposits of Simsboro sandstone in the Rockdale Delta was limited to 30 ft/d, giving a maximum transmissivity of 15,200 ft²/d.

Having an average hydraulic conductivity for a model layer less than the average measured value can be justified to the extent that (1) total layer transmissivity needs to take into account the part of the aquifer not made up of permeable sandstone, (2) wells of low permeability may be underrepresented in the database because they are not tested, and (3) the model layer includes parts of the formation downdip of the base of freshwater not included in the measured sample population.

Most of the Hooper Formation in the study area has assigned values of horizontal hydraulic conductivity of between 0.1 and 10 ft/d (fig. 48). In the same area, hydraulic conductivity of the Simsboro Formation, averaged over the thickness of the aquifer, is 10 to more than 30 ft/d (fig. 49). The geometry or architecture of hydraulic conductivity as mapped

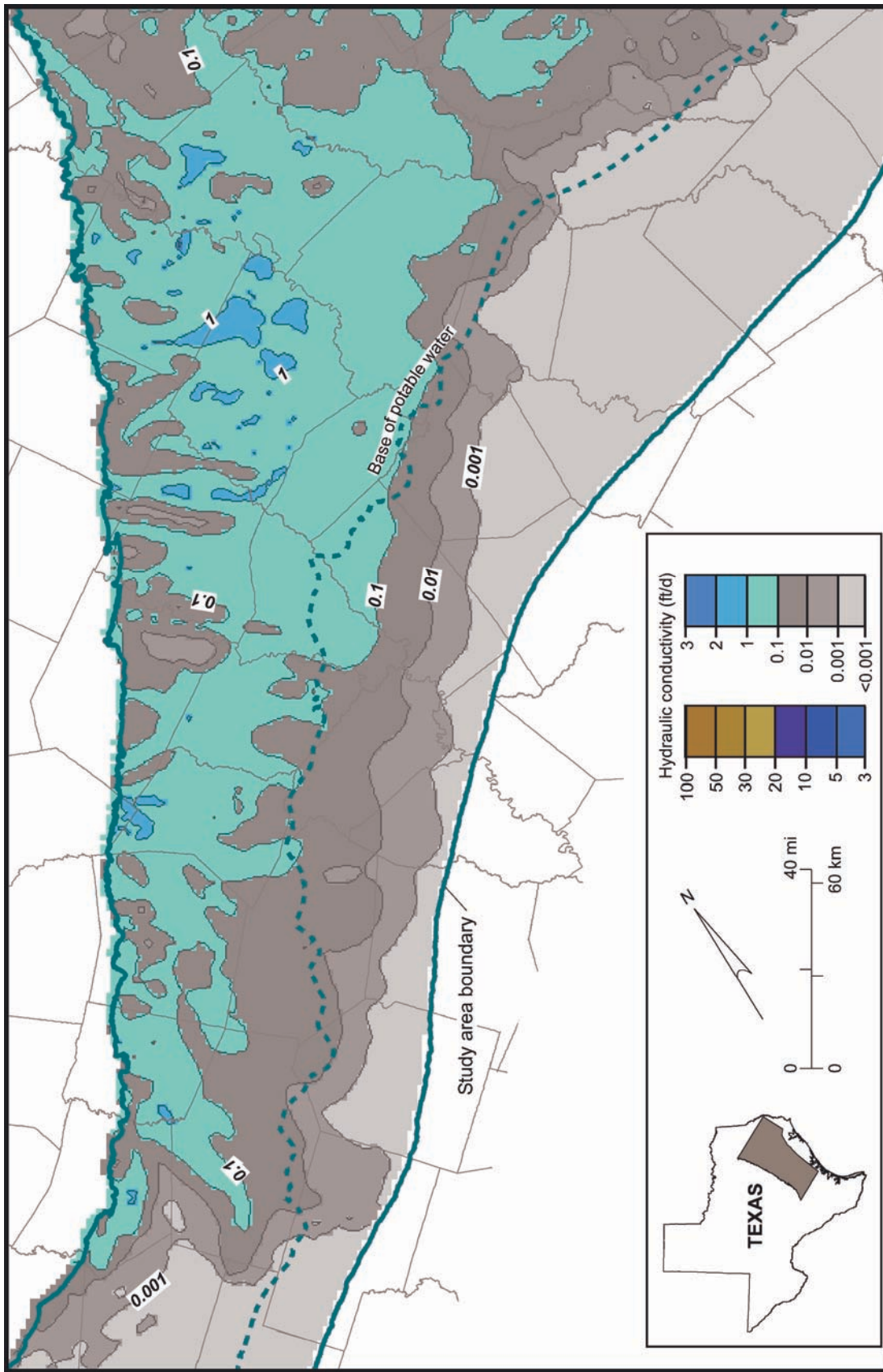


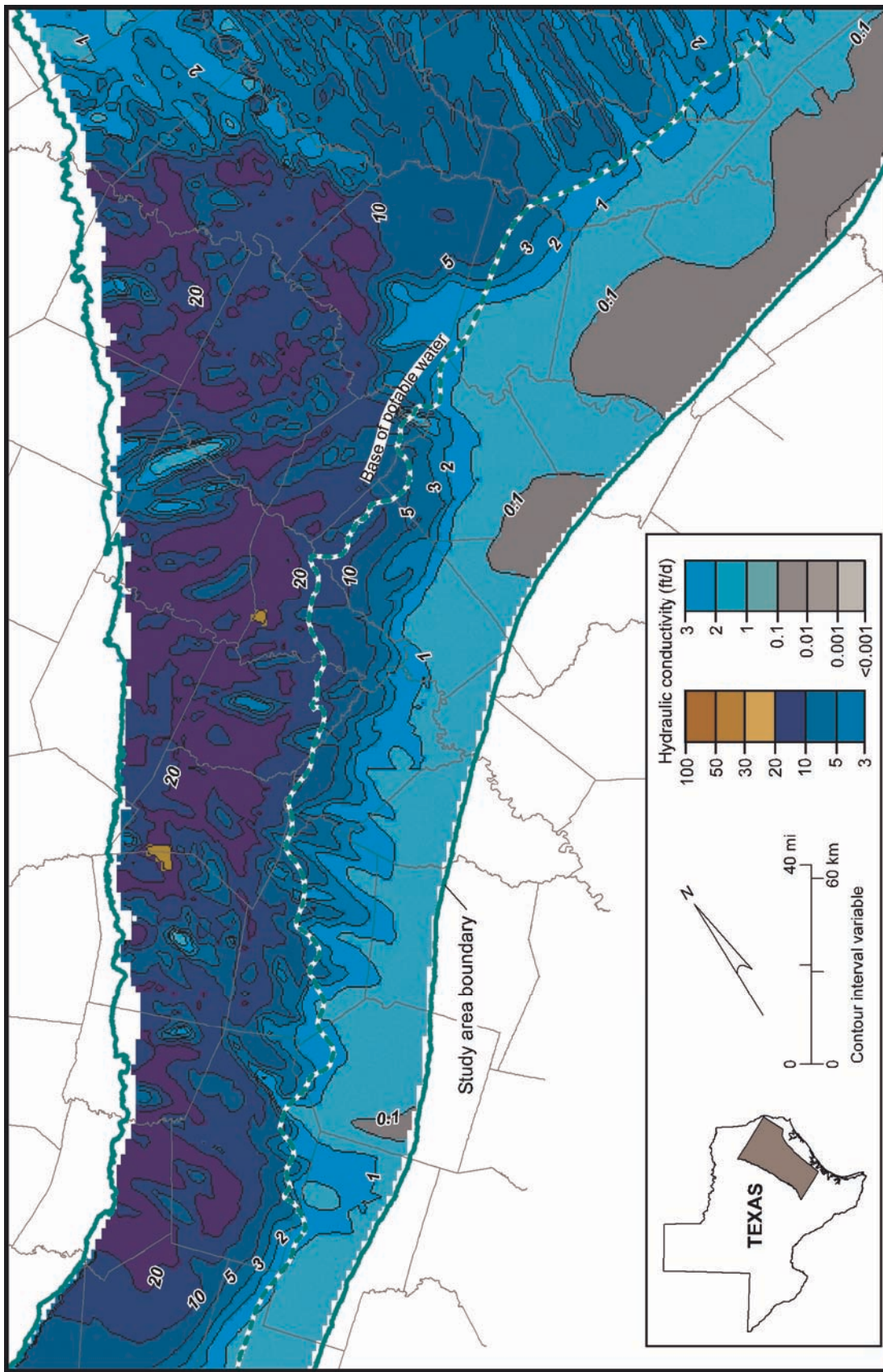
Figure 48. Map of average hydraulic conductivity in the Hooper Formation. Method of calculation described in text.

in the Simsboro Formation and other units reflects the assumption that sandstone thickness is locally correlated with hydraulic conductivity. The areas of high hydraulic conductivity in the Simsboro Formation (fig. 49) correspond to areas of greater sandstone thickness (fig. 12).

Average horizontal hydraulic conductivities of the Hooper and Calvert Bluff Formations are similar (figs. 48, 50; table 6). Hydraulic conductivity of the Carrizo Formation is greatest to the southwest. In the southwest part of the study area, Carrizo sandstones have high hydraulic conductivity in Gonzales and Wilson Counties. In the northern part of the study area, high hydraulic conductivity also corresponds to areas with greater thickness of sandstone in the Carrizo Formation (figs. 13, 51).

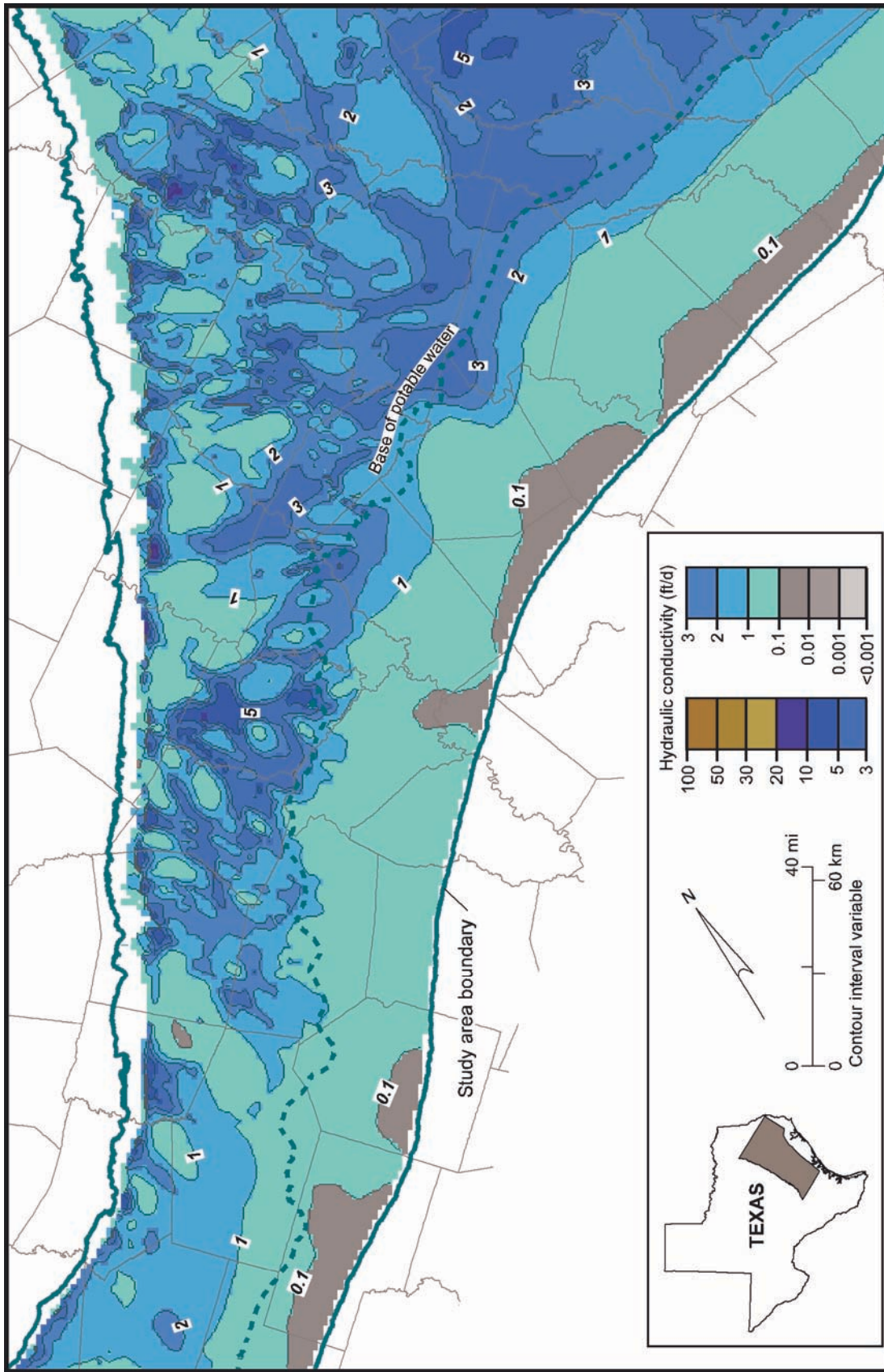
The values of vertical hydraulic conductivity calculated using equation 4 were used as initial estimates in the model. Vertical anisotropy of the calibrated model is about 10^{-3} for the Carrizo, Simsboro, and Hooper layers and about 10^{-4} for the Calvert Bluff layer (table 6). Fogg and others (1983) used an anisotropy of 10^{-4} in their model of the Carrizo–Wilcox aquifer in parts of Freestone and Leon Counties, with 10^{-3} as an upper limit. Given other parameter values, 10^{-4} was used to give a good match of the vertical gradient in hydraulic head. They noted that 10^{-4} is much smaller than the commonly assumed ratios for sandstone aquifers.

Specific storage is a proportionality factor between the difference in water inflow and outflow rates and the rate of change of hydraulic head. It measures the volume of water released as a result of expansion of water and compression of the porous media per unit volume and unit decline in hydraulic head. Specific storage \times aquifer thickness equals the storativity of the aquifer, which is equal to the volume of water released from a vertical column of the aquifer per unit surface area of the aquifer and unit decline in hydraulic head. Specific storage has units of 1/length and storativity is dimensionless.



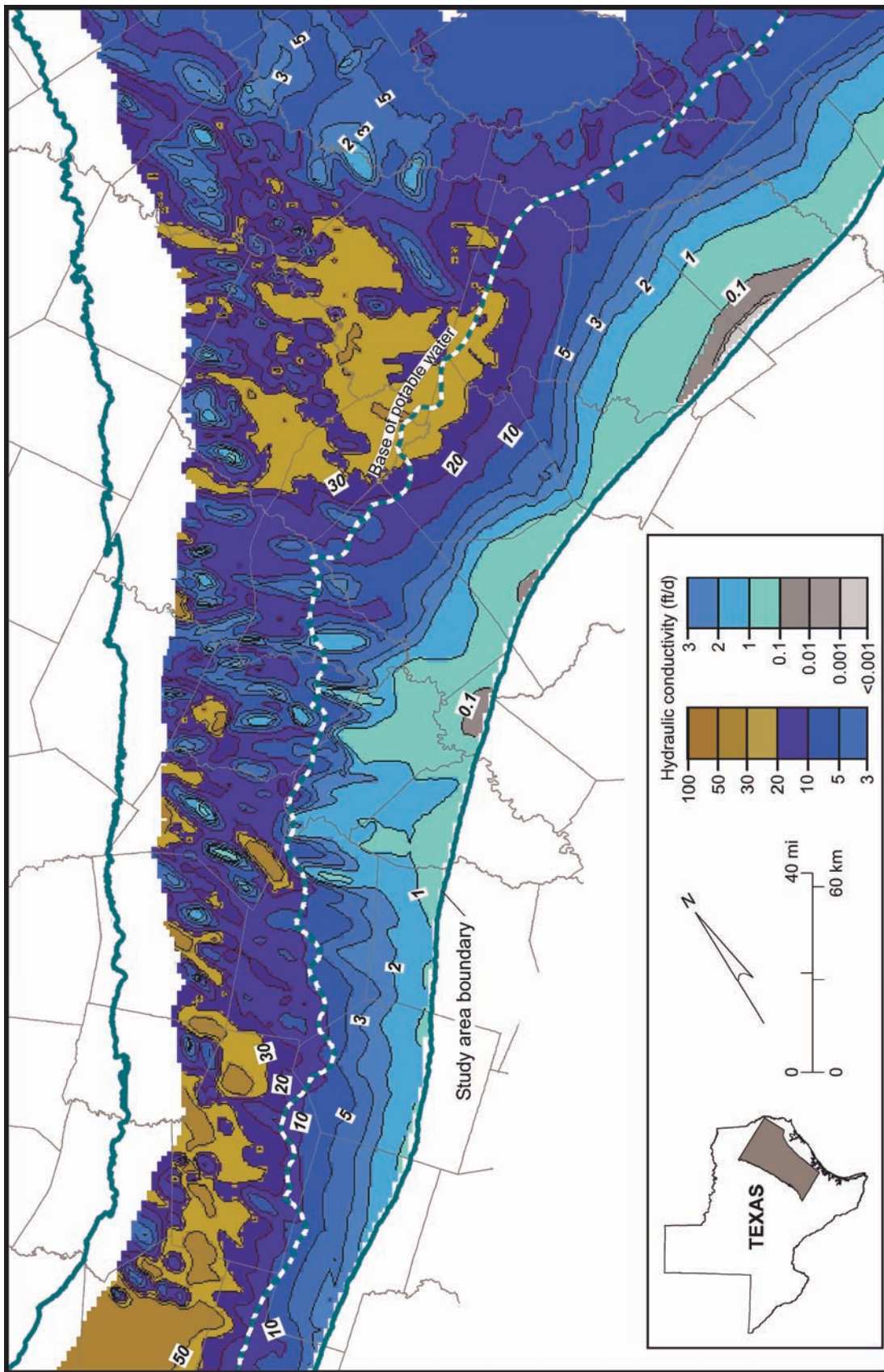
QA01811(e)c

Figure 49. Map of average hydraulic conductivity in the Simsboro Formation. Method of calculation described in text.



QA41811c1e

Figure 50. Map of average hydraulic conductivity in the Calvert Bluff Formation. Method of calculation described in text.



QAd1811(b)E

Figure 51. Map of average hydraulic conductivity in the Carrizo Formation. Method of calculation described in text.

Mace and others (2000c) compiled data on specific storage and the coefficient of storage (storativity). All reported results in Mace and others (2000c) are for the confined part of the aquifer. Values of specific storage average $10^{-5.7} \text{ ft}^{-1}$, $10^{-4.7} \text{ ft}^{-1}$, and $10^{-4.9} \text{ ft}^{-1}$ in the Carrizo Formation (three data points), Calvert Bluff Formation (four data points), and Simsboro Formation (five data points), respectively. Storativity ranges between 10^{-6} and 10^{-1} in the Carrizo–Wilcox aquifer and averages $10^{-3.5}$ (Mace and others, 2000c).

4.9 Well Discharge

Most pumping from the Carrizo–Wilcox aquifer in the study area has been for municipal public-water supply, manufacturing, and rural domestic water uses. These three uses have made up more than 60 percent of total pumping from the aquifer in the period from 1980 through 2000 (fig. 52; tables 7, 8). In the 1980's, lignite mines began pumping greater amounts of groundwater as part of mining operations. Water withdrawal related to all types of mining activities made up an estimated 25 percent of total production in 2000. Irrigation and stock water uses have made up another 10 to 15 percent of total pumping. This percentage does not include pumping from the Brazos River alluvium. Water use for power, for example, for cooling water for electricity-generating plants, makes up less than 3 percent of total groundwater pumping from the Carrizo–Wilcox aquifer in the study area. The Simsboro and Carrizo layers are the most productive parts of the Carrizo–Wilcox aquifer in the study area, and most pumping has been from these two layers. The Simsboro aquifer is the main development zone for the municipal well field supplying Bryan and College Station in Brazos County. The Carrizo aquifer is the main productive horizon on the

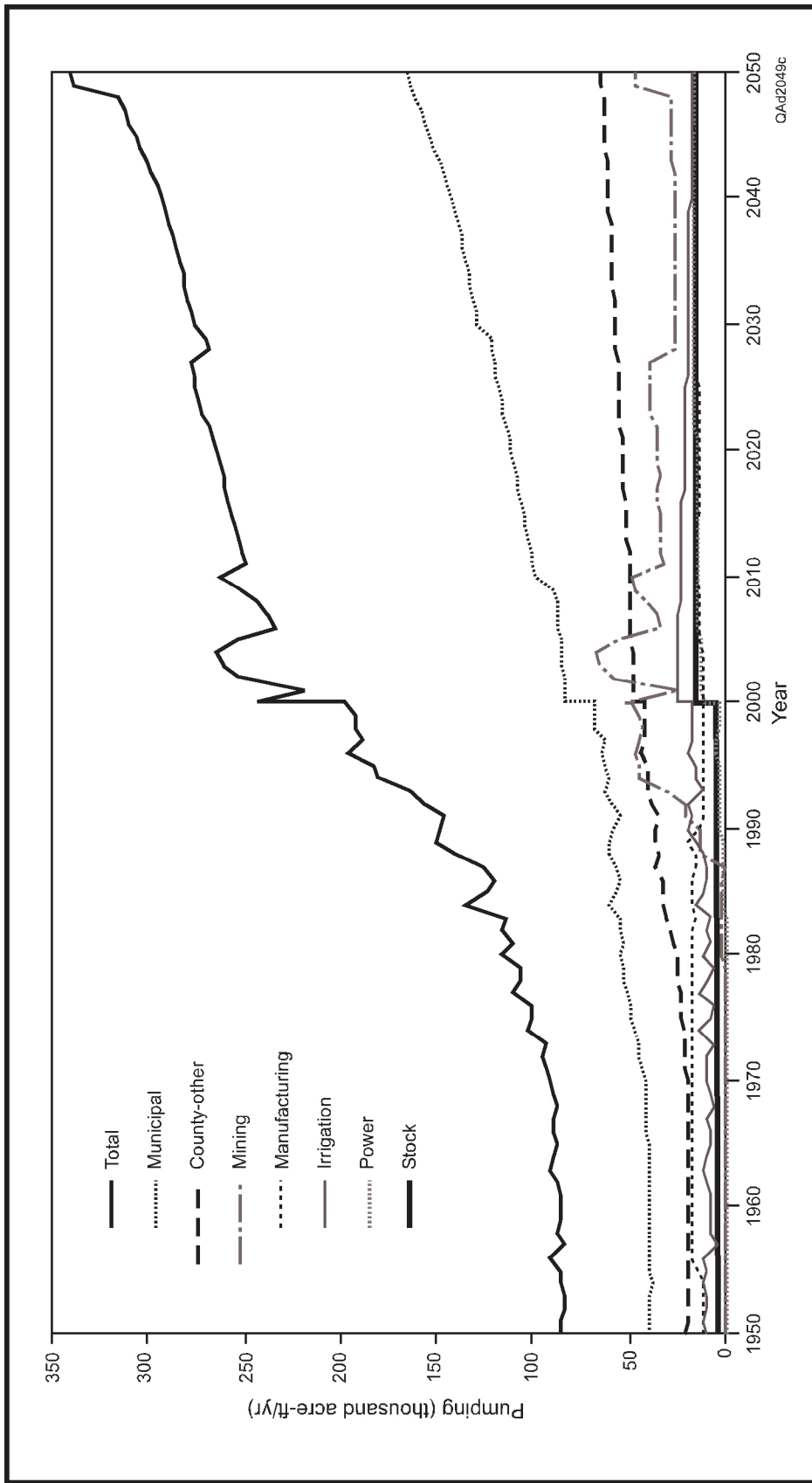


Figure 52. Total groundwater withdrawals from the Carrizo–Wilcox aquifer in the study area. Values for 1980 through 2000 are based on TWDB water-use survey information. Values for 1950 through 1980 are derived from 1980 estimates as described in text. Predictions for 2000 through 2050 are based on predicted dry demands estimated by Regional Water Planning Groups.

Table 7. Rates of groundwater withdrawal (acre-feet per year) from the Carrizo-Wilcox aquifer as assigned within the study area.

County	1980	1990	2000	2010	2020	2030	2040	2050
Anderson	3,552	5,529	8,050	6,789	6,773	6,815	6,783	6,909
Angelina	29,893	24,580	24,405	20,152	19,249	20,450	21,601	23,569
Bastrop	6,002	7,064	9,539	18,049	21,987	20,725	22,083	23,362
Bexar	112	187	64	3,535	3,436	2,456	2,496	2,176
Brazos	20,176	25,303	31,100	39,706	45,110	44,547	48,770	52,421
Burleson	1,157	1,142	1,281	3,338	3,395	3,436	3,495	3,629
Caldwell	2,718	3,896	3,494	7,608	7,972	8,312	8,363	8,390
Cherokee	6,695	7,078	7,664	4,207	4,327	4,530	4,714	5,001
Falls	62	51	40	893	895	904	913	923
Fayette	4	5	5	0	0	0	0	0
Freestone	2,298	2,487	2,889	3,078	3,061	3,084	3,116	3,137
Gonzales	2,639	4,134	2,438	15,693	20,146	29,488	35,093	44,620
Guadalupe	2,308	2,939	1,995	7,623	9,580	11,679	13,193	15,830
Henderson	3,385	4,180	4,517	4,245	4,247	4,252	4,241	4,314
Houston	760	574	866	1,465	1,469	1,475	1,483	1,488
Karnes	1,155	116	95	21	9	4	2	1
Lee	2,007	2,881	3,064	55,737	57,853	58,378	60,173	67,104
Leon	1,838	2,751	2,642	5,570	5,152	5,187	5,291	5,488
Limestone	1,289	2,656	2,246	11,530	11,590	11,725	11,913	12,224
Madison	0	80	48	1,773	1,726	1,684	1,627	1,580
Milam	2,904	15,105	35,448	21,654	21,131	21,127	21,770	23,072
Nacogdoches	6,576	8,007	8,942	7,679	8,150	8,995	9,785	10,532
Navarro	8	7	3	12	12	12	12	12
Robertson	7,070	8,353	22,760	26,695	27,279	30,983	32,125	33,370
Rusk	177	174	167	329	350	374	379	396
San Augustine	154	112	101	341	336	340	338	341
Smith	1,611	2,520	3,050	1,084	1,187	1,302	1,433	1,571
Van Zandt	634	750	829	548	851	767	814	833
Wilson	9,109	15,223	15,976	12,667	11,373	10,183	10,571	11,053
Total	116,293	147,884	193,718	282,021	298,646	313,214	332,577	363,346

Table 8a. Rate of groundwater withdrawal (acre-feet per year) for municipal public water supply from the Carrizo-Wilcox aquifer as assigned in the model.

County	1980	1990	2000	2010	2020	2030	2040	2050
Anderson	672	770	571	534	524	519	512	508
Angelina	17,251	14,555	15,759	12,776	12,547	13,550	14,408	15,812
Bastrop	2,254	1,890	3,242	7,765	8,171	11,356	12,000	13,040
Bexar	77	108	0	985	1,121	1,082	1,113	1,108
Brazos	17,923	22,451	27,878	37,866	42,944	42,277	46,663	50,515
Burleson	776	720	769	791	810	838	853	879
Caldwell	1,492	1,843	1,800	4,187	4,590	5,143	5,452	5,767
Cherokee	4,461	4,134	4,704	2,328	2,273	2,271	2,358	2,469
Falls	0	0	0	0	0	0	0	0
Fayette	0	0	0	0	0	0	0	0
Freestone	964	1,001	1,084	1,178	1,243	1,298	1,320	1,343
Gonzales	996	1,207	1,291	12,230	16,822	26,311	31,969	41,534
Guadalupe	0	0	548	242	232	254	272	277
Henderson	946	1,214	1,141	1,085	1,097	1,117	1,125	1,160
Houston	281	0	273	639	642	647	649	649
Karnes	0	0	0	0	0	0	0	0
Lee	1,093	1,683	1,469	24,367	26,280	27,957	29,673	36,470
Leon	604	720	662	1,227	1,270	1,348	1,422	1,510
Limestone	0	0	0	1,143	1,129	1,131	1,138	1,217
Madison	0	80	48	1,051	1,013	984	930	884
Milam	1,517	1,496	1,119	15,314	14,783	14,781	15,428	16,739
Nacogdoches	4,668	5,066	5,022	1,355	1,565	1,865	2,220	2,680
Navarro	0	0	0	0	0	0	0	0
Robertson	4,423	3,914	4,254	5,626	6,107	9,819	10,640	11,625
Rusk	0	0	0	0	0	0	0	0
San Augustine	0	0	0	0	0	0	0	0
Smith	0	0	0	72	80	81	85	91
Van Zandt	0	0	0	0	0	0	0	0
Wilson	1,451	1,883	2,117	2,369	2,458	2,603	2,754	2,928
Total	61,849	64,735	73,751	135,130	147,701	167,232	182,984	209,205

Table 8b. Rate of groundwater withdrawal (acre-feet per year) for rural domestic water supply from the Carrizo-Wilcox aquifer as assigned in the model.

County	1980	1990	2000	2010	2020	2030	2040	2050
Anderson	2,224	4,413	6,787	5,528	5,590	5,662	5,646	5,774
Angelina	2,310	2,645	3,288	2,057	2,058	2,118	2,123	2,211
Bastrop	1,678	4,101	5,050	7,018	8,120	9,315	10,019	10,247
Bexar	26	68	50	2,550	2,316	1,375	1,383	1,067
Brazos	2,251	2,790	3,106	1,838	2,166	2,275	2,107	1,911
Burleson	366	410	494	1,188	1,213	1,213	1,246	1,342
Caldwell	1,102	1,549	1,530	2,374	2,454	2,343	2,177	1,965
Cherokee	2,109	2,118	2,519	1,296	1,409	1,502	1,587	1,662
Falls	60	49	38	234	236	245	254	264
Fayette	4	5	5	0	0	0	0	0
Freestone	793	960	1,243	1,122	1,050	1,024	1,034	1,031
Gonzales	486	795	914	745	719	698	702	710
Guadalupe	978	1,517	1,374	5,424	7,303	9,298	10,662	13,158
Henderson	1,768	2,344	2,609	2,534	2,536	2,523	2,502	2,534
Houston	459	545	531	709	708	707	709	713
Karnes	54	65	91	0	0	0	0	0
Lee	575	946	1,216	1,691	1,749	1,819	1,906	2,044
Leon	666	1,127	717	1,002	1,078	1,157	1,243	1,343
Limestone	862	965	853	1,199	1,232	1,302	1,379	1,477
Madison	0	0	0	168	162	157	149	141
Milam	1,143	1,016	1,255	1,178	1,188	1,189	1,187	1,179
Nacogdoches	1,644	2,509	2,629	3,943	4,242	4,769	5,219	5,475
Navarro	8	7	3	0	0	0	0	0
Robertson	598	765	846	764	712	692	693	691
Rusk	138	141	143	283	303	328	332	349
San Augustine	136	92	86	274	269	271	269	272
Smith	1,602	2,510	3,042	991	1,086	1,201	1,328	1,460
Van Zandt	467	548	604	499	783	679	697	701
Wilson	850	1,550	1,831	2,654	2,927	3,207	3,897	4,571
Total	25,357	36,550	42,854	49,263	53,609	57,069	60,450	64,292

Table 8c. Rate of groundwater withdrawal (acre-feet per year) for mining water supply from the Carrizo-Wilcox aquifer as assigned in the model.

County	1980	1990	2000	2010	2020	2030	2040	2050
Anderson	0	0	0	168	93	61	40	31
Angelina	0	0	0	0	0	0	0	0
Bastrop	0	1	0	3,228	5,650	0	0	0
Bexar	0	0	0	0	0	0	0	0
Brazos	0	0	0	0	0	0	0	0
Burleson	0	0	0	0	0	0	0	0
Caldwell	0	0	0	16	10	4	0	0
Cherokee	81	125	0	47	23	49	61	76
Falls	0	0	0	0	0	0	0	0
Fayette	0	0	0	0	0	0	0	0
Freestone	18	20	7	32	23	21	21	22
Gonzales	0	0	0	10	9	8	8	9
Guadalupe	0	0	0	198	200	202	207	213
Henderson	265	102	394	164	144	129	115	102
Houston	0	0	0	0	0	0	0	0
Karnes	1,101	52	3	21	9	4	2	1
Lee	0	0	0	26,074	26,224	25,005	25,001	25,000
Leon	0	0	0	1,045	508	384	327	335
Limestone	398	366	447	872	913	976	1,080	1,214
Madison	0	0	0	72	66	56	54	56
Milam	0	12,271	32,537	0	0	0	0	0
Nacogdoches	11	0	0	0	0	0	0	0
Navarro	0	0	0	0	0	0	0	0
Robertson	0	0	11,396	8,572	8,572	8,572	8,572	8,572
Rusk	0	0	0	0	0	0	0	0
San Augustine	0	0	0	0	0	0	0	0
Smith	0	0	0	0	0	0	0	0
Van Zandt	0	0	0	0	0	0	0	0
Wilson	0	0	0	82	48	27	20	14
Total	1,874	12,937	44,784	40,601	42,492	35,498	35,508	35,645

Table 8d. Rate of groundwater withdrawal (acre-feet per year) for manufacturing and industrial water supply from the Carrizo-Wilcox aquifer as assigned in the model.

County	1980	1990	2000	2010	2020	2030	2040	2050
Anderson	346	0	0	139	146	152	165	176
Angelina	10,332	7,380	5,357	5,319	4,643	4,782	5,070	5,546
Bastrop	76	23	30	38	46	54	64	75
Bexar	1	1	1	0	0	0	0	0
Brazos	0	0	14	0	0	0	0	0
Burleson	0	0	0	145	158	171	182	194
Caldwell	1	0	0	65	69	74	79	84
Cherokee	0	0	0	0	0	0	0	0
Falls	0	0	0	0	0	0	0	0
Fayette	0	0	0	0	0	0	0	0
Freestone	0	0	0	0	0	0	0	0
Gonzales	0	0	0	654	687	701	751	797
Guadalupe	19	0	0	1,448	1,548	1,643	1,784	1,926
Henderson	0	0	0	99	106	119	135	154
Houston	0	0	0	12	14	16	19	21
Karnes	0	0	0	0	0	0	0	0
Lee	0	0	0	0	0	0	0	0
Leon	161	308	675	191	192	193	194	195
Limestone	0	0	0	0	0	0	0	0
Madison	0	0	0	82	85	87	94	99
Milam	0	0	0	0	0	0	0	0
Nacogdoches	21	0	0	874	874	874	872	874
Navarro	0	0	0	0	0	0	0	0
Robertson	28	24	0	51	61	72	84	98
Rusk	0	0	0	0	0	0	0	0
San Augustine	0	0	3	0	0	0	0	0
Smith	0	0	0	0	0	0	0	0
Van Zandt	0	0	0	0	0	0	0	0
Wilson	167	47	1	45	53	49	57	66
Total	11,152	7,783	6,081	9,162	8,682	8,987	9,550	10,305

Table 8e. Rate of groundwater withdrawal (acre-feet per year) for irrigation water supply from the Carrizo-Wilcox aquifer as assigned in the model.

County	1980	1990	2000	2010	2020	2030	2040	2050
Anderson	166	30	360	124	124	124	124	124
Angelina	0	0	0	0	0	0	0	0
Bastrop	1,655	734	938	0	0	0	0	0
Bexar	0	0	0	0	0	0	0	0
Brazos	0	0	0	0	0	0	0	0
Burleson	0	0	0	0	0	0	0	0
Caldwell	51	497	156	967	850	746	655	574
Cherokee	44	431	135	50	50	50	50	50
Falls	0	0	0	0	0	0	0	0
Fayette	0	0	0	0	0	0	0	0
Freestone	0	48	32	6	6	6	6	6
Gonzales	531	2,002	104	1,062	916	777	669	577
Guadalupe	1,262	1,390	41	311	296	282	268	255
Henderson	91	19	18	0	0	0	0	0
Houston	0	0	39	37	37	35	38	38
Karnes	0	0	0	0	0	0	0	0
Lee	165	103	211	143	139	136	132	128
Leon	0	0	0	0	0	0	0	0
Limestone	0	0	0	0	0	0	0	0
Madison	0	0	0	0	0	0	0	0
Milam	0	53	301	286	283	281	278	276
Nacogdoches	0	140	1,016	1,035	1,035	1,035	1,035	1,035
Navarro	0	0	0	0	0	0	0	0
Robertson	1,700	1,807	1,847	2,222	2,222	2,222	2,222	2,222
Rusk	0	0	0	0	0	0	0	0
San Augustine	0	0	0	0	0	0	0	0
Smith	0	0	0	0	0	0	0	0
Van Zandt	0	0	0	0	0	0	0	0
Wilson	6,499	11,642	11,919	7,517	5,887	4,297	3,844	3,474
Total	12,164	18,896	17,117	13,760	11,845	9,991	9,321	8,759

Table 8f. Rate of groundwater withdrawal (acre-feet per year) for power water supply from the Carrizo-Wilcox aquifer as assigned in the model.

County	1980	1990	2000	2010	2020	2030	2040	2050
Anderson	0	0	0	0	0	0	0	0
Angelina	0	0	0	0	0	0	0	0
Bastrop	0	0	0	0	0	0	0	0
Bexar	0	0	0	0	0	0	0	0
Brazos	0	58	103	0	0	0	0	0
Burleson	0	0	0	0	0	0	0	0
Caldwell	0	0	0	0	0	0	0	0
Cherokee	0	0	0	86	172	257	257	343
Falls	0	0	0	0	0	0	0	0
Fayette	0	0	0	0	0	0	0	0
Freestone	101	163	110	204	204	199	199	200
Gonzales	0	0	0	993	993	993	993	993
Guadalupe	0	0	0	0	0	0	0	0
Henderson	0	0	0	0	0	0	0	0
Houston	0	0	0	0	0	0	0	0
Karnes	0	0	0	0	0	0	0	0
Lee	0	0	0	1,750	1,750	1,750	1,750	1,750
Leon	0	0	0	0	0	0	0	0
Limestone	0	1,292	916	6,889	6,889	6,889	6,889	6,889
Madison	0	0	0	0	0	0	0	0
Milam	0	0	0	3,250	3,250	3,250	3,250	3,250
Nacogdoches	0	0	0	0	0	0	0	0
Navarro	0	0	0	0	0	0	0	0
Robertson	0	1,527	4,035	7,756	7,902	7,902	8,211	8,459
Rusk	0	0	0	0	0	0	0	0
San Augustine	0	0	0	0	0	0	0	0
Smith	0	0	0	0	0	0	0	0
Van Zandt	0	0	0	0	0	0	0	0
Wilson	0	0	0	0	0	0	0	0
Total	101	3,040	5,164	20,928	21,160	21,240	21,549	21,884

Table 8g. Rate of groundwater withdrawal (acre-feet per year) for stock water supply from the Carrizo-Wilcox aquifer as assigned in the model.

County	1980	1990	2000	2010	2020	2030	2040	2050
Anderson	144	317	332	296	296	296	296	296
Angelina	0	0	0	0	0	0	0	0
Bastrop	340	315	280	0	0	0	0	0
Bexar	8	10	13	0	0	0	0	0
Brazos	0	0	0	0	0	0	0	0
Burleson	15	12	18	1,214	1,214	1,214	1,214	1,214
Caldwell	72	7	9	0	0	0	0	0
Cherokee	0	270	305	401	401	401	401	401
Falls	2	2	2	659	659	659	659	659
Fayette	0	0	0	0	0	0	0	0
Freestone	423	295	412	535	535	535	535	535
Gonzales	626	130	129	0	0	0	0	0
Guadalupe	49	31	32	0	0	0	0	0
Henderson	315	501	354	363	363	363	363	363
Houston	20	29	23	69	68	69	68	67
Karnes	0	0	0	0	0	0	0	0
Lee	173	149	168	1,711	1,711	1,711	1,711	1,711
Leon	407	597	588	2,105	2,105	2,105	2,105	2,105
Limestone	29	33	31	1,427	1,427	1,427	1,427	1,427
Madison	0	0	0	400	400	400	400	400
Milam	243	269	237	1,627	1,627	1,627	1,627	1,627
Nacogdoches	232	293	275	472	434	452	440	468
Navarro	0	0	0	12	12	12	12	12
Robertson	322	316	382	1,704	1,704	1,704	1,704	1,704
Rusk	39	33	24	46	46	46	47	46
San Augustine	18	20	12	67	67	68	69	69
Smith	9	11	8	20	20	20	20	20
Van Zandt	167	202	224	49	68	88	117	132
Wilson	143	101	109	0	0	0	0	0
Total	3,796	3,943	3,967	13,177	13,157	13,197	13,215	13,256

north side of the study area, where the Simsboro sands are thin. Lufkin, Jacksonville, and other cities in East Texas get groundwater from the Carrizo aquifer. Carrizo sandstones also thicken to the south, providing groundwater resources, for example, in Gonzales County.

There are two issues associated with pumping: how much pumping there has been through time and where it has been located. Because most pumping has not been volumetrically metered, it is generally estimated indirectly, making it a possibly large source of calibration error in this and other numerical models. Accurate estimates of water withdrawals by pumping have been found to be key to calibrating predictive groundwater models (Konikow, 1986).

We relied on the results of water-use surveys (WUS) conducted by the TWDB to estimate groundwater use in the study area. TWDB reports WUS survey results by aquifer for river basins within counties and cross-listed by cities and industries responding to the survey. Annual pumping reported by river basin was aggregated by county for each of the main water-use groups: irrigation, manufacturing, mining, municipal, power, rural domestic, and stock. Municipal, manufacturing, and power water use was associated where possible with specific wells identified by user. In some cases we had to assume locations of wells near cities. Total annual pumping by user was prorated equally among all identified wells.

The TWDB developed predictive pumpage data sets for 2000, 2010, 2020, 2030, 2040, and 2050, subdivided into seven water-use categories. The source of the data sets was water-demand projections from the regional water plans as contained in Volume II of the 2002 State Water Plan (SWP) (TWDB, 2002). TWDB compared demand projections, currently available supplies, and associated strategies for water user groups listed in the SWP for the 2000-through-2050 planning cycle. TWDB adjusted predicted pumpage estimates so that the value to be used in the various GAM models did not exceed projected demands. Records associated with groundwater use were assigned to various aquifers.

5.0 CONCEPTUAL MODEL OF GROUNDWATER FLOW

The conceptual model of flow in the Carrizo–Wilcox aquifer includes the following points (fig. 53):

- Groundwater flows primarily from outcrop recharge areas, especially where sandy soils are present in the Carrizo and Simsboro Formations (Henry and Basciano, 1979), to discharge areas in low-lying areas such as river bottomlands, to wells, and to deeper regional flow paths including cross-formational flow.
- Recharge rates vary with soil properties; there is more recharge to the Simsboro and Carrizo aquifers than to other layers of the aquifer.
- Some flow paths are relatively short and remain in the unconfined part of the aquifer. These short flow paths beneath the outcrop are from upland areas toward discharge zones in low-lying areas.
- Other flow paths pass deeper into the confined part of the aquifer. Much of the recharge to the outcrop is discharged to rivers and streams or evapotranspired.
- Most groundwater contribution to the base flow of rivers and streams crossing the outcrop is from the Simsboro and Carrizo Formations.
- The proportion of recharge that reaches the confined aquifer increases with increased pumping as discharge to rivers and streams and evapotranspiration in the outcrop area decreases.
- Cross-formational flow of groundwater within the Carrizo–Wilcox aquifer is probably directed mostly downward beneath the upland areas that cross surface-water divides and mostly upward beneath low-lying river bottomlands (Fogg and others, 1983; Dutton, 1999), although this pattern may change with groundwater withdrawal from wells.

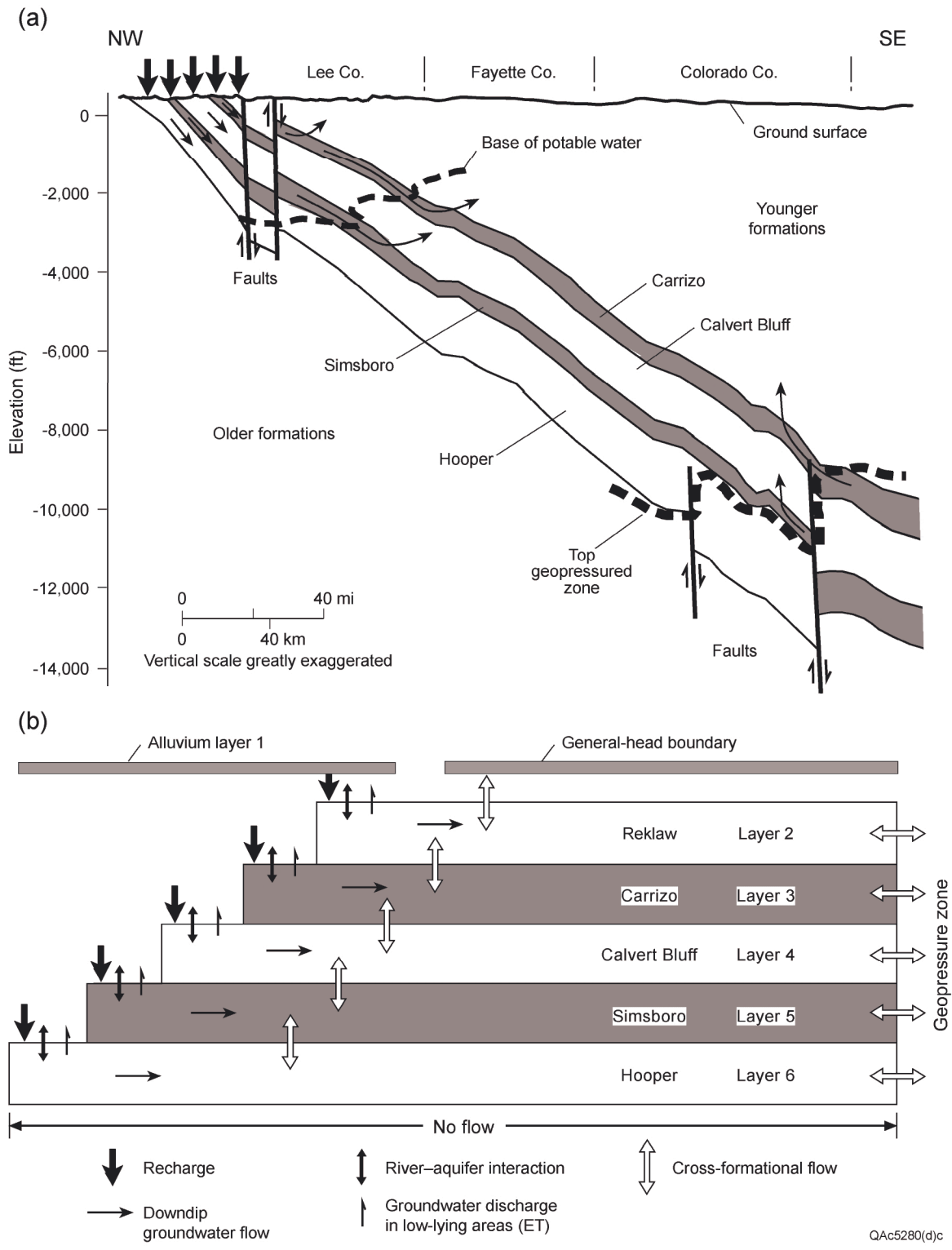


Figure 53. Conceptual model of the aquifer showing (a) hydrostratigraphic cross section with recharge and groundwater movement within and between model layers and (b) how the conceptual model translates into the computer model of the aquifer. Modified from Dutton (1999).

- Groundwater recharged in the upland outcrop areas follows arcuate flow paths moving toward the areas beneath stream valleys, where there is a tendency for upward discharge into the overlying formation.
- Some amount of water passes into the deeper part of the basin beyond the zone of freshwater. Increased concentrations of dissolved solids occurs along flow paths from the outcrop and are a result of ion exchange, dissolution of the mineral grains that make up the formation, and diffusion of residual salts out of low-permeability claystone and siltstone beds.
- Faults in the Karnes-Milano-Mexia Fault Zone disrupt the hydrologic continuity of the aquifers, probably affecting the extent of downdip, movement of groundwater, and width of the freshwater zone in the aquifers (fig. 27).
- At depths of more than 8,000 ft in the Wilcox Group there is a transition from normally pressured to geopressured conditions. The Wilcox Growth Fault Zone coincides approximately with the updip boundary of the geopressured zone. There has been a small amount of leakage of fluids upward and out of the geopressured zone into the deep part of the Carrizo–Wilcox aquifer downdip of the base of freshwater. Between the base of freshwater and the Wilcox Growth Fault Zone is a broad zone of convergence of the two flow systems where lateral flow may be very slow and where vertical flow may predominate.
- Pumping rate increased only slightly between 1950 and 1980. Total pumping rate has accelerated during the past 20 years (fig. 52). Part of the growth in groundwater withdrawal has been related to operations at lignite mines.
- Pumping rate is expected to continue to increase between 2000 and 2050, but at a slower rate than that of the past decade. Pumping will increase from the

Bryan-College Station well field but will be fairly steady from the Lufkin-Angelina County well field. Additional well fields will be established or grow because many municipalities and industries will meet future needs by drilling new wells and increasing their withdrawal from the Carrizo–Wilcox aquifer. Mining will continue to extract a significant volume of groundwater for mining operations, but after increasing in withdrawal rate during the period from 1990 through 2010, production of groundwater is expected to remain steady or to decrease.

6.0 MODEL DESIGN

Model design involves selecting the code, size of model cells, and layers used to represent the aquifer. Models represent approximations and simplifications of a natural system. Assumptions and compromises due to the conceptual model, objectives, input data, software capabilities, and schedule and budget for developing a model influence the results, accuracy, and applicability of a model. Different combinations of input data can result in different model predictions. Model design and calibration are attempts at constraining possible simulation results. We designed this model to agree as much as possible with our conceptual model of the occurrence and movement of groundwater in the central Carrizo–Wilcox aquifer.

6.1 Code and Processor

The choice of code is necessary to ensure that important processes, including recharge, interaction of groundwater and surface water, groundwater ET, pumping at wells, and boundary fluxes in the aquifer, are modeled appropriately. This study used MODFLOW-96 (Harbaugh and McDonald, 1996) to solve the flow equation according to the finite-difference method (Anderson and Woessner, 1992). MODFLOW is a widely tested and used groundwater-modeling software that includes modules needed for simulating the hydrologic processes in the aquifer. Processing MODFLOW (PMWIN version 5.3.0; Chiang and Kinzelbach, 2001) was used as the modeling interface to help load and package data into the formats needed for running simulations in MODFLOW and for looking at simulation

results. We developed and ran the model on a Dell Optiplex GX400 with a 1.8 GHz Pentium 4 Processor and 1 GB RAM running Windows 2000.

6.2 Layers and Grid

The lateral extent of the model roughly corresponds to natural hydrologic boundaries on the southwest, west, and southeast: (1) updip limit of the outcrop of host formations, (2) base or downdip limit of freshwater, and (3) presumed groundwater flow paths to the south. The southwestern boundary lies near the San Antonio River (fig. 2). The northwestern boundary is at the limit of the outcrop of the formations that make up the aquifer. The southeastern boundary coincides with the Wilcox Growth Fault Zone that roughly marks the updip limit of geopressed conditions in the aquifer (fig. 14). The northeast boundary of the study area runs from the aquifer outcrop in Van Zandt County, across part of the East Texas Basin, part of the Sabine Uplift, and then continues into the deep part of the Carrizo–Wilcox aquifer. We set an arbitrary boundary along this line. Groundwater flow paths in the vicinity of the lateral boundary on the northeastern side of the model have not remained constant during the past 20 to 50 yr owing to pumping in the vicinity of Jacksonville, Lufkin, Tyler, and other cities. Use of the northern Carrizo–Wilcox model may provide more representative results in this overlap area (fig. 3). The southwestern boundary of the northern Carrizo–Wilcox model is sufficiently distant from the pumping centers in Jacksonville, Lufkin, and Tyler that results are not affected by the boundary condition.

We defined six model layers. The bottom four layers represent the main parts of the Carrizo–Wilcox aquifer in the study area. Groundwater in the Hooper, Simsboro, Calvert Bluff, and Carrizo Formations is modeled in layers 6, 5, 4, and 3, respectively

(figs. 10, 54 through 57). In MODFLOW layers are numbered from top to bottom.

Layer 6 is the basal unit of the model; we assumed that no flow of groundwater occurs between the Hooper Formation and the underlying Midway Formation. Layer 2 represents the Reklaw Formation (fig. 58), which functions as a confining layer or aquitard between the Carrizo–Wilcox aquifer and the overlying Queen City aquifer. Layer 2 in the model has the role of applying a boundary condition across the top of the model. The uppermost layer 1 represents alluvium in the valleys of the Colorado, Brazos, and Trinity Rivers (fig. 59). Some of the active cells assigned in layers 2 through 5 are beneath the alluvium of layer 1 but above the uppermost bedrock layer. Using MODFLOW, we found it necessary to create additional active cells in these layers to allow a connection between the alluvium modeled in layer 1 and the underlying bedrock layer. These additional cells are apparent in figures 55 through 58 as narrow northwestward extensions of the active cells of model layers.

The model grid consists of 273 columns and 177 rows of square model cells that measure 1 mi on a side. This grid-cell size is considered small enough to reflect the density of data for building and calibrating the model, while large enough for the model to be manageable. Uniform grid-cell dimensions simplify the use of digital mapping and spreadsheets to input data into the model. There are 289,926 cells in the 273-column \times 177-row \times 6-layer model. Only 120,477, or about 42 percent, of these are active cells representing the aquifer at which calculations are made. Layer 1 has only 383 active cells, whereas layers 2 through 6 have more than 21,000 active cells each (21,857 in layer 2, 22,602 in layer 3, 24,560 in layer 4, 25,067 in layer 5, and 26,008 in layer 6). Cell thickness represents the thickness of model layers (for example, figs. 23 through 26).

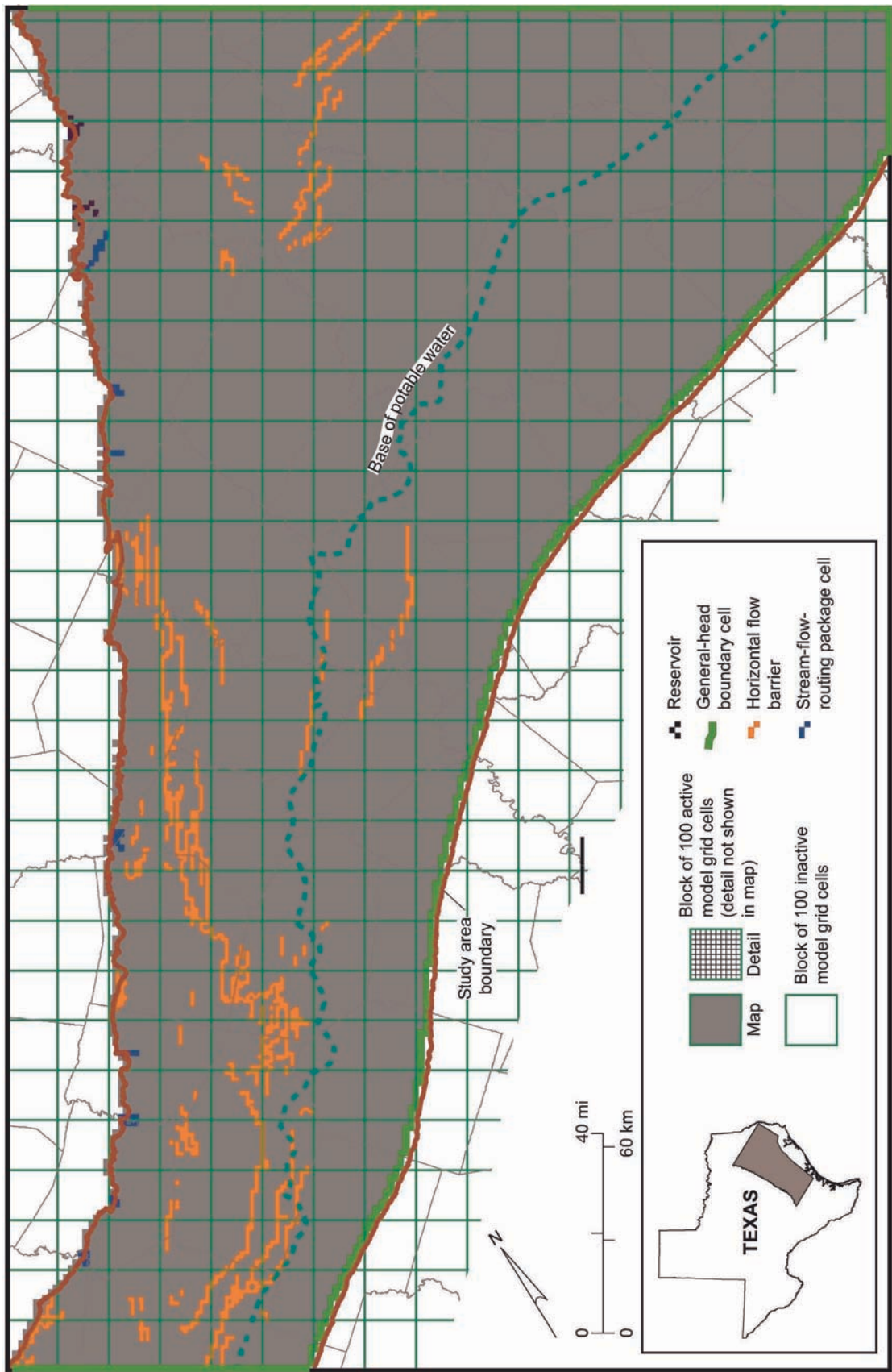


Figure 54. Location of active cells in model layer 6, representing groundwater in the Hooper Formation, and the position of boundary cells.

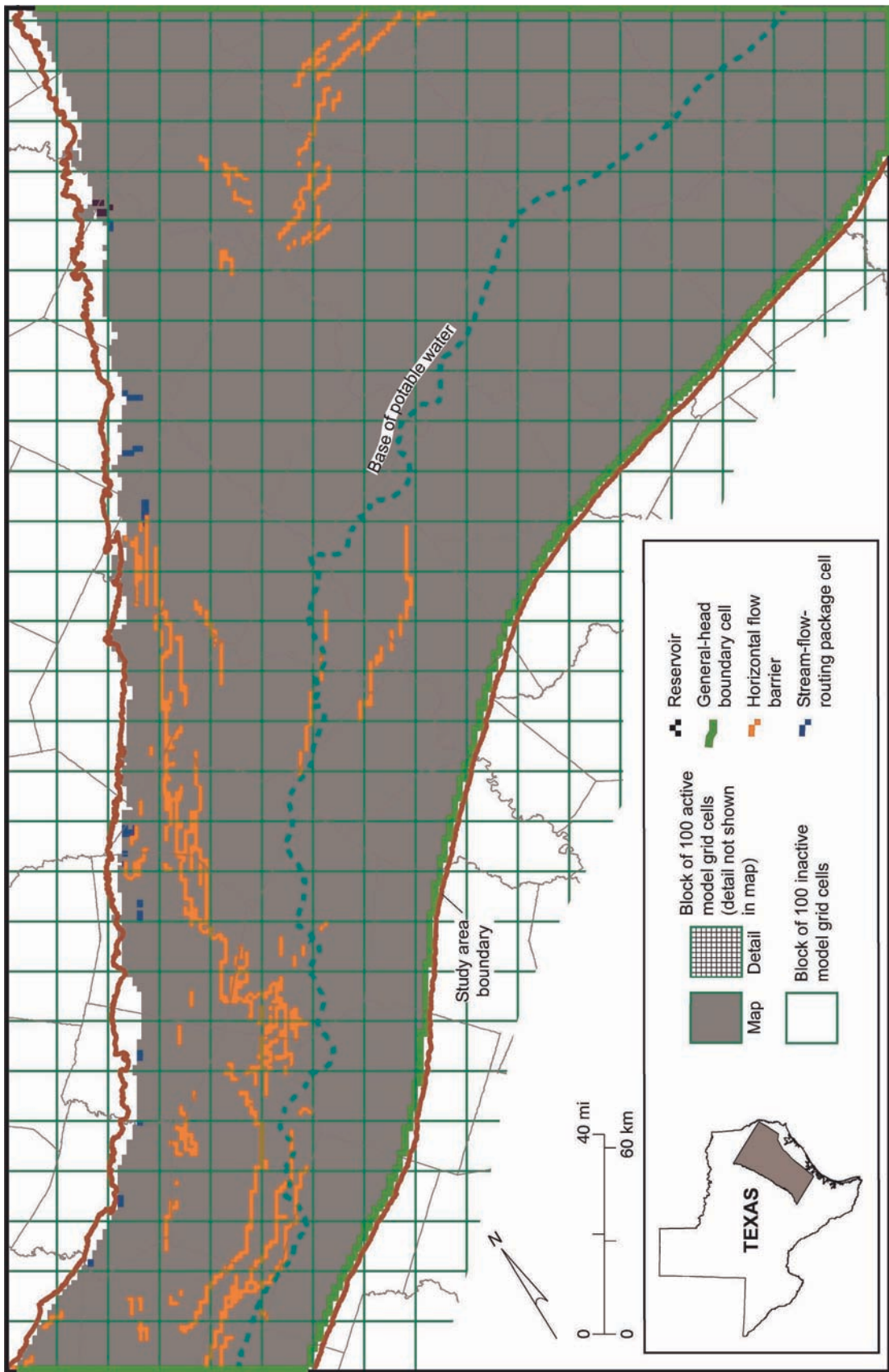


Figure 55. Location of active cells in model layer 5, representing groundwater in the Simsboro Formation, and the position of boundary cells.

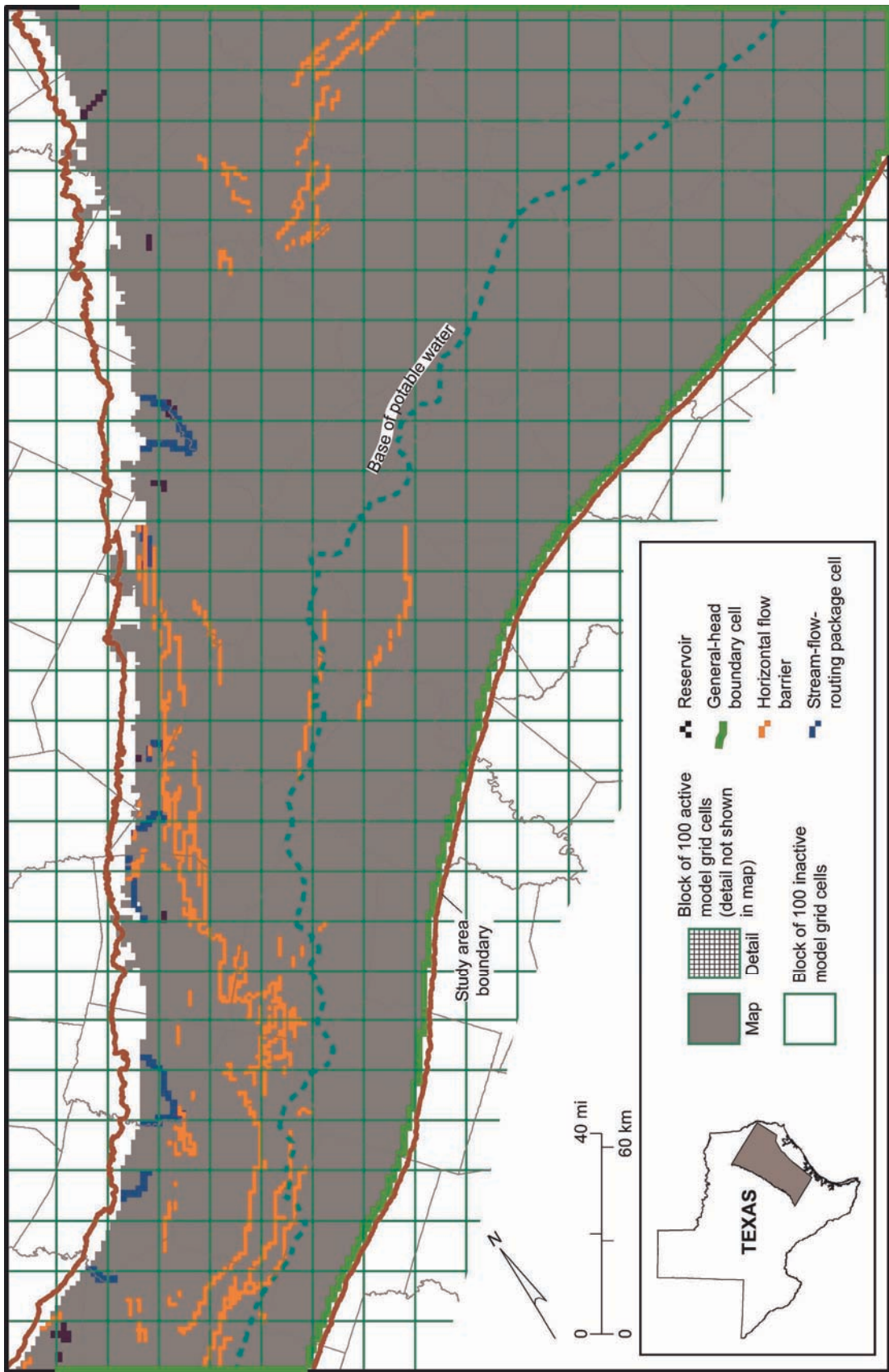


Figure 56. Location of active cells in model layer 4, representing the Calvert Bluff Formation, and the position of boundary cells.

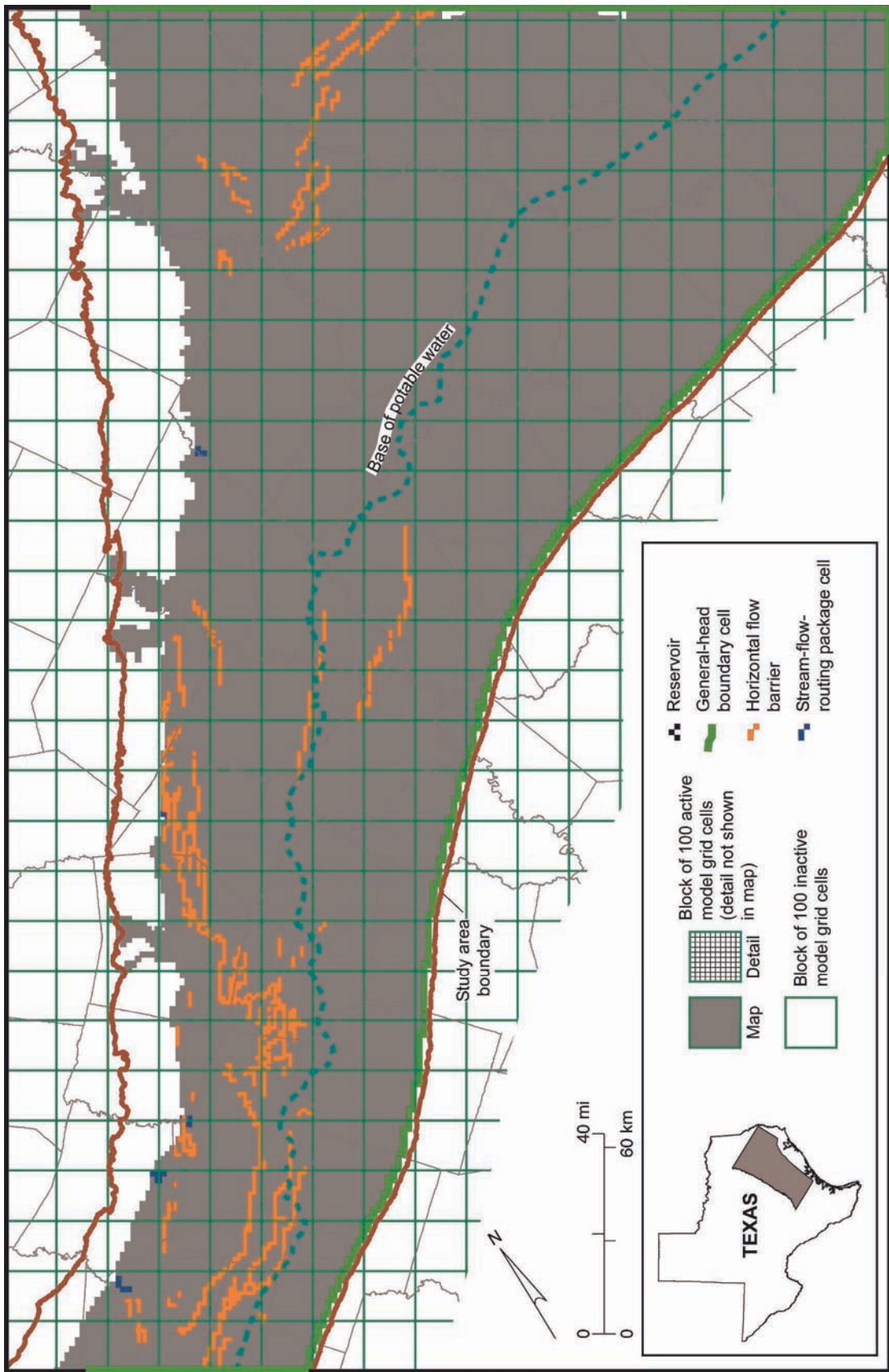
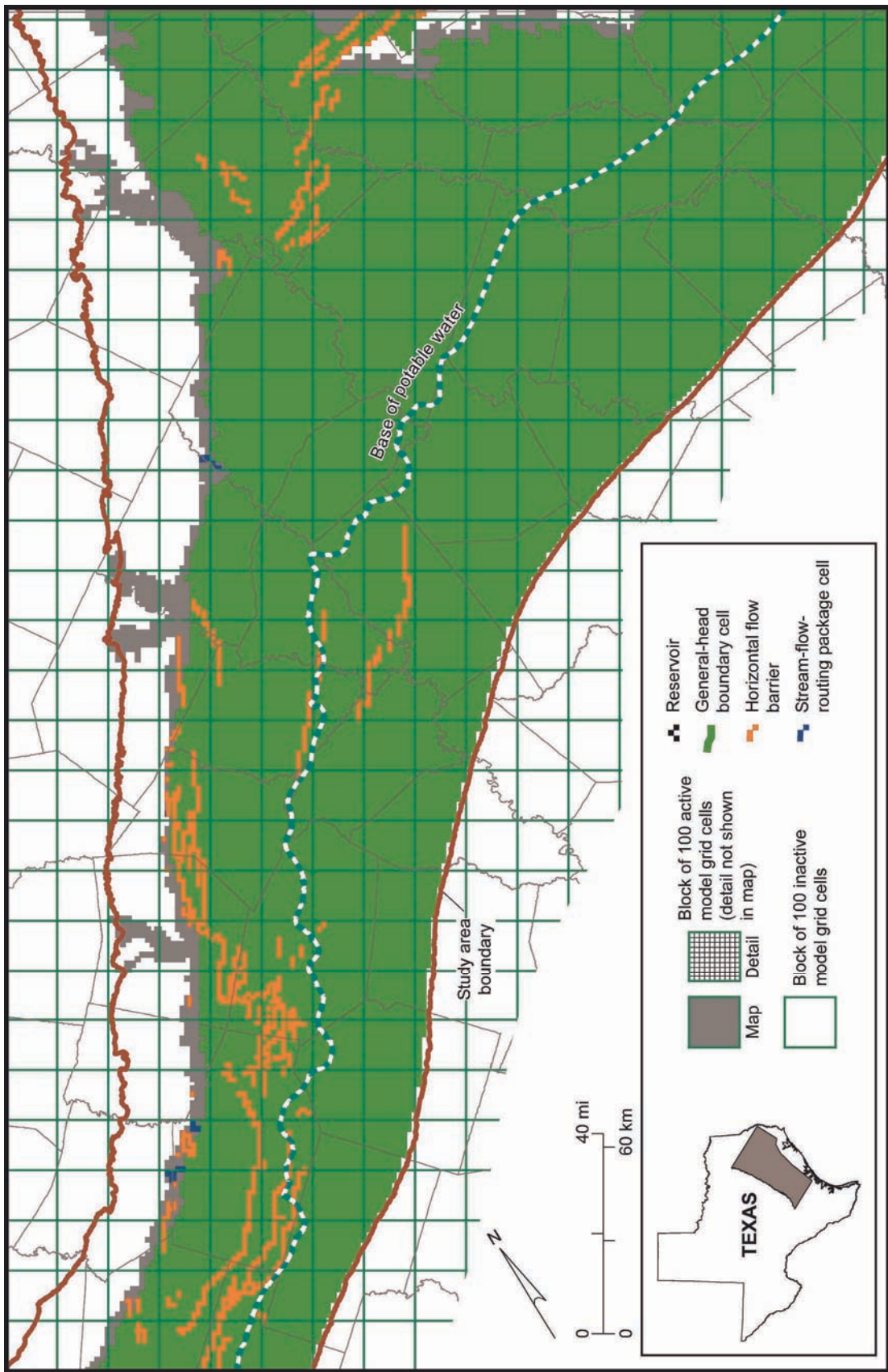


Figure 57. Location of active cells in model layer 3, representing the Carrizo Formation, and the position of boundary cells.



QA42039c

Figure 58. Location of active cells in model layer 2, representing the Reklaw Formation, and the position of boundary cells.

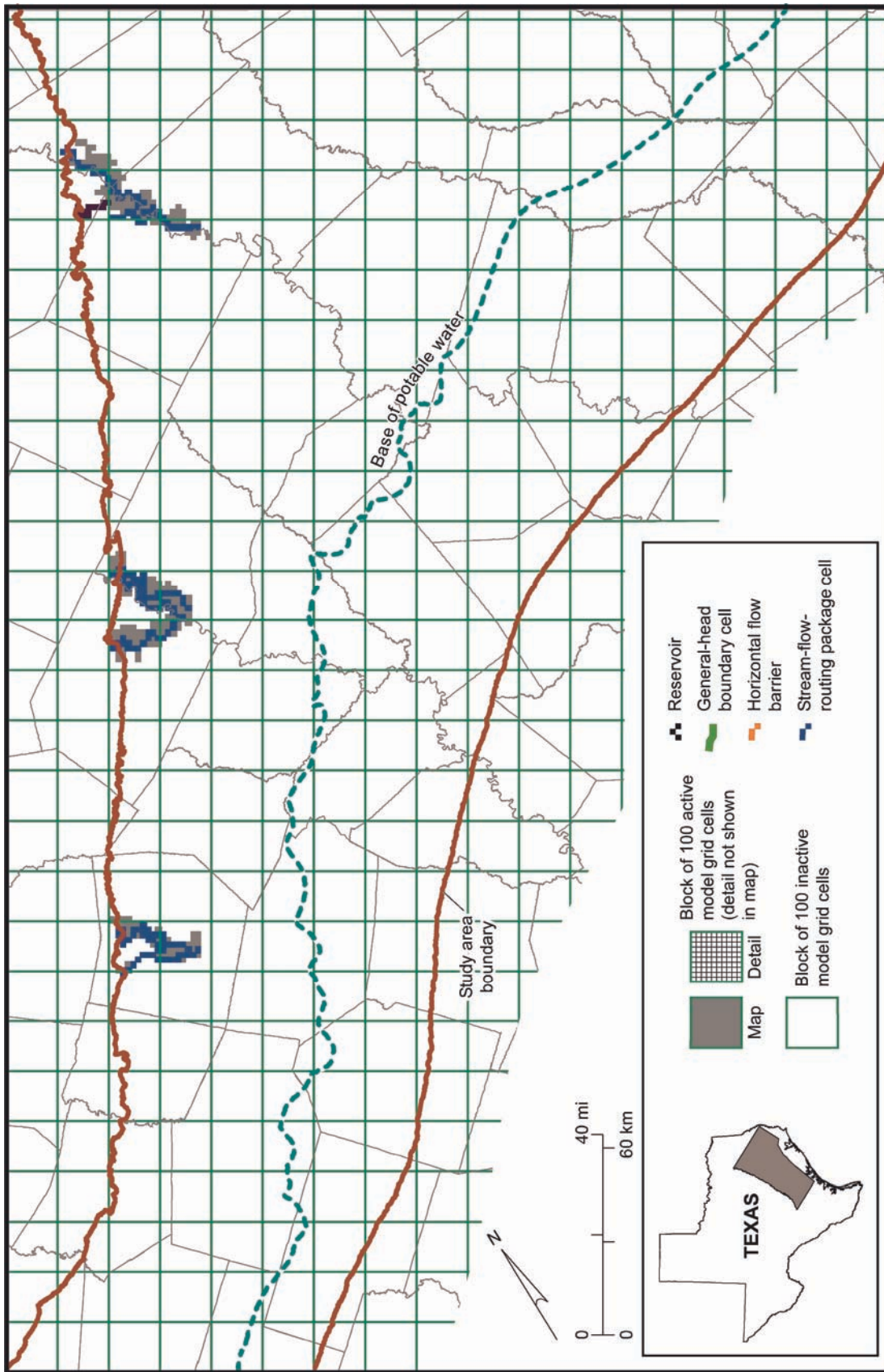


Figure 59. Location of active cells in model layer 1, representing alluvium in the Colorado, Brazos, and Trinity River systems, and the position of boundary cells.

Rows of the model were aligned parallel to the strike of the Wilcox outcrop on the northwestern side of the study area. The model grid origin (X_0 , Y_0) is located at GAM coordinates of 5,382,716 ft Easting and 18,977,220 ft Northing with the x axis rotated 58° positive or counterclockwise. The geographic projection parameters for the model grid and hydrogeologic data are given in table 9.

6.3 Boundary Conditions

Boundary conditions account for movement of water into and out of the model domain and represent the natural flow and pumping in the aquifer. Boundary conditions for the Carrizo–Wilcox aquifer are applied in the model using standard modules in MODFLOW. Boundary values were applied to all six faces of the model (top, bottom, and sides). Boundary conditions for the top or upper surface of model layers variously included MODFLOW's recharge, stream-flow routing, evapotranspiration (ET), and general-head boundary (GHB) packages. The bottom of the model was set as a no-flow boundary; we assumed that there is no appreciable exchange of groundwater between the Hooper and the underlying Midway Formations (fig. 10), both of which have a large proportion of low-permeability claystone. The updip (northwestern) boundary of each layer was also defined as a no-flow boundary. The GHB boundary package was applied to the downdip (southeast), northeast, and southwest sides of the model. The horizontal flow barrier and well packages of MODFLOW were applied internal to the model.

Table 9. Projection parameters for the model grid and hydrogeologic data.

Projection	Albers equal area conic
Units	Feet
Datum	North American Datum (NAD) 1983
Spheroid	GRS80
Central meridian	-100.00000
Reference latitude	31.25000°
First standard parallel	27.00000°
Second standard parallel	35.00000°
False easting	4921250.00000 (U.S. survey feet)
False northing	19685000.00000 (U.S. survey feet)

6.3.1 Recharge

Recharge was applied to the outcrop of each formation represented in the model, including alluvium in layer 1 and the Reklaw Formation in layer 2, as well as the parts of the Carrizo–Wilcox aquifer in layers 3 through 6. The procedure for calibrating steady-state recharge rates focused on scaling recharge rate for each outcrop cell between a minimum and maximum rate for each layer (table 10). We initially varied recharge rate also with respect to precipitation in the steady-state model. Model calibration showed, however, that higher recharge rates associated with higher precipitation rates in the north and northeast parts of the model area resulted in water levels that were simulated to be higher than measured. Recharge rate in each cell for the steady-state period (RST_{cell}) was calculated by

- (1) Estimating annual average precipitation ($P_{aver,cell}$) in each cell.
- (2) Mapping vertical hydraulic conductivity of soil (K_s ; fig. 41).
- (3) Deriving scaled soil hydraulic conductivity (K_{ss}) by linearly scaling K_s from 0 to 1, where 1 corresponds to a K_s value of 1.75 ft/d and above (every $K_s > 1.75$ ft/d is set to 1.75 ft/d). The threshold value of 1.75 ft/d was determined by examining the statistical distribution of soil conductivities.
- (4) Making initial estimates of the maximum and minimum recharge rates (R_{min} and R_{max} , respectively) for each layer. Minimum and maximum recharge rates assigned to alluvium (layer 1) cells are equal to those calculated for the underlying formation. Soil hydraulic conductivity used in the procedure for layer 1, however, is the value calculated for the soil developed on alluvium. Maximum and minimum recharge rates were adjusted during model calibration. Recharge applied to layer cells can be less than R_{min} because of the scaled soil hydraulic conductivity ($K_{ss} \leq 1$). R_{min} is the

Table 10. Calibrated values of minimum and maximum recharge rate by layer.

Unit	Layer	R_{min}^* Minimum recharge rate (inches/yr)	R_{max}^* Maximum recharge rate (inches/yr)
Reklaw	2	0.3	0.4
Calvert Bluff	3	3.33	3.91
Carrizo	4	0.8	0.8
Simsboro	5	2.6	3.9
Hooper	6	1.2	1.2

* Both R_{min} and R_{max} are maximum values; that is, for example, R_{min} is the largest minimum recharge rate that would be assigned to a cell in the layer. Few cells are assigned these upper-limit values because of scaled soil hydraulic conductivity.

maximum recharge that can be assigned to a cell that has the least precipitation in a layer. R_{max} is the maximum recharge that can be assigned to a layer's cell with the greatest precipitation.

- (5) Finding the slope and intercept (u and v , respectively) of the line that relates recharge rate $R_{s,cell}$ for each cell to average precipitation for the same cell,

$$R_{s,cell} = uP_{aver,cell} + v, \quad (5)$$

by simultaneously solving the two equations (6) and (7) that relate minimum and maximum recharge to minimum and maximum precipitation:

$$R_{min} = uP_{min} + v \quad (6)$$

and

$$R_{max} = uP_{max} + v \quad (7)$$

Minimum recharge rate corresponds to the whole outcrop minimum precipitation ($P_{min}=28.7$ inch/year), whereas maximum recharge rate corresponds to the whole outcrop maximum precipitation ($P_{max}=51.3$ inch/year). Because the steady-state model represents a long period of time (at least 100 yr), we assigned recharge using a long-term average of precipitation. Average long-term (1940 through 1997) precipitation was extrapolated for each model cell from National Weather Service station data. Station coverage was not as uniform prior to 1940.

- (6) Multiplying scaled recharge rate $R_{s,cell}$ by scaled soil hydraulic conductivity K_{SS} to obtain final cell recharge rate at steady State RST_{cell} :

$$RST_{cell} = K_{SS} \times R_{s,cell} \quad (8a)$$

$$RST_{cell} = K_{SS} \times (uP_{aver,cell} + v) \quad (8b)$$

$$RST_{cell} = K_{SS} \left(\frac{(P_{aver,cell} - P_{min})(R_{max} - R_{min})}{P_{max} - P_{min}} + R_{min} \right) \quad (9)$$

Some K_{SS} values are as low as 10^{-3} or 10^{-4} ; these cells are given small recharge rates.

For the transient model, recharge rate calculated for each outcrop cell (RTR_{cell}') differed according to each year's precipitation. Annual and monthly recharge rates were determined from scaled soil hydraulic conductivity and the difference between the actual and average precipitation rate. Transient model calibration involved adjusting the dimensionless scaling coefficient (q) relating change in scaled recharge rate $R_{s,cell}'$ and change in precipitation rate:

$$R_{s,cell}' = uP_{aver,cell} + v + q(P_{cell} - P_{aver,cell}) \quad (10a)$$

$$RTR_{cell}' = K_{SS} \times R_{s,cell}' \quad (10b)$$

$$RTR_{cell}' = K_{SS} (uP_{aver,cell} + v + q(P_{cell} - P_{aver,cell})) \quad (10c)$$

Years with higher precipitation rates were assumed to have higher recharge rates. To ensure that assigned recharge rate was positive, we set a lower limit of 0.1 inch/yr (2.3×10^{-5} ft/day) to the scaled recharge rate $R_{s,cell}'$. The actual value assigned to the model cell (RTR_{cell}) was the greater of either the calculated recharge rate or the minimum recharge of 0.1 inch/yr \times the scaled soil conductivity,

$$RTR_{cell} = \max(RTR_{cell}', 2.3 \times 10^{-5} K_{SS}) \quad (11)$$

where RTR_{cell}' , $R_{s,cell}'$, and K_{SS} are expressed in ft/day. The scaling coefficient (q) was determined by calibration procedure to be 0.06. The higher q is, the higher the range of recharge for a given cell.

For the predictive model we assigned a constant recharge rate for normal years using an average precipitation calculated from 1960 through 1997 data, excluding the effect of the

1950s drought of record from the calculation of the normal year recharge rate. Recharge rate was assigned to future drought years using equations 10 and 11 according to the difference between precipitation in those drought years and the average (1960 through 1997) precipitation rate. Monthly recharge during the drought years was kept uniform. We assumed that drainage from the unsaturated zone to the water table does not cease during a drought year.

6.3.2 Interaction of Surface Water and Groundwater

6.3.2.1 Stream-Flow Routing

All layers in this model include some number of cells in which streams or reservoirs are simulated. Both the stream-flow routing package and the reservoir package in MODFLOW use similar algorithms to simulate interaction between groundwater and surface water. For a given model cell, a water-surface elevation is assigned to the stream or reservoir, and this water level is compared with the calculated head in the aquifer. If the water level in the stream or reservoir is greater than the head in the aquifer, water will flow from the surface-water body into the aquifer as a function of the conductance of the bed sediments and the difference in heads. If the head in the aquifer is greater than the water level of the surface-water body, water will flow from the aquifer to the stream.

MODFLOW's stream-flow routing package was used to represent the interaction of groundwater and surface water in streams and river channels. The stream-flow routing package keeps track of the volume of surface water assumed to be in the river channel moving from cell to cell from upstream to downstream. Discharge from the aquifer adds to the volume of flow tracked in the river course. Water that moves from the river to the

aquifer is subtracted from the surface-water flow. The stream-flow routing package precludes water loss from exceeding the amount of water in the stream reach.

Three parameters describe the movement of water in and out of model cells: river stage, river-bottom elevation, and riverbed hydraulic conductance. We used data on surface-water stage heights from USGS gaging stations to define stream stage in the model, rather than selecting the option in the stream-flow routing package of calculating stream stage in reaches from Manning's equation. Hydraulic conductance is a function of the length, width, thickness, and hydraulic conductivity of the alluvium that transmits water between the channel and the aquifer (Harbaugh and McDonald, 1996). Length of individual stream reaches in each grid cell was measured on 1:24,000 scale USGS Topographic Quadrangle maps using an ArcView® utility. Width was estimated using several methods. For major rivers, published USGS data on river width at gaging stations (Slade, 2002) was referenced; an average of the widths from the nearest upstream and downstream gages was used throughout the outcrop reach. For smaller streams in which the width varied significantly throughout the reach, widths were increased from a few feet in the headwaters to a few tens of feet at the downstream end. Hydraulic conductivity and streambed thickness were initially estimated at one ft/d and 1 ft, respectively. Streambed conductance, assumed to be uniform along the length of any stream within each layer, was adjusted during model calibration to improve the match between simulated and targeted estimates of base flow. Streambed conductance was set over the Simsboro and Carrizo aquifers (layers 5 and 3, respectively) to values greater than those set over the Hooper, Calvert Bluff, and Reklaw aquitards (layers 6, 4, and 2, respectively). Adjustments were made for those cells that initially simulated losing reaches because, overall, the rivers are gaining across the width of

the outcrop of the Carrizo–Wilcox aquifer. Initial values of conductance also incorporated representative values of alluvium thickness. Stream flow is most sensitive to streambed conductance in a losing cell but not very sensitive to even an order-of-magnitude change in conductance in gaining cells.

Three sets of calibration targets were developed for evaluating how well the model represents interaction of surface water and groundwater. One set uses gaged information from Cibolo Creek, East Yegua Creek, Guadalupe River, Little Brazos River, Middle Yegua Creek, Navasota River, San Antonio River, San Marcos River, Tehuacana Creek, and Upper Keechi Creek. A second set uses results of low-flow studies on Cibolo Creek and the Colorado River. The third calibration set, based on the unit base-flow rate unitized per watershed in the outcrop of the Carrizo–Wilcox aquifer, is applied to the Brazos and Trinity Rivers for which gaged data for the study area were unavailable. Base flow is contributed mainly from the Simsboro and Carrizo aquifers. The unitized rates were adjusted to represent the watershed area crossing the outcrop of these aquifers.

6.3.2.2 Surface-Water Reservoirs

Any grid cell with more than half the cell area covered by surface water was represented in MODFLOW's reservoir package (figs. 54 through 59). Reservoir representation assumes that the entire grid cell is subject to inundation (that is, no partial inundation is simulated), so the length and width of reservoir cells default to the full dimensions of the grid cell. Average land-surface elevations were taken from topographic maps, whereas average water surface in the reservoirs was obtained from USGS hydrologic records. The same value of reservoir conductance was assigned to all reservoirs; there were insufficient data to do otherwise. As previously mentioned, an indirect estimate of reservoir

leakage at Lake Limestone provided a basis for assuming a reservoir conductance of 0.00001 ft/day.

6.3.3 Evapotranspiration

MODFLOW's evapotranspiration (ET) package was used, along with the stream-flow routing package, to simulate natural discharge of groundwater from the unconfined parts of the Carrizo–Wilcox aquifer (layers 6 to 3), the Reklaw aquitard (layer 2), and alluvium in layer 1. The parameters of the ET package in MODFLOW are the maximum ET rate, the elevation at which the maximum rate is applied (the ET surface), and the depth below the top of a cell at which the ET is assumed to be zero (extinction depth). Whereas the ET package is turned on for each cell representing the outcrop of a layer, groundwater discharge is indicated only if the elevation of the simulated water level is higher than the elevation of the extinction depth.

Initial values of the maximum ET rate were set to the average net lake evaporation rate (fig. 9) and varied across the outcrop. During calibration we adjusted a cutoff value to set a minimum value of 14 inches/yr for the maximum ET rate. The cutoff value applied mainly to the northeast section of the model in the Sabine Uplift area. Extinction depth was adjusted during calibration. The optimal value of extinction depth varies with cell thickness and depth to water in the cell. In the conceptual model, ET removal of groundwater occurs mainly in the river bottomlands and not across the upland surface-water divides. The net evaporation rate (pan evaporation rate minus annual precipitation) was used instead of a pan evaporation rate because the former better represents groundwater withdrawal by evapotranspiration once short-term infiltration in the unsaturated zone has been removed.

6.3.4 General-Head Boundary

The general-head boundary (GHB) package of MODFLOW is used to account for movement of water into and out of model cells. Two parameters are specified in the GHB package: GHB hydraulic conductance and hydraulic head (GHB head) at the boundary. The GHB hydraulic conductance is the proportionality constant between the flow and the difference in simulated and boundary hydraulic heads. By analogy to Darcy's Law, the proportionality constant for the northeast and southwest boundaries may be envisioned as the product of hydraulic conductivity, cell thickness, and row width, divided by column width. Thus, initial values of GHB conductance for the northeast and southwest boundaries were set equal to transmissivity. Calibration was made in the transient model to determine what value of GHB conductance gives a good calibration between simulated and observed water levels near the northeast and southwest boundaries. In transient model calibration, we determined the distance from the model edge at which simulated water levels did not respond as we adjusted GHB conductance from 0 to very large. As discussed later, the transient model responds more than the steady-state model to GHB conductance on the northeast and southwest boundaries because GHB heads there account for the effect of drawdown from groundwater withdrawal outside of the model. We interpolated transient GHB heads from maps of observed water levels in the Carrizo-Wilcox aquifer layers along the northeast model boundary. GHB conductance and transmissivity have units of length-squared/time (L^2/t).

GHB boundary cells were assigned to that part of layer 2 representing the nonoutcrop part of the Reklaw Formation to represent the exchange of groundwater between the Carrizo-Wilcox and Queen City aquifers. GHB head values represent the water level in the overlying Queen City aquifer. Values of the GHB conductance applied to layer 2 represent

the vertical hydraulic conductivity of the Reklaw aquitard. Initial GHB conductance values for layer 2 were a uniform 10^{-4} ft²/d. Water levels in the Queen City aquifer (fig. 30) have remained fairly constant during the past 50 yr, as previously discussed. Water levels are higher than in the Carrizo–Wilcox aquifer across the upland areas and lower than in the Carrizo–Wilcox aquifer in the river valleys.

The GHB package was also assigned along the downdip northeast and southwest boundaries of model layers 6 through 3, representing the Hooper aquitard, the Simsboro aquifer, the Calvert Bluff aquitard, and the Carrizo aquifer (figs. 54 through 57, respectively). The downdip boundary represents the exchange of groundwater across the Wilcox Growth Fault Zone between normally pressured and geopressured zones. For the steady-state model, we set the GHB head along the downdip boundary to match the mapped values of head shown in figures 28 and 29. The same GHB head was applied to each of these four layers. GHB conductance was assigned by trial and error. Very low values of GHB conductance, for example, less than 0.001 ft²/d, make the boundary behave as a no-flow boundary. Values of approximately 0.01 to 0.5 ft/d vary linearly along the downdip boundary from southwest to northeast. This range allows enough inflow of water from the boundary for the model to roughly match the updip-directed gradient in hydraulic head mapped across the deep Wilcox Group (figs. 28, 29). It is likely that fluid levels along the boundary have decreased locally in compartmentalized reservoirs during the past few decades owing to the withdrawal of natural gas from gas reservoirs.

The GHB boundary along the southwest side of the model was kept unchanged for the calibration and verification period representing pre-2000 conditions. This lack of change is justified by the small changes in water levels recorded in that part of the model area. The GHB boundary imposes a downdip gradient in water level in the aquifer. We varied the

GHB head assigned to the northeastern boundary of the model, accounting for the presence of well fields with large amounts of pumping just to the northeast of the study area, for example, at Tyler in Smith County. We projected predevelopment, 1980, 1990, and 2000 water-level maps for the Simsboro and Carrizo aquifers onto the northeastern boundary. We used linear interpolation to assign GHB heads for every model stress period. The GHB head for layer 4 was set to the average of the GHB heads in layers 3 and 5. Parameters for the GHB package in the transition between the hydropressured boundaries on the southwest and northeast sides of the model and the geopressured boundary on the downdip side of the model were assigned by linear interpolation.

6.3.5 Horizontal-Flow Barrier

The Karnes-Milano-Mexia Fault Zone breaks up the continuity of aquifer layers between the outcrop and subsurface. Rather than attempt to vary the hydrologic properties of the individual layers of the model, we used the horizontal-flow barrier (HFB) package of MODFLOW to impede lateral movement of groundwater. Between adjacent model cells (Hsieh and Freckleton, 1993), the HFB package specifies a hydraulic characteristic term that is equal to either hydraulic conductivity divided by thickness of the barrier material (units of $1/t$) for an unconfined (variable transmissivity) zone or transmissivity divided by the thickness of the barrier material (units of L/t) for a confined (constant transmissivity) zone. The HFB boundary was applied both to the updip normal faults with down-to-the-coast displacement, where blocks of Calvert Bluff, for example, are juxtaposed adjacent to high-permeability Simsboro material, and to the antithetic faults that form the southeastern side of the grabens typical of this extensional fault zone. The HFB package was applied to all layers (figs. 54 through 58) except for layer 1, representing alluvium. Dutton (1999) also used the

HFB package and varied HFB hydraulic characteristic proportional to the amount of throw on the several major fault strands included in his model. This model of the central part of the Carrizo–Wilcox aquifer includes a greater number of HFB cells; uniform conductances were applied regardless of fault displacement. The hydraulic characteristic of the fault zone was adjusted during model calibration. Initial estimates of the HFB hydraulic characteristic were 2×10^{-4} ft/d for cells in the confined part of the Carrizo–Wilcox aquifer, and 2×10^{-5} d⁻¹ for cells in the unconfined part.

6.3.6 Wells

Groundwater withdrawal for municipal, manufacturing, and power uses was associated with specific wells identified by the water user group. In some cases we had to assume a location of a well, especially for the predictive model. Total annual pumping by user group was prorated equally among all identified wells for that group. Figure 60a, b shows the allocation of pumping assigned to the model to represent municipal and manufacturing water supplies in 2000.

Pumping for irrigation, mining, rural domestic, and stock uses was distributed areally on the basis of land use and other information (fig. 60c–f). Irrigation was distributed mainly on the basis of Geographic Information Systems (GIS) coverages from 1989 and 1994 TWDB surveys. Some irrigated tracts of land are identified in both surveys; some land is designated as irrigated on only one survey. We made the assumption that any parcel of land identified in either survey constituted an area where groundwater was extracted for irrigation. We excluded areas where identified irrigation land falls within boundaries of municipal (population more than 500) areas. Some counties have listed irrigation use but no land

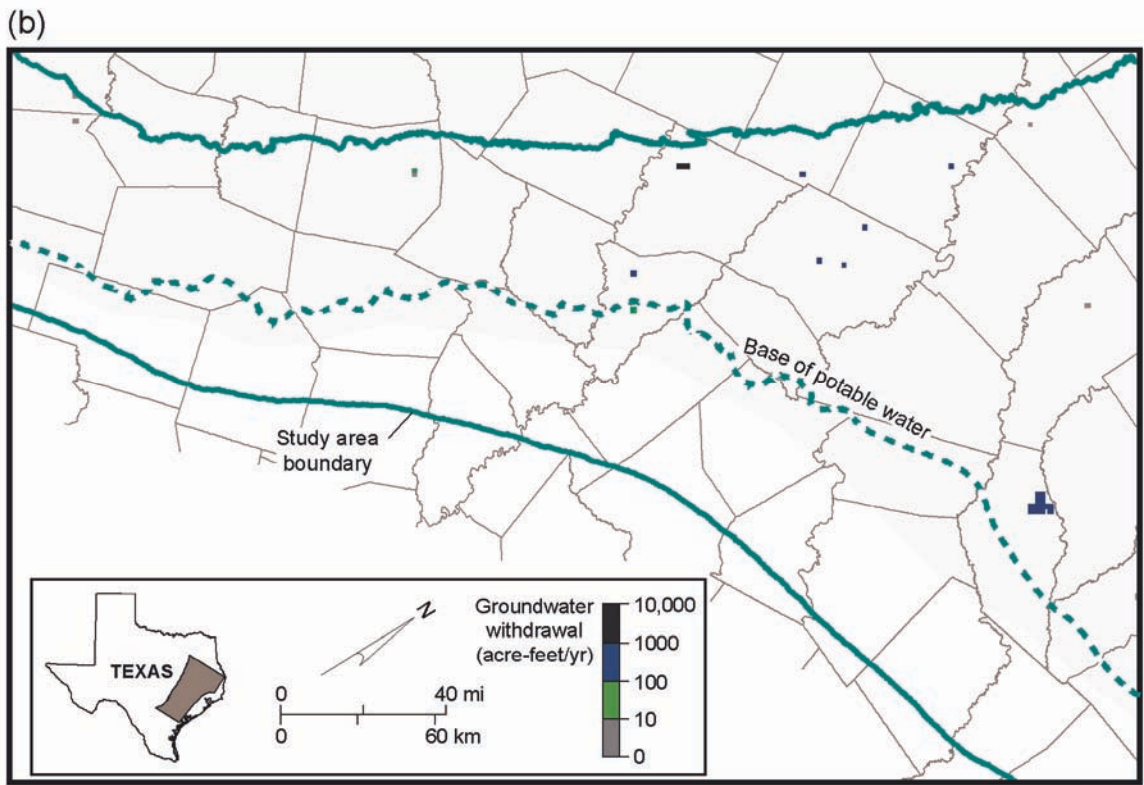
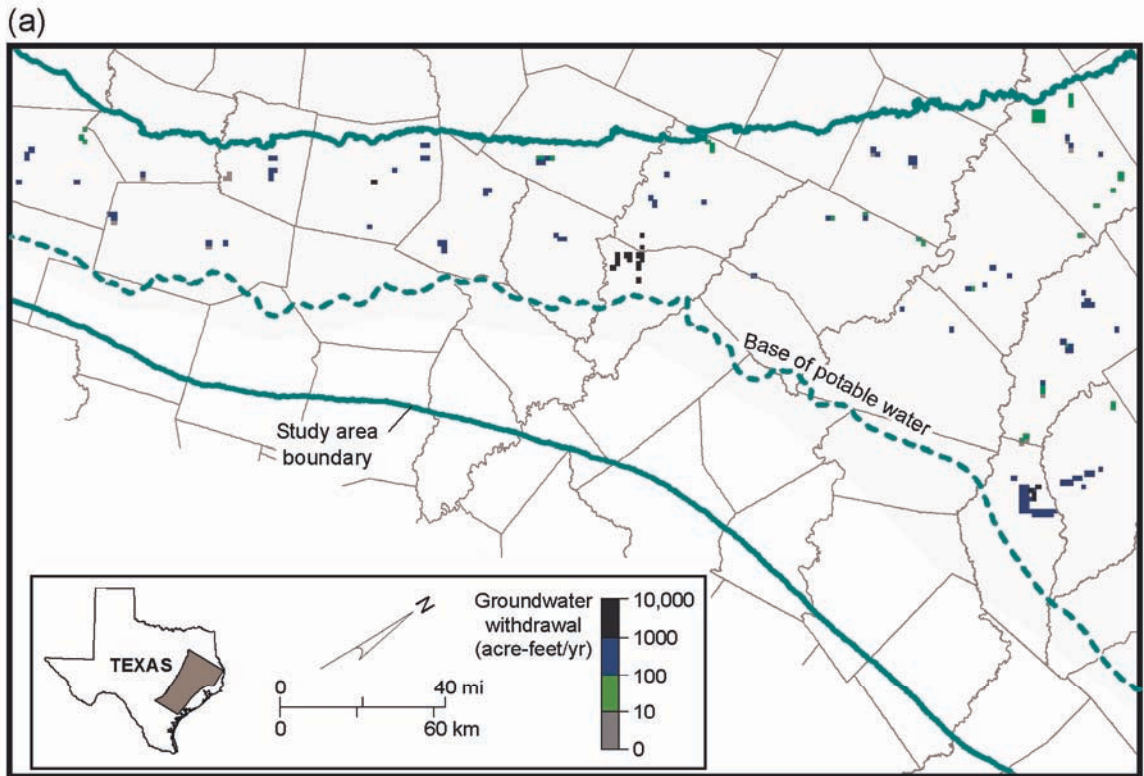
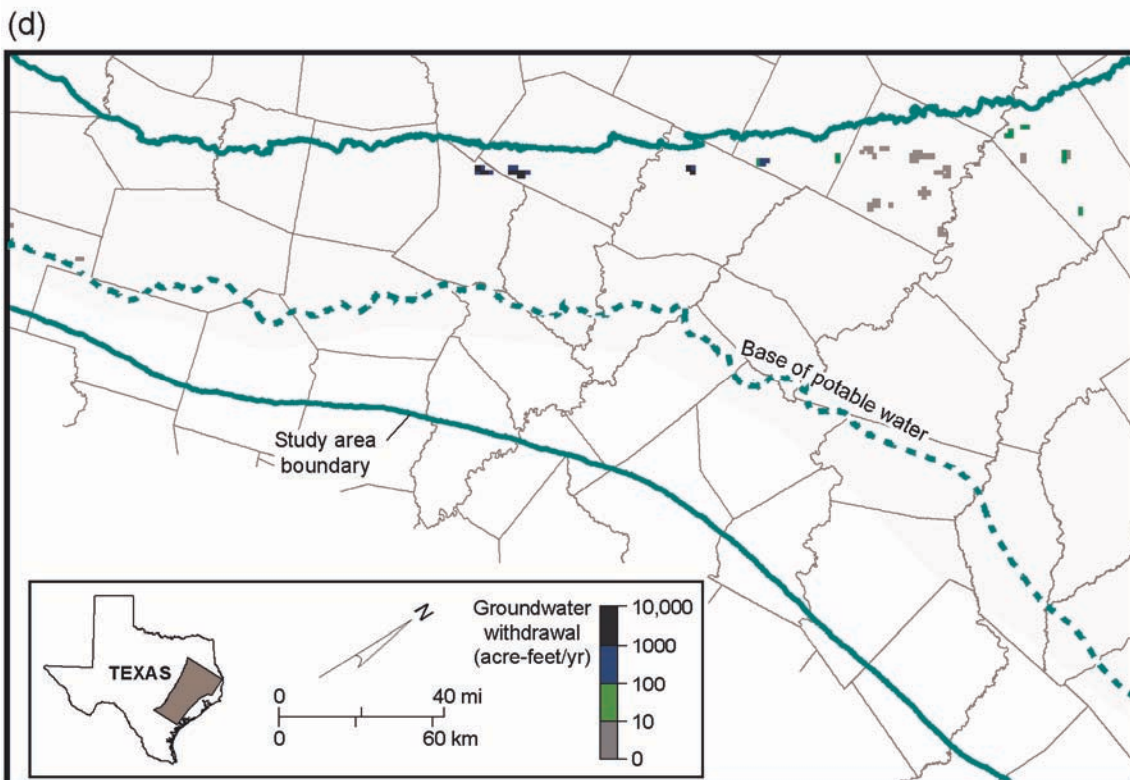
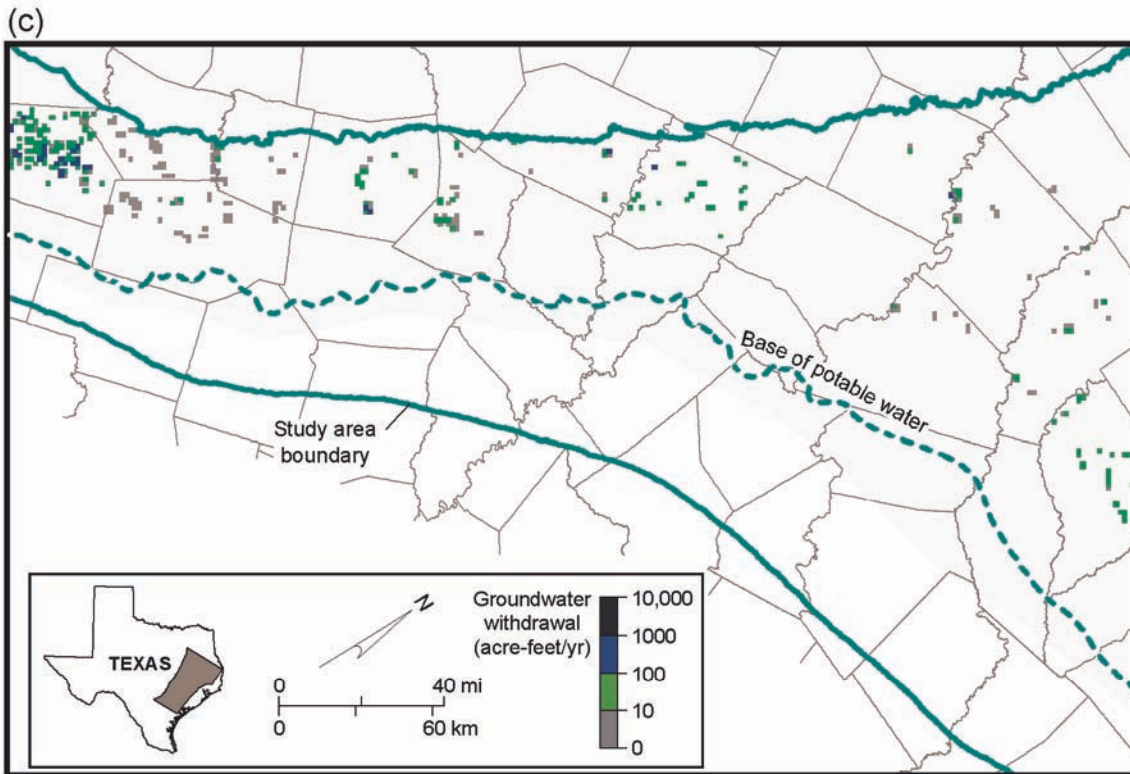


Figure 60. Distribution of groundwater withdrawal in 2000 for (a) municipal and (b) manufacturing and power supplies.



QAd2287(b)x

Figure 60 (continued). Distribution of groundwater withdrawal in 2000 for (c) irrigation supply and (d) mining-associated activity.

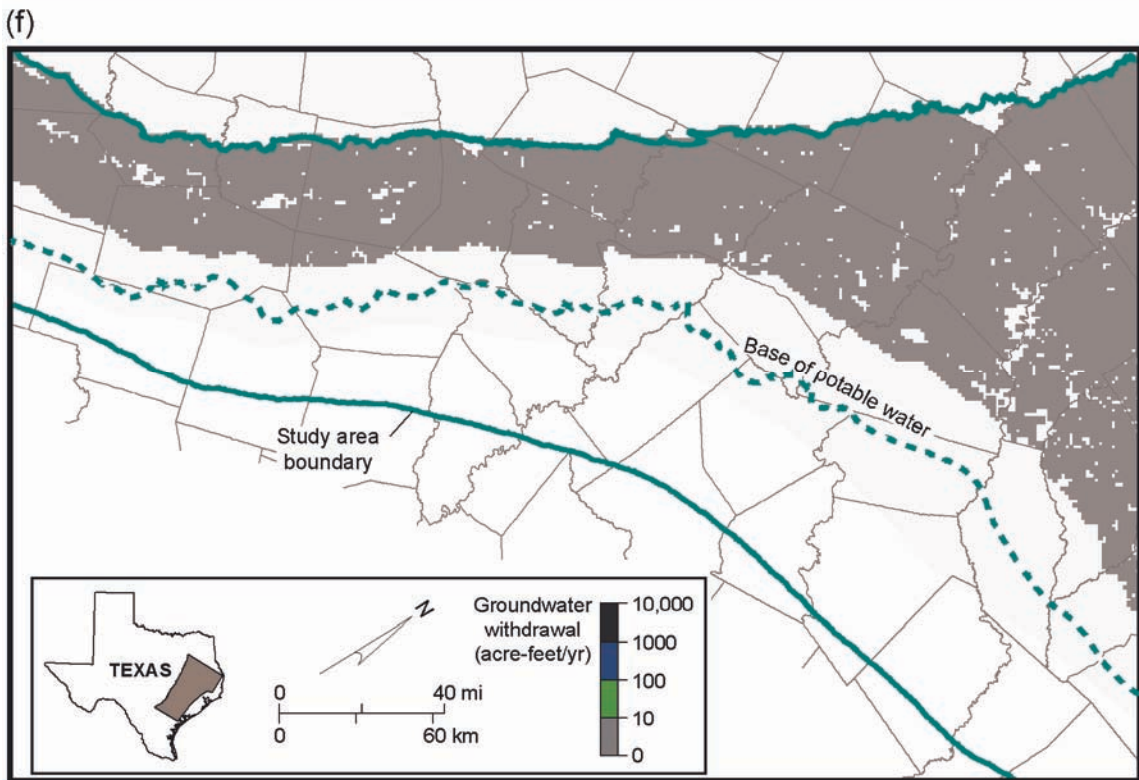
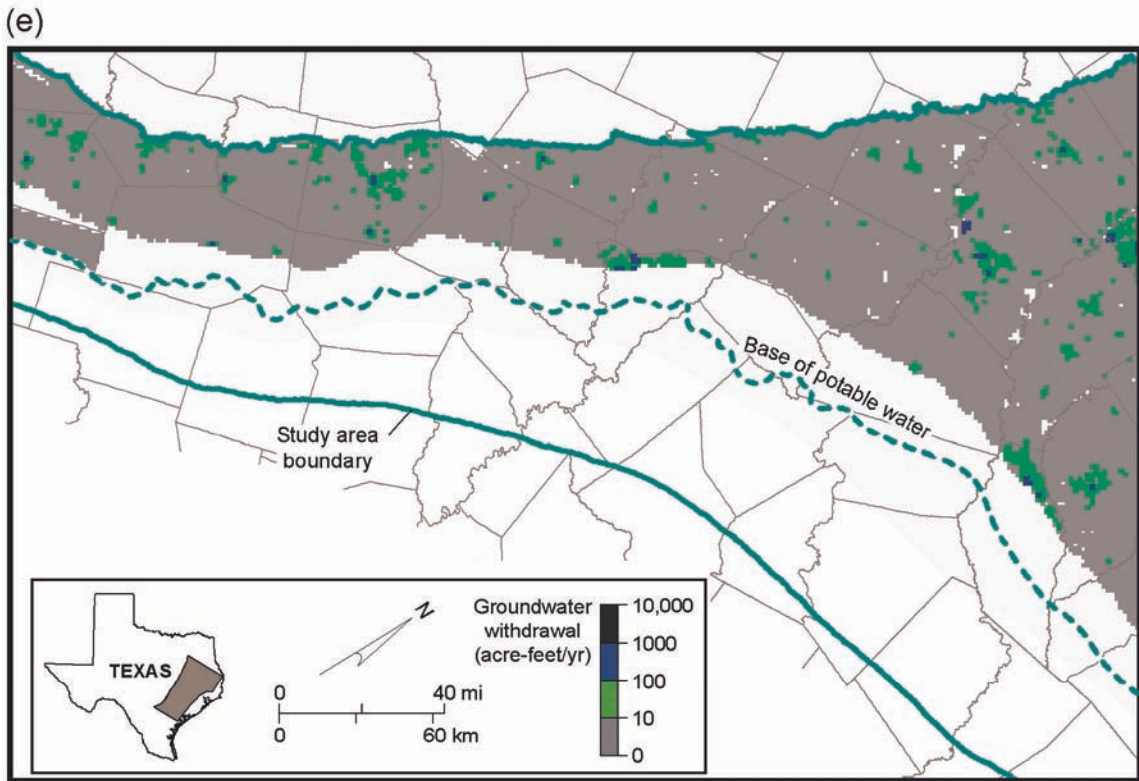


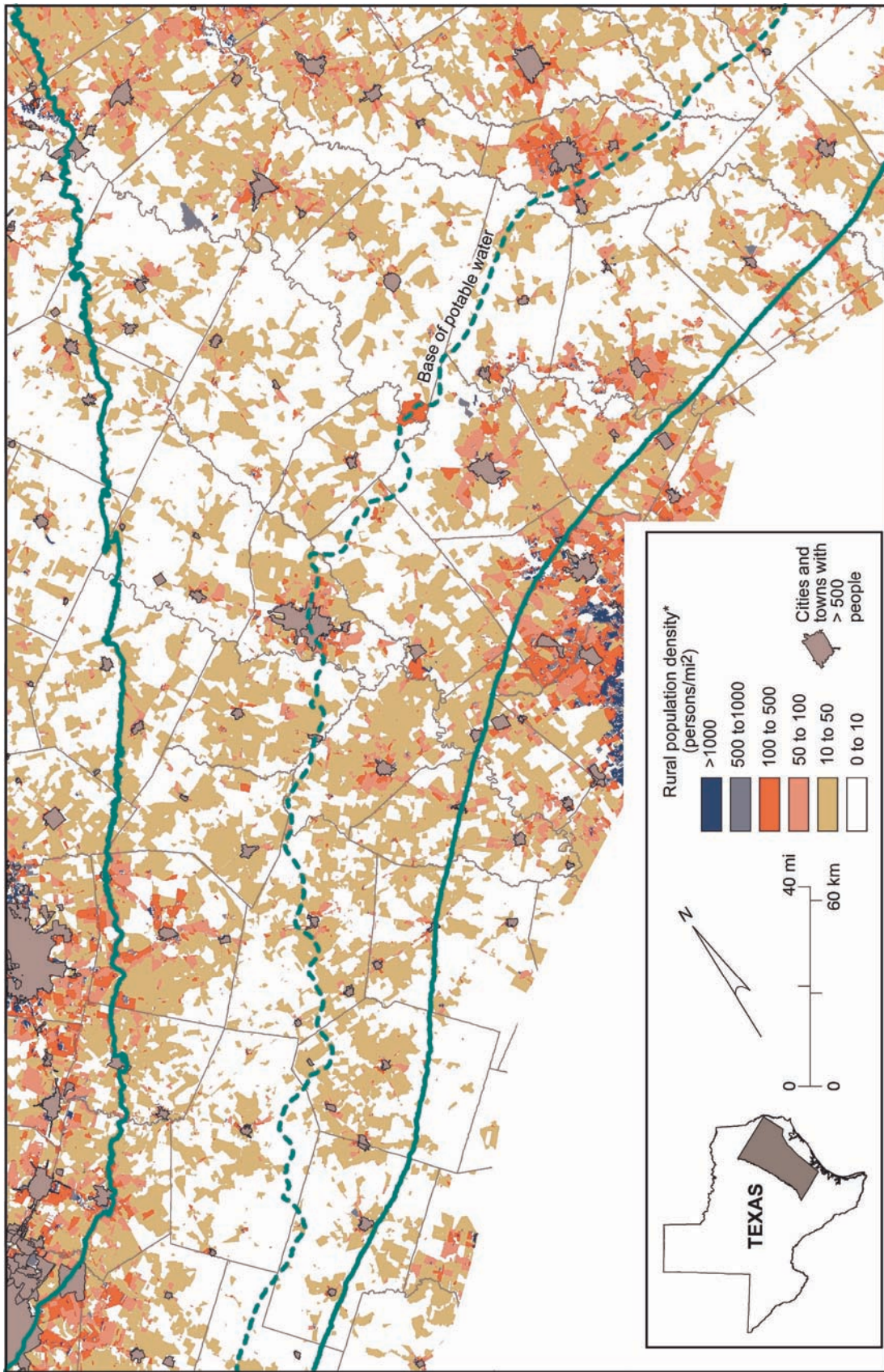
Figure 60 (continued). Distribution of groundwater withdrawal in 2000 for (e) rural domestic and (f) livestock supplies. QAd2287(c)x

identified in the 1989 or 1994 survey. For these counties we distributed pumping to irrigation water wells included in the TWDB online groundwater database.

Groundwater extraction for mining (fig. 60d) was assigned using partly land-use information presented in GIS format and partly additional information. Land use for which groundwater was assumed to have been produced for mining included strip mines, quarries, and gravel pits. Information on groundwater extraction rates at the Sandow Mine in Milam County, the Three Oaks Mine in Lee County, and the Walnut Creek Mine in Robertson County was based on information contained in permit files at the Railroad Commission of Texas (Bob Harden, 2001, written communication).

Rural domestic use was distributed on the basis of 1990 and 2000 census results (fig. 61). Population in census tracts, excluding municipal areas with more than 500 people, was linked to the grid of model cells. Population was linearly interpolated for model cells between 1990 and 2000. Population before 1990 was prorated by the ratio of county-total population in the year of interest to the 1990 population. Rural domestic water use was distributed to model cells (fig. 60e) on the basis of the proportion of total population accounted for by each model-cell area.

Stock water use (fig. 60f) was mapped according to land-use information also presented in GIS format. Groundwater extraction for stock watering was assigned for parcels identified as having land uses of (1) cropland and pasture, (2) confined feeding operations, or (3) herbaceous, shrub and brush, and mixed rangeland. Acreage associated with each mapped land parcel was totaled per county. County total groundwater use was prorated to individual parcels on the basis of their percentage of county totals. The land-use coverage was for the mid-1970s to early 1980s. We assumed that these water uses had the same proportional distribution in other years included in the model.



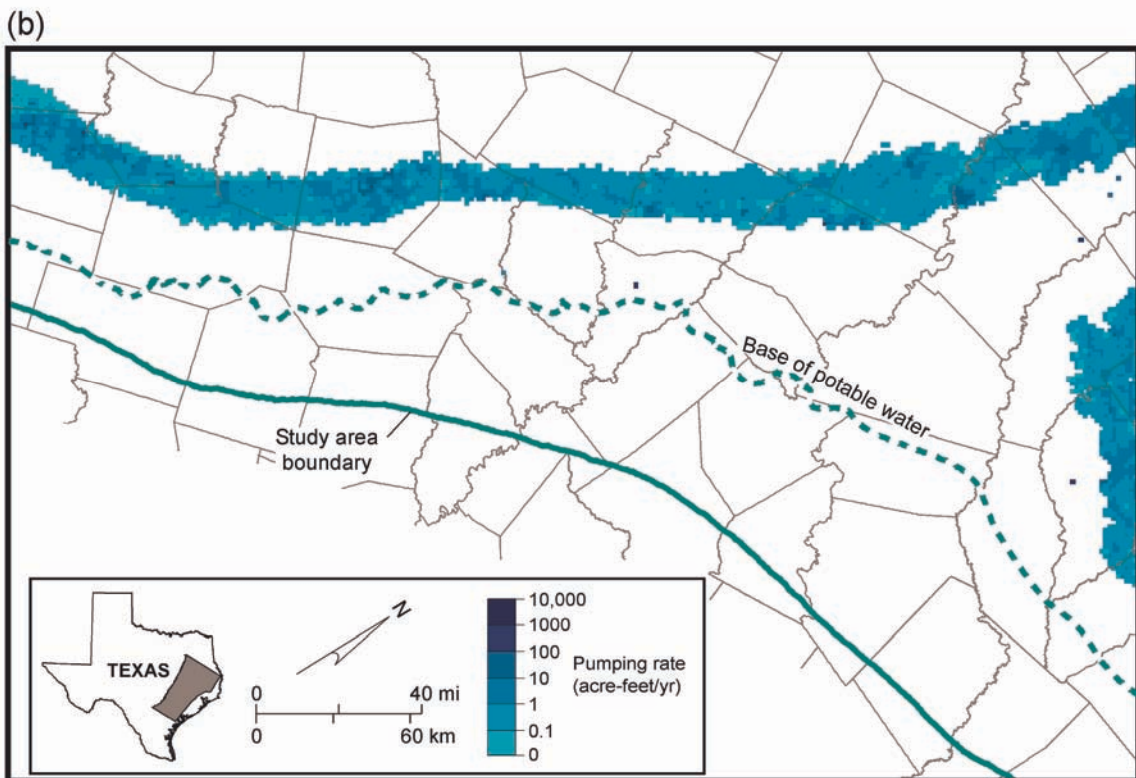
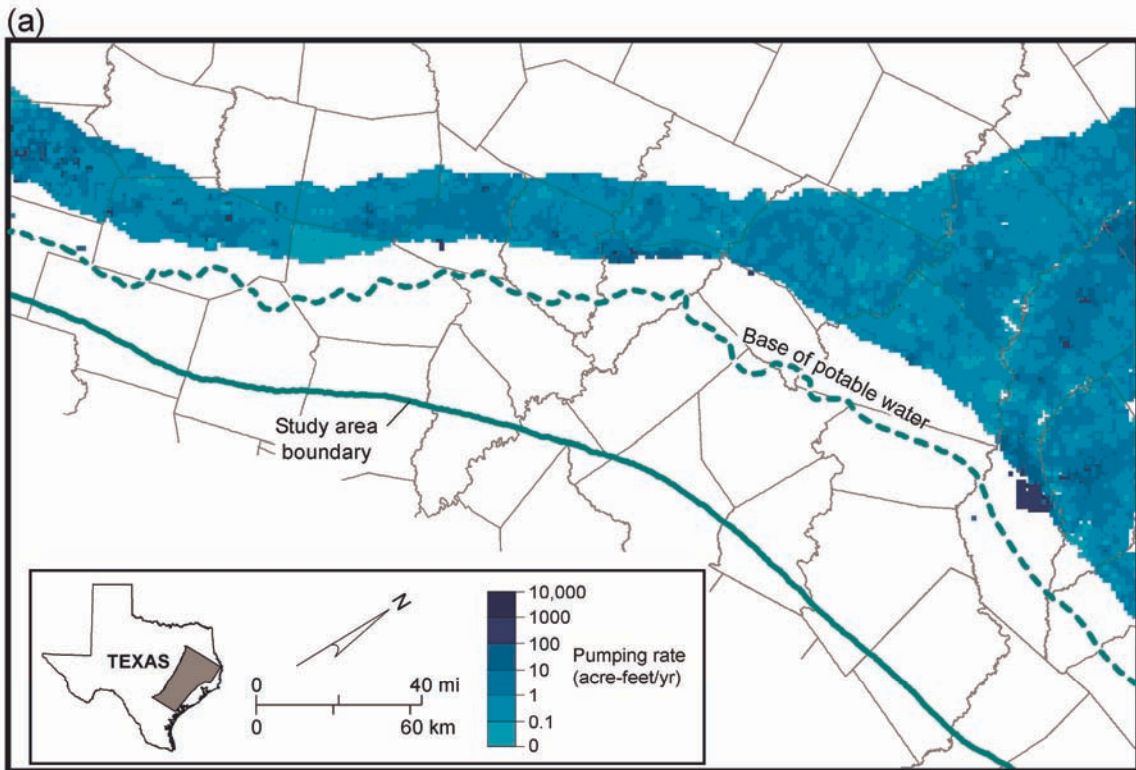
QAD1811(jc)

Figure 61. Map of population density in rural parts of the study area, excluding cities and towns with more than 500 people.

Pumping allocated by well was assigned to model layers on the basis of well information where available. Well information in the TWDB groundwater database can include aquifer, well depth, and screen interval. We cross checked the elevation of the well bottom against elevations of the top and bottom of model cells where wells were assigned. In some cases results did not agree with the aquifer designation. For some wells we assigned model layer on the basis of assignments for other nearby wells.

Pumping used for rural domestic, stock, and irrigation was assigned to model layer (figs. 62, 63) on the basis of well depth. We assumed that few wells for rural domestic, stock, or irrigation would be completed in the Hooper or the Calvert Bluff aquitards if the wells could be completed in the Simsboro or Carrizo aquifer, respectively. Also, we assumed that where depth to the Carrizo aquifer increased, rural domestic, stock, and irrigation wells would be drilled into the overlying Queen City aquifer. This assumption resulted in a downdip limit of pumping in each model layer for rural domestic, stock, and irrigation uses. Pumping was also split between the Carrizo and Simsboro aquifers in part of the East Texas Basin and in Bastrop County (figs. 62, 63).

Pumping in the Lufkin-Angelina County well field occurs at the downdip limit of pumping in layer 3, approximately 10 mi from the limit of potable water in the Carrizo–Wilcox aquifer (figs. 62a, 63a). Depth to the top of the Carrizo aquifer in the well field is more than 900 ft. No pumping was assigned to the deepest, downdip part of the aquifer, as previously explained. Likewise, pumping from the downdip part of the Calvert Bluff aquitard is assumed to be limited where the aquifer is overlain by the full section of the Carrizo aquifer (figs. 62b, 63b). The Bryan-College Station well field straddles the line between Brazos and Robertson Counties. We assumed that most pumping from the Hooper aquitard is generally near its outcrop because of the depth of drilling and water quality. Individual wells



QAd2053(a)c

Figure 62. Variation in total rate of groundwater withdrawal in 1990 in (a) Carrizo aquifer and (b) Calvert Bluff aquitard.

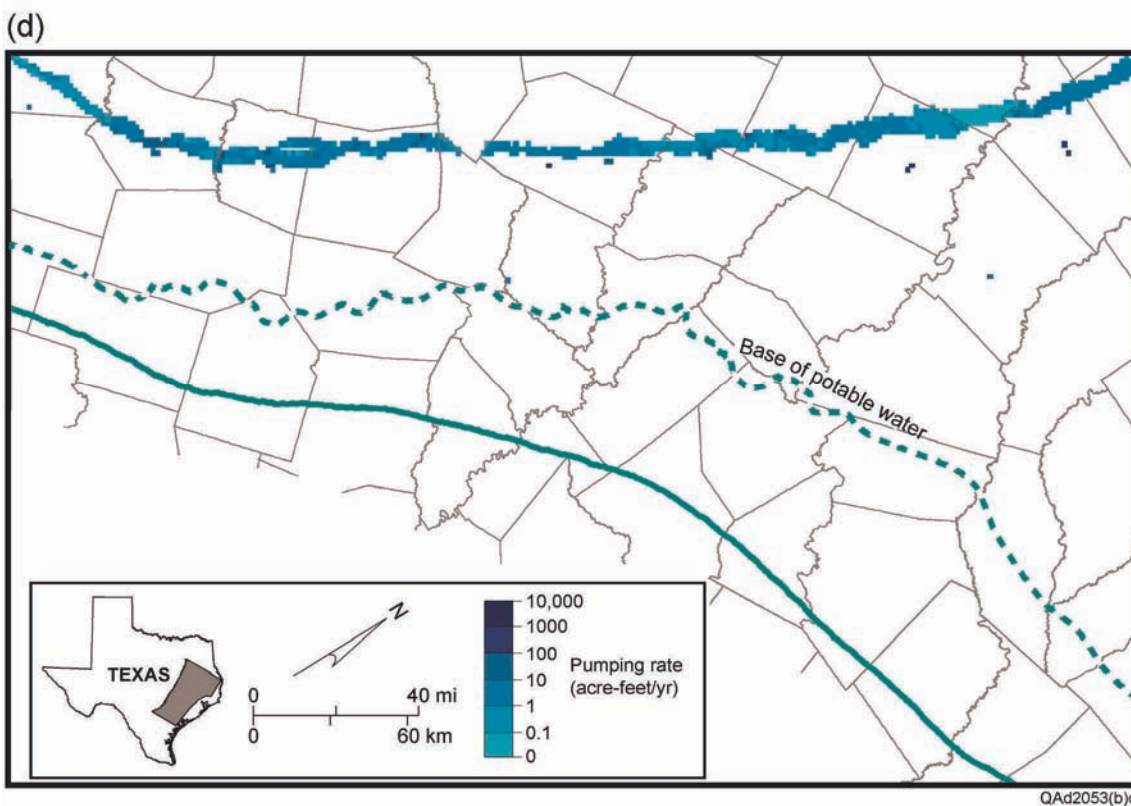
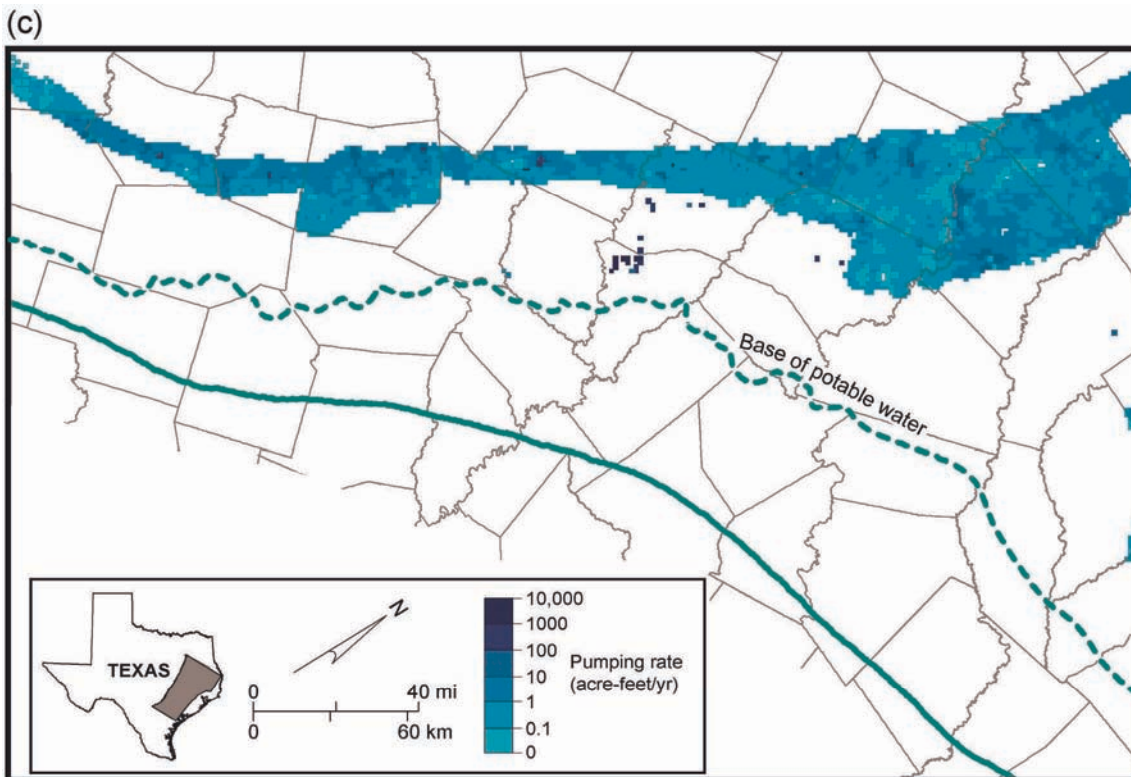
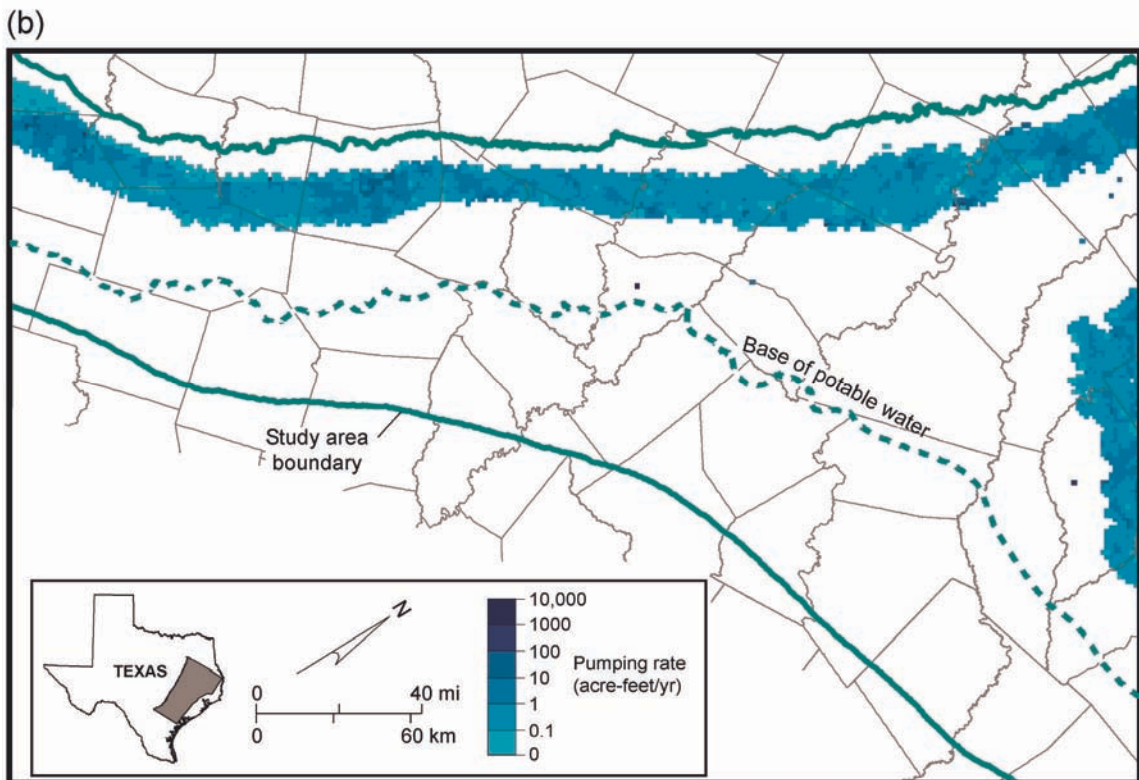
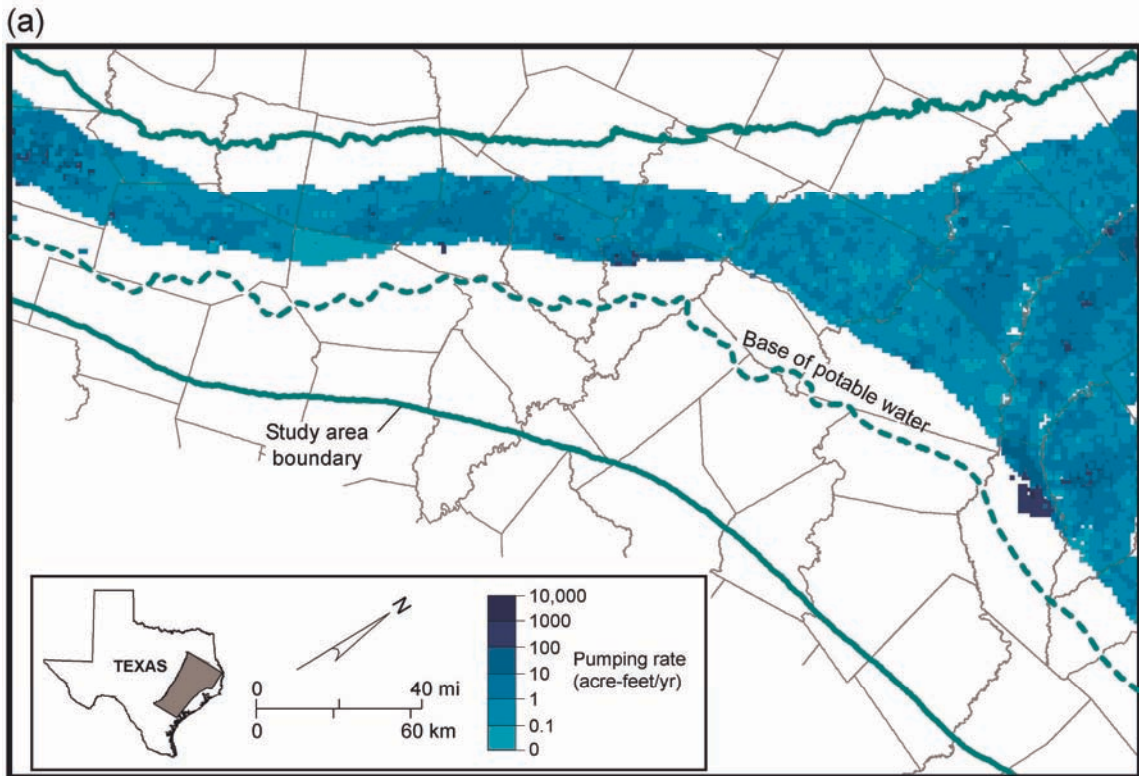


Figure 62 (continued). Variation in total rate of groundwater withdrawal in 1990 in (c) Simsboro aquifer and (d) Hooper aquitard.



QAd2054(a)c

Figure 63. Variation in total rate of groundwater withdrawal in 2000 in (a) Carrizo aquifer and (b) Calvert Bluff aquitard.

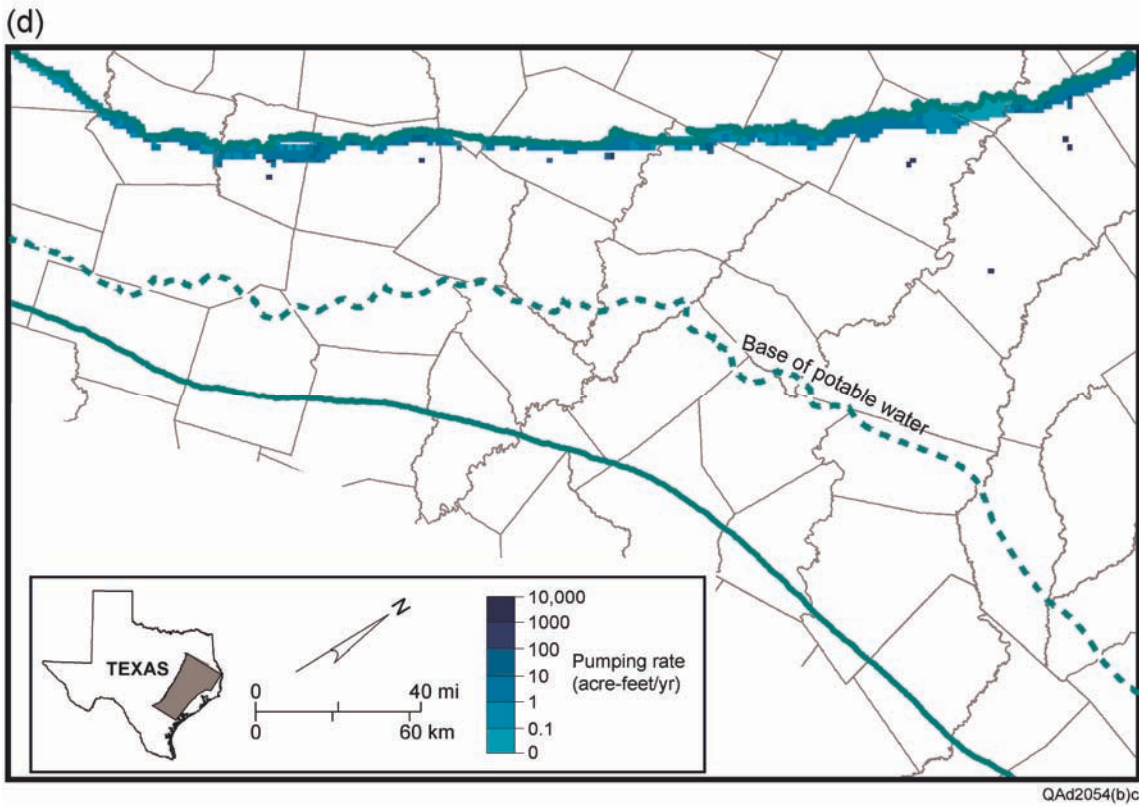
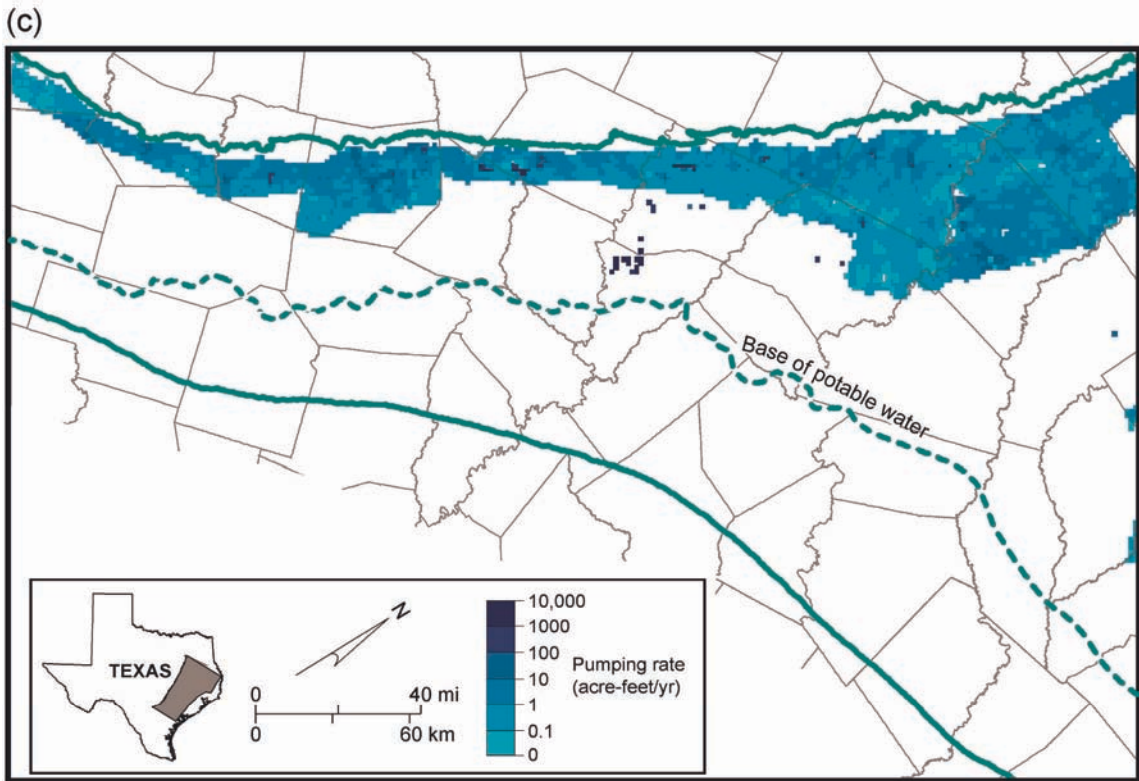


Figure 63 (continued). Variation in total rate of groundwater withdrawal in 2000 in (c) Simsboro aquifer and (d) Hooper aquitard.

in Freestone, Anderson, and Henderson Counties in the Hooper aquitard are deeper and show that this assumption is not valid everywhere.

The TWDB developed predictive pumpage data sets for 2000, 2010, 2020, 2030, 2040, and 2050, subdivided into seven water-use categories. The source of the data sets was water-demand projections from the regional water plans as contained in Volume II of the 2002 State Water Plan (SWP) (TWDB, 2002). TWDB compared demand projections, currently available supplies, and associated strategies for water user groups listed in the SWP for the 2000-through-2050 planning cycle. TWDB adjusted predicted pumpage estimates so that the value to be used in the various GAM models did not exceed projected demands. Records associated with groundwater use were assigned to various aquifers.

The various regional water plans present information on how future supplies from the Carrizo–Wilcox aquifer will be obtained, such as by drilling one or more additional wells to expand a city’s well field. Other plans do not provide specific information. Where additional wells are specifically mentioned, we added scheduled groundwater withdrawal to cells located in the vicinity of the well field. If additional wells were not targeted as a strategy, we simply increased the pumping rate from the enumerated wells in a city’s well field. Similarly, new groundwater withdrawal for manufacturing was assigned to model cells in appropriate locations. Increases in groundwater withdrawal for power was simulated by increased pumping from previously used model cells. Changes in pumping for irrigation, mining, rural domestic, and stock water uses were generally handled by prorating the amounts across the cells used in the 2000 simulation unless other information was available.

The Region K regional water plan identified the Carrizo–Wilcox aquifer as a water-management strategy for the City of Pflugerville in Travis County. The TWDB pumping rate for this strategy ranges from 700 acre-ft/yr in 2000 to 1,453 acre-ft/yr in 2050. This pumping

was assigned to the Simsboro aquifer in the vicinity of Elgin, Bastrop County, which is the productive area of the aquifer nearest the City of Pflugerville.

The Region G regional water plan identified the Carrizo–Wilcox aquifer as a water-management strategy to meet Williamson County water needs. Predicted groundwater withdrawal ranges from less than 1,000 acre-ft/yr in 2001 to more than 18,000 acre-ft/yr in 2050. Identified users included the cities of Bartlett, Brushy Creek, Florence, Georgetown, Granger, Hutto, Leander, Round Rock, Taylor, and Thrall, as well as water-supply corporations supplying rural domestic users. This predicted groundwater withdrawal was split between the Carrizo and Simsboro aquifers and allocated in the model to Lee County using the footprint defined in the Trans-Texas Water Program (HDR Engineering, 1998) and previously simulated in the Dutton (1999) model.

The Region L regional water plan identified the Carrizo–Wilcox aquifer as part of several water-management strategies to meet water needs for the City of San Antonio. In late 1998, a contract between Alcoa Inc. (ALCOA), San Antonio Water System (SAWS), and San Antonio’s City Public Service (CPS) was announced for transfer of groundwater produced from mining operations in Bastrop, Lee, and Milam Counties to provide municipal water supply to the City of San Antonio. Previously, groundwater extracted from the Simsboro aquifer as part of mining operations was discharged and released as surface water. Most of that released water would be transferred to SAWS. Additional pumping beyond that required for mining operations, however, was anticipated. This transfer was adopted as water-management strategy Simsboro SCTN-3 in the South Central Texas Region L water plan. The rate specified in the TWDB City Municipal Master Predictive data set for this strategy is approximately 50,600 acre-ft/yr in 2000, decreasing to about 31,500 acre-ft/yr in 2010, and then gradually increasing to about 38,700 acre-ft/yr in 2050.

To allocate this groundwater withdrawal, we assumed the total SAWS transfer would always be greater than the amount being pumped as part of mining operations, requiring additional pumping. We determined the additional amount of groundwater withdrawal needed to meet the targeted amount for transfer and allocated that amount to cells representing the Simsboro aquifer in the vicinity of the projected mining operations around the Sandow and Three Oaks mines in Bastrop, Lee, and Milam Counties. We assumed that 5,000 acre-ft/yr of ground water would be retained by ALCOA for on-site use.

Additional Region L water-management strategies referred to as the Carrizo aquifer–Gonzales and Bastrop (CZ-10D) plan and the Carrizo aquifer–Schertz-Seguin Water Supply Project identified the Carrizo–Wilcox aquifer in Gonzales County as a source of groundwater for municipal, manufacturing, and power-generation needs. This withdrawal was assigned to the Carrizo aquifer in the western part of Gonzales County. Model cells were designated for the simulation with the assistance of the Gonzales County Conservation District.

6.4 Model Parameters

Model parameters, including elevations of the top and bottom of layers, horizontal and vertical hydraulic conductivities, coefficient of storage (storativity), and specific yield, were distributed and assigned to model cells using a combination of Surfer® and ArcView®, and Microsoft Excel.

The top and bottom of layers were mapped from a digital database. Merging of the spatially dissimilar data sets required the use of geographic information systems (GIS) and geostatistical software packages. Once compiled, initial layer elevation data sets were checked for vertical consistency through surface subtraction using the triangulated irregular

network method of surface interpolation. Insertion of control points at appropriate locations corrected areas showing vertical discrepancies. Geostatistical methods were used to interpolate the structure surface across that part of the model with sparse or no data. This process included calculation of layer thickness, kriging the thickness surface throughout the model area, recalculation of layer boundary elevation from the kriged surface, and merging the recalculated elevation surface into data-poor zones. The complete layer boundary elevation surfaces were then draped onto points representing the model cell centroids. Particular attention was made to improving the accuracy of structural mapping across the Karnes-Milano-Mexia Fault Zone and in extrapolating the structural surfaces across the outcrop where the formations thin. Mapping of structure surfaces was coordinated for the central, southern, and northern GAM models of the Carrizo–Wilcox aquifer to ensure consistency.

We used Surfer® to interpolate gridded values of hydraulic conductivity. Input files for each layer included the measured data from Mace and others (2000c) and digitized traces of contours of hydraulic conductivity hand drawn by a geologist to take into account variations in thickness of sandstones. Once we had values of horizontal hydraulic conductivity, layer thickness, and sandstone thickness assigned to each model cell, we used a Fortran program to calculate equations 3 and 4 for horizontal and vertical hydraulic conductivity for the cells. Further adjustment was needed to match calculated values to well-known values, for example, in the vicinity of the Bryan-College Station well field. Other adjustments were made where initially calculated values appeared much higher than the statistical distribution (Mace and others, 2000c) would predict. We set the upper limit of hydraulic conductivity in the Simsboro aquifer to approximately 30 ft/d. Further corrections were needed to extrapolate results across the outcrop.

MODFLOW uses the dimensionless coefficient of storage, or storativity, to determine the volume of water released from a vertical column of a model layer per unit surface area and unit decline in hydraulic head. For cells in which the simulated hydraulic head is below the top of a cell, for example, cells representing the unconfined aquifer in the outcrop, MODFLOW switches to using specific yield to determine the volume of water released from a vertical column of a model layer per unit surface area and unit decline in hydraulic head. Storativity is a function of porosity, compressibility of water, and elasticity of the formation. We assumed that rock elasticity decreases as the sediment undergoes compaction and lithification during burial. Detrital minerals dissolve and additional minerals precipitate as cement in the pores of sediment, further changing porosity (Loucks and others, 1986) and elasticity. We accordingly varied storativity as a function of depth and texture of the aquifer matrix (for example, sandstone versus claystone).

Calibration involved specifying the range between maximum storativity at shallow depth and minimum storativity at greater depth and the effect of sand content. The calibrated model used a maximum baseline storativity of $10^{-3.5}$ (3.16×10^{-4}) at the updip edge of the confined aquifer in each layer and a minimum baseline storativity of $10^{-4.5}$ (3.16×10^{-5}) at the downdip limit of potable water (figs. 64 through 67). The more saline zone at depth was assigned a baseline storativity of $10^{-4.5}$. Storativity of the confined part of the Reklaw aquitard was also set to a uniform $10^{-4.5}$ (fig. 68). Storativity assigned in the model (S) for the Carrizo–Wilcox aquifer was adjusted from the baseline value (S_z) to reflect sand content in each layer using equation 12:

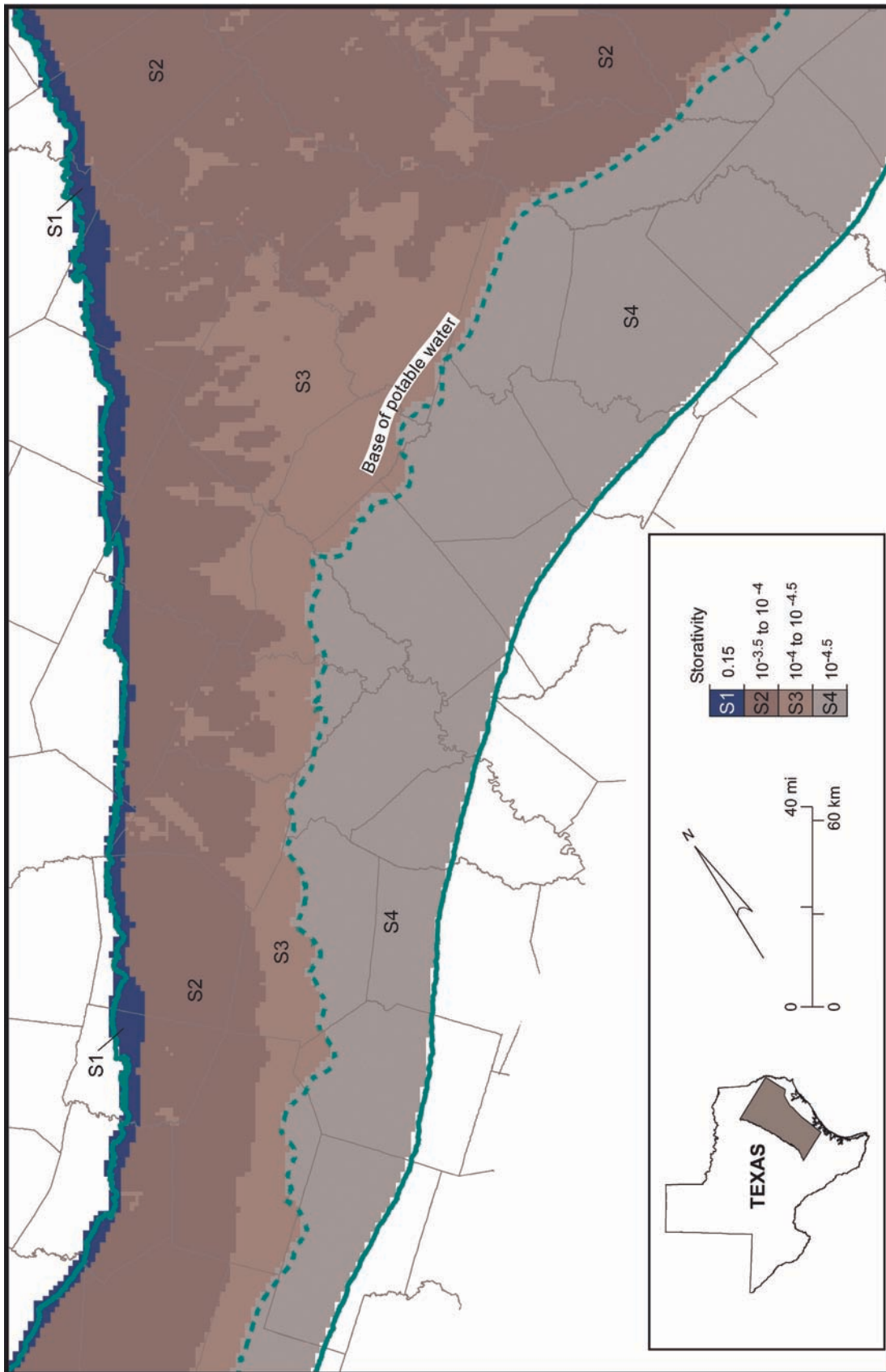
$$\begin{aligned} \text{Log}(S) &= \text{Log}(S_z) + \text{SPF}, \text{ where} \\ \text{SPF} &= (0.5 - \text{Sand content})/0.5 \end{aligned} \tag{12}$$

As *Sand content* for any cell of the model layer approaches 100 percent, the *SPF* term goes to -1 and reduces storativity by an order of magnitude. Likewise, as *Sand content* approaches 0 percent, the *SPF* term goes to 1 and increases storativity by an order of magnitude.

Specific yield was set to 0.15 for the Simsboro and Carrizo aquifers and to 0.10 for the Hooper, Calvert Bluff, and Reklaw aquitards. Specific yield of alluvium (layer 1) and of the additional cells in layers beneath the alluvium was set to 0.25.

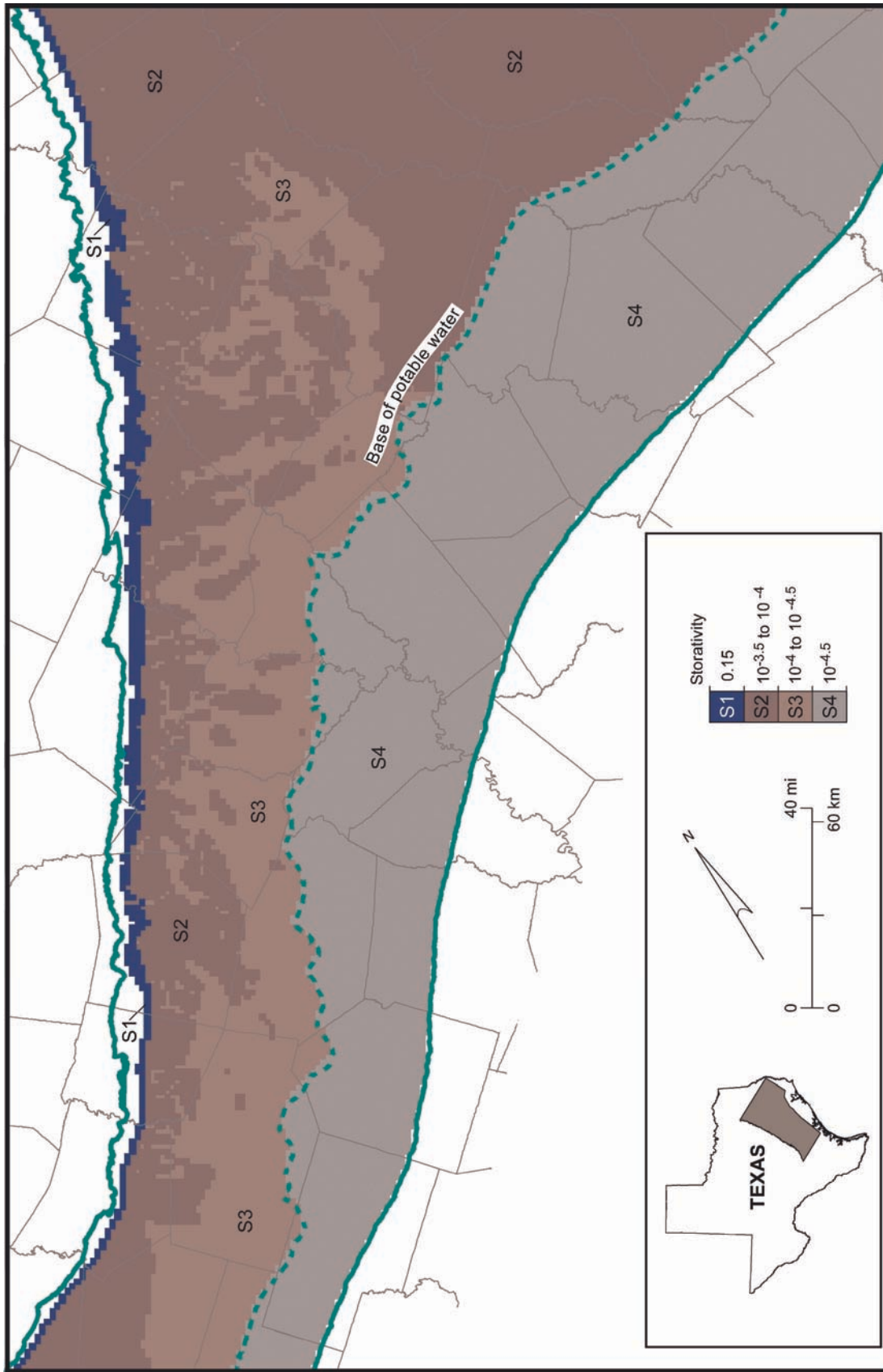
We made layer 1, representing the alluvium, an unconfined layer in which transmissivity varies with saturated thickness. The additional cells in layers 2 through 5 beneath the alluvium of layer 1 were considered extensions of the alluvium and were given a thickness of 0.1 ft. Because water level must lie above the top of these cells, that is, within the alluvium cells in layer 1, the additional cells in layers 2 through 5 are specified as confined but given a storage coefficient equal to that of the alluvium (0.25). In initial simulations, however, setting horizontal and vertical hydraulic conductivities of the additional cells equal to those of layer 1 increased the convergence time required for the simulation. Accordingly, the calibrated horizontal and vertical hydraulic conductivities of the additional cells were set to 1 ft/d.

Layers 2 through 6 were set as confined/unconfined. We allowed MODFLOW to calculate transmissivity from input values of hydraulic conductivity and layer and saturated thickness as appropriate. Storativity was specified as a model input. We used the Strongly Implicit Procedure (SIP) with a convergence criterion of 0.001 ft.



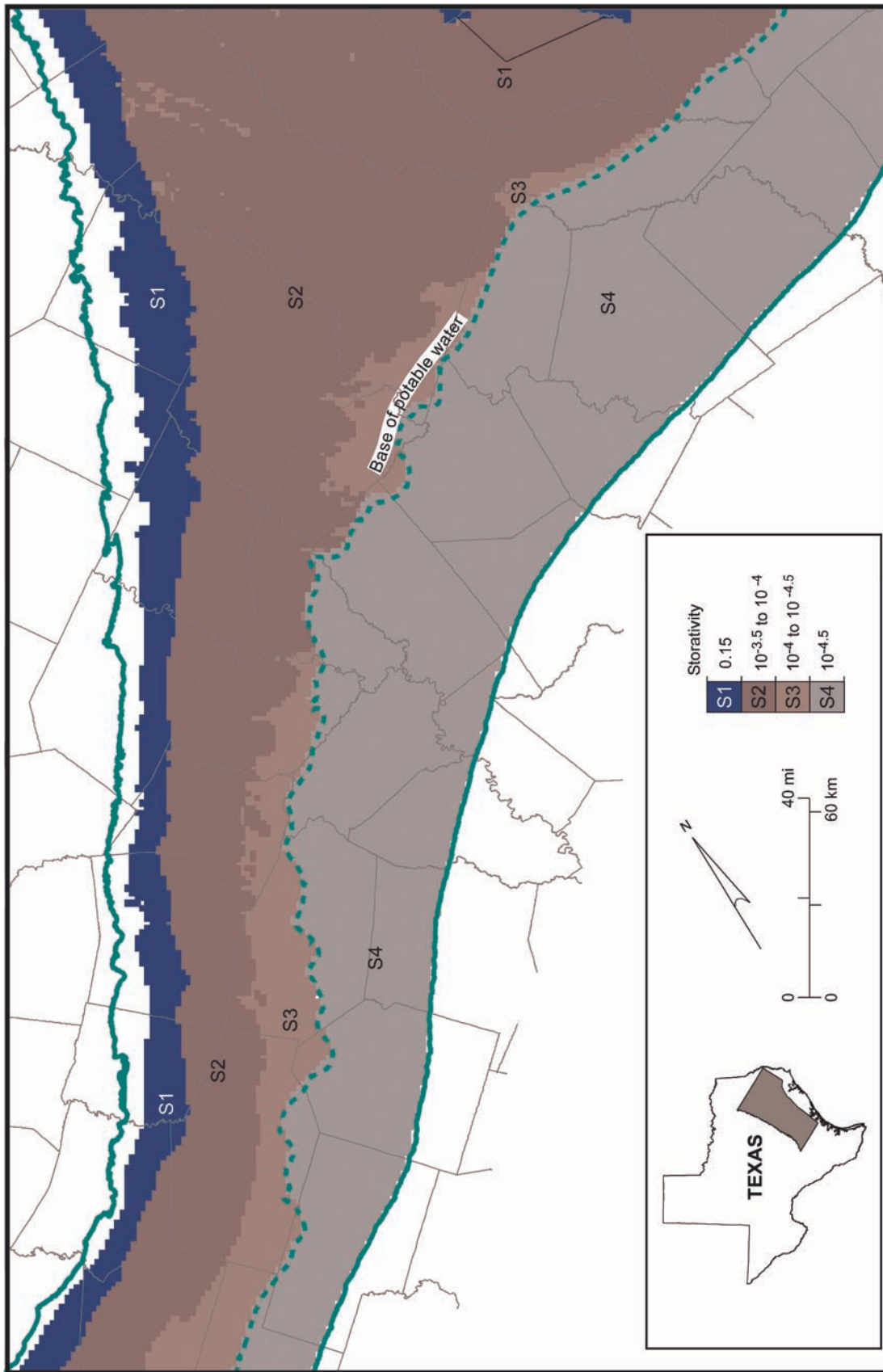
QA02278(e)c

Figure 64. Storativity assigned to model cells representing the Hooper aquitard (layer 6).



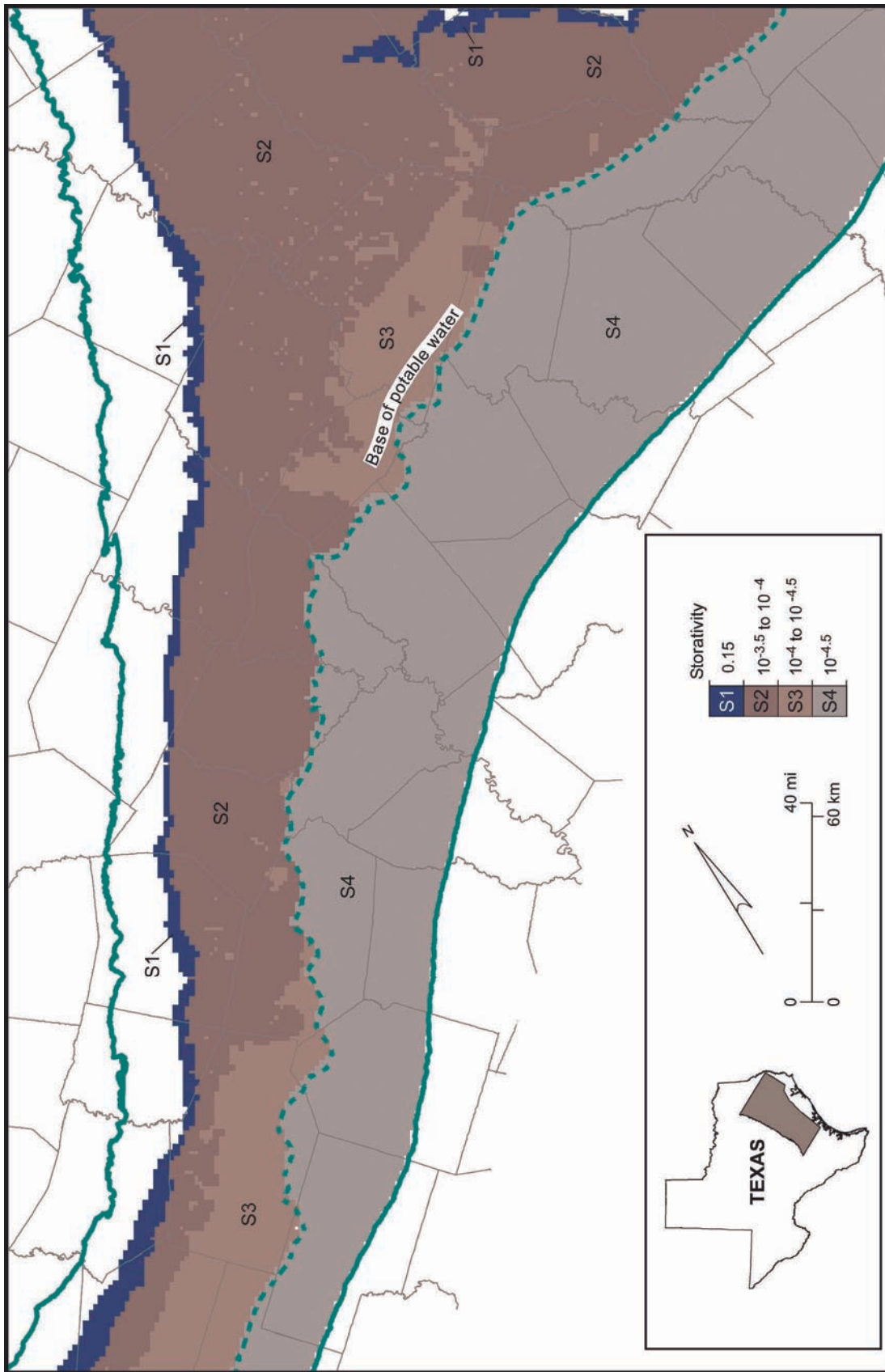
QA02278(b)c

Figure 65. Storativity assigned to model cells representing the Simsboro aquifer (layer 5).



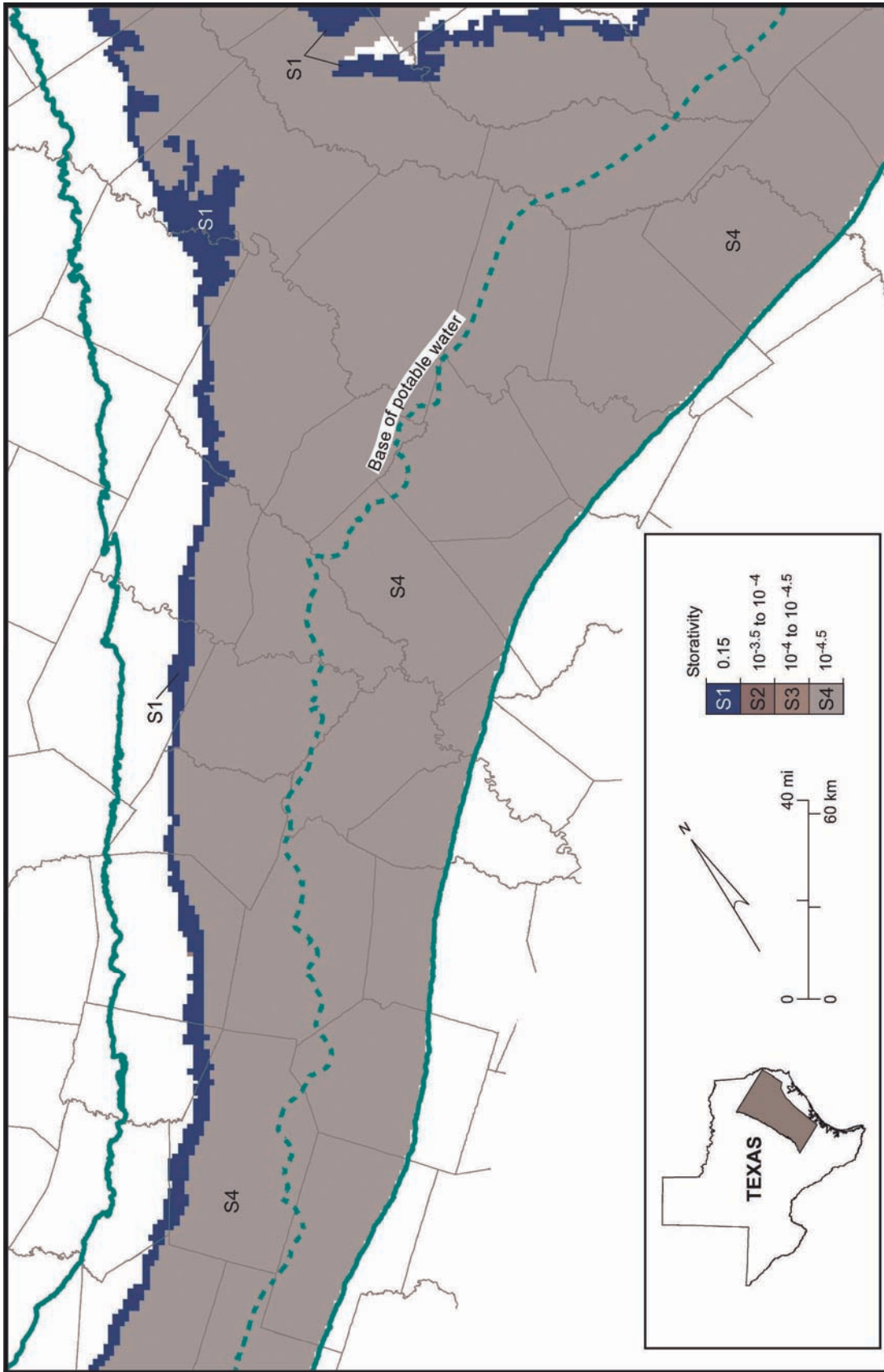
QA4278(c)

Figure 66. Storativity assigned to model cells representing the Calvert Bluff aquitard (layer 4).



QAd2278(d)jc

Figure 67. Storativity assigned to model cells representing the Carrizo aquifer (layer 3).



QAd2278(e)c

Figure 68. Storativity assigned to model cells representing the Reklaw aquitard (layer 2).

7.0 MODELING APPROACH

The modeling sequence included

- (1) Setting up and calibrating the steady-state version of the model. The steady-state model was used to make initial adjustments of model parameters, including hydraulic conductivities, recharge, parameters for the stream-flow routing and ET packages, GHB boundaries, and horizontal-flow barrier (HFB) parameters.
- (2) We set up a transient version of the model for calibration against the period of record from 1950 through 1990, with emphasis on the last 10 yr. We included pumping for the early part of the period at approximately the same rate as in 1980. We assumed that pumping rates did not vary greatly during this period, except in the well fields, and variation was estimated from changes in population. Moving the starting date for the transient model to 1950 decreases the influence of initial conditions on model results for the 1990 calibration. During the calibration phase we made further adjustments to all model parameters, including storativity.
- (3) The verification period ran from 1991 through 2000. Results for this period suggest how well the model may perform as a predictive tool.
- (4) The model was used to predict water-level changes during the period from 2000 through 2050 as an example of its use in predicting future conditions in the aquifer. Pumping rates for the predictive simulations were developed by the TWDB from Regional Water Planning Group projections. We used average recharge rates for predictive stress periods except for the last 36 month-long stress periods of each simulation.

The steady-state model was first established using the steady-state solution feature of MODFLOW. The steady-state model later was combined with the transient model and solved in a 100-yr stress period (effectively 1851 through 1950) with 200 time steps. The transient model for 1951 through 1990 and 1991 through 2000 was run with 1-yr stress periods, except that month-long stress periods were included for the drought years of the 1980s (1987 through 1989) and the 1990s (1995 through 1997). Most stress periods were solved using one time step with fewer than 200 iterations. For some stress periods in which pumping rates changed appreciably we had to increase the number of time steps to ensure convergence; at most, 5 time steps were used for annual stress periods or 10 time steps for month-long stress periods.

The 2000-through-2050 predictive simulations included a number of runs:

- (1) a run for 2000 through 2010, with 120 month-long stress periods, ending with drought-of-record recharge rates for the last 36 month-long periods (2007 through 2010);
- (2) a run for 2000 through 2020, with 10 annual stress periods, followed by 120 month-long stress periods, and ending with drought-of-record recharge rates for the last 36 month-long periods (2018 to 2020);
- (3) a run for 2000 through 2030, with 20 annual stress periods, followed by 120 month-long stress periods, and ending with drought-of-record recharge rates for the last 36 month-long periods (2028 through 2030);
- (4) a run for 2000 through 2040, with 30 annual stress periods followed by 120 month-long stress periods, and ending with drought-of-record recharge rates for the last 36 month-long periods (2038 through 2040);

- (5) a run for 2000 through 2050, with 40 annual stress periods, followed by 120 month-long stress periods, and ending with drought-of-record recharge rates for the last 36 month-long periods (2048 through 2050); and
- (6) a run for 2000 through 2050 with average recharge rates.

The only change in simulation of normal precipitation versus drought-of-record years was the use of different recharge rates. Pumping rates and their monthly variations were not changed to reflect changes in demand under drought conditions.

Five criteria were used for evaluating the quality of model calibration and verification. First, the difference between simulated and observed water levels was calculated for the steady-state model and end of 1990, as well as for the end of 2000. The number of measured water levels available for comparison were greater for 1990 and 2000 than for the steady-state model. Few data were available for the steady-state calibration, and they occurred in a narrow range near the outcrop with little variation in water-level elevation. Model calibration is measured by three calculated errors: root mean squared error (RMSE), mean absolute error (MAE), and mean error (ME) (Anderson and Woessner, 1992, p. 238-241). The increase in range of measured water levels and the increase in number of measurements result in an improvement in model performance in this model (a decrease in the ratio of RMSE to the range of water levels in the data set), except for layer 6, representing the Hooper aquitard.

The second calibration measure is minimizing the residual differences between simulated and observed water levels. One calibration goal is that the residual should also show no spatial bias.

A third calibration criterion is that the simulated and measured water levels for individual monitoring wells should match through time. We chose monitoring wells with

long-duration records in each layer of the Carrizo–Wilcox aquifer for hydrograph matching. Owing to error inherited from the steady state calibration, however, a simulated hydrograph may parallel the measured hydrograph but be offset by some baseline shift. To compensate for such baseline shift, we calculated the RMSE of hydrographs by

- (1) Estimating the trend of the measured water levels and the trend of simulated water levels through time to exclude anomalous outlier data,
- (2) Determining the baseline shift needed to adjust each simulated hydrograph to minimize the difference with a measured hydrograph, and
- (3) Calculating the RMSE between the measured water level and the shifted value of the simulated water level.

The RMSE and baseline shift are reported on each hydrograph in section 9.1.

The fourth calibration measure is comparison of rates of simulated and observed base-flow discharge to streams. As previously mentioned, stream-flow calibration numbers include results from historical low-flow studies, base-flow separation studies between gaged stations, and base flow unitized for the size of the watershed in the Carrizo–Wilcox outcrop. All base-flow calibration targets do not have the same quality.

A fifth calibration requirement is that the numerical difference in the water budget between inflow and outflow should be less than 1 percent.

Our approach for building the model was to use as much geological and hydrological information as possible. Improving calibration involved a combination of fixing obvious errors in model input, recognizing reported water levels that were invalid or assigned to the wrong aquifer layer, and adjusting those parameters that are not well constrained by data, such as vertical hydraulic conductivity and storativity. We minimized other cell-by-cell adjustments to not “overcalibrate” the model, a stated desire of the GAM models.

8.0 STEADY-STATE MODEL

The steady-state, or predevelopment, version of the model represents an approximation of the aquifer before the construction of water wells and pumping of groundwater. Predevelopment conditions are not as well known as later conditions in the aquifer because there are few records of early water-level measurements. We assume, however, that because water levels did not change much during the decades of the 1970s through 1990s, except in the vicinity of high-production well fields, that predevelopment water levels were not greatly different than recorded in the earliest measurements.

We used the steady-state model to evaluate our initial model construction; provide consistent starting conditions for the transient calibration; adjust model parameters, including horizontal and vertical hydraulic conductivity, recharge, parameters for the stream-flow routing and ET packages, GHB boundaries, and horizontal-flow barrier (HFB) parameters; and to assess the sensitivity of simulation results to model properties. The steady-state model initially was set up and solved in one long (100-yr) stress period. The model later was incorporated into the transient model as the first stress period and assigned a 100-yr duration. Additional adjustment of these parameters was performed during calibration of the transient model.

8.1 Calibration

During steady-state calibration, we adjusted model parameters to improve the matches between simulated and observed water levels and simulated and observed base flow in rivers. The need to adjust some parameters became apparent mainly as a result of transient

runs. We chose not to adjust horizontal hydraulic conductivity much beyond obvious data-input corrections. We assumed that horizontal hydraulic conductivity to be one of the better-constrained variables in the model because of the number of hydrologic tests and number of well logs controlling the maps of sandstone content. Vertical hydraulic conductivities for layers representing the Carrizo–Wilcox aquifer were adjusted to ensure that the vertical anisotropy (K_v/K_h) ratio was within expected ranges.

We found that we needed to decrease vertical hydraulic conductivity for layer 2 (Reklaw aquitard) across part of the East Texas Basin where water levels in the Queen City aquifer (and assigned as the layer 2 GHB head value) are greater than 500 ft. A vertical hydraulic conductivity (K_v) of 10^{-4} ft/d, as initially applied, allowed so much downward-directed, cross-formational leakage of water that simulated heads in the Carrizo aquifer were too high. An adjusted K_v of 10^{-6} ft/d was assigned in the East Texas Basin area. A similar adjustment was made for the GAM model of the northern part of the Carrizo–Wilcox aquifer (Intera and Parsons Engineering Science, 2002a). Further study is needed to evaluate the hydrogeological properties of the Reklaw aquitard and its influence on movement of groundwater between the Queen City and Carrizo–Wilcox aquifers.

Steady-state calibration sets the initial balance between the amount of water entering the aquifer as recharge and the amount leaving the aquifer in the outcrop as either base-flow discharge to rivers and streams or groundwater ET. Initial interpretation of field studies of recharge results suggested that recharge to the Simsboro aquifer could be as low as 1 inch/yr. When we applied that rate, model simulation results could not match the stream-flow calibration targets. Results from the completed field study are consistent with those of previous studies (fig. 40). Average steady-state recharge rates assigned to the outcrop of the Simsboro and Carrizo aquifers in the calibrated model were 2.1 and 2.9 inches/yr,

respectively (figs. 69, 70). Average recharge rates assigned to the outcrop of the Hooper, Calvert Bluff, and Reklaw aquitards were 0.5, 0.4, and 0.2 inches/yr, respectively.

During calibration we set a minimum value of the maximum ET rate, which applied mainly in the Sabine Uplift area on the northeast side of the model. The smallest value of maximum ET rate was set to 14 inches/yr. Extinction depth was also adjusted during model calibration and set at 15 ft.

With the calibration of parameters for recharge rate, discharge to rivers and streams, ET, and hydrological properties, no model cells go dry during the steady-state simulation.

Resulting simulated water levels for the predevelopment or steady-state condition in the Simsboro and Carrizo aquifers are shown in figures 71 and 72, respectively. The simulated water levels are reasonably similar to those according to early data (figs. 28, 29). Simulated water level in the Simsboro aquifer (fig. 71) also reflects a main feature of the observed potentiometric surface map (fig. 28), which is the relatively flat gradient in water level across the central part of the study area. Water levels are above 300 ft across the Sabine Uplift at the northeastern boundary. Lower water-level elevations are shown to the southeast beneath the Angelina River valley as previously mentioned. Simulated water-level elevation in the Carrizo aquifer (fig. 72) decreases from about 450 to 500 ft in the outcrop to less than 300 ft in the central part of the model, with lower water-level elevation to the southeast beneath the Angelina River valley. The shape of the potentiometric surface of the Carrizo aquifer also shows the effect of the Sabine Uplift and the low topography of the Angelina River valley.

Overall, the model does a good job in matching predevelopment water levels (fig. 73), considering the sparse data (fig. 74, table 11). The root mean square error (RMSE) is 19 ft for the Carrizo aquifer (sample size = 33) and 25 ft for the Simsboro aquifer

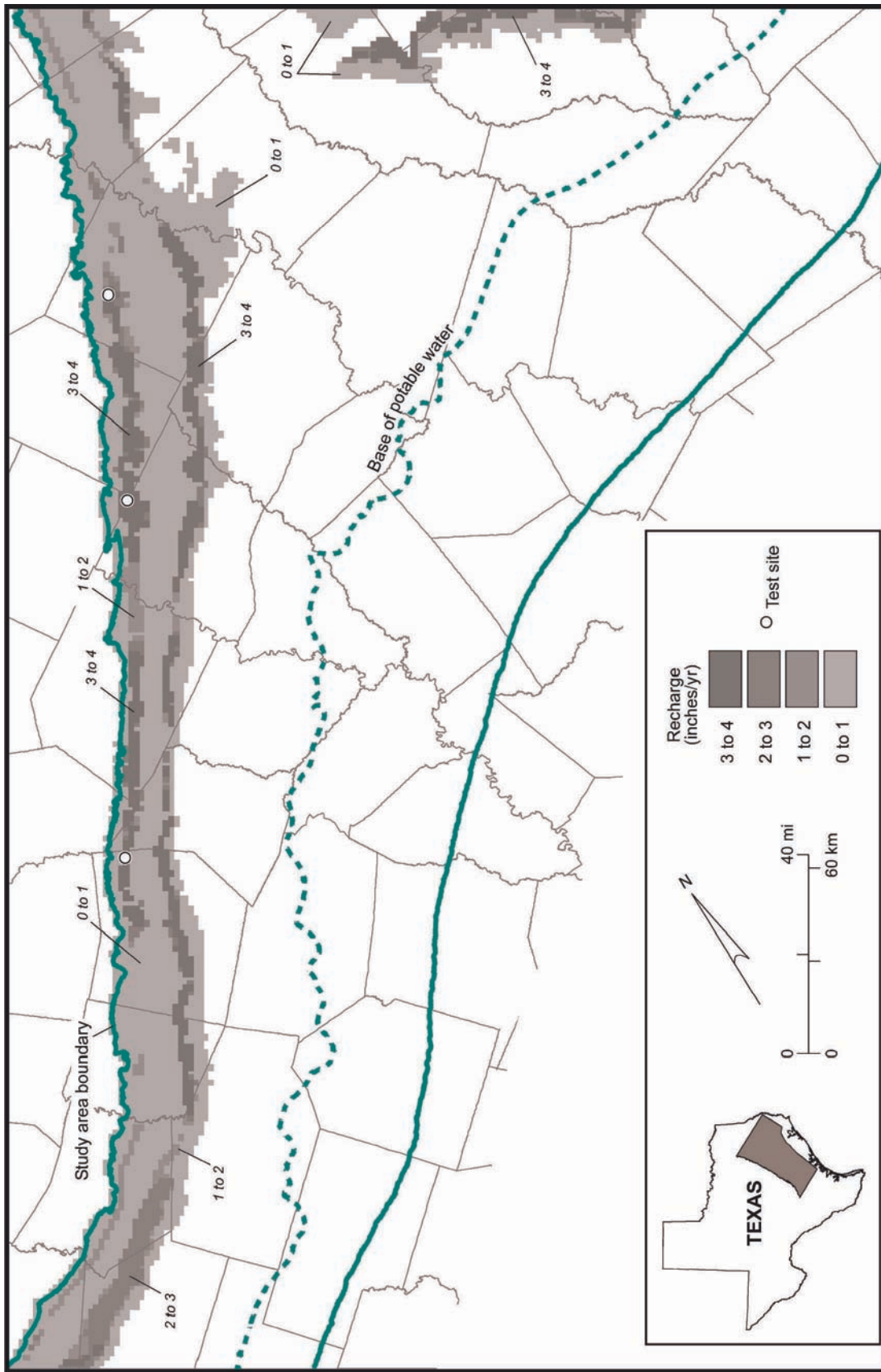


Figure 69. Recharge rate estimated on the basis of soil properties and results of previous studies. Test sites for using environmental tracers for estimating recharge rate were located in the outcrop of the Simsboro aquifer in Bastrop, Lee, Robertson, and Freestone Counties. Approach for assigning recharge to the model is described in section 6.3.1.

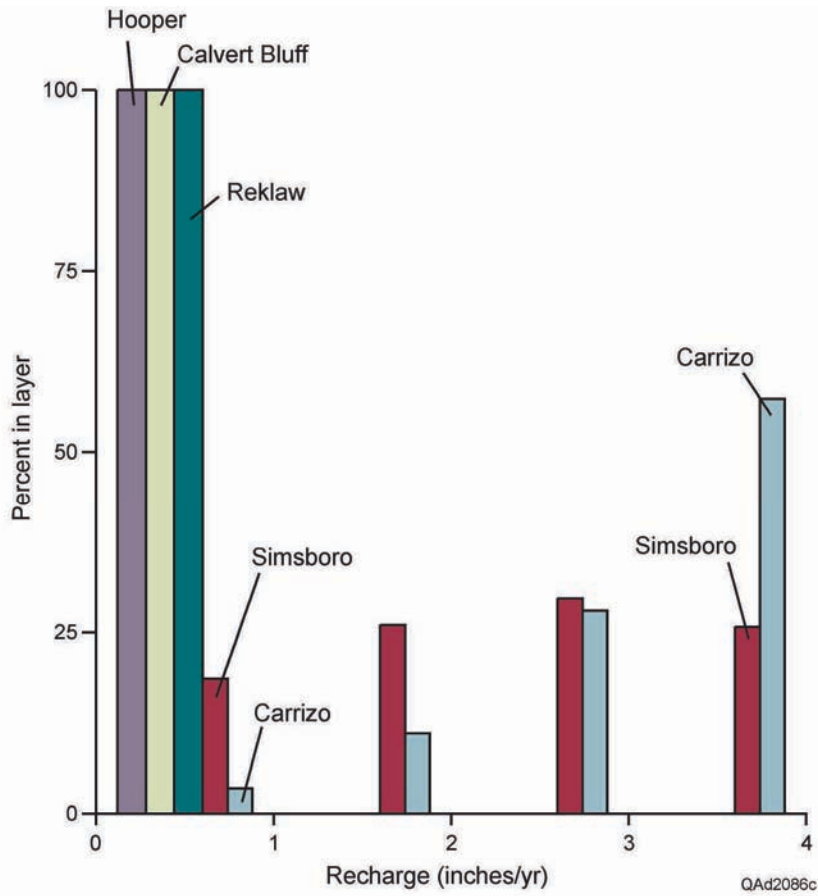
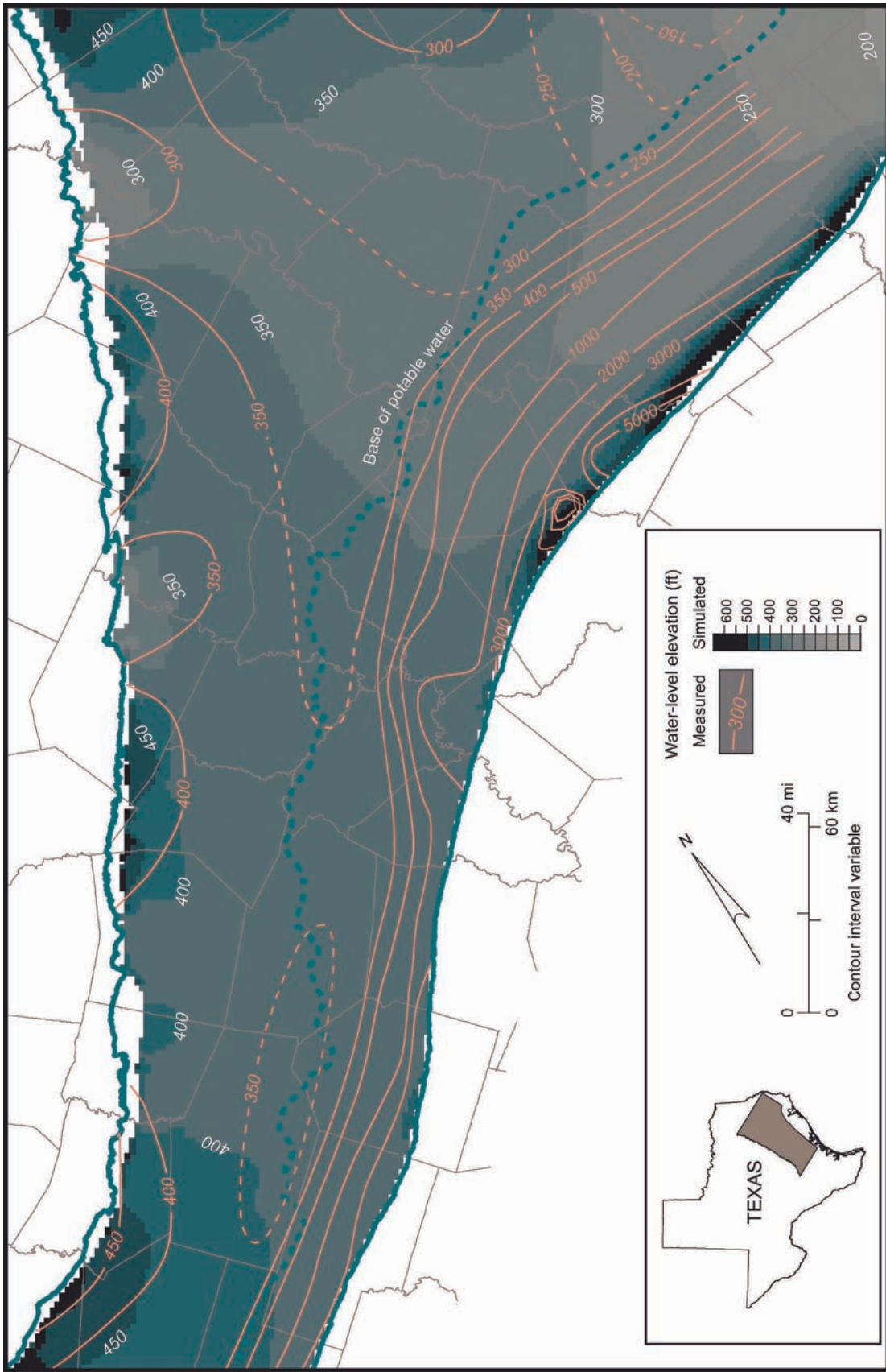
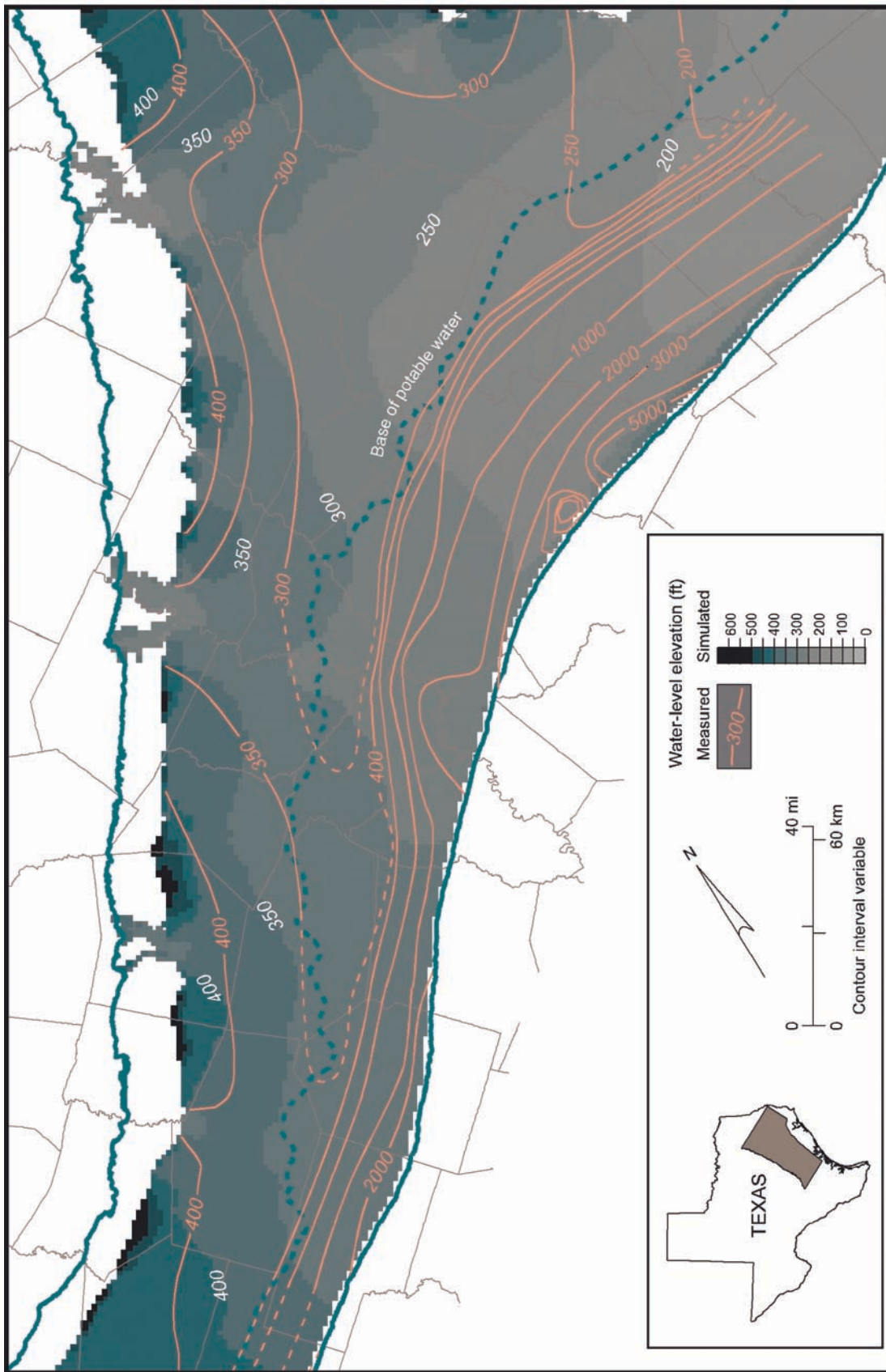


Figure 70. Histogram of recharge rates applied in the model. Most recharge is applied in the outcrop of the Simsboro and Carrizo aquifers.



QA02262(b)(c)

Figure 71. Simulated water levels for the Simsboro aquifer in the study area under predevelopment or steady-state (1950) conditions and comparison with measured contours.



QA4282(e)jc

Figure 72. Simulated water levels for the Carrizo aquifer in the study area under predevelopment or steady-state (1950) conditions and comparison with measured contours.

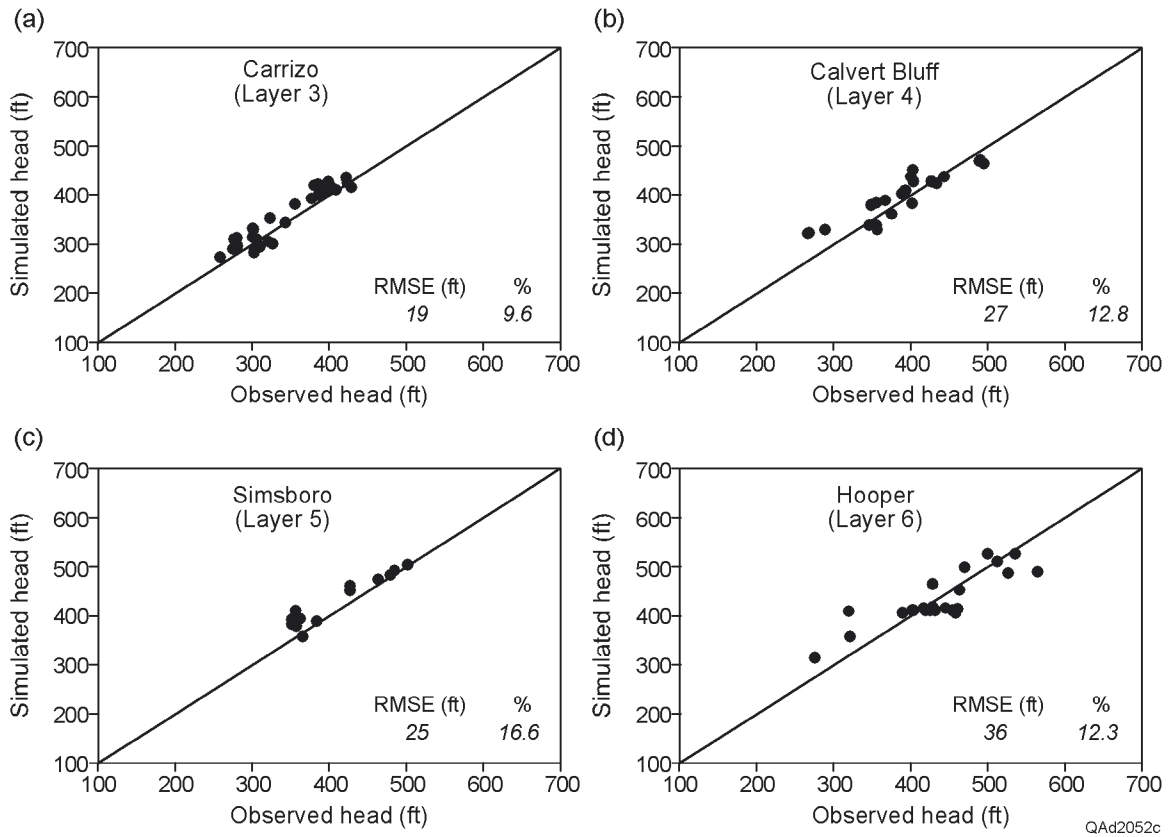


Figure 73. Comparison of simulated and measured water levels in the steady-state simulation of model layers representing the Carrizo–Wilcox aquifer. Well locations are shown in figure 74.

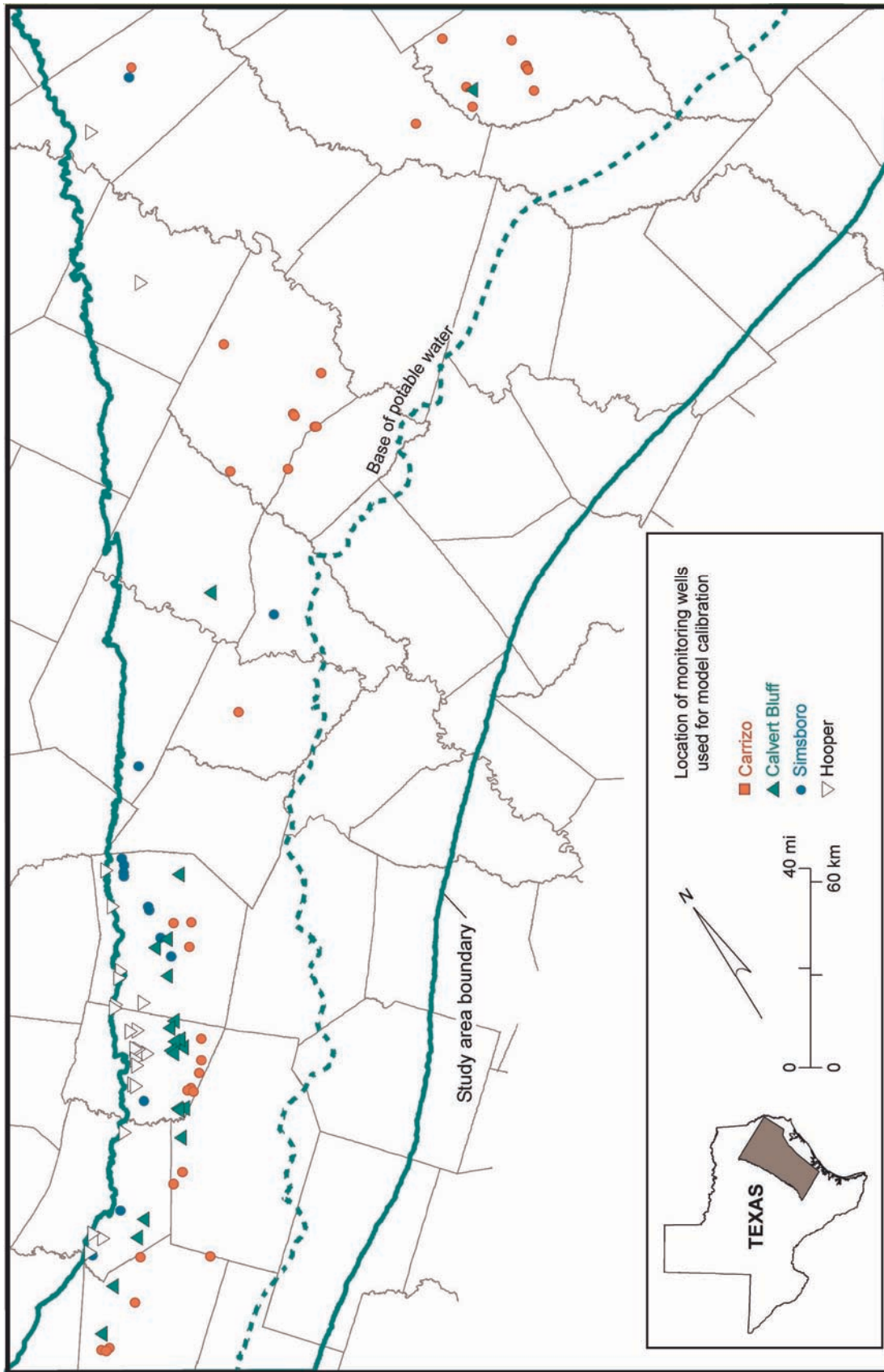


Figure 74. Location of water-level measurements used in calibration of the steady-state version of the model shown in figure 73.

Table 11. Summary of model calibration and verification statistics.

Model	Unit	Layer no.	Root mean squared error (ft)	Mean absolute error (ft)	Mean error (ft)	Number of data points	RMSE/ Δh (%)*
Steady state	Carrizo	3	19.0	16.0	7.7	33	9.6
	Calvert Bluff	4	27.2	23.5	7.6	23	12.0
	Simsboro	5	24.9	19.5	18.2	13	16.6
	Hooper	6	35.5	27.9	-2.9	23	12.3
1990	Carrizo	3	49.4	34.9	23.0	115	6.8
	Calvert Bluff	4	37.5	27.6	10.3	64	9.4
	Simsboro	5	36.1	25.6	17.4	42	10.0
	Hooper	6	42.9	33.0	16.6	42	12.6
2000	Carrizo	3	42.7	31.9	25.4	80	5.7
	Calvert Bluff	4	37.5	29.5	8.1	49	9.5
	Simsboro	5	48.9	35.9	23.7	32	9.8
	Hooper	6	46.3	36.5	20.1	32	12.8

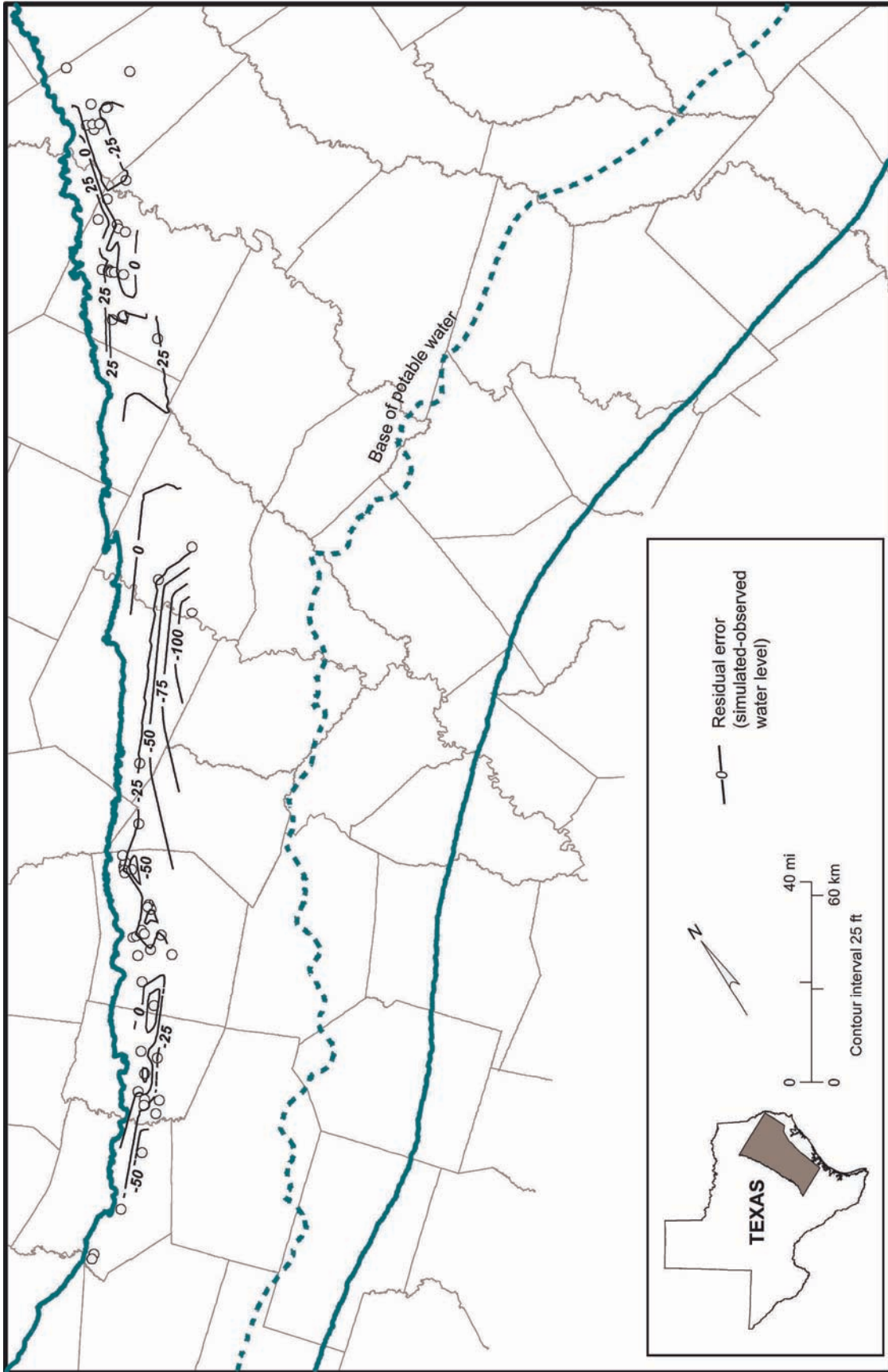
* RMSE is root mean square error (column 4); Δh is range in water level in data. Ratio is expressed in percent.

(sample size = 13). The RMSE values are 9.6 and 16.6 percent, respectively, of the range in water level among the observation wells. The range of measurements for the Simsboro aquifer in the steady-state calibration data set is 150 ft (table 11). Table 11 also reports other calibration statistics, including mean absolute error and mean error. The mapped residual or difference in estimated and simulated water levels for the Simsboro aquifer is shown in figure 75. There are sparse data with which to interpolate a residual across the model area. Most of the model area has a residual of ± 25 ft, which is consistent with the calculated RMSE for the aquifer (table 11). The model underestimates one measurement in Robertson County by more than 100 ft. The residual error for the Carrizo aquifer is also less than ± 25 ft (fig. 76).

Table 12 shows the estimated simulated base flow to the 21 streams and the 5 river basins included in this study. The model generally underpredicts the estimated base flow of the major streams. Simulated base flow is 29 percent of estimated base flow of the Guadalupe River, and 48, 61, and 24 percent of estimated base flow for the Colorado, Brazos, and Trinity Rivers, respectively. Simulation results better match estimated base flow for smaller streams. Most reaches are gaining; stream losses simulated for a set of model cells are typically less than 15 percent of the stream gains. The Simsboro and Carrizo aquifers are the main contributors to base flow. The Hooper and Calvert Bluff aquitards contribute little to stream flow in comparison.

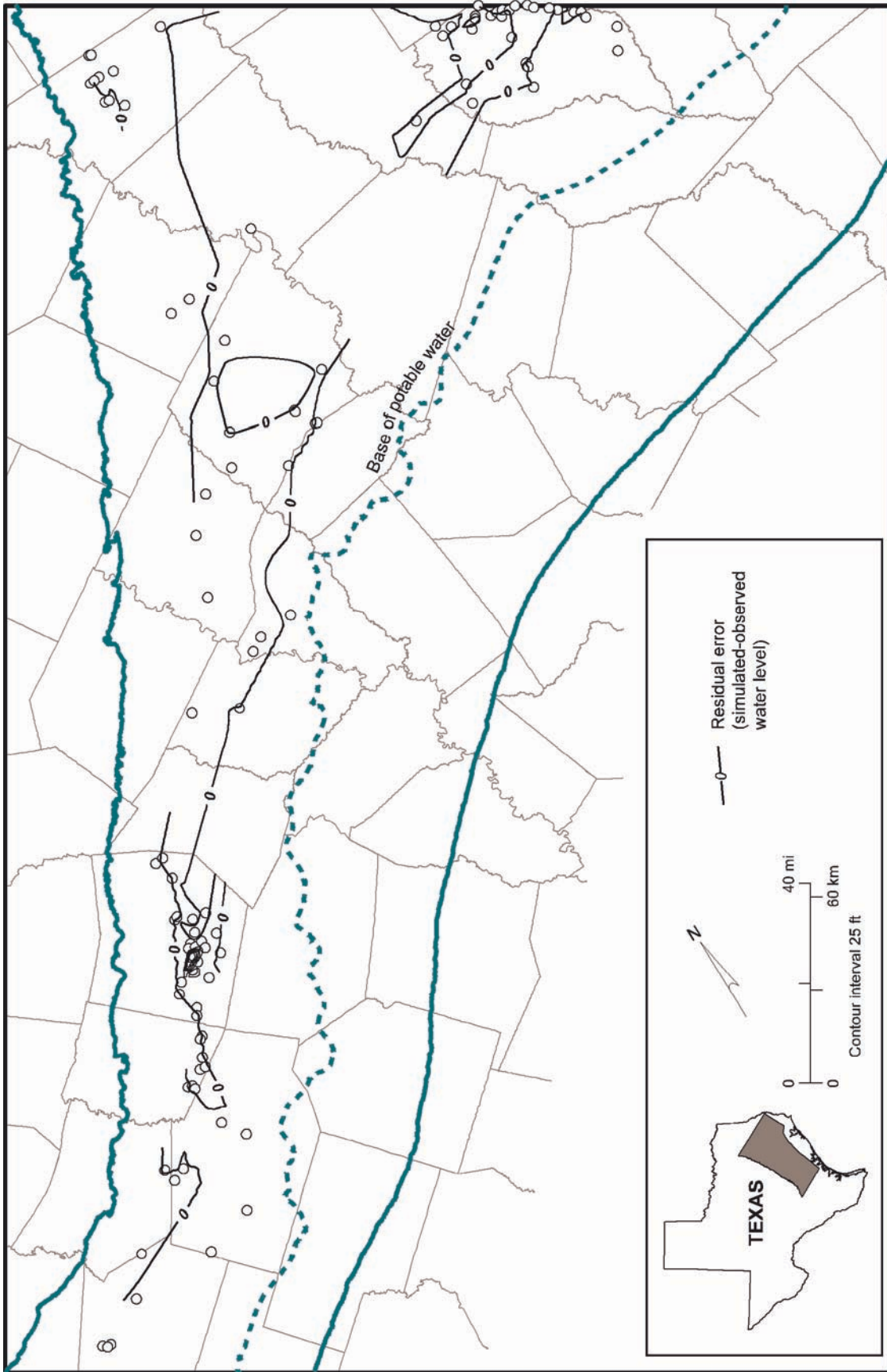
8.2 Sensitivity Analysis

We analyzed the sensitivity of the predevelopment model to horizontal and vertical hydraulic conductivity, recharge, ET, stream conductance, and general-head boundary



QA42289x

Figure 75. Map of residual differences between simulated and measured water levels for the Simsboro aquifer (layer 5) for the steady-state calibration.



QA0228Bx

Figure 76. Map of residual differences between simulated and measured water levels for the Carrizo aquifer (layer 3) for the steady-state calibration.

Table 12. Simulated groundwater discharge to streams.

River basin/stream	Estimated total discharge* (acre-ft/yr)	Percent of estimated base flow	Simulated total discharge (acre-ft/yr)		
			Steady state	1990	2000
<i>San Antonio River Basin Total</i>			20,400	18,300	18,000
San Antonio River	13,700	104	14,200	13,800	13,700
Cibolo Creek	6,700	93	6,200	4,500	4,300
<i>Guadalupe River Basin Total</i>			14,700	11,500	12,000
Guadalupe River	10,900	29	3,200	2,300	2,500
San Marcos River	11,100	104	8,900	7,500	7,800
Plum Creek			2,600	1,700	1,700
<i>Colorado River Basin Total</i>			12,500	11,000	10,800
Cedar Creek	26,100	48 ¹	3,100	2,900	2,900
Colorado River			6,900	6,000	6,000
Big Sandy Creek			2,500	2,100	1,900
<i>Brazos River Basin Total</i>			32,000	27,700	25,600
Middle Yegua Creek	5,200	93	4,800	4,100	3,700
East Yegua Creek	2,200	58	1,300	700	700
Brazos River	23,400	61 ²	4,300	4,000	3,900
Little River			6,100	5,500	5,300
Little Brazos River			1,300	1,200	1,200
Walnut Creek			2,600	1,700	600
Duck Creek	2,200	79	1,800	1,500	1,400
Steele Creek	8,100	119 ³	2,100	1,900	1,900
Navasota River			5,800	5,400	5,300
Big Creek			1,900	1,700	1,600
<i>Trinity River Basin Total</i>			11,200	10,700	10,500
Upper Keechi Creek	3,800	110	4,200	4,000	4,000
Tehuacana Creek	4,700	59	2,800	2,700	2,700
Trinity River	17,800	24	4,200	4,000	3,800
<i>Total</i>	135,900	67	90,800	79,200	76,900

* Rounded to nearest 100 acre-ft/yr

¹ Sum of Colorado River, Cedar Creek, Big Sandy Creek

² Sum of Brazos River, Little River, Little Brazos River, Walnut Creek

³ Sum of Navasota River, Steele Creek, Big Creek

(GHB) head and GHB conductance. Each of these input parameters was increased uniformly by 10 percent and 20 percent above the calibrated value and decreased 10 percent and 20 percent below the calibrated value. Trial-and-error adjustment showed that the steady-state model was not very sensitive to changes in the HFB hydraulic characteristic term. Further tests during the transient model calibration showed no reason to change the initial estimates of the HFB hydraulic characteristic.

Hydraulic conductivity, specific yield, ET, and GHB conditions were changed on a layer basis in layers 3 and 5, whereas recharge and stream conductance were changed modelwide. Sensitivity was measured as the mean difference (MD) between simulated water level for the calibrated model (h_{cal}) and simulated water level for the sensitivity run (h_{sens}):

$$MD = \frac{1}{n} \sum_{i=1}^n (h_{sens,i} - h_{cal,i}) \quad (13)$$

Results of the sensitivity analysis indicate that steady-state simulation of the Simsboro aquifer is most sensitive to

- recharge rates (fig. 77c),
- horizontal conductivity of the Simsboro aquifer (fig. 77a), and
- GHB heads imposed on the lateral boundaries of the Simsboro aquifer (fig. 77a).

Results are also sensitive to increases of more than 10 percent in GHB heads in layer 2 (fig. 77c). Sensitivity of model results to other parameters is an order of magnitude smaller (fig. 77). Variation of parameters in the Carrizo aquifer (layer 3) has only a slight impact on

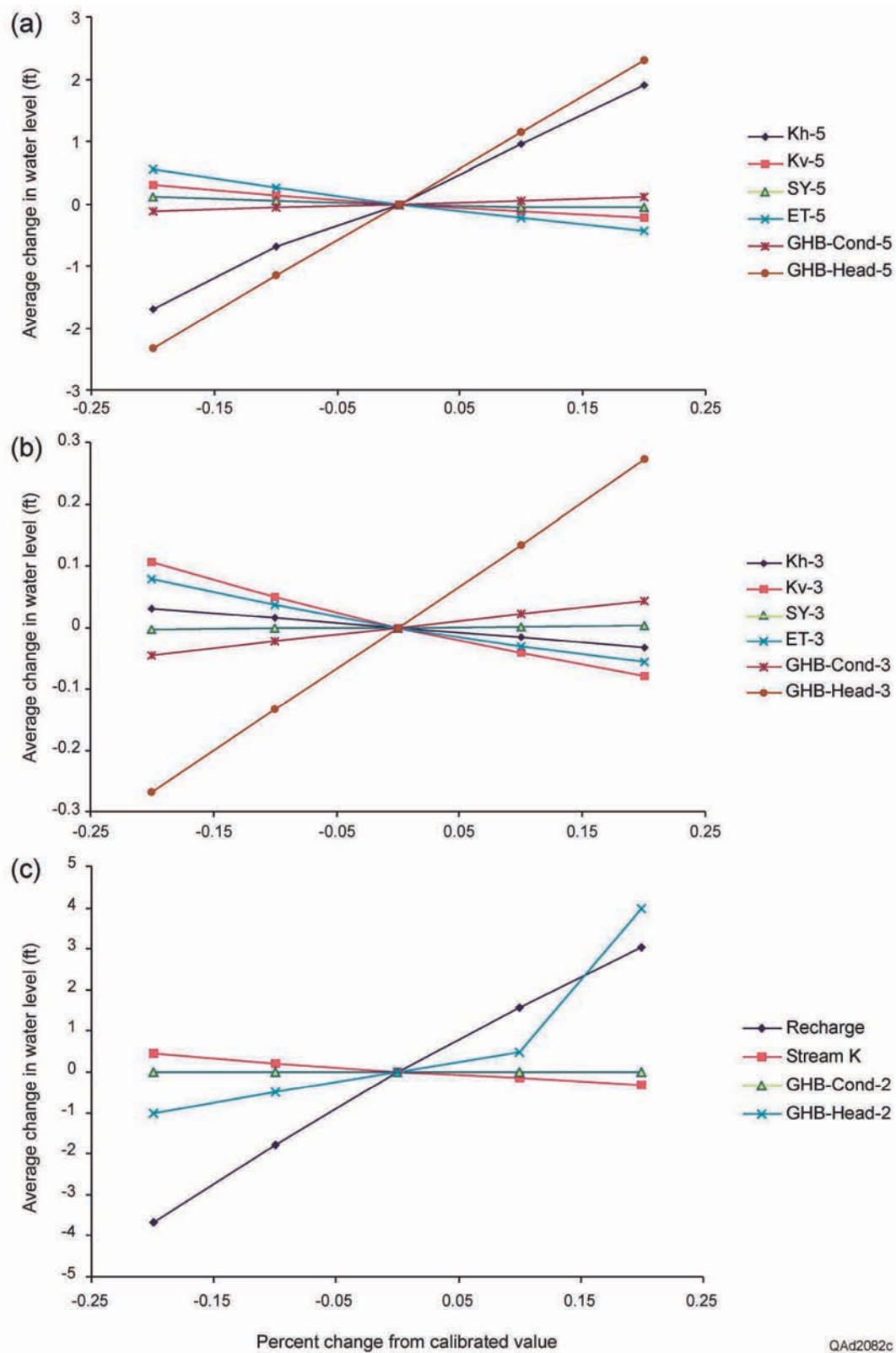


Figure 77. Sensitivity of predicted water levels in the Simsboro aquifer (layer 5) of the steady-state model to changes in parameter values for the (a) Simsboro aquifer (layer 5), (b) Carrizo aquifer (layer 3), and (c) recharge rate, streambed conductance, and the GHB boundary on the Reklaw aquitard (layer 2).

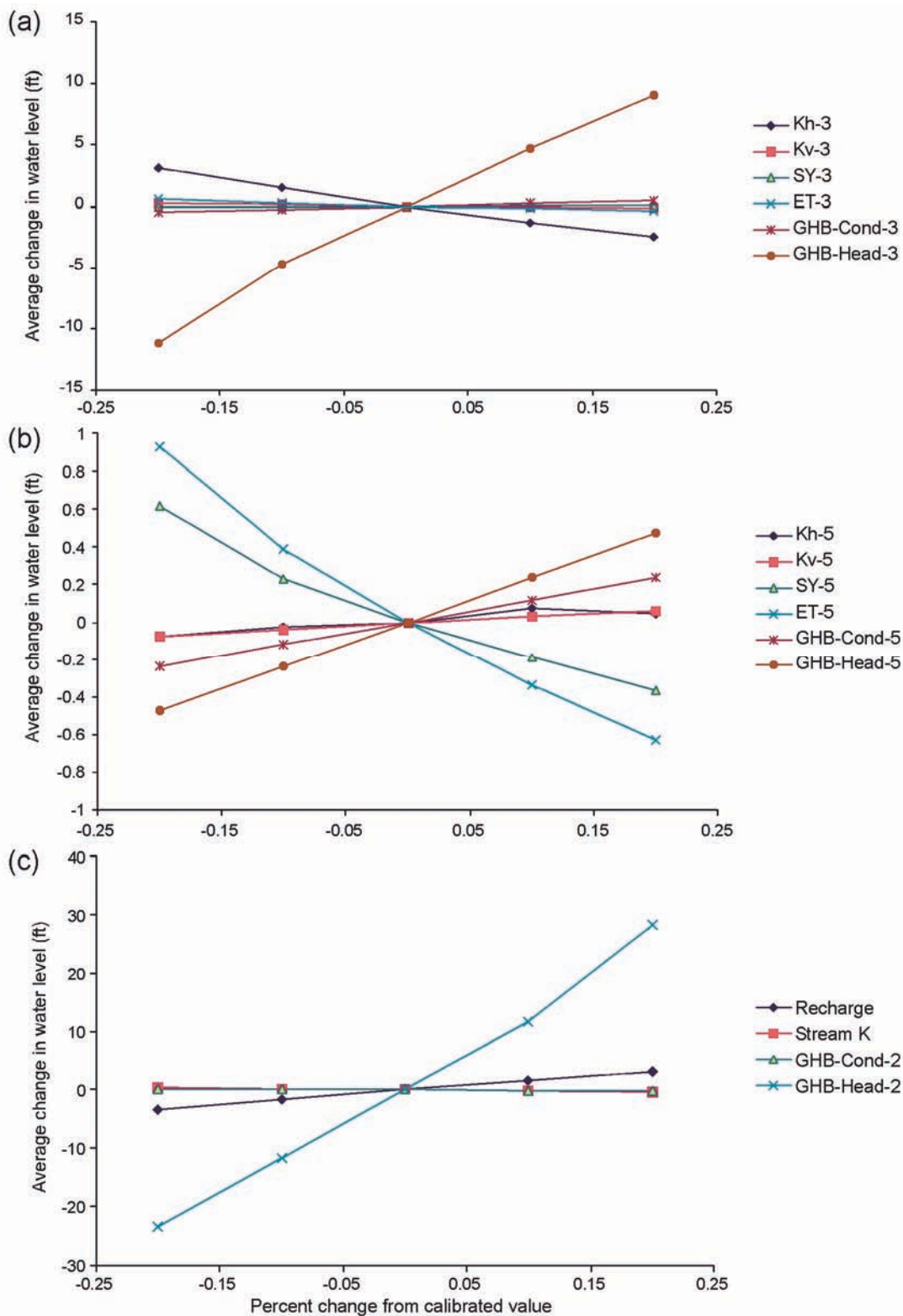
water levels in the Simsboro layer (fig. 77b); note the difference in vertical scale between figure 77a and b. Steady-state simulation results for the Carrizo aquifer are most sensitive to

- GHB heads imposed from layer 2 (fig. 78c), and
- GHB heads imposed on the boundaries of the Carrizo aquifer (fig. 78a).

Model results for the Carrizo aquifer are less sensitive to recharge and horizontal conductivity (fig. 78a, c). Variation of parameters in layer 5 has only a slight impact on water levels in the Carrizo layer (fig. 78b); note the difference in vertical scale between figure 78a and b.

8.3 Water Budget

Table 13 summarizes the water budget calculated for the steady-state model. Recharge provides 10 times more water overall than the GHB boundaries, except for the Reklaw aquitard (layer 2), which is dominated by that boundary (fig. 58). Simulated ET removes approximately 75 percent of total (gross) recharge. Simulated ET removes almost 100 percent of recharge to alluvium (layer 1) and to aquitard layers 2, 4 and 6. Approximately 60 percent of recharge in the Simsboro and Carrizo aquifers is removed by groundwater ET. The water-balance error for the steady-state model, which is the difference between inflow and outflow for the model, is less than 0.01 percent. Net recharge is the flux of groundwater moving from the unconfined to the confined part of the aquifer and is estimated by summing the simulated fluxes across the flow faces of model cells at the boundary between the unconfined and confined zones. Net recharge rates to the Simsboro and Carrizo layers average 0.5 and 0.3 inches/yr, respectively, in the steady-state model. Figure 79 illustrates the water budget of the steady-state model, with a block diagram showing the inflow to and outflow from the model area.



QAd2081c

Figure 78. Sensitivity of predicted water levels in the Carrizo aquifer (layer 3) of the steady-state model to changes in parameter values for the (a) Carrizo aquifer (layer 3), (b) Simsboro aquifer (layer 5), and (c) recharge rate, streambed conductance, and the GHB boundary on the Reklaw aquitard (layer 2).

Table 13. Water budget for the calibrated steady-state model (1,000 acre-ft/yr). Positive values are inflow to the aquifer; negative values are discharge from the aquifer. Annual rates determined from the last time step (12 mo long) of the 1-yr steady-state stress period.

Layer	Recharge	Net recharge	ET	Stream leakage	Reservoir leakage	GHB Reklaw	GHB downdip boundary	GHB NE boundary	GHB SW boundary	Wells	Cross-formational flow	Change in storage	Water balance error (%)
Alluvium (1)	12.6	0	-13.3	-26.3	0	0	0	0	0	0	27.0	0	-0.005
Reklaw (2)	13.7	-5.6	-20.5	-0.6	0	-36.9	0	0	0	0	44.2	0	-0.007
Carrizo (3)	117.2	11.9	-72.4	-32.5	0	0	2.4	-0.9	18.3	0	-32.1	0	-0.003
Calvert Bluff (4)	45.4	-9.3	-39.6	-13.5	0	0	2.3	13.1	0.2	0	-7.9	0	-0.006
Simsboro (5)	59.4	14.8	-31.1	-13.3	0	0	2.2	4.6	0.2	0	-22.0	0	-0.004
Hooper (6)	24.6	4.3	-15.9	-4.4	0	0	1.4	3.5	0.0	0	-9.2	0	-0.001
ALL	272.9	16.1	-192.8	-90.6	0	-36.9	8.4	20.2	18.6	0	0	0	-0.005

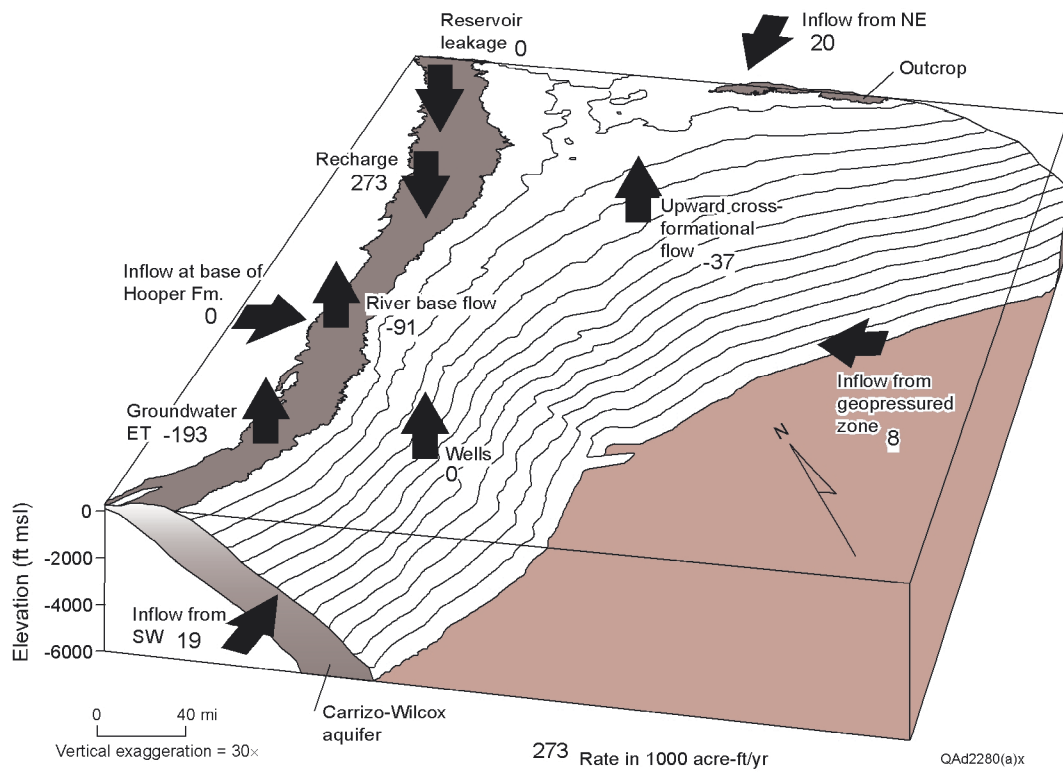


Figure 79. Block diagram of the Carrizo–Wilcox aquifer representing the components of the steady-state model.

9.0 TRANSIENT MODEL

After we calibrated the initial predevelopment version of the model, we added stress periods to represent the aquifer from 1951 through 1990. Moving the starting date for the transient model to 1951 decreases the influence of initial conditions on model results for the 1990 calibration. During the calibration phase we made further adjustments to all model parameters, including horizontal and vertical hydraulic conductivity, recharge, parameters for the stream-flow routing and ET packages, GHB boundaries, horizontal-flow-barrier (HFB) parameters, specific storage, and specific yield.

9.1 Calibration and Verification

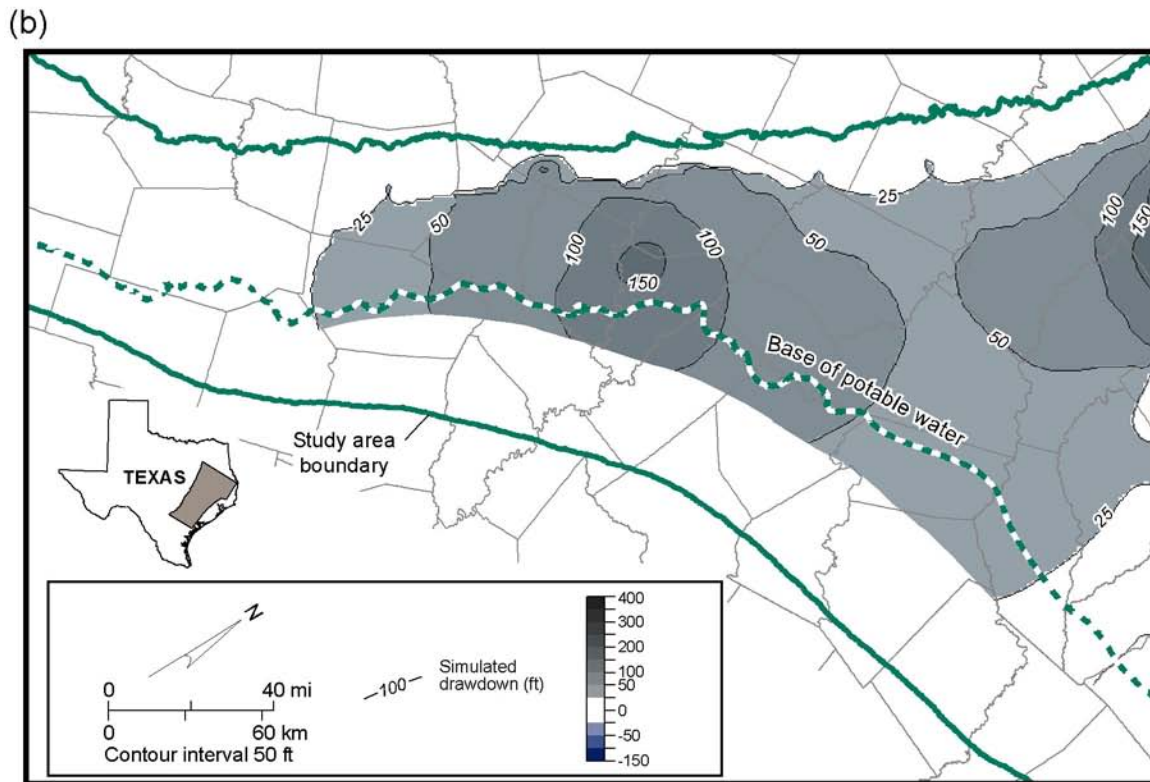
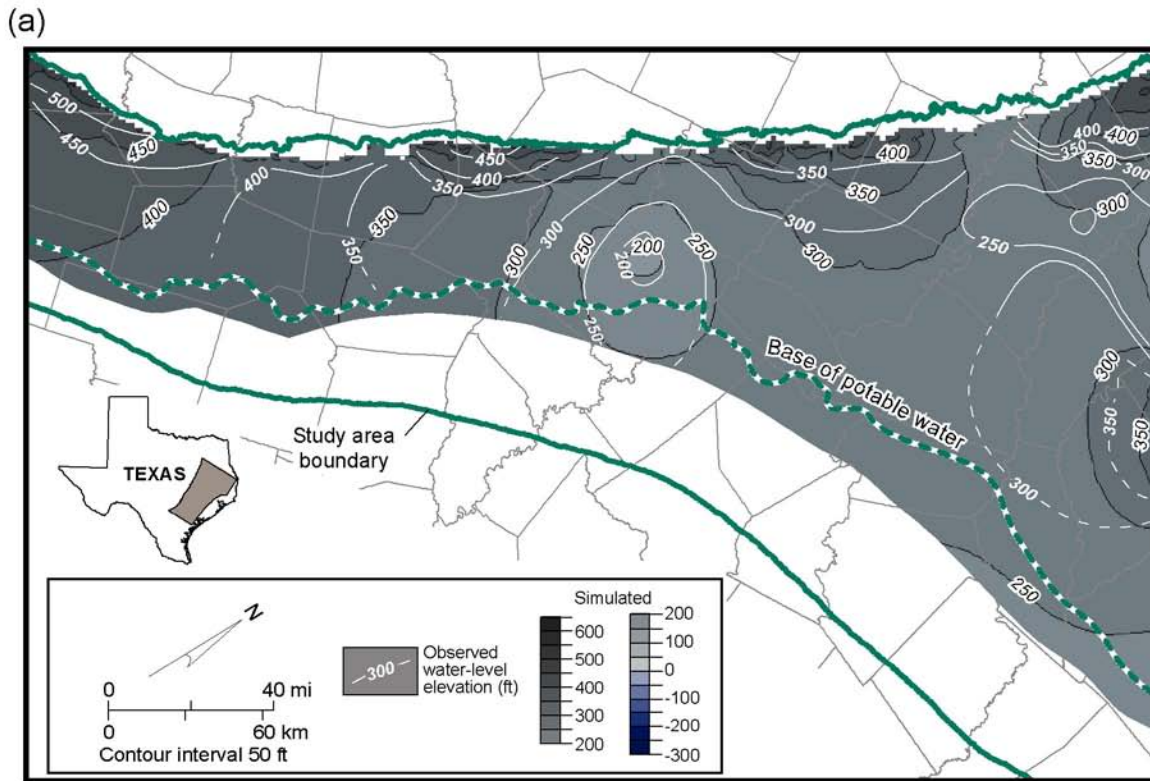
The period from 1980 through 2000 has the best available estimates of total pumping rates for each county. We projected the 1980 estimates backward to 1950 by assuming that pumping rates did not vary greatly except in municipal well fields. Municipal and rural domestic pumping rates for 1950 through 1979 were distributed through time on the basis of county population. Irrigation rates were varied on the basis of annual rainfall. Other pumping rates were held at 1980 levels (fig. 52).

During transient model calibration we adjusted the GHB heads along the northeast boundary of the model to account for the areas of drawdown related to groundwater withdrawal outside of the model in Smith County (Intera and Parsons Engineering Science, 2002a). In addition, we varied GHB conductance from 0 to very large for the northeast boundary. A GHB conductance of 0 makes the boundary equivalent to a no-flow boundary. A large GHB conductance imposes the greatest effect of the boundary on the model.

The distance at which the model responds to further increases in GHB conductance asymptotically approaches the maximum distance of 30 to 40 miles of the northeast boundary. The value of GHB conductance we used (set equal to transmissivity) allows the imposed GHB heads to have an effect extending into the model approximately 15 to 20 miles. Because the three GAM models were designed with overlaps, it may be more suitable to use either the northern or southern GAM models (Intera and Parsons Engineering Science, 2002a, 2002b) within 30 to 40 miles of the northeast or southwest boundaries of the central GAM model.

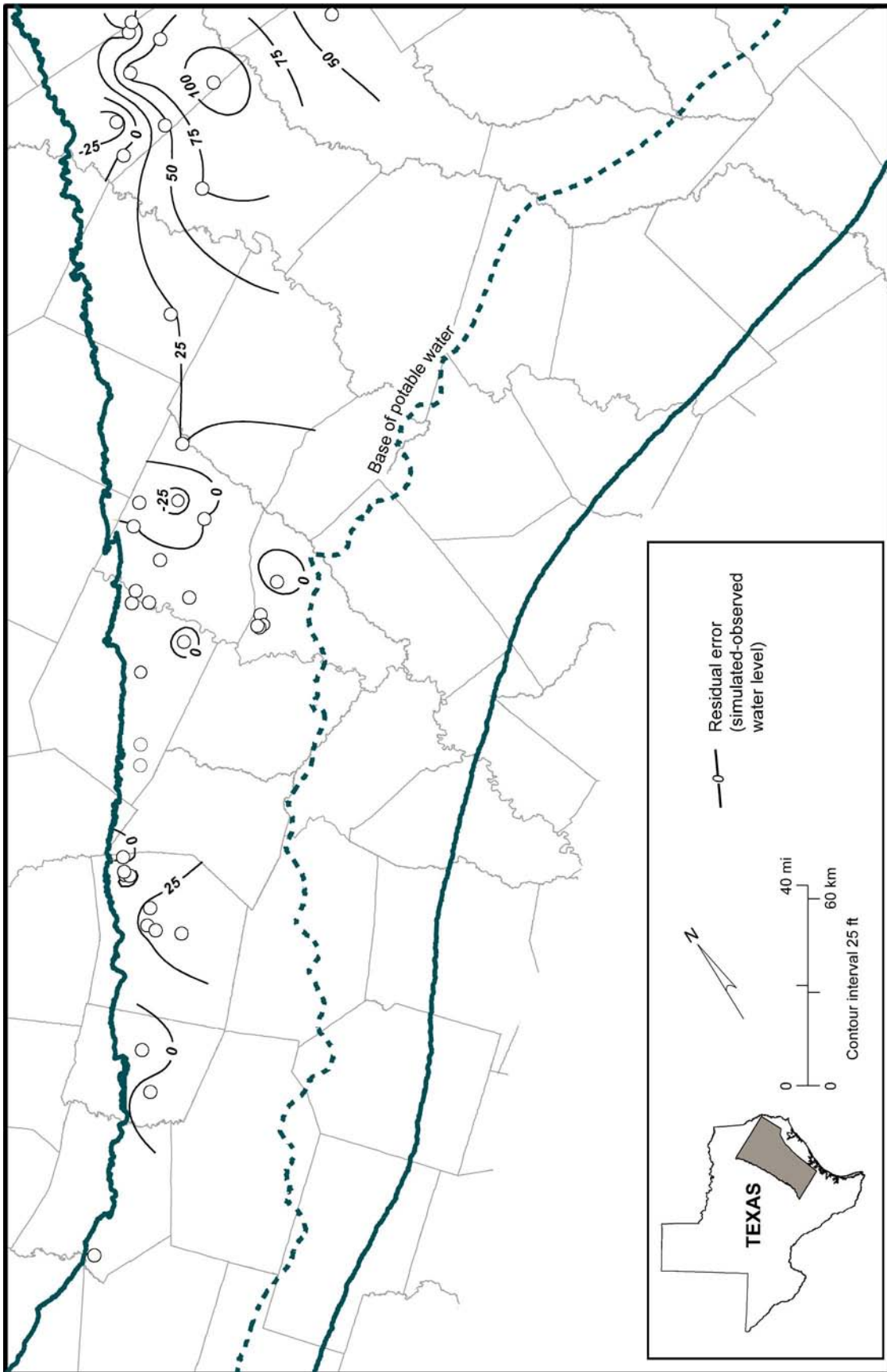
Simulated water levels for 1990 reflect the effects of groundwater withdrawal in the artesian part of the Carrizo–Wilcox aquifer (fig. 80). The model generally does a good job in matching water levels and drawdown in the Simsboro and Carrizo aquifers. The simulated water level as of 1990 at the center of the Bryan-College Station well field in the Simsboro aquifer is within 15 ft of the reported levels (figs. 80a, 81); simulated drawdown slightly overestimates actual drawdown in the Simsboro aquifer. The RMSE comparing simulated and observed water levels in the Simsboro aquifer for 1990 is 36 ft (fig. 82, table 11). Whereas this is larger than the 25-ft RMSE calculated for the steady-state calibration, it is a smaller fraction (10.0 percent) of the range in observed water levels (363 ft) and is based on three times the number of data points available for the steady-state calibration (n=42; table 7).

The RMSE comparing simulated and observed water levels in the Carrizo aquifer for 1990 is 49 ft (fig. 82a); 6.8 percent of the range in observed water levels (table 11). The dominant feature in the map of simulated water levels for 1990 in the Carrizo aquifer is the drawdown related to withdrawal of groundwater in the Lufkin-Angelina County well field



QAd2078c

Figure 80. Maps for the Simsboro aquifer (layer 5) showing (a) simulated and observed 1990 water level and (b) drawdown from 1950 through 1990.



QA42063C

Figure 81. Map of residual differences between simulated and measured water levels for the Simsboro aquifer (layer 5) for the 1990 calibration.

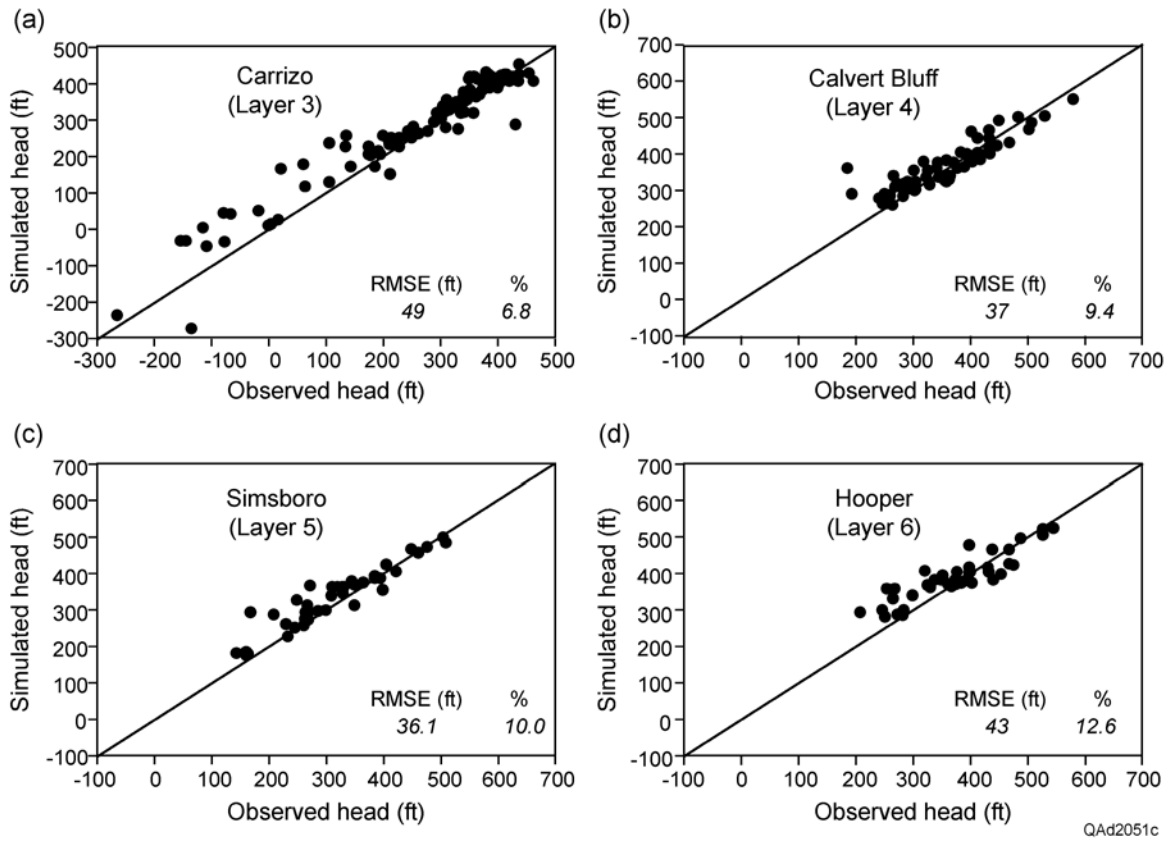
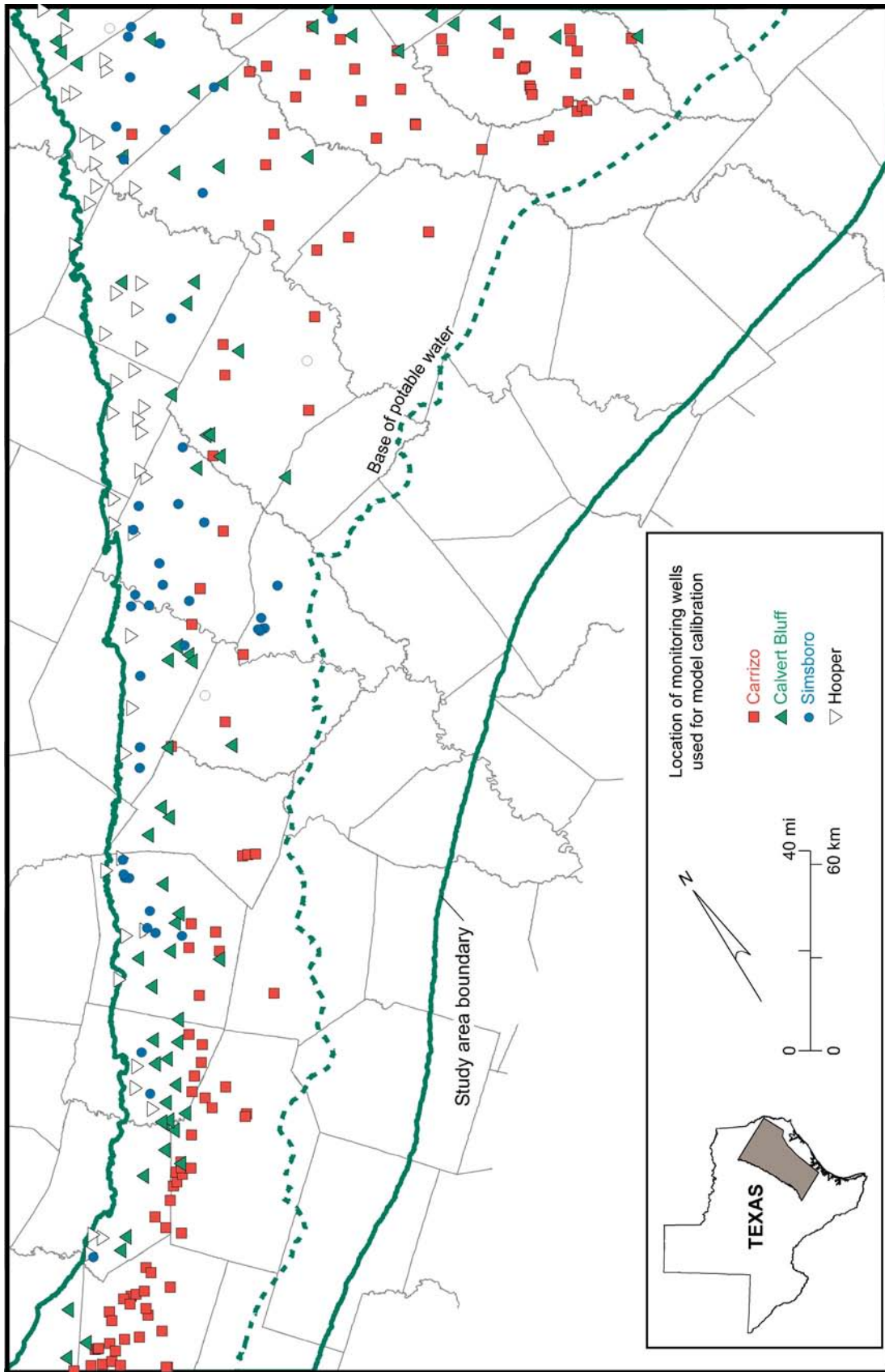


Figure 82. Comparison of simulated and observed water levels for the 1990 calibration. Well locations are shown in figure 83.



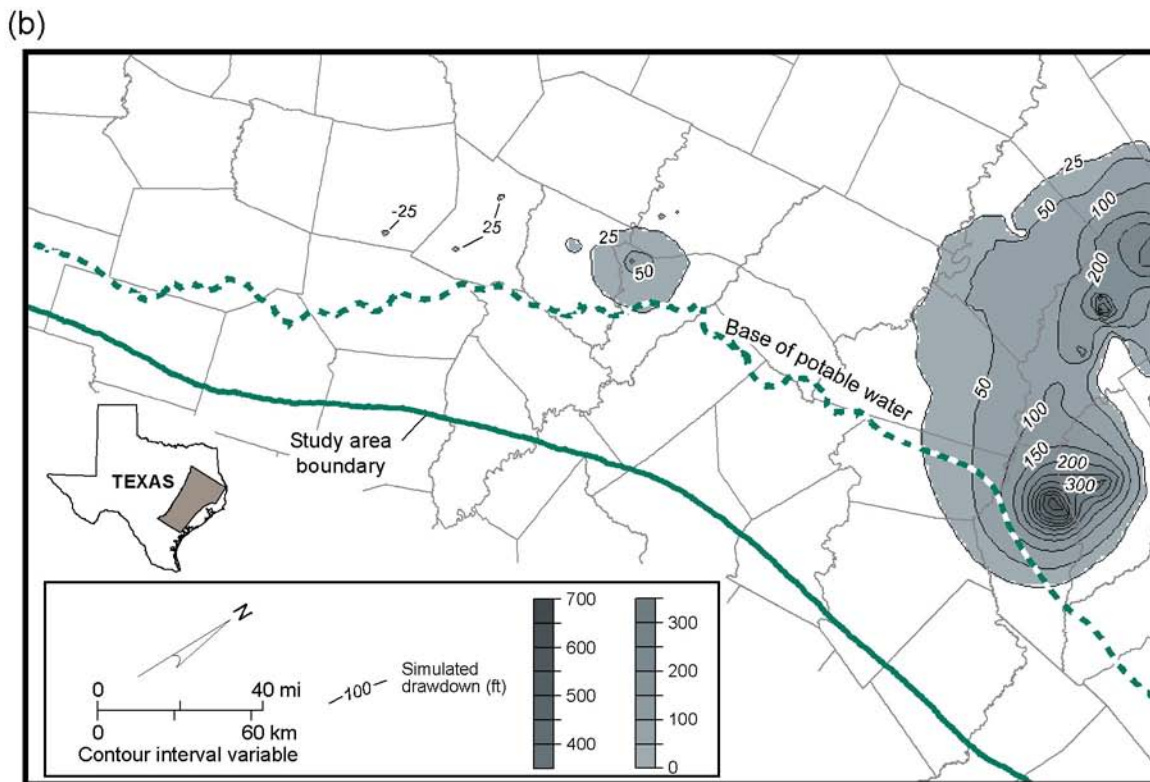
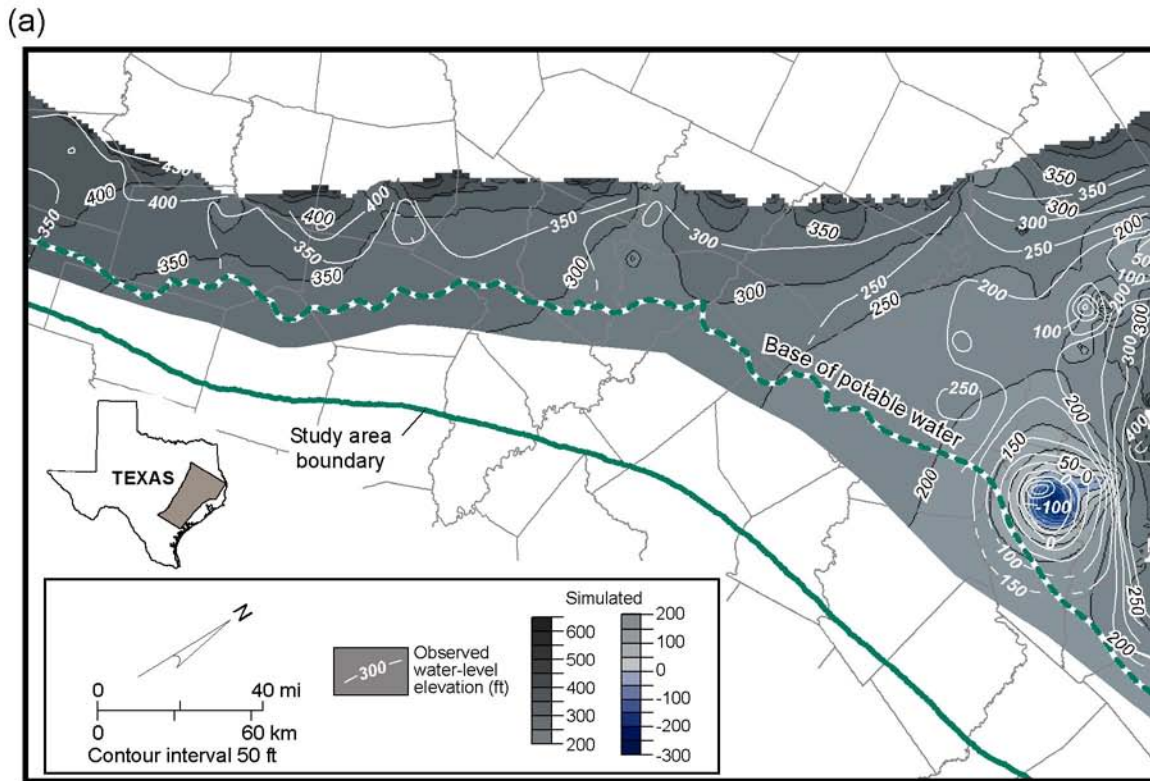
QA41814(c)

Figure 83. Location of wells used to develop the 1990 calibration of the model shown in figure 82.

(fig. 84). Whereas in most parts of the study area the match between simulated and observed water levels is within ± 25 ft, the biggest differences between simulated and observed water levels in the Carrizo aquifer are near the northeastern boundary of the model. The model overestimates drawdown in northern Anderson County and in the Lufkin-Angelina County well field by more than 125 ft (fig. 85). Part of the discrepancy may be due to an effect of the model's northeast boundary on simulation results. Other factors could include errors in pumping rates, storativity, and vertical permeability between the Carrizo and Reklaw layers.

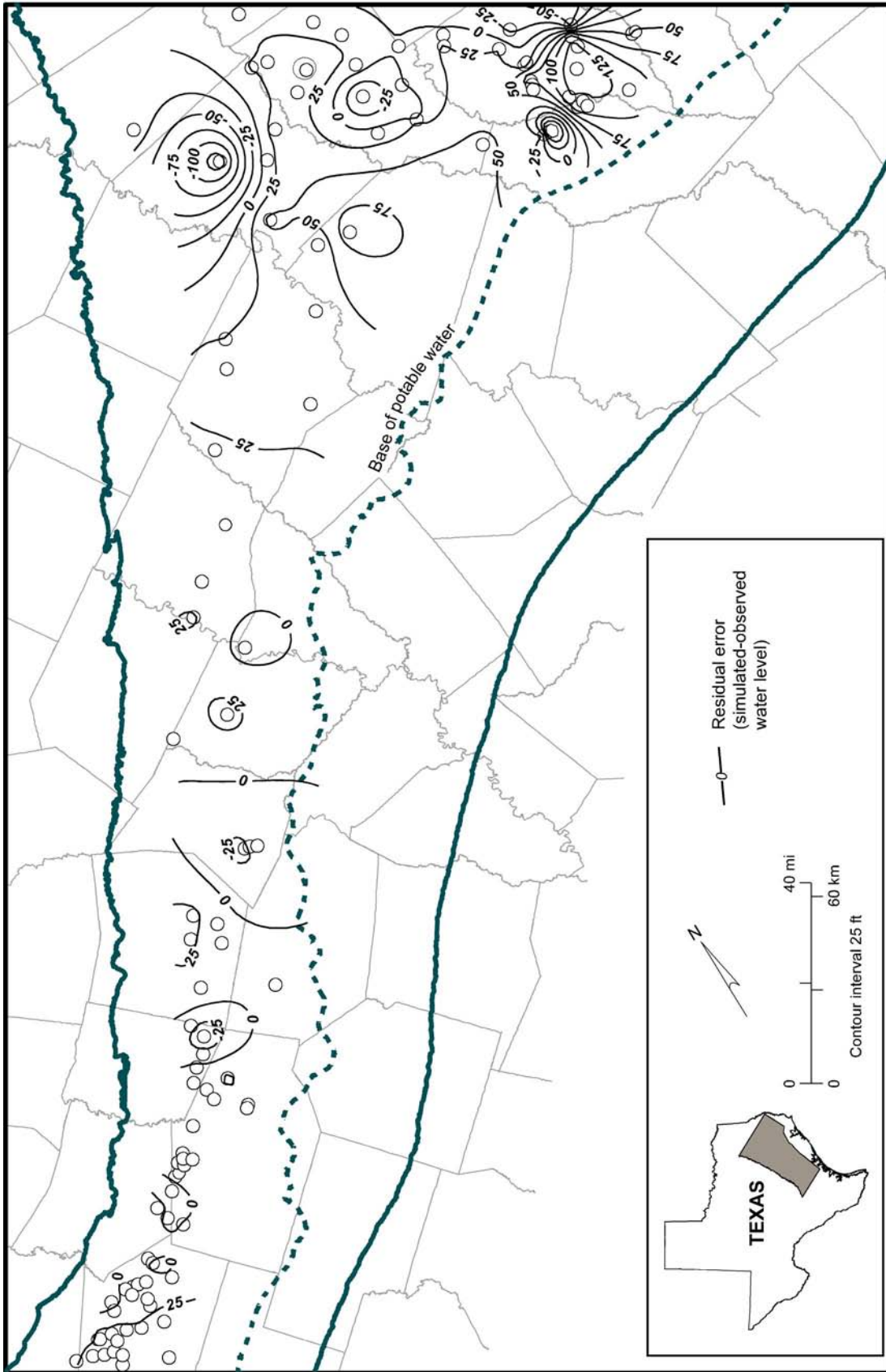
Water levels simulated in the Hooper and Calvert Bluff aquitards for 1990 are shown in figures 86a and 87a, respectively. The RMSE values comparing simulated and observed water levels in the Hooper and Calvert Bluff aquitards for 1990 are 43 (fig. 82d) and 38 (fig. 82b) ft, respectively.

The number of water-level observations for use in model calibration is smaller for 2000 than for 1990 (table 11). The range in observed water levels measured in the Simsboro and Carrizo aquifers, however, increased from 1990 to 2000 (table 11). Applying the calibrated model to the 1991 through 2000 verification period shows a slightly improved match between simulated and observed water levels (fig. 88, table 11) partly because of the increased range of water-level elevations, a result of continued groundwater withdrawal. The simulated water level as of 2000 at the center of drawdown in the Bryan-College Station well field is about 115 ft above sea level (fig. 90a). This is 100 ft above the reported most drawn-down water levels. For 2000 the model underestimates the amount of maximum drawdown since 1950. Drawdown in the Simsboro aquifer in northern Brazos and southern Robertson Counties before 2000 is estimated to have been more than 300 ft (fig. 90b). In most areas the simulated and observed water levels match within ± 30 ft; simulated water levels tend to overestimate observed water levels at depth in the confined aquifer (fig. 91).



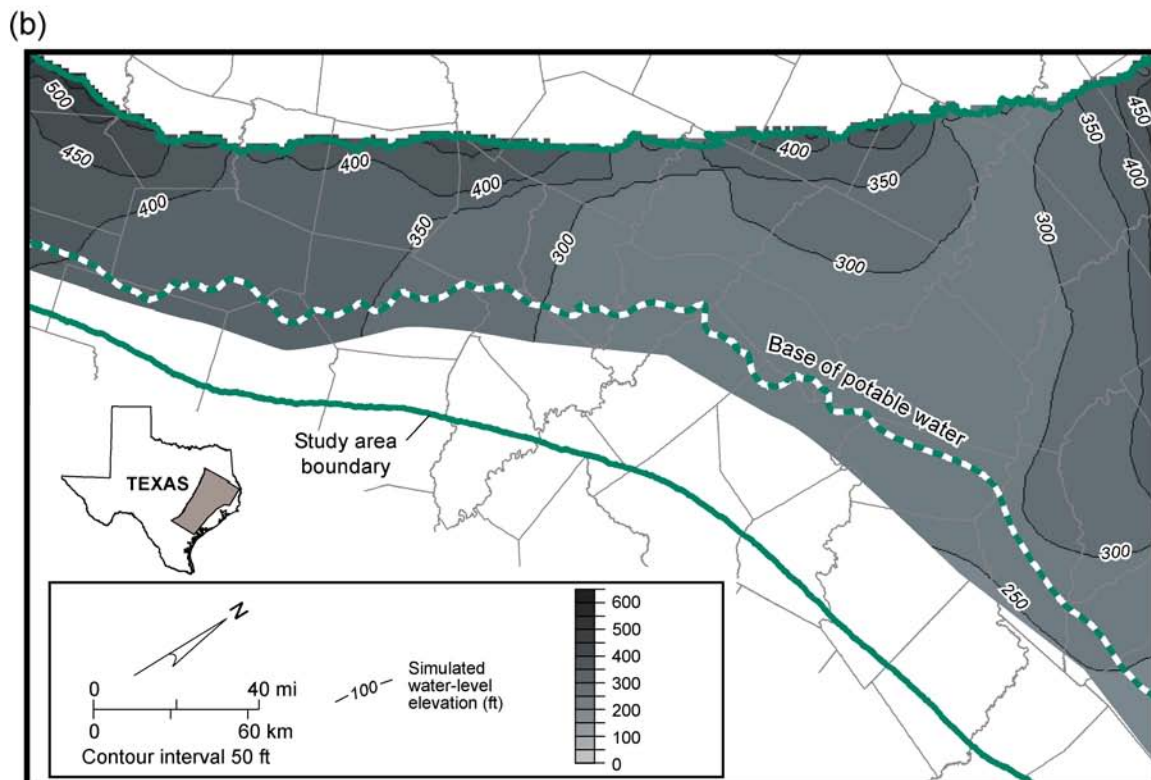
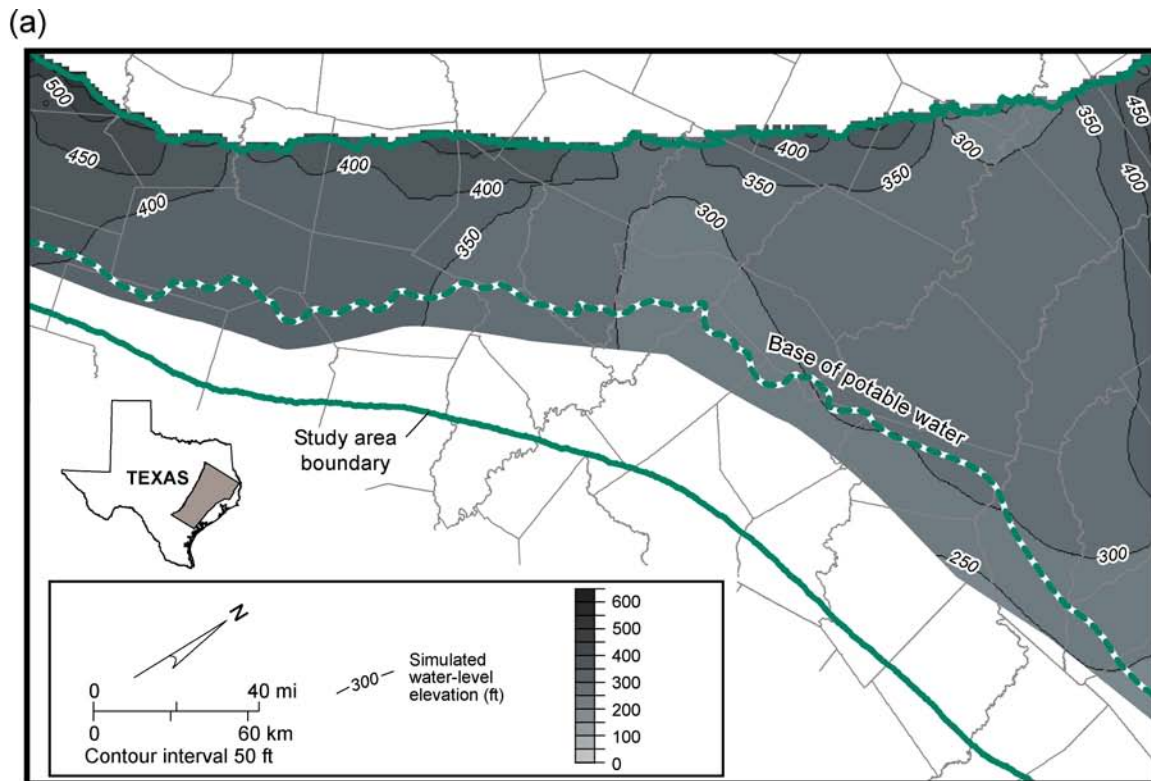
QAAd2077c

Figure 84. Maps for the Carrizo aquifer (layer 3) showing (a) simulated and observed 1990 water level and (b) drawdown from 1950 to 1990.



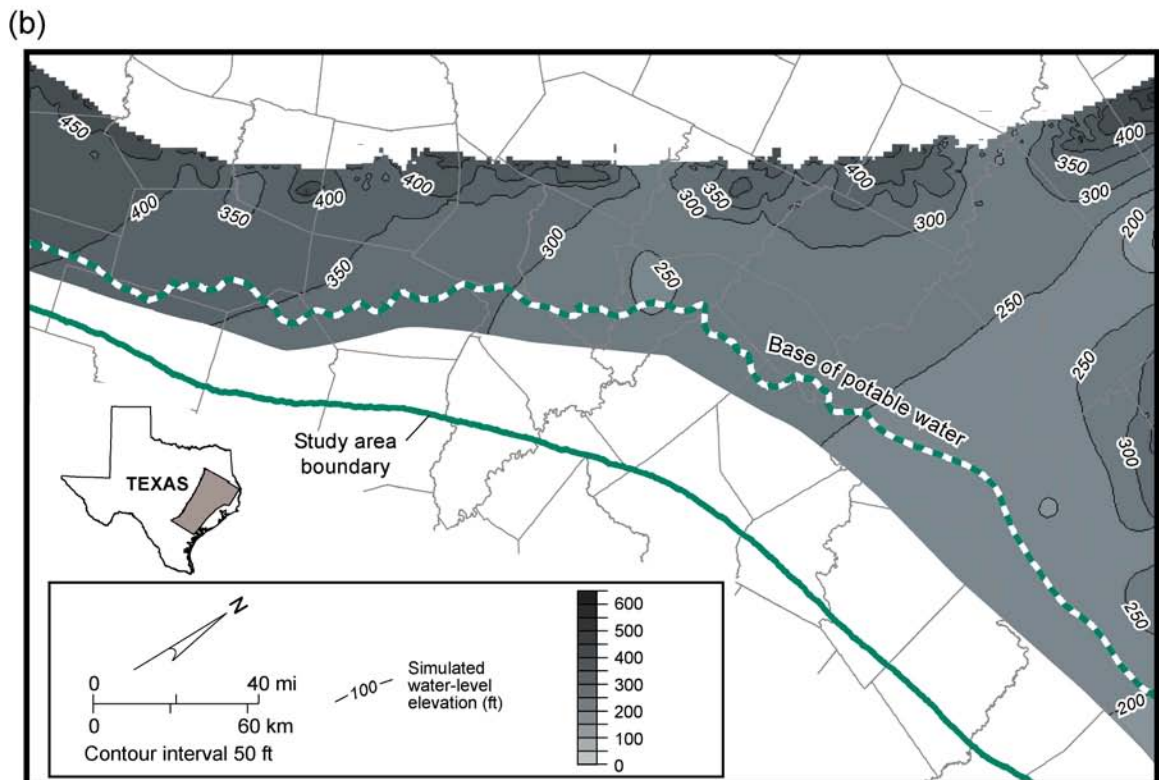
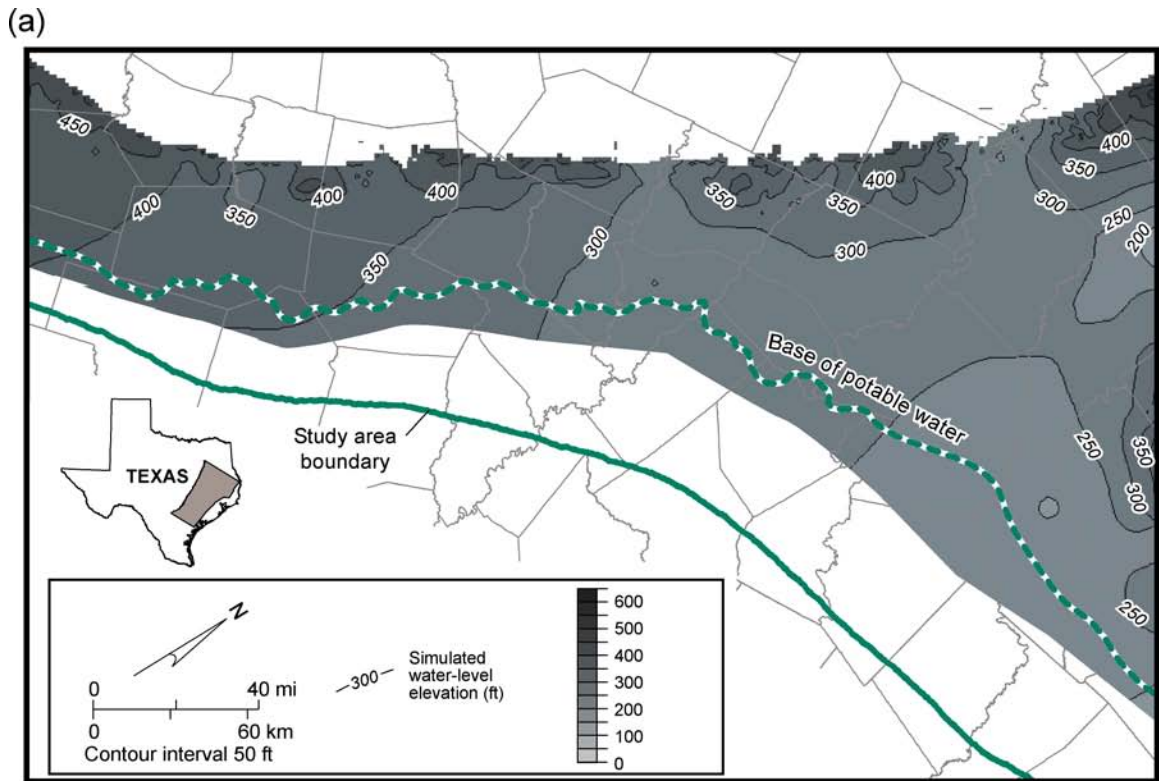
QA42064c

Figure 85. Map of residual differences between simulated and measured water levels for the Carrizo aquifer (layer 3) for the 1990 calibration.



QAd2263c

Figure 86. Maps of water level in the Hooper Formation (layer 6) in (a) 1990 and (b) 2000.



QAd2264c

Figure 87. Maps of water level in the Calvert Bluff Formation (layer 4) in (a) 1990 and (b) 2000.

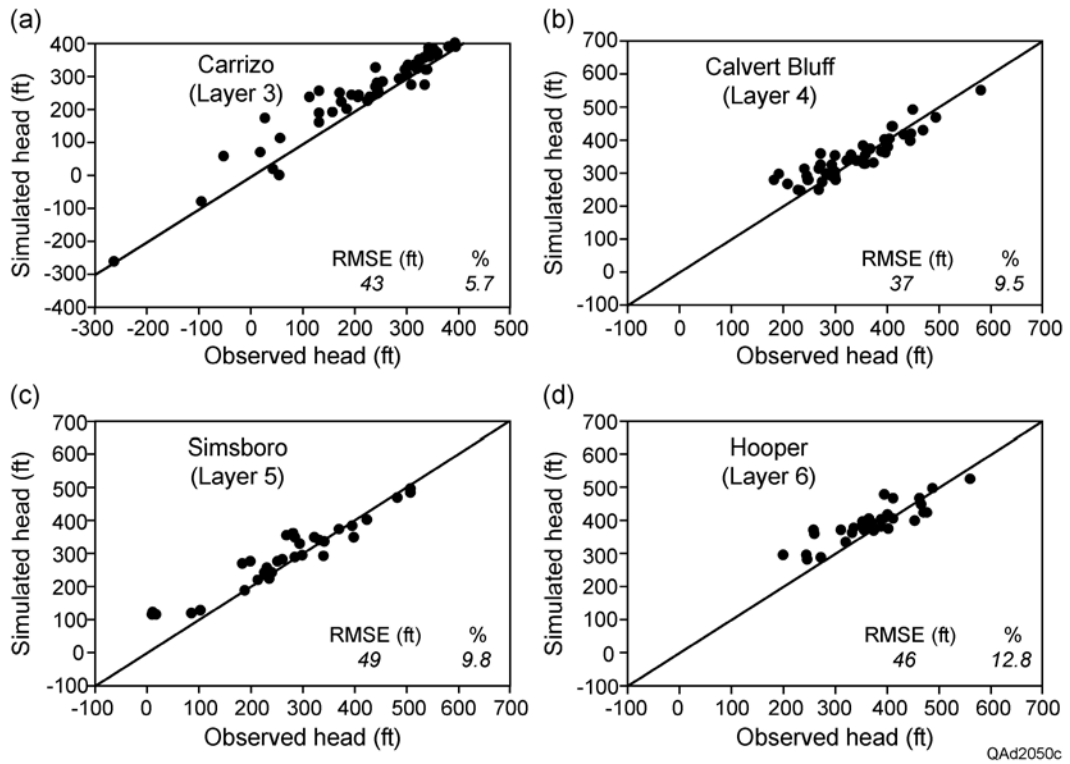
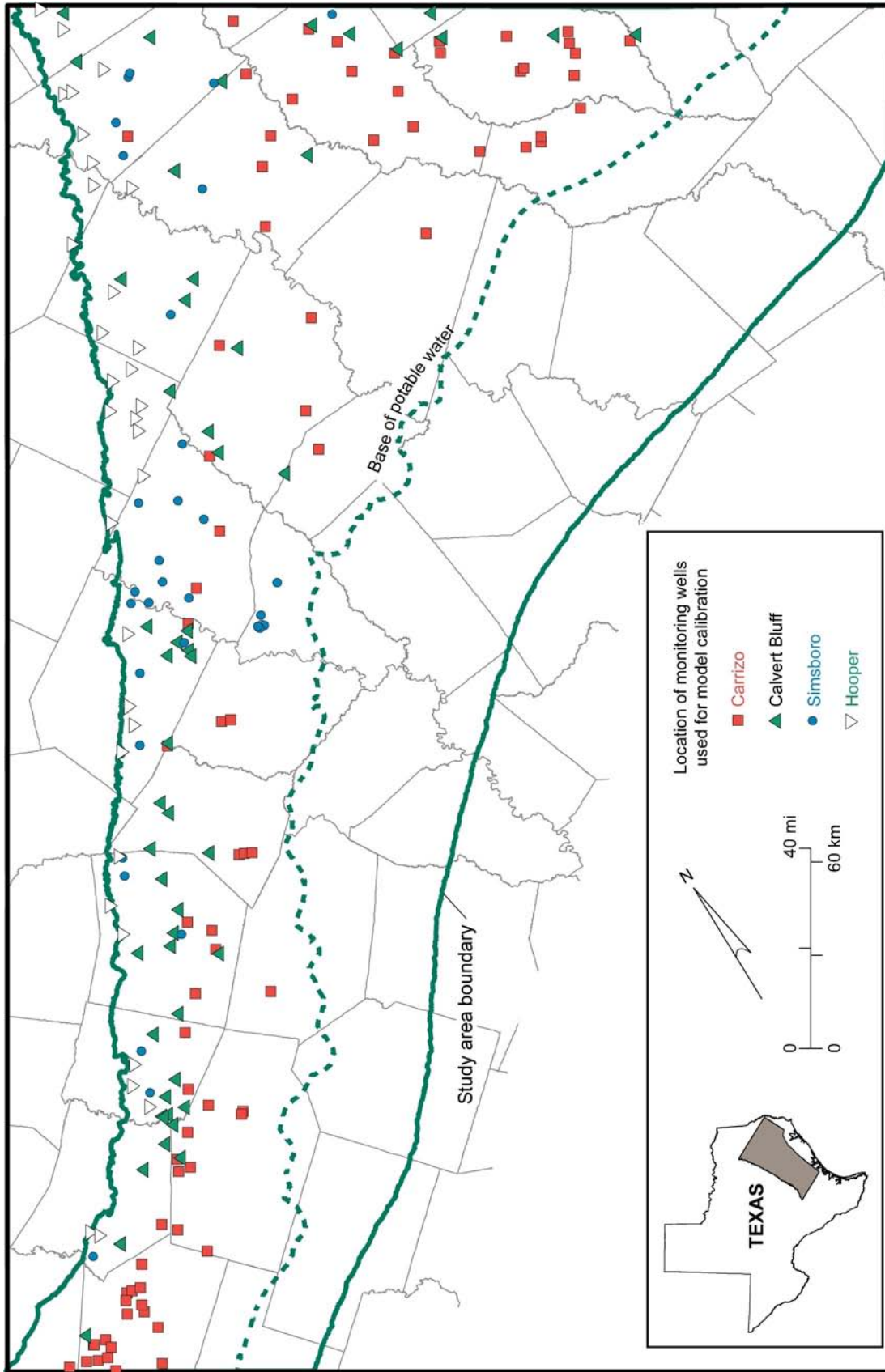
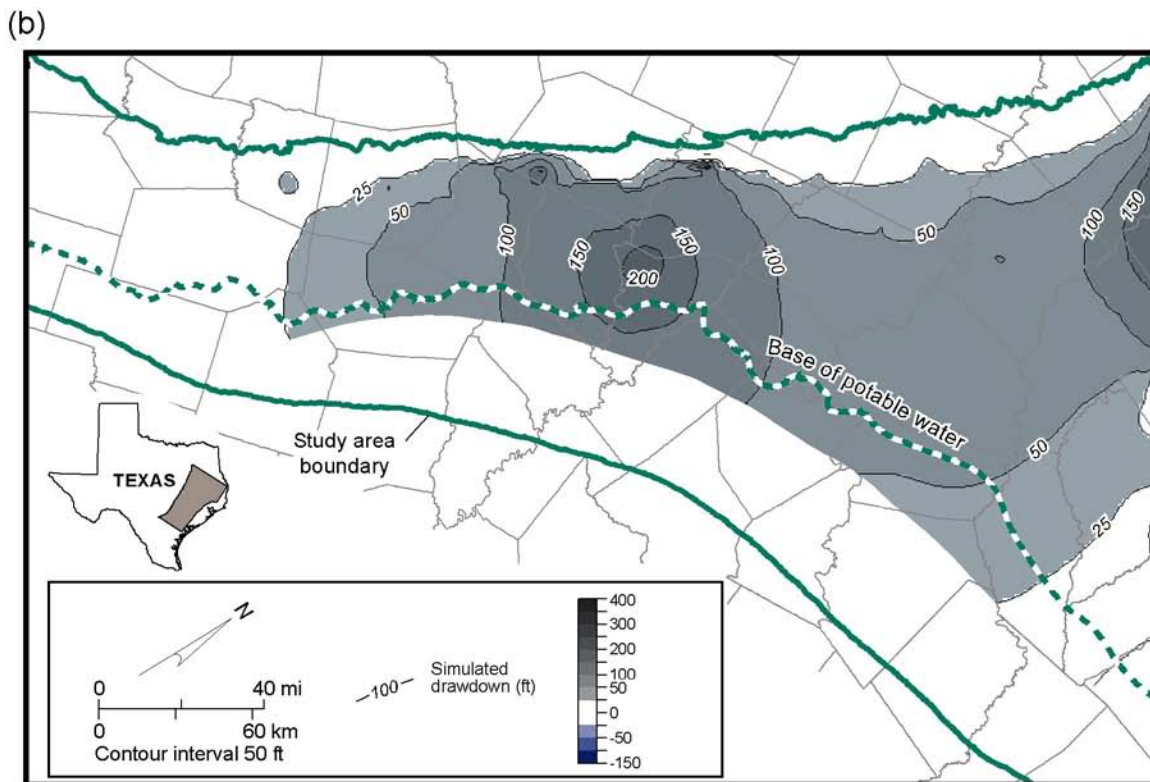
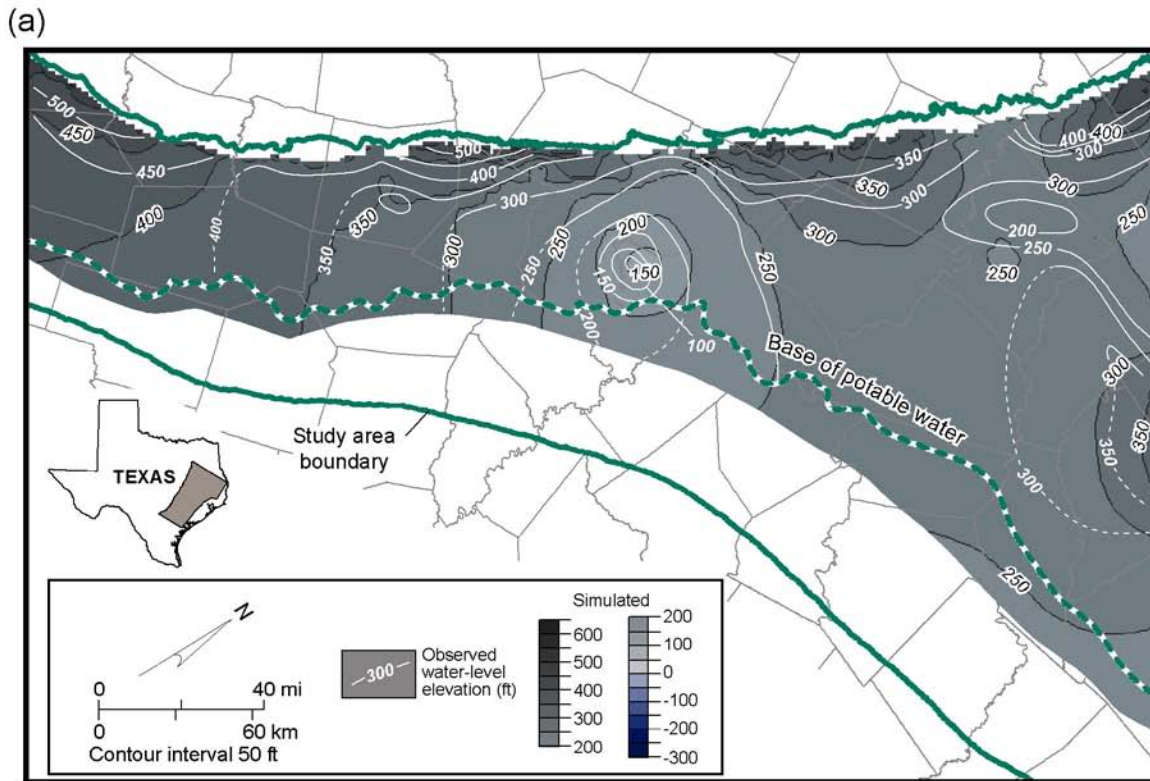


Figure 88. Comparison of simulated and observed water levels for the 2000 calibration. Well locations are shown in figure 89.



QA41814(0)c

Figure 89. Location of wells used to develop the 2000 calibration of the model shown in figure 88.



QAd2080c

Figure 90. Maps for the Simsboro aquifer (layer 5) showing (a) simulated and observed 2000 water level and (b) drawdown from 1950 through 2000.

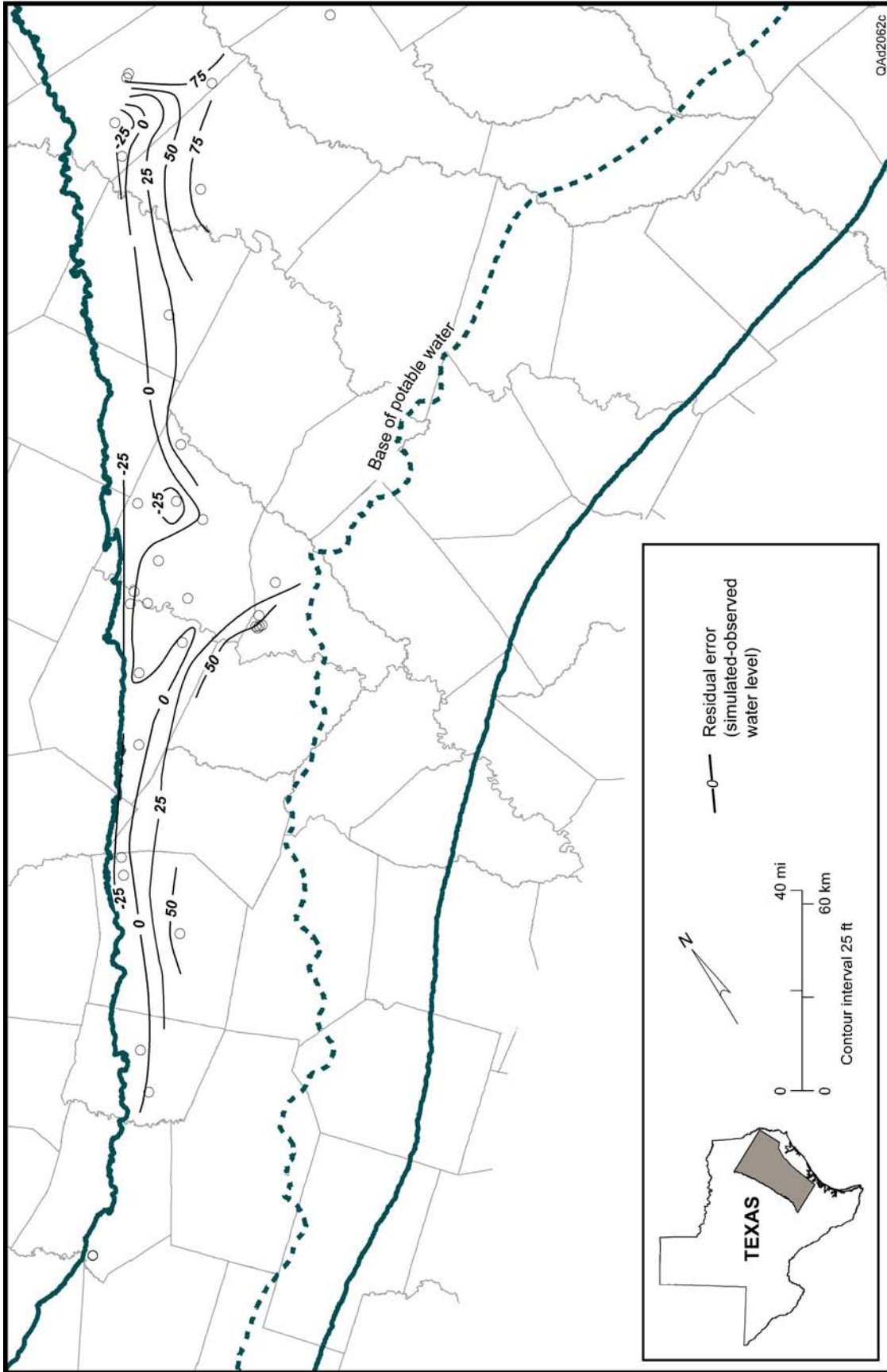
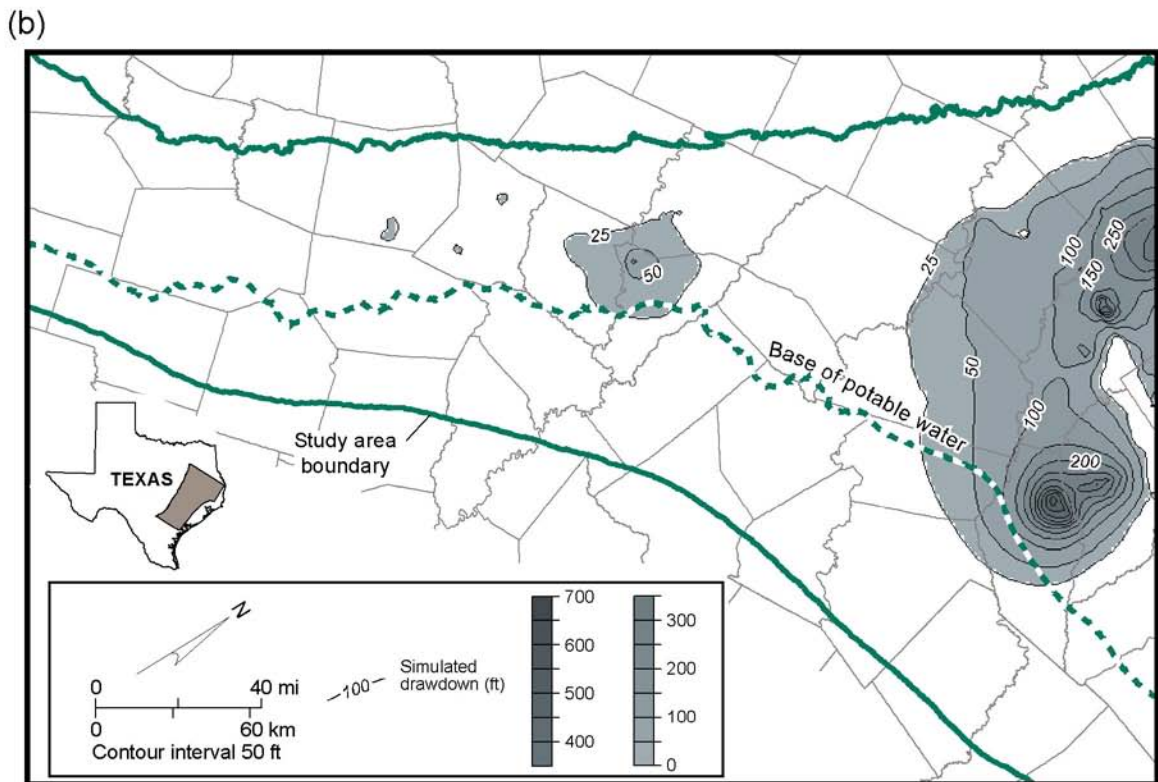
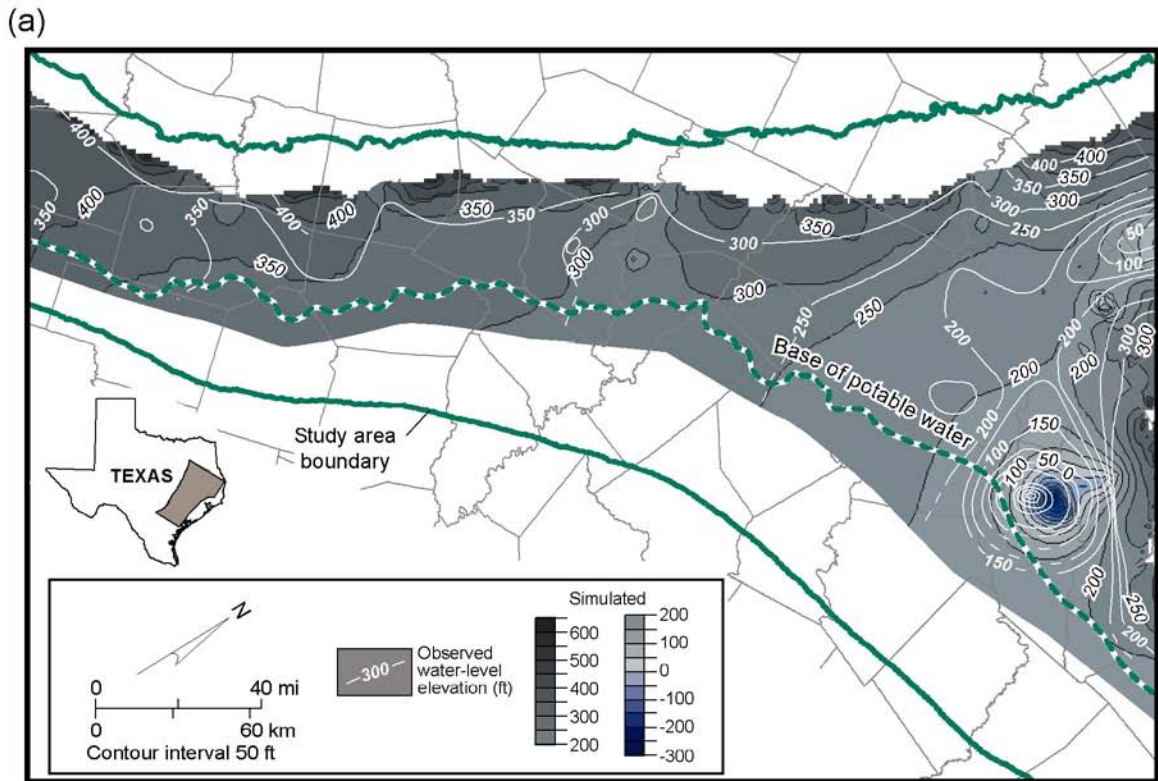


Figure 91. Map of residual differences between simulated and measured water levels for the Simsboro aquifer (layer 5) for the 2000 calibration.

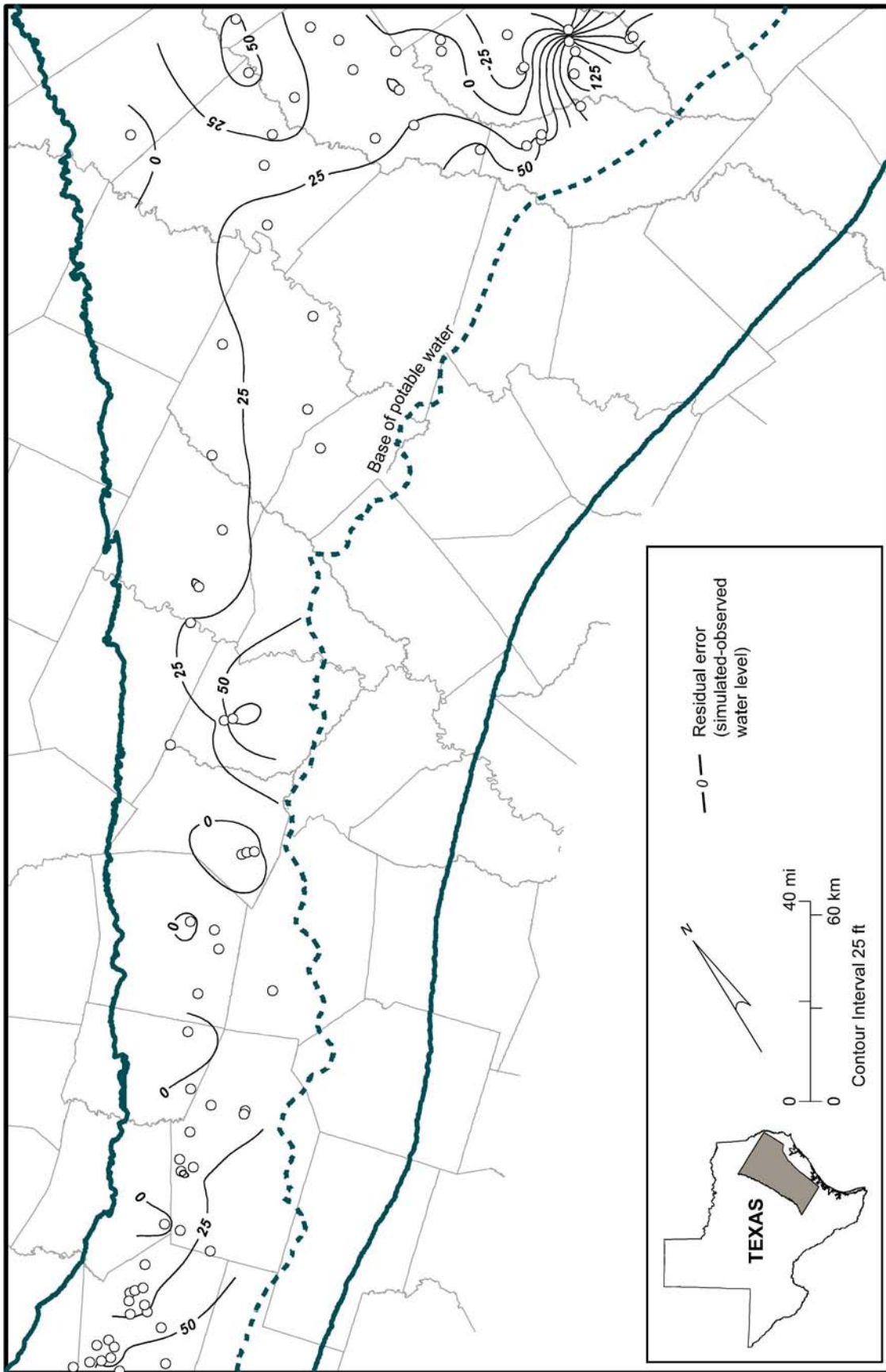
The RMSE comparing simulated and observed water levels in the Carrizo aquifer for 2000 is 43 ft (fig. 82a). During the 1990s, water-level elevation in the Lufkin-Angelina County well field decreased by approximately another 50 ft to more than 300 ft below sea level (fig. 92a). Total drawdown since 1950 is estimated to have been almost 600 ft. The model simulation for 2000 overestimates drawdown in the Lufkin-Angelina County well field by about 30 ft (fig. 93). The Bryan-College Station well field includes withdrawal from the Carrizo aquifer. Artesian drawdown in the vicinity of that well field is influenced by the Karnes-Milano-Mexia Fault Zone (fig. 14), represented in the model using the horizontal-flow-barrier (HFB) package of MODFLOW. The effect of the fault zone is to impede the movement of water from the outcrop toward the well field and results in the “cone of depression” being elongated in a northeast-southwest trend. In most of the study area the match between simulated and observed water levels is within ± 30 ft in the Carrizo aquifer (fig. 93). The largest apparent discrepancy is near the northeastern boundary of the study area. The northern Carrizo–Wilcox model (Intera and Parsons Engineering Science, 2002a) may provide more representative simulation results for the Carrizo aquifer layer within about 30 to 40 mi of the northeastern boundary, including Anderson, Angelina, Cherokee, Rusk, San Augustine, Smith, and Van Zandt Counties.

Water levels simulated in the Hooper and Calvert Bluff aquitards for 2000 are shown in figures 86b and 87b, respectively. The RMSE values comparing simulated and observed water levels in the Hooper and Calvert Bluff aquitards for 2000 are 46 ft (fig. 88d) and 38 ft (fig. 88b), respectively.



QAd2079c

Figure 92. Maps for the Carrizo aquifer (layer 3) showing (a) simulated and observed 2000 water level and (b) drawdown from 1950 through 2000.



QA42061C

Figure 93. Map of residual differences between simulated and measured water levels for the Carrizo aquifer (layer 3) for the 2000 calibration.

Hydrographs shown in figures 94 through 97 give another comparison of how well the model simulates water levels in both aquifers and aquitards. The hydrographs show how the model performs at specific locations through time and are similar to others in the study area but not shown in this report. Some simulation hydrographs show an abrupt change in water level in 1950, which is when simulated pumping was started in the model. The influence of the change from steady state to transient has little effect on the transient model calibration for the period from 1980 through 1990. For the periods of 1987 through 1989 and 1995 through 1997, monthly fluctuations in water level are simulated. The water-level change shows an annual cycle that responds to a range in pumping rate that is approximately two times greater in summer than in winter. The greater annual fluctuation for water levels in and near the Bryan-College Station well field (for example, wells 59-21-209 and 59-21-409 in Brazos County [fig. 95]) is proportional to the greater annual rate of pumping in that area. The hydrograph for well 59-11-703 in Milam County (fig. 95) shows the onset of increased groundwater withdrawal in that county for mining operations.

Overall, the match between simulated and observed hydrographs is good. Calculated values of RMSE and baseline shift, as explained in section 7.0, are given for each hydrograph (figs. 94 through 97). RMSE ranges between 1 and 32 ft for these representative hydrographs. The match for well 37-35-701 in Angelina County (fig. 97) again shows that the model overestimates drawdown in the Carrizo aquifer in the Lufkin-Angelina County well field. The range of annual fluctuation in water levels during the periods of 1987 through 1989 and 1995 through 1997 for that well is proportional to the amount of pumping in the well field. The fluctuation is determined more by the two-fold variation in pumping rate than by storativity. Changing storativity by an order of magnitude decreased the annual water-level fluctuation by about 20 percent.

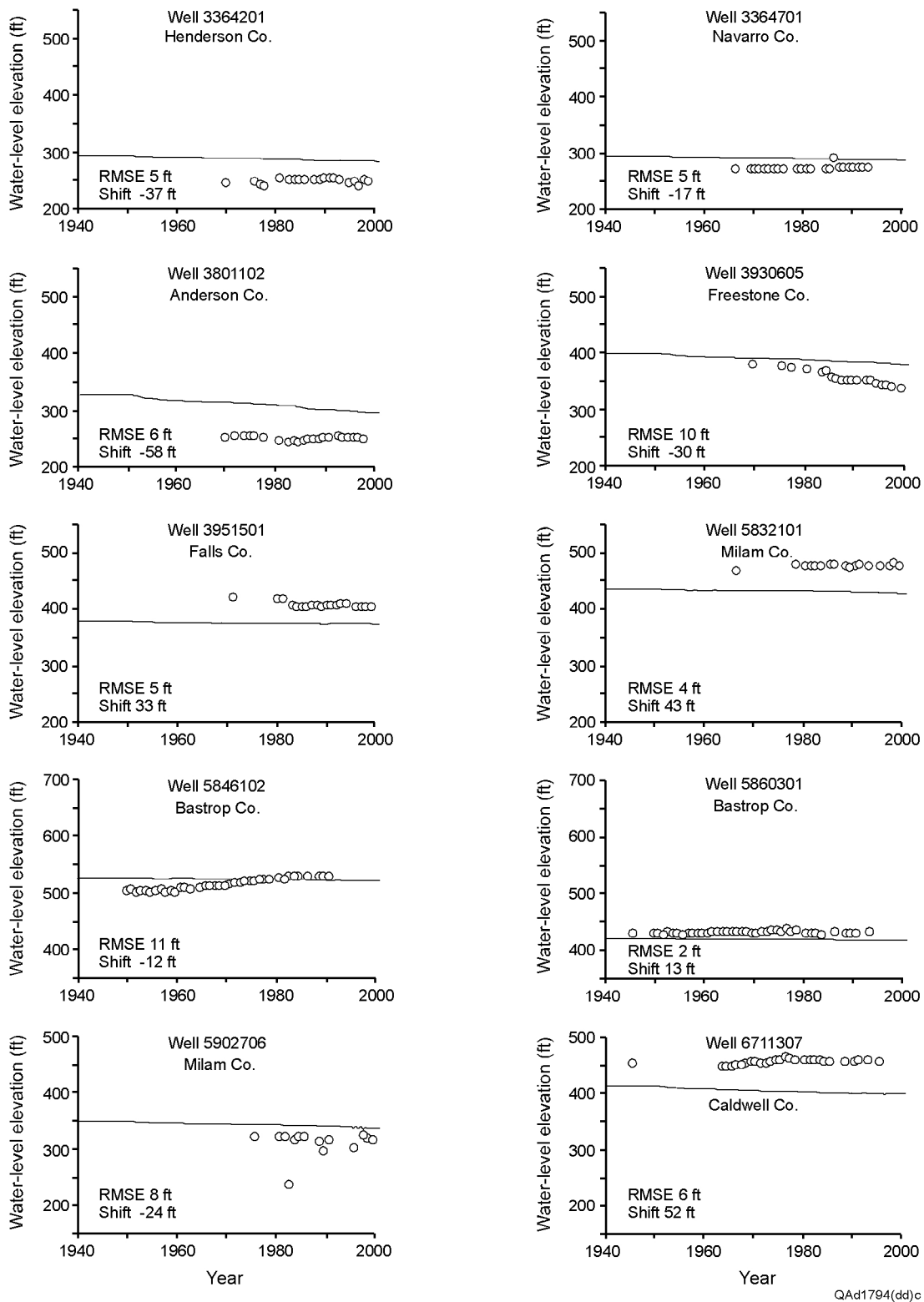


Figure 94. Comparison of simulated and observed water-level hydrographs for 10 wells in the Hooper aquitard (layer 6). Well locations are shown in figure 36.

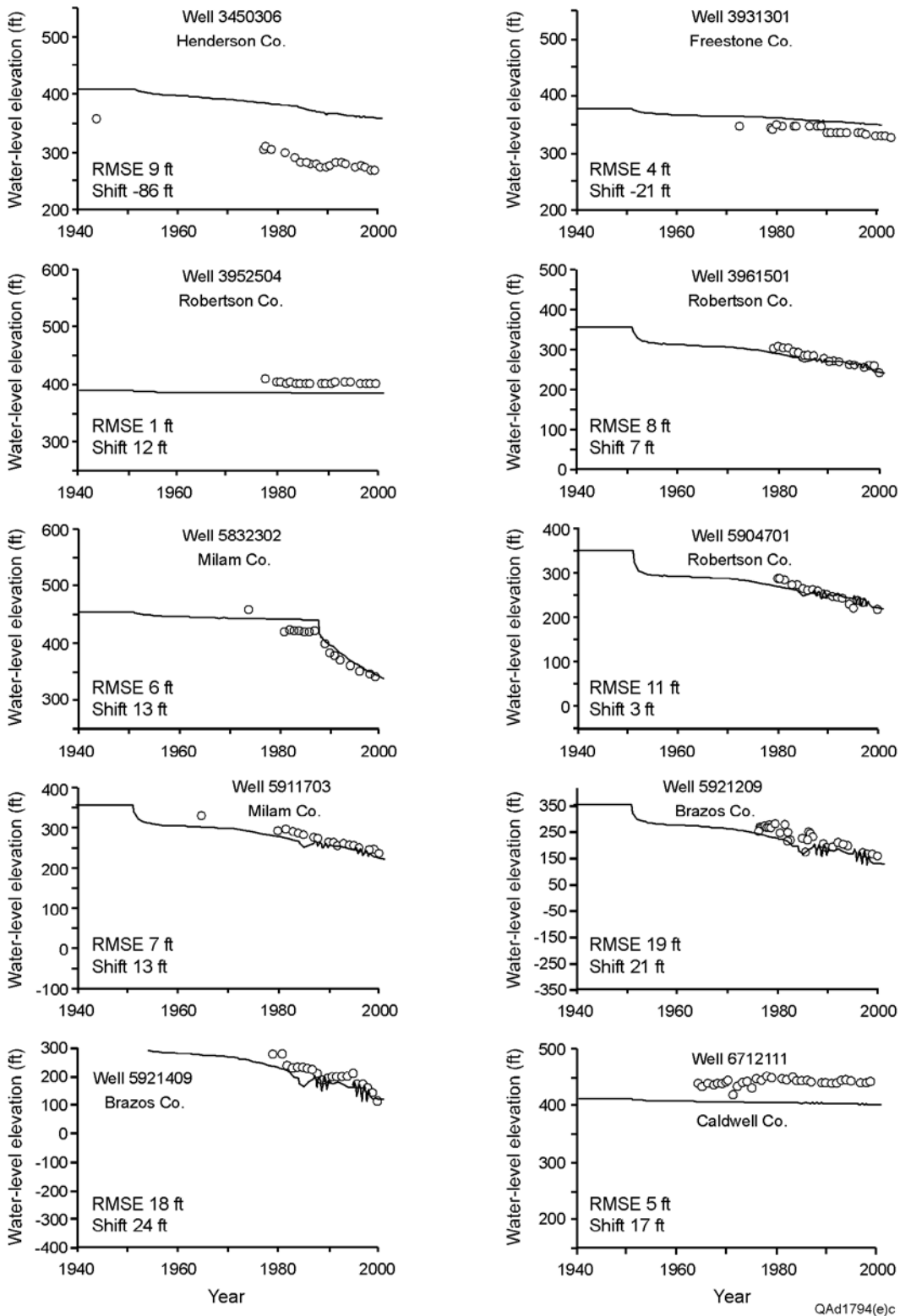
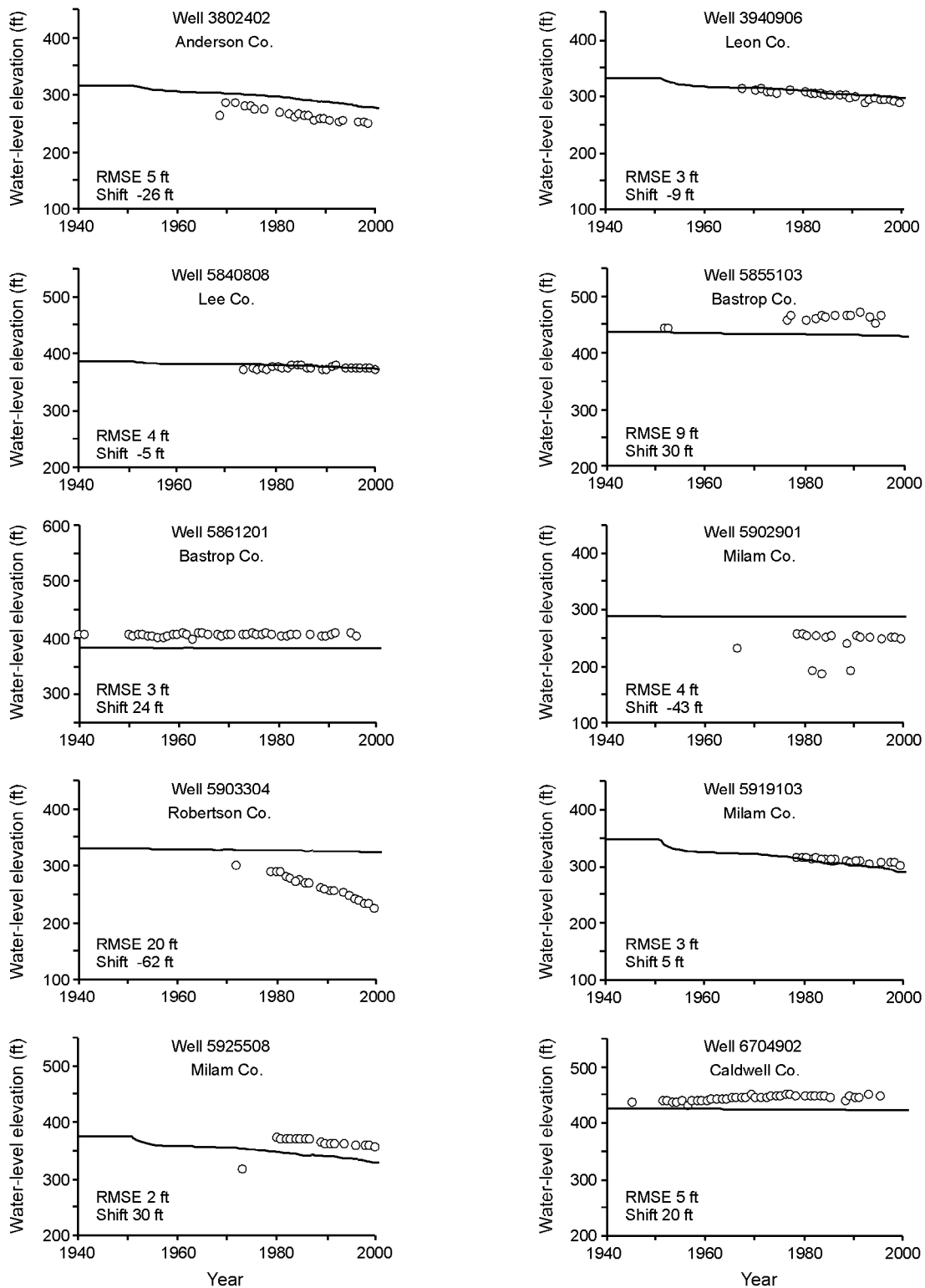


Figure 95. Comparison of simulated and observed water-level hydrographs for 10 wells in the Simsboro aquifer (layer 5). Well locations are shown in figure 36.



QAAd1794(bb)c

Figure 96. Comparison of simulated and observed water-level hydrographs for 10 wells in the Calvert Bluff aquitard (layer 4). Well locations are shown in figure 36.

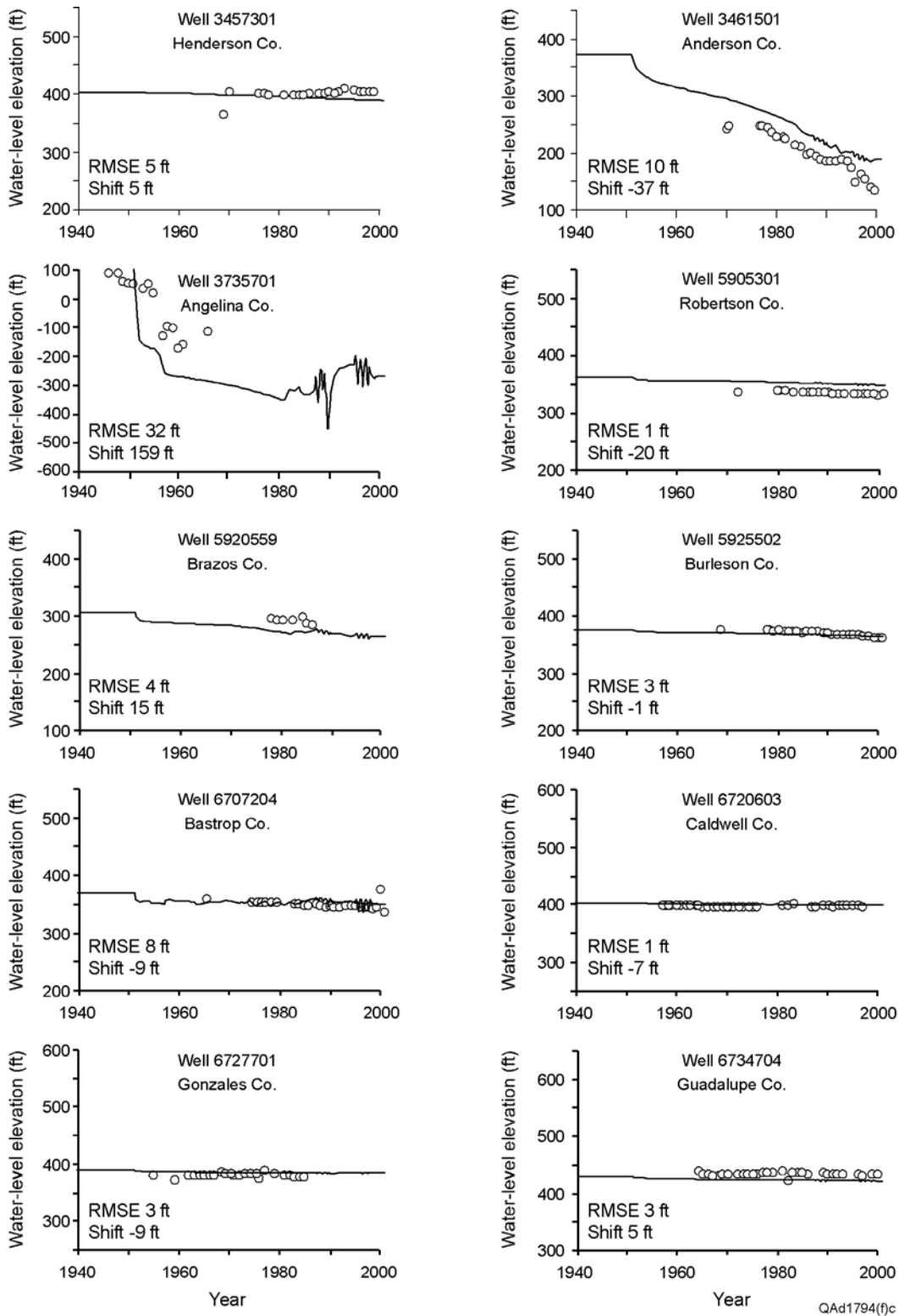


Figure 97. Comparison of simulated and observed water-level hydrographs for 10 wells in the Carrizo aquifer (layer 3). Well locations are shown in figure 36.

Rate of discharge to streams simulated for the transient model period is similar to the steady state, average base-flow rate. Simulated rate of base-flow discharge fluctuates with annual rates of recharge; there is also a trend of decreasing base-flow rate through time (fig. 98, table 14). This simulated decrease in base flow most likely reflects a simulated decline in water levels in the aquifer outcrop attributed to increased pumpage. It should be noted, however, that base-flow estimates show no long-term trend. Because recent precipitation records were not available in the Internet source, average precipitation for the period 1960 through 1997 are used for 1998 through 2000, resulting in a constant simulated recharge for this period as well. Most model cells are simulated as gaining reaches through the transient model period. Stream losses are approximately 6 percent of stream gains. The Simsboro and Carrizo aquifers contribute essentially all of the discharge to the rivers and streams. Because of their low hydraulic conductivity and slow rates of groundwater movement, the Hooper and Calvert Bluff aquitards contribute very little base flow to streams. Groundwater ET simulated for 2000 is shown in figure 99. Most of the ET is focused in low-lying topographical areas flanking streams. Some ET is also simulated for areas between streams according to how the ET package parameters are set.

9.2 Water Budget

Water budgets for the transient model change each year with changes in recharge rate and pumping (fig. 98). Annual recharge rates applied to the model were greater or less than average in proportion to how much precipitation was greater or less than average. In addition, the GHB heads on the northeastern boundary of the model were varied in long-term trends to account for movement of groundwater out of the study area toward well fields,

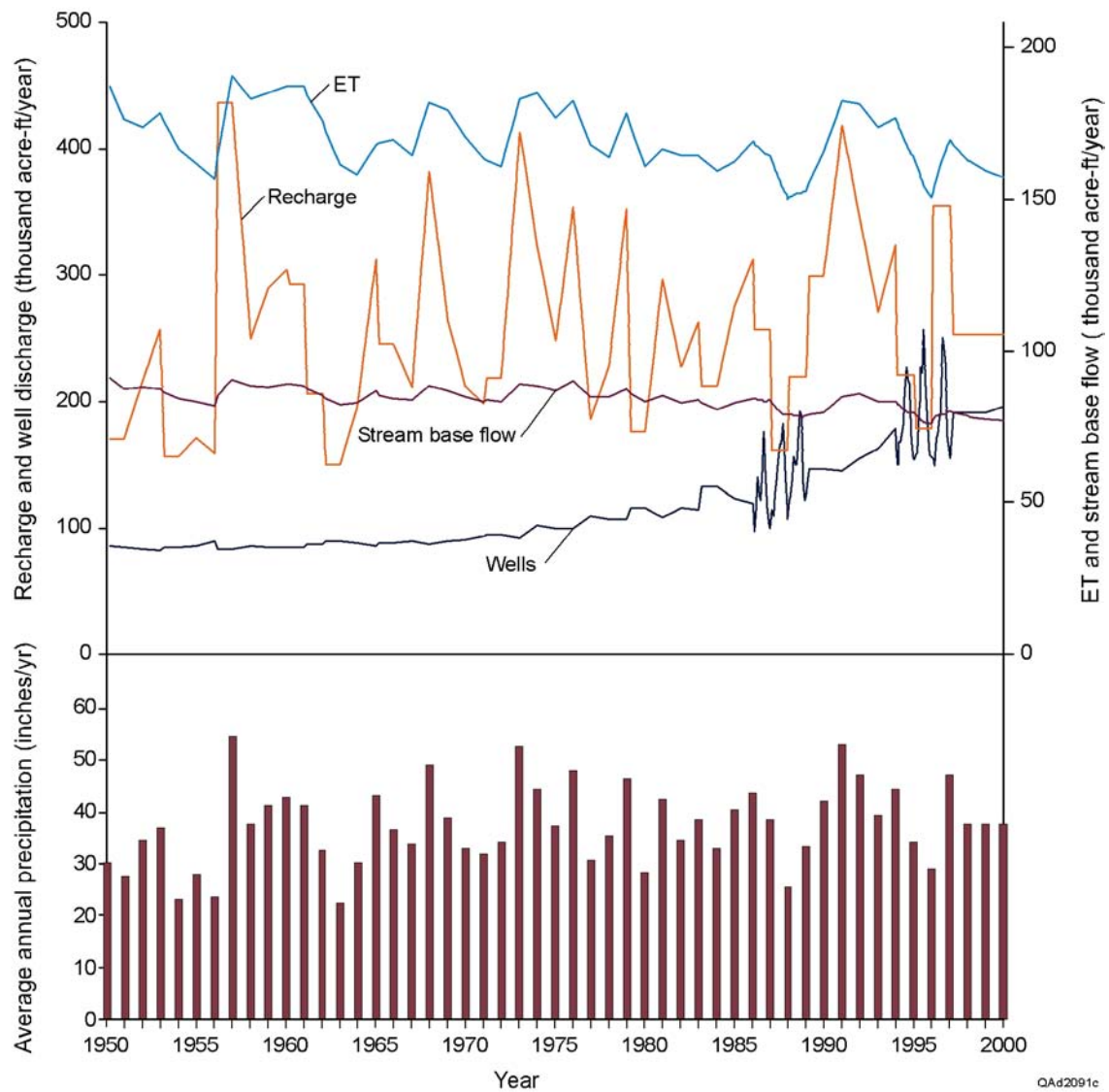


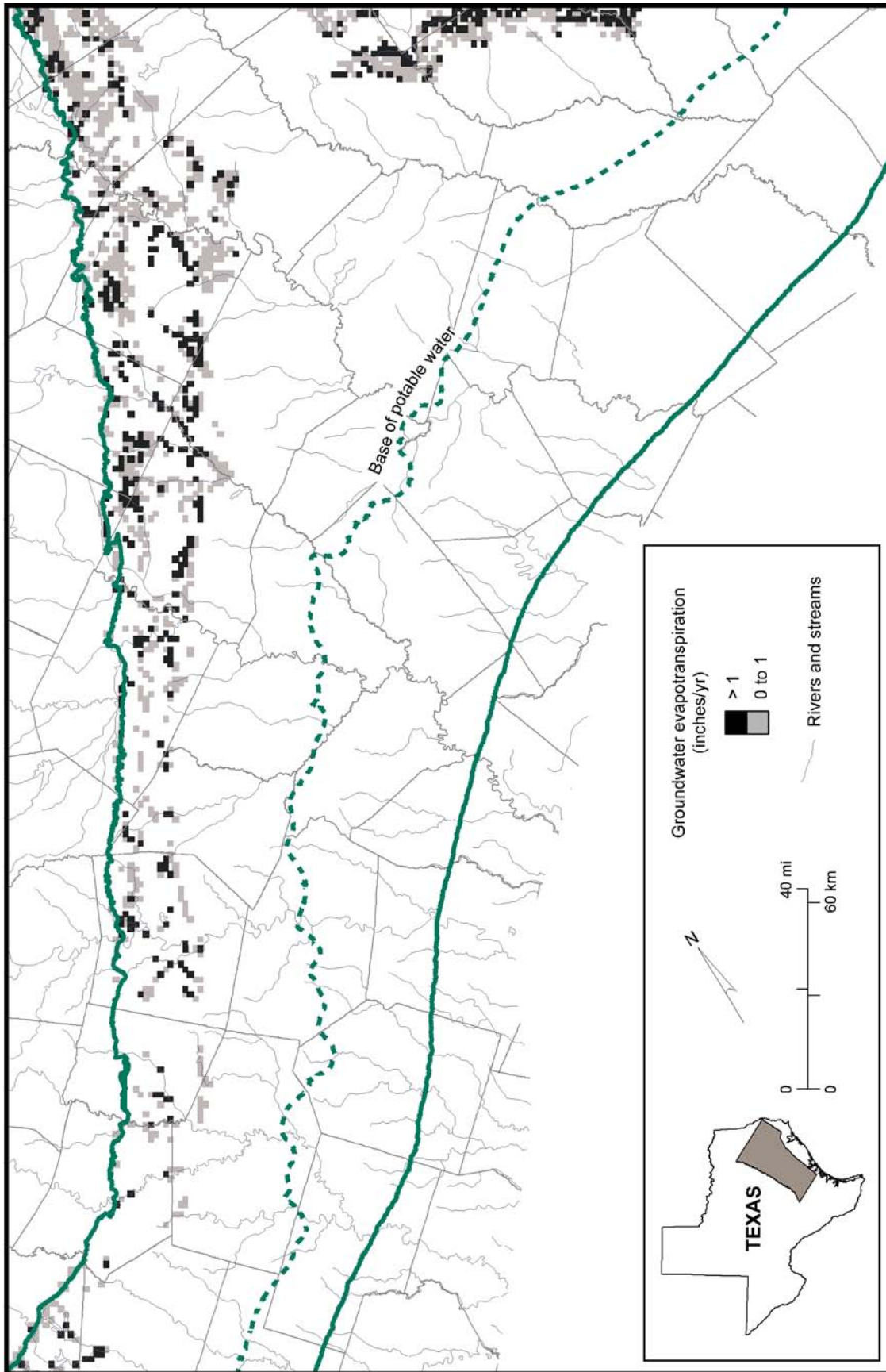
Figure 98. Changes in simulated ET and base-flow discharge to stream with variation in recharge and pumping rates.

Table 14a. Water budget for the calibrated steady-state and transient models (1000 acre-ft/yr). Positive values are inflow to the aquifer; negative values are discharge from the aquifer. Annual rates are for a 12-month long time step for steady state and 2000 budgets and projected from five 2.4-month long time steps for 1990.

Layer	Recharge	Net recharge	ET	Stream leakage	Reservoir leakage	GHB Reklaw	GHB downdip boundary	GHB NE boundary	GHB SW boundary	Wells	Cross-formational flow	Change in storage	Water balance error (%)
<u>Steady state</u>													
Alluvium (1)	12.6	0	-13.3	-26.3	0	0	0	0	0	0	27.0	0	-0.005
Reklaw (2)	13.7	-5.6	-20.5	-0.6	0	-36.9	0	0	0	0	44.2	0	-0.007
Carrizo (3)	117.2	11.9	-72.4	-32.5	0	0	2.4	-9	18.3	0	-32.1	0	-0.003
Calvert Bluff (4)	45.4	-9.3	-39.6	-13.5	0	0	2.3	13.1	0.2	0	-7.9	0	-0.006
Simsboro (5)	59.4	14.8	-31.1	-13.3	0	0	2.2	4.6	0.2	0	-22.0	0	-0.004
Hooper (6)	24.6	4.3	-15.9	-4.4	0	0	1.4	3.5	0.0	0	-9.2	0	-0.001
ALL	272.9	16.1	-192.8	-90.6	0	-36.9	8.4	20.2	18.6	0	0	0	-0.005
<u>1990</u>													
Alluvium (1)	13.8	0	-12.4	-23.9	0.6	0	0	0	0	0	22.2	-0.4	0.001
Reklaw (2)	28.8	-5.1	-23.1	-0.5	0	7.2	0	0	0	0	-1.5	-10.9	0.001
Carrizo (3)	122.9	23.9	-64.3	-29.5	0	0	2.4	2.4	26.4	-74.8	13.6	0.9	0.005
Calvert Bluff (4)	59.2	-3.1	-32.9	-11	2.1	0	2.3	15.0	0.7	-10.4	-23.3	-1.6	0.001
Simsboro (5)	62.8	32.1	-23.5	-10.8	0.4	0	2.3	1.3	0.3	-56.2	8.8	14.7	-0.011
Hooper (6)	30.7	8.8	-13.5	-3.4	1.1	0	1.5	8.8	0	-6.4	-19.8	1	-0.015
ALL	318.2	56.6	-169.7	-79.1	4.2	7.2	8.5	27.5	27.3	-147.8	0	3.7	-0.001
<u>2000</u>													
Alluvium (1)	12.9	0	-11.9	-23.7	0.6	0	0	0	0	0	21.7	0.3	-0.005
Reklaw (2)	14.8	-4.9	-21.5	-0.6	0	7.8	0	0	0	0	-3.1	2.6	-0.007
Carrizo (3)	118.4	25.6	-64.7	-29.3	0	0	2.4	0.7	27.1	-78.0	11.1	12.3	-0.003
Calvert Bluff (4)	47.4	-0.2	-31.9	-10.8	2.1	0	2.4	10.3	0.8	-11.4	-28.4	19.6	-0.006
Simsboro (5)	60.2	42.8	-21.9	-9.5	0.4	0	2.3	2.2	0.3	-98.0	22.0	42.0	-0.004
Hooper (6)	25.4	10.7	-13.5	-3.4	1.1	0	1.5	9.6	0	-6.2	-23.2	8.7	-0.001
ALL	279.2	74.1	-165.4	-77.2	4.2	7.8	8.5	22.8	28.1	-193.6	0	85.6	-0.005

Table 14b. Water budget for the transient model (1000 acre-ft/yr) for drought years 1988 and 1996. Positive values are inflow to the aquifer; negative values are discharge from the aquifer. Annual rates are totaled from 12 1-month time steps.

Layer	Recharge	Net recharge	ET	Stream leakage	Reservoir leakage	GHB Reklaw	GHB down dip boundary	GHB NE boundary	GHB SW boundary	Wells	Cross-formational flow	Change in storage	Water balance error (%)
<u>1988</u>													
Alluvium (1)	6.9	0	-12.1	-24.1	0.6	0	0	0	0	0	26.7	2.0	-0.002
Reklaw (2)	3.9	-5.1	-18.6	-0.6	0	4.9	0	0	0	0	-1.0	11.4	0.001
Carrizo (3)	92.9	22.9	-62.9	-29.9	0	0	2.4	2.1	25.0	-71.1	9.8	31.7	0.002
Calvert Bluff (4)	8.6	-3.3	-31.9	-11.6	2.1	0	2.3	14.6	0.6	-9.6	-22.8	47.6	-0.002
Simsboro (5)	44.2	31.5	-23.8	-10.9	0.4	0	2.3	2.3	0.2	-53.4	6.2	32.6	-0.002
Hooper (6)	9.1	8.7	-12.9	-3.5	1.1	0	1.5	8.4	0	-6.8	-18.9	22.1	-0.003
ALL	165.7	54.7	-162.2	-80.5	4.2	4.9	8.5	27.3	25.8	-140.9	0	147.3	0.000
<u>1996</u>													
Alluvium (1)	9.1	0	-12.1	-23.9	0.6	0	0	0	0	0	24.7	1.6	-0.002
Reklaw (2)	4.0	-4.9	-19.7	-0.6	0	5.6	0	0	0	0	-1.7	12.4	0.000
Carrizo (3)	99.7	25.3	-64.2	-29.2	0	0	2.4	1.7	27.5	-78.9	9.6	31.4	0.002
Calvert Bluff (4)	15.3	-1.5	31.0	-10.8	2.1	0	2.3	12.6	0.8	-12.1	-27.2	47.9	-0.001
Simsboro (5)	49.0	42	-22.0	-9.8	0.4	0	2.3	1.8	0.3	-93.8	16.5	55.5	0.000
Hooper (6)	14.2	9.7	-12.9	-3.3	1.1	0	1.5	9.2	0	-6.5	-22.0	18.8	-0.003
ALL	191.2	70.5	-161.9	-77.6	4.2	5.6	8.5	25.4	28.5	-191.4	0	167.7	0.000



QAd2290x

Figure 99. Map of aquifer discharge simulated as groundwater evapotranspiration for 2000.

for example, at Tyler and Henderson, Texas. The components of the water budget for 1990 and 2000 are reported in table 14 and illustrated in figure 100.

During the period included in the transient model, most recharge is simulated as being discharged to rivers and streams or taken up by ET. The rate of net recharge increases and ET decreases as pumpage increases, although these responses are obscured by annual variations in recharge rate shown in table 14. Net recharge, or movement from the unconfined to confined zones, is simulated to be 1.5 and 0.6 inches/yr in 2000 for the Simsboro and Carrizo aquifers, respectively, an increase from the steady-state model. Net recharge was estimated by summing the simulated fluxes across the flow faces of model cells at the boundary between the unconfined and confined zones; this tally takes into account cross-formational flow and change in storage in the unconfined zone. From 1950 through 2000, net recharge is simulated to have increased by 58,000 acre-ft/yr, whereas simulated stream flow decreased by 13,000 acre-ft/yr and groundwater ET decreased by 28,000 acre-ft/yr (fig. 98). Historical base-flow estimates, as previously noted, show no long-term decrease.

The GHB boundary applied to the Reklaw aquitard (layer 2) changes from net discharge out of the Carrizo–Wilcox aquifer to net inflow to the aquifer (table 14). The two largest reservoirs in the outcrop of the Carrizo–Wilcox aquifer, Lake Limestone and Richland-Chambers Reservoirs, were simulated as contributing most of the 4,200 acre-ft/yr simulated as leakage to the Carrizo–Wilcox aquifer from surface-water reservoirs (table 15). As previously stated, few data exist on historical leakage from these reservoirs, and the predicted losses are uncalibrated. The reservoir leakage accounts for about 1.5 percent of the water budget in the model.

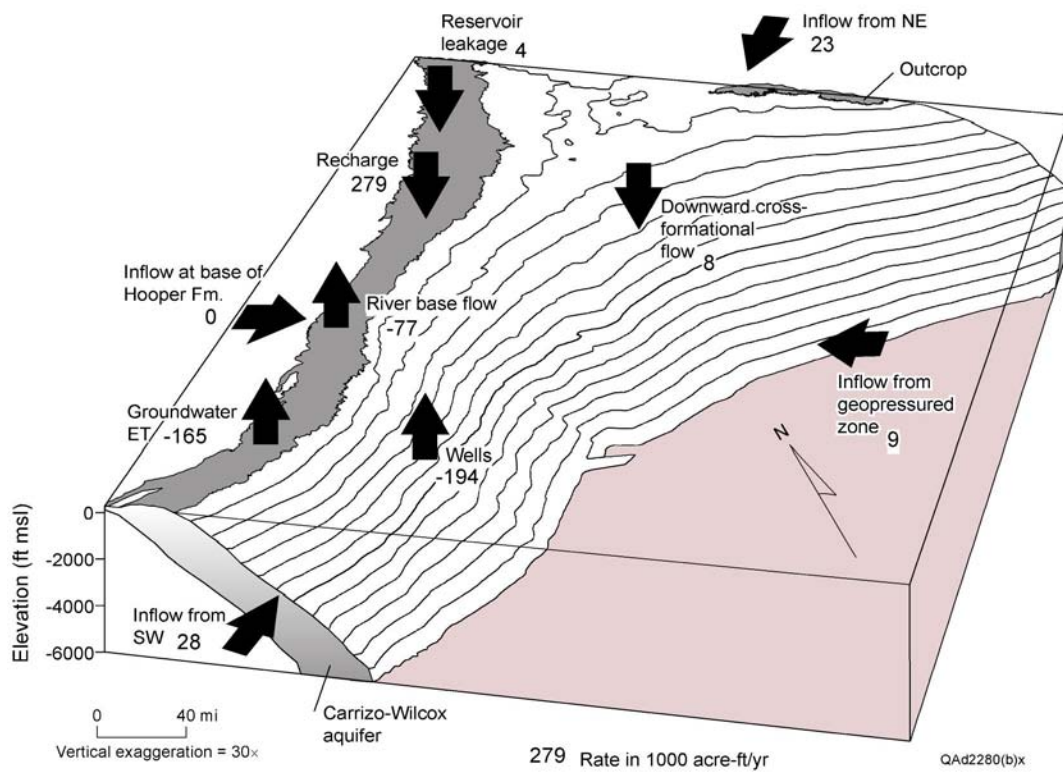


Figure 100. Block diagram of the Carrizo–Wilcox aquifer representing the components of the transient model for 2000.

Table 15. Simulated leakage of water to the Carrizo–Wilcox aquifer from surface-water reservoirs.

Reservoir	Total leakage (acre-ft/yr)	
	<u>1990</u>	<u>2000</u>
Lake Bastrop	120	120
Cedar Creek Reservoir	950	950
Fairfield Lake	120	120
Richland-Chambers Reservoir	1,060	1,040
Calaveras Lake	450	450
Lake Limestone	1,130	1,130
Twin Oak Reservoir	170	170
Alcoa Lake	40	40
Braunig Lake	180	180
Total	<u>4,220</u>	<u>4,200</u>

At the end of the historical period, no model cells are simulated as having gone dry in any layer. There is a narrow band adjacent to the outcrop where the width of the unconfined part of the aquifer grows as cells change from artesian to unconfined. The water-balance error for the 1990 and 2000 dates in the transient model is less than 0.01 percent.

9.3 Sensitivity Analysis

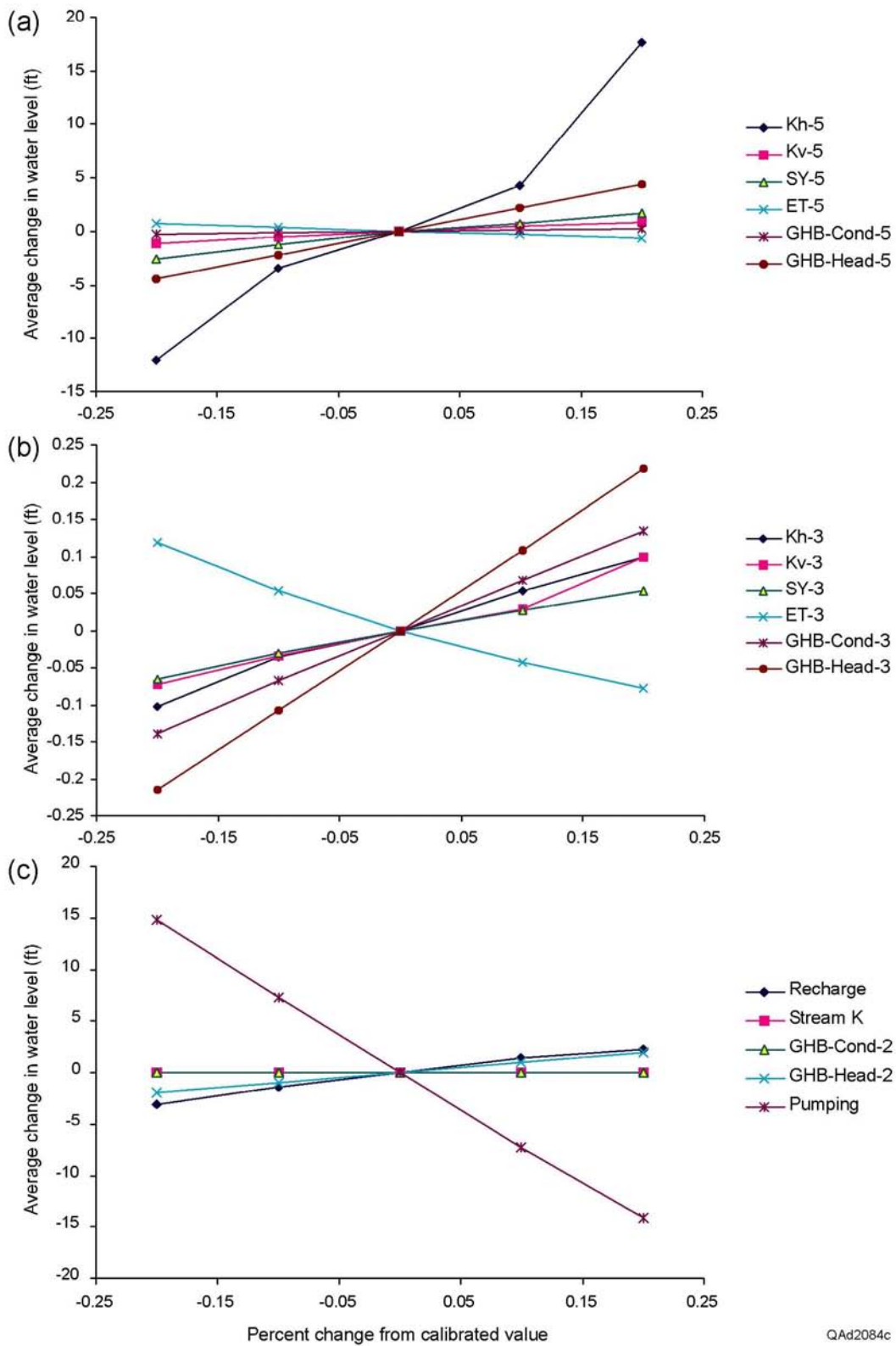
Results of the sensitivity analysis for the transient period (figs. 101, 102) are consistent with those for the steady-state analysis (figs. 77, 78). Simulated water levels in layer 5 (Simsboro aquifer) in the transient model are most sensitive to

- pumping rate (fig. 101c),
- horizontal hydraulic conductivity of the Simsboro aquifer (layer 5) (fig. 101a), and
- storativity (fig. 103b).

The results are also sensitive to recharge rate and the GHB heads in the Reklaw aquitard (fig. 101c) and at the northeastern and southwestern boundaries of the model. Changing the GHB conductance on the northeastern boundary from 0 (no-flow) to a large number has an effect on water levels within about 30 to 40 mi of the boundary.

Water levels are also sensitive to pumping rates. The transient model is less sensitive to recharge rates and horizontal conductivity than is the steady-state model. The same conclusions apply to the Carrizo aquifer (fig. 102)

Storativity was varied by one order of magnitude on each side of the calibrated value for each model layer. Changing storativity assigned to model cells can have a dramatic impact on drawdown in well fields but, on average, the model is less sensitive to storativity



QAd2084c

Figure 101. Sensitivity of predicted water levels in the Simsboro aquifer (layer 5) in the transient model to changes in parameter values for the (a) Simsboro aquifer (layer 5), (b) Carrizo aquifer (layer 3), and (c) other parts of the model.

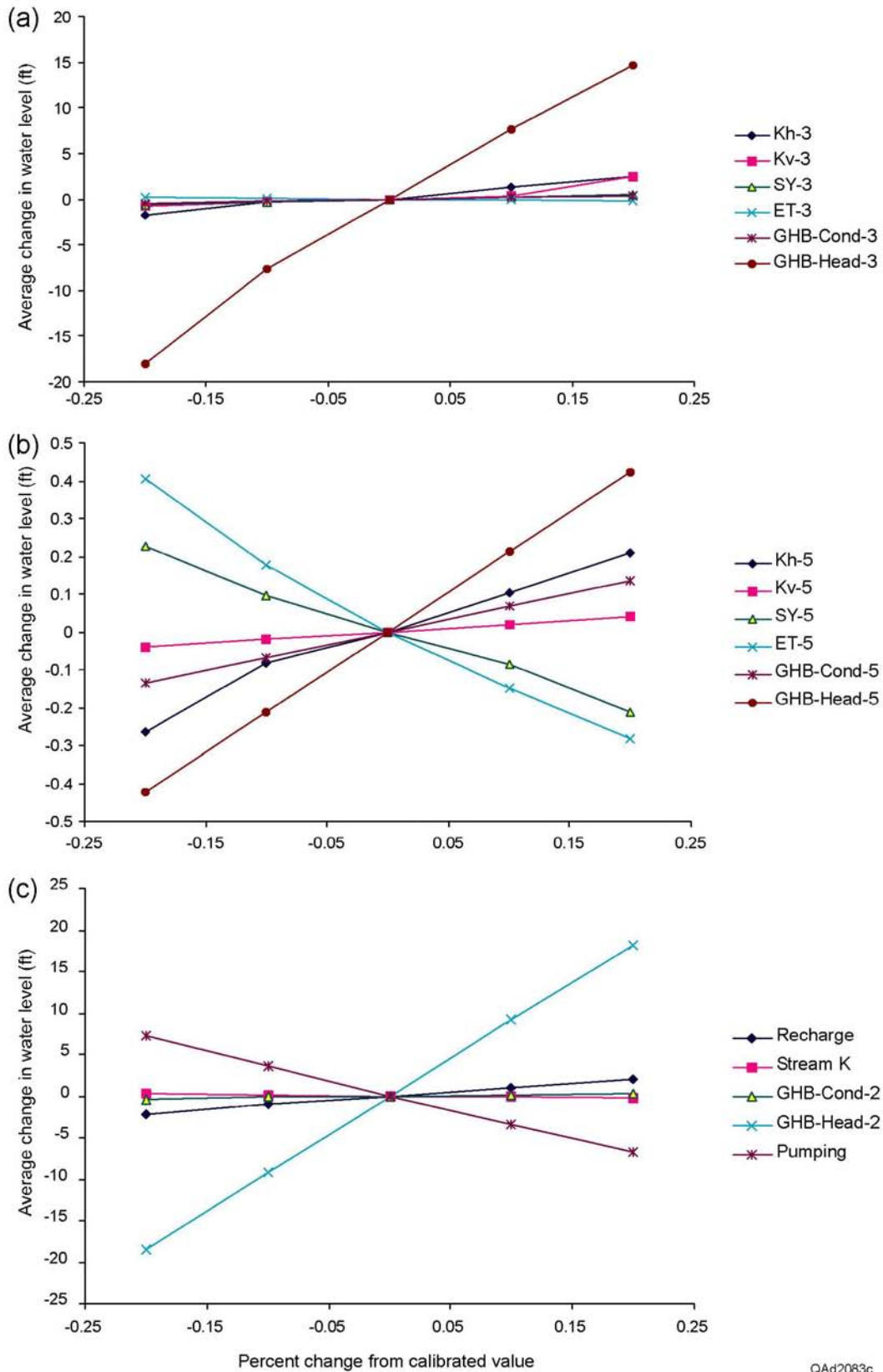


Figure 102. Sensitivity of predicted water levels in the Carrizo aquifer (layer 3) in the transient model to changes in parameter values for the (a) Carrizo aquifer (layer 3), (b) Simsboro aquifer (layer 5), and (c) other parts of the model.

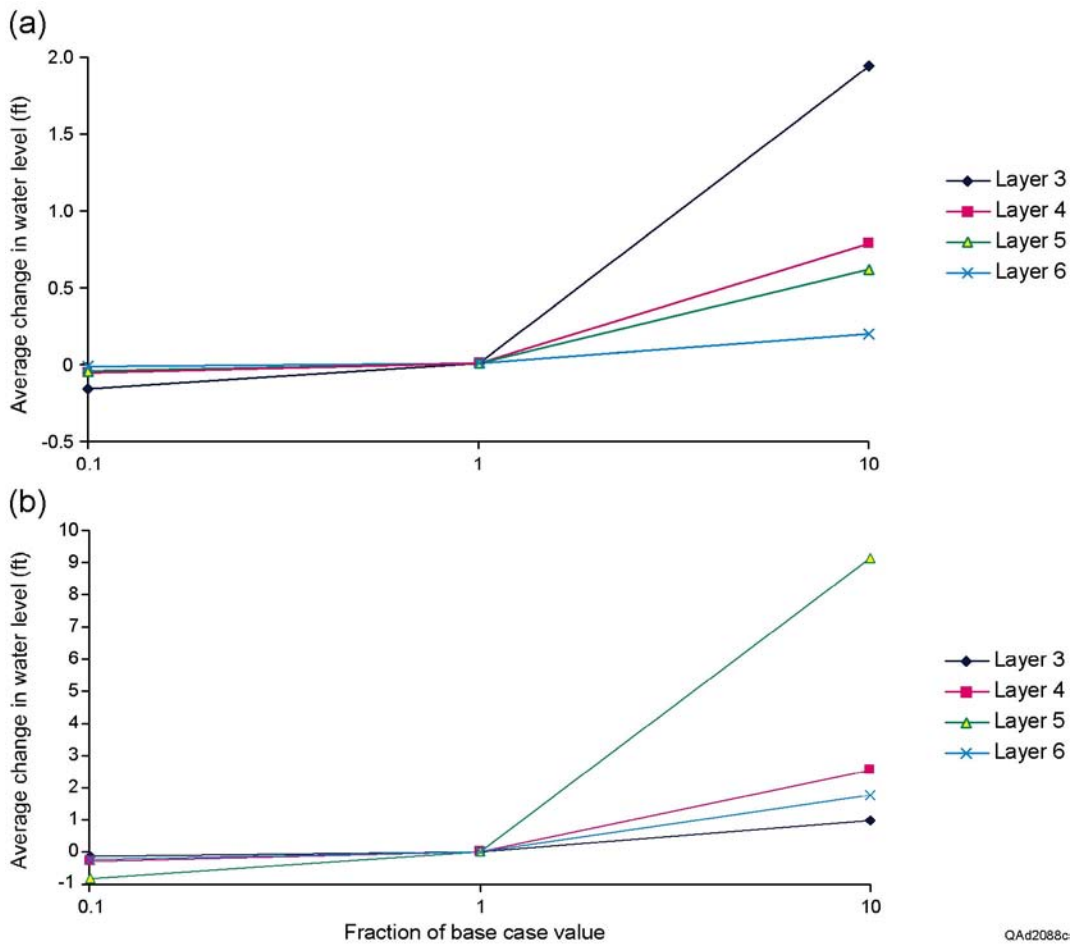


Figure 103. Sensitivity of simulated water levels to order-of-magnitude changes in storativity for the (a) Carrizo aquifer (layer 3), and (b) Simsboro aquifer (layer 5). Note difference in vertical scales.

than to other parameters (fig. 103). Figure 104 shows the sensitivity of several water-level hydrographs to order-of-magnitude differences in storativity. The examples are for wells that show a large amount of drawdown among those of figures 95 and 97; hydrographs for wells with little drawdown are not very sensitive to storativity.

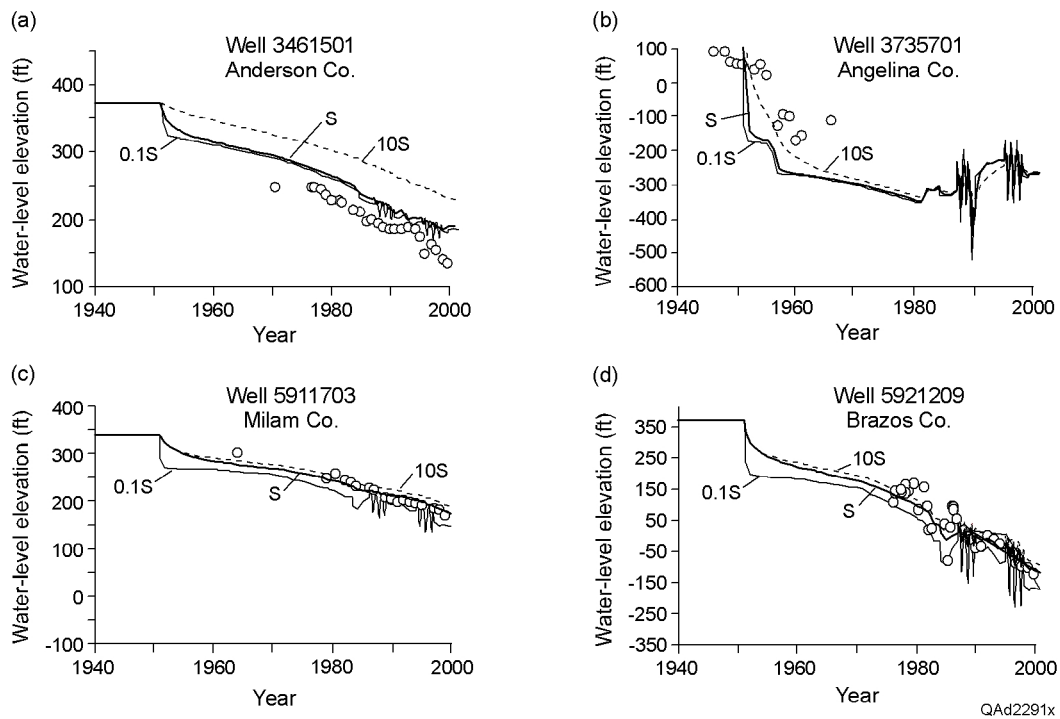


Figure 104. Sensitivity of simulated water levels (lines) in the Carrizo (a, b) and Simsboro (c, d) aquifers to differences in storativity. Location of wells in figure 36. Open circles = measured water levels.

10.0 PREDICTIONS

The purpose of developing the GAM model of the central part of the Carrizo–Wilcox aquifer is to provide a tool for evaluating changes in water level and stream flow for various expected or proposed changes in pumping rates and other activities impacting groundwater. To demonstrate the use of the model in predicting future water levels, base-line predictive simulations were run that include predicted pumping rates. The projected pumping rates for 2000 through 2050 were derived from a TWDB analysis of the demands and supplies of surface water and groundwater, along with possible water-management strategies, included in the Regional Water Plans prepared by Regional Water Planning Groups. These predictive runs were summarized in section 7.0. GHB heads for 2000 on the northeast and southwest boundaries were held constant in the predictive model from 2001 through 2050. The following section shows predicted water levels in the aquifer layers and predicted drawdown relative to the modeled 2000 water levels.

10.1 Predictive Results

A range in predicted water-level changes is shown in well hydrographs in figures 105 through 108 for the Hooper aquitard, the Simsboro aquifer, the Calvert Bluff aquitard, and the Carrizo aquifer, respectively. These extend the hydrographs of figures 94 through 97 from 2000 through 2050. Several of the hydrographs show a discontinuity—a step or jump—at 2000. This jump reflects differences in data sources for pumping rates used in the model. Pumping assigned to the historical model was derived from the water-use surveys conducted by the TWDB. Predicted pumping is based on the projections by regional

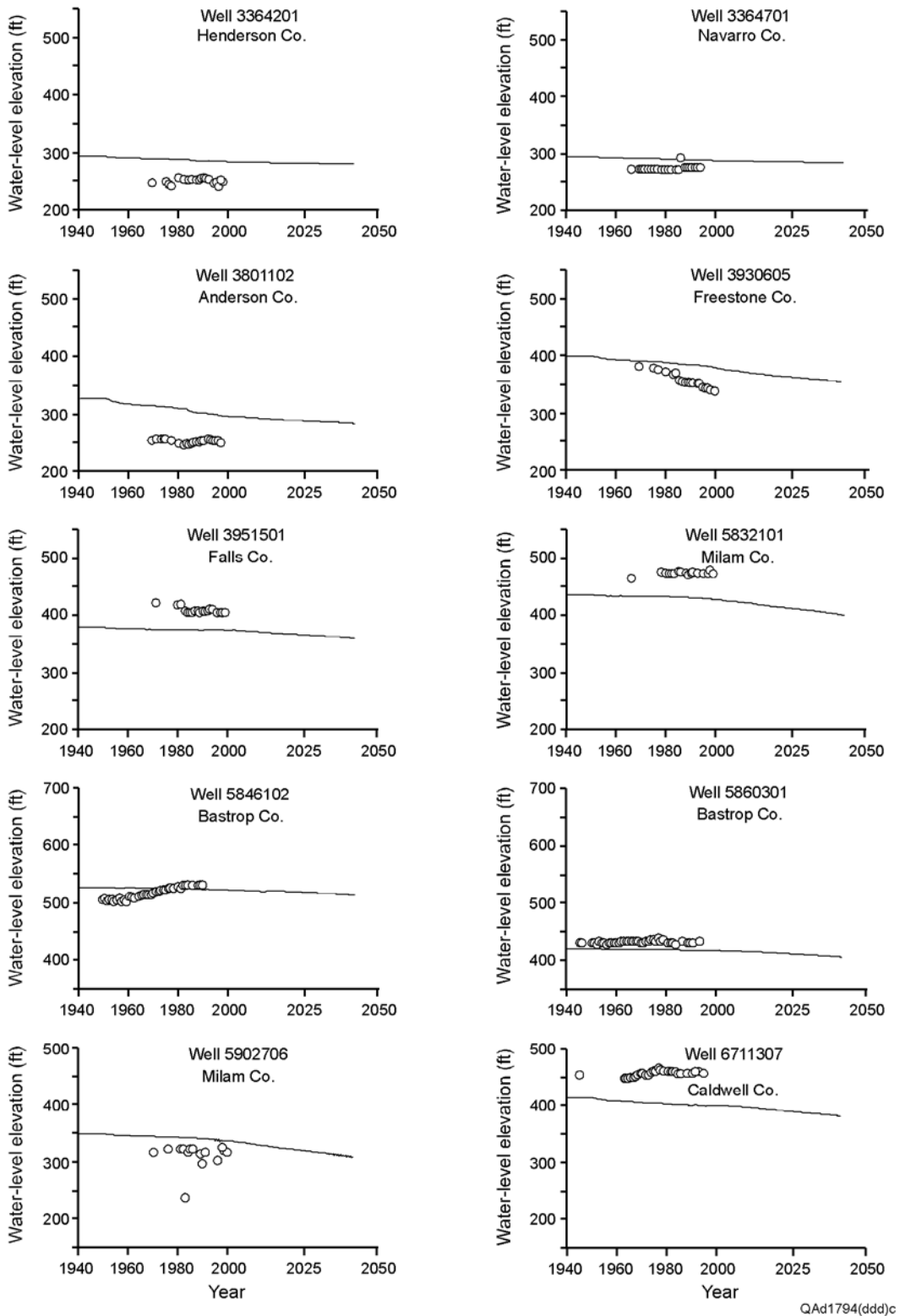
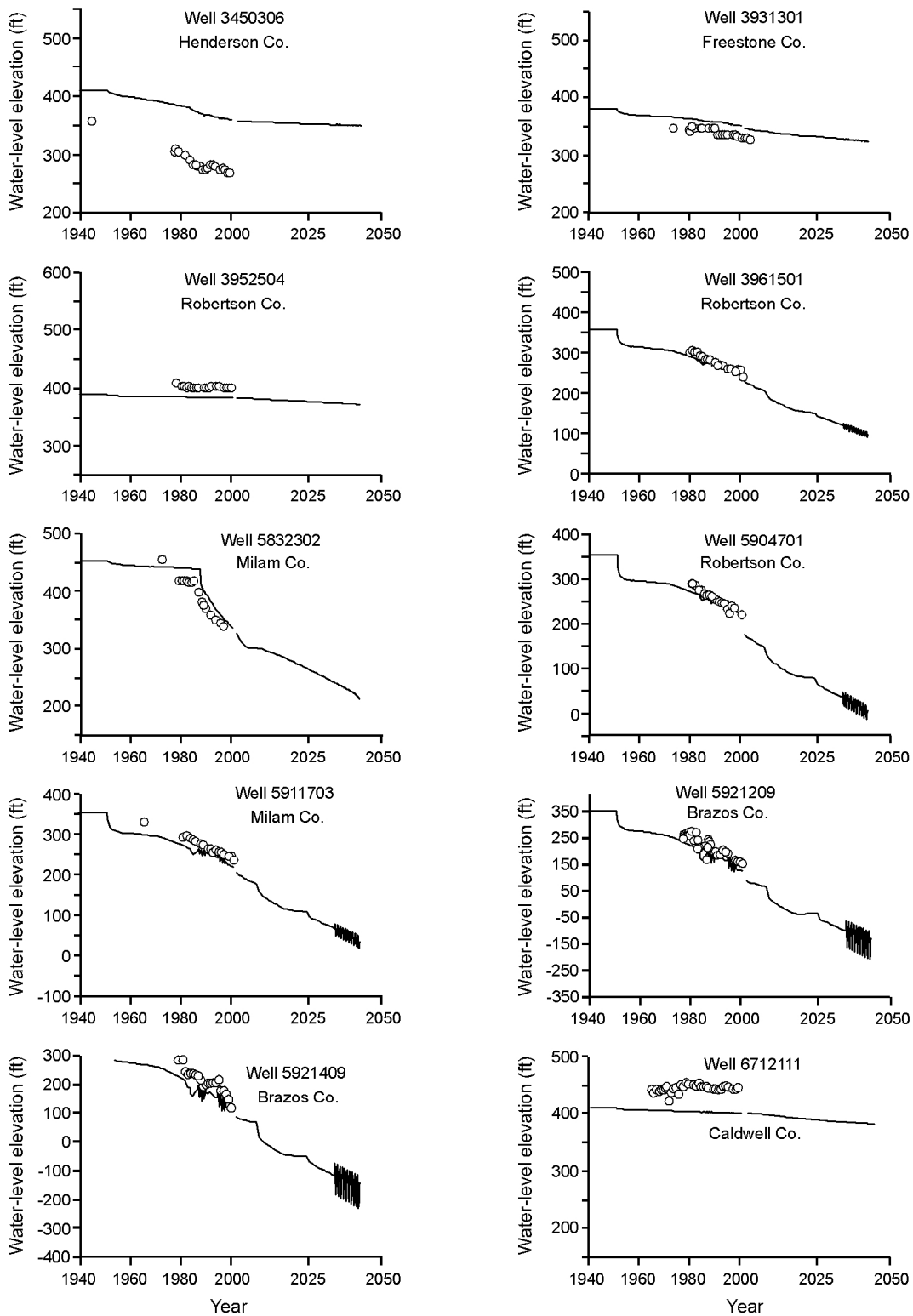


Figure 105. Simulated hydrographs showing predicted water levels through 2050 for wells in the Hooper aquitard (layer 6). Well locations are shown in figure 36.



QAd1794(h)c

Figure 106. Simulated hydrographs showing predicted water levels through 2050 for wells in the Simsboro aquifer (layer 5). Locations of wells shown in figure 36.

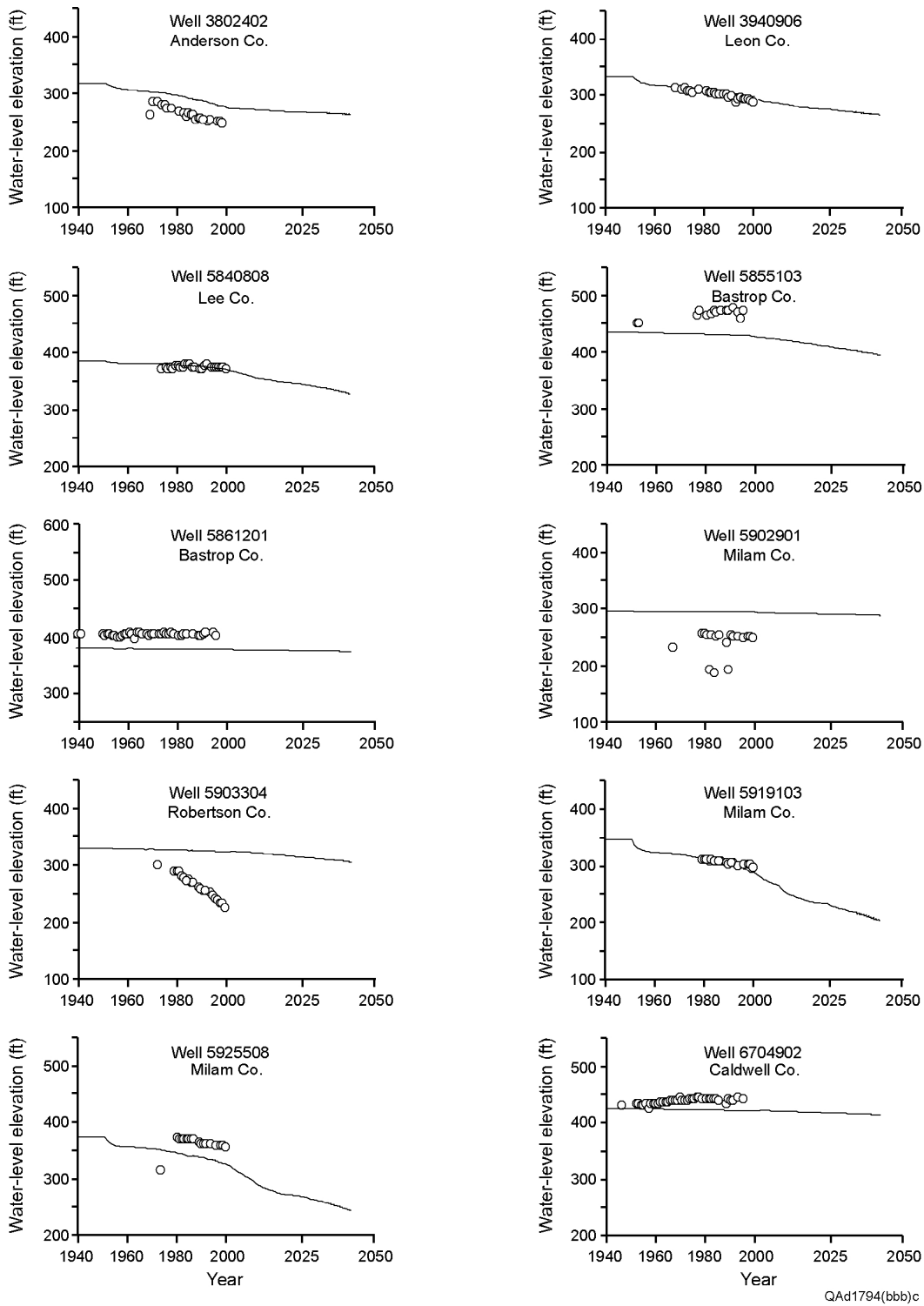


Figure 107. Simulated hydrographs showing predicted water levels through 2050 for wells in the Calvert Bluff aquitard (layer 4). Well locations are shown in figure 36.

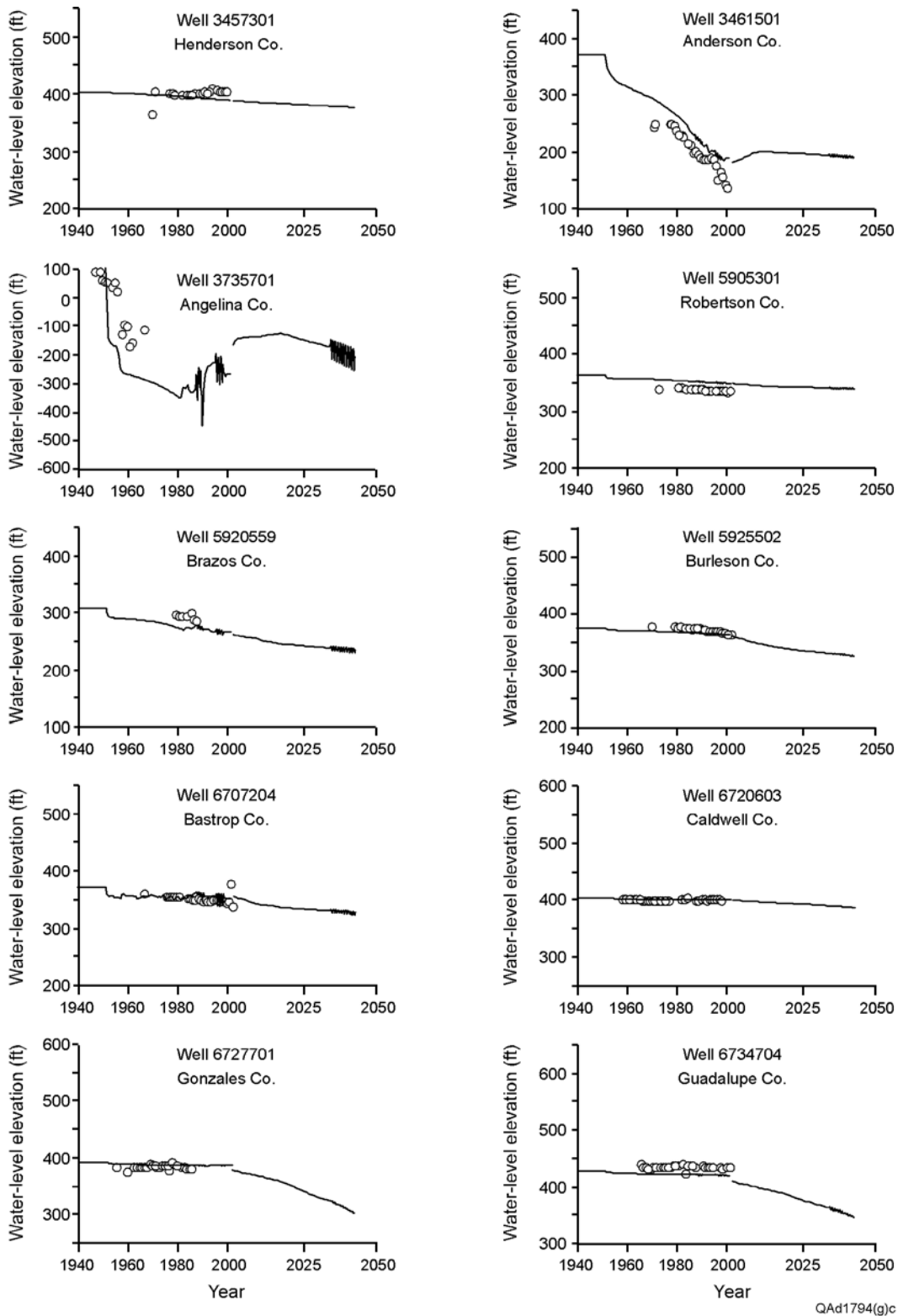
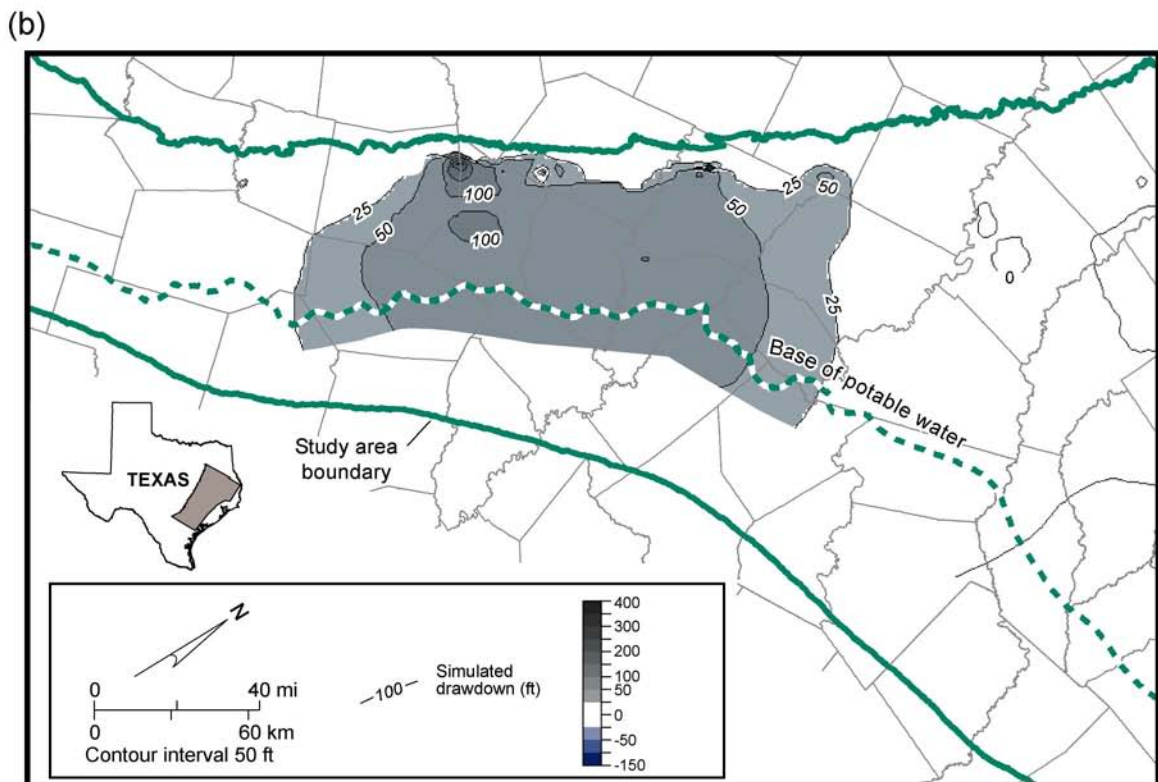
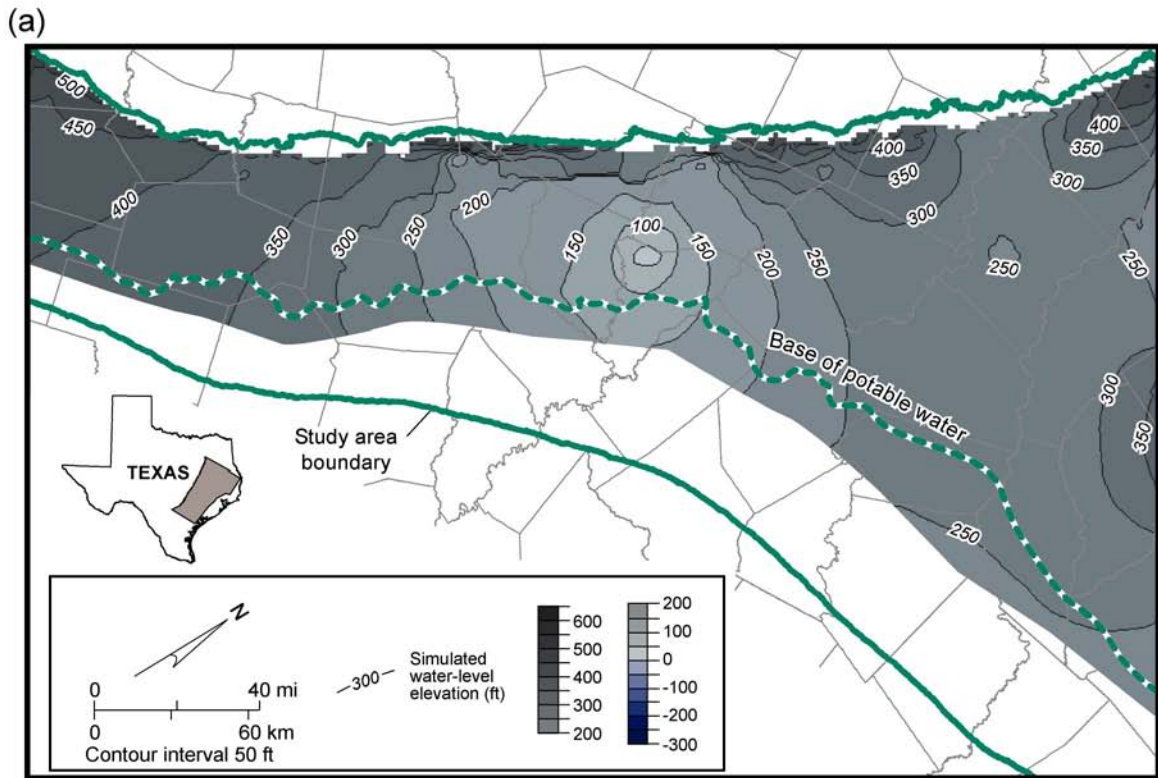


Figure 108. Simulated hydrographs showing predicted water levels through 2050 for wells in the Carrizo aquifer (layer 3). Locations of wells shown in figure 36.

water planning groups. Overall, the historical and predicted pumping rates match well at 2000 (fig. 52). Most of the difference is in assumed rates for municipal supply and irrigation. Differences can be significant for individual counties, but across the entire model and water-use categories the differences partly cancel out.

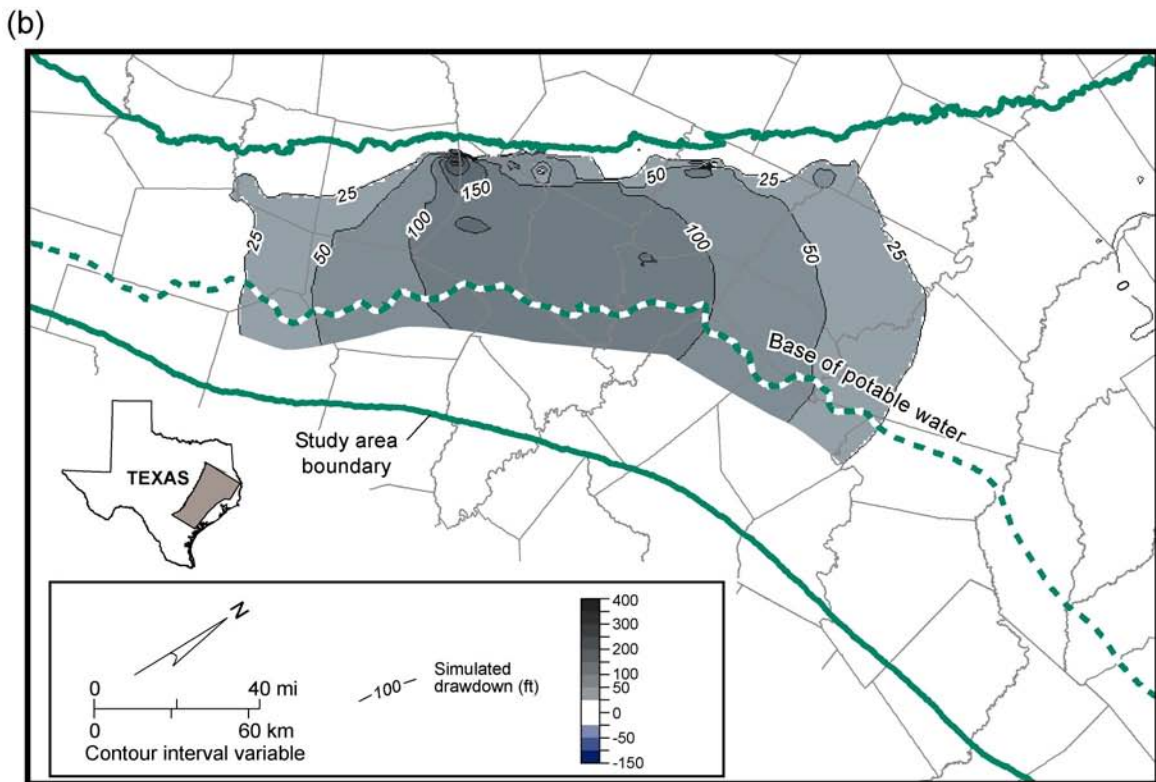
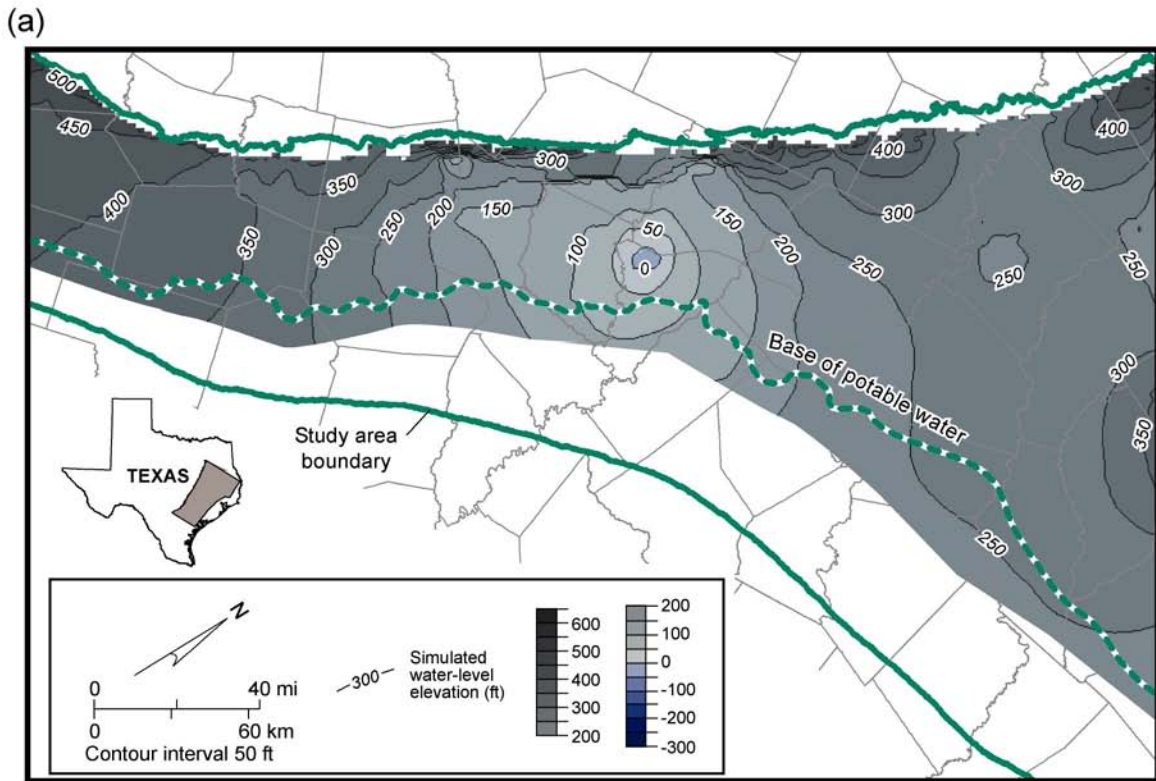
Other hydrograph features between 2000 and 2050 show predicted changes that are noteworthy. Long-term rates of drawdown in the vicinity of the Bryan-College Station well field (for example, wells in Brazos and Robertson Counties, fig. 105) are relatively constant from 1980 through 2050. Little change in rate of drawdown is predicted for other wells more distant from the well field. The last 10 yr of the 2000-through-2050 simulation consists of 120 1-month stress periods in which pumping rates were varied to allow an evaluation of annual fluctuations in water level. Winter and summer pumping rates used in the model differ by a factor of about 2 (see fig. 98 for the 1987–89 and 1995–97 periods). The differences reflect monthly changes in assumed rates for municipal, industrial, rural domestic, and irrigation rates. Annual fluctuations in water level are proportional to total pumping rates. Water-level response is less sensitive to specific storage than to pumping rate. Thus, wells close to the pumping centers show greater water-level fluctuations.

Figures 109 through 113 show predicted changes in water levels in the Simsboro aquifer for the periods from 2010, 2020, 2030, 2040, and 2050, respectively. Obvious predicted changes in the Simsboro aquifer are (1) increase in the area where drawdown exceeds 25 ft and (2) increase in drawdown to almost 300 ft between 2000 and 2050 in parts of Brazos and Lee Counties. Water levels remain above the top of the confined part of the Simsboro aquifer through 2050. Drawdown is attributed to the continued growth in groundwater withdrawal from the Bryan-College Station well field, development of a



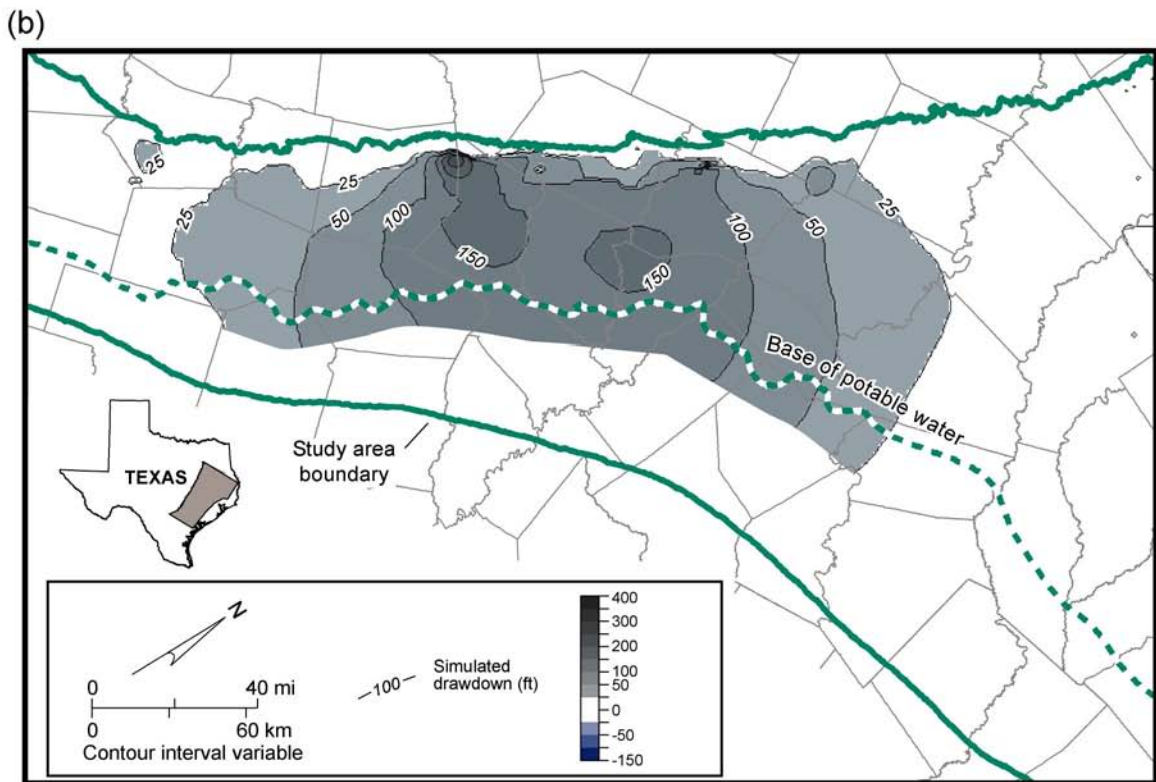
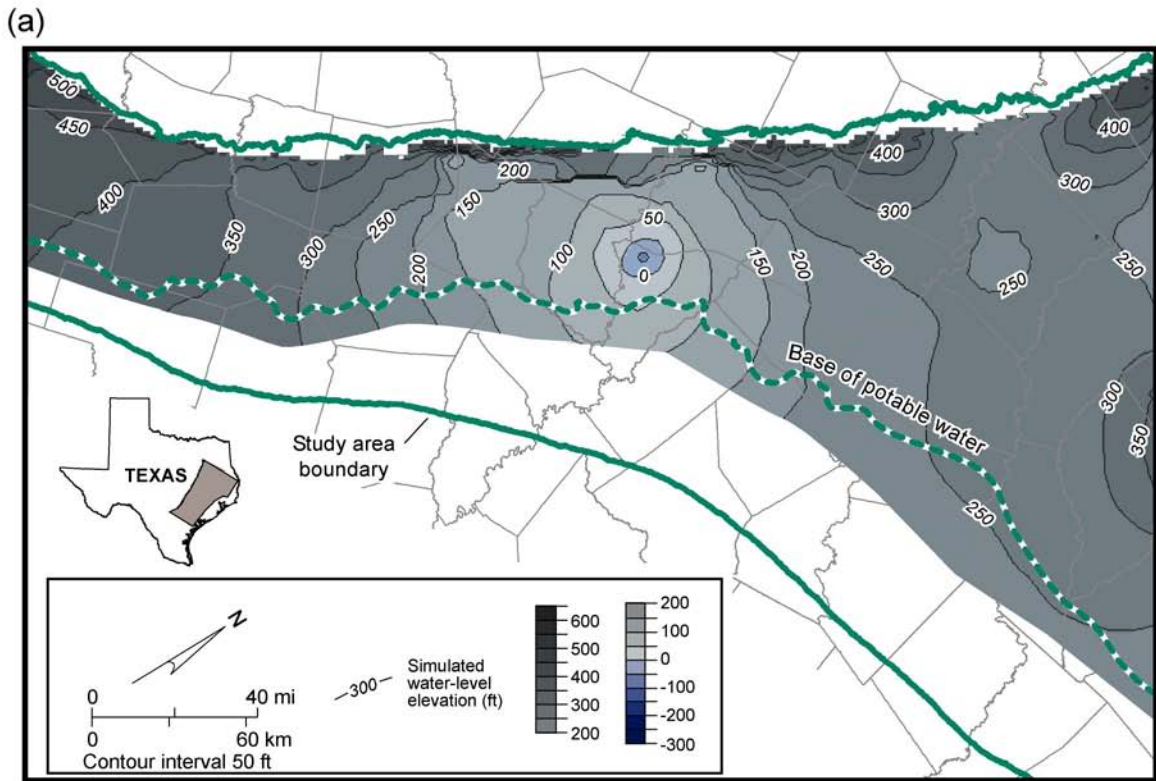
QAd2265c

Figure 109. Maps for the Simsboro aquifer (layer 5) showing predicted (a) 2010 water level and (b) drawdown from 2000 through 2010 assuming drought-of-record recharge from 2008 through 2010.



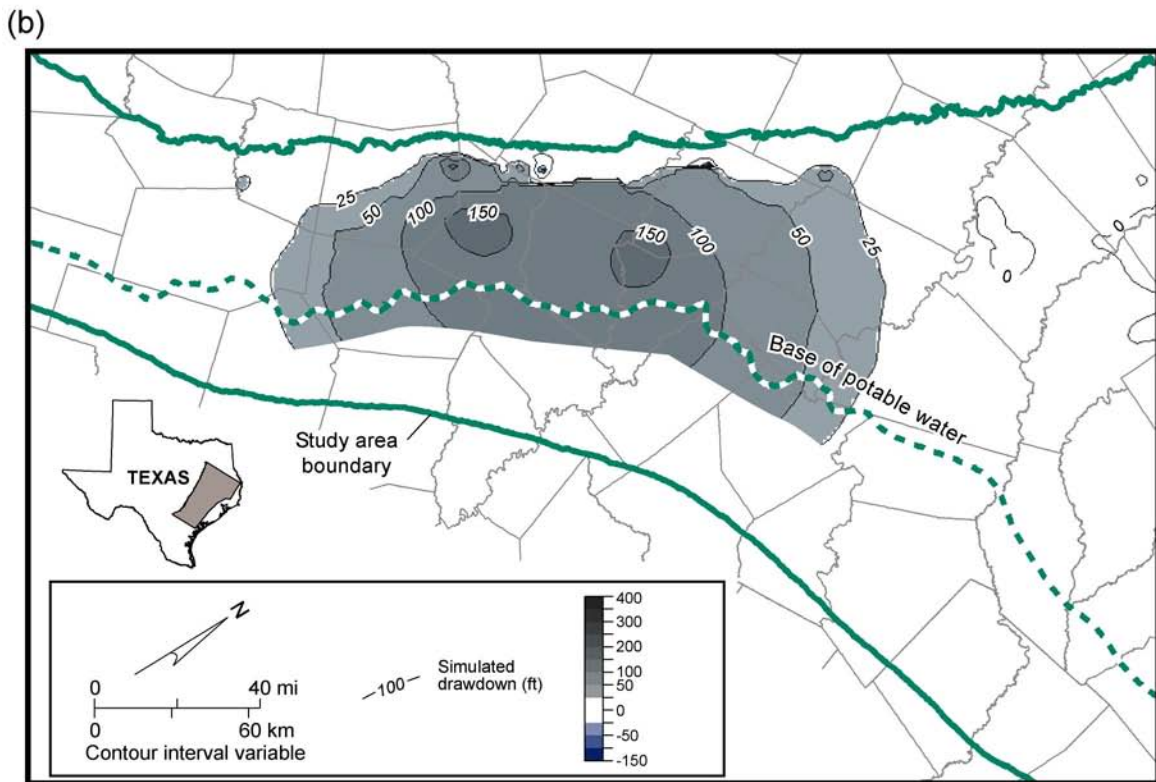
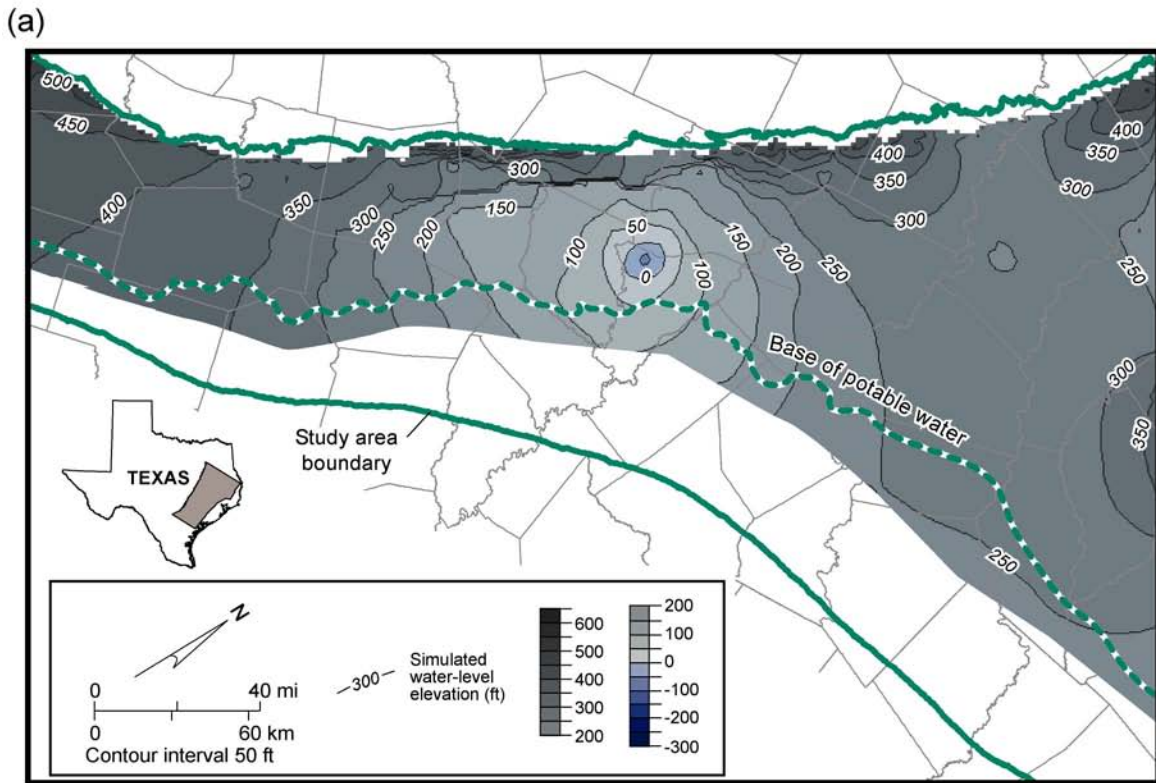
QAd2266c

Figure 110. Maps for the Simsboro aquifer (layer 5) showing predicted (a) 2020 water level and (b) drawdown from 2000 through 2020 assuming drought-of-record recharge from 2018 through 2020.



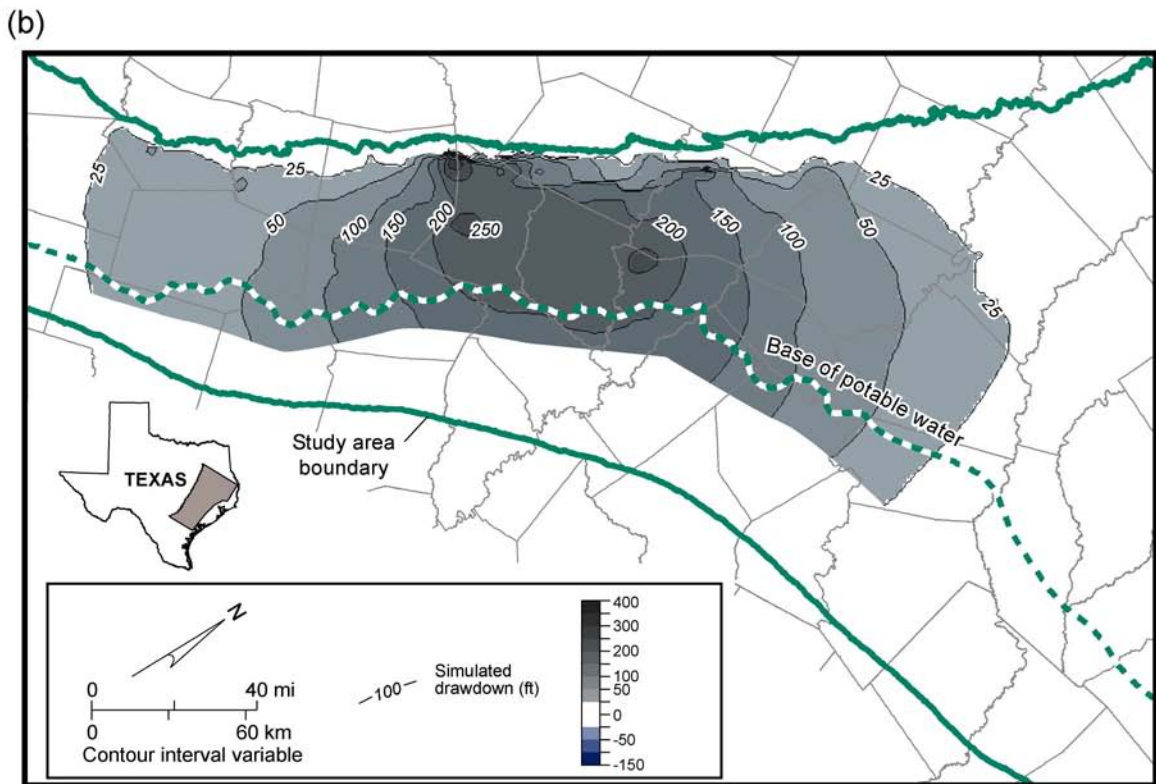
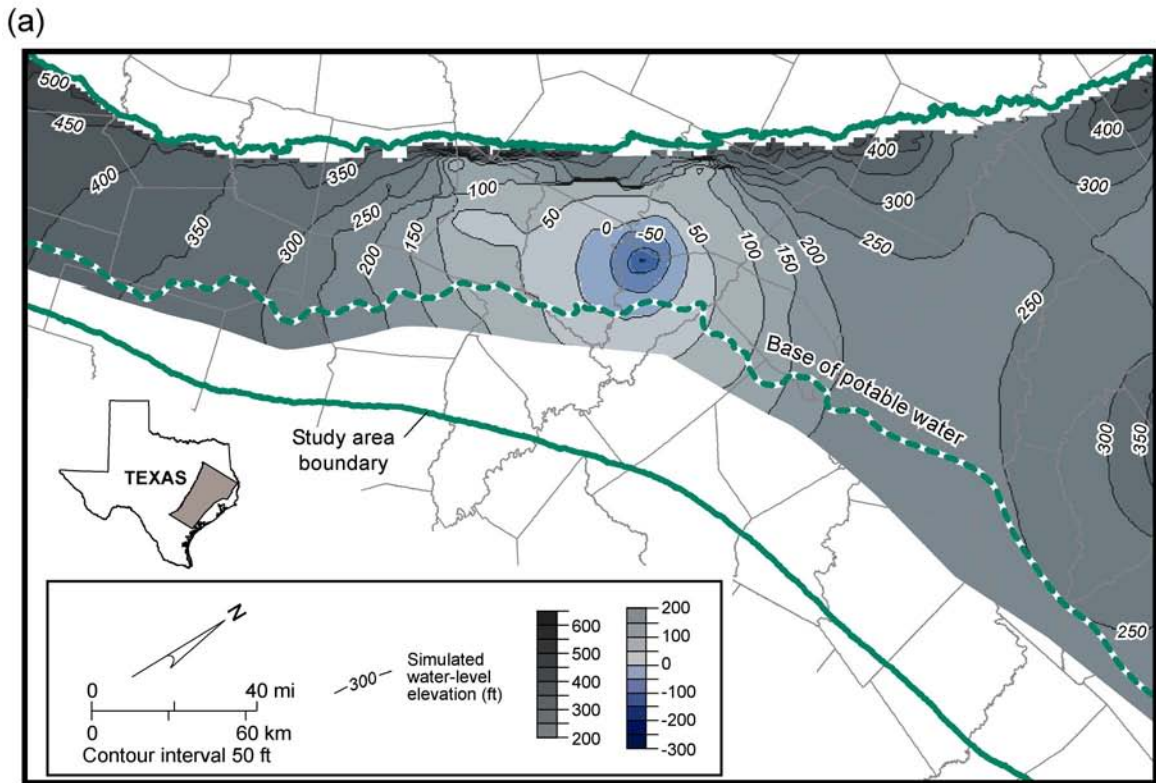
QAd2267c

Figure 111. Maps for the Simsboro aquifer (layer 5) showing predicted (a) 2030 water level and (b) drawdown from 2000 through 2030 assuming drought-of-record recharge from 2028 through 2030.



QAd2268c

Figure 112. Maps for the Simsboro aquifer (layer 5) showing predicted (a) 2040 water level and (b) drawdown from 2000 through 2040 assuming drought-of-record recharge from 2038 through 2040.



QAd2269c

Figure 113. Maps for the Simsboro aquifer (layer 5) showing predicted (a) 2050 water level and (b) drawdown from 2000 through 2050 assuming drought-of-record recharge from 2048 through 2050.

well field in Lee County to meet Williamson County water needs, and other increases in withdrawal from the aquifer.

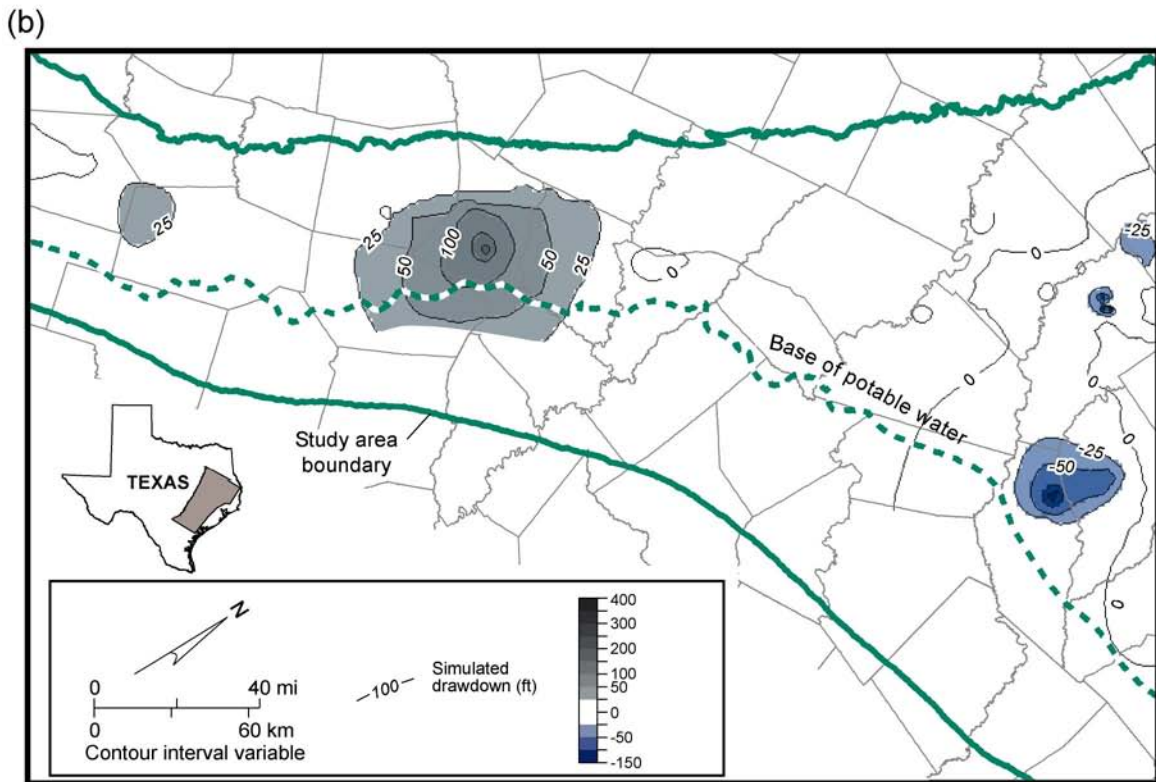
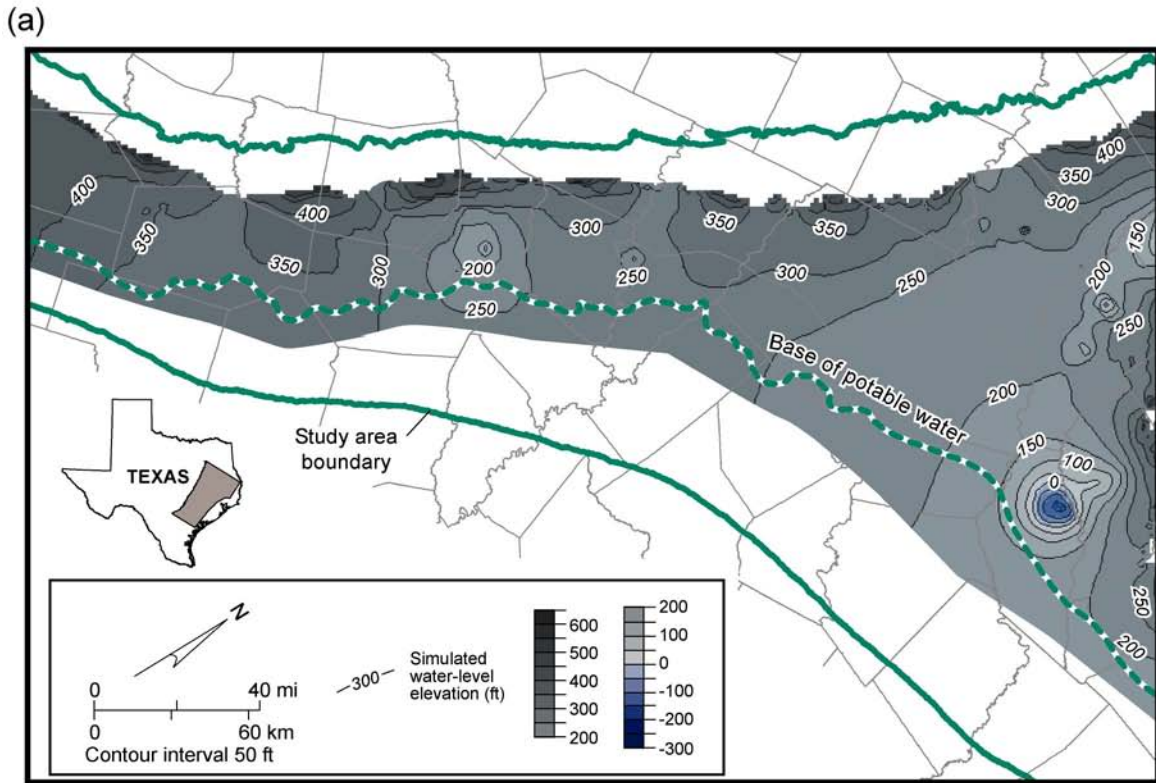
The water-level drawdown maps (for example, fig. 109b) show the area near the northeastern study boundary to have slightly negative (<0) drawdown. This prediction is an artifact of the assumed pumping rates for many of the counties near the boundary. It is unlikely that water levels will show significant recovery unless regional decreases in pumping rates are realized.

Additional drawdown in the central part of the study area is due to withdrawal of groundwater for a well field assigned to Lee County as part of the Brazos G Regional Water Plan strategy to meet Williamson County water needs. Part of that volume was assigned to the Carrizo aquifer and part to the Simsboro aquifer, using the footprint defined in the Trans-Texas Water Program (HDR Engineering, 1998). The spread of the area of drawdown around these projects is affected by the Karnes-Milano-Mexia Fault Zone (fig. 14). Water-level contours in figures 109 through 113 come close together and define a steep gradient in hydraulic head across the fault zone. Groundwater withdrawal associated with mining operations and groundwater withdrawal for transfer to the City of San Antonio in Bastrop and Lee Counties on the updip (northwestern) side of the fault zone adds to the regional drawdown.

Drawdown of the water levels in the Simsboro aquifer is predicted to grow to more than 100 ft by 2010, relative to 2000 water levels, and to almost 300 ft by 2050. By 2050, therefore, the model predicts that the historical (1950 through 2000) drawdown (fig. 90) will be doubled in the deeper artesian part of the aquifer, assuming that project pumping rates are realized. The water levels, however, remain above the top of the Simsboro aquifer. Predictions of the amount of drawdown and incidence of change from artesian to unconfined

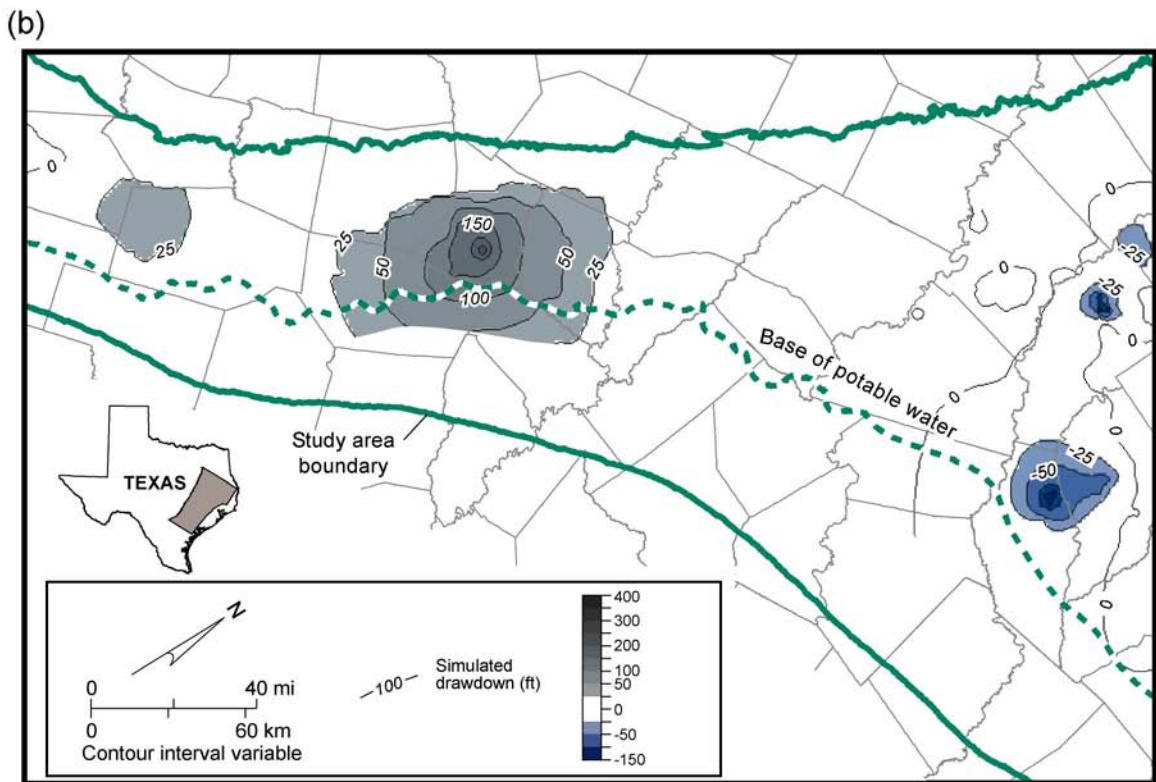
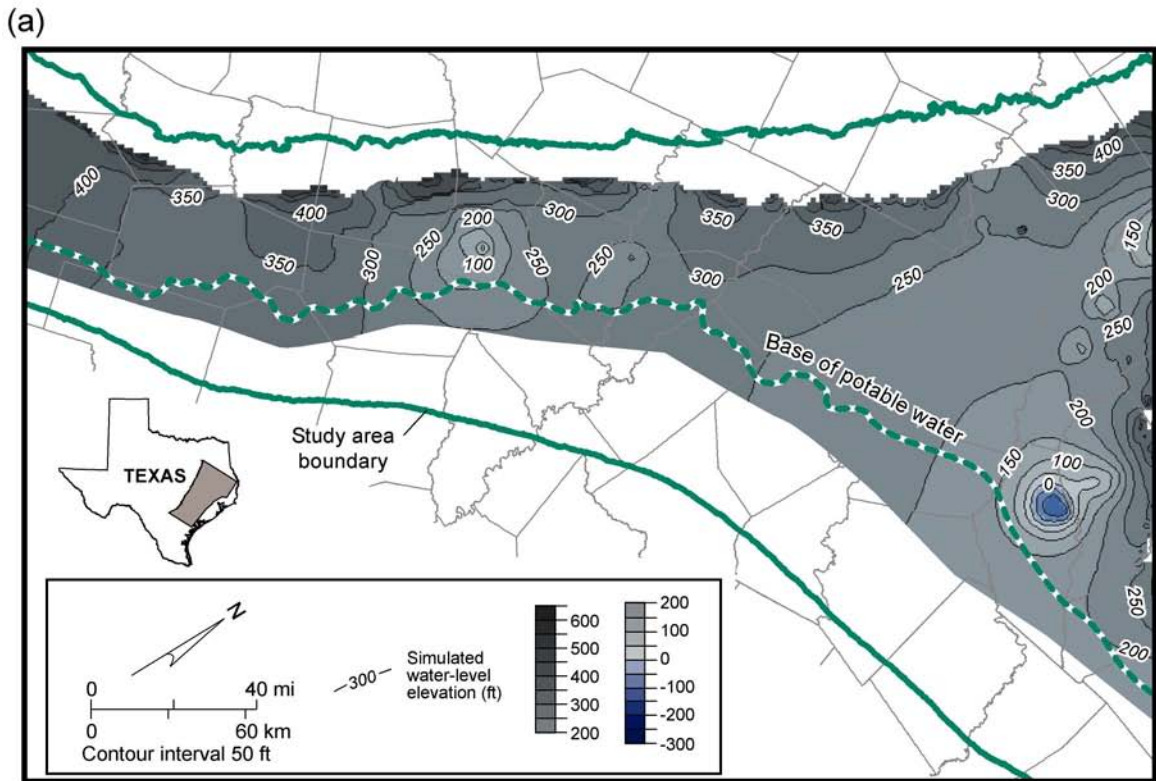
conditions nearer the outcrop is very sensitive to the assumed distribution or concentration of pumping represented in various model cells. As previously mentioned, the only change in simulation of normal precipitation and drought-of-record years was the use of different recharge rates. Pumping rates and their monthly variations were not changed to reflect changes in demand under drought conditions. For normal precipitation years in the predictive model, we used a constant recharge rate calculated from the average precipitation for 1960 through 1997 by the same equations used to estimate recharge for the transient model. Using 1960 through 1997 data excluded the effect of the 1950s drought of record from the calculation of the normal year recharge rate. Monthly recharge during the drought years was calculated from the precipitation of drought-of-record years (1954 through 1956). We kept monthly recharge rate constant during the drought in the predictive model because we assumed that drainage from the unsaturated zone to the water table in the Carrizo–Wilcox aquifer would not cease during a 3-yr drought.

Figures 114 through 118 show predicted changes in water levels in the Carrizo aquifer from 2000 through 2010, 2020, 2030, 2040, and 2050, respectively. The Carrizo drawdown maps also show areas of water-level recovery (drawdown values <0) in the northeast side. These are artifacts of the differences in historical and predictive pumping data from the TWDB and Regional Water Planning Groups. Other features are noteworthy. In the center of the model area, drawdown is due to pumping of groundwater from the Carrizo aquifer from the Bryan-College Station well field near the Brazos–Robertson County line, and from a Lee County well field assumed to be the source of water for Williamson County needs, as previously mentioned. Drawdown increases relative to 2000 water levels in Lee and adjacent counties. Also, several strategies in the South Central Texas Region L



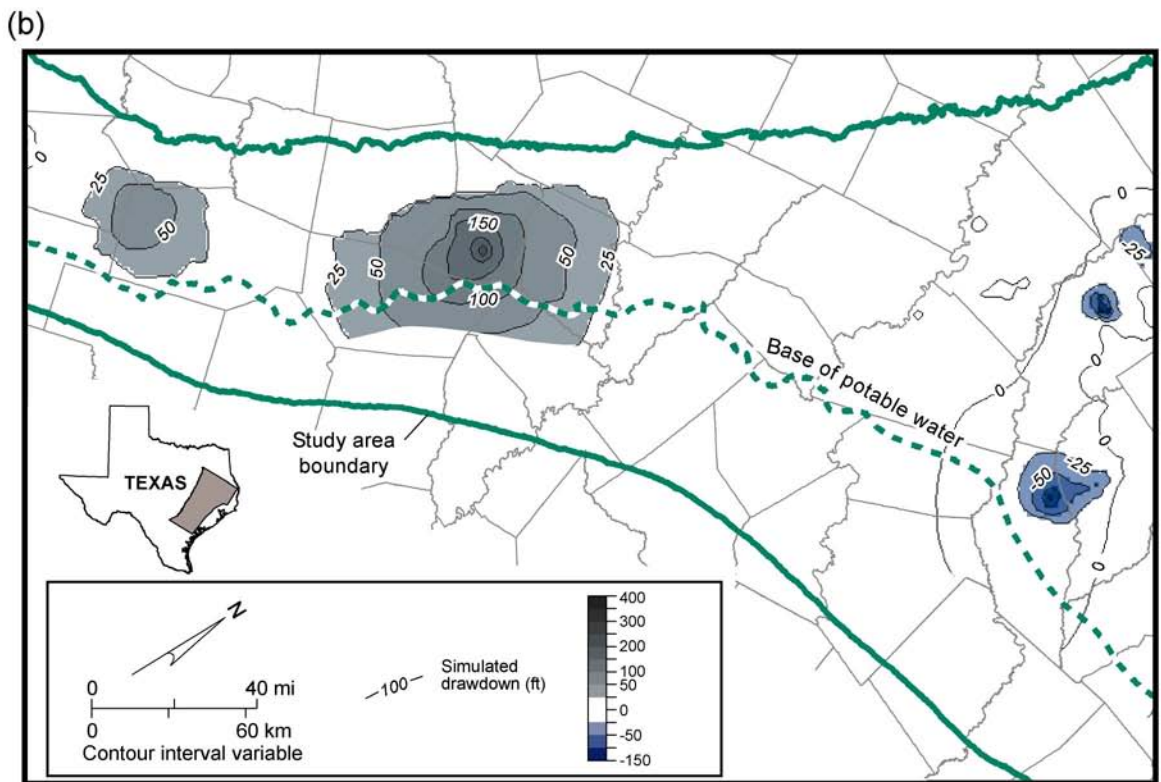
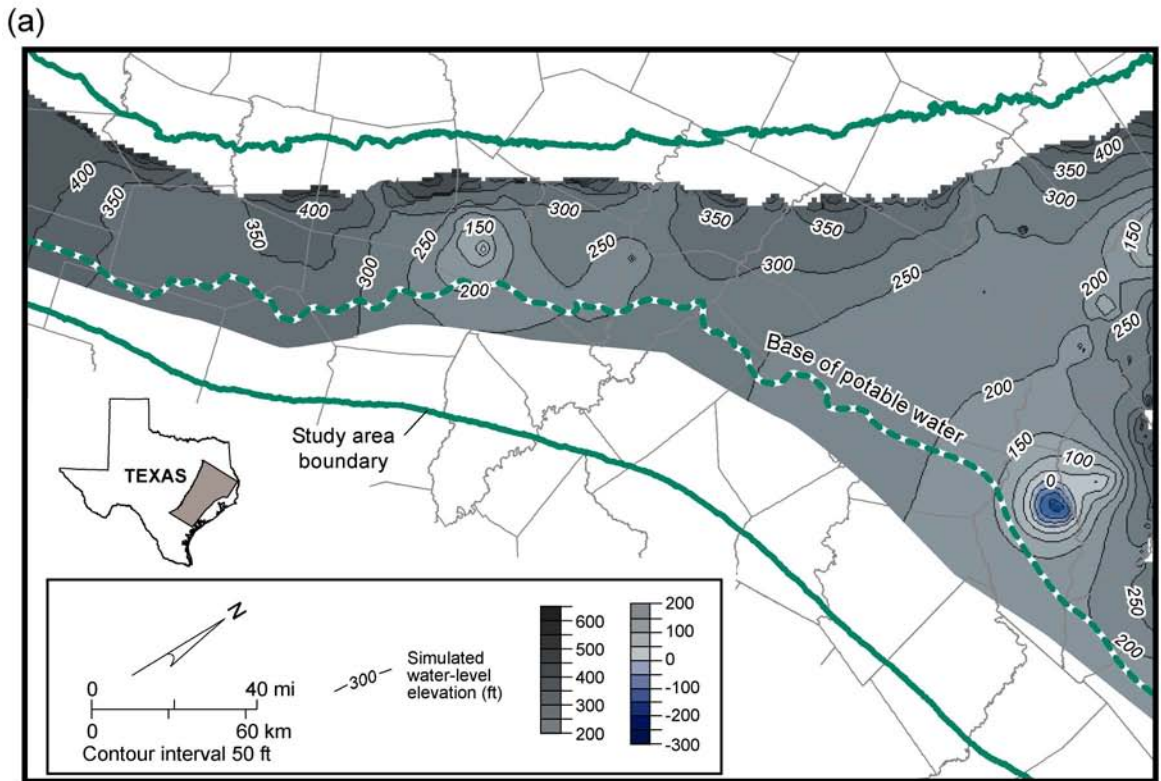
QAd2270c

Figure 114. Maps for the Carrizo aquifer (layer 3) showing predicted (a) 2010 water level and (b) drawdown from 2000 through 2010 assuming drought-of-record recharge from 2008 through 2010.



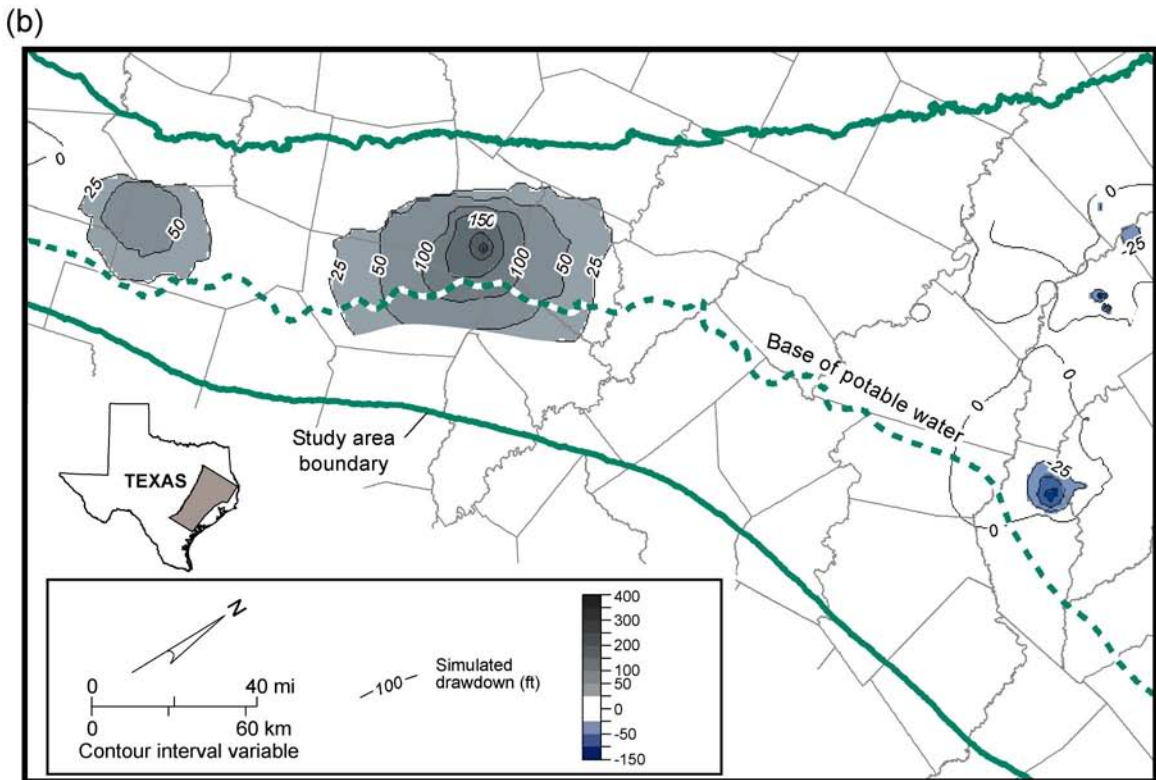
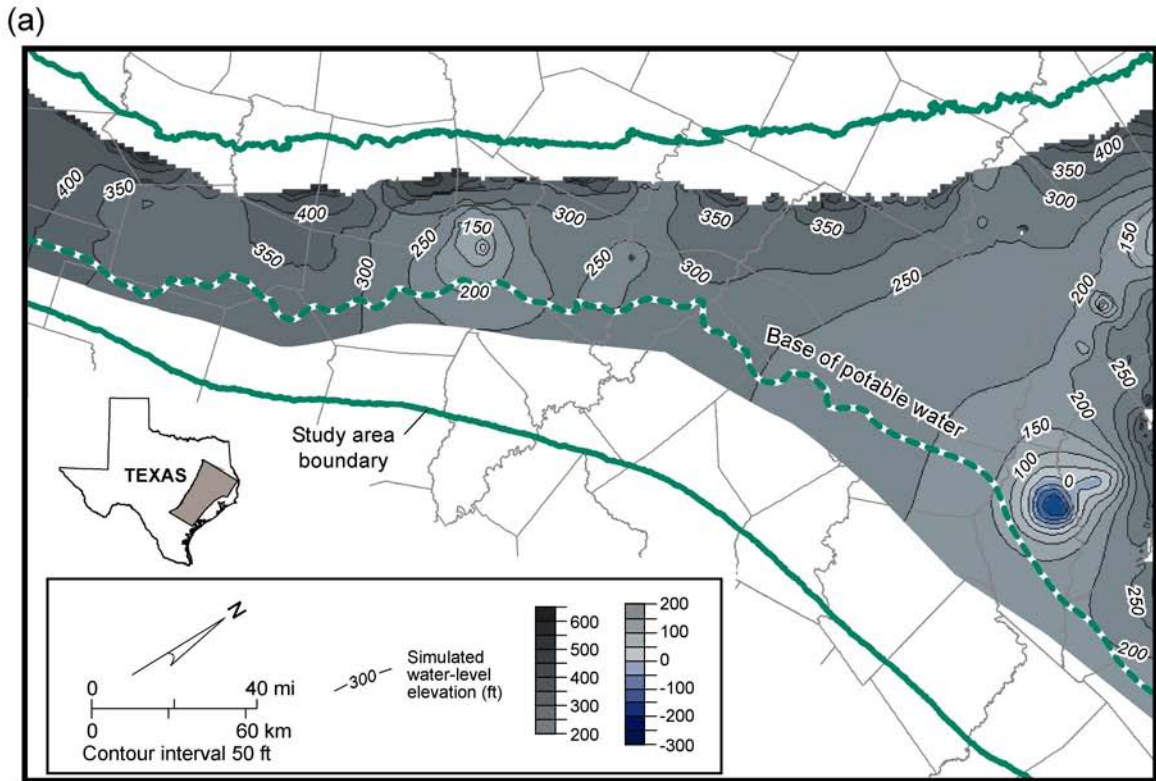
QAd2271c

Figure 115. Maps for the Carrizo aquifer (layer 3) showing predicted (a) 2020 water level and (b) drawdown from 2000 through 2020 assuming drought-of-record recharge from 2018 through 2020.



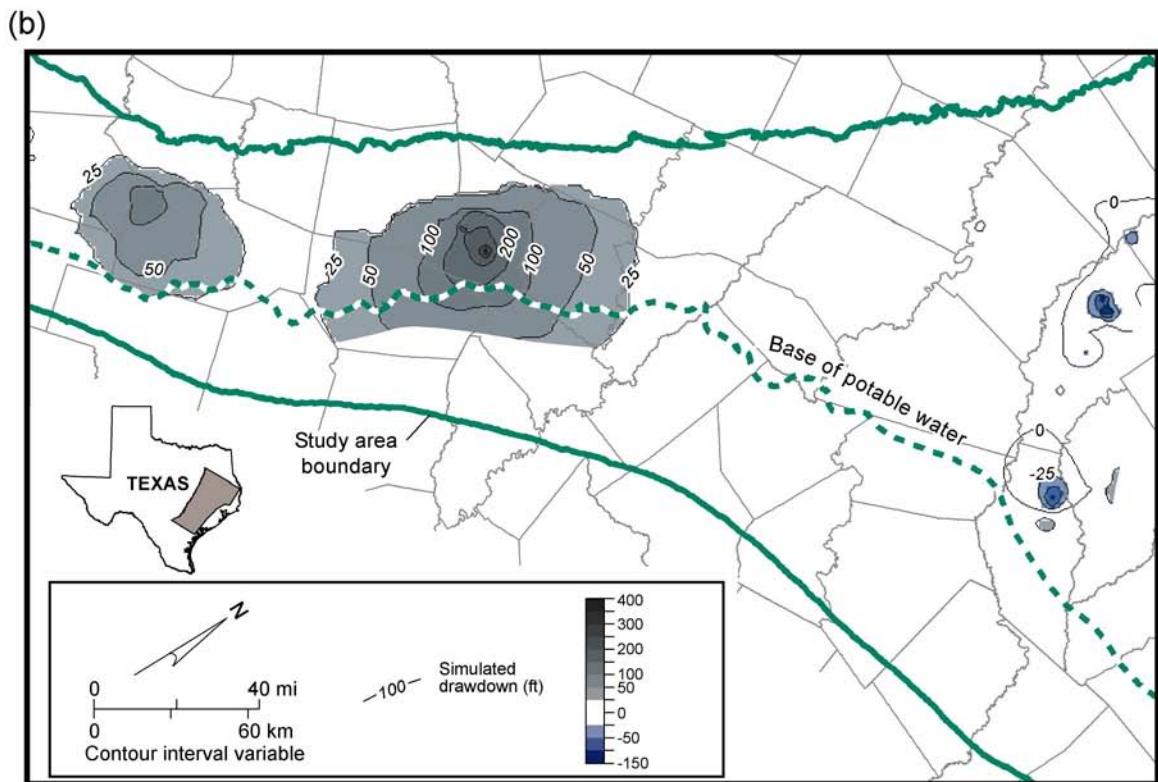
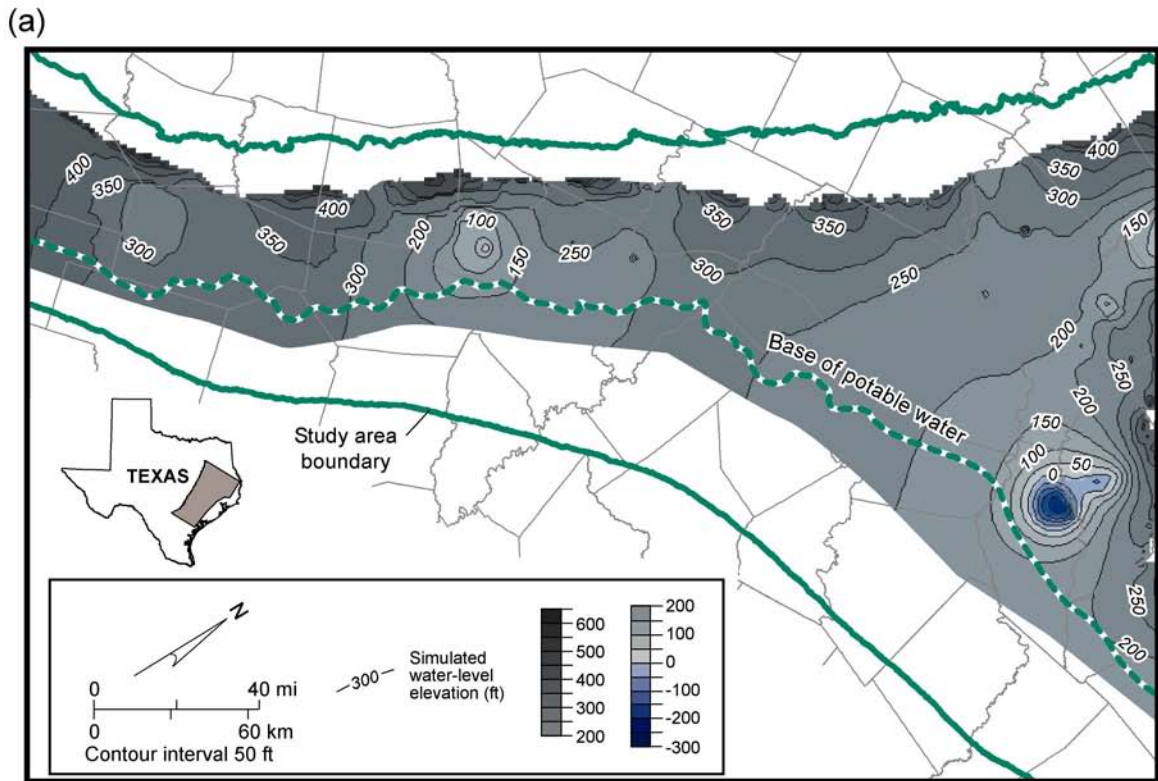
QAd2272c

Figure 116. Maps for the Carrizo aquifer (layer 3) showing predicted (a) 2030 water level and (b) drawdown from 2000 through 2030 assuming drought-of-record recharge from 2028 through 2030.



QAd2273c

Figure 117. Maps for the Carrizo aquifer (layer 3) showing predicted (a) 2040 water level and (b) drawdown from 2000 through 2040 assuming drought-of-record recharge from 2038 through 2040.



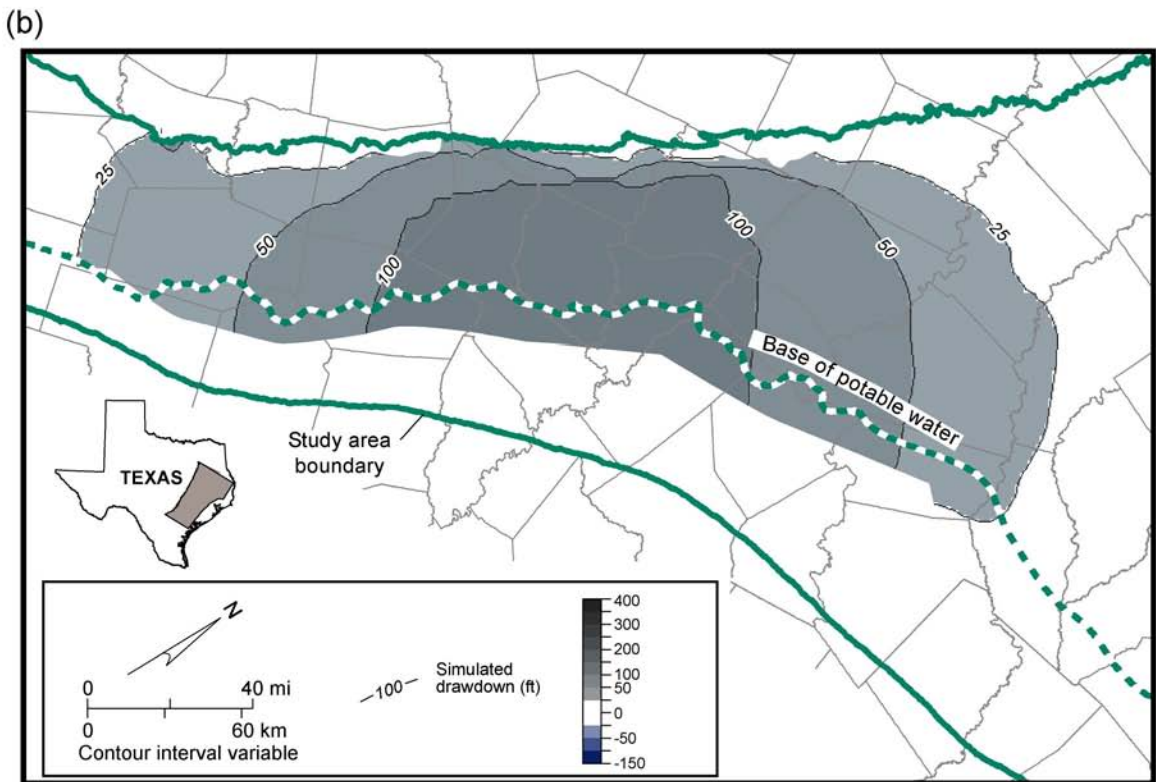
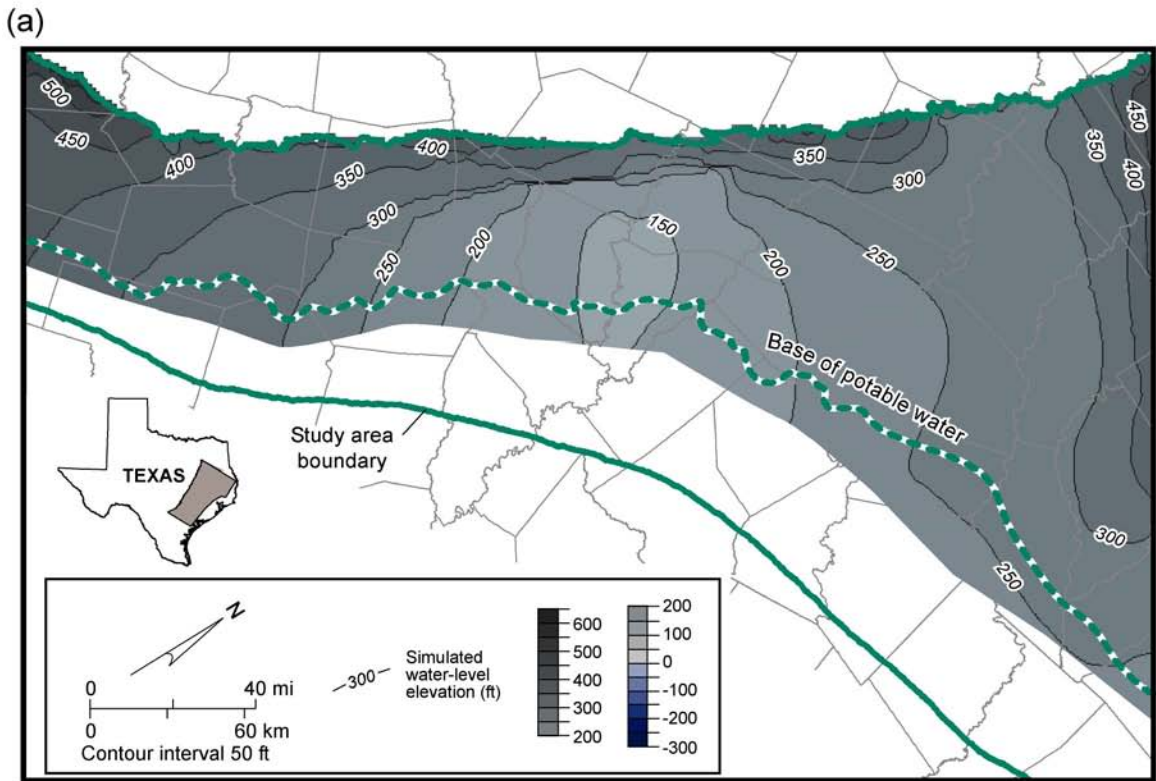
QAd2274c

Figure 118. Maps for the Carrizo aquifer (layer 3) showing predicted (a) 2050 water level and (b) drawdown from 2000 through 2050 assuming drought-of-record recharge from 2048 through 2050.

water plan identify the Carrizo aquifer in western Gonzales County as a source of groundwater. Drawdown in the Carrizo aquifer in western Gonzales County is predicted to be less than 100 ft over the 2000-through-2050 period (fig. 118).

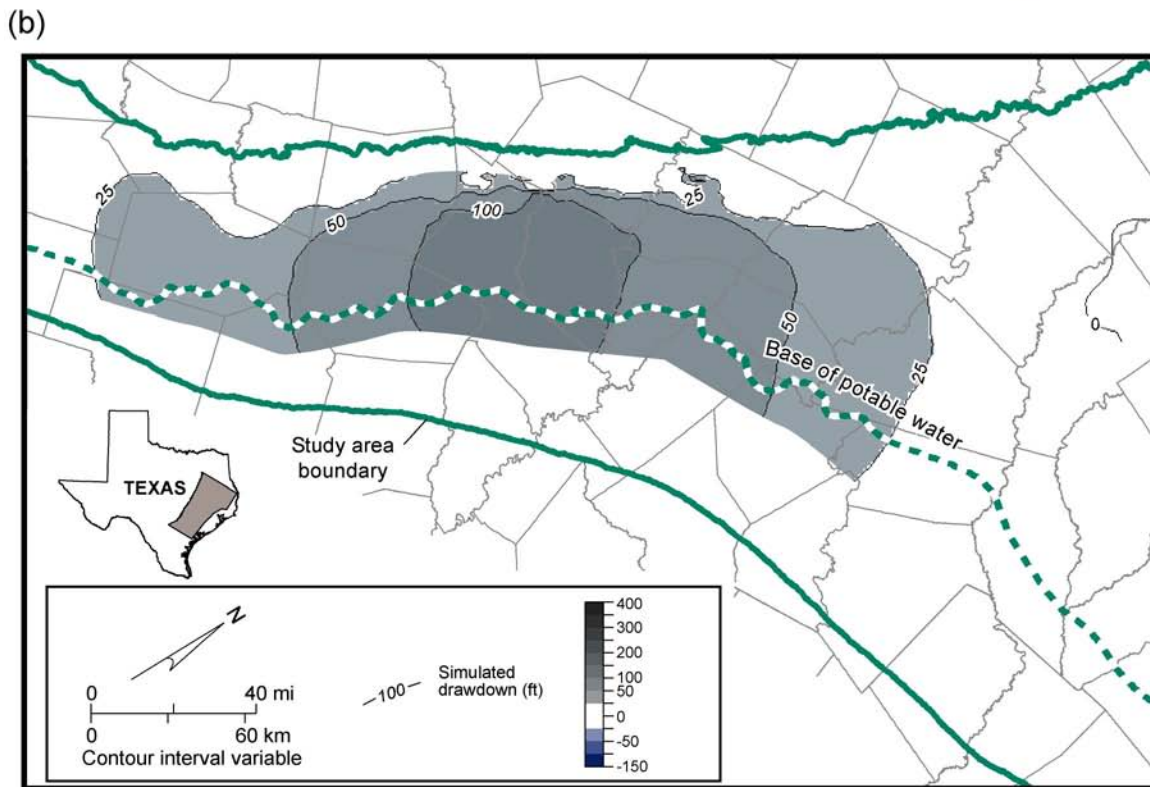
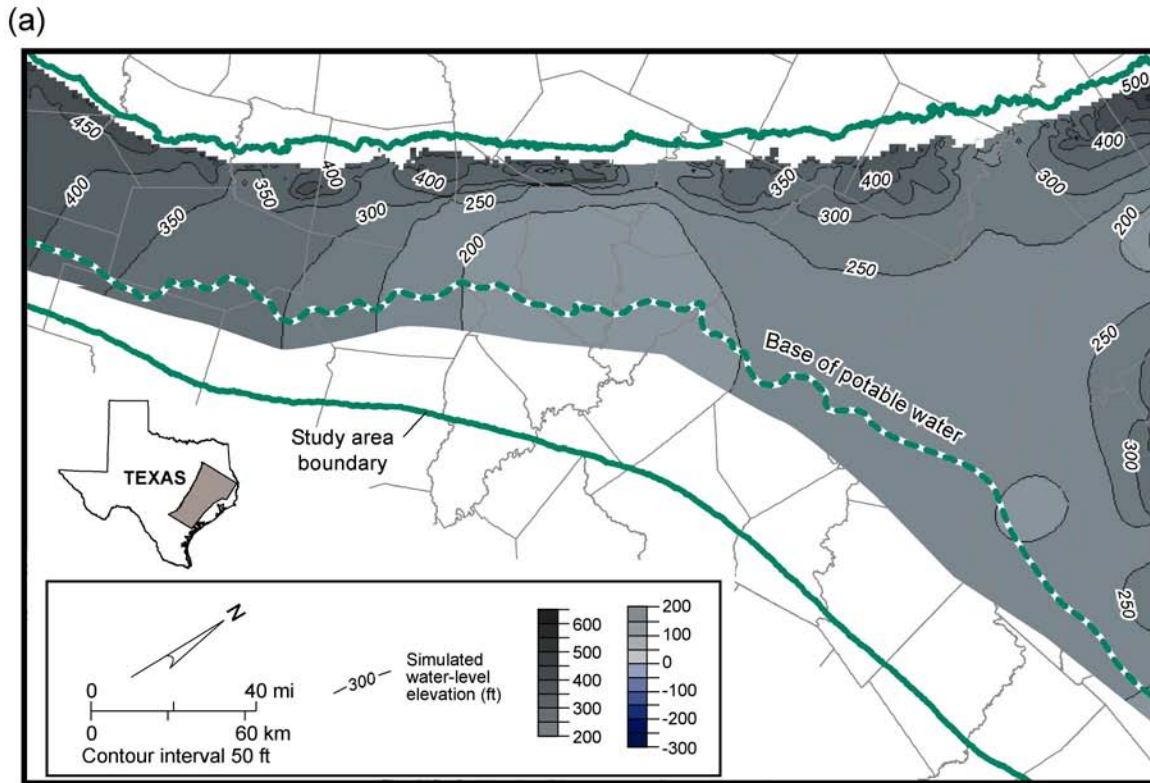
Figures 119 and 120 show predicted 2050 water levels and drawdown, relative to 2000 water levels, in the Hooper and Calvert Bluff Formations. About 30 model cells at the updip limit of the outcrop of the Hooper aquitard (layer 6) are simulated as going dry by 2050. These are the only model cells that go dry during the historical and predictive simulations. That these cells go dry in the model reflects the interaction of pumping and recharge rates, cell thickness, specific yield, and hydraulic conductivity assigned to that part of the model. Groundwater withdrawal assigned to these model cells represents mainly rural domestic water use, estimated on the basis of census information. Finding good yields of potable groundwater near the updip limit of the Hooper aquitard can be problematic. Future pumping rates from the updip Hooper aquitard will most likely be limited by well yield and water quality.

Some drawdown in the Hooper and Calvert Bluff aquitards is predicted from cross-formational flow. The Carrizo–Wilcox aquifer is a “leaky” aquifer in which some of the water pumped from well fields in the Simsboro and Carrizo aquifers derives from cross-formational leakage. The model predicts that such cross-formational flow accounts for more than 25 ft of water-level change in the Hooper aquitard (fig. 118b). Most of the predicted drawdown in the Calvert Bluff aquitard (>50 ft, fig. 120b) is a result of cross-formational leakage to that part of the Simsboro aquifer with more than 100 ft of drawdown (compare figs. 120b and 113b).



QAd2275c

Figure 119. Maps for groundwater in the Hooper Formation (layer 6) showing predicted (a) 2050 water level and (b) drawdown from 2000 through 2050 assuming drought-of-record recharge from 2048 through 2050.



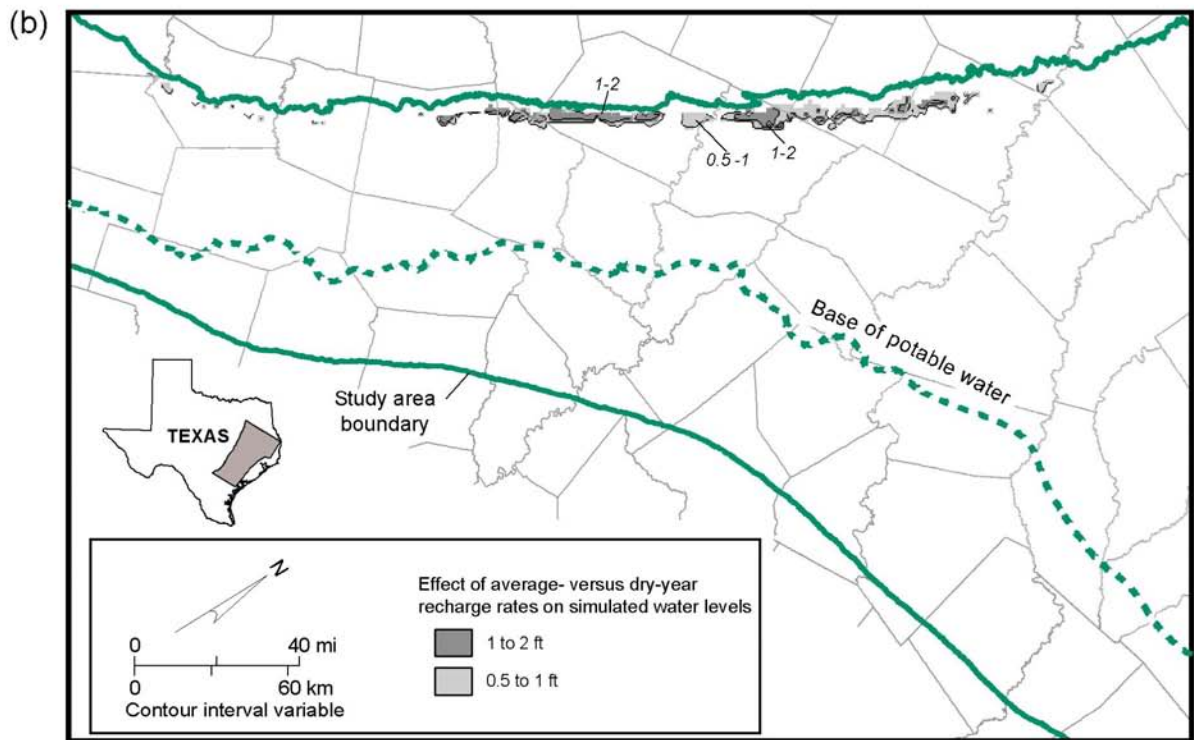
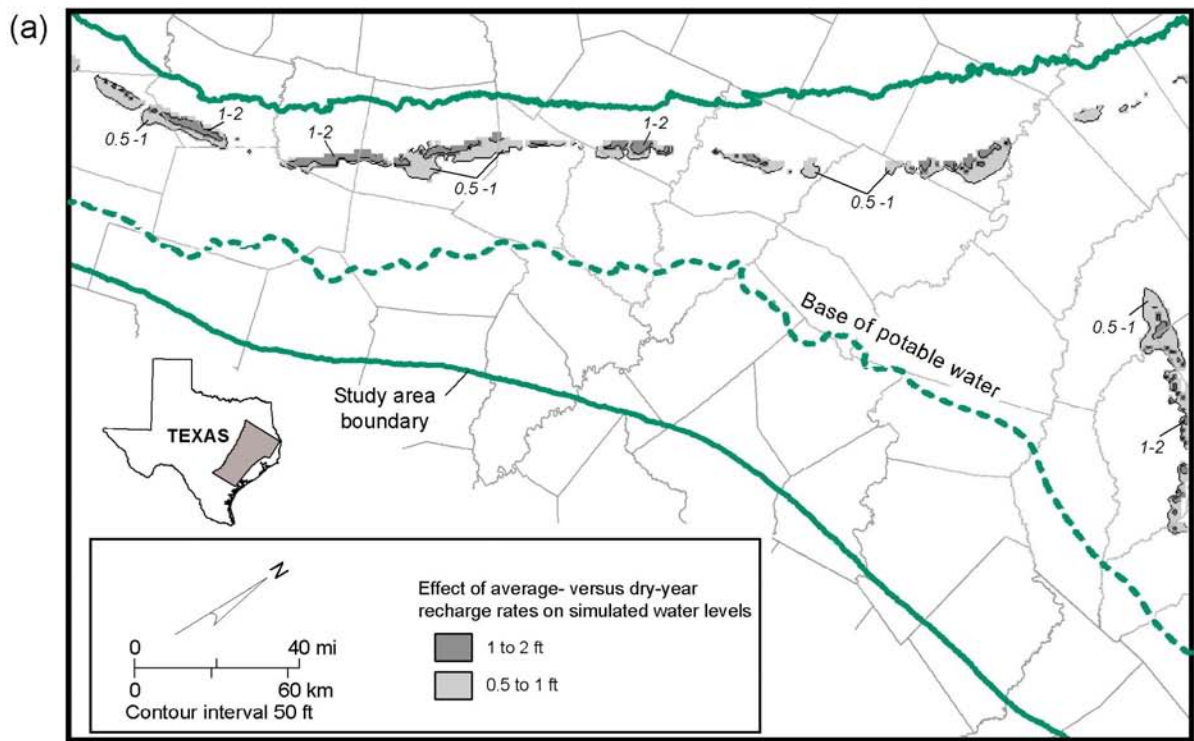
QAd2276c

Figure 120. Maps for groundwater in the Calvert Bluff Formation (layer 4) showing predicted (a) 2050 water level and (b) drawdown from 2000 through 2050 assuming drought-of-record recharge during 2048 through 2050.

Model simulation results shown in figures 109 through 120 include average recharge except for drought-of-record recharge rates applied in the last 3 yr of each simulation. Another simulation from 2000 through 2050 did not include the 3-yr drought-level recharge rates. Water levels predicted for 2050 using average and drought-level recharge rates differ by less than 5 ft and only near the outcrop (fig. 121a, b).

10.2 Water Budget

Table 16 presents the water budget for the preceding predictive simulations. Average recharge was used except for the last 3 yr of each simulation, for which we used a recharge rate predicted from precipitation during the 1954 through 1956 drought of record. GHB head at lateral boundaries of layers and assigned to layer 2 were kept constant at 2000 levels. Groundwater withdrawal (wells) is predicted to increase from approximately 194,000 to 363,000 acre-ft/year. This increase results in some changes in the water budget, but the main characteristics and trends are similar to those of the historical transient water budget (table 14). ET and base-flow discharge to streams are predicted to generally decrease as predicted water levels decline in the outcrop. Stream loss is approximately 21 percent of the stream gains; rivers and streams overall remain as gaining streams through 2050. Comparison of the simulated 2050 water levels with average versus drought-of-record recharge shows that recharge, ET, and stream gains are reduced during the predicted drought. Figure 122 illustrates the major components of the water budget in a block diagram for comparison with figures 79 and 100 for the steady-state and transient (2000) model. The model predicts a further reduction in base flow in all streams



QAd2293x

Figure 121. Difference for the end of 2050 in simulated water levels in (a) Carrizo aquifer (layer 3) and (b) Simsboro aquifer (layer 5) assuming average versus drought-of-record rates of recharge.

Table 16. Water budget for the predictive model (1000 acre-ft/yr). Average recharge for 2010 to 2050; simulation ends with drought of record recharge. Positive values are inflow to the aquifer; negative values are discharge from the aquifer. Annual rates from a 12-month long time step for 2000 and totaled from 12 1-month stress periods for 2010 through 2050.

Layer	Recharge	Net recharge	ET	Stream leakage	Reservoir leakage	GHB Reklaw	GHB down dip boundary	GHB NE boundary	GHB SW boundary	Wells	Cross-formational flow	Change in storage	Water balance error (%)
<u>2000</u>													
Alluvium (1)	12.9	0	-11.9	-23.7	0.6	0	0	0	0	0	21.7	0.3	-0.005
Reklaw (2)	14.8	-4.9	-21.5	-0.6	0	7.8	0	0	0	0	-3.1	2.6	-0.007
Carrizo (3)	118.4	25.6	-64.7	-29.3	0	0	2.4	0.7	27.1	-78.0	11.1	12.3	-0.003
Calvert Bluff (4)	47.4	-0.2	-31.9	-10.8	2.1	0	2.4	10.3	0.8	-11.4	-28.4	19.6	-0.006
Simsboro (5)	60.2	42.8	-21.9	-9.5	0.4	0	2.3	2.2	0.3	-98.0	22.0	42.0	-0.004
Hooper (6)	25.4	10.7	-13.5	-3.4	1.1	0	1.5	9.6	0	-6.2	-23.2	8.7	-0.001
ALL	279.2	74.1	-165.4	-77.2	4.2	7.8	8.5	22.8	28.1	-193.6	0	85.6	-0.005
<u>2010</u>													
Alluvium (1)	5.8	0	-10.8	-21.3	0.6	0	0	0	0	0	23.3	2.4	-0.002
Reklaw (2)	4.5	-4.9	-16.3	-0.5	0	32.7	0	0	0	0	-31.1	10.7	-0.002
Carrizo (3)	90.3	30.6	-55.5	-26.3	0	0	2.4	-0.1	28.7	-110.5	32.2	38.8	0.002
Calvert Bluff (4)	9.3	0.7	-23.4	-7.2	2.1	0	2.4	10.9	0.9	-13.1	-42.6	60.8	-0.005
Simsboro (5)	43.1	50.8	-16.1	-4.8	0.4	0	2.3	2.2	0.5	-146.4	47.5	71.3	-0.001
Hooper (6)	6.3	12.3	-9.3	-2.3	1.1	0	1.5	9.7	0	-12.1	-29.3	34.4	-0.001
ALL	159.2	89.5	-131.5	-62.3	4.3	32.7	8.5	22.8	30.0	-282.1	0	218.4	-0.001
<u>2020</u>													
Alluvium (1)	5.8	0	-9.9	-19.7	0.6	0	0	0	0	0	20.7	2.5	-0.003
Reklaw (2)	4.5	-4.9	-16.1	-0.4	0	43.2	0	0	0	0	-42.2	11.0	-0.002
Carrizo (3)	90.3	32.5	-54.3	-25.1	0	0	2.4	0.1	29.4	-119.8	39.5	37.6	0.002
Calvert Bluff (4)	9.3	2.2	-21.7	-6.1	2.2	0	2.4	11.1	0.9	-13.8	-46.5	62.2	-0.004
Simsboro (5)	43.1	48.5	-14.8	-3.3	0.4	0	2.3	2.5	0.5	-152.0	59.2	62.2	0.001
Hooper (6)	6.3	14.2	-8.6	-2.1	1.1	0	1.5	9.9	0	-12.5	-30.7	35.0	0.000
ALL	159.2	92.5	-125.4	-56.7	4.3	43.2	8.5	23.7	30.8	-298.0	0	210.5	0.000

Table 16 (continued). Water budget for the predictive model (1000 acre-ft/yr). Average recharge for 2010 to 2050; simulation ends with drought of record recharge. Positive values are inflow to the aquifer; negative values are discharge from the aquifer. Annual rates from a 12-month long time step for 2000 and totaled from 12 1-month stress periods for 2010 through 2050.

Layer	Recharge	Net recharge	ET	Stream leakage	Reservoir leakage	GHB Reklaw	GHB downdip boundary	GHB NE boundary	GHB SW boundary	Wells	Cross-formational flow	Change in storage	Water balance error (%)
<u>2030</u>													
Alluvium (1)	5.8	0	-9.1	-18.4	0.6	0	0	0	0	0	18.5	2.5	-0.003
Reklaw (2)	4.5	-4.9	-15.9	-0.4	0	49.4	0	0	0	0	-48.7	11.1	-0.002
Carrizo (3)	90.3	35.2	-53.4	-23.7	0	0	2.4	0.3	30.8	-131.5	45.6	39.4	0.002
Calvert Bluff (4)	9.3	3.1	-20.6	-5.3	2.2	0	2.4	11.5	0.9	-14.5	-48.5	62.6	-0.004
Simsboro (5)	43.1	46.9	-13.9	-2.3	0.4	0	2.3	2.8	0.5	-153.5	64.6	56.2	0.001
Hooper (6)	6.2	14.8	-8.1	-1.9	1.1	0	1.5	10.1	0	-12.4	-31.5	35.1	0.001
ALL	159.1	95.2	-121.0	-52.0	4.3	49.4	8.5	24.6	32.1	-312.0	0	206.9	0.000
<u>2040</u>													
Alluvium (1)	5.8	0	-8.6	-17.1	0.6	0	0	0	0	0	16.8	2.5	-0.002
Reklaw (2)	4.5	-4.9	-15.7	-0.3	0	55.5	0	0	0	0	-55.1	11.1	-0.002
Carrizo (3)	90.3	37.1	-52.7	-22.2	0	0	2.4	0.4	32.3	-140.4	50.1	39.9	0.002
Calvert Bluff (4)	9.3	4	-19.6	-4.6	2.2	0	2.4	11.7	1	-15.2	-50.9	63.6	-0.004
Simsboro (5)	43.1	46.1	-13.3	-1.7	0.4	0	2.3	3.1	0.5	-162.5	71.8	56.5	0.000
Hooper (6)	6.2	15.4	-7.8	-1.8	1.1	0	1.5	10.3	0	-12.9	-32.7	36	0.001
ALL	159.1	97.7	-117.7	-47.8	4.4	0	8.5	25.5	33.8	-331.1	0	209.6	0.000

Table 16 (continued). Water budget for the predictive model (1000 acre-ft/yr). Average recharge for 2010 to 2050; simulation ends with drought of record recharge. Positive values are inflow to the aquifer; negative values are discharge from the aquifer. Annual rates from a 12-month long time step for 2000 and totaled from 12 1-month stress periods for 2010 through 2050.

Layer	Recharge	Net recharge	ET	Stream leakage	Reservoir leakage	GHB Reklaw	GHB downdip boundary	GHB NE boundary	GHB SW boundary	Wells	Cross-formational flow	Change in storage	Water balance error (%)
<u>2050</u>													
Alluvium (1)	5.8	0	-8.1	-15.9	0.6	0	0	0	0	0	15.1	2.5	-0.003
Reklaw (2)	4.5	-4.8	-15.6	-0.3	0	64.0	0	0	0	0	-64.0	11.3	-0.002
Carrizo (3)	90.3	40	-52.1	-20.7	0	0	2.4	0.6	34.6	-156.0	57.4	43.6	0.002
Calvert Bluff (4)	9.3	5	-18.6	-3.9	2.2	0	2.4	12.1	1.2	-16.1	-54.0	65.5	-0.004
Simsboro (5)	43.1	45.7	-12.9	-1.2	0.4	0	2.3	3.4	0.5	-196.4	80.1	80.7	0.001
Hooper (6)	6.2	16	-7.4	-1.6	1.1	0	1.5	10.4	0	-13.5	-34.6	37.7	0.001
ALL	159.1	101.9	-114.8	-43.6	4.4	64.0	8.6	26.5	34.4	-381.9	0	241.4	0.000

2050 (simulation ends with average recharge for 1960 to 1997)

Layer	Recharge	Net recharge	ET	Stream leakage	Reservoir leakage	GHB Reklaw	GHB downdip boundary	GHB NE boundary	GHB SW boundary	Wells	Cross-formational flow	Change in storage	Water balance error (%)
Alluvium (1)	12.9	0	-8.5	-17.0	0.6	0	0	0	0	0	11.3	0.6	-0.002
Reklaw (2)	14.8	-4.7	-19.3	-0.3	0	63.9	0	0	0	0	-62.3	3.2	-0.002
Carrizo (3)	118.4	42.4	-58.4	-21.6	0	0	2.4	0.6	34.3	-156.0	58.6	21.7	0.002
Calvert Bluff (4)	47.4	6.1	-22.5	-5.0	2.2	0	2.4	12.0	1.1	-16.1	-53.7	32.3	-0.001
Simsboro (5)	60.2	47.9	-15.6	-1.6	0.4	0	2.3	3.4	0.5	-196.4	80.6	66.2	0.000
Hooper (6)	24.9	17.4	-9.2	-1.9	1.1	0	1.5	10.4	0	-13.5	-34.5	21.2	-0.001
ALL	278.6	109.1	-133.5	-47.4	4.4	63.9	8.6	26.4	36.0	-381.9	0	145.1	0.000

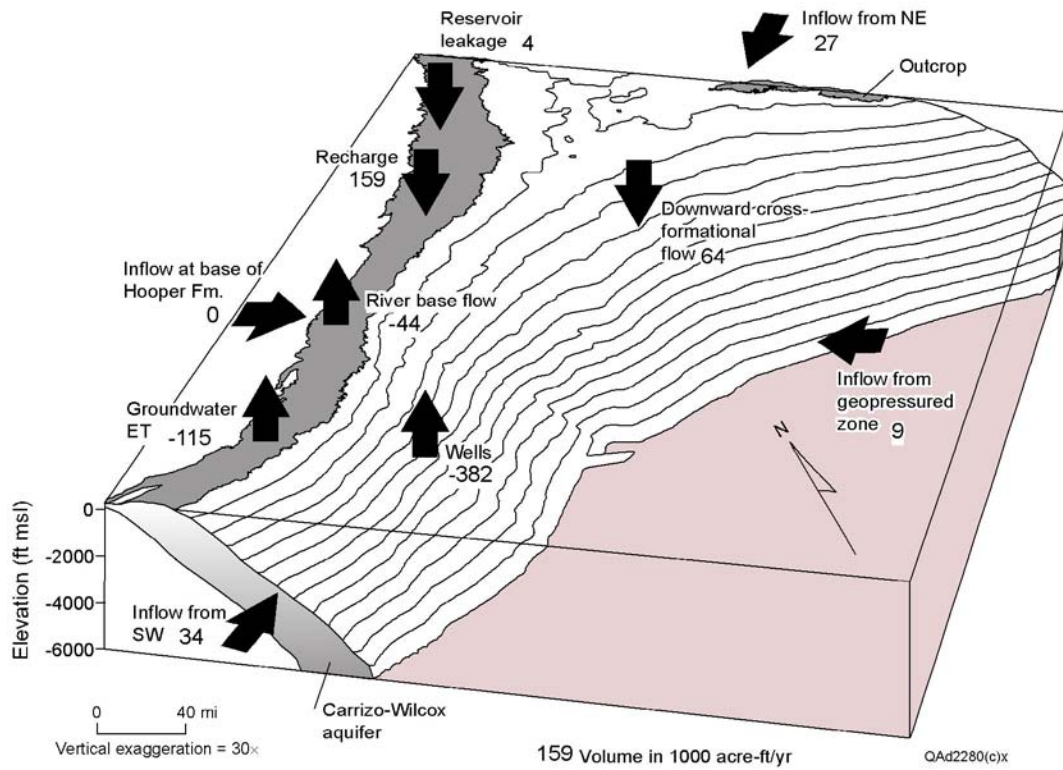


Figure 122. Block diagram of the Carrizo–Wilcox aquifer representing the components of the predictive model for 2050.

with increased pumping through 2050 (table 17). Base flow, however, is a small fraction of total stream flow. Historical data show no reduction in base flow.

Predicted water budgets also show that inflow from the GHB boundary continues to increase. The greatest inflow is from the top boundary of the model assigned to the Reklaw aquitard (layer 2) and to the lateral boundary assigned to the Carrizo aquifer (layer 3). The layer-3 inflow indicates that there is a net inflow to the model area across the northeastern boundary, mostly related to water-level drawdown in the vicinity of Angelina and Nacogdoches Counties.

An increase by an order of magnitude of the storage coefficient would double the inflow from the Calvert Bluff Formation into the Carrizo Formation and also increase the stream flow from the Simsboro Formation (table 18). A decrease by an order of magnitude of the storage coefficient would not have a major impact on the budget. Pumping changes of 10 percent have again a major impact on cross-formational flow from the Calvert Bluff Formation and on stream discharge from the Simsboro Formation.

Table 17. Simulated groundwater discharge to streams for the predictive model.

	Total discharge* (acre-ft/yr)		
	Steady state	2000	2050 ¹ DOR
<i>San Antonio River Basin Total</i>			
San Antonio River	20,500	18,000	14,600
Cibolo Creek	14,200	13,700	12,900
<i>Guadalupe River Basin Total</i>	6,200	4,300	1,700
Guadalupe River	14,700	12,100	600
San Marcos River	3,200	2,500	-1,200
Plum Creek	8,900	7,800	2,300
<i>Colorado River Basin</i>	2,600	1,700	-500
Cedar Creek	12,400	10,800	6,100
Colorado River	3,100	2,900	2,500
Big Sandy Creek	6,900	6,000	3,500
<i>Brazos River Basin Total</i>	2,500	1,900	100
Middle Yegua Creek	31,800	25,700	12,600
East Yegua Creek	4,800	3,700	1,300
Brazos River	1,300	700	0
Little River	4,300	3,900	2,600
Little Brazos River	6,100	5,300	2,500
Walnut Creek	1,300	1,200	700
Duck Creek	2,600	600	0
Steele Creek	1,800	1,400	1,000
Navasota River	2,100	1,900	1,300
Big Creek	5,800	5,300	2,100
<i>Trinity River Basin Total</i>	1,900	1,600	1,100
Upper Keechi Creek	11,100	10,500	9,100
Tehuacana Creek	4,200	4,000	3,300
Trinity River	2,800	2,700	2,300
San Antonio River	4,200	3,800	3,400
<i>Total</i>	90,600	77,200	42,900

* Rounded to nearest 100 acre-ft/yr

¹ DOR: Drought of Record

Table 18. Sensitivity of predicted 2050 water budget (with drought of record) to changes in storativity and pumping rate. Positive percent shows increase with respect to baseline 2050 drought-of-record results (table 16).

<u>Sensitivity to change in storativity (percent difference)</u>										
Layer	Recharge	ET	Stream leakage	Reservoir leakage	GHB	Wells	Flow upper cell face	Flow lower cell face	Change in storage	
<u>Storativity × 10</u>										
Alluvium (1)	0.0	6.6	6.9	0.0	0.0	0.0	0.0	11.3	-2.6	
Reklaw (2)	0.0	1.0	3.2	0.0	-14.8	0.0	11.3	-23.2	0.0	
Carrizo (3)	0.0	2.0	1.9	0.0	-1.4	0.0	-23.2	114.9	8.2	
Calvert Bluff (4)	0.0	7.9	16.9	-0.9	-5.5	0.0	114.9	-18.9	6.3	
Simsboro (5)	0.0	4.7	41.4	-3.3	-26.0	0.0	-18.9	12.1	8.9	
Hooper (6)	0.0	9.8	23.4	-0.9	-8.8	0.1	12.1	0.0	16.8	
ALL	0.0	3.9	6.9	-1.0	-10.0	0.0	-98.1	-98.1	8.8	
<u>Storativity × 0.1</u>										
Alluvium (1)	0.0	-0.6	-0.7	0.0	0.0	0.0	0.0	-1.2	0.4	
Reklaw (2)	0.0	-0.1	-0.4	0.0	1.7	0.0	-1.2	2.6	0.0	
Carrizo (3)	0.0	-0.2	-0.2	0.0	0.1	0.0	2.6	-13.1	-0.8	
Calvert Bluff (4)	0.0	-0.8	-2.0	0.1	0.6	0.0	-13.1	2.1	-0.7	
Simsboro (5)	0.0	-0.5	-5.0	0.4	2.7	0.0	2.1	-1.5	-0.9	
Hooper (6)	0.0	-1.0	-2.9	0.1	0.9	0.0	-1.5	0.0	-2.0	
ALL	0.0	-0.4	-0.8	0.1	1.1	0.0	11.1	11.1	-0.9	

Table 18 (continued). Sensitivity of predicted 2050 water budget (with drought of record) to changes in storativity and pumping rate. Positive percent shows increase with respect to baseline 2050 drought-of-record results (table 16).

Sensitivity to change in pumping rate (percent difference)											
Layer	Recharge	ET	Stream leakage	Reservoir leakage	GHB	Wells	Flow upper cell face	Flow lower cell face	Change in storage		
<u>Pumping (+10%)</u>											
Alluvium (1)	0.0	-3.1	-4.5	0.0	0.0	0.0	0.0	-7.1	3.6		
Reklaw (2)	0.0	-0.7	-8.5	0.0	15.4	0.0	-7.1	23.3	3.0		
Carrizo (3)	0.0	-1.3	-4.2	0.0	4.8	10.0	23.3	-28.2	7.3		
Calvert Bluff (4)	0.0	-3.6	-12.4	0.7	3.4	10.0	-28.2	13.2	5.4		
Simsboro (5)	0.0	-3.0	-41.9	2.1	8.3	9.7	13.2	5.8	11.9		
Hooper (6)	-0.3	-3.8	-10.3	0.3	2.1	7.3	5.8	0.0	6.0		
ALL	0.0	-2.1	-6.4	0.6	9.6	9.7	52.0	52.0	7.9		
<u>Pumping (-10%)</u>											
Alluvium (1)	0.0	3.5	4.8	0.0	0.0	0.0	0.0	7.5	-3.6		
Reklaw (2)	0.0	0.7	9.2	0.0	-15.5	0.0	7.5	-23.7	-3.2		
Carrizo (3)	0.0	1.4	4.5	0.0	-4.9	-10.0	-23.7	28.4	-6.7		
Calvert Bluff (4)	0.0	3.9	12.8	-0.7	-3.5	-10.0	28.4	-13.6	-5.5		
Simsboro (5)	0.0	3.3	40.0	-2.9	-8.6	-10.0	-13.6	-5.8	-12.4		
Hooper (6)	0.1	4.1	10.5	-0.3	-2.2	-9.5	-5.8	0.0	-6.7		
ALL	0.0	2.3	6.6	-0.7	-9.7	-10.0	-53.2	-53.2	-8.1		

11.0 LIMITATIONS OF THE MODEL

Typical limitations of numerical models of groundwater flow include (1) quality and quantity of input data, (2) assumptions and simplifications used in developing the model, and (3) the scale of application of the model (Mace and others, 2000a). These affect where and what kind of situation the model is applicable and how predictions may be made, interpreted, and used.

11.1 Input Data

The amount of geological control and other information used in building the model varies according to data category.

- Mapping and input of horizontal hydraulic conductivity is well constrained by test data (Mace and others, 2000c) and regional maps of the thickness of major sandstones. Model parameters are also well constrained by data for the Bryan-College Station well field.
- Top and bottom elevations of aquifer layers are generally well defined by abundant well logs and well drillers' reports. Assignment of layer elevation was coordinated between the northern, central, and southern Carrizo–Wilcox aquifer models. Inconsistencies between data sets were resolved. Setting the downdip boundary at the updip limit of the Wilcox Group Growth Faults required extending our structure maps well past the base of freshwater. It was beyond the scope of this aquifer modeling study, however, to map the deep structural elevation with as much resolution as the freshwater part of the

aquifer. In addition, structural and hydrologic properties associated with the Yoakum Channel, located in the southern part of the study area (Xue and Galloway, 1995), were not differentiated. Also, structure around salt domes in the East Texas Basin was not resolved precisely using the square-mile grid cells.

- Extrapolating subsurface structure data to the outcrop limit, however, can include greater uncertainty than structure mapping in the confined aquifer. A slight error in interpolated elevation on the base of a model layer is insignificant at depth, where model layers are from 300- to more than 1,000-ft thick. For the first few rows of active cells representing the aquifer outcrop, however, cell thickness can be less than 50 ft. A 10- to 20-ft interpolation error can result in major misrepresentations of aquifer transmissivity and saturated thickness in the outcrop.
- This study provided some of the first field measurements of recharge rates for the Carrizo–Wilcox aquifer. Preliminary results suggest that these “environmental tracers” have the potential to be useful tools for estimating recharge. But many more tests will be needed to answer questions about how many samples and what sampling density are needed to adequately characterize local and regional variations in recharge rates within each model layer. Also, different tracers yield slightly different results that require subjective discernment to reconcile. Nonetheless, field results for this study are consistent with previous modeling studies. Assigning recharge rates in space on the basis of soil permeability and through time on the basis of

proportional differences in precipitation rates appears to have yielded reasonable values for model input.

- The predicted water-level response to a future drought of record included only changes in recharge rates, not pumping. Sensitivity analysis shows that predictive model results will be much more sensitive to an increase in pumping rate than to a decrease in recharge rates. Evaluation of aquifer change during future drought, therefore, needs a protocol for varying pumping rates during the drought.
- GHB heads were assigned on the northeastern boundary to account for drawdown induced by pumping outside of the study area, for example, near Tyler in Smith County and Henderson in Rusk County. Changing the GHB conductance on the northeastern boundary from 0 (no-flow) to a large number has an effect on water levels within about 30 to 40 mi of the boundary. These GHB heads were kept constant during predictive simulations. The predictive water budgets suggest an increase in inflow to the study area across the northeastern boundary, mainly related to the well fields in Angelina and Nacogdoches Counties near the boundary. The northern Carrizo–Wilcox aquifer model (Intera and Parsons Engineering Science, 2002a) may provide more representative simulation results for the Carrizo aquifer layer within about 30 to 40 mi of the northeastern boundary, including Anderson, Angelina, Cherokee, Rusk, San Augustine, Smith, and Van Zandt Counties.
- The Karnes-Milano-Mexia Fault Zone displaces the aquifer layers and breaks up their hydrologic continuity between the outcrop and deeper artesian zone. The horizontal flow barrier (HFB) package of MODFLOW was used to

represent these hydrologic discontinuities. The shape and growth of areas of drawdown around centers of pumping near the fault zone, for example, in Bastrop, Lee, Burleson, Milam, and Robertson Counties, are highly influenced by the compartments in the aquifer set up by these faults. The same may also apply to southeastern Gonzales County in the vicinity of the Karnes Trough Fault Zone.

- The annual stress periods used during this study do not account for seasonal variability of stream flow. Several streams in the study area are intermittent, flowing during winter months following recharge during a period when ET is low. Although the intermittent streams receive less base-flow discharge than the larger, perennial streams, the seasonal variability is not represented in the annual model.

11.2 Assumptions

Important and basic assumptions included in our model include

- The base of the Carrizo–Wilcox aquifer at the Midway Group–Hooper Formation contact is impermeable; there is no exchange of groundwater between these units. Both the Midway and the Hooper Formations generally have low hydraulic conductivity, so this assumption would seem valid. This boundary assumption, however, may need to be reevaluated locally if groundwater were to be developed on a large scale from one of the Hooper Formation channel-sand deposits at depth.

- Groundwater historically leaves the confined part of the Carrizo–Wilcox aquifer by cross-formational flow across the Reklaw aquitard to either (1) river bottomlands in the Reklaw Formation outcrop or (2) discharge into the Queen City aquifer. Upward-directed discharge is focused in the river bottomlands where the down-gradient hydraulic heads are low. There is generally downward leakage into the Carrizo–Wilcox aquifer beneath upland areas. We had to reduce the vertical hydraulic conductivity assigned to the Reklaw aquitard in the East Texas Basin to locally restrict the amount of downward flow into the Carrizo aquifer, where water levels in the Queen City aquifer are especially high. We assumed that Queen City water levels remained constant during the historical and predictive simulations. Hydrograph data for the Queen City aquifer generally support this assumption. Additional study planned by the TWDB for 2003 through 2004 is expected to lead to a better understanding of the interaction of the Queen City and Carrizo–Wilcox aquifers.
- We assumed that under pre-1950 conditions there was a slight inflow of groundwater into the deeply buried part of the Wilcox Group (depths of 3,000 to 10,000 ft) from the geopressured zone. In addition, significant volumes of natural gas have been withdrawn from gas reservoirs in the Wilcox Growth Fault Zone during the past 50 yr. It is unknown whether equivalent hydraulic head at the updip margin of the geopressured zone has decreased or whether change in equivalent hydraulic head has been local in compartmentalized gas reservoirs. We also have assumed that a calculated equivalent brine-density hydraulic head is a satisfactory estimate of hydraulic head for calculating

hydraulic gradient. Nonetheless, the updip limit of the growth fault zone is a significant physical boundary in the deep Wilcox Group. The structural traps that hold oil and gas reservoirs are also physical boundaries for the circulation of water. Whereas we think that the rate of groundwater flow is very small in the deep Wilcox aquifer at depths greater than 5,000 ft (Dutton and others, 2002), the area in which artesian pressures are drawn down around the Bryan-College Station well field extends well into the deep Wilcox aquifer. Assumptions on how the deep downdip boundary is assigned could have some effect on predicted water levels for that well field as its drawdown depth doubles over the next 50 yr.

- We used conventional formation stratigraphy to subdivide the Carrizo–Wilcox aquifer into four layers representing the Hooper aquitard, the Simsboro aquifer, the Calvert Bluff aquitard, and the Carrizo aquifer. Groundwater flow through the aquifer, however, is more continuous. Subdividing each layer would give more intralayer resolution of vertical gradients in water level and vertical movement of groundwater. Our assumption of four hydrologic layers may yield simulation results that suggest that model cells near the outcrop have changed from artesian to unconfined conditions. This result may be an artifact of the simplified layering of the model. The vertical gradient in hydraulic head may be more continuous than shown in simulations.

11.3 Scale of Application

The model is most accurate in simulating regional gradients and long-term trends in water levels. The Simsboro and Carrizo aquifers, from which 90 percent of the groundwater in the aquifer system is withdrawn, have more hydrologic data than have the Hooper and Calvert Bluff aquitards. Whereas more effort has been put into calibrating the Simsboro and Carrizo layers of the model, the model should give reasonable results for the Calvert Bluff aquitard. Calibration is poorest for the Hooper aquitard.

The square-mile-grid cell size limits the applicability of the model at a local level. The model would not be appropriate in its present form for the detailed work needed for designing and locating individual wells in well fields. The model may be used to assess regional water-resource implications of the withdrawal of groundwater from well fields. In addition, corrections for apparent drawdown may be needed to apply model results, calculated for the center of grid cells, to individual wells and their pumping cycles. Similarly, stream base flow is not predicted accurately for individual model cells.

The model is well suited for making comparisons between various groundwater-withdrawal scenarios. Running the model with and without a particular well field project, for example, and subtracting the differences in simulated water levels for a given year will show the differences in water level that could be attributed to that well field project. Such comparisons can also be made for differences in boundary conditions or model parameters for a better understanding of how these might affect model results. An advantage is that such comparisons cancel out effects of assumptions, boundary conditions, and nonvaried parameters and their uncertainties. Scenario comparison may be complicated near the outcrop where transmissivity can differ between the scenarios.

MODFLOW-96 as provided in PMWIN can handle reservoirs located only in the first layer of the model. A simple modification of the subroutine RES1.FOR and recompilation of the MODFLOW-96 code with a Lahey Fortran 95 allowed production of complete results for reservoirs as presented in this report.

12.0 FUTURE IMPROVEMENTS

Several areas in which the model may be improved were beyond the scope of this study. They include further review of existing information, as well as the collection and scientific analysis of additional data.

First, the baseline future pumping rates used in the predictive model do not in all cases appear to be continuous with the historical estimates from the TWDB water-use surveys. Pumping during the 2000-through-2010 period, for example, is likely to be similar to what was experienced during 1990 through 2000.

Second, there remain significant gaps in basic hydrologic data on the aquifer, in particular for recharge rates, ET rates, vertical hydraulic conductivity, and specific storage.

- Relying on model estimates of recharge rate has some limitation because correct recharge rates require other model parameters to be well known. Environmental tracers have some potential to constrain model rates of recharge because tracers inherently average estimated rates over long (for example, 10- to 50-yr) periods. Because each tracer has some associated uncertainty, multiple tracers need to be applied with the goal of finding consistent results. Recent advances in developing a variety of tracers (Scanlon and others, 2002) make these techniques accessible for potential application to aquifers in Texas.
- ET rates and stream leakage both remove a large amount of water from the unconfined aquifer beneath the outcrop. This removal has a significant impact on net recharge, as inferred from the water budgets. Improved approaches to characterizing and calibrating the nonstream discharge of groundwater in

river bottomlands are needed. Modeling software such as the Soil Water Assessment Tool (SWAT) may be useful (Srinivasan and Arnold, 1994).

- Vertical hydraulic conductivity (K_v) is almost never measured in the field owing to the impracticality of making the long-term measurements needed to detect small changes in water level (Neuzil, 1999). Additional research may be warranted for a better understanding of how K_v should be assigned in heterogeneous aquifers.
- All predictive models with pumping are sensitive to specific storage. Direct measurements on specific storage are rare because they typically require paired observation and pumping wells within a radius of influence during a hydrologic test. Many models make the assumption that specific storage is uniform (for example, Intera and Parsons Engineering Science, 2002a, b). Specific storage in the confined part of the Carrizo–Wilcox aquifer and other aquifers may vary by one to three orders of magnitude. Obvious geological controls include consolidation, cementation, and other diagenetic processes that affect the elasticity of the aquifer matrix. Petrographic studies document that such diagenetic changes can be predicted as a function of depth. Elasticity of sandstone, claystone, and other common aquifer media also differs (Domenico and Schwartz, 1990). In some places, the diagenetic history is complex, with burial and exhumation resulting in a complex evolution of a rock's elastic properties. Additional research on how specific storage could be predicted on the basis of known or measurable rock properties and burial depth should be pursued.

- Additional research is needed for water quality issues to be understood, as well as water resources of the Carrizo–Wilcox aquifer. As previously described, this study advanced the understanding of how regional circulation of groundwater in the Carrizo–Wilcox aquifer is influenced by the Karnes–Milano–Mexia Fault Zone and the geopressured zone that starts in the Wilcox Growth Fault Zone (Dutton and others, 2002). The area of artesian drawdown in the Simsboro aquifer centered at well fields in Lee, Brazos, and Robertson Counties is expected to encounter the downdip boundary of the model, where total dissolved solids exceed 50,000 mg/L. Preliminary analysis suggests that groundwater flow rates are extremely slow in the deep artesian part of the aquifer, and water-quality impacts from the downdip boundary are not expected to be detectable. Although existing information indicates that it is not an issue, water quality might change owing to cross-formational flow and leakage of poor-quality water out of clay beds (Henry and others, 1979; Dutton, 1985).
- It was previously noted that there are fewer water-level data for model validation for 2000 than there were for model calibration in 1990. During the 1990s the number of water-level measurements being recorded by the State of Texas decreased compared with 1980s’ data collection owing to changes in budget priorities. Additional water-level data will be needed for postaudits of the performance of this and other models in the future. Continued collection of hydrologic data by the State of Texas is important in order to meet water resources needs.

13.0 CONCLUSIONS

We developed a numerical model of the occurrence and movement of groundwater in the central part of the Carrizo–Wilcox aquifer in Texas as part of a Statewide program to create models for use in evaluating groundwater availability in major and minor aquifers. This model is one of three overlapping models of the Carrizo–Wilcox aquifer. Development of the three models was coordinated to ensure model results in the overlap areas are as consistent as possible.

The central model divides the Carrizo–Wilcox aquifer into four layers, which represent, from bottom to top, the Hooper, Simsboro, Calvert Bluff, and Carrizo Formations. Two additional model layers represent (a) the Reklaw aquitard that overlies the Carrizo–Wilcox aquifer and (b) stream-bed alluvium through which groundwater moves from the bedrock aquifers to stream channels. There are 120,477 active cells in the six model layers.

We followed a standard protocol in constructing the numerical model. We developed the conceptual model of groundwater flow and defined aquifer properties on the basis of our review of previous work and file data, new field studies of recharge rates, and an original analysis of data on gas pressures and chemical composition of groundwater. Our modeling approach included (1) setting up and calibrating a steady-state version of the model without pumping; (2) calibrating a transient model of the period from 1950 through 1990, with emphasis on 1980 through 1990; (3) extending the model simulation through 2000 for verification of “predicted” 2000 water levels; (4) analyzing sensitivity of model results to input parameters; and (5) demonstrating the use of the model as a predictive tool by simulating water levels, drawdown, and stream flow for the 2000-to-2050 period with pumping rates derived from Regional Water Planning Groups water-demand projections.

Average steady-state recharge rates assigned to the Simsboro and Carrizo aquifers are 2.1 and 2.9 inches/yr, respectively. These rates are consistent with the 1- to 4-inch/yr rates indicated by previous studies and our field measurements of environmental tracers. In comparison, average recharge rates assigned to the Hooper, Calvert Bluff, and Reklaw aquitards in the model are 0.5, 0.4, and 0.2 inches/yr, respectively.

The steady-state model was calibrated to water levels measured between 1901 and 1950 and to the results of low-flow studies in streams and rivers. Overall, the model does a good job in matching the predevelopment water levels, considering the sparse data. Root Mean Square Error (RMSE) of simulated and observed water levels in the Simsboro aquifer is 25 ft, which is about 17 percent of the narrow range of water level reported for 13 observation wells. RMSE for the steady-state calibration of the Carrizo aquifer is 19 ft, less than 10 percent of the water-level drop across the observation wells. Model results match field observations that most stream base flow is discharged from the Simsboro and Carrizo Formations. The model generally under predicts the estimated base flow of the Guadalupe, Colorado, Brazos; and Trinity Rivers but better matches estimated base flow for smaller streams. The steady-state model is most sensitive to changes in (1) hydraulic heads assigned to the Reklaw aquitard (layer 2) using MODFLOW's General Head Boundary (GHB) package, (2) GHB heads imposed on the lateral boundaries of the Simsboro and Carrizo aquifers, (3) recharge rates, and (4) horizontal conductivity of the Simsboro and Carrizo aquifers. The GHB heads assigned to the upper boundary of the model are based on water levels in the Queen City aquifer, which overlies the Reklaw aquitard. The model estimates that under predevelopment conditions, net rates of recharge to the Simsboro and Carrizo layers averages 0.4 and 0.2 inches/year, respectively. Net recharge is the calculated amount of recharge per unit area of the outcrop that moves downdip from the unconfined

to the confined part of the aquifer or is taken into storage in the unconfined aquifer.

The model shows that net recharge rates to aquitard layers of the model are very small under predevelopment conditions.

We were able to obtain a good calibration and verification of the historical model as measured by comparison of measured and simulated water levels. RMSE errors for the Simsboro and Carrizo aquifers for the 1990 calibration year are 36 and 49 ft, respectively, or 10 and 7 percent of the range in water level recorded in water wells. RMSE errors for the 2000 verification year are 49 ft in the Simsboro aquifer and 43 ft in the Carrizo aquifer, less than 10 and less than 6 percent, respectively, of the observed range in water level in the Simsboro and Carrizo aquifers. The match of simulated and observed water-level hydrographs generally is very good. Annual fluctuations in water level simulated with monthly stress periods are proportional to the seasonal range in pumping rate and also match observed short-term water-level fluctuations. Simulated water levels in the transient model are more sensitive to pumping rates and horizontal conductivity than to storativity and recharge rates. The water budget of the transient model shows that net recharge rates may have slightly increased while ET and stream flow may have decreased during the past several decades. The transient-model water budget also indicates that more water now moves downward into the Carrizo–Wilcox aquifer than moves upward to the Queen City aquifer, a reversal of the predevelopment trend.

We used the calibrated model to simulate 2000-through-2050 water levels for the central Carrizo–Wilcox aquifer study area. Each predictive simulation ended with drought-of-record conditions with reduced recharge rates. The model predicts that the largest future drawdown of as much as 300 ft, compared to 2000 water levels, will be in the Simsboro aquifer in the area centered on Brazos, Lee, and Robertson Counties. Artesian water levels,

however, remain well above the top of the aquifer. The increased drawdown reflects the predicted increase in rate of groundwater withdrawal for the Bryan-College Station well field, a new well field in Lee County providing water to Williamson County, and additional pumping in Bastrop, Lee, and Milam Counties for transfer to Bexar County and other increased withdrawal rates. The model predicts that the simulated rivers and streams will remain gaining through 2050.

A numerical model such as this one for the central part of the Carrizo–Wilcox aquifer includes many approximations and simplifications of an aquifer system. Those assumptions and simplifications, along with the quality and quantity of input data, size and geometry of the model grid, and assumptions about future pumping rates, can impact the accuracy of model predictions. This model was designed for use as a tool for answering regional-scale questions about groundwater availability. The model would not be appropriate for designing and locating individual wells in well fields or predicting water-level changes at individual wells. The model is well suited for making comparisons between various scenarios. Additional aquifer studies and post-audits of the model will improve the calibration of the model.

14.0 ACKNOWLEDGMENTS

Many people contributed in various ways to this aquifer-modeling project. Approximately 35 people regularly attended and participated in the eight Stakeholder Advisory Forums held in Austin, Bastrop, Bryan, and Hearne, Texas. The Stakeholders included members of the public, as well as representatives of groundwater conservation districts, regional water planning groups, municipal utilities, industry, and local, State, and Federal government agencies. Their encouraging comments, suggestions, and data are appreciated. We also thank Barry Miller of the Gonzales County Underground Water Conservation District for helping us with model locations to represent 2000-through-2050 well fields and Larry Land of HDR Engineering for reviewing with us the various water strategies adopted by the South Central Texas Region L Water Planning Group. We also appreciate the cooperation of Van Kelley, Rainer Senger, Neil Deeds, and Dennis Fryar at Intera, Inc., who were responsible for developing GAM models for the northern and southern Carrizo–Wilcox aquifer. Coordination of the three models was an important part of the GAM project.

James Bene, Michael Jaffre, Jamie Wilson, and Joel Zimmerman at R. W. Harden and Associates, Inc., made many contributions in constructing model input files, making model calibration runs, using MT3DMS modeling software to evaluate the downdip boundary, and discussing modeling results.

At the Bureau of Economic Geology, Bridget Scanlon and Bob Reedy conducted the field study to estimate recharge. Bob Reedy also helped prepare model input data. Eugene Kim accessed pressure data for Wilcox Group gas fields. Scott Hamlin and Paul Knox mapped hydraulic conductivity in the study area. Katie Kier, Thandar Phyu, and

Thet Naing assisted with GIS analysis, model input data, and preparation of report and data model materials. Katie Kier also mapped TDS in the study area. The report was edited by Lana Dieterich under the direction of Susie Doenges, Editor in Chief. Illustrations were prepared by Patricia Alfano, Jana S. Robinson, David M. Stephens, and John T. Ames, and the report manuscript was laid out and the cover was designed by Jamie H. Coggin, all under the direction of Joel L. Lardon, Graphics Manager.

We also gratefully acknowledge the contributions made by TWDB staff, including Robert Mace (Project Manager for the central Carrizo–Wilcox GAM model), Roberto Anaya, Cindy Ridgeway, Richard Smith, and Shao-Chih (Ted) Way. Cindy Ridgeway and her staff set up the data sets for historical and predictive pumping demands, saving us much effort in data preparation. TWDB staff consistently provided helpful suggestions for improving the study as part of their reviews of the conceptual model, steady-state and transient numerical models, and predictive model results.

The views and conclusions contained in this draft report and the GAM CW-c groundwater model reflect those of the Bureau of Economic Geology and should not be interpreted as necessarily representing the opinions, either expressed or implied, of R. W. Harden and Associates, Inc., HDR Engineering, Inc., or the official policies or records of the Texas Water Development Board.

15.0 REFERENCES

- Amyx, J. W., Bass, D. M., Jr., and Whiting, R. L., 1960, Petroleum Reservoir Engineering: New York, McGraw-Hill, 610 p.
- Anders, R. B., 1957, Ground-water geology of Wilson County, Texas: Austin, Texas Water Development Board, Report B5701.
- ____ 1960, Ground-water geology of Karnes County, Texas: Austin, Texas Water Development Board, Report B6007.
- Anderson, M. P., and Woessner, W. W., 1992, Applied groundwater modeling, simulation of flow and advective transport: New York, Academic Press, 381 p.
- Arnow, T., 1959, Ground-water geology of Bexar County, Texas: Austin, Texas Water Development Board, Report B5911.
- Ashworth, J. B., and Hopkins, J., 1995, Aquifers of Texas: Austin, Texas Water Development Board Report 345, 69 p.
- Ayers, W. B., Jr., and Lewis, A. H., 1985, The Wilcox Group and Carrizo Sand (Paleogene) in East-Central Texas: depositional systems and deep-basin lignite: The University of Texas at Austin, Bureau of Economic Geology, 19 p. + 30 pl.
- Baker, B., Duffin, G., Flores, R., and Lynch, T., 1990, Evaluation of water resources in part of Central Texas: Texas Water Development Board, Report R319.

- Barnes, V. E., compiler, 1992, Geologic map of Texas: The University of Texas at Austin, Bureau of Economic Geology, 4 sheets.
- Bebout, D. G., Weise, B. R., Gregory, A. R., and Edwards, M. B., 1982, Wilcox Sandstone reservoirs in the deep subsurface along the Texas Gulf Coast: their potential for production of geopressured geothermal energy: The University of Texas at Austin, Bureau of Economic Geology Report of Investigations No. 117, 125 p.
- Bethke, C. M., 1986, Inverse hydrologic analysis of the distribution and origin of Gulf Coast-type geopressured zones: *Journal of Geophysical Research*, v. 91, no. B6, p. 6535–6545.
- Brill, J. P. and Beggs, H. D., 1974, Two-phase flow in pipes: The Hague, University of Tulsa INTERCOMP Course.
- Bureau of Economic Geology, 1992, Geology of Texas: The University of Texas at Austin, page-sized map.
- Chiang, W. H., and Kinzelbach, W., 2001, 3D-Groundwater modeling with PMWIN: a simulation system for modeling groundwater flow and pollution: New York: Springer, 346 p.
- Collins, E. W., 1995, Structural framework of the Edwards aquifer, Balcones Fault Zone, Central Texas: *Gulf Coast Association of Geological Societies Transactions*, v. 45, p. 135–142.
- Collins, E. W., Hovorka, S. D., and Laubach, S. E., 1992, Fracture systems of the Austin Chalk, North-Central Texas, *in* Schmoker, W., Coalson, E. B., and Brown, C. A., eds.,

- Geological studies relevant to horizontal drilling: examples from western North America: Rocky Mountain Association of Geologists, p. 129–142.
- Collins, E. W., and Laubach, S. E., 1990, Faults and fractures in the Balcones fault zone, Austin region, central Texas: Austin Geological Society, Guidebook 13, 34 p.
- Cronin, J. G., and Wilson, C. A., 1967, Ground water in the flood-plain alluvium of the Brazos River, Whitney Dam to vicinity of Richmond, Texas: Austin, Texas Water Development Board, Report R041, 206 p.
- Dillard, J. W., 1963, Availability and quality of ground water in Smith County: Texas Water Development Board, Report B6302.
- Domenico, P. A., and Schwartz, F. W., 1990, Physical and chemical hydrogeology: New York, John Wiley, 824 p.
- Duffin, G., 1991, Evaluation of water resources in Bell, Burnet, Travis, Williamson and parts of adjacent counties, Texas: Texas Water Development Board, Report R326.
- Dutton, A. R., 1982, Hydrochemistry of the unsaturated zone at Big Brown lignite mine, East Texas: The University of Texas at Austin, Master's Thesis, 259 p.
- ____ 1985, Brackish water in unsaturated confining beds at a Texas lignite mine: Ground Water, v. 23, no. 1, p. 42–51.
- ____ 1990, Vadose-zone recharge and weathering in an Eocene sand deposit, East Texas, U.S.A.: Journal of Hydrology, v. 114, p. 93–108.

- ____ 1999, Groundwater availability in the Carrizo–Wilcox aquifer in Central Texas—numerical simulations of 2000 through 2050 withdrawal projections: The University of Texas at Austin, Bureau of Economic Geology Report of Investigations No. 256., 53 p.
- Dutton, A. R., Harden, R. W., and Kier, K. S., 2002, Convergence between hydro pressured and geopressed zones in the Wilcox Group, Central Texas Gulf Coast: Gulf Coast Association of Geological Societies Transactions 2002, v. 52.
- Ewing, T. E., 1990, Tectonic map of Texas: The University of Texas at Austin, Bureau of Economic Geology, scale 1:750:000.
- Fisher, W. L., and McGowen, J. H., 1967, Depositional systems in the Wilcox Group of Texas and their relationship to occurrence of oil and gas: Gulf Coast Association of Geological Societies Transactions, v. 17, p. 105–125.
- Fogg, G. E., Kaiser, W. R., and Ambrose, M. L., 1991, The Wilcox Group and Carrizo Sand (Paleogene) in the Sabine Uplift area, Texas: ground-water hydraulics and hydrochemistry: The University of Texas at Austin, Bureau of Economic Geology, 70 p. + 19 pls.
- Fogg, G. E., and Kreitler, C. W., 1982, Ground-water hydraulics and hydrochemical facies in Eocene aquifers of the East Texas Basin: The University of Texas at Austin, Bureau of Economic Geology Report of Investigations No. 127, 75 p.
- Fogg, G. E., Seni, S. J., and Kreitler, C. W., 1983, Three-dimensional ground-water modeling in depositional systems, Wilcox Group, Oakwood salt dome area, East Texas:

The University of Texas at Austin, Bureau of Economic Geology Report of Investigations No. 133, 55 p.

Folk, R. L., 1968, Petrology of sedimentary rocks: Austin, Hemphill Publishing Company, 182 p.

Follett, C. R., 1966, Ground-water resources of Caldwell County, Texas: Texas Water Development Board, Report R012.

____ 1970, Ground-water resources of Bastrop County, Texas: Texas Water Development Board, Report R109, 138 p.

____ 1974, Ground-water resources of Brazos and Burleson Counties, Texas: Texas Water Development Board, Report 185, 194 p.

Foster, M. D., 1950, The origin of high sodium bicarbonate waters in the Atlantic and Gulf Coastal Plains: *Geochimica et Cosmochimica Acta*, v. 1, p. 33–48.

Galloway, W. E., Ewing, T. E., Garrett, C. M., Tyler, Noel, and Bebout, D. G., 1983, Atlas of major Texas oil reservoirs: The University of Texas at Austin, Bureau of Economic Geology, 139 p.

Guyton and Associates, 1970, Ground-water conditions in Angelina and Nacogdoches Counties, Texas: Texas Water Development Board, Report R110.

____ 1972, Ground-water conditions in Anderson, Cherokee, Freestone, and Henderson Counties, Texas: Texas Water Development Board, Report R105.

- Hall, S. A., 1990, Channel trenching and climatic change in the southern U.S. Great Plains: *Geology*, v. 18, p. 342–345.
- Hamlin, H. S., 1988, Depositional and ground-water flow systems of the Carrizo-Upper Wilcox, South Texas: The University of Texas at Austin, Bureau of Economic Geology Report of Investigations No. 175, 61 p.
- Harbaugh, A. W., and McDonald, M. G., 1996, User's documentation for MODFLOW-96, an update to the U.S. Geological Survey modular finite-difference ground-water flow model: U.S. Geological Survey Open-File Report 96-485, 56 p.
- Harrison, W. J., and Summa, L. L., 1991, Paleohydrology of the Gulf of Mexico basin: *American Journal of Science*, v. 291, no. 2, p. 109-176.
- Hatcher, R. D., 1995, *Structural geology, principles, concepts, and problems*, 2nd edition: Prentice Hall, Inc., 525 p.
- HDR Engineering, 1998, Trans-Texas Water Program, north central study area, phase II report, volume 1, integrated water supply plans: variously paginated.
- Henry, C. D., and Basciano, J. M., 1979, Environmental geology of the Wilcox Group lignite belt, East Texas: The University of Texas at Austin, Bureau of Economic Geology Report of Investigations No. 98, 28 p.
- Henry, C. D., Basciano, J. M., and Deux, T. W., 1979, Hydrology and water quality of the Eocene Wilcox Group: significance for the lignite development in East Texas: *Gulf Coast Association of Geological Societies Transactions*, v. 29, p. 127–135.

- Hosman, R. L., and Weiss, J. S., 1991, Geohydrologic units of the Mississippi Embayment and Texas coastal uplands aquifer systems, south-central United States: U.S. Geological Survey Professional Paper 1416-B.
- Hovorka, S. D., and Dutton, A. R., 2001, Aquifers of Texas: The University of Texas at Austin, Bureau of Economic Geology, page-sized map.
- Hsieh, P. A., and Freckleton, J. R., 1993, Documentation of a computer program to simulate horizontal-flow barriers using the U.S. Geological Survey's modular three-dimensional finite-difference ground-water flow model: U.S. Geological Survey Open-File Report 92-477, 38 p.
- Intera and Parsons Engineering Science, 2002a, Groundwater availability model for the northern Carrizo–Wilcox aquifer: Draft report prepared for Texas Water Development Board, September, variously paginated.
- _____ 2002b, Groundwater availability model for the southern Carrizo–Wilcox aquifer: Draft report prepared for Texas Water Development Board, September, variously paginated.
- Jackson, M. P. A., 1982, Fault tectonics of the East Texas Basin: The University of Texas at Austin, Bureau of Economic Geology Geological Circular 84-2, 31 p.
- Jones, P. H., 1975, Geothermal and hydrocarbon regimes, northern Gulf of Mexico Basin, *in* Dorfman, M. H., and Deller, R. W., eds., Proceedings, First Geopressed Geothermal Energy Conference, June 2–4, Austin, Center for Energy Studies: The University of Texas at Austin, p. 15–89.

Kaiser, W. R., 1978, Depositional system in the Wilcox Group (Eocene) of east-central Texas and the occurrence of lignite, *in* Kaiser, W. R., ed., Proceedings, 1976 Gulf Coast Lignite Conference: geology, utilization, and environmental aspects: The University of Texas at Austin, Bureau of Economic Geology Report of Investigations No. 90, 276 p.

____ 1990, The Wilcox Group (Paleocene-Eocene) in the Sabine Uplift area, Texas: depositional systems and deep-basin lignite: The University of Texas at Austin, Bureau of Economic Geology, Special Publication, 20 p.

Konikow, L. F., 1986, Predictive accuracy of a ground-water model—lessons from a postaudit: *Ground Water*, v. 24, no. 2, p. 173–184.

Kosters, E. C., Bebout, D. G., Seni, S. J., Garrett, C. M., Brown, L. F., Jr., Hamlin, H. S., Dutton, S. P., Ruppel, S. C., Finley, R. J., and Tyler, Noel, 1989, Atlas of major Texas gas reservoirs: The University of Texas at Austin, Bureau of Economic Geology, 161 p.

Kuiper, L. K., 1985, Documentation of a numerical code for the simulation of variable density ground-water flow in three dimensions: U.S. Geological Survey, Water-Resources Investigations Report 84-4302.

Land, L. S., and Macpherson, G. L., 1992, Origin of saline formation waters, Cenozoic section, Gulf of Mexico sedimentary basin: *American Association of Petroleum Geologists Bulletin*, v. 76, no. 9, p. 1344–1362.

Larkin, T. J., and Bomar, G. W., 1983, Climatic atlas of Texas: Austin, Texas, Department of Water Resources, Report LP-192, 151 p.

Lasser, Inc., 2000, Texas production database: Digital CD-ROM.

Loucks, R. G., Dodge, M. M., and Galloway, W. E., 1986, Controls on porosity and permeability in lower Tertiary sandstones along the Texas Gulf Coast: The University of Texas at Austin, Bureau of Economic Geology Report of Investigations No. 149, 78 p.

Mace, R. E., Chowdhury, A. H., Anaya, Roberto, and Way, Shao-Chih (Ted), 2000a, Groundwater availability of the Trinity Aquifer, Hill Country, Texas: numerical simulations through 2050: Texas Water Development Board Report 353, 117 p.

Mace, R. E., Mullican, W. F., III, and Way, Ted (Shao-Chih), 2000b, Estimating groundwater availability in Texas, *in* Proceedings, 1st Annual Texas Rural Water Association and Texas Water Conservation Association Water Law Seminar: water allocation in Texas: the legal issues, Austin, Texas, January 25–26, 2001, Section 1, 16 p.

Mace, R. E., Smyth, R. C., Xu, L., and Liang, J., 2000c, Transmissivity, hydraulic conductivity and storativity of the Carrizo–Wilcox aquifer in Texas, The University of Texas at Austin, Bureau of Economic Geology, final report submitted to the Texas Water Development Board, 76 p.

McGowen, J. H., Proctor, C. V., Jr., Haenggi, W. T., Reaser, D. F., and Barnes, V. E., 1972, Dallas sheet: The University of Texas at Austin, Bureau of Economic Geology, scale 1:250,000.

- Morton, R. A., and Land, L. S., 1987, Regional variations in formation water chemistry, Frio Formation (Oligocene), Texas Gulf Coast: American Association of Petroleum Geologists Bulletin, v. 71, no. 9, p. 191–206.
- Murray, G. E., 1961, Geology of the Atlantic and Gulf Coast Province of North America: New York, Harper Brothers, 692 p.
- Nance, H. S., Laubach, S. E., and Dutton, A. R., 1994, Fault and joint measurements in Austin Chalk, Superconducting and Super Collider Site, Texas: Gulf Coast Association of Geological Societies Transactions, v. 44, p. 521–532.
- Neuzil, C. E., 1994, How permeable are clays and shales?: Water Resources Research, v. 30, no. 2, p. 145–150.
- Parker, C. A., 1974, Geopressures and secondary porosity in the deep Jurassic of Mississippi: Gulf Coast Association of Geological Societies Transactions, v. 24, p. 69–80.
- Peckham, R. C., 1965, Availability and quality of ground water in Leon County: Texas Water Development Board, Report B6513.
- Piper, A. M., 1944, A graphic procedure in the geochemical interpretation of water analyses: American Geophysical Union, Transactions, v. 25, p. 914–923.
- Proctor, C. V., Jr., Brown, T. E., McGowen, J. H., Waechter, N. B., and Barnes, V. E., 1974, Austin sheet: The University of Texas at Austin, Bureau of Economic Geology, scale 1:250,000.

- Proctor, C. V., Jr., Brown, T. E., Waechter, N. B. Aronow, S., and Barnes, V. E., 1974, Seguin sheet: The University of Texas at Austin, Bureau of Economic Geology, scale 1:250,000.
- Proctor, C. V., Jr., McGowen, J. H., Haenggi, W. T., and V. E. Barnes, 1970, Waco sheet: The University of Texas at Austin, Bureau of Economic Geology, scale 1:250,000.
- Rettman, P. L., 1987, Ground-water resources of Limestone County, Texas: Texas Water Development Board, Report R299.
- Rogers, L. T., 1967, Availability and quality of ground water in Fayette County, Texas: Texas Water Development Board, Report R056, 134 p.
- Ryder, P. D., 1988, Hydrogeology and predevelopment flow in the Texas Gulf Coast aquifer systems: U.S. Geological Survey, Water-Resources Investigations Report 87-4248, 109 p.
- Ryder, P. D., and Ardis, A. F., 1991, Hydrology of the Texas Gulf Coast aquifer systems: U.S. Geological Survey Open-File Report 91-64, 147 p.
- Salvador, A., 1991, Chapter 14: Origin and development of the Gulf of Mexico basin, *in* Salvador, A., ed., The Gulf of Mexico Basin: The Geological Society of America, The Geology of North America, vol. J, p. 53–72.
- Sandeen, W. M., 1987, Ground-water resources of Rusk County, Texas: Texas Water Development Board, Report R297.

- Scanlon, B., Dutton, A. R., and Sophocleos, M., 2002, Groundwater recharge in Texas:
<http://www.twdb.state.tx.us/gam/resources/RechRept.pdf>.
- Shafer, G. H., 1965, Ground-water resources of Gonzales County, Texas: Texas Water Development Board, Report R004.
- ____ 1966, Ground-water resources of Guadalupe County, Texas: Texas Water Development Board, Report R019.
- ____ 1974, Ground-water resources of Brazos and Burleson Counties, Texas: Texas Water Development Board, Report R185.
- Shelby, C. A., Pieper, M. K., Wright, A. C., Eargle, D. H., and Barnes, V. E., 1968, Palestine sheet: The University of Texas at Austin, Bureau of Economic Geology, scale 1:250,000.
- Slade, R. M., Jr., Bentley, J. T., and Michaud, D., 2002, Results of streamflow gain-loss studies in Texas with emphasis on gains from and losses to major and minor aquifers, Texas, 2000: U.S. Geological Survey Open File Report 02-068.
- Srinivasan, R., and Arnold, J. G., 1994, Integration of basin-scale water quality model with GIS: Water Resources Bulletin, AWRA, v. 30, no. 3, p. 453–462.
- Tarver, G. R., 1966, Ground-water resources of Houston County, Texas: Texas Water Development Board, Report R018.
- ____ 1968, Ground-water resources of Polk County, Texas: Texas Water Development Board, Report R082.

Texas Water Development Board, 2002, Water for Texas—2002: Document No. GP-7-1, 156 p.

Thompson, G. L., 1966, Ground-water resources of Lee County, Texas: Texas Water Development Board, Report R020.

____ 1972, Ground-water resources of Navarro County, Texas: Texas Water Development Board, Report R160.

Thorkildsen, D., and Price, R. D., 1991, Ground-water resources of the Carrizo–Wilcox aquifer in the Central Texas region: Texas Water Development Board, Report 332, 73 p.

Thorkildsen D., Quincy, R., and Preston, R., 1989, A digital model of the Carrizo–Wilcox aquifer within the Colorado River Basin of Texas: Texas Water Development Board, Report LP-208, 67 p.

Tóth, J., 1978, Cross-formational gravity flow of groundwater: A mechanism of the transport and accumulation of petroleum (The generalized hydraulic theory of petroleum migration): American Association of Petroleum Geologists, Studies in Geology, p. 121–167.

Wahl, T. L., 2001, BFI Version 4.12, A computer program for computing an index to base flow: U.S. Geological Survey.

Wermund, E. G., 1996a, Physiography of Texas: The University of Texas at Austin, Bureau of Economic Geology, 1 pl.

- Wermund, E. G., 1996b, River basin map of Texas: The University of Texas at Austin, Bureau of Economic Geology, 1 pl.
- White, D. E., 1973, Ground-water resources of Rains and Van Zandt Counties, Texas: Texas Water Development Board, Report R169.
- Williamson, A. K., Grubb, H. F., and Weiss, J. S., 1990, Ground-water flow in the Gulf Coast aquifer systems, South Central United States—A preliminary analysis: U.S. Geological Survey, Water-Resources Investigations Report 89-4071.
- Wilson, C. A., 1967, Ground-water resources of Austin and Waller Counties, Texas: Texas Water Development Board, Report R068.
- Xue, L., 1994, Genetic stratigraphic sequences and depositional systems of the lower and middle Wilcox strata, Texas Gulf Coast Basin: The University of Texas at Austin, Ph.D. dissertation, 202 p.
- Xue, L., and Galloway, W. E., 1995, High-resolution depositional framework of the Paleocene middle Wilcox strata, Texas coastal plain: American Association of Petroleum Geologists Bulletin, v. 79, no. 2, p. 205–230.

APPENDIX A

COLLECTION AND ANALYSIS OF ENVIRONMENTAL TRACERS FOR ESTIMATION OF RECHARGE RATES IN THE GAM MODEL OF THE CENTRAL CARRIZO-WILCOX AQUIFER

by

Robert C. Reedy, Bridget R. Scanlon, and Alan R. Dutton
Bureau of Economic Geology

Site Description

The study area is in the outcrop area of the Simsboro Formation in the central part of the Carrizo-Wilcox aquifer (fig. A-1). The Simsboro Formation generally consists of coarse-grained sediments, and recharge studies focused on this unit because recharge rates were expected to be higher in this than in other units of the Wilcox Group. The topography consists of rolling hills with relief of about 100 to 200 ft. The groundwater depth was not known a priori because very few wells in the Texas Water Development Board database were located in this unit. The regional climate is subtropical humid (Larkin and Bomar, 1983). Long-term (50 yr) mean annual precipitation in the central part of the Carrizo-Wilcox aquifer ranges from 29 inches in the southwest to 48 inches in the northeast of the modeled area.

METHODS

Theory

Environmental Tracers

Chloride

Chloride in the unsaturated zone or groundwater has been widely used to estimate recharge (Allison and Hughes, 1978; Scanlon, 1991; 2000; Phillips, 1994). Chloride in precipitation and dry fallout is transported into the unsaturated zone with infiltrating water. Chloride concentrations increase through the root zone as a result of evapotranspiration because chloride is nonvolatile and is not removed by evaporation or by plant transpiration.

Below the root zone chloride concentrations should remain constant if recharge rates have not varied over time. Qualitative estimates of relative recharge rates can be estimated using chloride concentrations if precipitation and dry fallout are the only sources of chloride to the subsurface. Chloride concentrations are inversely related to recharge rates: low chloride concentrations indicate high recharge rates because chloride is flushed out of the system, whereas high chloride concentrations indicate low recharge rates because chloride accumulates as a result of evapotranspiration. Quantitative estimates of recharge can also be calculated using the chloride mass balance approach, which balances chloride input (precipitation and dry fallout, P) times the chloride concentration in precipitation (C_p) with chloride output (recharge rate times chloride concentration in the unsaturated zone pore water or groundwater (C_{uz} or C_{gw})):

$$PC_p = RC_{uz} = RC_{gw} \quad R = \frac{PC_p}{C_{uz}} = \frac{PC_p}{C_{gw}} \quad (1)$$

The age of the pore water at any depth in the unsaturated zone can also be estimated by dividing the cumulative mass of chloride from the surface to the depth of interest by the chloride input. There are many assumptions associated with the chloride mass balance approach: one-dimensional, vertically downward, piston water movement, no surface runoff, and no subsurface sources or sinks of chloride. The validity of these assumptions is difficult to determine; however, the sandy soils in the Simsboro Formation should result in predominantly piston flow and negligible runoff. This coarse-grained unit is expected to have no connate water from original marine deposition of these sediments; however, this assumption would not be valid for the low-permeability units in the Carrizo-Wilcox aquifer, such as the Hooper and Calvert Bluff Formations.

The chloride input to the system was estimated from chloride deposition in precipitation from the National Atmospheric Deposition Program (NADP, <http://nadp.sws.uiuc.edu/>). Data from seven stations in the immediate vicinity of the study area were interpolated. Chloride concentrations reported by the NADP represent wet precipitation and do not include any dry deposition. To account for dry deposition, chloride concentrations from NADP were increased by a factor of two, which was suggested Izbicki (personal communication, 2001). Because the uncertainties in the CMB approach are greater than the spatial variability in

chloride input, an average value of chloride input (0.9 mg/L) was used for the entire study area. An average value of precipitation (37.4 inches) was also used in the analysis.

Tritium

Historical tracers or event markers, such as bomb-pulse tritium (^3H), have been used widely in the past to estimate recharge (Egboka and others, 1983; Robertson and Cherry, 1989). Tritium is used to trace water movement because it is part of the water molecule. Tritium is a radioactive isotope of hydrogen with a half-life of 12.32 yr. Tritium occurs naturally in the atmosphere and enters the subsurface primarily through precipitation. Tritium fallout increased as a result of atmospheric nuclear testing that began in the early 1950s and peaked in 1963 (fig. A-2). The presence of bomb-pulse tritium in groundwater indicates that a component of the groundwater is young ($< \sim 50$ yr old). Bomb-pulse ^3H concentrations have been greatly reduced as a result of radioactive decay; therefore, the use of ^3H to date groundwater is generally being replaced by the use of tritium/helium-3 ($^3\text{H}/^3\text{He}$). Tritium decays to the noble gas helium-3. Tritium and tritiogenic helium-3 combined behave as a nondecaying tracer, and the ratio of ^3He to ^3H can be used to estimate the age of the groundwater (age being defined as the time since water entered the saturated zone):

$$t = -\frac{1}{\lambda} \ln \left[1 + \frac{^3\text{He}_{\text{trit}}}{^3\text{H}} \right] \quad (2)$$

where λ is the decay constant ($\ln 2/t^{1/2}$; 0.05626), $t^{1/2}$ is the ^3H half-life (12.32 yr), and $^3\text{He}_{\text{trit}}$ is tritiogenic ^3He . Use of this equation assumes that the system is closed (does not allow ^3He to escape) and is characterized by piston flow (no hydrodynamic dispersion). The age of the water at the sampling point can then be used to determine the water velocity from the water table to the midpoint of the well screen depth. The recharge rate can then be calculated by dividing the velocity by the average porosity of the sediments.

Field and Laboratory Methods

Water Content and Chloride

Boreholes were installed primarily in open fields that the landowners claimed had been cleared for at least 40 yr. Seven boreholes were drilled in outcrop areas of the Carrizo-Wilcox aquifer in Bastrop, Lee, Robertson, and Freestone Counties (fig. A-1,

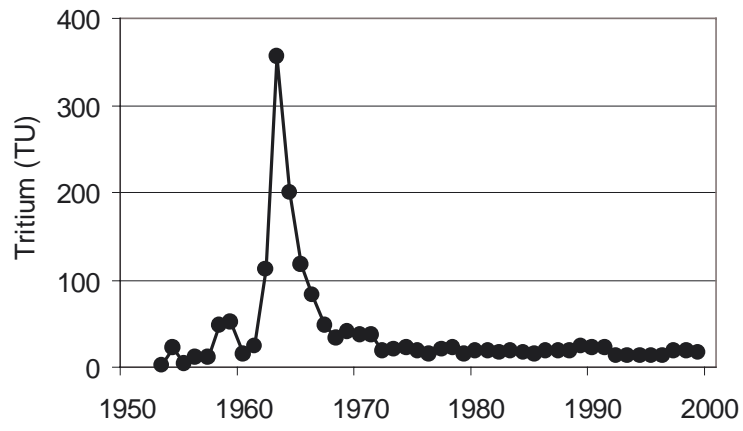


Figure A-2. Average annual atmospheric tritium fallout for Ottawa, Ontario.

table A-1). The boreholes were drilled with a hollow-stem auger without any drilling fluid, and samples were collected with a split spoon. Sediment samples were collected for laboratory measurement of water content and chloride concentrations. Gravimetric water content was measured in the laboratory by oven drying samples at 105°C for 24 to 72 hr. To determine chloride content, double-deionized water was added to the dried sediment sample in a 1:1 ratio by weight. Samples were agitated on a reciprocal shaker for 4 hr. The supernatant was centrifuged and filtered through 0.45- μ m filters. Chloride was analyzed by ion chromatography (detection limit 0.1 mg/L) at the New Mexico Bureau of Mines. Chloride concentrations are expressed as mg Cl per L of pore water.

Tritium and Tritium/Helium

Groundwater samples were collected from all seven wells for tritium analysis and from three wells for tritium/helium analysis. The samples for tritium analysis were collected through the drill stem and stored in 1-L bottles with polyseal caps. These samples were sent to the University of Miami Tritium Laboratory (<http://www.rsmas.miami.edu>) for tritium analysis using gas proportional counting with enrichment. Selection of the three wells for tritium/helium analysis was based on relatively shallow depths to unconfined groundwater (<50 ft). Wells were completed for tritium/helium sampling by inserting PVC pipe (2-inch ID) inside the drill stem, with screen lengths varying from 0.75 to 1.5 ft at the well bottom. The drill stem was pulled back to the surface and 20/40-sieve sand was packed around the well screens. The well annulus was backfilled to above the water table with cuttings, and a 5-ft-thick bentonite grout plug was installed. A 10-inch ID PVC pipe section 8 ft long was installed over the well pipe, and cuttings were backfilled to the ground surface. The ground surface around the wellhead was covered with a plywood plate, mounded with cuttings, and caps were installed on both the well and the outer protective PVC pipes. Well development was accomplished by surge-pumping until there was no visible sediment in the produced water. Water samples were pumped to the surface using a submersible pump (Redi-Flo 2, Grundfos Pumps Corp., Olathe, KS) that was connected to 3/16-inch ID plastic tubing. Flow rates ranged from approximately 0.2 to more than 2 gallons per minute during sampling. Approximately three well-bore volumes of water were produced prior to sample collection. Water samples for helium analysis were collected in copper tubes (3/8-inch ID),

Table A-1. Location of sampled boreholes, property owners, dates drilled, borehole depth, static water level below land surface (bls), and number of chloride samples collected in the unsaturated zone.

Borehole	County	Latitude	Longitude	Date drilled	Elevation (ft)	Total depth (ft bls)	Static water level (ft bls)	No. of Cl samples
CW-1	Bastrop	30.2917	-97.3056	2/6/2002	495	103.8	74.80	37
CW-2	Lee	30.3872	-97.2911	3/4/2002	578	53.3	43.25	30
CW-3	Freestone	31.6892	-96.2917	3/5/2002	505	53.7	41.30	28
CW-4	Freestone	31.8006	-96.2139	3/6/2002	400	38.8	24.80	26
CW-5	Freestone	31.8389	-96.1992	3/7/2002	395	18.5	10.50	15
CW-6	Robertson	31.1850	-96.6503	3/8/2002	485	48.6	37.35	25
CW-7	Robertson	31.1689	-96.6281	3/9/2002	485	78.5	76.70	33

with a down-stream valve used to apply back pressure on the pump to ensure that dissolved gases remained under pressure in the sample. Finally the copper tubes were sealed at both ends with refrigeration clamps while under pressure. A total of four samples, each containing approximately 18 mL, were collected at each site.

Helium concentrations in the samples were measured at the University of Utah. Water vapor and CO₂ were removed initially at -95°C and -195°C, respectively. Then N₂ and O₂ were removed by reaction with Zr-Al alloy, and Ar and Ne were adsorbed onto activated charcoal at -195°C and at -233°C, respectively. Helium isotope ratios (³He/⁴He) and concentrations were analyzed on a VG 5400 rare-gas mass spectrometer. ³He/⁴He ratios are reported relative to the atmospheric ratio (R_{air}) using air helium as the absolute standard.

RESULTS

Water Content and Chloride Concentrations

The average water content in each of the profiles was not highly variable and ranged from 0.13 to 0.18 g/g (fig. A-3, table A-2). Minimum water contents ranged from 0.04 to 0.08 g/g. Maximum water contents ranged from 0.22 to 0.40 g/g and indicate that in some areas the sediments were close to saturation. Although the texture of the sediments was not analyzed in the laboratory, spatial variability in water content could be qualitatively related to variations in texture from core descriptions. Water contents were highest near the water table in most profiles.

Average chloride concentrations in the unsaturated zone ranged from 23 to 519 mg/L (fig. A-3, table A-2). Variability in mean chloride concentrations was high locally, as shown by differences in mean concentrations in CW1 and CW2 and in CW3, CW4, and CW5. Chloride concentrations were also highly variable within each profile as shown by differences in maximum and minimum concentrations (table A-2). There was no systematic variation in chloride concentrations with depth. Recharge rates were calculated for the portion of the profiles that generally represented the last 50 yr where possible. In some cases recharge rates were so low that a 50-yr section corresponded to a very narrow depth interval.

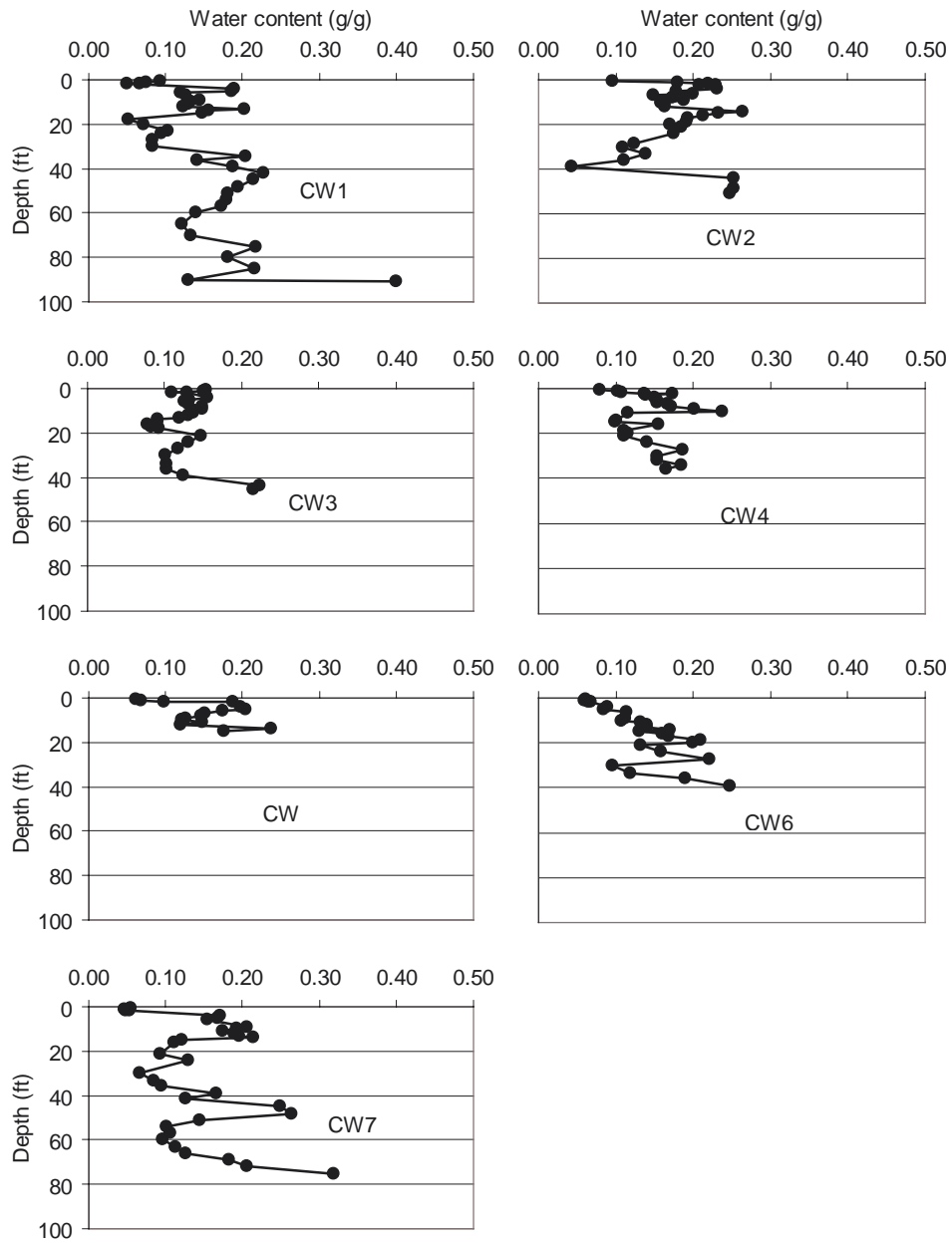


Figure A-3. Water content (weight basis) with depth.

Table A-2. Water content, chloride concentration, and recharge (rech) based on unsaturated zone (uz) chloride concentrations, chloride concentrations in groundwater (gw) and associated recharge rates, and age of the chloride profile.

BH no.	Water content uz (g/g)			Chloride uz (mg/L)			Rec (uz)	Cl (gw)	Rech (gw)	Age base
	mean	min.	max.	mean	min.	max.	(in/yr)	(mg/L)	(in./yr)	(yr)
CW-1	0.21	0.08	0.34	245	10	1907	0.79	180	0.20	2815
CW-2	0.18	0.04	0.26	23	11	37	1.42	25	1.34	110
CW-3	0.13	0.08	0.22	35	12	125	1.02	5	6.22	112
CW-4	0.14	0.08	0.24	259	51	1131	0.24	32	1.06	846
CW-5	0.15	0.06	0.24	325	145	684	0.20	22	1.54	360
CW-6	0.13	0.06	0.25	239	72	560	0.20	33	1.02	700
CW-7	0.14	0.05	0.32	518	52	2206	0.20	107	0.31	2480

Recharge rates generally ranged from 0.2 to 1.4 inch/yr. The time required for chloride to accumulate in each profile ranged from 110 to 2,815 yr.

Groundwater chloride concentrations were generally lower than those in the unsaturated zone (5 to 180 mg/L) (tables A-2, A-3). Recharge rates based on the chloride mass balance approach ranged from 0.2 to 6.2 inches/yr. Recharge rates based on groundwater chloride were generally higher than those based on unsaturated zone chloride (CW3-CW6). In some cases; however, the recharge rates from the two data sets were similar (CW2, CW7). The lower recharge rate calculated for CW1 may not be representative of recharge in this area because groundwater was confined in this well. In addition, the low recharge rate for CW7 may reflect additional chloride from connate water because clay content was high in this borehole. The higher recharge rate at CW3 may represent focused recharge from ponded conditions because water was ponded in the vicinity of the borehole during drilling. Therefore, representative recharge rates based on groundwater chloride concentrations range from 1 to 1.5 inch/yr. The generally higher recharge rates based on groundwater chloride relative to unsaturated zone chloride are considered more representative of the regional system, whereas the unsaturated-zone data indicate that locally recharge rates are lower. Preferential flow may also result in lower chloride concentrations in the groundwater relative to the unsaturated zone.

Groundwater Tritium and Tritium/Helium

Groundwater tritium concentrations ranged from 0.76 to 3.57 TU (table A-4). These tritium levels were much greater than the detection limit for tritium (~ 0.2 TU) and indicate that a component of the water was recharged in the last 50 yr. Tritium/helium was also used to date the water in wells CW3, CW4, and CW6. There were problems with analysis of ^3He in water samples from CW6. ^3He concentrations were low in well CW3 and much higher in well CW4. The low ^3He concentrations in CW3 indicate a short residence time of the water of 2.2 yr, whereas the much higher ^3He concentrations in CW4 indicate a residence time of 21.4 yr. The times represent the time of ^3He accumulation since it was isolated from the unsaturated zone. Water velocities were calculated by dividing the distance between the water table and the center of the well screen by the age of the water and resulted in

Table A-3. Water content and chloride concentrations in soil samples from boreholes CW1-CW7.

Depth (ft)	Water content (g/g)	Chloride (mg Cl/kg soil)	Chloride (mg Cl/L water)	Depth (ft)	Water content (g/g)	Chloride (mg Cl/kg soil)	Chloride (mg Cl/L water)
CW1				CW2			
0.5	0.09	1.90	20.33	0.5	0.10	2.10	21.94
1.0	0.07	1.00	13.38	1.0	0.18	2.90	16.17
1.5	0.07	1.30	19.76	1.5	0.22	3.40	15.46
2.0	0.05	1.00	19.86	2.0	0.21	3.20	15.46
4.0	0.19	5.70	30.15	2.5	0.23	2.63	11.41
5.0	0.19	1.80	9.70	4.0	0.23	4.56	19.76
6.0	0.12	5.29	44.32	5.0	0.18	4.82	27.00
7.0	0.13	8.63	68.32	6.0	0.20	5.11	25.54
9.0	0.15	7.00	48.28	7.0	0.15	4.51	30.42
10.0	0.13	4.01	30.10	8.0	0.17	4.70	27.18
11.0	0.13	4.32	33.15	9.0	0.19	4.60	24.54
12.0	0.12	4.81	39.02	10.0	0.16	4.34	27.35
13.0	0.20	5.20	25.65	11.0	0.16	4.39	26.99
14.0	0.16	11.01	70.69	12.0	0.16	4.80	29.28
15.0	0.15	11.01	74.15	14.0	0.26	6.30	23.85
18.0	0.05	3.10	61.02	15.0	0.23	6.88	29.52
20.0	0.07	3.20	44.41	16.0	0.21	5.50	25.88
23.0	0.10	3.94	38.01	17.0	0.19	4.00	20.72
24.0	0.09	4.10	43.46	19.0	0.19	2.92	15.24
27.0	0.08	3.50	41.83	20.0	0.17	3.20	18.78
30.0	0.08	6.10	73.74	21.0	0.18	4.00	21.73
34.5	0.20	37.00	180.91	24.0	0.18	3.62	20.59
36.0	0.14	10.00	70.98	28.3	0.12	3.30	26.67
39.0	0.19	24.00	128.27	30.0	0.11	2.83	26.00
42.0	0.23	29.98	131.29	33.3	0.14	3.31	23.93
45.0	0.21	13.00	60.68	36.0	0.11	2.80	25.42
48.0	0.20	66.19	339.42	39.0	0.04	0.53	12.24
51.0	0.18	154.76	854.09	44.0	0.25	4.93	19.51
54.0	0.18	294.71	1649.57	48.3	0.25	6.29	24.99
57.0	0.17	329.80	1906.69	51.0	0.25	9.25	37.34
60.0	0.14	130.12	929.65				
65.0	0.12	59.07	489.77				
70.0	0.13	67.06	502.48				
75.0	0.22	60.16	277.50				
80.0	0.18	64.98	359.86				
85.0	0.22	31.02	143.89				
90.0	0.13	27.04	207.76				

Table A-3 (continued). Water content and chloride concentrations in soil samples from boreholes CW1-CW7.

Depth (ft)	Water content (g/g)	Chloride (mg Cl/kg soil)	Chloride (mg Cl/L water)	Depth (ft)	Water content (g/g)	Chloride (mg Cl/kg soil)	Chloride (mg Cl/L water)
CW3				CW4			
0.5	0.15	1.82	11.83	0.5	0.08	17.62	221.78
1.0	0.15	5.41	35.92	1.0	0.10	18.70	184.11
1.5	0.11	1.61	14.76	1.5	0.11	20.53	191.51
2.0	0.13	2.40	18.62	2.0	0.14	17.51	127.81
4.0	0.16	4.09	26.24	2.5	0.17	17.94	103.86
5.0	0.13	4.53	34.33	3.0	0.14	25.82	185.20
6.0	0.13	3.88	30.86	4.0	0.15	28.53	189.35
7.0	0.13	3.44	26.40	5.0	0.15	16.24	105.51
8.0	0.15	4.78	32.08	6.0	0.15	27.39	178.61
9.0	0.15	4.01	27.03	7.0	0.17	21.06	126.68
10.0	0.14	4.10	30.15	8.0	0.17	23.20	134.59
11.0	0.14	4.16	30.16	9.0	0.20	29.83	148.30
12.0	0.13	4.00	30.43	10.0	0.24	12.22	51.48
13.0	0.12	4.70	39.30	11.0	0.12	22.39	192.89
14.0	0.09	3.12	34.20	14.0	0.10	10.96	109.11
15.0	0.09	2.90	31.92	15.0	0.10	21.06	211.24
16.0	0.08	2.86	36.68	16.0	0.16	18.03	116.10
17.0	0.08	3.38	41.08	19.0	0.11	19.13	174.31
18.0	0.09	4.10	44.30	20.0	0.12	22.59	196.36
21.0	0.15	5.22	35.22	21.0	0.11	90.24	814.25
24.0	0.13	4.12	31.41	24.0	0.14	157.71	1130.63
27.0	0.12	5.31	44.89	27.0	0.19	74.99	401.65
30.0	0.10	5.57	55.00	30.0	0.15	47.06	307.55
33.7	0.10	3.90	37.87	32.1	0.15	72.01	471.45
36.0	0.10	4.40	42.69	34.0	0.18	47.73	258.85
39.0	0.12	15.50	124.72	36.0	0.16	66.81	405.76
43.7	0.22	4.37	19.58				
45.5	0.21	2.81	13.10				
CW5				CW6			
0.5	30.10	32.32	522.16	0.5	0.06	34.28	559.51
1.0	32.42	17.47	254.34	1.0	0.06	20.03	334.21
1.5	30.66	19.32	196.47	1.5	0.06	17.12	266.52
2.0	32.15	37.94	202.70	1.9	0.07	14.78	218.53
4.0	30.71	28.74	144.88	4.0	0.09	10.16	114.76
5.0	30.52	68.59	336.05	5.0	0.08	28.76	344.56
6.0	30.55	119.84	683.88	6.0	0.11	31.74	279.91
7.0	29.98	86.04	569.48	9.0	0.11	18.58	164.38
8.0	31.10	55.67	382.62	10.0	0.11	30.66	284.84
9.0	30.06	52.15	412.04	11.0	0.13	24.93	188.30
10.0	30.19	24.86	206.03	12.0	0.14	24.89	176.96

Table A-3 (continued). Water content and chloride concentrations in soil samples from boreholes CW1-CW7.

Depth (ft)	Water content (g/g)	Chloride (mg Cl/kg soil)	Chloride (mg Cl/L water)	Depth (ft)	Water content (g/g)	Chloride (mg Cl/kg soil)	Chloride (mg Cl/L water)
CW5				CW6			
11.0	30.16	32.44	219.27	13.0	0.14	20.02	143.09
12.0	29.98	39.36	329.65	14.0	0.17	12.34	72.48
14.0	30.06	46.36	195.36	15.0	0.13	17.62	134.98
15.0	30.08	37.94	214.79	16.0	0.16	24.48	153.71
				17.0	0.17	26.68	158.20
				19.0	0.21	25.24	120.20
				20.0	0.20	29.61	148.56
				21.0	0.13	28.71	216.90
				24.0	0.16	31.72	201.20
				27.0	0.22	39.70	179.09
				30.0	0.10	36.43	379.23
				33.6	0.12	53.83	452.71
				36.0	0.19	57.81	303.81
				39.0	0.25	92.91	375.35
CW7							
0.5	0.06	34.28	559.51				
1.0	0.06	20.03	334.21				
1.5	0.06	17.12	266.52				
1.9	0.07	14.78	218.53				
4.0	0.09	10.16	114.76				
5.0	0.08	28.76	344.56				
6.0	0.11	31.74	279.91				
9.0	0.11	18.58	164.38				
10.0	0.11	30.66	284.84				
11.0	0.13	24.93	188.30				
12.0	0.14	24.89	176.96				
13.0	0.14	20.02	143.09				
14.0	0.17	12.34	72.48				
15.0	0.13	17.62	134.98				
16.0	0.16	24.48	153.71				
17.0	0.17	26.68	158.20				
19.0	0.21	25.24	120.20				
20.0	0.20	29.61	148.56				
21.0	0.13	28.71	216.90				
24.0	0.16	31.72	201.20				
27.0	0.22	39.70	179.09				
30.0	0.10	36.43	379.23				
33.6	0.12	53.83	452.71				
36.0	0.19	57.81	303.81				
39.0	0.25	92.91	375.35				

Table A-4. Results of ^3He , ^4He , ^{20}Ne , ^{40}Ar , and N_2 measurements, and calculated tritogenic helium-3 ($^3\text{He}^*$) and $^3\text{H}/^3\text{He}$ ages.

BH no.	^3H (TU)	^3H error (2σ TU)	R/Ra [†]	^4He cc STP/g [‡]	^{20}Ne cc STP/g	^{40}Ar cc STP/g	N_2 cc STP/g	$^3\text{He}^*$ TU	Age (yr)
CW-1	0.76	0.18							
CW-2	3.25	0.22							
CW-3	3.3	0.22	1.072	4.41E-08	1.99E-07	4.72E-04	0.0150	0.4	2.2
CW-4	3.57	0.24	1.072	9.35E-08	2.97E-07	7.04E-04	0.0251	21.4	34.5
CW-5	2.43	0.2							
CW-6	3.05	0.2	0.986	5.80E-08	2.59E-07	5.66E-04	0.0184	-7.1	
CW-7	1.1	0.18							

[†] R is the $^3\text{H}/^4\text{He}$ ratio of the sample; Ra is the $^3\text{H}/^4\text{He}$ ratio of the air standard

[‡] STP Standard temperature and pressure

^3H error reported as two standard deviations (2σ)

velocities of 0.4 (CW4) to 4 ft/yr (CW3). Recharge rates of 1.6 (CW4) to 16.7 inches/yr (CW3) were calculated by multiplying the velocities by the average porosity of 0.35. The recharge rate for CW4 of 1.6 inch/yr is similar to that estimated from the groundwater chloride concentration. The recharge rate for CW3 of 16.7 inches/yr is higher than that estimated from groundwater chloride concentration of 6.2 inches/yr.

DISCUSSION

The results of this study indicate that there is no systematic variation in recharge rates spatially. There was more variability locally in one area than there was between different areas. Recharge rates based on groundwater chloride ranged from 0.2 to 1.3 inch/yr in the southern zone and from 0.3 to 1.2 inch/yr in the northern zone. The low recharge rates in the southern and northern sampling areas may be related to confined conditions because these boreholes were deeper and overlain by clay-rich sediments relative to nearby boreholes.

Groundwater chloride concentrations seem to provide the most reliable recharge estimates and indicate that the average recharge rate ranges from about 1 to 1.5 inch/yr. The high recharge rate estimated for well CW-3 may be related to additional inputs of chloride from ponded water at the surface in nearby regions. Recharge rates based on unsaturated-zone chloride concentrations were generally lower than those estimated from groundwater chloride. This discrepancy in recharge rates may result from groundwater chloride not representing vertical recharge from the land surface in the area immediately overlying the well and generally lower recharge rates in the sampled unsaturated zones.

REFERENCES

- Allison, G. B., and Hughes, M. W., 1978, The use of environmental chloride and tritium to estimate total recharge to an unconfined aquifer: *Australian Journal of Soil Resources*, v. 16, p. 181–195.
- Egboka, B. C. E., Cherry, J. A., Farvolden, R. N., and Frind, E. O., 1983, Migration of contaminants in groundwater at a landfill: a case study. 3. Tritium as an indicator of dispersion and recharge: *Journal of Hydrology*, v. 63, p. 51–80.

- Larkin, T. J., and Bomar, G. W., 1983, Climatic atlas of Texas: Austin, Texas, Department of Water Resources, Report LP-192, 151 p.
- Phillips, F. M., 1994, Environmental tracers for water movement in desert soils of the American Southwest: Soil Science Society of America Journal, v. 58, p. 14–24.
- Robertson, W. D., and Cherry, J. A., 1989, Tritium as an indicator of recharge and dispersion in a groundwater system in Central Ontario: Water Resources Research, v. 25, p. 1097–1109.
- Scanlon, B. R., 1991, Evaluation of moisture flux from chloride data in desert soils: Journal of Hydrology, v. 128, p. 137–156.
- _____ 2000, Uncertainties in estimating water fluxes and residence times using environmental tracers in an arid unsaturated zone: Water Resources Research, v. 36, p. 395–40.

APPENDIX B

Surface Water–Groundwater Interaction in the Central Carrizo-Wilcox Aquifer

by
David O'Rourke and Ken Choffel
HDR Engineering Services, Inc.

B-1.0 Introduction

Herein we present the approach and findings of a study on the interaction between surface water and groundwater (SW/GW) in the central Carrizo-Wilcox aquifer and the simulation of this interaction in the Groundwater Availability Model (GAM). The geographic scope of this investigation focuses on the aquifer between the San Antonio River and the Trinity River. Rivers and streams were represented using the Stream Package of MODFLOW, while lakes and reservoirs were represented using the Reservoir Package of MODFLOW.

The following creeks and rivers were represented in the model (fig. B-1):

- San Antonio River
- Cibolo Creek
- Guadalupe River
- San Marcos River
- Plum Creek
- Cedar Creek
- Colorado River
- Big Sandy Creek
- Middle Yegua Creek
- East Yegua Creek
- Little River
- Brazos River
- Little Brazos River
- Walnut Creek
- Duck Creek
- Steele Creek
- Navasota River
- Big Creek
- Upper Keechi Creek
- Tehuacana Creek
- Trinity River

The following lakes and reservoirs were also represented in the model (fig. B-1):

- Braunig Lake
- Calaveras Lake
- Lake Bastrop
- Alcoa Lake
- Twin Oaks Reservoir
- Lake Limestone
- Richland-Chambers Reservoir
- Fairfield Lake
- Cedar Creek Reservoir

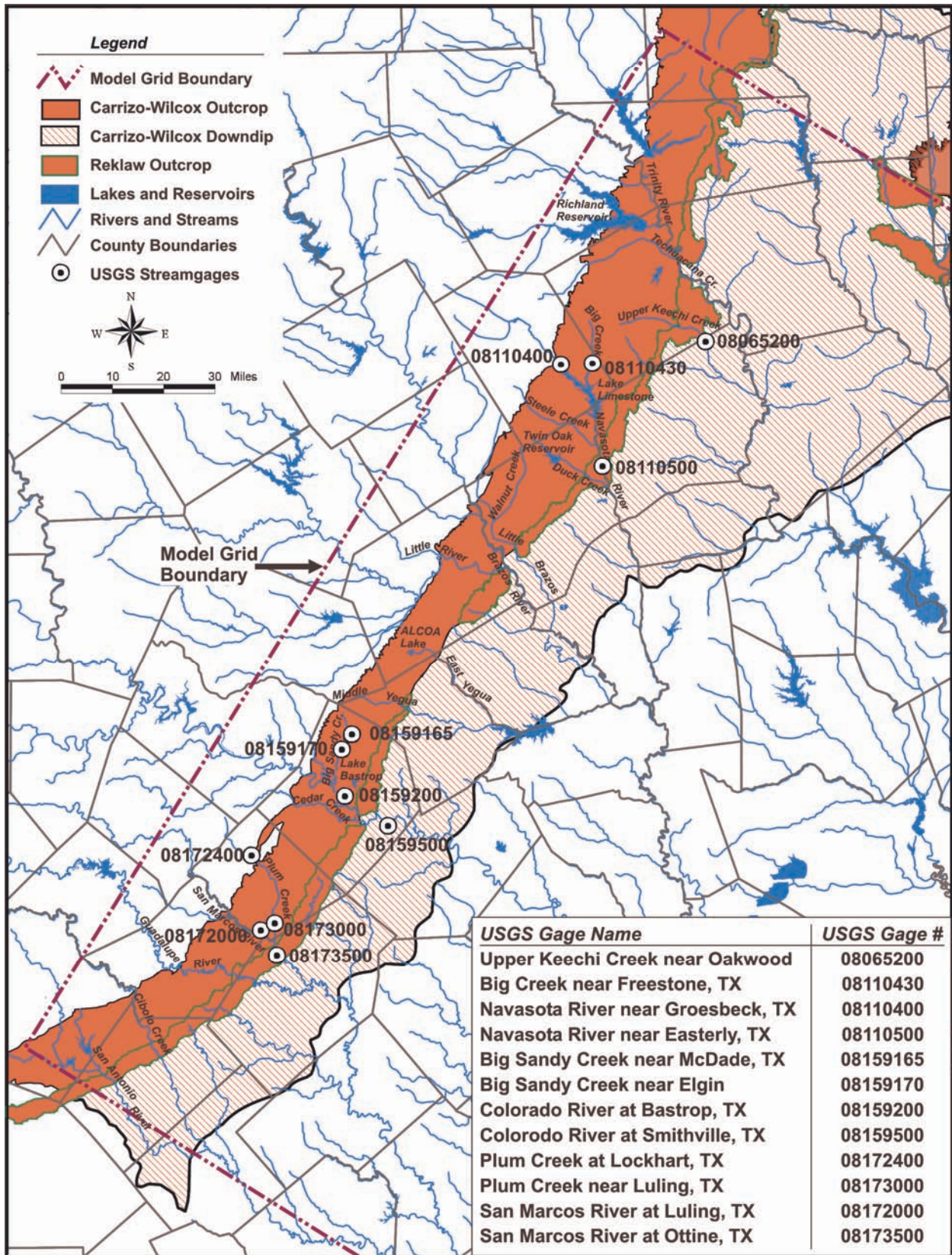


Figure B-1. Central Carrizo GAM surface-water feature.

There are two primary goals of this investigation. The first is to compile physical data and to calculate parameters for all streams and reservoirs simulated and to incorporate these data and parameters into the model framework. The second is to estimate calibration/verification targets for SW/GW interaction within the model domain for use from 1980 through 2000. The methodology for these analyses is described in the following sections.

B-2.0 Surface Water-Groundwater Interaction

B-2.1 Physical Processes and Measurement

Streams and aquifers interact on the aquifer's outcrop. If the water table is above the streambed and slopes toward the stream, the stream is receiving groundwater from the aquifer and is called a gaining reach (i.e., it gains flow as it moves through the reach). If the water table is below the streambed and slopes away from the stream, the stream is losing water to the aquifer and is called a losing reach. In some cases, streams have an intermittent base flow, which is usually associated with wet winter conditions and dry, hot summer conditions. For large rivers such as the Colorado, Brazos, and Trinity, there are significant alluvium deposits that buffer the stream from direct connection with the regional aquifer. (The Brazos Alluvium is significant enough to be classified as one of the minor aquifers of the state.) Because of the regional scale of the GAM and because insufficient data were available to quantify the interaction between the Carrizo-Wilcox and the alluvium, the system was modeled as having direct interaction between the Carrizo-Wilcox and the stream.

As the Carrizo-Wilcox aquifer dips below the land surface and becomes confined, it loses the potential to interact with surface water; thus, all significant interaction occurs in the outcrop. We therefore represented streams only in the outcrop cells of the model, and data for consideration in the analysis were limited to sources located on or near the aquifer outcrop.

Results were applied to both gaged and ungaged watersheds in the outcrop cells of the model to develop targets for the model calibration.

Reservoirs also have a significant impact on the local groundwater regime. As reservoirs are filled, impounded water leaks into the underlying geologic formations until equilibrium between the reservoir water level and the surrounding water table is achieved.

B-2.2 MODFLOW Representation of SW/GW Interaction

Both the stream package and the reservoir package in MODFLOW use similar algorithms to simulate interaction between groundwater and surface water. For a given model cell, a surface-water elevation is assigned to the stream or reservoir, and this water level is compared with the calculated head in the aquifer. If the water level in the stream or reservoir is greater than the head in the aquifer, water will flow from the surface-water body into the aquifer as a function of the conductance of the bed sediments and the difference in heads. If the head in the aquifer is greater than the water level of the surface-water body, water will flow from the aquifer to the stream (fig. B-2). The quantity of flow in either direction is calculated by

$$Q=C*dh \tag{1}$$

where Q = discharge (L^3/T), C is conductance of streambed or reservoir sediments (L^2/T), and dh is difference in head between the surface water and groundwater (L). Conductance is a lumped parameter calculated by

$$C=KLW/M \tag{2}$$

where K is hydraulic conductivity (L/T), L is length of stream (or reservoir) reach in grid cell (L), W is width of stream (or reservoir) reach in grid cell (L), and M is thickness of streambed or reservoir sediments (L).

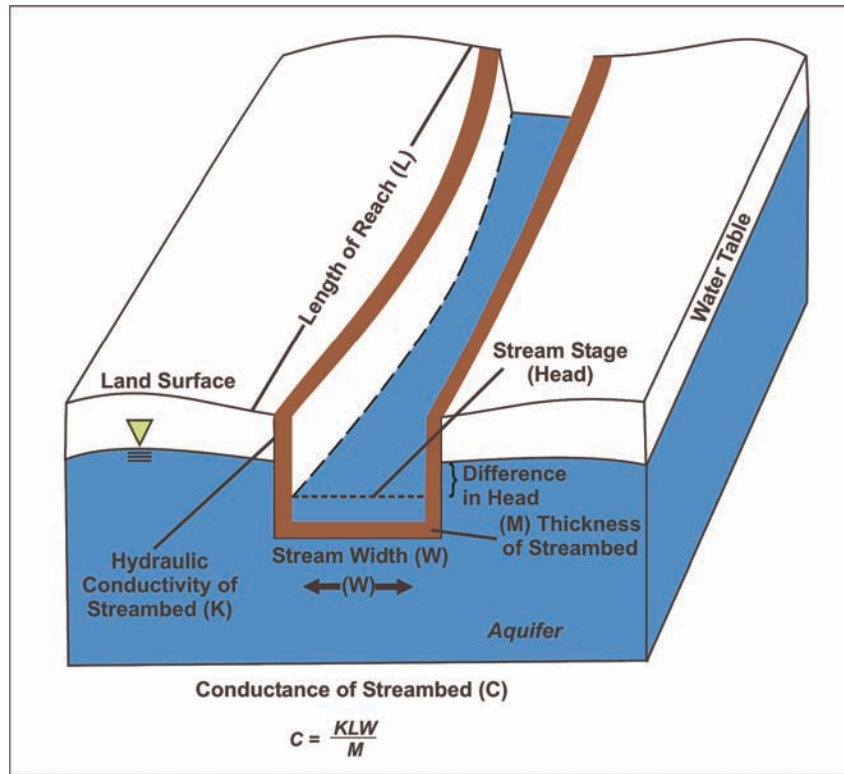


Figure B-2. MODFLOW representation of surface-water-groundwater interaction.

These parameters were assigned as follows. Length of individual stream reaches in each grid cell was measured on 1:24,000-scale USGS Topographic Quadrangle maps using an ArcView utility. Width was estimated using several methods. For major rivers, published USGS data on river width at gaging stations (Slade, 2002) was referenced; an average of the widths from the nearest upstream and downstream gages was used throughout the outcrop reach. For smaller streams, in which the width varied significantly throughout the reach, widths were increased from a few feet in the headwaters to a few tens of feet at the downstream end. Hydraulic conductivity and streambed thickness were initially estimated at 1 ft/d and 1 ft, respectively; however, it was anticipated that conductance values would be adjusted during calibration.

For reservoir simulation, any grid cell with more than half the cell area covered by surface water in TWDB GIS coverage was represented in the Reservoir Package. Reservoir representation assumes that the entire grid cell is subject to inundation (i.e., no partial inundation is simulated), so the length and width of reservoir cells default to the full dimensions of the grid cell. Average land-surface elevations were derived from topographic maps, while average water surface in the reservoirs was obtained from USGS hydrologic records.

B-3.0 Methods to Estimate Interaction of Surface Water and Groundwater

Two methods were employed to characterize SW/GW interaction in the model domain. In the first, details of historical low flow studies conducted on any streams across the Carrizo-Wilcox aquifer within the model domain were reviewed. In the second, data from stream gages located on the outcrop were analyzed using techniques of base-flow separation to obtain quantitative estimates of groundwater discharge to the streams.

B-3.1 Low-Flow Studies

The first method of investigation into Carrizo-Wilcox groundwater–surface-water interaction was to examine historical low-flow studies that had been conducted by the USGS or other agencies on rivers or streams that crossed the outcrop of the Carrizo-Wilcox aquifer. Low-flow studies involve performing flow measurements at many locations on a stream within a short period of time, when flows are low and no significant surface runoff is occurring in the study reach. One low-flow study was conducted on the Colorado River in 1918. Low-flow studies were conducted on Cibolo Creek in 1949, 1963, and 1968. Although, in most cases, the specific locations of the outcrop boundaries were not identified in the original data, comparison of recorded river mile data with known landmarks allowed identification of the approximate boundaries of the aquifer outcrop in these studies.

Figures B-3 and B-4 depict the results of these low-flow studies. In all four studies, the flow increased as the stream crossed the aquifer outcrop, indicating gaining conditions at the time the studies were performed.

In the 1918 Colorado River study, the flow increased from about 61 to 97 cfs across the aquifer outcrop, an increase of 36 cfs (fig. B-3a). The flow at the Smithville gage during this study was 101 cfs. For comparison with historical flows, a flow-duration curve was generated for daily flows at the Smithville station (fig. B-3b), and the flow of 101 cfs is exceeded 99.9 percent of the time (in fact, only 16 daily flows out of 17,573 were lower than 101 cfs). This figure indicates that even during conditions of extremely low flow, the Colorado River is still a gaining reach across the outcrop of the Carrizo-Wilcox aquifer. The flow increase documented in the 1918 study may be compared with the results obtained from the model to estimate the low end of

**1918 USGS Colorado River Low Flow Investigation
Flow Measurements Across Carrizo-Wilcox and Reklaw Outcrops**

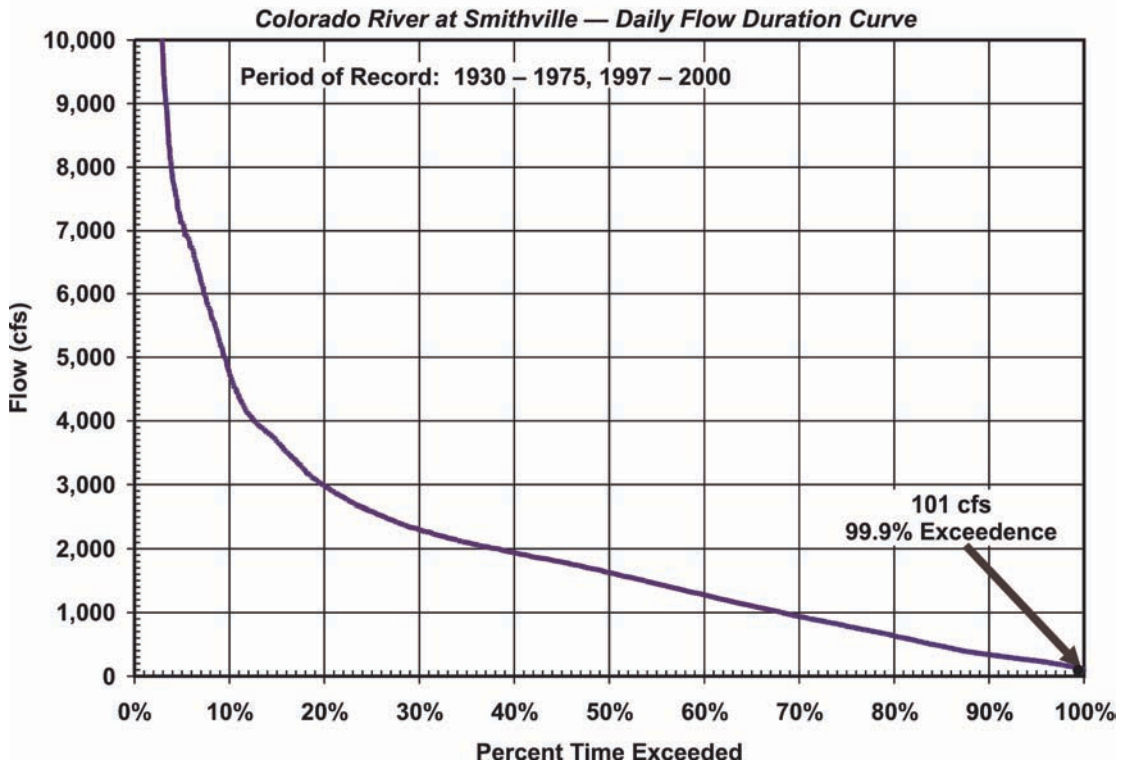
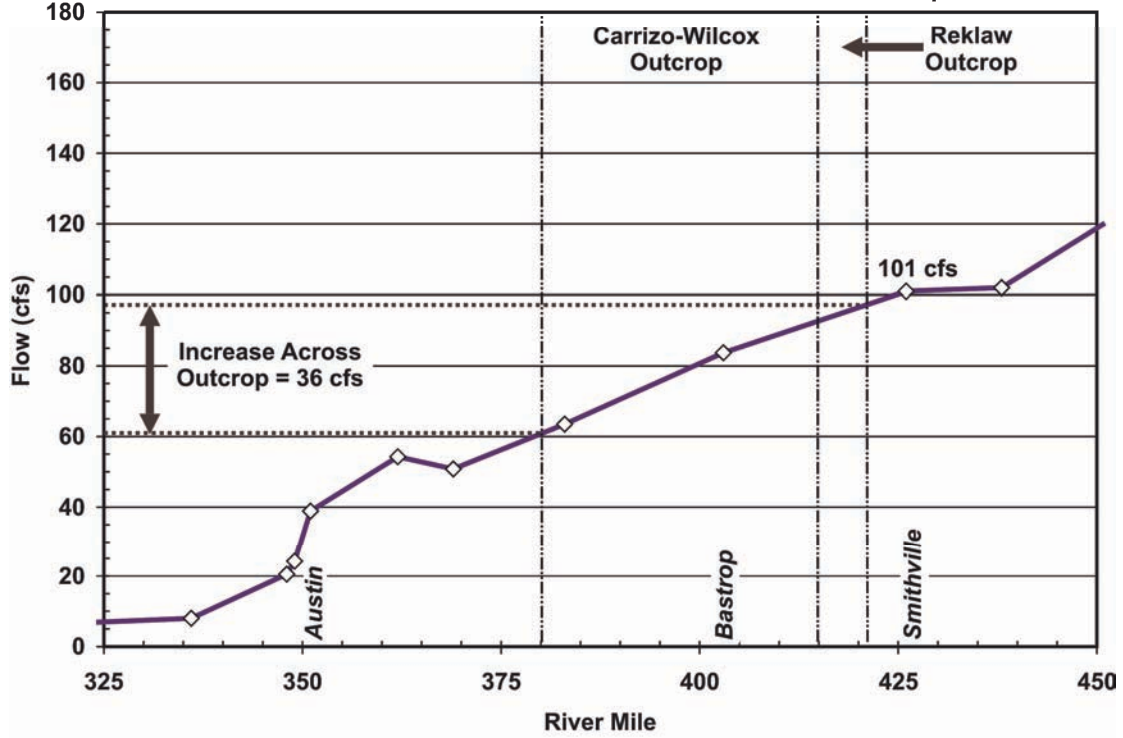
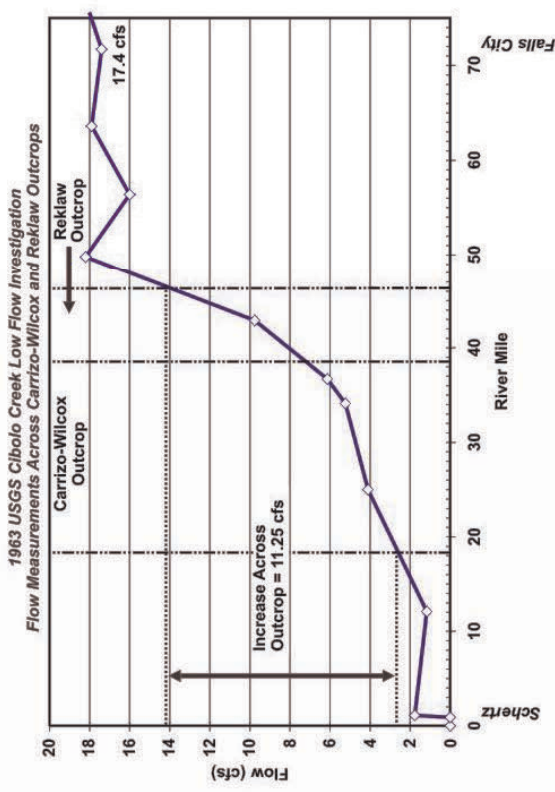
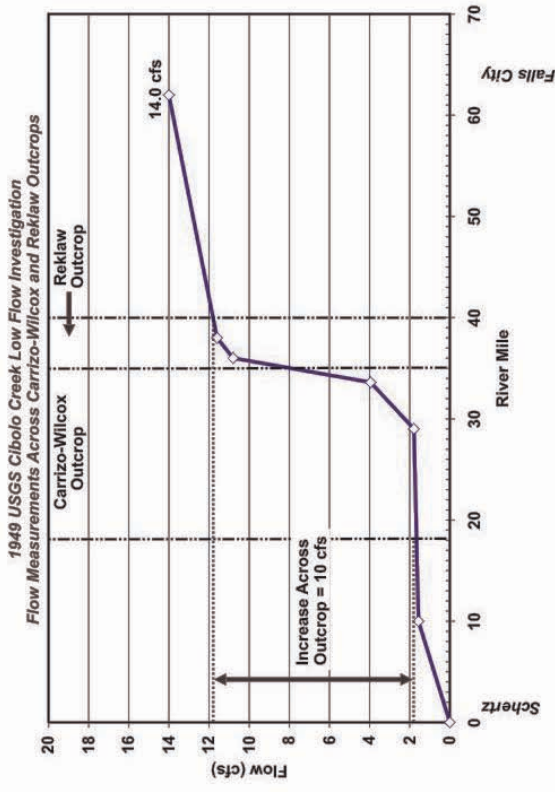


Figure B-3. Colorado River low-flow investigation.



Note: Variation between studies in Schertz – Falls City river distance reflects original data.

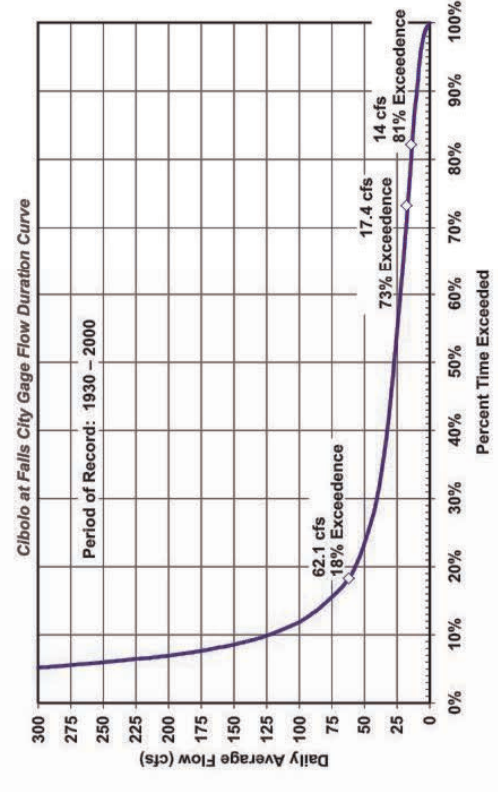
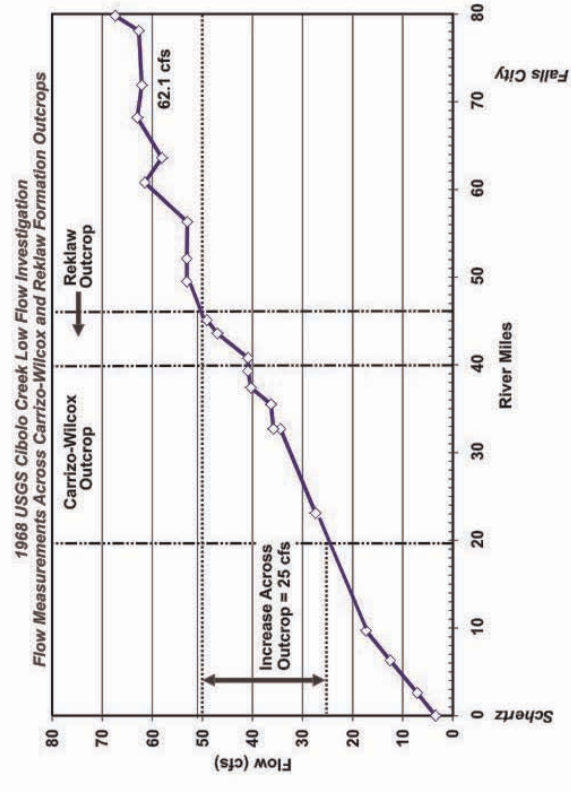


Figure B-4. Cibolo Creek Low Flow Investigations

groundwater discharge in the Colorado River across the outcrop (i.e., few, if any, modeled aquifer discharge quantities should be less than this value).

In the Cibolo Creek studies, the flow increases across the outcrop were about 10 cfs (0.38 cfs/mi) in the 1949 study (fig. B-4a), 11.25 cfs (0.5 cfs/mi) in the 1963 study (fig. B-4b), and 25 cfs (1 cfs/mi) in the 1968 study (fig. B-4c). Examination of a daily-flow duration curve generated for the Falls City stream gage (fig. B-4d) indicates that these studies spanned a wide range of flow conditions. For example, in the 1949 study, flow at Falls City was 14.0 cfs, a daily value that is exceeded 81 percent of the time, indicating fairly low-flow conditions. By contrast, in the 1968 study, flow at Falls City was 62.1 cfs, a daily value that is exceeded only 18 percent of the time, indicating relatively higher flow conditions. Therefore, Cibolo Creek is consistently gaining on the outcrop over this wide range of flow conditions. Although no studies exist during extreme low-flow conditions (as on the Colorado), these data indicate that Cibolo Creek may be expected to be a gaining reach during most conditions, and the specific quantities of discharge from the aquifer to the stream documented in these studies may be compared to the results obtained from the model on Cibolo Creek to check for consistency.

B-3.2 Base-Flow Studies

The portion of a stream's flow that is not directly influenced by runoff is considered to be its base flow. Unlike other water-budget components such as pumping, it is a cumulative result from a diffuse source over all the bed and banks of the stream in the watershed. It is therefore not directly measurable. Base flow is determined using graphical techniques for separation of base flow from the total stream flow. For this project, base-flow separation was performed on daily

flow data using the Base Flow Index (BFI) program, jointly maintained by the USGS and U.S. Bureau of Reclamation (Wahl and Wahl, 2001). BFI uses the Standard Hydrologic Institute Method for base-flow separation; this method identifies sudden rises in the hydrograph typical of storm-induced runoff and separates the total stream flow into daily time series of base flow and storm flow for each gage. Figure B-5 presents an example of this process on data from Big Sandy Creek at McDade. It is important to note that this is an approximate method and that for any given day the program may under- or overpredict base flow, although the long-term accuracy of the method is commonly accepted.

In order to quantify the amount of groundwater discharge provided to streams by the Carrizo-Wilcox aquifer in the model domain, the following methodology was used. Stream-flow records were reviewed to determine all gages historically located on or near the aquifer outcrop. These data were narrowed to identify any combination of stream gages that specifically bracketed flow on the Carrizo-Wilcox outcrop. By isolating stream reaches located entirely on the outcrop, the influence of hydrologic factors external to the base flow from the Carrizo aquifer was minimized. Outcrop-specific stream reaches may be defined using one of three types of gage arrangements, as depicted in the schematic drawings in figure B-6. In Type 1, only one gage is necessary for a headwater watershed located on the outcrop (a, fig. B-6) (i.e., all of the contributing watershed area is above a single gage and is located on the outcrop, as in the case of Big Creek near Freestone and Upper Keechi Creek near Oakwood). In Type 2, two gages on the same stream may define an outcrop reach (b, fig. B-6) if both gages are located near the outcrop boundaries and all or most of the intervening drainage area is located on the outcrop, as in the case of Navasota River, Big Sandy Creek, and Plum Creek. Finally, in Type 3, three gages may

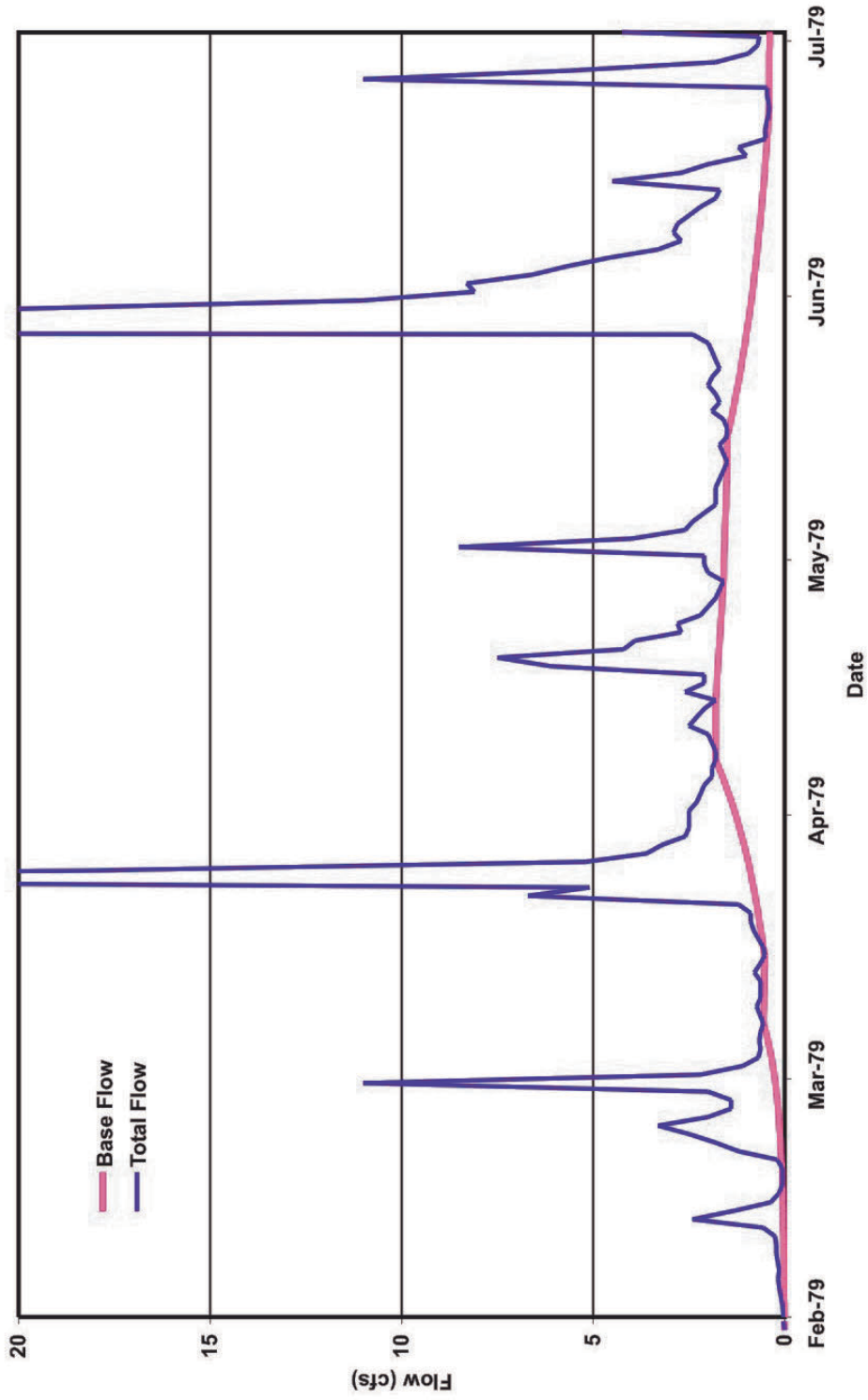


Figure B-5. Baseflow Separation — Big Sandy Creek near McDade, TX

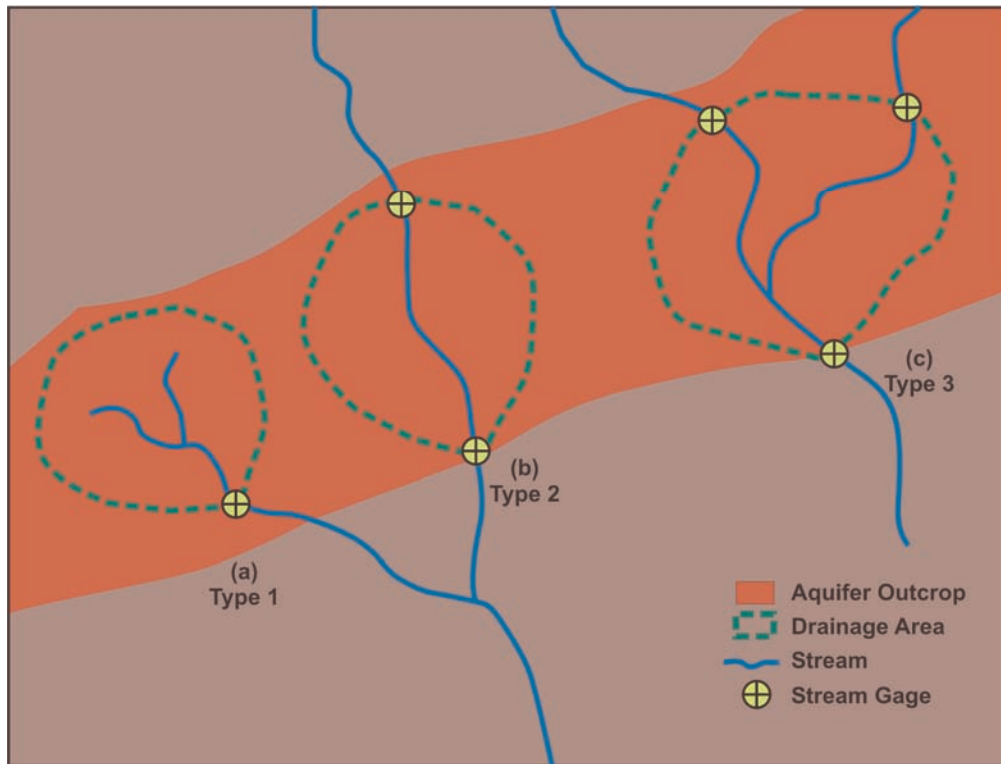


Figure B-6. Schematic stream-gage configurations for estimating base flow.

be used (c, fig. B-6) if all three reaches of a stream confluence are gaged, as in the case of the San Marcos River/Plum Creek confluence.

The stream gages used to define the study reaches are summarized in table B-1, and presented in figure B-1. The study reaches identified that meet the previously described criteria to estimate base-flow gains and losses on the Carrizo-Wilcox outcrop are presented in table B-2.

A brief description of the unique aspects of each reach and its associated gages analyzed within the framework of this investigation follows.

- Upper Keechi Creek (Type 1). Gage #08065200: Upper Keechi near Oakwood, TX. Period of record May 1962–September 2000. This reach has its headwater drainage located entirely on the outcrops of the Carrizo-Wilcox and Reklaw Formations. It is an intermittent stream. The gage is located near the downstream extent of the Reklaw Formation.
- Big Creek (Type 1). Gage #08110430: Big Creek near Freestone, TX. This reach has its headwaters on the Carrizo-Wilcox outcrop and is an intermittent stream. This gage was established to monitor inflows into Lake Limestone from Big Creek.
- Navasota River (Type 2). Upstream Gage #08110400: Navasota River near Groesbeck, TX. Downstream gage #08110500: Navasota River near Easterly, TX. The Easterly gage is located near the downstream edge of the Reklaw Formation. The Groesbeck gage is located near the upstream extent of the aquifer. It was discontinued and moved farther upstream in 1979 in association with the construction of the dam that created Lake Limestone.

Table B-1. Stream-gage summary.

<i>USGS gage name</i>	<i>USGS gage number</i>	<i>Drainage area (mi²)</i>	<i>Gage datum (fsl)</i>	<i>Period of record</i>
Upper Keechi Ck near Oakwood, TX	08065200	150	240.11	5/1/62-9/30/01
Big Ck near Freestone, TX	08110430	97	362.94	7/1/78-9/30/00
Navasota Rv near Groesbeck, TX	08110400	311	358.84	3/1/65-4/30/79
Navasota Rv near Easterly, TX	08110500	968	271.46	4/1/24-9/30/00
Big Sandy Ck near McDade TX	08159165	39	422	7/13/1979-9/30/85
Big Sandy Ck near Elgin, TX	08159170	64	392	7/12/79-9/30/85
Colorado Rv at Bastrop, TX	08159200	28576	307.38	3/1/60-9/30/00
Colorado Rv at Smithville, TX	08159500	28968	270.14	8/1/30-9/24/75, 10/6/97-9/30/00
Plum Ck at Lockhart, TX	08172400	112	431.19	5/1/59-9/30/01
Plum Ck near Luling, TX	08173000	309	321.27	4/1/30-9/30/01
San Marcos Rv at Luling, TX	08172000	838	322.05	5/1/39-9/30/01
San Marcos Rv at Ottine, TX	08173500	1249	285.20	7/1/15-1/31/43

Table B-2. Stream reaches used in base-flow study.

<i>Reach name</i>	<i>Reach type</i>	<i>USGS gage number</i>		<i>Outcrop in drainage area (mi²)</i>	<i>Common period of record</i>
		<i>Upstream</i>	<i>Downstream</i>		
Upper Keechi Creek	1	NA ¹	08065200	150	5/28/62-9/30/00
Big Creek	1	NA	08110430	97	7/1/78-9/30/00
Navasota River	2	08110400	08110500	566	3/1/65-4/30/79
Big Sandy above McDade	1	NA	08159165	64	7/13/1979-9/30/85
Big Sandy above Elgin	1	NA	08159170	39	7/13/1979-9/30/85
Colorado River	2	08159200	08159500	394	3/1/60-9/24/75, 10/6/97-9/30/00
Plum Creek	2	08172400	08173000	142	5/1/59-9/30/93
San Marcos River/Plum Creek	3	08173000 08172000	08173500	96	5/1/39-1/31/43

Notes: ¹NA = Not applicable. Type 1 reaches are headwaters defined by a single gage.

- Big Sandy Creek (Type 1). Upstream gage #08159165: Big Sandy Creek near Elgin, TX. Downstream gage #08159170: Big Sandy Creek near McDade, TX. These gages were temporarily operated from 1979 through 1985, or 6 years. Big Sandy Creek is an intermittent stream, located primarily on the Calvert Bluff Formation. For this study, each gage was considered independently as a Type 1 headwater gage to avoid inaccuracies associated with subtraction of daily rating-derived flow estimates.
- Colorado River (Type 2). Upstream gage #08159200: Colorado River at Bastrop, TX. Downstream gage #08159500: Colorado River at Smithville, TX. The Smithville gage is actually located slightly downstream from the top of the Reklaw Formation, which is in turn obscured by the Colorado River alluvial deposits. However, because of the close proximity of the gage to the outcrop edge and the connective effect of the alluvium, a simplifying assumption was made that the intervening drainage area was in the outcrop. These time-series data had the additional complicating factors of being influenced by major releases from the Highland Lakes for deliveries to rice farmers during the growing season, approximately March through September. Identifying and analyzing only periods of time when no reservoir releases were being made and no significant precipitation was occurring minimized the effect of these releases.
- Plum Creek (Type 2). Upstream gage #08172400 (Plum Creek at Lockhart, TX). Downstream gage #08173000 (Plum Creek near Luling, TX). Just downstream from the Lockhart gage, the stream passes over a small outcrop area that is part of the underlying Midway Formation then reenters the Carrizo-Wilcox outcrop. Plum Creek is an intermittent stream.

- San Marcos River (Type 3). Upstream gages #08172000 (San Marcos at Luling, TX) and #08173000 (Plum Creek near Luling, TX). Downstream gage #08173500 (San Marcos River at Ottine, TX). These three gages define a reach of the San Marcos River where it receives flow from Plum Creek, a major tributary on the outcrop of the Carrizo-Wilcox aquifer. Daily data exist for all three of these gages for approximately 3.5 yr.

Base-flow separation was performed on the data for all identified stream gages with common periods of record. The difference in base flow between the upstream and downstream gages is used as an estimate of the amount of groundwater discharge from the aquifer to the stream in the reach between the two gages. Data from Water Availability Models (WAM) prepared for the TNRCC were reviewed to identify any significant water rights or return flows located between the gages; accordingly, base-flow estimates were adjusted for the Colorado and Navasota Rivers, but in neither case was this adjustment significant when compared with the total base flow.

Once the quantification of base-flow change was completed for each of the seven stream reaches on the outcrop of the Carrizo-Wilcox aquifer, this discharge was then converted to unit values by dividing the base-flow change by the intervening drainage area on the outcrop between the gages. This calculation yielded a value of change in base flow per unit area (af/yr/mi²) of Carrizo-Wilcox outcrop drained. A summary of these data is presented in figure B-7. A flow duration curve was generated from the unit daily values, showing the percentage of time that each flow value was exceeded during the period of record. The flow duration curves for all seven study reaches are presented in figure B-8. Basic flow statistics, including maximum, minimum,

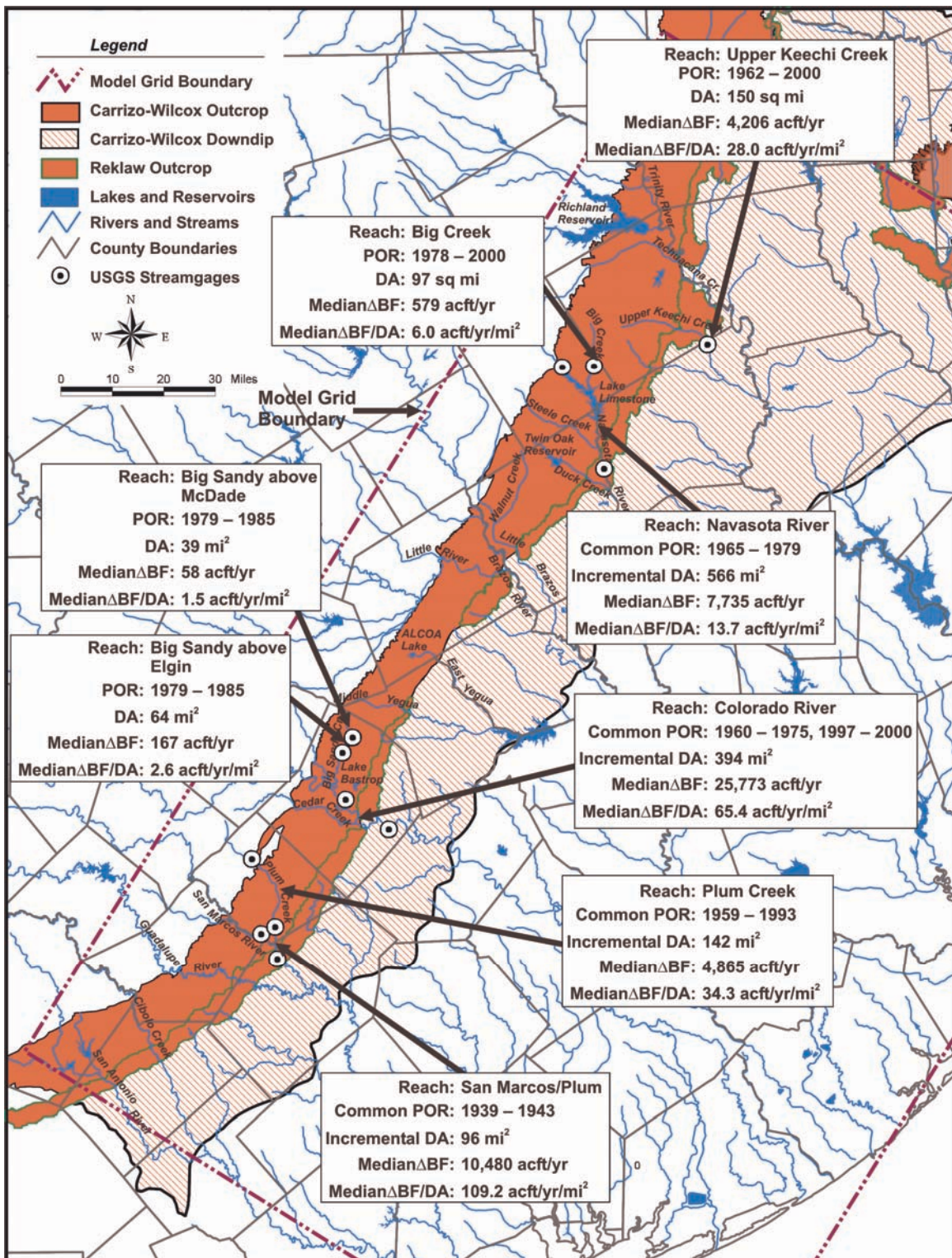


Figure B-7. Base-flow separation analysis results.

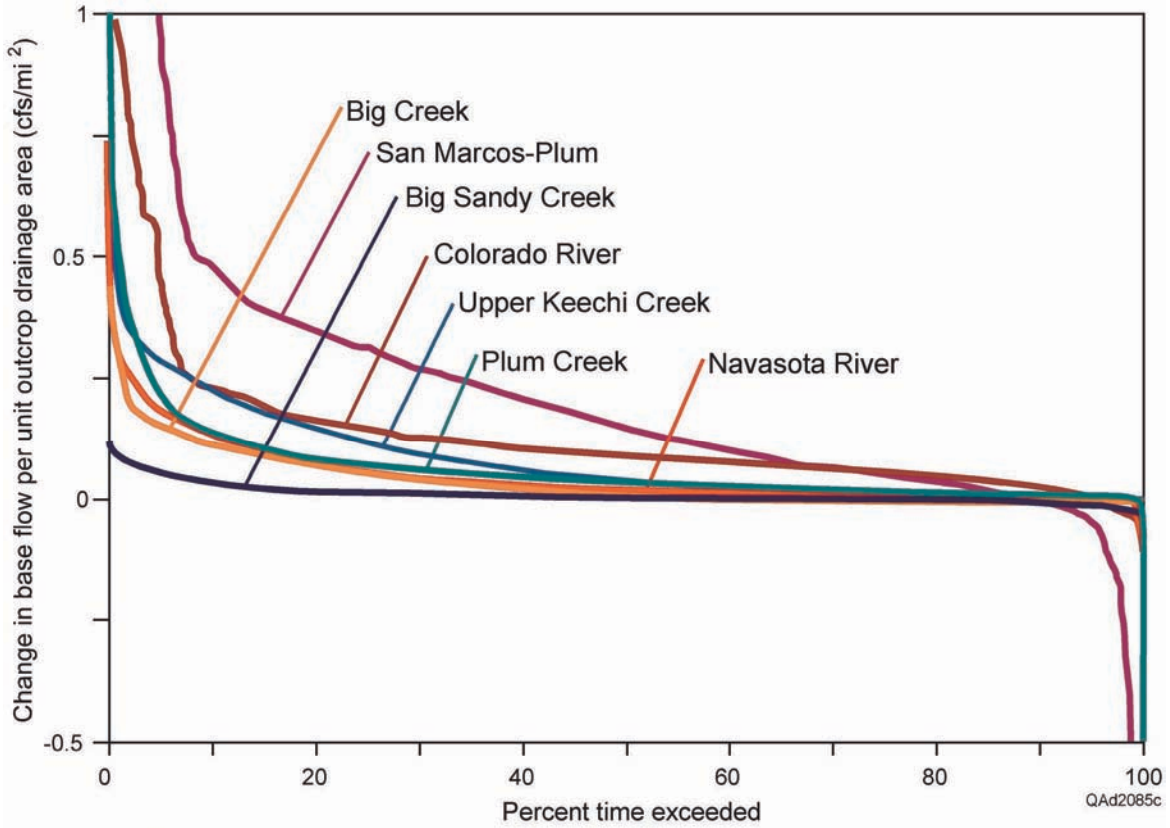


Figure B-8. Base-flow increase across the Carrizo–Wilcox outcrop, unitized by area of drainage basin in the outcrop. Base-flow increase assumed to reflect the discharge of groundwater from the Carrizo–Wilcox aquifer. Most of the discharge is from the Simsboro and Carrizo Formations.

median, and flows from the 10th and 90th percentiles, were calculated and are presented in table B-3. The application of these values is described in the Section B-4.

B-4.0 Model Application

As discussed previously, the physical processes of aquifer discharge are variable in quantity, diffuse in source, and cumulative in nature. The ultimate purpose of the data analysis described in Section B-3 is to develop specific numerical targets of groundwater flux between the aquifer and the streams for use during model calibration. Calibration targets for both the steady-state and the transient models are needed. We satisfied this requirement using the methods described in subsections B-4.1 and B-4.2.

B-4.1 Steady-State Model Calibration

For the steady-state model, the following approach was used to develop calibration targets. Because there is no variation in heads or storage in a steady-state simulation, a single value was necessary for each calibration target location on outcrop streams. Initially it was determined that for the steady-state calibration, calibration targets would be located at the downstream edge of the outcrop, thereby incorporating all tributary contribution to the stream prior to leaving the outcrop. Ultimately, calibration targets were developed for all modeled streams, and for each modeled stream, a “reference stream” was selected from the seven study reaches analyzed. This “reference stream” is the analyzed stream reach that most closely approximates the ungaged, modeled stream in size and location. Steady-state targets were derived by multiplying the median values of base-flow increase per unit area of the reference stream times the outcrop drainage area for the modeled stream at the target location. For example, of the seven streams analyzed, the Brazos River (which did not have adequate gage

Table B-3. Statistics from base-flow analysis of selected stream reaches (acre-feet/yr/mi²). Results based on median increase in base flow in the reach in the outcrop.

	Big Sandy above McDade	Big Sandy above Elgin	Big Creek	Upper Keechi
Period of record	1979-1985	1979-1985	1978-2000	1962-2000
Median	1.50	2.61	5.97	28.04
Maximum	46.77	54.47	320.95	492.32
Minimum	0	0	0	0
10th Percentile	0	0	0	0.10
90th Percentile	22.45	20.77	82.25	163.48
	Navasota River	Plum Creek	Colorado River	San Marcos- Plum
Period of record	1965-1979	1959-1993	1960-1975, 1997- 2000	1939-1943
Median	14.33	34.26	65.72	109.17
Maximum	618.61	1028.90	754.97	7082.08
Minimum	-92.62	-1245.59	-48.50	-1347.62
10th Percentile	1.38	6.12	18.98	0
90th Percentile	110.21	136.58	166.05	349.22

data for the analysis) most closely resembles the Colorado River. Therefore, the median unit base-flow value for the Colorado (66 af/yr/mi²) was multiplied by the outcrop drainage area for the Brazos River (380 mi²) to obtain a steady-state calibration target for the farthest downstream cell of the Brazos River. In this way, the appropriate unit base-flow increase calculated during the previous analysis may be applied to any ungaged stream and watershed within the model domain to produce a reasonable calibration target. (Although included in the study analysis, the data for the San Marcos River-Plum Creek confluence were ultimately not used as a reference stream because of both the relative brevity of the period of record [3.5 yr] and the ambiguity associated with apportioning the calculated base flows between the two tributary streams.) A summary of steady-state calibration targets developed in this process is presented in table B-4.

B-4.2 Transient Model Calibration

Because transient models simulate multiple stress periods in which heads, flux, and storage change with time, they require more extensive calibration targets than steady-state simulations. This GAM was calibrated and verified to the historical period of 1980 through 2000. The analysis presented in Section B-3 resulted in two separate approaches to developing transient calibration targets. The first involves matching time-specific data from the analysis at particular stream-gage locations for any of the study streams that had data within the 1980 through 2000 calibration period. The second involves using the base-flow duration statistics generated during the analysis as a guide for evaluating the time series at streams for which no specific data within the 1980 through 2000 time period was known. The following paragraphs discuss these approaches.

Table B-4. Steady-state conditions of calibration targets for selected watersheds.

River name	Calibration target cell ¹			Outcrop in drainage area (mi ²)	Reference stream ²	Estimated base-flow increase across outcrop (af/yr) ^{3, 4}
	Layer	Row	Column			
San Antonio River	2	22	5	208	Colorado	13,700
Cibolo Creek	2	27	16	196	Plum Creek	6,700
Guadalupe River	2	36	41	202	Colorado	13,300 (10,900) ⁴
San Marcos River	2	39	49	367	Colorado	24,100 (11,100) ⁴
Colorado River	1	39	85	495	Colorado	32,500 (26,100) ⁴
Middle Yegua Creek	2	33	112	151	Plum	5,200
East Yegua Creek	3	33	125	65	Plum	2,200
Brazos River	1	36	151	380	Colorado	25,000 (20,000) ⁴
Little Brazos River	1	37	153	234.5	Navasota	3,400
Duck Creek	3	40	178	164	Plum	2,200
Navasota River	2	43	181	566	Navasota	8,100
Upper Keechi Creek	3	39	218	134	Upper Keechi	3,800
Tehuacana Creek	1	29	231	329	Navasota	4,700
Trinity River	1	39	229	651	Colorado	42,800 (17,800) ⁴
Total						187,700 (135,900)⁴

Notes:

¹ Target cell at extreme downstream location of stream on outcrop.

² Reference stream is one of the seven streams quantitatively analyzed that most resembles the modeled stream in location and area.

³ Estimate obtained by multiplying median unit base-flow increase of reference stream by outcrop drainage area of modeled stream.

⁴ The estimated base flow for the Colorado has been revised from 32,500 acre-ft/yr to 26,100 acre-ft/yr, which corresponds to the value of 36 cfs of the 1918 low flow study (Fig. B-3). As a consequence, all stream flows derived from the Colorado River data, except the San Antonio River, have been multiplied by a correction factor of 26100/32500~0.8: new estimated base flows for Guadalupe and Brazos Rivers are 11,100 acre-ft/yr and 20,000 acre-ft/yr, respectively. In addition, it was observed that the Simsboro and Carrizo Formations contribute most to the stream base flow, whereas the Hooper, Calvert Bluff, and Reklaw Formations contribute very little. Approximately 25 percent of the Colorado drainage basin is located on the Simsboro and Carrizo Formations. The same is true of the Guadalupe and Brazos Rivers. However, the San Marcos and Trinity Rivers need an additional correction because the Simsboro and Carrizo Formations cover only 14 and 12 percent of the river drainage area, respectively. The new estimated base-flow increase for the San Marcos and Trinity Rivers is then 24,100 x 0.8 x 0.14/0.25 ~11,100 acre-ft/yr and 42,800 x 0.8 x 0.12/0.25 ~17,800 acre-ft/yr, respectively (multiplications not exact because of rounding).

The first calibration target approach simply applies annual base-flow increases calculated during the study. Of the seven streams examined in the quantity analysis, five (all but Navasota and San Marcos Rivers) have at least some data in the calibration period. For those streams, the annual median change in base flow attributed to each stream reach was used as an annual calibration target for any year in which data existed. These calibration targets are presented in table B-5.

Several of the modeled streams have no specific data in the 1980 through 2000 time period. In these instances, the second calibration target approach was used. We derived transient calibration targets by trying to match the duration curve statistics generated for the appropriate reference stream. Only base flows between 10 and 90 percent were considered for calibration statistics because many outliers are included in the extremes owing to (1) gage inaccuracies, (2) time lag for propagation of flow between upstream and downstream gages, and (3) inaccuracies in the base-flow program. Flows from the 10th percentile (Q_{10}) were used to estimate the minimum quantity of discharge from the aquifer to the streams, and flows from the 90th percentile (Q_{90}) were used to estimate the maximum of base-flow discharge from the aquifer to the streams. The median was selected instead of the average as a representative value of the middle range of flows to diminish the influence of extreme outliers in the data set. Therefore, after an appropriate reference stream is selected (as with the steady-state targets), the median, 10th, and 90th percentile unitized base-flow increases from the reference stream are multiplied times the outcrop area for any modeled stream to produce estimates for the median, minimum, and maximum groundwater flux expected between the aquifer and the stream at any target location. This is not a “hard” calibration target in the traditional sense; there is no specific numerical target associated with a particular stress period. However, it defines a target base-flow

Table B-5. Calculated 1980–2000 annual base-flow increases for selected study reaches.

<i>Stream</i>	<i>Upper Keechi Creek</i>	<i>Plum Creek</i>	<i>Big Creek</i>	<i>Big Sandy Creek</i>	<i>Colorado River</i>
<i>Target cell (L, R, C)</i>	<i>3, 39, 218</i>	<i>4, 33, 55</i>	<i>4, 27, 201</i>	<i>4, 26, 96</i>	<i>(Reach between 1, 32, 88 and 1, 39, 85)</i>
1980	8,900	3,100	1,800	384	*
1981	3,300	5,500	900	329	*
1982	6,200	4,600	1,600	286	*
1983	10,600	4,000	2,800	780	*
1984	6,000	2,900	1,800	239	*
1985	8,000	9,200	3,000	835	*
1986	7,200	13,800	1,900	*	*
1987	7,300	11,700	3,300	*	*
1988	3,300	4,000	1,700	*	*
1989	4,500	2,100	900	*	*
1990	9,300	1,900	1,800	*	*
1991	20,700	800	6,300	*	*
1992	19,900	30,000	7,700	*	*
1993	16,400	14,800	3,600	*	*
1994	11,100	*	2,400	*	*
1995	13,700	*	3,800	*	*
1996	2,000	*	1,000	*	*
1997	9,100	*	3,100	*	*
1998	12,400	*	4,600	*	132,750
1999	11,200	*	2,200	*	80,514
2000	3,900	*	500	*	56,551
	8,900	4,300	2,200	357	

range to compare against the range of flux values calculated by the model. Calibration targets developed using this method are summarized in table B-6.

B-5.0 Discussion

The methodology developed to quantify the interaction between groundwater and surface water attempts to develop specific numerical estimates of quantities that are not directly measurable. Simplifying assumptions were made in order to facilitate the analysis. Several factors may affect the accuracy of the estimates. This section briefly discusses these factors.

The estimates provided by the base-flow methodology may somewhat underestimate aquifer discharge because stream-channel losses due to evaporation and transpiration are occurring between the two gages' measuring points. What is actually measured using this methodology is groundwater discharge from the aquifer minus evapotranspiration losses in the intervening reach. However, this is a valid target for model calibration, when considering a model design that represents evapotranspiration.

In addition, this statistical approach may overestimate the seasonal and year-to-year variability of groundwater discharge to streams. If viewed as a simple system in the context of Darcy's Law, with groundwater flow direction perpendicular toward the stream, the quantity of discharge (Q) to the stream is

$$Q=KiA \tag{3}$$

where: K is hydraulic conductivity, i is hydraulic gradient of groundwater flow, and A is cross-sectional area of flow. Of these factors, hydraulic conductivity and cross-sectional area of flow remain constant with time. The hydraulic gradient is a factor of lateral flow distance (x-direction), which remains constant, and the vertical head (z-direction), which changes. However, groundwater level fluctuations in the outcrop are generally only on the order of 5 to 10 ft, and

Table 6. Calibration targets for transient conditions (acre-feet/yr)

River Name	Calibration Target Cell ¹		Outcrop in Drainage Area (mi ²)	Reference Stream ²	Minimum flow increase across outcrop ³	Median flow increase across outcrop ⁴	Maximum flow increase across outcrop ⁵
	Layer	Row					
San Antonio River	2	22	5	Colorado	4,000	13,700	34,500
Cibolo Creek	2	27	16	Plum Creek	1,200	6,700	26,900
Guadalupe River	2	36	41	Colorado	3,800	13,300	33,500
San Marcos River	2	39	49	Colorado	7,000	24,200	60,900
Plum Creek ⁶	4	36	52	Plum Creek	900	4,800	19,500
Cedar Creek	1	36	84	Plum Creek	1,500	8,700	34,900
Colorado River	1	39	85	Colorado	9,400	32,700	82,200
Big Sandy Creek	4	28	91	Big Sandy Ck	0 ⁷	100	1,500
Middle Yegua Creek	2	33	112	Plum Creek	900	5,100	20,700
East Yegua Creek	3	33	125	Plum Creek	400	2,200	8,900
Little River	1	34	150	Navasota	200	3,400	27,000
Brazos River	1	36	151	Colorado	7,200	25,100	63,100
Little Brazos River	1	37	153	Navasota	200	3,300	25,800
Walnut Creek	1	28	159	Plum Creek	800	4,600	18,500
Duck Creek	3	40	178	Plum Creek	1,000	5,600	22,500
Steele Creek	3	39	184	Plum Creek	1,000	5,400	21,900
Navasota River	2	43	181	Navasota	600	7,900	62,300
Big Creek	4	29	196	Big Creek	0	600	7,700
Upper Keechi	3	39	218	Upper Keechi	0	3,800	21,800
Tehuacana Creek	1	29	231	Navasota	300	4,600	36,200
Trinity River	1	39	229	Colorado	12,400	43,000	108,100

1. Target cell located at farthest downstream location of stream on outcrop, except as noted.
2. Reference stream is the one of the seven streams quantitatively analyzed which most resembles the modeled stream in location and area.
3. Obtained by multiplying median unitized base-flow increase of reference stream by outcrop drainage area of modeled stream. See text for details.
4. Obtained by multiplying 10th percentile unitized base-flow increase of reference stream by outcrop drainage area of modeled stream. See text for details.
5. Obtained by multiplying 90th percentile unitized base-flow increase of reference stream by outcrop drainage area of modeled stream. See text for details.
6. Stream name in bold indicates that target cell location is coincident with USGS gage location rather than farthest downstream location.
7. Reported minimum estimates of zero reflect 10th percentile flows from analyzed streams. Annual average minimum flows will likely be greater than zero.

with all other factors essentially remaining constant, it may be argued that the quantity of aquifer discharge does not vary as markedly as indicated from the base-flow methodology presented here. In addition, a succession of large storms would tend to increase the base-flow estimate if there were not adequate time between storms for the hydrograph recession limb to return to its prestorm level.

In addition, the relative altitude of a stream gage or the degree of incision of a river channel may affect the amount of groundwater discharge because a deeply incised channel will offer a cross-sectional area through which groundwater may enter the river that is larger than a gently sloping floodplain with no significant incision. There is no consideration of factors such as gage altitude or stream incision in this analysis.

An additional factor that is lost in the context of annual stress periods is the seasonal variability of stream flow. As previously mentioned, several of the streams modeled in this GAM are intermittent, going dry during the hottest summer months but maintaining flow through the winter. Although the intermittent streams analyzed have smaller values of groundwater flux than perennial streams, this variability is not represented in an annual model; future work that incorporates shorter stress periods should attempt to simulate this seasonal variability.

It has been suggested that recent groundwater development would result in values of groundwater discharge that are lower than historical, predevelopment values. However, the unit annual values calculated during the base-flow analysis were examined and revealed no evidence of a decreasing trend with time. As discussed previously, seasonal variability in base flow for perennial streams may not fluctuate as significantly as indicated by the base-flow analysis results.

B-6.0 Reference

Wahl, T. L., and Wahl, K. L., 2001, BFI Version 4.12, A Computer Program for Computing an Index to Base Flow: U.S. Bureau of Reclamation and U.S. Geological Survey.

APPENDIX C

DERIVATION OF HYRAULIC CONDUCTIVITY

Horizontal and vertical hydraulic conductivity were derived from (1) measured estimates of hydraulic conductivity compiled by Mace and others (2000), (2) maps of sandstone thickness (Bebout and others [1982], Ayers and Lewis [1985], Fogg and others [1983b], Xue [1994]), and (3) structural information on layer elevations and thickness. This appendix documents how values of horizontal and vertical hydraulic conductivity were derived and assigned to model grid cells.

Our approach to mapping hydraulic conductivity followed these steps:

- (1) We used ArcView to post the field-estimates of hydraulic conductivity compiled by Mace and others (2000). Additional work was needed to assign the Mace and others (2000) data to specific model layers on the basis of well depth, screened interval, and designated aquifer code. Data were posted on maps as the logarithm (base 10) of the reported hydraulic conductivity.
- (2) On top of the posted values of hydraulic conductivity, we overlaid maps of the net thickness of sandstone in the aquifer layers. To account for the entire study area we used sandstone-thickness maps from Bebout and others (1982), Ayers and Lewis (1985), Fogg and others (1983b), and Xue (1994). To supplement these maps, we posted and contoured values of sandstone thickness for part of Gonzales County inferred from additional logs.
- (3) We contoured hydraulic conductivity by hand using the thickness of sandstones as an interpretive guide. Our conceptual model was that hydraulic conductivity is greatest along the axes of sand channels because (a) that is where the coarse-grained sands are

concentrated and low-permeability silts and clays tend to be absent and (b) thick sandstones tend to be better interconnected and have a higher effective hydraulic conductivity (Fogg and others, 1983a). We found qualitative but mappable local correlation between sandstone thickness and hydraulic conductivity.

(4) We traced and digitized the contoured maps of hydraulic conductivity and sandstone thickness.

(5) We used Surfer to interpolate values of hydraulic conductivity (still in log-base 10 units) and sandstone thickness for each active cell of model grid for the Hooper aquitard (layer 6), Simsboro aquifer (layer 5), Calvert Bluff aquitard (layer 4), and Carrizo aquifer (layer 3).

(6) We calculated an average value of horizontal and vertical hydraulic conductivity (K_h and K_v , respectively) for each active cell in the Hooper aquitard (layer 6), Simsboro aquifer (layer 5), Calvert Bluff aquitard (layer 4), and Carrizo aquifer (layer 3). We used equations A-1 and A-2 to weight hydraulic conductivity by sand thickness. Equation A-1 gives an arithmetic average for horizontal hydraulic conductivity and equation A-2 gives a harmonic mean for vertical hydraulic conductivity

$$K_h = (K_{hs} \times b_s + K_{hc} \times b_c)/B \quad (A-1)$$

$$K_v = B/[(b_s/K_{vs}) + (b_c/K_{vc})] \quad (A-2)$$

where K_{hs} and b_s are the horizontal hydraulic conductivity and total cell thickness of sand, respectively; K_{hc} and b_c are horizontal hydraulic conductivity and total cell thickness of non-sand (clay, silt, and lignite) materials, respectively; and B is total cell thickness. The values of K_{hs} and b_s were determined in step (5) above; b_c was determined from total cell thickness minus sand thickness. Total cell thickness (B) was calculated

from the top and bottom of grid cells. We assumed that K_{hc} was 9×10^{-4} ft/d. We assumed that local anisotropy is 0.1 for sandstone beds and 0.01 for clay, silt, and lignite beds.

Adjustments were made to the initial cell estimates of horizontal and vertical hydraulic conductivity during model construction and calibration.

- (1) We smoothed the values of hydraulic conductivity in the outcrop of layer 5 representing the Simsboro aquifer. If the value in row i was less than 20 percent of the value in row $i+1$ in the outcrop, for any given column, we set the hydraulic conductivity of the cell in row i to the value for the cell of row $i+1$.
- (2) Another correction for the outcrop of the Hooper and Calvert Bluff aquitards (layers 6 and 4, respectively) was where too large a value of vertical hydraulic conductivity was calculated because sand makes up most or all of the section. If the estimated K_v was more than twice the assigned value of K_{hc} , we limited K_v for the cell to the mean value for the layer.
- (3) We made sure default values were assigned to additional cells in layers between the active cells representing alluvium in layer 1 and the uppermost active cell of bedrock layers 6 through 3.
- (4) Maximum hydraulic conductivity of thick deposits of Simsboro sandstone in the Rockdale Delta was limited to 30 ft/d, giving a maximum transmissivity of 15,200 ft²/d.
- (5) We selectively adjusted hydraulic conductivity in four zones of layer 5 representing the Simsboro aquifer where model-calculated values of transmissivity, or the range in transmissivity, were deemed too high in

comparison to field data. These adjustments decreased the range of assigned values in the targeted zones. These zones included:

- (a) The area within columns 164 to 168 and rows 27 to 29 in the vicinity of the Walnut Creek Mine in Robertson County,
- (b) The area within columns 145 to 153 and rows 46 to 54 in the vicinity of the Bryan-College Station well field in Brazos and Robertson Counties,
- (c) The area within columns 117 to 140 and rows 29 to 33 in the vicinity of the Sandow Mine in Milam County, and
- (d) The area within columns 101 to 105 and rows 27 to 33 in the vicinity of the Three Oaks Mine in Bastrop and Lee Counties.

Transmissivity for each cell in zone (a) was decreased by 30,000 ft²/d to no less than 30,000 ft²/d. In zone (b), transmissivity was increased by 30,000 ft²/d to as much as approximately 113,700 ft²/d. In zone (c) and (d), the adjustment of transmissivity was linearly scaled. In zone (c) the maximum decrease in transmissivity of -50,000 ft²/d was assigned to cells with an initial transmissivity of as much as 113,000 ft²/d; the decrease in transmissivity was scaled to 0 for cells with an initial transmissivity of less than 40,000 ft²/d. For zone (d) we increased transmissivity, again by scaling the adjustment. The maximum increase in transmissivity of +30,000 ft²/d was assigned to cells with an initial transmissivity as small as 5,000 ft²/d; the increase in transmissivity was scaled to 0 for cells with an initial transmissivity of more than 40,000 ft²/d. The recalculated transmissivities were then divided by cell thickness to provide hydraulic conductivity as the model input parameter.

- (6) We increased K_v of layer 6 representing the Hooper aquitard in all cells by a factor of 10 to improve the model calibration of simulated and observed water levels. And (7), we globally adjusted vertical hydraulic conductivity by layer by slightly shifting the average and decreasing or increasing the standard deviation of vertical hydraulic conductivity to better reproduce the expected ratio of K_v/K_h from the conceptual model (Table C-1).

Table C-1. Comparison of initial and adjusted values of hydraulic conductivity (horizontal [K_h] and vertical [K_v]) assigned in the model

		K_h		K_v		K_v/K_h	
		initial	adjusted	initial	adjusted	initial	adjusted
Carrizo (Layer 3)	$10^{\mu_{\log[-]}}$	6.4	6.2	5.5×10^{-4}	1.3×10^{-3}	8.6×10^{-5}	2.1×10^{-4}
	$\sigma_{\log[-]}$	0.62	0.60	0.78	0.62	0.75	0.49
Calvert Bluff (Layer 4)	$10^{\mu_{\log[-]}}$	0.91	0.91	2.8×10^{-5}	9.7×10^{-5}	3.1×10^{-5}	1.1×10^{-4}
	$\sigma_{\log[-]}$	0.51	0.51	0.09	0.12	0.49	0.48
Simsboro (Layer 5)	$10^{\mu_{\log[-]}}$	2.6	2.6	1.4×10^{-4}	9.5×10^{-4}	5.5×10^{-5}	3.7×10^{-4}
	$\sigma_{\log[-]}$	0.80	0.80	0.62	0.58	0.76	0.53
Hooper (Layer 6)	$10^{\mu_{\log[-]}}$	0.91	0.49	1.1×10^{-5}	3.5×10^{-5}	1.2×10^{-5}	7.1×10^{-5}
	$\sigma_{\log[-]}$	1.7	1.5	0.12	0.38	1.6	1.1

$10^{\mu_{\log[-]}}$ Mean value calculated as geometric mean of log-transformed variable

$\sigma_{\log[-]}$ Standard deviation calculated from log-transformed variable

References

- Ayers, W. B., Jr., and Lewis, A. H., 1985, The Wilcox Group and Carrizo Sand (Paleogene) in East-Central Texas: depositional systems and deep-basin lignite: The University of Texas at Austin, Bureau of Economic Geology, 19 p. + 30 pl.
- Bebout, D. G., Weise, B. R., Gregory, A. R., and Edwards, M. B., 1982, Wilcox Sandstone reservoirs in the deep subsurface along the Texas Gulf Coast: their potential for production of geopressed geothermal energy: The University of Texas at Austin, Bureau of Economic Geology Report of Investigations No. 117, 125 p.
- Fogg, G. E., Seni, S. J., and Kreitler, C. W., 1983a, Three-dimensional ground-water modeling in depositional systems, Wilcox Group, Oakwood salt dome area, East Texas: The University of Texas at Austin, Bureau of Economic Geology Report of Investigations No. 133, 55 p.
- Fogg, G. E., Kaiser, W. R., and Ambrose, M. L., and Macpherson, G. L., 1983b, Regional aquifer characterization for deep-basin lignite mining, Sabine Uplift area, northeast Texas: The University of Texas at Austin, Bureau of Economic Geology Geological Circular 83-3, 30 p.
- Xue, L., 1994, Genetic stratigraphic sequences and depositional systems of the lower and middle Wilcox strata, Texas Gulf Coast Basin: The University of Texas at Austin, Ph.D. dissertation, 202 p.

APPENDIX D

RESPONSES TO TECHNICAL AND ADMINISTRATIVE COMMENTS ON THE DRAFT AND DRAFT FINAL TECHNICAL REPORTS

Comments pertaining to the Draft Report were provided on December 12, 2002.
Additional comments on the Draft Final Report are appended at the end of the list.

DRAFT REPORT

DRAFT REPORT - OVERALL COMMENTS

1. Some characters did not translate when PDF was created. Please ensure a good translation with final report.

[Response]: We have revised and checked our procedure for converting to pdf files to ensure a good translation with final report.

2. Formation and aquifer names should always refer to a noun (i.e. aquifer, formation, etc.).

[Response]: We have added nouns as suggested in most places. In a few places such as table columns where space was limited we have left out the nouns.

3. Mining and SAWS-ALCOA pumping are described in mixed ways in the report. It might be good to explain the history and planned use and then be consistent when describing effects in the report (partly a stakeholder comment).

[Response]: We added text in section 6.3.6 Wells, that describes regional water plan water management strategies.

4. Additional discussion on how the predictive pumping was assigned would be useful and was requested by a stakeholder.

[Response]: We added text in section 6.3.6 Wells that describes how the predictive pumping was assigned.

DRAFT REPORT- TABLE OF CONTENTS

1. 9.2: Please fix margin indent

[Response]: Corrected.

2. Figure 6: Please remove '13' from figure title

[Response]: Corrected.

3. Figures 56 through 61, 99, 100: Please refer to formation and aquifer as the primary descriptor and then the layer. Note that layers are not referred to consistently in the figure captions.

[Response]: Corrected.

4. Figure 62: 'aquifer' should be 'aquifers'
[Response]: Corrected.
5. Figures 65, 66, 68, 84, 85, 86: Please add 'aquifer' after 'Simsboro' and 'Carrizo.'
Note that 'Simsboro,' 'Carrizo,' 'Wilcox,' and other formation and aquifer names should be followed by aquifer or appropriate geologic name in the report.
[Response]: Corrected.
6. Figure 70: Please include rest of caption
[Response]: Corrected.
7. Figure 76: Please verify year. Appear that it should be 2000 instead of 1990.
[Response]: Corrected.

DRAFT REPORT- ABSTRACT

1. Page 1, 1st paragraph: "Groundwater withdrawal from the central part of the Carrizo-Wilcox..." Please define what you mean by 'central part.'
[Response]: Sentence added that states "This model covers the central section of the Carrizo-Wilcox aquifer as defined by the surface-water divide between the San Antonio and Guadalupe Rivers to the southwest and the surface-water divide between the Trinity and Neches Rivers to the northeast." Previous sentence revised to introduce the three models.
2. Page 1, 2nd paragraph: "...water-use survey estimates of historical and future groundwater withdrawals..." Water-use survey estimates apply only to historical withdrawals. Please change sentence to reflect this.
[Response]: "and future" was deleted.

DRAFT REPORT- 1.0 INTRODUCTION

1. Page 4, 1st paragraph: See comment 40 under *DRAFT REPORT - SECTION 4.0: HYDROLOGIC SETTING*
[Response]: Text revised to say "Groundwater production is predominantly for municipal public-water supply, manufacturing, and rural domestic uses." These make up more than 50 percent of total withdrawal.
2. Page 4, 2nd paragraph: "Groundwater availability is defined as the total amount of groundwater available from an aquifer under a predefined development scenario chosen by the Regional Water Planning Groups." This statement is not true. Please change.
[Response]: Text revised to "Estimating groundwater availability for the 50-yr planning period in Texas involves information on aquifer management goals, environmental issues, rules and regulations, and scientific understanding of how an aquifer works (Mace and others, 2001)."
3. Page 5, 1st line: "...pumpage increased by from 10,600" Please remove 'by.'
[Response]: Corrected

4. Page 5, 2nd paragraph: Please repair the bad break at end of paragraph between "the" and "Carrizo-Wilcox."

[Response]: Corrected

5. Page 5, 3rd paragraph: Discussion on transient calibration and verification indicates that the quality of calibration and verification was assessed only by comparing simulated water levels to measured water levels at the end of the decades. However, there should have also been a comparison to water-level changes over time during the decades. Please change the sentence to reflect this.

[Response]: Five calibration criteria were checked. Text has been revised to reflect this.

6. Page 5, 3rd paragraph, discussion on projected pumping demands: The RWPGs did not provide projected pumping demands. The RWPGs provided projected demands and supplies with possible water management strategies. The TWDB did an analysis to assign the demands to groundwater and surface water sources. Please change this sentence to reflect this.

[Response]: Text revised to state that Groundwater withdrawal for the 50-yr period was derived from a TWDB analysis of the demands and supplies of surface water and groundwater, along with possible water management strategies, projected by the Regional Water Planning Groups.

7. Page 7, 1st paragraph: Please change "stakeholder meetings" to "stakeholder advisory forums."

[Response]: Corrected

8. Page 7, 2nd paragraph: Please list GCDs first and RWPGs second.

[Response]: Corrected

DRAFT REPORT- 2.0 STUDY AREA

1. Figure 5: Please add a date (as of...) to the figure. Note that several GCDs have been confirmed since the map was prepared.

[Response]: Corrected

2. Section 2.1, Page 14: Note that the predictive model requires the use of an average precipitation from 1960 to most recent data. Please add a description of this time period for precipitation.

[Response]: Text revised to state that since the steady-state model represents a long period of time (at least 100 yr), we assigned recharge for the steady-state calibration using a long-term average (1940 to 1997) precipitation, whereas or the predictive model we assigned a constant recharge rate for normal years using an average precipitation calculated from 1960 to 1997 data. This excludes the effect of the 1950s drought of record from the calculation of the normal year recharge rate.

3. Page 14, paragraph 2: “Average annual precipitation during the period from 1900...” should be “Annual precipitation during the period from 1900...”
[Response]: Corrected
4. Figure 6. Please label drainage basins.
[Response]: Corrected
5. Figure 7. Consider using thicker contours (difficult to resolve with county lines).
[Response]: Corrected
6. Figures 7, 8, and 9: Please add a reference to the data source to the figure.
[Response]: Figure 7 on precipitation is from www.twdb.state.tx.us/mapping/gisdata.htm.
Figure 9 on average net lake evaporation rate is from data at <http://hyper20.twdb.state.tx.us/Evaporation/evap.html>.
7. Figure 11: The same color is used for Pleistocene etc. and Simsboro Fm. Please change color scheme so all the divisions can be clearly identified.
[Response]: Corrected
8. Figure 11: Two boxes in the legend have no name. Please address.
[Response]: Corrected
9. Section 2.2, page 28,4th sentence: Please add "and" to the sentence.
[Response]: Corrected
10. Section 2.2: Please review the width of the outcrop as referenced in the report. The report says less than 2 miles wide, but it appears from the geology map that it is more than 20 miles wide.
[Response]: Additional detail added to expand clarity. Formations are not formally broken out south of the Colorado River and north of the Trinity River. The width of the Wilcox Group is given for those areas.

DRAFT REPORT- 3.0 PREVIOUS WORK

1. Section 2.2, page 29: Please explain what the Newby flow unit is.
[Response]: Added text to identify the Newby Member of the Reklaw Formation.

DRAFT REPORT - 4.0: HYDROLOGIC SETTING

1. Figure 15, page 35: For A'-A", there appears to be a horst in Lee County. It seems more likely that there would be a graben or normal faulting toward the coast. The horst feature shows up in Lee County where no faulting is indicated on Figure 34. Faulting in Bastrop County in Figure 34 does not appear on the cross section. Also note that the Simsboro appears to thicken in the horst. Please review Figures 34 and 35 for accuracy and make any needed changes.
[Response]: Revised. Not all faults were shown on the figure leading to an impression of a geologic structure that is not present. Other revisions made as suggested.

2. Figure 16, page 36: For C-C', '10,000' should be '-10,000.'

[Response]: Corrected.

3. Section 4.1: Hydrostratigraphy section discusses the Quaternary alluvium while ignoring Queen City, Sparta, and Yegua (?) aquifers. Need to either add brief discussion of missing aquifers or explain why Quaternary alluvium important to the modeling effort. Important to discuss Queen City as its hydraulic heads are added to the model.

[Response]: Text added to discuss Queen City and Sparta aquifers.

4. Section 4.2, page 39: It is unclear which data was used where and how for creating the structure maps. Please add more detail on methods (i.e. were maps digitized from reports, how many new data points and where).

[Response]: Information added on sources of information and how data were reconciled.

5. Section 4.2: Later sections indicate that the Reklaw Fm. was included as a layer. Therefore, please include a figure showing the top of the Reklaw Fm.

[Response]: Added figure 22 showing structure of top of Reklaw Formation.

6. Section 4.2: Later sections indicate that the alluvium was included as a layer in the model. Please include a discussion on how the thickness of alluvium was assessed and describe the thicknesses.

[Response]: Additional text added to page 39 of draft report as follows: "Alluvial deposits associated with the Colorado, Brazos, and Trinity Rivers likely have a significant impact on the interaction of surface water and groundwater in the outcrop of the Carrizo-Wilcox aquifer. Areal limits of the alluvium associated with the Colorado, Brazos, and Trinity Rivers were digitized from McGowen and others (1987), Proctor and others (1988), Proctor and others (1993a), Proctor and others (1993b), and Shelby and others (1993). The upper surface of the alluvium was taken as ground surface and assigned by draping USGS DEM data onto model cell centroids in the areas underlain by alluvium. Thickness of alluvium was estimated from data on well depth and well-screen position (Wilson, 1967; http://www.twdb.state.tx.us/data/waterwell/well_info.html). The lower surface of alluvium was mapped by subtracting alluvium thickness from DEM for each model cell."

7. Figures 18 through 21: Not sure what the extended blue areas are near the up-dip limit of the outcrop. Please address.

[Response]: Map information for additional cells between the alluvium in layer 1 and the uppermost active bedrock model layer has been masked in all figures except for figures 55 to 58 which show the active model cells.

8. Figures 22-25: Please remove 'Model' from legends.

[Response]: Corrected.

9. Page 50, paragraph 4: The 3,000 mg/l TDS contour represents the base of 'potentially potable water', not 'freshwater' (1,000 mg/l TDS).

[Response]: Corrected in all maps.

10. Page 51. 3,000 mg/l is limit of slightly saline or potentially potable water.

[Response]: Corrected.

11. Section 4.4.1, page 55: Unclear how reported water levels in the College-Bryan Station well field were adjusted. Please explain in more detail.

[Response]: Text added as follows to page 55 of draft report: Water-level measurements taken when a well is not pumping are considered static water-level measurements. Simulated water levels reflect drawdown caused by groundwater withdrawal assigned to model cells. Adjusting static water levels for the Bryan-College Station well field is appropriate for comparison to simulated results for model cells. The adjustment followed the method of Anderson and Woessner (1992). An initial water-level recovery was estimated using the known transmissivity, average pumping rate, and assumed elapsed recovery time. Initial recovery was projected to an equivalent for a 1-mi grid cell. The correction factor is small relative to measured and simulated changes in water level.

12. Figure 26. Cannot clearly see contours, especially in the freshwater part of the aquifer.

[Response]: Corrected.

13. Section 4.4.2, page 60, 3rd paragraph: "This seems more probable..." Please explain why it seems more probable.

[Response]: Text revised to delete phrase and rewritten for clarity.

14. Section 4.4.2: Figure 27 shows a large cone of depression in Gonzales County in the freshwater part of the aquifer, and Figure 27 and 28 show cones of depression in the deep down-dip part of the aquifer. Cones of depression are not consistent with a pre-development potentiometric surface. Please explain why these features are in the map. If appropriate, please update the map.

[Response]: Figure revised to not show data from oil and gas fields at which calculated equivalent hydraulic heads were below local trends and which probably have been affected by gas production.

15. Section 4.4.2, Figure 27: The lower right-hand corner of the map in the freshwater part of the aquifer shows hydraulic heads going down. There are no data points to support this. Please add a discussion in the text as to why this may be realistic. Also, please check the values of the contours in this area: the two contours have the same value of '200.'

[Response]: Draft report on page 59 (1st paragraph) identified our interpretation that the topographic elevation of <100 ft msl in the lower Angelina River valley must influence the hydraulic head in the Carrizo-Wilcox aquifer and define the 'base level' of the aquifer. This point is repeated as needed in the revised text.

16. Section 4.4.2., Figure 28: The lower right-hand corner of the map in the fresh-water part of the aquifer shows hydraulic heads going down. There are no data points to support this. Please add a discussion in the text as to why this may be realistic.

[Response]: Draft report on page 59 (1st paragraph) identified our interpretation that the topographic elevation of <100 ft msl in the lower Angelina River valley must influence the hydraulic head in the Carrizo-Wilcox aquifer and define the 'base level' of the aquifer. This point is repeated as needed in the revised text.

17. Section 4.4.2, Page 61: "One implication of the reversal in gradient of hydraulic head..." suggests that there is a reversal of hydraulic gradient, but it has not been previously discussed (there is discussion that gradient has changed, but not magnitude and not reversal). Please rewrite to reflect actual analysis. Also please check the logic of the sentence: "One implication...that there may have been..." Even if there wasn't a hydraulic gradient reversal, there still may have been a stagnation zone. This may also be the appropriate place to discuss how a change would affect the aquifer given that the boundary is assumed to remain the same in subsequent modeling.

[Response]: Added text to 3rd paragraph on page 60 to more clearly identify the reversal in gradient. It was beyond scope to discuss how a change would affect the aquifer given that the boundary is assumed to remain the same in subsequent modeling.

18. Figure 30: Please add dashed lines where appropriate to this figure for the water-level elevations as done in figures 29 and 31.

[Response]: Corrected.

19. Figure 34: Well 37-17-902 and others appear to be beyond where Calvert Bluff is defined. Please review the location of these wells.

[Response]: Well locations were reviewed.

20. Figure 36: Note that well 37-17-902 on figure 34 does not have a hydrograph in this figure. Please review well numbers between figure 34 and figures 33, 35, 36, and 37.

[Response]: Only the 40 wells included as hydrographs remain in the revised figure.

21. Section 4.2: Please add a map/discussion of water levels in the Queen City aquifer (referred to earlier as being assigned to the Reklaw).

[Response]: New figure 30 presents the 'predevelopment' map of the Queen City aquifer.

22. Section 4.4.3, page 61, 1st paragraph: Page 61, para. 4. The first two sentences appear to conflict with each other.

[Response]: Corrected and paragraph rewritten.

23. Section 4.4.3, pages 61-62: What were the pre-development hydraulic heads in the Bryan-College Station and Lufkin-Angelina County well fields?

[Response]: Text added to state predevelopment hydraulic heads in the Bryan-College Station and Lufkin-Angelina County well fields.

24. Section 4.5: Please include discussion on how figure 39 was developed.

[Response]: Figure 39 has been moved and renumbered as figure 69. In its place in the section on recharge is a map of soil hydraulic conductivity, the basis for mapping recharge rates. The recharge section was extensively rewritten to spell out the method of calculation.

25. Section 4.5: Please discuss 'rejected recharge.'

[Response]: Paragraph added on rejected recharge. "Rejected recharge is the concept that much of the water that reaches the water table as recharge in the unconfined part of the aquifer does not travel downdip into the confined part of the aquifer. Rejected recharge leaves the unconfined part of the aquifer by discharge to seeps and springs in valleys, discharge to rivers and streams, evapotranspiration in river bottomland areas. Rejected recharge generally does not include withdrawal of groundwater by wells in the unconfined aquifer. The water that cycles through the unconfined aquifer, therefore, is not available for withdrawal by wells in the confined part of the aquifer. Captured recharge is the concept that drawdown of water levels in the confined part of the aquifer increases the gradient in hydraulic head and draws more groundwater from the unconfined to confined parts of the aquifer. In addition, drawdown of water levels in the unconfined aquifer, owing to pumping of wells in either the unconfined or confined parts of the aquifer, results in a decrease in the discharge of groundwater to rivers and streams and may reduce actual evapotranspiration. Groundwater that is "captured" by the confined aquifer reflects a change in the water budget of the aquifer."

26. Section 4.5: Please clarify the assignment of recharge to the Hooper and Calvert Bluff.

[Response]: Recharge to the Hooper and Calvert Bluff was handled the same way as recharge for other layers and this is explained in the revised text.

27. Section 4.5: Later in the report, recharge is reported for the Reklaw as a model result. Please explain how this was assigned (may be more appropriate to discuss in the calibration section).

[Response]: Recharge to the Reklaw was handled the same way as recharge for other layers and this is explained in the revised text. Methodology is given in section 6.0 and deleted out of section 4.0. Results are given in section 8.0.

28. Section 4.5: Please outline assumptions used in the chloride recharge estimation.

[Response]: Text added: "The primary assumptions of the chloride mass balance approach are that water movement is downward and there are no subsurface sources or sinks of chloride. The first assumption is valid because in broad areas between surface water bodies the main direction of water movement is vertical and the direction in the hydrogeologic setting of the study area the direction of net flow of water in the

unsaturated zone is downward. The second assumption also is reasonable for these tests in the Simsboro Formation outcrop (Dutton, 1985, 1990).”

29. Figure 43: Please include the outcrop of the Carrizo-Wilcox aquifer (referred to in the text).

[Response]: Added as suggested.

30. Figure 44b: Please change 'csf' to 'cfs' on y-axis of plot.

[Response]: Corrected.

31. Figure 45: Please change 'cfs/m⁻²' to 'cfs/mi²' on the y-axis.

[Response]: Corrected.

32. Section 4.6: Please discuss streambed conductance.

[Response]: Text added.

33. Section 4.6: Please discuss hydraulic connection of lakes to aquifers.

[Response]: Text added.

34. Table 4: Unclear what "Field data (fig. 46)" means in the Table. Please clarify or remove.

[Response]: Line revised to refer to Mace and others (2000) data in figure 46.

35. Section 4.7, bottom of page: Sentence is cut off. Please include all of the sentence.

[Response]: Corrected.

36. Figures 48, 49, 50: Not sure what the extended blue areas are near the up-dip limit of the outcrop. Please address.

[Response]: Map information for additional cells between the alluvium in layer 1 and the uppermost active bedrock model layer has been masked in all figures except for figures 55 to 58 which show the active model cells.

37. Section 4.7, page 90: “...(for example, figs. 12,~~14~~13)” should be 'figs. 12 and 13.'

[Response]: Corrected.

38. Section 4.7, last paragraph: Please include more information on how specific storage was assigned to the model. We need to be able to reproduce assigned values.

[Response]: Several paragraphs added to section 6 to discuss how storativity was assigned. Text reorganized between sections 4 and 6.

39. Section 4.7: Please include a discussion on horizontal anisotropy.

[Response]: Text added. “There is appreciable lateral heterogeneity in hydrogeologic properties related to the original depositional systems and subsequent burial diagenesis of the sediments that make up the Carrizo-Wilcox aquifer. Much of the heterogeneity

reflects the variations in thickness of sandstones (figs. 12, 13). The thick major sands may have greater hydraulic conductivity than thinner sands, and also have greater lateral continuity (Fogg and others, 1983). We assume that the aquifer and aquitard materials are isotopic in the horizontal direction. This means that horizontal hydraulic conductivity is the same regardless of direction.”

40. Section 4.8, 1st paragraph: Logic: Most pumping is from municipal and manufacturing, but accounts for only one third of total pumping. Please address.

[Response]: Text revised. “Most pumping from the Carrizo-Wilcox aquifer in the study area has been for municipal public-water supply, manufacturing, and rural domestic water uses. These three uses have made up more than 60 percent of total pumping from the aquifer in the period from 1980 through 2000.”

41. Section 4.8, 3rd paragraph, 2nd sentence: "Because there are few measurements of historical pumping..." is too broad a statement. Our water-use survey collects reported measured values of pumping for municipal and industrial uses of water.

[Response]: Text revised to say that “because most pumping has not been volumetrically metered, it is generally estimated indirectly...”

42. Figure 51: Please change '200' to '2000.'

[Response]: Corrected.

43. Section 4.8: Please show a map showing the distribution of irrigation pumping.

[Response]: New figure 60 added with 6 maps that show 200 pumping allocation for municipal, manufacturing, irrigation, mining, rural domestic, and stock.

44. Section 4.8, page 115, paragraph 3: Please explain why mining was distributed based on land use rather than using specific well locations.

[Response]: As discussed during the TWDB review of the transient model calibration, we had found few enumerated wells in counties to which mining pumping was to be assigned. The decision was made to use land use for those counties where we lacked adequate information to distribute pumping to wells. For Bastrop, Lee, and Milam County we had specific information available to assign well locations for mining.

45. Table 6a: Please explain why there is a increase in pumping in Lee County (stakeholder comment).

[Response]: Text added in section 6 to relate predictive pumping to the regional water plan water management strategies, and to explain how the pumping was allocated to the model. The Region G regional water plan identified the Carrizo-Wilcox aquifer as a water management strategy to meet Williamson County water needs. Predicted groundwater withdrawal ranges from less than 1,000 acre-ft/yr in 2001 to more than 18,000 acre-ft/yr in 2050. Identified users included the cities of Bartlett, Brushy Creek, Florence, Georgetown, Granger, Hutto, Leander, Round Rock, Taylor, and Thrall and also water-supply corporations supplying rural domestic users. This predicted groundwater withdrawal was split between the Carrizo and Simsboro aquifers and allocated in the model to Lee County using the footprint defined in the Trans-Texas

Water Program (HDR Engineering, 1998) and previously simulated in the Dutton (1999) model. Predicted pumping ranged from less than 1,000 acre-ft/yr in 2001 to more than 18,000 acre-ft/yr in 2050.

46. Please discuss evapotranspiration.

[Response]: Section 4.7 added on Groundwater Evapotranspiration

47. TNP is not a mine but a power plant (whose new name is Twin Oaks Power Plant) (stakeholder comment).

[Response]: Corrected.

DRAFT REPORT - 5.0: CONCEPTUAL MODEL OF GROUNDWATER FLOW

1. Page 124, 3rd bullet: Evapotranspiration is not discussed in Hydrologic Setting section. Please discuss in the Hydrologic Setting section or remove from conceptual model.

[Response]: Section 4.7 added to discuss Groundwater Evapotranspiration.

2. Page 124, 3rd bullet: Net recharge is not discussed in Hydrologic Setting section. Please discuss in the Hydrologic Setting section or remove from conceptual model.

[Response]: Net recharge discussed using the term 'rejected recharge' in added text to section 4.0.

3. Page 124, 4th bullet: "Most groundwater contribution to the base flow of rivers and streams crossing the outcrop is from the Simsboro and Carrizo." This concept is not discussed in the Hydrologic Setting section. Please discuss in the Hydrologic Setting section or remove from conceptual model.

[Response]: The statement that base flow is mainly from the Simsboro and Carrizo aquifers has been added to section 4.6.

4. Page 124, 5th bullet: "The proportion of recharge that reaches the confined aquifer changes with increased pumping." This concept is not discussed in the Hydrologic Setting section. Please discuss in the Hydrologic Setting section or remove from conceptual model.

[Response]: This has been added to the discussion of rejected recharge added to page 74 of the draft report.

5. Page 124, 6th bullet: Cross-formational flow. This concept is not discussed in the Hydrologic Setting section. Please discuss in the Hydrologic Setting section or remove from conceptual model.

[Response]: Discussion of Cross-formational flow has been added to page 59 of the draft report in discussion on water levels.

6. Page 124, 7th bullet: "...where there is a tendency for upward discharge into the overlying formation." This concept is not discussed in the Hydrologic Setting section. Please discuss in the Hydrologic Setting section or remove from conceptual model.

[Response]: Discussion of Cross-formational flow has been added to page 59 of the draft report in discussion on water levels.

7. Page 126, 3rd bullet: Flow rates. This concept is not discussed in the Hydrologic Setting section. Please discuss in the Hydrologic Setting section or remove from conceptual model.

[Response]: The reference to groundwater ages and flow rates has been deleted.

DRAFT REPORT - 6.0: MODEL DESIGN

1. Section 6.2, page 129, bottom of page: Please fix the 'stutter sentence' that begins on this page and continues onto page 136.

[Response]: Corrected.

2. Section 6.2, page 136, end of 1st paragraph: Please discuss in more detail assigning active cells beneath the active cells in layer 1 (i.e. how thick and what hydraulic properties were assigned).

[Response]: Text added to section 6.2 to discuss the additional cells: Some of the active cells assigned in layers 2 through 5 are beneath the alluvium of layer 1 but above the uppermost bedrock layer. It was necessary using MODFLOW to create additional active cells in these layers to allow a connection between the alluvium modeled in layer 1 and the underlying bedrock layer. These additional cells are apparent in figures 55 to 58 as narrow northwestward extensions of the active cells of model layers." Additional text on properties added to section 6.4

3. Section 6.2, page 136: In addition to the grid origin, please discuss/present the projection parameters.

[Response]: Added table 9 with projection information.

4. Section 6.3.1, page 17: Please remove discussion of recharge results to the calibration section. This section should only be discussing procedures.

[Response]: Text reorganized between sections 4, 6, and 8. Revised section 6 text focuses on procedures.

5. Section 6.3.2, 3rd paragraph: "Hydraulic conductance is the product of the width, length, and thickness of the alluvium." This is incorrect. Please include the correct definition of hydraulic conductance.

[Response]: Revised to state that "Hydraulic conductance is the function of the width, length, and thickness" and additional explanation added.

6. Section 6.3.3, page 140: "It is applied over a broad area..." Please be more specific.
[Response]: Changed statement and revised two paragraphs to discuss how ET was assigned.

7. Section 6.3.3, page 140: "The two parameters of the ET package in MODFLOW are the maximum ET rate applied at ground surface..." This is incorrect. The ET package assigns an "ET surface," which is not necessarily the ground surface. Please address.

[Response]: Text revised to state that "The parameters of the ET package in MODFLOW are the maximum ET rate, the elevation at which the maximum rate is applied (the ET surface), and the depth below the top of a cell at which the ET is assumed to be zero (extinction depth). While the ET package is turned on for each cell representing the outcrop of a layer, groundwater discharge is indicated only if the elevation of the simulated water level is higher than the elevation of the extinction depth."

8. Section 6.3.5, page 141: "...water levels in the Queen City have remained fairly constant during the past 50 yr." This was not shown in the Hydrologic Setting sections. Please include an analysis of water levels in the Queen City in the Hydrologic Setting section to substantiate this claim.

[Response]: Text added to section 4.4.2 describing the water levels of the Queen City aquifer.

9. Section 6.3.5, page 142: "We accordingly adjusted the GHB boundary to represent a decrease in fluid pressure." In Section 4.4.2, you say that it was beyond the scope of the project to map transient changes in fluid pressure in this zone. If an analysis was done, please include it in Section 4.4.2. If an analysis was not done and heads were adjusted on this boundary, then please discuss how this was done and why.

[Response]: It was incorrectly stated that the GHB boundary was changed. The boundary was kept constant. This has been restated in the revised report.

10. Section 6.3.5, page 142: "The GHB boundary along the southwestern side of the model was kept unchanged for the calibration and verification period..." The parameters assigned to this boundary have not been previously discussed. Please discuss.

[Response]: The parameters assigned to the GHB boundary have been added to section 6.3.4.

11. Section 6.3.5, page 142: "GHB conductance was set to the value of aquifer transmissivity." Hydraulic conductance is not equivalent to transmissivity. Please review how conductance was assigned to the model.

[Response]: GHB conductance has units of length-squared/time (L^2/t), the same as transmissivity. Transmissivity of model cells was used the initial estimate of GHB conductance in model calibration for the northeast and southwest boundaries. Trial-and-error adjustment determined how far the boundary effect would extend into the model area and what value gave the best match to estimated water level.

12. Section 6.3.5, page 142: Please explain why gaps were left in the GHB in the northeastern and southeastern corners of the model.

[Response]: In the draft model we left the interval between the hydro pressured and geopressed domains and lateral no flow boundaries. To close up the gaps in the GHB package we used linear interpolation to assign GHB heads in the convergence zone between the hydro pressured and geopressed domains. This is stated in the revised text.

13. Section 6.3: Please explain what boundary condition was used for the bottom of the model.

[Response]: Text added to state that a no flow boundary was used for the base of the model between the Hooper and Midway.

14. Section 6.3: Please explain what boundary condition was used for the outcrop of the Reklaw Fm.

[Response]: Text added to start of section 6.0 to state that “Boundary values were applied to all six faces of the model (top, bottom, and sides). Boundary conditions for the top or upper surface of model layers variously included MODFLOW’s recharge, stream-flow routing, evapotranspiration (ET), and general-head boundary (GHB) packages. The bottom of the model was set as a no-flow boundary; we assumed there is no appreciable exchange of groundwater between the Hooper and the underlying Midway Formations (fig. 10), both of which have a large proportion of low-permeability claystone. The updip (northwestern) boundary of each layer was also defined as a no-flow boundary. The GHB boundary package was applied to the downdip (southeastern), northeastern, and southwestern sides of the model. The horizontal flow barrier and wells packages of MODFLOW were applied internal to the model.”

15. Section 6.3: Please show a map of active cells in Layer 1.

[Response]: Figure 59 shows the active cells in the revised draft report; we changed the map to better distinguish which cells are active.

16. Section 6.3: Wells are mentioned as a boundary condition in the introduction, but not mentioned in discussion. Please include of wells as boundary conditions.

[Response]: A new section 6.3.6 on wells is included that incorporates some text previously given in section 4.

17. Section 6.3: Please include a discussion of reservoirs and how assigned in model.

[Response]: A new section 6.3.2.2 on Surface-Water Reservoirs has been added.

18. Section 6.3.2: Please discuss whether or not Manning’s roughness coefficient was used in stream-flow routing and what the source of the data was.

[Response]: We used data on surface-water stage heights from USGS gauging stations to define stream stage in the model, rather than selecting the option in the stream-flow routing package of calculating stream stage in reaches from Manning’s equation. Statement added to text.

19. Section 6.4: "Specific yield was assigned as a function of depth and sandstone in the aquifers." Either here or in the Hydrologic Setting section, please discuss this approach in more detail.

[Response]: Section 6.4 includes discussion of how storativity was assigned.

20. Please include a map showing where horizontal flow barriers were used.

[Response]: Figures 54 to 58 now include the HFB package cells.

DRAFT REPORT - 7.0: MODELING APPROACH

1. Page 147: "The increase in range of measured values and the increase in number of measurements mean that apparent model performance improves with time..." This is not a universal occurrence. Please adjust text to reflect this.

[Response]: This was revised to read more clearly as a model-specific rather than general result, and the exceptions were pointed out.

2. Page 147: Please discuss calibration criteria for the steady-state model.

[Response]: Five model criteria are presented in the revised text.

3. Page 147: "The third calibration measure is mapping the residual differences..." "third" should be "second."

[Response]: Corrected.

4. Page 147: There are other required calibration measures: (1) Water balance is less than 1 percent and (2) RMS error for fitting hydrographs. Please include these in the discussion and, in the case of RMS error for hydrographs, in the report.

[Response]: Corrected and added.

DRAFT REPORT - 8.0: STEADY-STATE MODEL

1. Section 8.0, page 149: "...one long time step." Please consider changing this to "...one long stress period."

[Response]: Text changed to "one long (100-yr) stress period."

2. Section 8.1, page 149: Please change "...applied allows enough..." to "...applied allowed enough..."

[Response]: Text changed to "...as initially applied, allowed so much..."

3. Table 7: Please fix formatting for RMSE/h for layer 3, steady-state.

[Response]: Corrected.

4. Table 8: Unclear why Big Creek and Duck Creek are not included in the calibration data set but, in the case of Big Creek, model results are compared to the sum. Please explain.

[Response]: Table 8 renumbered as table 12 and revised. Big Creek had always been included in the calibration data set, the "*" in table 8 of the draft report was a typo. Duck Creek was not in the initial steady state calibration data set but it has been added.

5. Table 8: Please include the percent of estimated base flow for the total base flow.
[Response]: Table 8 (renumbered to 12) revised to include percent of estimated base flow.
6. Tables 8, 9, 10, and 11: Please add "Values rounded to..." to the caption.
[Response]: Corrected.
7. Section 8.2, 1st sentence: Please remove "specific yield" from the list of sensitivity parameters.
[Response]: Corrected.
8. Table 9: Please include a reminder of which layers correspond to which aquifers/formations.
[Response]: All tables and figures that list a number for a layer also include a layer name, although for space reasons we did not include a noun, e.g., Simsboro (5).
9. Section 8.0: Please include a map comparing measured and simulated water levels.
[Response]: The simulated water levels for the Simsboro and Carrizo in the revised report include superposed trace of contours from the estimated water-level maps.
10. Section 8.0: Please include a map showing the residuals between measured and simulated water levels.
[Response]: Residuals (simulated minus observed water levels) have been added for the Simsboro and Carrizo aquifers.
11. Section 8.1, page 150: "Improved model results came from varying the maximum ET rate according to regional trends in net lake-surface evaporation." Unclear if figure 9 was used or a generalization of figure 9. Please clarify. If a generalization was used, please include a map to show final calibrated values.
[Response]: Maximum ET rates are set to the net lake-surface evaporation or 14 in/yr, whichever is greater as described in Section 4 of the report. The same data set was used to build figure 9.
12. Please report the water balance error.
[Response]: The water balance error is included in each budget table and summarized in the text as less than 0.01 percent.
13. Need a discussion on how horizontal flow barriers were calibrated.
[Response]: We state that "Trial-and-error adjustment showed that the steady-state model was not very sensitive to changes in the HFB hydraulic characteristic term. Further tests during the transient model calibration showed no reason to change the initial estimates of the HFB hydraulic characteristic."

DRAFT REPORT - 9.0: TRANSIENT MODEL

1. Section 9.1: Please include a map of measured water levels vs. simulated water levels.

[Response]: The 1990 and 2000 simulated water levels for the Simsboro and Carrizo in the revised report include superposed trace of contours from the estimated water-level maps. Residuals maps also are included.

2. Figure 72: The model does not do well in matching water levels in the northeastern part of the model although it is stated that the model ‘generally’ matches the observed water levels. Please add more discussion as to why this area is error.

[Response]: Revised text adds statement to page 165 of the draft report that “other factors could include errors in pumping rate, storativity, and vertical permeability between the Carrizo and Reklaw layers.

3. Section 9.1: Please include the RMSE for the hydrographs.

[Response]: RMSE and Shift are given in each of the 40 hydrographs shown through 2000.

4. Figure 83: The last three years show the same value for precipitation. Please review and address as appropriate.

[Response]: The latest mappable precipitation data we had available at the start of the project was 1997 and so we use that year’s value for 1998 through 2000. This is mentioned in the text.

5. Please report the water balance error.

[Response]: The water balance error is included in each budget table and summarized in the text as less than 0.01 percent.

6. Table 10: Please include a note on the time period the change in storage represents.

[Response]: Comments have been added to the three water budget tables (steady state, transient, and predictive). In general the annual rates are totals or averages for a year and not extrapolated from part of a year, e.g., a 12-month time step or 12 1-month stress periods. For 1990 we did end up having to extrapolate from a 2.4 month time step to the rest of the year.

7. Section 9.3: Please include several hydrographs showing sensitivity to hydrologic parameters.

[Response]: New figure 104 shows several hydrographs showing sensitivity to hydrologic parameters for the Carrizo and Simsboro. We made other hydrographs; hydrographs are only visibly sensitive if they show large amounts of drawdown.

8. Please include a budget for 1990 and the drought of the 1990s.

[Response]: Table 14b includes a budget for the maximum drought years of 1988 and 1996.

9. Please provide a map of the final calibrated specific storage.

[Response]: Figures 64 to 68 show the final calibrated storativity.

DRAFT REPORT - 10.0: PREDICTIONS

1. Section 10, 1st paragraph: "...pumping rates projected by the Regional Water Planning Groups..." See comment 6 in the DRAFT REPORT- 1.0 INTRODUCTION.

[Response]: [Response]: Text revised to state that the projected pumping rates for 2000 to 2050 were derived from a TWDB analysis of the demands and supplies of surface water and groundwater, along with possible water management strategies, included in the Regional Water Plans prepared by Regional Water Planning Groups.

2. Section 10.1, page 199, 1st paragraph: "... water strategy..." should be "...water management strategy..."

[Response]: Corrected.

3. Section 10.1, page 199, 2nd paragraph: "The model predicts that combining too much pumping in a few closely spaced cells yields simulation results that can include dewatering of cells." Does this mean that the predictive runs include dewatered cells in the large well field areas? If this is the case, then please discuss the implications of this on model results (i.e. underestimated drawdowns).

[Response]: Text rewritten and quoted phrase deleted. In the revised model, about 30 model cells at the updip limit of the outcrop of the Hooper aquitard (layer 6) are simulated as going dry by 2050. These are the only model cells that go dry during the historical and predictive simulations (no cells go dry as of 2000). That these cells go dry in the model reflects the interaction of pumping and recharge rates, cell thickness, specific yield, and hydraulic conductivity assigned to that part of the model. Groundwater withdrawal assigned to these model cells represents mainly rural domestic water use, estimated on the basis of census information. Finding good yields of potable groundwater near the updip limit of the Hooper aquitard can be problematic. Future pumping rates from the updip Hooper most likely will be limited by well yield and water quality.

These cells going dry does have an effect on the water budget, we lose as much as 3,000 acre-ft/yr from the simulation in 2050, mainly from stock and rural domestic pumping, that had been assigned to these edge cells of the outcrop.

4. Section 10: Please include a discussion of how the drought of record was defined and how it compares to normal precipitation.

[Response]: Draft report section 2.1 on physiography and climate stated that the period from 1954 through 1956 included 3 of the 10 driest years since 1940 and can be defined as the drought of record for the area (fig. 8). The driest years during the decades of the 1980s and 1990s were 1988 (average of 29.4 inches/yr) and 1996 (average of 38.1 inches/yr).

We also point out in section 6.1 that recharge rate was assigned to future drought years using according to the difference between precipitation in those drought years and the average (1960 to 1997) precipitation rate, the same methodology for assigning recharge as a function of precipitation and soil characteristic for any year. Monthly recharge during the drought years was kept uniform because we assume that drainage from the unsaturated zone to the water table does not cease during a drought year.

5. Please change "Simsboro" in the captions of figures 94 through 98 to "Carrizo."
[Response]: Corrected.

6. Table 11: Pumping rates do not agree with those shown in Table 5. Please address.

[Response]: Some of the difference was rounding error, some was more dry cells in the draft version of the model. There remains a slight difference (<1 percent) between revised tables 5 and 16, which replace tables 5 and 11, which probably relate to the 30 Hooper cells going dry.

7. Table 11: Parts of Table 11 do not agree with model output.

[Response]: Some difference may be from draft version of the flow model saved for the data model that incorporated corrections and improvements after the draft report had already been committed to production.

8. Table 11: Please specify which stress period the budgets apply to (i.e. the last monthly stress period or the sum of the 12 stress periods for a year).

[Response]: Comment added to table stating that the budget is calculated from sum of the 12 1-month stress periods that make up each decadal-year simulation.

9. Figure 101: Please label what (a) and (b) are.

[Response]: Parts (a) and (b) are identified in the caption.

DRAFT REPORT - 11.0: LIMITATIONS OF THE MODEL

1. Section 11.2, page 215, 1st bullet: Extraneous period occurs after Wilcox in three places.

[Response]: Corrected.

DRAFT REPORT - 12.0: FUTURE IMPROVEMENTS

1. 2nd paragraph: "In some cases there are significant discrepancies between the estimates for future pumping developed by the regional water planning groups and the TWDB that need to be resolved." The RWPGs did not develop datasets for future pumping. Please revise this statement.

[Response]: Sentence was deleted.

2. Page 219, 1st bullet: Please specify who in the Federal government.

[Response]: Reference is revised to cite publication by Neuzil (1994) on assessment of low-permeability materials.

3. Page 220, 1st bullet: “Additional research is needed for water quality”
Please add 'for.'
[Response]: Corrected.

DRAFT REPORT - 13.0: CONCLUSIONS

No comments

DRAFT REPORT - APPENDIX A

1. Section A-3.1: All of the superscripts in this section are not “super,” they need to be raised. Specifically degree symbols and mass numbers.
[Response]: Corrected.

DRAFT REPORT - APPENDIX B

1. Page B-4, equation 1: Please define ‘dh.’
[Response]: The term ‘dh,’ with units of length (L) was defined in the draft report in the line immediately following equation (1).
2. Page B-4, equation 2: Is it ‘m’ as shown in the equation or ‘M’ as in the definition?
[Response]: Corrected; lower case changed to upper case.

DRAFT REPORT - FIGURES

The following figures are not readable when photocopied in black and white (see RFP Attachment 1 page 25/40, “figures shall be designed such that a black and white photocopy is readable”). If possible please use different line types, symbols, or shades of gray rather than different colors:

Figures 11, 12, 13, 34, 44, 48, 50, 52, 53, 54, 64, 70, 76

[Response]: Per discussion with the Project Manager, it is our understanding that the original TWDB intent was that color figures be readable when printed as an original to a standard office-quality black and white printer, as has been set for the reporting standard in the 2002 GAM technical specifications. We believe these figures meet this requirement.

DRAFT REPORT - MODEL

No comment. Model runs, although there are some differences between the water budget in the model and the budget presented in the report.

CZWX c GAM Review – Part B: Project Data

Did we get all of the data files we requested? No
Is the data organized in the way we requested? No

Introduction:

It is imperative that we receive enough source data to completely rebuild the groundwater model from scratch and reproduce all report figures and tables should it be necessary. In other words, if a new model grid resolution and/or orientation was needed, there should be sufficient data to create a new model for the study area. Moreover, there should be enough data to regenerate any or all of the intermediate derivative data with updated information. This source and intermediate derivative data should be organized under the SRCDATA folder/directory according to the guidelines set forth in Attachments 1 & 2 of the RFP. An empty directory tree structure was provided to facilitate the organization of the project data. The empty directory tree structure is available for download in zip format at http://www.twdb.state.tx.us/gam/resources/gam_tree.zip.

It is also required that all final model parameter and variable/stress data be delivered in a database format that can easily be referenced to each and every model grid cell. In other words, there should be enough cell-referenced data to regenerate all or update any individual cell value of the required MODFLOW or PMWIN input files. The file format of these databases may be in Excel 97, Access 97, or in an ESRI GIS format compatible with ArcView 3.2 or ArcInfo 7.21. Each sheet, table, or coverage should be attributed with the appropriate model grid cell-reference information as set forth in Attachments 1 & 2 of the RFP. These data sets should be organized under the GRDDATA folder directory and within the appropriate sub-folders/directories. The GRDDATA OUTPUT folder and its sub-folders/directories may be omitted or left empty.

Finally, the actual MODFLOW 96 and PMWIN 5.0 formatted files for both INPUT and OUTPUT must be organized as set forth in Attachments 1 & 2 of the RFP. Separate folders/directories must be used for 1) the calibrated steady-state model files; 2) the calibrated transient model files; 3) the verification transient model files; 4) and each of the decadal transient predictive model simulation run files.

Review Summary:

The data provided by the CZWX_c contractor are missing some required data sets as listed in sections below. Listing files are needed within each folder/directory listing all file names or groups of file names and their contents. Contractor did not follow data model organization as requested in RFP.

[Response]: It is our understanding that we need to provide files and documentation in the format and software used for their construction. Data sets worked up in Excel or Surfer will be reported in Excel or Surfer. It is not required to construct ArcView coverages solely for the purpose of providing a GIS coverage if that data was otherwise developed. Access was not much used during this project.

Hard copy listing files were provided with the data model; digital versions of the file listings will be included in the final data model.

Some metadata files had incorrect spatial reference information or missing altogether. Metadata files should include enough information to determine data source, data processing methods, data units, and correct spatial parameters (for GIS coverages) for each data set, table, worksheet, and/or coverage. Moreover, the GIS coverages may have been projected with incorrect NAD 27 datum instead of correct NAD 83 datum since state and county coverages do not match exactly with TWDB state and county GAM coverages. The datum error results in various horizontal shifts from less than 100 ft. to more than 3,000 ft in various directions in various places.

[Response]: It is our understanding the 100 to 3,000 ft error originated from our using TWDB data early in the project that had been posted on the TWDB website with truncated projection reference information. BEG had discovered this error in related work for the SHP Ogallala GAM project and passed this information along through that contractor to the TWDB, after which the web site information was changed. Unfortunately, this error was not brought to the attention of the CW-c GAM project team and it was not previously corrected. The cited spatial shift is the same as that observed resulting from the truncation errors.

Our corrective action has been to redownload and save to the data model as many coverages as possible to recreate. Not all of the sequence of calculations could be followed through late in the project for all coverages. Few of the coverages using TWDB data with this error had a significant effect on model design or results. The shift is small compared to model grid-cell size and especially with respect to the large distances between control data.

The NAD27 versus NAD83 issue we believe is a different problem. The NAD27 labels in the metafiles are incorrect in most if not all cases and are being corrected in the revised data model. We had used a software package to automatically generate the metadata files; it defaulted the NAD27 statement for all files. This is corrected in the revised data model.

File nomenclature is inconsistent such that it is extremely difficult to associate data files with metadata files. Consistency should be kept throughout with regard to file suffix (ie. .TXT or .MET). Furthermore, file prefix should be same for metadata file as for its associated data file(s). Additional comments below listed under expected data model organization.

[Response]: The revised data model includes more consistency in file naming.

Pumpage data sets are unacceptable due to missing data fields and poor or missing documentation.

[Response]: Additional data and documentation are being included in the several file sets used to generate the pumping input files for the model.

DRIVE:\CZWX_c\grddata\input\hydraul

NO DATA OR FOLDER FOUND – model cell-referenced hydraulic parameters should go here.

[Response]: The input, output, and documentation of ArcView, Surfer®, Excel, and Fortran-based calculations that generated the values of horizontal and vertical permeability will be loaded into this directory.

DRIVE:\CZWX_c\grddata\input\ibnd

Need a listing file listing name of each file or grouped set of files and their contents or purpose within each folder.

[Response]: Digital versions of the file listings will be included in the final data model for this directory.

Access97 database is acceptable except for needed metadata file describing fields and field units.

[Response]: ASCII files will be used to present metadata information on data fields and field units

DRIVE:\CZWX_c\grddata\input\stress\ststate\drns

NO DATA OR FOLDER FOUND – model cell-referenced hydraulic parameters should go here along with required documentation.

[Response]: No drain package was used in the model.

DRIVE:\CZWX_c\grddata\input\stress\ststate\evt

NO DATA OR FOLDER FOUND – model cell-referenced hydraulic parameters should go here along with required documentation.

[Response]: The TWDB data on net lake evaporation was used to estimate maximum ET rate. Gridded data based on this information are included in this directory.

ET input parameters were constant through time; they did not vary with stress period and are the same for steady state, transient, and predictive models. The same files and documentation will be placed in the respective folders to make them available for each model.

DRIVE:\CZWX_c\grddata\input\stress\ststate\rech

Difficult to ascertain whether this data is actually in grid format due to lack of documentation. More detailed documentation is needed to explain each of the Excel files and final recharge values. For example, what are the files ppte_avr_1951-1997_3avr.xls and Set-Rech-File2.1.xls used for? What values are used for drought of record periods of the predictive simulations? The recharge files need much more organization as detailed under by Attachment 2 of RFP.

[Response]: The same methodology was used for estimating recharge for the steady state, transient, and predictive models. The key information for generating recharge input for the model include (1) maps of precipitation through time by model cell, derived from NWS station measurements, and (2) soil permeability, derived from STATSGO coverage. Calculations from the derived gridded data were done in Excel. These files and

documentation will be placed in the respective folders to make them available for each model.

File names will be simplified and tied to metafile information more clearly with consistent naming.

DRIVE:\CZWX_c\grddata\input\stress\ststate\res

NO DATA OR FOLDER FOUND – model cell-referenced reservoir package parameters should go here.

[Response]: There were no reservoirs in the steady state (1850-1950) model.

DRIVE:\CZWX_c\grddata\input\stress\ststate\strm

NO DATA OR FOLDER FOUND – model cell-referenced stream package parameters should go here along with required documentation.

[Response]: Streamflow routing input parameters were constant through time; they did not vary with stress period and are the same for steady state, transient, and predictive models. The same files and documentation will be placed in the respective folders to make them available for each model.

We will provide an Excel file listing model cell-referenced stream package parameters with required documentation.

DRIVE:\CZWX_c\grddata\input\storage

NO DATA OR FOLDER FOUND – model cell-referenced hydraulic parameters should go here along with required documentation.

[Response]: We generated storativity values for the model grid in Excel. These files will be placed here with documentation.

DRIVE:\CZWX_c\grddata\input\stress\ststate\well

Need a listing file listing name of each file or grouped set of files and their contents or purpose within each folder.

[Response]: There was no pumping in the steady-state (1850-1950) model.

The Excel spreadsheets for calibration and predictive pumpage are acceptable but each need a metadata file describing fields and field units. Pumpage data sets must contain WUG_ID and WUG_Name relationship as specified by RFP.

The predevelopment municipal pumpage Excel file has no reference to model cell_id, row, or column as required by Attachment 2 of RFP. Other ASCII pumpage data also have no reference to model cell_id, row, or column as required by Attachment 2 of RFP. None of the predevelopment data sets have metadata files associated with them.

DRIVE:\CZWX_c\grddata\input\stress\trans\drns

NO DATA OR FOLDER FOUND – model cell-referenced hydraulic parameters should go here along with required documentation.

[Response]: No drain package was used in the model.

DRIVE:\CZWX_c\grddata\input\stress\trans\evt

NO DATA OR FOLDER FOUND – model cell-referenced hydraulic parameters should go here along with required documentation.

[Response]: The TWDB data on net lake evaporation was used to estimate maximum ET rate. Gridded data based on this information are included in this directory.

ET input parameters were constant through time; they did not vary with stress period and are the same for steady state, transient, and predictive models. The same files and documentation will be placed in the respective folders to make them available for each model.

DRIVE:\CZWX_c\grddata\input\stress\trans\rech

Difficult to ascertain whether this data is actually in grid format due to lack of documentation. More detailed documentation is needed to explain each of the excel files and final recharge values. For example, what are the files ppte_avr_1951-1997_3avr.xls and Set-Rech-File2.1.xls used for? What values are used for drought of record periods of the predictive simulations? The recharge files need much more organization as detailed under by Attachment 2 of RFP.

[Response]: The same methodology was used for estimating recharge for the steady state, transient, and predictive models. The key information for generating recharge input for the model include (1) maps of precipitation through time by model cell, derived from NWS station measurements, and (2) soil permeability, derived from STATSGO coverage. Calculations from the derived gridded data were done in Excel. These files and documentation will be placed in the respective folders to make them available for each model.

File names will be simplified and tied to metafile information more clearly with consistent naming.

DRIVE:\CZWX_c\grddata\input\stress\trans\res

NO DATA OR FOLDER FOUND – model cell-referenced reservoir package parameters should go here along with required documentation.

[Response]: Information on reservoirs used to select the model cells to which reservoirs were assigned will be listed in this directory. The limited coverage on reservoirs, consisting of where reservoirs are in order to assign those reservoirs > 1 cell, will be added.

DRIVE:\CZWX_c\grddata\input\stress\trans\strm

NO DATA OR FOLDER FOUND – model cell-referenced stream package parameters should go here along with required documentation.

Streamflow routing input parameters were constant through time; they did not vary with stress period and are the same for steady state, transient, and predictive models. The same files and documentation will be placed in the respective folders to make them available for each model.

DRIVE:\CZWX_c\grddata\input\stress\trans\well

Need a listing file listing name of each file or grouped set of files and their contents or purpose within each folder.

[Response]: We created master input files of pumping rates for the transient model and the predictive model. These revised files will be placed here with documentation.

The Excel spreadsheets for calibration and predictive pumpage are acceptable but each need a metadata file describing fields and field units. Pumpage data sets must contain WUG_ID and WUG_Name relationship as specified by RFP.

[Response]: Documentation and metadata files on pumping rates will be provided with WUG_ID and WUG_Name relationship.

The predevelopment municipal pumpage Excel file has no reference to model cell_id, row, or column as required by Attachment 2 of RFP. Other ASCII pumpage data also have no reference to model cell_id, row, or column as required by Attachment 2 of RFP. None of the predevelopment data sets have metadata files associated with them.

[Response]: The Excel file will have an added key column with the required model cell_id information.

DRIVE:\CZWX_c\grddata\input\struct

Need a listing file listing name of each file or grouped set of files and their contents or purpose within each folder.

[Response]: We will provide a file with grid cell bottom and top listed with respect to model cell_id and associated metadata files.

Access97 database is acceptable except for needed metadata file describing fields and field units.

DRIVE:\CZWX_c\modflow\modfl_96\input\ststate

Need a listing file listing name of each file or grouped set of files and their contents or purpose within each folder.

There is only one set of MODFLOW formatted files and cannot easily determine whether they are for steady-state, transient, or predictive run(s). Steady-state is assumed. Need more documentation for these files.

[Response]: It is our understanding that the requirement is that the steady state model be incorporated as the first long stress period of the transient model so that any future

changes will be readily incorporated. Therefore, the steady state model is the first stress period of the transient model. We have not separated these models for the purpose of the data model. The same MODFLOW files will be saved here as in the DRIVE:\CZWX_c\modflow\modfl_96\input\trans directory.

DRIVE:\CZWX_c\modflow\modfl_96\input\trans

NO DATA OR FOLDER FOUND – MODFLOW formatted ASCII files for transient runs should go here along with required documentation.

[Response]: It is our understanding that the requirement is that the steady state model be incorporated as the first long stress period of the transient model so that any future changes will be readily incorporated. Therefore, the first stress period of the transient model is the steady state run (100-yr long). We have not separated these models for the purpose of the data model. The same MODFLOW files will be saved here as in the DRIVE:\CZWX_c\modflow\modfl_96\ input\ststate directory.

DRIVE:\CZWX_c\modflow\modfl_96\input\pred

NO DATA OR FOLDER FOUND – MODFLOW formatted ASCII files for predictive runs should go here along with required documentation.

[Response]: The multiple predictive (2010, 2020, 2030, 2040, and 2050) MODFLOW model files will be saved here.

DRIVE:\CZWX_c\modflow\pmwin_50\input\ststate

Need a listing file listing name of each file or grouped set of files and their contents or purpose within each folder.

There is only one set of PMWIN5.0 formatted files and cannot easily determine whether they are for steady-state, transient, or predictive run(s). Steady-state is assumed. Need more documentation for these files.

[Response]: It is our understanding that the requirement is that the steady state model be incorporated as the first long stress period of the transient model so that any future changes will be readily incorporated. Therefore, the steady state model is the first stress period of the transient model. We have not separated these models for the purpose of the data model. The same PMWIN-5.3 files will be saved here as in the DRIVE:\CZWX_c\modflow\modfl_96\input\trans directory.

DRIVE:\CZWX_c\modflow\pmwin_50\input\trans

NO DATA OR FOLDER FOUND – PMWIN5.0 formatted files for transient runs should go here along with required documentation.

[Response]: It is our understanding that the requirement is that the steady state model be incorporated as the first long stress period of the transient model so that any future changes will be readily incorporated. Therefore, the first stress period of the transient model is the steady state run (100-yr long). We have not separated these models for the

purpose of the data model. The same PMWIN-5.3 files will be saved here as in the DRIVE:\CZWX_c\modflow\modfl_96\input\ststate directory.

DRIVE:\CZWX_c\modflow\pmwin_50\input\pred

Need a listing file listing name of each file or grouped set of files and their contents or purpose within each folder.

PMWIN5.0 formatted files for predictive runs should go here along with required documentation.

[Response]: The multiple predictive (2010, 2020, 2030, 2040, and 2050) PMWIN-5.3 model files will be saved here.

DRIVE:\CZWX_c\modflow\pmwin_50\refdx

Need a listing file listing name of each file or grouped set of files and their contents or purpose within each folder.

[Response]: Digital versions of the file listings will be included in the final data model for this directory and information the contents or purpose of each file will be included.

DRIVE:\CZWX_c\scrdata\bndy

Need a listing file listing name of each file or grouped set of files and their contents or purpose within each folder.

[Response]: Digital versions of the file listings will be included in the final data model for this directory and information the contents or purpose of each file will be included.

Coverages may have incorrect spatial projection parameter (Datum should be NAD 83 instead of NAD 27).

[Response]: Please see comment in review summary.

Missing coverages for counties, census, and any other boundary(s) used in study or report.

[Response]: Coverage for counties, census, and any other boundaries will be moved or copied into this directory.

DRIVE:\CZWX_c\scrdata\clim

Need a listing file listing name of each file or grouped set of files and their contents or purpose within each folder.

[Response]: Digital versions of the file listings will be included in the final data model for this directory and information the contents or purpose of each file will be included.

Coverages may have incorrect spatial projection parameter (Datum should be NAD 83 instead of NAD 27).

[Response]: Please see comment in review summary.

If modelcells_Netevaporation.xls was used for ET package, it should be located under DRIVE:\CZWX_c\grddata\input\stress\trans\evt folder.

[Response]: The files will be moved to the appropriate location.

The NOAA_annualppt_bystation_allmodelboxes.xls file needs further explanation for each of the worksheets as well as purpose of this data set.

[Response]: Additional information will be provided for this and related files.

Unsure what purpose of modelgrid_mergedwith_soil&k&ppt.xls data is for (recharge or soils analysis?). This data set needs more detailed documentation with regard to purpose and processing method(s) for each worksheet. This data set also appears to be a copy of same named file under SOILS folder.

[Response]: This is a master file that brought together key information on precipitation and soils that was used to calculate recharge. Thus it has potential cross-listing value and was included in more than one directory. Additional information on the file and its purpose will be included.

DRIVE:\CZWX_c\scrdata\cnsv

Need a listing file listing name of each file or grouped set of files and their contents or purpose within each folder.

[Response]: Digital versions of the file listings will be included in the final data model for this directory and information the contents or purpose of each file will be included.

Coverages may have incorrect spatial projection parameter (Datum should be NAD 83 instead of NAD 27).

[Response]: Please see comment in review summary.

Missing landuse coverage and associated documentation.

[Response]: Land use is one of the main conservation-file coverage. Its information will be relocated to this directory.

DRIVE:\CZWX_c\scrdata\geol

Need a listing file listing name of each file or grouped set of files and their contents or purpose within each folder.

[Response]: Digital versions of the file listings will be included in the final data model for this directory and information the contents or purpose of each file will be included.

Coverages may have incorrect spatial projection parameter (Datum should be NAD 83 instead of NAD 27).

[Response]: Please see comment in review summary.

Data sets under NET_SANDS folder should be located under the DRIVE:\CZWX_c\scrdata\subhyd folder.

[Response]: The files will be moved to the appropriate location.

Need structural surfaces interpreted from source point data sets.

[Response]: Several disparate data sets used to map structure surface are spatially dissimilar, so merging them required both GIS and geostatistical software packages. Layer elevations were checked for vertical consistency by mapping layer thickness calculated with a triangulated irregular network method in AutoCAD. False points inserted at appropriate locations corrected areas with a vertical discrepancy. Layer elevations were extended to areas lacking geophysical control data by kriging layer thickness, recalculating layer elevations from the kriged surface, and merging the recalculated elevation surface into data-poor areas. The interpreted surface, therefore, was actually a back-calculation directly into the model grid cells.

No cross-sections used in study? If yes, cross-sections must be provided under this folder.

[Response]: Cross sections were prepared using paper photocopies of geophysical logs hung together on room-sized poster sections. Visual information from the sections was used to guide the contouring of structure data in map view. These cross sections were scanned and traced for the purpose of generating figures 15 and 16 in the report.

DRIVE:\CZWX_c\scrdata\geom

Need a listing file listing name of each file or grouped set of files and their contents or purpose within each folder.

[Response]: Digital versions of the file listings will be included in the final data model for this directory and information the contents or purpose of each file will be included.

Coverages may have incorrect spatial projection parameter (Datum should be NAD 83 instead of NAD 27).

[Response]: Please see comment in review summary.

A physiography coverage is required by RFP.

[Response]: Please see comment in review summary. The study area lies entirely within the Interior Coastal Plains, part of the Gulf Coastal Plain, as stated in the draft report. A digitized version of a physiographic map was not required for development of the conceptual model or flow model.

DRIVE:\CZWX_c\scrdata\geop

NO DATA FOUND – geophysical data should go here if used in study.

[Response]: No digitized geophysical data were obtained for this study.

DRIVE:\CZWX_c\scrdata\soil

Need a listing file listing name of each file or grouped set of files and their contents or purpose within each folder.

[Response]: Digital versions of the file listings will be included in the final data model for this directory and information the contents or purpose of each file will be included.

Coverages may have incorrect spatial projection parameter (Datum should be NAD 83 instead of NAD 27).

[Response]: Please see comment in review summary.

The data set modelgrid_mergedwith_soil&k&ppt.xls needs more detailed documentation with regard to purpose and processing method(s) for each worksheet.

[Response]: This is a master file that brought together key information on precipitation and soils that was used to calculate recharge. Thus it has potential cross-listing value and was included in more than one directory. Additional information on the file and its purpose will be included.

DRIVE:\CZWX_c\scrddata\subhyd

Need a listing file listing name of each file or grouped set of files and their contents or purpose within each folder.

[Response]: Digital versions of the file listings will be included in the final data model for this directory and information the contents or purpose of each file will be included.

Coverages may have incorrect spatial projection parameter (Datum should be NAD 83 instead of NAD 27).

[Response]: Please see comment in review summary.

The various “county”.xls files all need a column header in addition to correct metadata documentation for each file. They appear to be data dumps from the TWDB groundwater database.

[Response]: The “county”.xls files were much used as a reference during this study. For example, to check whether reported formation of observation water wells were in the correct layer when they seemed to be out of calibration. Each county file has the basic information on well data, water levels, and water quality. The files are as downloaded from the TWDB web site, where they are posted without header information. We will add information from the TWDB Groundwater Data Dictionary defining the respective column headings.

Some of the header information is also missing from the calvertblufftds228_gam.shp point coverage.

[Response]: This will be corrected.

Need source and intermediate derivative coverages used to spatially distribute stock, irrigation, and domestic other pumpage data. Pumpage data sets must contain WUG_ID and WUG_Name relationship as specified by RFP. Pumpage data must also be related to model layer(s).

[Response]: The various intermediate files in constructing the master pumping input files will be included and described and will include WUG_ID and WUG_Name information.

Layer information is saved in the final pumping master file. Layer assignments for specific wells were checked by comparing aquifer code, if present, to position of the bottom of the well and layer elevation surfaces. Non-point source pumping was assigned on the basis of layer elevation and other assumptions.

Need spatially distributed water levels interpreted from point data as used in report.
[Response]: We will provide the data files used in making maps and the derived Surfer files.

Need spatially distributed conductivity fields interpreted from point data as used in report.
[Response]: Hydraulic conductivity maps were composed from Mace and others (2000) point data, Ayers and Lewis (1985) maps of sandstone thickness, and digitized tracing of hand-drawn contours. These information were gridded in Surfer and back interpolated to the model grid. Further subjective adjustments were made during model calibration in the PMWIN and Excel environments.

Need spatially distributed specific yield and porosity fields if available and/or used in report.
[Response]: We will include the data from Mace and others (2000) in this directory.

Need to specify point coverage used for target water levels and hydrographs used for calibration and verification.
[Response]: We will include the ArcView shape files that listed the ~97 wells for which hydrographs were constructed. Hydrographs were built in Excel using a macro, which will be provided. Of these hydrographs we chose 40 that were representative for inclusion in the report.

DRIVE:\CZWX_c\scrddata\surhyd

Need a listing file listing name of each file or grouped set of files and their contents or purpose within each folder.
[Response]: Digital versions of the file listings will be included in the final data model for this directory and information the contents or purpose of each file will be included.

The GAM Reservoir Package Data_0729.xls and GAM Reservoir Package Data_0729.xls model grid referenced data sets and their associated metadata files belong in their appropriate folders under the folder
DRIVE:\CZWX_c\grddata\input\stress\ as required by Attachment 2 of RFP.

[Response]: The files will be moved to the appropriate location.

The Base Flow Index (BFI) computer program used to generate baseflow estimates must be included along with documentation.
[Response]: BFI is a public domain program and will be provided in a zipped format.

The watershed_clipped_streams shape file does not appear to have complete coverage of study area nor is its purpose understood. Need better documentation and possibly complete coverage.

[Response]: We will download a new coverage of streams and provide in the data model to replace this.

Coverages may have incorrect spatial projection parameter (Datum should be NAD 83 instead of NAD 27).

[Response]: Please see comment in review summary.

Metadata files needed for each ArcView coverage rather than one metadata file for all coverages in addition to needing full spatial data parameter information (ie. NOT just “GAM coordinate system”).

[Response]: Metadata files needed for each ArcView coverage will be provided.

Some of the coverages belong under the DRIVE:\CZWX_c\scrdata\bndy\ folder such as the tx_cntys_2m_albers, tx_state_2m_albers, grid_gam, and carizo_gam shape files.

[Response]: The files will be moved to the appropriate location.

Finally, it appears that the coverages may not have been projected correctly since the state and county coverages do not match up exactly with GAM coordinate system.

[Response]: Please see comment in review summary.

DRIVE:\CZWX_c\scrdata\tran

Need a listing file listing name of each file or grouped set of files and their contents or purpose within each folder otherwise, these files are acceptable.

[Response]: Digital versions of the file listings will be included in the final data model for this directory and information the contents or purpose of each file will be included.

Coverages may have incorrect spatial projection parameter (Datum should be NAD 83 instead of NAD 27).

[Response]: Please see comment in review summary.

DRAFT FINAL REPORT

Comments pertaining to the Draft Final Report were provided on February 6, 2003. Comments in quotes (“ ”) paraphrase comments previously made on the Draft Report as cited above in this appendix. Numbering refers to original numbering of comments on the Draft Report. Page numbers refer to pages in the Draft Final Report.

DRAFT REPORT - OVERALL COMMENTS

4. "Additional discussion on how the predictive pumping was assigned would be useful and was requested by a stakeholder." Please change "...water user groups listed in the WUG's listed in the SWP..." on p. 157 to "...water user groups listed in the SWP..." or something appropriate.

[Response]:Redundancy eliminated and text revised to state “ water user groups listed in the SWP...”

DRAFT REPORT- 2.0 STUDY AREA

5. "Figures 7, 8, and 9: Please add a reference to the data source to the figure." This comment was not addressed. Reference cited in comment, but the figures still require a reference.

[Response]:References given in responses to comments have been added to the figure captions.

DRAFT REPORT - 4.0: HYDROLOGIC SETTING

11. "Section 4.4.1, page 55: Unclear how reported water levels in the College-Bryan Station well field were adjusted. Please explain in more detail." Please also include a page number for the Anderson and Woessner reference.

[Response]:The citation to Anderson and Woessner (1992, p. 147-149) has been added to the text.

DRAFT REPORT - 6.0: MODEL DESIGN

5. "Section 6.3.2, 3rd paragraph: 'Hydraulic conductance is the product of the width, length, and thickness of the alluvium.' This is incorrect. Please include the correct definition of hydraulic conductance." Hydraulic conductance is also a function of hydraulic conductivity.

[Response]:The text has been revised to state that “ hydraulic conductance is a function of the length, width, thickness, and hydraulic conductivity of the alluvium...(Harbaugh and McDonald (1996).”

11. "Section 6.3.5, page 142: 'GHB conductance was set to the value of aquifer transmissivity.' Hydraulic conductance is not equivalent to transmissivity. Please review how conductance was assigned to the model." Although the dimensions of

hydraulic conductance and transmissivity are the same, they are very different parameters with potentially different magnitudes. Conductance is the product of hydraulic conductivity and cross-sectional area of flow divided by the length of the flow path. Transmissivity is the product of hydraulic conductivity and the thickness of the aquifer. We do not find discussion on how GHB conductance was adjusted in the discussion of the steady-state calibration although the text here suggests some assigned values with initial values.

[Response]: This comment involves several points that are clarified in the revised text (see page 148 in Final Report):

(1) The use of transmissivity as an initial estimate of GHB conductance applies only to the NE and SW lateral boundaries of the model. The downdip and layer 2 GHB boundaries are handled differently, as discussed in several following paragraphs. This accounts for the 'potentially different magnitudes' perceived in the comment. GHB conductance on the NE and SW lateral boundaries is much greater than on the downdip boundary.

2) The approximation of GHB conductance by transmissivity is by analogy to Darcy's Law. The GHB conductance for the northeast and southwest boundaries may be envisioned as the product of hydraulic conductivity, cell thickness, and row width, divided by column width.

3) Calibration of GHB conductance is mentioned in chapters 8 and 9. Since the GHB boundary on the north side is mainly used to represent the drawdown of water levels outside of the model, for example in a well field near Tyler, Smith County, Texas, adjustment of the GHB boundary was done in the transient model rather than the steady state model. The model was not very sensitive to change of the GHB conductance by ± 10 percent, so we marked how far into the model water levels would appreciably change with change in GHB conductance and left the GHB conductance the same as transmissivity.

DRAFT REPORT - 9.0: TRANSIENT MODEL

3. "Section 9.1: Please include the RMSE for the hydrographs." The correction caused Figure 93 to lose the lines of simulated results.

[Response]: The RMSE and shift hydrograph information have been restored:

CZWX c GAM Review – Part B: Project Data

Our review of the contractor's response to our comments project data will occur when the files are delivered.

APPENDIX D-ADDENDUM

RESPONSES TO TECHNICAL AND ADMINISTRATIVE COMMENTS ON THE FINAL TECHNICAL REPORT

Comments pertaining to the Draft Report were provided on December 12, 2002. Additional comments on the Draft Final Report are appended at the end of the list contained in Appendix D. The following responses are to comments on the Final Report provided on March 26, 2003.

FINAL REPORT REVIEW:

1. No additional comments. However, the comments on the model may affect tables in the report.

[Response]: There is one typographical error on table 13 and one on table 14a. In addition, a clarifying note could be added to the title of table 14a. These corrections could be accomplished with an errata page and the three revised table sheets included on an additional CD.

MODEL REVIEW:

1. Model results do not appear to match results shown in tables in the report. Specific comments:

[Response]: Most review observations are based on choosing one part of the model output to estimate the average annual rates, whereas BEG generally summed total annual rate for calculating the table numbers. So mostly there is no need for table revision as the numbers are correct. There are two minor typographical errors to be corrected.

- Steady-state run (Table 13, 14a)

Data match model run results except GHB for layer 3.

[Response]: Errata. The data entry for Carrizo (3) under column GHB NE boundary should be -0.9 instead of -9.

- 1988 (Table 14b)

Well pumpage (layers 3-5), cross-formational flow (layer 1) , and change in storage (layers 3 and 5) deviate significantly from model results.

[Response]: (1)Errata. The data entry for Alluvium (1) under column Cross-formational flow should be 26.7 instead of 0.

(2) The change in storage number is correct as given in the table. As stated in the table, annual rates are totaled from 12 1-month long time steps. We understand TWDB has looked at the last (or first?) time step only and extrapolated to the annual average rate, which results in a different value.

- 1990 (Table 14a)

Change in storage (layer 2) differs from model results.

[Response]: The change in storage number is correct as given in the table. As stated in the table, annual rates are projected from the last 2.4-month long time step for 1990. We understand TWDB used the first time step in making this comment. Line 3 of the table title could be changed to read “budgets and projected from a the last 2.4-month long time step for 1990. (delete strikethrough, insert underlined text).

- 1996 (Table 14b)

Well pumpage and change in storage (layers 3 and 5) differ significantly from model run.

[Response]: The numbers for well pumpage and change in storage are correct as given in the table. As stated in the table, annual rates are totaled from 12 1-month long time steps. We understand TWDB used the first time step in making this comment, and that accounts for the perceived disparity.

- 2010 (Table 16)

Well pumpage (layers 3, and 5) and change in storage (layers 3 and 5) differ from model results.

[Response]: The numbers for well pumpage and change in storage are correct as given in the table. As stated in the table, annual rates are totaled from 12 1-month stress periods. We understand TWDB used one stress period for 2010 in making this comment, and that accounts for the perceived disparity.

- 2020 (Table 16)

Well pumpage (layers 3 and 5) and change in storage (layers 3 and 5) differ from model results.

[Response]: The numbers for well pumpage and change in storage are correct as given in the table. As stated in the table, annual rates are totaled from 12 1-month stress periods. We understand TWDB used one stress period for 2020 in making this comment, and that accounts for the perceived disparity.

- 2030 (Table 16)

Well pumpage (layers 3 and 5) and change in storage (layers 3 and 5) differ from model results.

[Response]: The numbers for well pumpage and change in storage are correct as given in the table. As stated in the table, annual rates are totaled from 12 1-month stress periods. We understand TWDB used one stress period for 2030 in making this comment, and that accounts for the perceived disparity.

- 2040 (Table 16)

Well pumpage (layers 3 and 5) and change in storage (layers 3 and 5) differ from model results.

[Response]: The numbers for well pumpage and change in storage are correct as given in the table. As stated in the table, annual rates are totaled from 12 1-month stress periods. We understand TWDB used one stress period for 2040 in making this comment, and that accounts for the perceived disparity.

- 2050: Average (Table 16)

Well pumpage (layers 3 and 5) and change in storage (layers 3 and 5) differ from model results.

[Response]: The numbers for well pumpage and change in storage are correct as given in the table. As stated in the table, annual rates are totaled from 12 1-month stress periods. We understand TWDB used one stress period for 2050 in making this comment, and that accounts for the perceived disparity.

- 2050: Drought (Table 16)

Well pumpage (layers 3 and 5) and change in storage (layers 3 and 5) differ from model results.

[Response]: The numbers for well pumpage and change in storage are correct as given in the table. As stated in the table, annual rates are totaled from 12 1-month stress periods. We understand TWDB used one stress period for 2050 in making this comment, and that accounts for the perceived disparity.

- Net recharge values in the report do not agree with the model.

[Response]: The statement given on page 225, “*Net recharge was estimated by summing the simulated fluxes across the flow faces of model cells at the boundary between the unconfined and confined zones; this tally takes into account cross-formational flow and change in storage in the unconfined zone.*” is correct. This estimate of net

recharge cannot be calculated from the information presented in tables 13, 14, or 16 because the components of cross-formational flow and change in storage for the unconfined part of the aquifers and aquitards is not separately listed. The number in the table is not the sum of 'Recharge' minus 'ET' minus 'Stream leakage.' It may be appropriate to revise perhaps as an Errata, the sentence on page 193 that says, "*Net recharge, defined here as gross recharge minus groundwater ET minus discharge to streams and rivers, is the amount of groundwater that moves from the outcrop into the confined part of the aquifer or is taken into storage in the unconfined part of the aquifer.*" That sentence taken literally would lead a reader to attempt to calculate Net recharge in the tables as the sum of the three mentioned columns. The sentence on page 193 could be replaced by "*Net recharge is the flux of groundwater moving from the unconfined to the confined part of the aquifer and is estimated by summing the simulated fluxes across the flow faces of model cells at the boundary between the unconfined and confined zones.*"

DATA REVIEW:

The data model provided by UTBEG is very well organized and documented. However, a few required items specified by the RFP were not found:

- DRIVE:\CZWX_c\grddata\input\stress\ststate\res
Although the readme file states that no reservoir package was used for the steady-state model runs, data is provided under this folder. Please verify that reservoir package was NOT used for the steady-state model runs.

[Response]: The reservoir package was not active for the stress period representing the steady-state phase of the model. Since TWDB required the steady-state period to be bundled with the transient period, the reservoir package is enabled in the transient model that includes steady state as the first stress period. Since the package is enabled, we duplicated the basic reservoir package information in this folder. The reservoir package is made inactive for the steady state period both by the impoundment date being later than the dates of the first stress period and by assigning a reservoir stage below the base of the model cells in which the reservoir is assigned.

- DRIVE:\CZWX_c\scrdata\bdndy
Census block-level data is required by RFP to distribute domestic-other pumpage. If not used please verify and/or explain ... otherwise please provide.

[Response]: Census block-level data were used (see figure 61 on page 156 and text on rural domestic pumping on page 155). This file was overlooked when loading the data model on the CD. An amendment to the data model will include the GIS coverage for the census data and also Excel files with census population for 1990 and 2000 assigned to grid cells.

- DRIVE:\CZWX_c\scrdata\subhyd
A BNDY.MDB Access data set was provided without any metadata file or its purpose. Please provide.

[Response]: This file presents data on water level elevations in the Queen City aquifer used to assign GHB boundary conditions in layer 2. It is companion to associated shape files. An amendment to the data model will include a metadata file documenting this Access file, which will be renamed “qn_wl_50.mdb” for consistency.